Olfactory Ensheathing Cells Moderate Astrocyte Inflammatory Activation

by

David Matthew Hale, BSc (Hons)

Submitted in fulfilment of the requirements for the Degree of
Doctor of Philosophy

Menzies Research Institute
University of Tasmania

August, 2011

STATEMENTS

Declaration of Originality

This thesis contains no material that has been accepted for a degree or diploma by the University of Tasmania or any other institution, except by way of background information and where duly acknowledged in the thesis. To the best of my knowledge and belief this thesis contains no material that infringes copyright or has been previously published or written by any other person except where due acknowledgement is made in the text of the thesis.

David M Hale

Authority of Access

This thesis is available for loan and limited copying in accordance with the *Copyright Act* 1968.

David M Hale

Ethical Conduct

The research associated with this thesis abides by the international and Australian codes on animal experimentation, the guidelines by the Australian Government's Office of the Gene Technology Regulator and the rulings of the Safety, Ethics and Institutional Biosafety Committees of the University.

David M Hale

ABSTRACT

The exceptional capacity for regeneration of olfactory sensory neurons in the olfactory epithelium and their axonal projections into the central nervous system (CNS) has led to extensive investigation of olfactory ensheathing cell (OEC) transplantation as a therapy to promote repair within the injured CNS. In those studies that report enhanced anatomical and functional recovery, the beneficial effects of OECs have been variously attributed to OECs re-myelinating axons, forming a supportive tract for axon growth across the boundary between the peripheral and central nervous systems or producing growth factors, cell adhesion molecules and extracellular matrix proteins that promote axon growth. This thesis investigates the possibility that OECs modulate the inflammatory activation of astrocytes and could thereby contribute to CNS injury repair after therapeutic transplantation.

Following CNS injury, factors released by damaged cells, activated microglia and invading peripheral immune cells activate surviving astrocytes in the lesion penumbra. The activated astrocytes undergo reactive astrogliosis and become another important source of inflammatory mediators. These inflammatory responses often lead to delayed secondary neuronal loss and tissue damage that can exceed the initial traumatic damage. In addition, astrogliosis leads to the development of a glial scar around the lesion that is a barrier to axonal regeneration. Therefore, moderation of astrocyte activation by transplanted OECs could potentially both protect neurons by moderating inflammation and promote axon regeneration by moderating astrogliosis and glial scarring.

The transcription factor nuclear factor-kappaB (NF-κB) is a key regulator of inflammatory responses, including many of the protein expression changes that characterize astrogliosis. NF-κB exists as inactive dimers in the cytoplasm of most cells and must translocate to the nucleus in order to regulate gene transcription. Phorbol myristate acetate (PMA) and calcium ionophore (PMA/ionophore) stimulation was found to induce rapid robust translocation of NF-κB to astrocyte nuclei ($p < 0.001$), providing an *in vitro* model of astrocyte inflammatory activation. NF-κB translocation was readily detectable by immunocytochemistry, providing a relatively simple, direct, unambiguous measure of this early key event in astrocyte activation. Subsequently, soluble factors released by microglia were found to similarly induce NF-κB translocation in astrocytes ($p < 0.001$), illustrating that this detection method can be utilised to investigate other inflammatory stimuli.

Most importantly, soluble factors released by OECs moderated the NF-κB translocation induced in astrocytes by either PMA/calcium ionophore or the microglia-derived factors ($p < 0.001$). Immunostaining confirmed that insulin-like growth factor-1 (IGF-1) was expressed by the cultured OECs and may have contributed to the moderation of astrocyte activation, since IGF-1 also significantly moderated ($p < 0.05$) the NF-κB translocation induced by either stimulus, albeit insufficiently ($p < 0.01$) to account in full for the OEC-induced moderation. OECs also significantly moderated the increased transcription of the NF-κB-regulated pro-inflammatory cytokine, granulocyte macrophage-colony stimulating factor (GM-CSF) in the activated astrocytes ($p < 0.01$). High levels of GM-CSF released by astrocytes can stimulate microglia to produce cytotoxic levels of pro-inflammatory cytokines that may further amplify and prolong inflammation. More severe inflammation leads to more severe astrogliosis, increased secondary neuronal damage and more extensive glial scarring, accompanied by increased deposition of axon growth-inhibitory extracellular matrix molecules. Hence, the identified moderation of astrocyte activation by OECs represents a plausible mechanism whereby transplanted OECs could facilitate neural repair after CNS injury. Furthermore, PMA/ionophore and the microglia-derived factors did not induce NF-κB translocation in OECs, suggesting that OECs transplanted into CNS injury sites could be resistant to pro-inflammatory stimuli and may be able to maintain the *in vitro* phenotype associated here with the amelioration of astrocyte activation.

CNS injury and the associated ischemia induces increases in intracellular calcium levels that can initiate inflammatory responses via NF-κB or, when excessive, cell death by necrosis or apoptosis. Calcium ionophore alone activated significantly more astrocytes than PMA alone ($p < 0.001$), with only a relatively small additive effect attributable to PMA, when astrocytes were treated simultaneously with PMA and ionophore. TUNEL assay demonstrated that at higher doses (250nM-1μM), calcium ionophore dose-dependently ($R^2 = 0.9996$) induced significant ($p < 0.001$) apoptosis of astrocytes. OECs did not appear to protect astrocytes against the ionophore-induced apoptosis and they became apoptotic more rapidly and at lower ionophore doses (125nM) than astrocytes. Consequently, OECs could become apoptotic due to excessive calcium influx if transplanted into ischemic regions of CNS lesions where there are high levels of extracellular calcium ions, glutamate and ATP. Disruption of the surviving vasculature during OEC transplantation could re-initiate ischemia and *in vivo* research may be required to determine the optimal timing and location for transplanting OECs. Both the OEC moderation of astrocyte activation and the absence of OEC inflammatory activation imply that if transplanted OECs survive, they are likely to enhance neuronal survival by moderating inflammation.

In summary, this thesis provides evidence that OECs moderate the inflammatory activation of astrocytes, thus providing a plausible mechanism that could contribute to improved neuroprotection and tissue regeneration in response to therapeutic OEC transplantation after CNS injury. IGF-1 was identified as soluble factor that may have contributed to the anti-inflammatory effects of the cultured OECs. Further research to identify and isolate the responsible soluble factors released by the OECs could lead to more precisely targeted molecular therapies. The *in vitro* model of astrocyte activation established during the thesis could be further utilised to investigate other CNS injury therapies.

ACKNOWLEDGEMENTS

Thanks to my supervisors Inn Chuah and Adrian West for their advice and support. Thanks also for advice, assistance and cooperation in the lab to Rob Gasperini, Shannon Ray, Jackie Leung, Emma Eaton, Michael Pankhurst, Adele Holloway, Julie Harris, Debbie Orchard, Chris Butler, Bill Bennett, Roger Chung, Adele Vincent, Graeme McCormack, Murray Plaister, Marcus Pollard, Steve Weston, Mark Cozens and many others. Thanks to Dadong Wang and Leanne Bischof from the CSIRO for their assistance with HCA Vision software.

PUBLICATIONS

The following publication has arisen during the period of candidature:

Leung JY, Chapman JA, Harris JA, **Hale D,** Chung RS, West AK, Chuah MI (2008) Olfactory ensheathing cells are attracted to and can endocytose bacteria. Cell Mol Life Sci 65:2732-2739.

Part of the research submitted in this thesis has been accepted for publication as follows:

Hale DM, Ray S, Leung JY, Holloway AF, Chung RS, West AK, Chuah MI (2010) Olfactory ensheathing cells moderate nuclear factor kappaB translocation in astrocytes. Mol Cell Neurosci (published online 11 September 2010).

Chuah MI, **Hale DM,** West AK (2010) Interaction of olfactory ensheathing cells with other cell types *in vitro* and after transplantation: Glial scars and inflammation. Exp Neurol (published online 18 August 2010).

The following presentations were based on research submitted in this thesis:

Hale, DM, Chuah MI, West AK (2007) Olfactory ensheathing cells restore an axon-growth permissive phenotype and inhibit apoptosis in astrocytes. Poster presentation at 7th IBRO world congress of Neuroscience, Melbourne, Australia.

Hale, DM, Ray S, Small DH, Chuah MI, West AK (2008) Olfactory ensheathing cells moderate NFκB translocation in rat cortical astrocytes *in vitro*. Poster presentation at SfN Neuroscience 2008 conference, Washington DC, USA.

ABBREVIATIONS

AP	activating protein
ADP	adenosine diphosphate
AMPA	alpha-amino-3-hydroxy-5-methylisoxazole-4-propionic acid
AQP	aquaporin
AraC	cytosine-β-D-arabinofuranoside
ATP	adenosine triphosphate
BBB	blood brain barrier
BDNF	brain-derived neurotrophic factor
BrdU	bromylated dUTP
BSA	bovine serum albumin
CAM	cell adhesion molecule
caMKII	calcium/calmodulin-dependent protein kinase
cAMP	adenosine 3'/5'-cyclic monophosphate
Ca^{2+}	calcium ion
CCL	chemokine
cDNA	complementary DNA
CFDA-SE	carboxy-fluorescein diacetate succinimidyl ester
CHIP	chromatin immunoprecipitation
CM	conditioned medium
CNS	central nervous system
CNTF	ciliary neurotrophic factor
COX	cyclooxygenase
CSPG	chondroitin sulphate proteoglycan
CXCL	chemokine receptor
DAG	diacylglycerol
Db-cAMP	dibutyryl-cyclic AMP
dH_2O	distilled water
DMSO	dimethyl sulphoxide
DMEM	Dulbecco's Modified Eagle's Medium

DMEM-10S	DMEM supplemented with 10% FCS
DNA	deoxyribonucleic acid
dNTP	deoxynucleoside 5’-triphosphate
DTT	dithiothreitol
dUTP	deoxyuridine 5’-triphosphate
EAAT	excitatory amino acid transporter
E. coli	Escherichia coli
EDTA	ethylene diamine tetraacetic acid
ELISA	enzyme-linked immunoabsorbant assay
EMSA	electrophoretic mobility shift assay
ERK	extracellular signal-regulated kinase
FCS	foetal calf serum
FGF	fibroblast growth factor
FITC	fluorescein isothiocyanate
GAPDH	glyceraldehyde 3-phosphate dehydrogenase
GAP43	growth-associated protein 43
GDNF	glial cell line-derived neurotrophic factor
GFAP	glial fibrillary acidic protein
GLAST	glutamate/aspartate transporter
GLT-1	glutamate transporter-1
GM-CSF	granulocyte macrophage-colony stimulating factor
GTP	guanosine 5-triphosphate
HB	Hoechst blue (33342) DNA dye
HEPES	N-2-hydroxyethyl piperazine-N-2-ethane sulphonic acid
HBSS	Hank’s Balanced Salt Solution
HRP	horseradish peroxidase
ICAM	intercellular adhesion molecule
IFN	interferon
IGF	insulin-like growth factor
IgG	immunoglobulin
IκB	inhibitor of nuclear factor kappaB

IKK	IκB kinase
IL	interleukin
iNOS	inducible nitric oxide synthase
IP3	inositol trisphosphate
JAK	janus tyrosine kinase
JNK	Jun N-terminal kinase
K^+	potassium ion
LIF	leukaemia inhibitory factor
LDL	low-density lipoprotein
LPA	lysophosphatidic acid
LPS	lipopolysaccharide
MAP	microtubule-associated protein
MAPK	mitogen-activated protein kinase
MCP	monocyte chemoattractant protein
MEM-H	Modified Eagle's Medium with HEPES
mGluR	metabotropic glutamate receptor
MHCII	major histocompatibility complex II
MIP	macrophage inflammatory protein
MKK	MAPK kinase
MMP	matrix metalloproteinase
mRNA	messenger RNA
MT	metallothionein
MTF	metal transcription factor
NADPH	nicotinamide adenine dinucleotide phosphate
Na/Ca	sodium/calcium ion exchanger
NFAT	nuclear factor of activated T-cells
NF-κB	nuclear factor-kappaB
NGF	nerve growth factor
NMDA	N-methyl-D-aspartate
NO	nitric oxide
OEC	olfactory ensheathing cell

P	phosphorylation
PAGE	polyacrylamide gel electrophoresis
PBS	phosphate buffered saline
PCR	polymerase chain reaction
PK	protein kinase
PKC	calcium-dependent protein kinase
PLC	phospholipase C
PLL	poly-L-lysine
PMA	phorbol-12-myristate-13-acetate
PNS	peripheral nervous system
P/I	PMA and calcium ionophore
$p75^{NTR}$	low affinity neurotrophin receptor
P2X	ionotropic purinergic receptor
P2Y	metabotropic purinergic receptor
RNA	ribonucleic acid
RNS	reactive nitrogen species
ROS	reactive oxygen species
RTK	receptor tyrosine kinase
S. aureus	Staphylococcus aureus
SCI	spinal cord injury
SDS	sodium dodecyl sulphate
SERCA	smooth endoplasmic reticulum calcium ATPase (pump)
SOD	superoxide dismutase
STAT	signal transducer and activator of transcription
TGF	transforming growth factor
TLR	toll-like receptor
TNF	tumour necrosis factor
TNFR	TNF receptor
TUNEL	terminal dUTP transferase nick end labelling
VEGF	vascular endothelial growth factor

TABLE OF CONTENTS

LIST OF TABLES AND FIGURES

CHAPTER 1: Introduction

1.0 Central nervous system injury

1.00 Neurons are vulnerable to injury

1.00.0 Central nervous system function depends on adequate blood supply

The structural and functional integrity of the central nervous system (CNS) depends on a continuous supply of oxygen and glucose from the cerebral vasculature (Iadecola and Nedergaard, 2007; Doyle et al., 2008; Candelario-Jalil, 2009). The disruption of this metabolite supply because of vascular damage is the major underlying cause of the neuronal and glial cell death resulting from CNS injury. Although constituting only about 2% of adult body weight, the brain consumes around 20% of the available oxygen and glucose in order to maintain the necessary activity of ion pumps for regulating neuronal membrane potentials and the constant synthesis of neurotransmitters and other signalling molecules (Gulbenkian et al., 2001; Edvinsson, 2006; Girouard and Iadecola, 2006; Zlokovic, 2008; del Zoppo, 2010). Brain tissue is highly perfused to cater for this high energy demand and the brain capillary density displays a remarkably heterogeneity that correlates with regional blood flow and energy use (Iadecola and Nedergaard, 2007). Changes in neural activity can induce highly localised changes in cerebral blood flow within seconds to match the oxygen and glucose supply to the local metabolic requirements. CNS blood vessels, neurons and glia constitute a functional 'neurovascular unit' (Fig. 1.0) where the close proximity of the different cells allows the necessary metabolite exchange and regulatory paracrine signalling (Iadecola and Nedergaard, 2007; Zlokovic, 2008; del Zoppo, 2010). The endothelial cells of arterioles and capillaries have a continuous basal lamina and a layer of contractile pericytes that regulate blood vessel diameter (Kida et al., 1993; Girouard and Iadecola, 2006; Zlokovic, 2008). Tight junctions between brain capillary endothelial cells together with the continuous basal lamina constitute the blood-brain barrier (BBB), which prevents potentially harmful macromolecules and pathogens in the blood from entering brain tissue (Abbott, 2002; Curin et al., 2006; Iadecola and Nedergaard, 2007; Zlokovic, 2008). The flattened end-feet of astrocyte processes are closely apposed on the basal lamina and interact with the

endothelial cells to regulate BBB permeability. The regulated movement of water, ions, glucose and other nutrients across the BBB between the capillary endothelial cells and the astrocyte end-feet is crucial to maintaining a suitable environment for normal neuronal function (Verkhratsky et al., 1998; Verkhratsky and Steinhauser, 2000; Zlokovic, 2008; Kwon et al., 2009).

1.00.1 Ischemia causes rapid neuronal death

Ischemia resulting from traumatic injury, stroke or cardiac arrest interrupts the supply of oxygen and glucose required for ATP production by glycolysis and oxidative phosphorylation, causing neuronal death within minutes (Johnston, 2005; Curin et al., 2006; Doyle et al., 2008; Candelario-Jalil, 2009). The glucose-dependent metabolism, high energy requirements and cellular specialisation of neurons makes them particularly sensitive to ischemic damage, although astrocytes and other glial cells are also susceptible (Xu et al., 2001; Swanson et al., 2004; Chen et al., 2005b; Giffard and Swanson, 2005). The CNS damage caused by ischemia is largely irreversible and often has fatal or severely disabling consequences depending on the location and extent of the neuronal damage (Stys, 2004; Ennis and Keep, 2006; Oechmichen and Meissner, 2006; Yamashima et al., 2007; Doyle et al., 2008; Segura et al., 2008; Candelario-Jalil, 2009). Following the initial cell death from ischemia and physical damage, a sequence of events leads to excessive glutamate-induced excitation culminating in 'excitotoxic' neuronal death (Coyle and Puttfarcken, 1993; Kannurpatti et al., 2000; Johnston, 2005; Villmann and Becker, 2007; Fernandez-Gomez et al., 2008). Without ATP, the membrane sodium and potassium pumps cannot maintain ionic gradients and membrane depolarisation occurs in neurons and astrocytes, releasing large amounts of glutamate, ATP and other neurotransmitters. Glutamate is the major excitatory neurotransmitter and the excessive extracellular levels initiate a positive feedback loop, causing further membrane depolarisation, ATP consumption and glutamate release. Blood glutamate levels are several fold higher than normal levels in the brain extracellular fluid and make an important additional contribution to excessive glutamate receptor activation following injury (Wagner, 2007). Activation of glutamate receptors on neurons and astrocytes releases calcium ions (Ca^{2+}) from intracellular stores (Lipton, 2001; Pivovarova et al.,

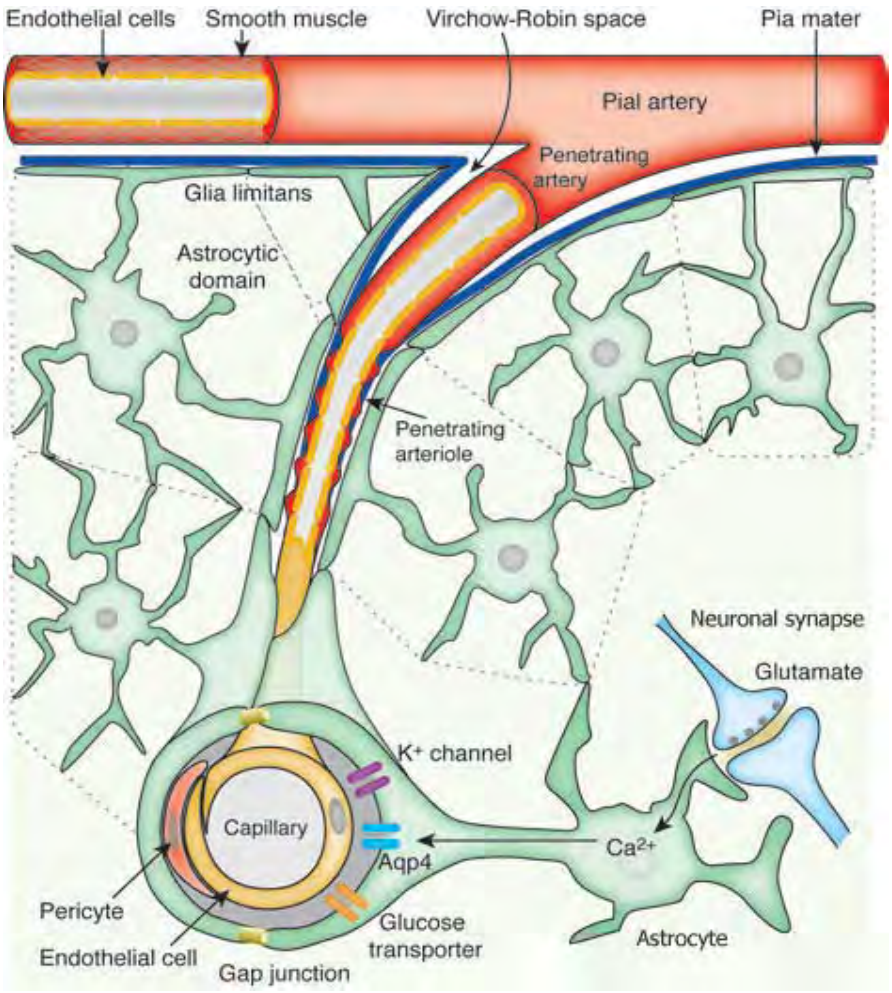

Figure 1.0 Astrocytes interact with synapses and blood vessels. Grey matter astrocytes extend fine processes that surround most synapses and large processes (end-feet) that are closely apposed on blood vessel walls. Pial arteries rest on the glia limitans, which envelops the brain surface. Astrocytes support synaptic transmission by taking up and recycling glutamate for re-use by neurons. Astrocytes also produce metabolic substrates for neuronal function and synapse formation. Grey matter astrocytes occupy exclusive spatial domains and consequently all of the ~160,000 synapses in an astrocytic domain are covered by processes from a single astrocyte. The end-feet of astrocytes cover >99% of the vascular surface facing capillary endothelial cells or the contractile pericytes. Vascular end-feet express several specialized proteins including the glucose transporter 2 for the rapid transfer of glucose from blood to neurons. Ion channels (e.g. potassium; K^+) , aquaporin 4 (Aqp4) and gap junction proteins in the end-feet regulate CNS extracellular homeostasis and may also be involved in the regulation of blood-flow to match neuronal demand, which could be signalled by glutamate stimulation of intracellular calcium (Ca^{2+}) signalling (adapted from Iadecola et al, 2007).

2004; Swanson et al., 2004; Smith et al., 2005; Wagner, 2007; Candelario-Jalil, 2009). Mitochondria attempt to take up the excess Ca^{2+} until high Ca^{2+} levels damage mitochondrial membranes and calcium is released back into the cytosol, together with cytochrome C and reactive oxygen species (ROS) from the mitochondrial respiratory chain (Dugan et al., 1995; Swanson et al., 2004; Blomgren and Hagberg, 2006; Wagner, 2007; Lai et al., 2009; Niizuma et al., 2009; Wang et al., 2009b). Cytochrome C then activates cytosolic proteases, initiating a cascade of cellular damage leading to neuronal apoptosis. Hypoxia also interrupts the respiratory chain of oxidative phosphorylation causing increased ROS generation, which is further catalysed by iron released from blood and damaged cellular proteins (Choi et al., 2005; Blomgren and Hagberg, 2006; Loh et al., 2006; Valko et al., 2007). The high levels of ROS including superoxide, nitric oxide and peroxynitrite generated by neurons and surrounding glia contribute to anoxic neuronal death by directly damaging neuronal proteins and membranes (Casetta et al., 2005; Blomgren and Hagberg, 2006; Forder and Tymianski, 2009; Niizuma et al., 2009).

1.00.2 Cerebral oedema is a consequence of blood brain barrier damage

Blood brain barrier (BBB) damage resulting from injury causes cerebral oedema due to the excessive influx of water from the blood into the extracellular space of the CNS (Lynch et al., 2002; Ishida et al., 2006; Ostrowski et al., 2006; Doyle et al., 2008; Risher et al., 2009; Zador et al., 2009). Cerebral oedema can be further increased by obstruction of the flow or drainage of the cerebrospinal fluid by the initial damage or subsequent haematoma development (Go, 1997; Lohdia et al, 2006). Oedema elevates intra-cranial pressure and restricts vascular perfusion and therefore exacerbates hypoxia and the related tissue damage. The clotting responses that limit systemic blood loss disrupt the supply of oxygen and metabolites leading to further cell death. Astrocyte swelling is a prominent early response to injury as a result of the inactivation of ion pumps in the hypoxic conditions and the excess water moving into astrocytes by osmosis (Panickar and Norenberg, 2005; Gunnarson et al., 2008; Laird et al., 2008; Sinke et al., 2008; Panickar et al., 2009; Risher et al., 2009; Zador et al., 2009). Astrocytes upregulate aquaporin water transport proteins in response to injury, assisting in the uptake and redistribution of excess water via gap junctions into the ventricular cerebrospinal fluid or the vascular

blood in undamaged CNS regions. However, excessive swelling can also rupture astrocyte plasma membranes causing necrotic cell death and releasing cellular contents into the extracellular space (Kimelberg, 2005; Panickar and Norenberg, 2005). Neurons also swell during oedema adding to neuronal damage and death because neurons do not express aquaporins to regulate water uptake (Risher et al., 2009).

1.01 The inflammatory response to CNS injury

1.01.0 CNS tissue damage initiates inflammation

The initial responses to CNS injury are followed by longer term changes involving complex cellular and molecular interactions extending well beyond the lesion site that may have systemic components (Fawcett and Asher, 1999; Chen and Swanson, 2003; Harukuni and Bhardwaj, 2006; Lucas et al., 2006; Floyd and Lyeth, 2007; Ayer and Zhang, 2008; Doyle et al., 2008; Fitch and Silver, 2008). Neurons and glia that die immediately, due to physical damage and ischemia, release ATP, glutamate, cytokines, prostaglandins, heat shock proteins, calcium and cellular debris. The entry of blood components and pathogens into the CNS following BBB damage can directly induce inflammation and generate neurotoxic products at injury sites (Stys, 2004; Choi et al., 2005; Ray, 2006; Whitney et al., 2009; Goldshmit et al., 2010). Inflammation is a stereotypical response of tissues to injury that has evolved to degrade toxic stimuli and restore tissue integrity in what is usually a beneficial and self-limiting healing process (Kracht and Saklatvala, 2002; Schwartz et al., 2006; Farooqui et al., 2007). Surrounding cells attempt to limit the injury and repair the damage (Ellison et al., 1999; Kracht and Saklatvala, 2002; Farooqui et al., 2007; Whitney et al., 2009). Dependent on the extent of injury, the acute inflammation resolves with wound healing and the restoration of tissue integrity. Although a similar sequence of events occurs following injury to the adult mammalian CNS, there is never a substantial restoration of normal tissue structure and function, even after relatively mild tissue damage. Removal of pathogens and damaged tissue usually requires some sacrifice of surrounding tissue prior to tissue regeneration for wound-healing (Schwartz, 2003, 2010). In the CNS, this tissue sacrifice is a particularly critical determinant of the capacity for recovery of normal function. The complex, precise network of neural connections required for motor and cognitive functions together with

the low inherent capacity for neurogenesis and axon regrowth in the adult CNS, decreases the likelihood of tissue repair and restoration of normal function (Schwartz et al., 1989; Yagita et al., 2001; Schwab, 2002; Nieto-Sampedro, 2003; Lie et al., 2004; Fawcett, 2006b; Das and Basu, 2008; Ruitenberg and Vukovic, 2008; Whitney et al., 2009).

1.01.1 Inflammation causes neuronal damage

Although the inflammation following CNS injury resembles that resulting from injury to any vascularised tissue (Ellison et al., 1999; Farooqui et al., 2007; Whitney et al., 2009; del Zoppo, 2010), the immune protection provided by the BBB and the highly specialised functions of CNS tissue ensure that there are also important differences (Whitney et al, 2009). Activated neurons and glia release cytokines and chemokines that recruit microglia, the resident CNS immune cells, and peripheral leukocytes to the injury site, where they proliferate and can differentiate into macrophages to phagocytose and remove pathogens and damaged tissue (Fawcett and Asher, 1999; Frangogiannis, 2007; Chen and Palmer, 2008; Matsumoto et al., 2008). Upregulation of adhesion molecules promotes leukocyte infiltration through capillary endothelial cells and retention in the damaged tissue. Local blood flow is augmented by increased production of prostaglandins and nitric oxide (NO) following induction of their respective enzymes, cyclooxygenase-2 (COX-2) and inducible NO synthase (iNOS) (Kracht and Saklatvala, 2002; Kim and de Vellis, 2005; Kim and Dustin, 2006; Kim et al., 2006). Under normal conditions only relatively low numbers of macrophages, T-cells and dendritic cells can enter the CNS parenchyma from the blood. BBB damage and altered permeability after injury (del Zoppo, 2010) allows the recruitment of large numbers of peripheral neutrophils, monocytes and lymphocytes to the lesion (Toews et al., 1998; Bush et al., 1999; Proescholdt et al., 2002; Babcock et al., 2003; Popovich et al., 2003; Frangogiannis, 2007; Gee et al., 2007; Longbrake et al., 2007; Matsumoto et al., 2007). Pro-inflammatory cytokines and other factors stimulate innate immune responses in both the recruited peripheral immune cells and resident microglia in the damaged tissue. Adaptive immune responses are triggered when lymphocytes that enter the lesion encounter novel CNS antigens. Following exposure to abnormal CNS proteins or molecules from blood in the altered post-injury environment, activated microglia can also participate in adaptive

immune responses, including antigen presentation (Stollg and Jander, 1999; Town et al., 2005; Hanisch and Kettenmann, 2007; Wagner, 2007; Yang et al., 2010). This activation of the immune cells initiates a massive release of pro-inflammatory and neurotoxic molecules from resident and invading cells (Feuerstein et al., 1994; Ellison et al., 1999; John et al., 2005; Kim and de Vellis, 2005; Mehta et al., 2007; Yagita et al., 2008; Pineau and Lacroix, 2009).

NO and other ROS generated by the activated immune cells can destroy invading micro-organisms but may also damage resident CNS cells that are compromised by injury or infection (Kim and Dustin, 2006). The injury and tissue repair responses continue over days and up to months and are associated with continuing apoptotic death of neurons because of their vulnerability to the cytotoxic effects of NO and other ROS (Profyris et al., 2004; Swanson et al., 2004; Casetta et al., 2005; Oechmichen and Meissner, 2006; Szeto, 2006; Mehta et al., 2007). The extent to which tissue repair is possible depends on the location and size of the region of damaged tissue. Growth factors, cytokines and other molecules released by activated astrocytes, microglia, macrophages, fibroblasts and endothelial cells during mild acute inflammation can stimulate neurogenesis and axon growth (Bregman et al., 1997; Namiki et al., 2000; Le and Esquenazi, 2002; Graef et al., 2003; Furukawa and Furukawa, 2007; Bunge, 2008). However, more severe and prolonged inflammation after CNS injury typically leads to increased secondary neuronal damage, increased infarct size, decreased neurogenesis and worse functional deficits (Bethea, 2000; Brahmachari et al., 2006; Yang et al., 2007; Jiang et al., 2008; Laird et al., 2008).

1.01.2 Four intracellular signalling pathways regulate inflammatory gene expression

The progress of inflammation and wound healing is determined by complex interactions involving inflammatory mediators produced by astrocytes, microglia, peripheral immune cells, neurons, progenitor cells, fibroblasts and endothelial cells (Chen and Swanson, 2003; Sandvig et al., 2004; Fawcett, 2006a; Farooqui et al., 2007; Chen and Palmer, 2008). The inflammation and wound healing involve extensive reorganisation of cells and tissues requiring the altered transcription of hundreds of genes to regulate the necessary protein synthesis (Ellison et al., 1999). Astrocytes, microglia and recruited immune cells

produce a variety of growth factors, cytokines and other factors that regulate cell survival, proliferation and differentiation for wound-healing (Ellison et al., 1999; Hernandez et al., 2002; Lu et al., 2004; Yang et al., 2004; John et al., 2005; Yang et al., 2007). Expression of most of these inflammatory genes is co-ordinated through the activation of four intracellular signalling pathways leading to transcriptional activation (Fig. 1.1) (Yamamoto and Gaynor, 2001; Kracht and Saklatvala, 2002; Saklatvala, 2007; Yang et al., 2007). These are the pathways leading to activation of the transcriptional regulator, nuclear factor-kappaB (NF-κB) and the phosphorylation cascades of the three types of mitogen-activated protein kinase (MAPK), the Jun N-terminal kinases (JNKs), the p38 MAPKs and the extracellular signal-regulated kinases 1 and 2 (ERK1/2) (Kyriakis and Avruch, 2001; Saklatvala, 2007; Wolter et al., 2008). Activation of the three MAPKs can promote inflammatory gene expression both through activation of NF-κB and other transcription factor families. While NF-κB translocation is necessary for robust inflammatory responses, full activation of inflammatory genes appears to require the assembly of a multi-protein activation complex at gene promoter regions associated with the synchronous activation of both NF-κB and a mitogen-activated (MAP) kinase pathway (Kracht and Saklatvala, 2002; Chen and Greene, 2004a). NF-κB like other "rapid-acting" primary transcription factors, including c-JUN, nuclear factor of activated T-cells (NFAT), and signal transducers and activators of transcription (STATs), facilitate the rapid inflammatory responses required for protection of cells against potentially harmful stimuli, since being present in cells in an inactive state, they do not require new protein synthesis before activation (Gilmore, 1999; Wolter et al., 2008). Amplification of the inflammatory response to injury can occur through signalling interactions between cells, within the intracellular signalling cascades and through the multiple complementary mechanisms for transcriptional regulation (Baeuerle and Henkel, 1994; Kracht and Saklatvala, 2002; Chen and Greene, 2004b).

1.01.3 Increased cytokine production can amplify inflammation

MAPK and NF-κB pathway activation (Fig. 1.2) by the initial injury leads to an inflammatory cascade that stimulates production of a range of cytokines, chemokines, adhesion molecules, extracellular matrix proteins, proteases and growth factors required

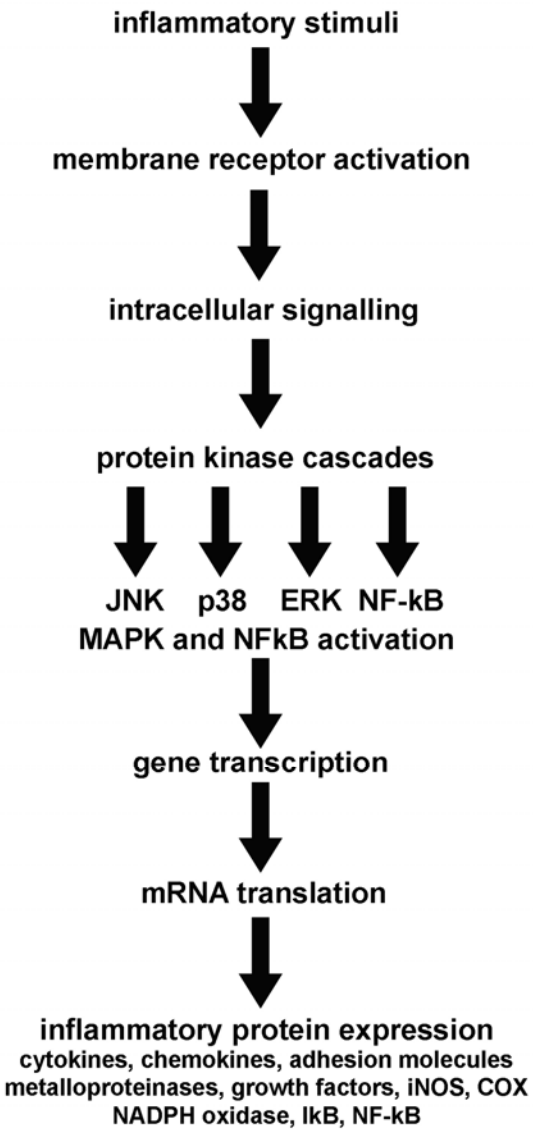

Figure 1.1 Flow chart of inflammatory gene regulation. Expression of most inflammatory genes is regulated through the activation of four intracellular signalling pathways leading to transcriptional activation. These are the pathways leading to activation of the transcriptional regulator, nuclear factor-kappaB (NF-κB) and the protein kinase phosphorylation cascades of the three types of mitogen-activated protein kinase (MAPK), the Jun N-terminal kinases (JNKs), the p38 MAPKs and the extracellular signal-regulated kinases 1 and 2 (ERK1/2). Inflammatory stimuli, including cytokines, chemokines, pathogens and excessive levels of neurotransmitters stimulate specific membrane receptors. Complex interactions follow within intracellular signalling pathways that lead to activation of the protein kinase cascades of the four major inflammatory signalling pathways. Gene transcription is followed by mRNA translation and increased protein expression (adapted from Kracht and Saklatvala, 2002).

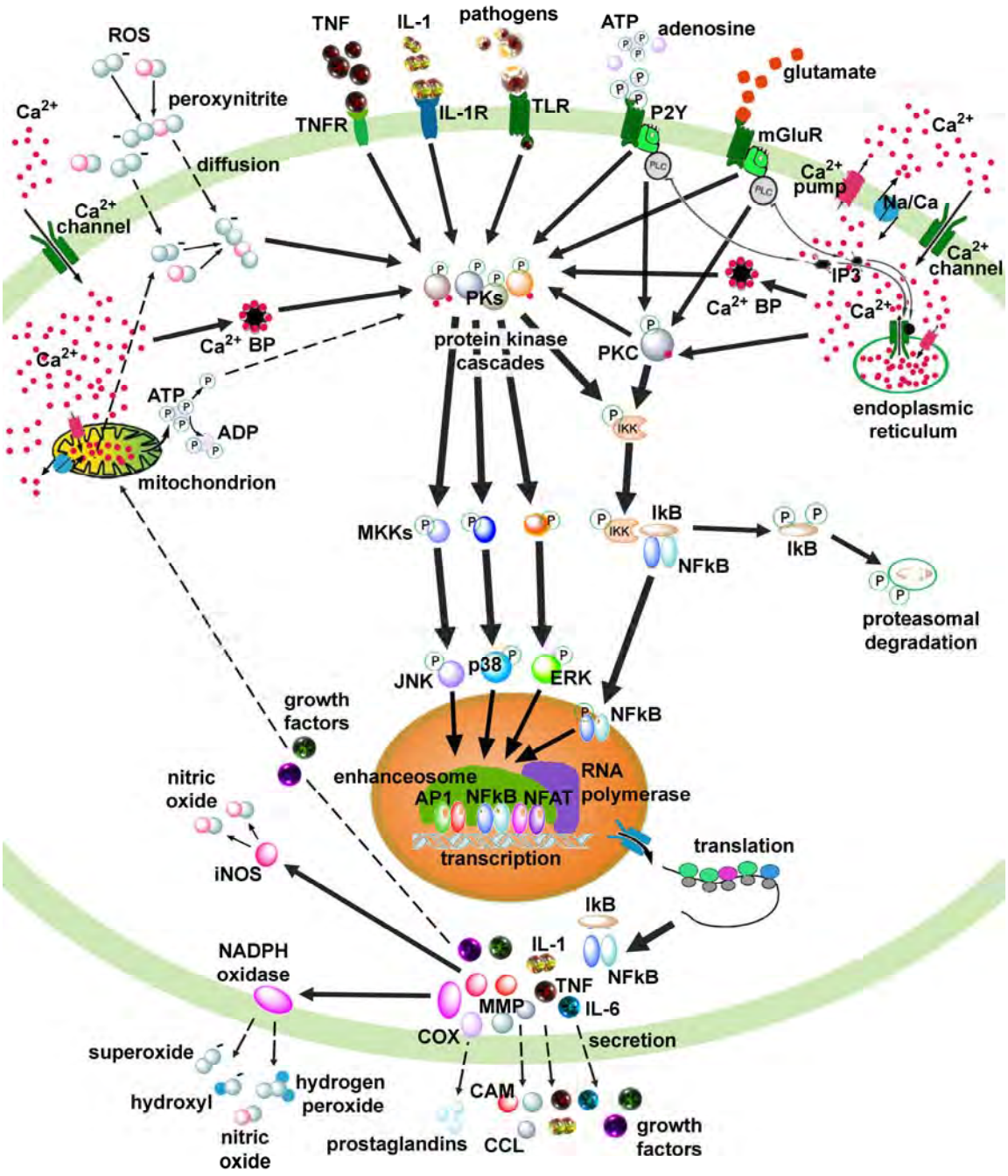

Abbreviations: AP-1, activating protein 1 CAM, cell adhesion molecule; Ca^{2+}BP, calcium binding protein; CCL, chemokine; COX, cyclo-oxygenase; ERK, extracellular-regulated kinase; IκB, inhibitor of NF-κB; IKK, IκB kinase; IL-1, interleukin-1; iNOS, inducible nitric oxide synthase; IP3, inositol trisphosphate; JNK, JUN-N-terminal kinase; MAPK, mitogen-activated protein kinase; mGluR, metabotropic glutamate receptor; MKK, MAPK kinase; MMP, matrix metalloproteinase; Na/Ca, sodium/calcium ion exchanger; NFAT, nuclear factor of activated T-cells; NF-κB, nuclear factor-κB; P, phosphorylation; PKC, calcium-dependent protein kinase; PKs, protein kinases; PLC, phospholipase C; P2Y, metabotropic purinergic receptor; ROS, reactive oxygen species; RTK, receptor tyrosine kinase; TLR, toll-like receptor; TNF, tumour necrosis factor.

Figure 1.2 The regulation of cellular inflammatory responses. Pro-inflammatory mediators including, IL-1, TNF, ATP, glutamate and pathogens trigger specific receptor activation leading to activation of protein kinases, elevation of intracellular calcium ion (Ca^{2+}) levels and indirectly via increased metabolism, to increased intracellular ROS and RNS production. Extracellular Ca^{2+} can also enter through membrane ion channels, while ROS and RNS released from nearby cells can diffuse through membranes. These factors lead to activation of the IκB kinase, ERK, JNK and p38 MAPK signalling pathways. These kinases phosphorylate either IκB and NF-κB, or the transactivation domains of AP-1 proteins, resulting in activation of both NF-κB and AP-1. Purine and glutamate stimulation of metabotropic receptors can release Ca^{2+} from internal stores, which activate NF-κB and MAPKs via PKC and other transcription factors, such as NFAT via Ca^{2+} binding proteins, such as calcineurin. Activation of at least one MAP kinase pathway is required in addition to NF-κB to promote strong transcription. Signals from these pathways converge at gene promoters by promoting chromatin remodelling via histone acetylation and phosphorylation. This is followed by the formation of multi-protein complexes, known as enhanceosomes. Within an enhanceosome, NF-κB and AP-1 interact with DNA, other transcription factors such as NFAT, co-activators and RNA polymerase. Variations within the enhanceosome composition result in activation of specific genes followed by mRNA translation and increased inflammatory protein expression. NF-κB promotes transcription of its own gene and its inhibitor (IκB), while many of the other inflammatory proteins are stimulators of the MAPK and NF-κB pathways. Increased intracellular calcium and growth factors can stimulate mitochondrial production of ATP to provide energy for the increased protein synthesis (adapted from Kracht and Saklatvala, 2002 and Carafoli, 2002).

for inflammation and subsequent wound-healing (Ellison et al., 1999; Meeuwsen et al., 2003a; Raghavendra Rao et al., 2003; John et al., 2005; Zhang et al., 2006). IL-1β and TNF-α are major initiating cytokines involved in inflammatory responses in the CNS and other tissues (Siren et al., 2001a; John et al., 2005; Panickar and Norenberg, 2005; Farooqui et al., 2007; Lambertsen et al., 2009). Transcription of both cytokines is promoted by NF-κB activation and their upregulation has been detected within an hour of CNS injury (John et al., 2005; Laird et al., 2008). IL-1β and TNF-α are also important secondary amplifiers of inflammation that promote their own production by macrophages and activated glia through their strong activation of NF-κB and the MAPKs (John et al., 2005; Saklatvala, 2007). Cytokines such as IL-6, IL-15 and interferon-γ (IFN-γ) can synergise with other stimuli to amplify the response (John et al., 2005; Satriotomo et al., 2006; Saklatvala, 2007; Gomez-Nicola et al., 2008; Gomez-Nicola et al., 2010).

1.02 Astrocyte activation has a crucial role in CNS injury responses

1.02.0 Reactive astrocytes are a major source of inflammatory mediators

Altered gene transcription following the inflammatory activation of astrocytes *in vivo* leads to a phenotype change known as astrogliosis, which is a prominent feature of CNS inflammation (Silver and Miller, 2004; Sofroniew, 2005; Fawcett, 2006a; Fernandez et al., 2007a; Fitch and Silver, 2008). Due to their size and abundance, the activated astrocytes are a major source of cytokines, chemokines, adhesion factors, extracellular matrix proteins, growth factors and other inflammatory mediators (Ellison et al., 1999; Panenka et al., 2001; Meeuwsen et al., 2003a; John et al., 2005; Khorooshi et al., 2008). Astrocytes are also the main contributors to wound healing and restoration of the extracellular matrix after CNS injuries (Hertel et al., 2000; Muir et al., 2002; Bundesen et al., 2003; Zhang et al., 2006; Gris et al., 2007). The high levels of extracellular glutamate, ATP, Ca^{2+} and many other factors in the hypoxic conditions after CNS injury, activate inflammatory gene transcription in astrocytes through the NF-κB and MAPK pathways (Neary and Kang, 2005; O'Riordan et al., 2006; Zeng et al., 2008b), with an increase in intracellular Ca^{2+} levels being an early event in the astrocyte activation (Neary and Kang, 2005; Smith et al., 2005; Weisman et al., 2005) (Fig. 1.2). Activated microglia release ROS, IL-1β, TNF-α and IL-6 (Giulian et al., 1994; Streit, 2000; Aloisi, 2001; Hanisch,

2002; Kim and de Vellis, 2005; Gosselin and Rivest, 2007), which also activate astrocytes via NF-κB to promote the expression of chemokines, including monocyte chemoattractant protein (MCP)-1, macrophage inflammatory proteins (MIPs) 1α and 2α, Gro and fractalkine as well as their respective receptors (Hughes et al, 2002; Babcock et al., 2003; Meeuwsen et al., 2003a; Bolin et al., 2005; John et al., 2005; Khorooshi et al., 2008; Held-Feindt et al., 2010; Schwartz et al., 2010). The location of reactive astrocytes in the injury penumbra and their proximity to the BBB enables them to generate a gradient of chemokines that attract resident microglia and circulating leukocytes towards the injured tissue (Ellison et al., 1999; Babcock et al., 2003; Meeuwsen et al., 2003a; John et al., 2005). The chemokines and adhesion molecules also promote the migration of neural progenitor cells, which further contribute to the complexity of the inflammatory signalling as they proliferate and differentiate in the lesion (Okada et al., 2004; Alonso, 2005; John et al., 2005; Faijerson et al., 2006; Tatsumi et al., 2008).

1.02.1 Reactive astrocytes form a protective glial scar

Over several days post-injury the GFAP-rich processes of reactive astrocytes are major contributors to the formation of a 'glial scar' (Figs. 1.3, 1.4) around the lesion that separates the core region of severely damaged tissue from the lesion penumbra (Fawcett and Asher, 1999; Silver and Miller, 2004; Sofroniew, 2005; Fitch and Silver, 2008). The increased immunoreactivity for GFAP exhibited by reactive astrocytes surrounding CNS lesions (Fig. 1.4) is a prominent feature of astrogliosis that is often used as an indication of the severity of inflammation (Krohn et al., 1999; Brahmachari et al., 2006). Although the functional significance of the increased GFAP immunoreactivity remains uncertain, it has been suggested that increased expression of GFAP could provide more binding sites for aquaporins, glutamate transporters and ion channels to help restore post-injury extracellular homeostasis (Wilhelmsson et al., 2006; Sullivan et al., 2007; Gunnarson et al., 2008). The glial scar is a dense tissue with many tightly interwoven astrocyte processes (Fig. 1.4B) and other cells surrounded by a specialised extracellular matrix with little extracellular space (Fawcett and Asher, 1999; Fitch and Silver, 2008). Neural progenitor cells are induced to proliferate and differentiate in the lesion where they make a major contribution to the population of reactive astrocytes that form the glial scar

(Alonso, 2005; Shen et al., 2010). A robust inflammatory response within the lesion may allow the removal of cellular debris and pathogens by migratory and resident phagocytes without compromising cells outside the glial scar (Faulkner et al., 2004; Sofroniew, 2005). The more moderate inflammatory responses of astrocytes in the penumbra (Fig. 1.4E) may then initiate processes leading to wound healing and tissue regeneration involving angiogenesis, gliogenesis, neurogenesis and the re-establishment of the BBB and a glial-pial boundary (Chen and Swanson, 2003; Faulkner et al., 2004; Sofroniew, 2005). Thus, as with scarring in other organs and tissues the glial scar may be an adaptive component of wound healing with protective functions. Any neurogenesis is more likely to occur outside the glial scar, in the perilesional penumbra, where inflammation is less severe (Kernie et al., 2001; Chen and Swanson, 2003; Panickar and Norenberg, 2005; Ito et al., 2006c; Doyle et al., 2008).

1.02.2 The glial scar is a barrier to axonal regeneration

Although the glial scar could limit tissue damage by protecting the penumbral tissue from excessive inflammation, it simultaneously presents a major barrier to the axon regrowth across the lesion required for the restoration of functional neural networks by surviving or regenerating penumbral neurons (Qiu et al., 2000; Silver and Miller, 2004; Fawcett, 2006b). The altered expression of chemokines, adhesion molecules, proteases, extracellular matrix components and cell surface receptors by reactive astrocytes serves to attract and retain microglia, neural progenitors and peripheral macrophages at injury sites (Babcock et al., 2003; Chen and Swanson, 2003; John et al., 2005). Since the motility of all cells is regulated by similar pathways affecting cytoskeletal dynamics (Suter and Forscher, 2000; Gallo and Letourneau, 2004; Hall, 2005), many of these same factors expressed by reactive astrocytes may also restrict regenerating axons to the lesion periphery (Sandvig et al., 2004; Goldshmit et al., 2006; Gross et al., 2007). While this could protect regenerating neurons from the cytotoxic conditions of the lesion it also prevents the re-establishment of neuronal connectivity for the recovery of normal CNS function.

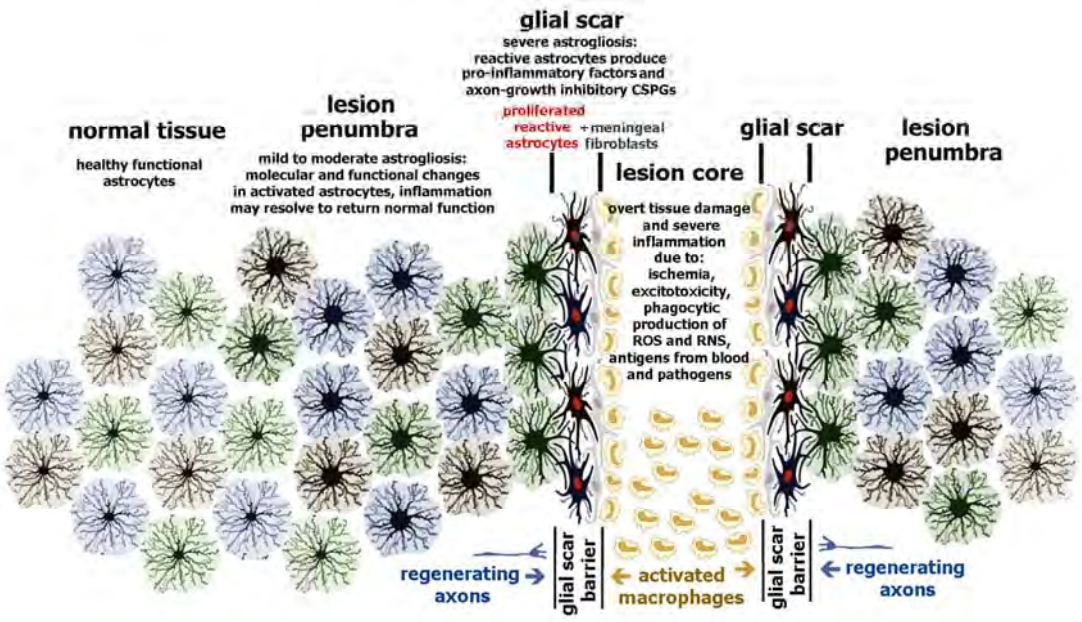

Figure 1.3 Reactive astrocytes and the glial scar. Severe reactive astrogliosis and glial scarring develop on the boundary of the lesion core, involving astrocyte proliferation (with red nuclei in figure) and invading meningeal fibroblasts (with grey nuclei in figure). Progenitor cells proliferate and differentiate into reactive astrocytes adding to the scar tissue. Reactive astrocytes in the scar have overlapping domains, extend long thickened GFAP-expressing processes towards the lesion and secrete axon-growth inhibitory chondroitin sulphate proteoglycans (CSPGs). Mature glial scars tend to persist for long periods and act as barriers not only to axon regeneration but also to inflammatory cells and so protect healthy tissue from the cytotoxic conditions of the lesion core. Astrocytes in the lesion penumbra exhibit mild to moderate reactive astrogliosis and remain in their exclusive domains although having thickened processes. Penumbral astrocytes show alterations in molecular expression and functional activity that vary with insult severity and may return to normal if inflammation resolves (adapted from Sofroniew, 2009).

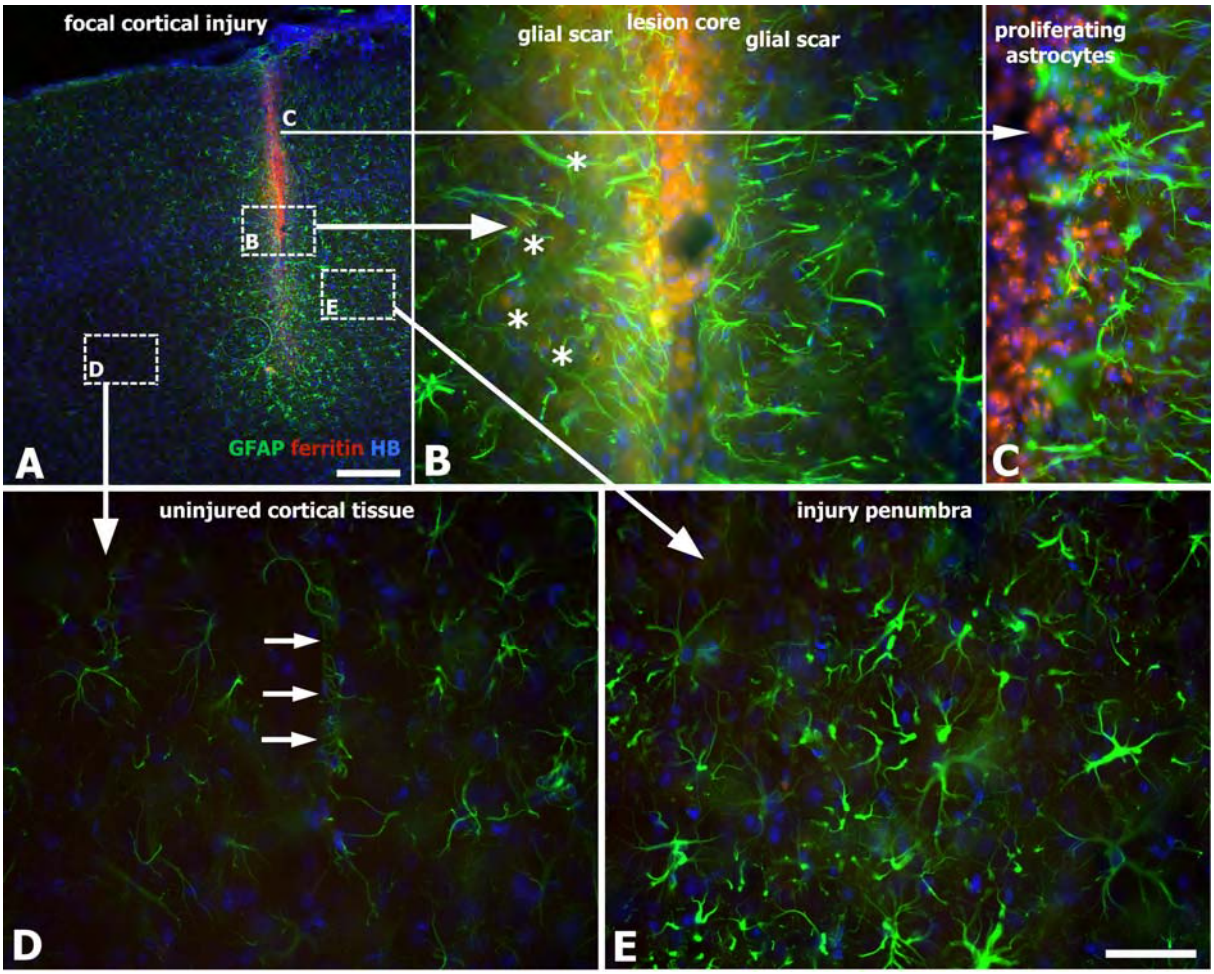

Figure 1.4 Reactive astrocytes surround a focal cortical injury lesion. A: 7 days after a 1.5mm deep, 22 gauge needle-stick injury in adult rat cortex, 50µm sagittal cryostat sections were immunostained for GFAP (green) to show astrocytes and ferritin (red) as a marker for activated macrophages. Nuclei were counterstained with Hoechst blue DNA stain (HB). Activated macrophages occupy the needle-stick injury lesion surrounded by reactive astrocytes with high intensity GFAP immunoreactivity. GFAP immunoreactivity gradually diminishes away from the lesion until reaching the usual low levels found in adult cortical astrocytes. Scale bar is 250µm. B: Enlargement of lesion and glial scar region from A. Most activated macrophages are confined to the lesion with some also appearing amongst the reactive astrocytes of the scar tissue (asterisks). Overlapping processes extend from the reactive astrocytes and surround the lesion. C: Small astrocytes with intense GFAP immunoreactivity on the lesion border are probably proliferating astrocytes that have differentiated from progenitor cells, which migrate to lesions. D: Astrocytes about 1mm from the lesion show normal adult cortical morphology with weak immunoreactivity for GFAP creating the appearance of spindly processes, which can be seen wrapped around a small descending blood vessel in the centre of the image (arrows). E: Astrocytes in the injury penumbra have processes showing thickened regions of strong GFAP immunoreactivity but remain predominantly within their exclusive domains. Scale bar is 50µm.

1.02.3 Extracellular matrix proteins and basal laminae inhibit axon-growth

The glial scar often appears to be a disorganised accumulation of reactive astrocytes, activated microglia, macrophages and fibroblasts surrounded by extracellular matrix (Fawcett and Asher, 1999; Nieto-Sampedro, 2003; Teng et al., 2008). Meningeal fibroblasts often contribute to the development of glial scar tissue (Fig. 1.3) by invading lesions where they proliferate and interact with reactive astrocytes (Lagord et al., 2002; Sandvig et al., 2004; Teng et al., 2008). The fibroblasts and reactive astrocytes secrete glycoproteins and proteoglycans to form layers of extracellular matrix in the glial scar. Deposition of chondroitin sulphate proteoglycans (CSPGs), particularly phosphacan, versican and brevican, by reactive astrocytes and fibroblasts into the extracellular matrix of the glial scar is considered to be a major factor in the inhibition of axon growth at the glial scar boundary of CNS lesions (Silver, 1994; Gilbert et al., 2005; Laabs et al., 2005; Smith and Strunz, 2005; Galtrey and Fawcett, 2007). Digestion of the CSPGs with the enzyme chondroitinase ABC has improved axon regrowth in several CNS injury models (Chau et al., 2004; Del Rio and Soriano, 2007; Bunge, 2008). The extracellular matrix layers resemble basal laminae with separate networks of type IV collagen and laminin cross-linked by fibronectin (Berry et al., 1983; Hermanns et al., 2006; Teng et al., 2008). The end-feet of astrocytes form a glia limitans-like structure against the basal laminae similar to the interaction with fibroblasts and blood vessel endothelial cells during developmental glia limitans formation. The glia limitans re-establishes a BBB around the lesion and walls off the fibrotic scar tissue preventing further penetration of the CNS by fibroblasts and blood cells. Extensive revascularisation also occurs in the lesion following the infiltration of endothelial cells, which proliferate and form new capillaries and there is often a permanent increase in capillary density within the damaged region (Jaeger and Blight, 1997; Stichel and Muller, 1998; Lagord et al., 2002). Reactive astrocytes interact with the endothelial cells to form basal laminae and a BBB around the capillaries, further increasing the complexity of the scar environment.

1.02.4 Glial scarring is more extensive in the spinal cord

The nature and extent of glial scarring varies considerably with differences in the relative contributions of perilesional astrocytes, migrating progenitor cells and invading

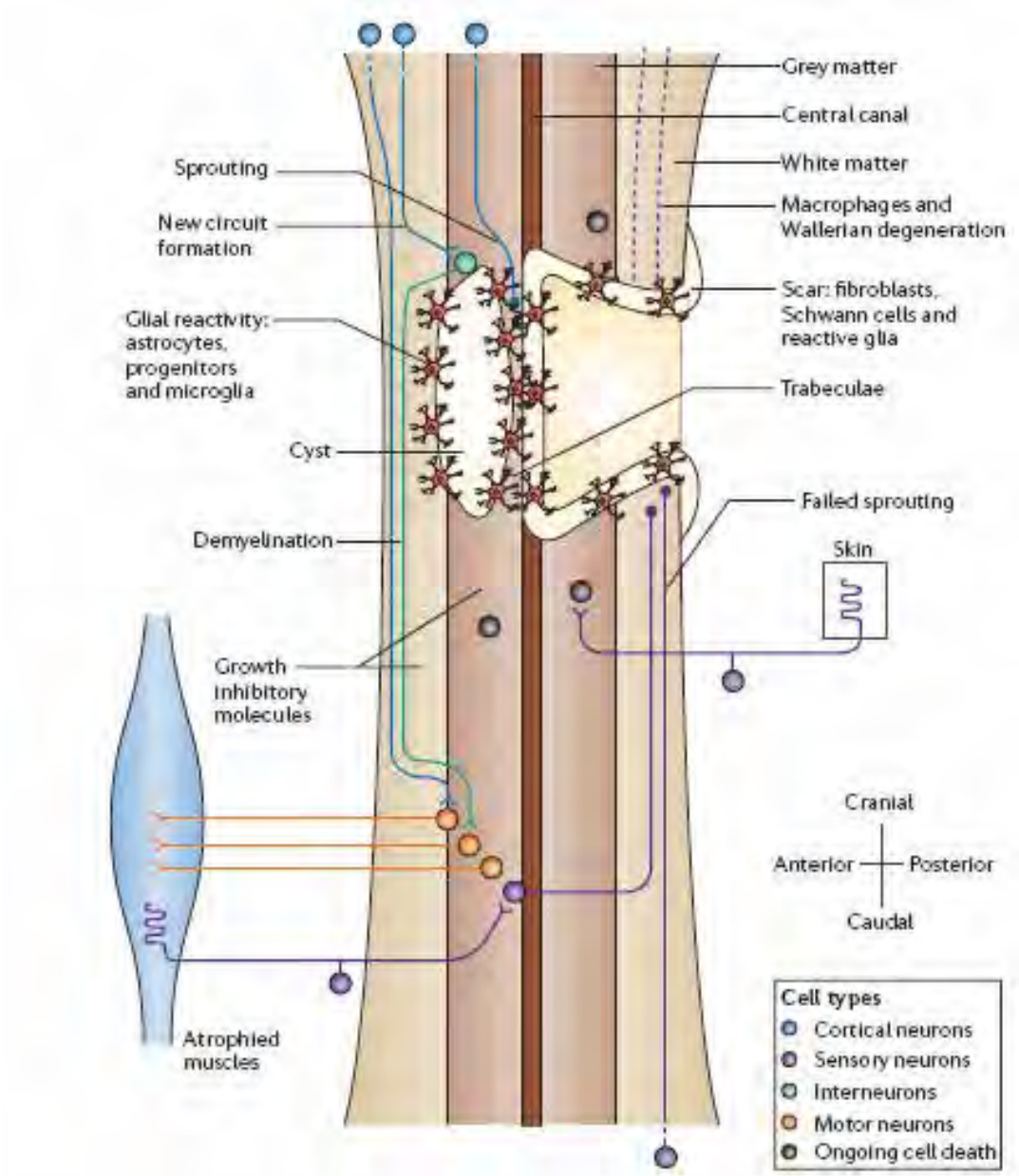

Figure 1.5 Spinal cord after injury. Schematic sagittal view through a region of cervical spinal cord injury (SCI), depicting a combination of features from different types of injury. Many cells die immediately, and progressively, after SCI. Cystic cavities usually form after contusion injury. After penetrating injury, cells from the peripheral nervous system (PNS) often invade the injury site and, in conjunction with CNS glial cells, form a connective tissue scar incorporating astrocytes, progenitor cells, meningeal fibroblasts and microglia, which presents a permanent barrier to axon regrowth. Many ascending and descending axons are interrupted and fail to regenerate over long distances. Some axons form new circuits via interneurons with collateral motor neurons in spared tissue. At the site of cyst formation, axons can sprout into trabeculae that are formed from ependymal cells. Disconnected myelinated axon segments are phagocytosed by macrophages. Some spontaneous remyelination occurs, largely by invasive PNS Schwann cells, to maintain motor function in some muscles, while denervated (non-spastic) muscles atrophy (adapted from Thuret, 2006).

fibroblasts that result from different injuries (Nieto-Sampedro, 2003; Silver and Miller, 2004; Fawcett, 2006b; Thuret et al., 2006; Teng et al., 2008). Glial scarring is usually less extensive in cortical grey matter injuries (Fig. 1.4) than in spinal cord (Fig. 1.5) and white matter injuries where there are more axons and high GFAP-expressing fibrous astrocytes predominate. In addition, the axon-growth inhibitory extracellular matrix components, brevican, versican, phosphacan and tenascin are more abundant in white matter (Bekku et al., 2009). Meningeal fibroblasts and Schwann cells often invade spinal cord injuries following glia limitans damage, while cystic cavities formed in the lesion core present an impassable physical barrier to axon regrowth (Fawcett, 2006b; Thuret et al., 2006). However, spinal cord injuries do not always completely sever the cord and some functional recovery may occur through stimulation of axonal sprouting or plasticity in spared collateral tracts (Li and Raisman, 1995; Raineteau and Schwab, 2001; Chuah et al., 2004).

1.03 Microglia are rapidly activated following CNS injury

1.03.0 Microglia are the resident CNS immune cells

Microglia are the principal immune effector cells of the CNS (Schwartz, 2003; Davalos et al., 2005; Hanisch and Kettenmann, 2007). Quiescent microglia are small cells with many long, fine highly-branched processes that appear to be actively sampling the environment of their exclusive domains within the healthy brain (Kloss et al., 1997; Davalos et al., 2005; Hanisch and Kettenmann, 2007). The most immediate activator of microglia following injury may be the physical disruption of ‘calming’ signals from neurons and astrocytes mediated by membrane-bound factors, such as fractalkine, which maintain a quiescent state in microglia (Hanisch and Kettenmann, 2007; Held-Feindt et al., 2010; Lauro et al., 2010). Fractalkine (or CX3CL1) is expressed by neurons and astrocytes (Hughes et al, 2002; Mizuno et al., 2003) and can promote leukocyte recruitment by increasing their adhesion to capillary endothelial cells (Ruitenberg et al., 2008; Schwartz et al., 2010). Binding of constitutively-expressed neuronal fractalkine to the specific CX3CR1 receptors on microglia has recently been shown to exert neuroprotective ‘calming’ effects that ameliorate microglial expression of pro-inflammatory cytokines (Cardona et al., 2006; Held-Feindt et al., 2010; Lauro et al., 2010). Microglia respond to

specific antigens through immune receptors, including toll-like receptors, and to non-specific indicators of damage through chemokine receptors (Davalos et al., 2005; Haynes et al., 2006; Block et al., 2007). Hence, a wide variety of inflammatory or antigenic signals can stimulate the transformation of microglia to a variety of reactive phenotypes, including a macrophage-like phenotype. There is a massive release of ATP and other purines, mainly from astrocytes damaged by traumatic or ischemic CNS injury, which rapidly activates microglia (Haynes et al., 2006; Kurpius et al., 2007; Pineau and Lacroix, 2009). Glutamate released from injured neurons and astrocytes can also activate microglia through metabotropic glutamate receptors and activation of NF-κB (Kaushal and Schlichter, 2008; Kataoka et al., 2009; Pineau and Lacroix, 2009). Toll-like receptor activation by heat shock proteins or extracellular matrix components released by proteases is another mechanism for the rapid activation of microglia by CNS injury (Lee and Lee, 2002; Hanisch et al., 2008; Pineau and Lacroix, 2009). Traumatic CNS injury immediately provokes targeted movement of microglial processes towards the injury site and increased transcription of inflammatory chemokines and cytokines occurs within five minutes (Davalos et al., 2005; Haynes et al., 2006; Hanisch and Kettenmann, 2007). Reactive microglia also upregulate their expression of proteins involved in immune complement cascades, membrane transport, cell motility and protein degradation (Gasque et al., 1997; Kurpius et al., 2007). Activated microglia adopt an amoeboid morphology and migrate to injury sites within hours where they proliferate and phagocytose cellular debris, including degenerating axons, dendrites and myelin (Davalos et al., 2005; Haynes et al., 2006; Hanisch and Kettenmann, 2007; Kurpius et al., 2007). While activated microglia may have a prominent role in immune responses in the penumbral region, the majority of immune cells that accumulate in the lesion (Fig. 1.3) within hours of injury appear to be peripheral leukocytes that enter from the blood (Liu et al., 1994; Fawcett and Asher, 1999; Babcock et al., 2003; Frangogiannis, 2007; Pineau et al., 2009). In the first 24 hours, chemokine expression by astrocytes recruits mainly neutrophils, with increasing numbers of monocyte-derived macrophages and lymphocytes being recruited over the following days and weeks. The peripheral immune cell recruitment is more extensive and is more likely to involve immune cell infiltration into the perilesional parenchyma following spinal cord injuries than for brain injuries (Schnell et al., 1999;

Schwartz, 2001; reviewed by Donnelly and Popovich, 2008). Immune activation of both the resident microglia and peripheral immune cells has conflicting effects on the injured CNS. The activated immune cells can protect against pathogenic invasion, phagocytose cellular debris and secrete a variety of neuroprotective and growth-promoting factors. However, they can also release pro-inflammatory cytokines, matrix metalloproteinases and toxic free radicals that can exacerbate inflammation and increase blood-brain barrier permeability leading to increased secondary neuronal and glial cell damage. The majority of microglia and peripheral monocytes recruited to CNS injury sites are rapidly induced to differentiate into activated macrophages that participate in robust immune responses with neurotoxic effects (Longbrake et al., 2007; Kigerl et al., 2009; Schechter et al., 2009; Schwartz, 2009, 2010). A more transient response may involve differentiation of macrophages into an anti-inflammatory phenotype with neuroprotective and regenerative activities. Invading T and B lymphocytes can react to CNS antigens to induce pathological autoimmune responses that can amplify macrophage activity to increase blood-brain barrier damage, oedema and neuronal injury (Ankeny et al., 2009; Ankeny and Popovich, 2009). There may also be a protective form of autoimmunity mediated by autoreactive T cells (Schwartz, 2001, 2009) and both T and B cells can secrete the neurotrophin BDNF (Donnelly and Popovich, 2008).

1.03.1 Phagocytic activity may increase cellular damage

Activated microglia, monocyte-derived macrophages and neutrophils all participate in the production of potentially neurotoxic levels of free radicals at CNS injury sites (Block et al., 2007; Wagner, 2007; Donnelly and Popovich, 2009; Yang et al., 2010). The membrane-bound enzyme NADPH oxidase, which catalyses the generation of superoxide free radicals, is the primary source of extracellular ROS released by activated microglia and other macrophages (Forman and Torres, 2001; Iles and Forman, 2002; Block et al., 2007; Sun et al., 2007; Wagner, 2007). NO generated by iNOS reacts with superoxide to form highly reactive and toxic peroxynitrite (Forman et al., 1998; Forman and Torres, 2001). Superoxide, NO and peroxynitrite can diffuse into micro-organisms and kill them by inactivating essential enzymes. ROS and reactive nitrogen species (RNS) along with lytic enzymes are also released into phagolysosomes to degrade phagocytosed antigens

and remnants of apoptotic and necrotic cells both after injury and during normal tissue maintenance (Forman and Torres, 2001; Farooqui et al., 2007; Harting et al., 2008). At high levels, ROS and RNS can induce apoptosis in intact cells by damaging proteins, lipids and nucleic acids (Forman and Torres, 2001; Chen and Palmer, 2008; Reed et al., 2009). High extracellular levels of NO and peryoxynitrite are particularly detrimental because their greater stability enhances diffusion through cell membranes to cause intracellular damage (Forman and Torres, 2001). Tissue remodelling is necessary for injury repair and the cytotoxic and phagocytic activities of macrophages removes compromised cells and debris, including injured axons and dendrites to provide space for regrowth and the establishment of new neural connections (Shih et al., 2006; Hanisch and Kettenmann, 2007). However, persisting high levels of ROS and RNS associated with macrophage activation in the lesion, can continue secondary neuronal damage for weeks after an injury (Si et al., 1997; Jia-Yi et al., 2006; Shih et al., 2006; Block et al., 2007; Hanisch and Kettenmann, 2007). The glial scar could protect penumbral tissue by confining severe neurotoxic macrophage activity to the lesion core (Sofroniew, 2008; Yang et al., 2010; Schwartz, 2010), because the instability of ROS and RNS ensures that they cannot diffuse far before being inactivated by reacting with other molecules (Forman and Torres, 2001). Glial scar extracellular matrix components, such as chondroitin sulphate proteoglycans, and possibly other factors produced by reactive astrocytes, may attract peripheral macrophages to the lesion border and direct their differentiation towards the phenotype with more neuroprotective and wound healing activity (Rolls et al., 2008; Schwartz, 2010). Following recruitment to the perilesional glial scar region, the complementary actions of these peripheral macrophages and activated microglia may be required for effective wound healing.

1.03.2 Microglia have concentration-dependent responses to ATP

The actions of activated microglia are thought to be generally neuroprotective although they can be neurotoxic depending on the phenotype adopted and the injury environment context (Schilling et al., 2001; Re et al., 2002; Schwartz, 2003; Hanisch and Kettenmann, 2007). Different modes of microglial activation may be regulated by microglial metabotropic (P2Y) and ionotropic (P2X) purinergic receptors that have concentration-

dependent responses to extracellular ATP (Re et al., 2002; Lai and Todd, 2006, 2008). Microglial P2Y activation by low to moderate ATP levels has been associated with neuroprotective IL-6 production, glutamate uptake and degradation, chemotaxis and phagocytic activity. However, at the high ATP levels associated with the lesion core and severe injuries, activation of P2X receptors induces expression of immediate early genes c-fos and c-jun and activates NF-κB and NFAT leading to expression of pro-inflammatory cytokines such as IL-1β, TNF-α and IFN-γ as well as prostaglandins, glutamate, NO, RNS and ROS (Kaya et al., 2002; Kim and de Vellis, 2005; Block et al., 2007; Kataoka et al., 2009). Excessive glutamate, TNF-α, RNS and ROS can all be neurotoxic while IL-1β and TNF-α can alter adhesion molecule expression in the endothelial tight junctions of the BBB promoting leukocyte and potentially pathogen entry to the brain parenchyma. P2X activation also induces microglial production of chemokines, such as MCP-1, MIP-1α and microglial response factor-1 that continue recruitment of leukocytes and microglia to the injury site (Kaya et al., 2002; Kataoka et al., 2009). Glutamate stimulation of microglial metabotropic glutamate receptors activates NF-κB resulting in increased TNF-α secretion. Activation of neuronal NF-κB by the ensuing high levels of TNF-α can induce caspase-dependent apoptosis (Kaushal and Schlichter, 2008). The P2Y mediated microglial activities may predominate in the lesion penumbra, where, because there is less cell damage, extracellular purine levels are likely to be lower than in the lesion infarct. P2Y activation by gradients of released purines may induce chemotaxis of microglia in the penumbra towards locally damaged cells or the lesion core. Higher purine levels in more severely damaged tissue could induce more robust and potentially neurotoxic activation of microglia through P2X receptors.

1.03.3 Interaction between astrocytes and microglia can amplify inflammation

Complex interaction between astrocytes and microglia regulates the severity, progression and resolution of inflammation (Hanisch, 2002; Kim and de Vellis, 2005; Block et al., 2007). Damaged astrocytes release ATP and other factors that activate microglia, which then, dependent on the degree of activation, release a variety of cytokines, chemokines, ROS and other inflammatory mediators. High levels of the pro-inflammatory cytokines

IL-1β, IL-6 and TNF-α, produced by microglia and other macrophages, induce more severe astrogliosis (Oh et al., 1993; Okada et al., 2004; John et al., 2005; Weisman et al., 2005; Kim et al., 2006). The reactive astrocytes increase their production of pro-inflammatory cytokines, including more IL-1β and TNF-α, chemokines, matrix metalloproteases, COX and iNOS (John et al., 2005; Kim et al., 2006; Laird et al., 2008). The consequent increase in astrocytic prostaglandins and NO production results in amplification of inflammation with further IL-1β and TNF-α production, increased BBB disruption, more secondary neuronal damage and increased infarct size (Schneider et al., 1999; Bethea, 2000; Brambilla et al., 2005b; Canellada et al., 2008). In addition, more severe astrogliosis leads to more extensive glial scarring with increased deposition of axon growth-inhibitory CSPGs (Lemons et al., 1999; Sandvig et al., 2004; Properzi et al., 2005). TNF-α induces increased expression of toll-like receptors (TLRs) by astrocytes and blood entering after CNS damage generates antigens that bind the TLRs, inducing further increases in IL-1β, TNF-α, iNOS and NO production (Konat et al., 2006; Phulwani et al., 2008). Activated astrocytes produce granulocyte macrophage-colony stimulating factor (GM-CSF) (Zaheer et al., 2002; Henze et al., 2005), which induces proliferation and immune activation of microglia to potentially further amplify the inflammatory response (Giulian et al., 1994; Fujita et al., 1996; Schilling et al., 2001).

1.04 The severity of astrocyte inflammation affects the potential for CNS repair

1.04.0 Reactive astrocytes have neuroprotective and regenerative actions

Neuronal viability after CNS injury is obviously dependent on the survival of astrocytes because of their normal physiological roles of providing metabolic support for neurons and maintaining extracellular homeostasis. As a consequence of these roles, astrocytes have large stores of metabolic substrates and high levels of anti-oxidant enzymes, which provide protection against ischemic damage (Swanson et al., 2004; Kintner et al., 2007) (Zhang et al, 2007; Takuma et al, 2004; Yu et al, 2007). Upregulation of glutamate transporters (Duan et al., 1999; Sullivan et al., 2007; Li et al., 2008a; Arranz et al., 2010) and increased production of anti-oxidants, such as ascorbate, glutathione and metallothionein by reactive astrocytes (Eddleston and Mucke, 1993; Penkowa et al., 1997; Aschner, 1998; Shih et al., 2003; Swanson et al., 2004; Chen et al., 2006b) may limit

neuronal excitotoxic damage by enhancing uptake of extracellular glutamate and detoxifying ROS. Lower levels of IL-1β and TNF-α, associated with the progression towards the resolution of inflammation, greater distance from the lesion core or less severe injuries, may favour astrocytic production of factors such as metallothionein (Wakida et al., 2007; Chung et al., 2008), erythropoietin (Li et al., 2008b), IL-6 (Penkowa et al., 2003; Bolin et al., 2005), transforming growth factor (TGF)β1 (Lin et al., 2006), ciliary neurotrophic factor (CNTF) (Albrecht et al., 2002), fibroblast growth factor (FGF) (Furukawa and Furukawa, 2007), brain derived neurotrophic factor (BDNF) (Giehl and Tetzlaff, 1996), vascular endothelial growth factor (VEGF) (Kalaria et al., 1998), nerve growth factor (NGF) (Oudega and Hagg, 1996) and insulin-like growth factor-1 (IGF-1) (Fernandez et al., 2007b) that have more neuroprotective and regenerative effects. Nerve growth factor (NGF) and brain-derived neurotrophic factor (BDNF) produced by astrocytes promote neuron survival and axon outgrowth (Zafra et al., 1992; Namiki et al., 2000; Meeuwsen et al., 2003a; Vargas et al., 2004). IGF-1 has anti-inflammatory actions (Pons and Torres-Aleman, 2000; Fernandez et al., 2007b) and together with FGF and VEGF promotes angiogenesis, proliferation of astrocytes and neurogenesis (Fernandez et al., 1999; Albrecht et al., 2002; Jung et al., 2006; Wang et al., 2006; Furukawa and Furukawa, 2007). TGFβ1 promotes angiogenesis (Vinals and Pouyssegur, 2001; Lagord et al., 2002; Gomes et al., 2005) and differentiation of neural progenitors into neurons (Chen and Palmer, 2008) or astrocytes (Lagord et al., 2002; Stipursky and Gomes, 2007). Erythropoietin is a neuroprotective factor that moderates astrogliosis, promotes angiogenesis and limits BBB disruption and oedema (Siren et al., 2001b; Diaz et al., 2005; Kretz et al., 2005; Li et al., 2008b) resulting in less tissue damage and improved functional recovery from CNS injury (Wakida et al., 2007; Li et al., 2008b). Metallothioneins are ubiquitous, small, zinc-binding proteins with anti-oxidant actions that are strongly upregulated by reactive astrocytes after injury (Hidalgo et al., 1994; Carrasco et al., 2000b; Wakida et al., 2007; Chung et al., 2008). Metallothionein 1/2 produced by reactive astrocytes protects neurons by binding excess zinc released from injured neurons and detoxifying ROS, (Dalton et al., 1994; Kumari et al., 2000; Katakai et al., 2001; Frederickson et al., 2004; Kruczek et al., 2009) while exogenous metallothionein 2A strongly promotes axon regeneration (Chung et al., 2003). Il-6

activation of the receptor associated janus tyrosine kinase (JAK), signal transducer and activator of transcription (STAT) and MAPK pathways promotes differentiation of neural progenitors into astrocytes (Fan et al., 2005; He et al., 2005; Nakanishi et al., 2007) and the transformation of astrocytes to a reactive phenotype (Justicia et al., 2000; Bolin et al., 2005), thereby contributing to glial scar development.

1.04.1 Moderation of astrogliosis can improve recovery from CNS injury

CNS injuries can vary from transient ischemic attacks or diffuse brain injuries where there may be only selective neuron and axonal damage without detectable functional consequences to severe traumatic injuries and stroke causing permanent serious functional deficits or death (Singleton and Povlishock, 2004; Panickar and Norenberg, 2005; Wagner, 2007; Doyle et al., 2008; Sofroniew, 2008). A similar variation in the degree of damage also occurs in individual injuries with distance from the lesion (Figs. 1.3, 1.4). At the lesion core there may be permanently damaged tissue or even a cell-free void following death of neurons and glia, whereas in the injury penumbra, the inflammatory responses of surviving astrocytes may enable some restoration of neuronal function. While reactive astrocytes produce neuroprotective and neurotrophic factors, more severe inflammation is associated with more severe astrogliosis, increased neuronal damage and glial scarring that is more inhibitory to regenerating axons (John et al., 2005; Fawcett, 2006a; Fernandez et al., 2007a; Laird et al., 2008). Numerous studies on anti-inflammatory treatments have produced evidence for improved neuronal survival and regeneration (Chen et al, 2008; Kunz et al, 2008; Zhang et al, 2008; Yenari and Han, 2006; Jatana et al, 2006; Kauppinen et al, 2008; Ginis et al, 2002) that has often been associated with the moderation of astrogliosis and glial scarring (Schneider et al., 1999; Fernandez et al., 2007a; Khorooshi et al., 2008; Phulwani et al., 2008; Sinke et al., 2008). However, differentiation and proliferation of astrocytes to establish the glial scar and close the lesion is an essential step in wound healing and may protect surviving neurons from the severe inflammatory responses in the lesion core (Sofroniew, 2005). Consequently, selective ablation of proliferating astrocytes after CNS injury results in a less organised glial scar that allows increased axonal regrowth into the lesion, but ultimately leads to increased oedema, inflammation and neuronal damage (Bush et al.,

1999; Horner and Gage, 2000; Faulkner et al., 2004). However, suppression of the inflammatory activation of astrocytes, rather than ablation of the scar-forming astrocytes, can ameliorate CNS injury damage and improve functional recovery (Brambilla et al., 2005b).

1.1 Olfactory ensheathing cells as a therapy for CNS injury

1.10 The olfactory neuronal pathway

The primary olfactory pathway (Fig. 1.6) has a remarkable capacity for continuous post-developmental neurogenesis and de novo growth of axons from the peripheral olfactory epithelium into the CNS (Doucette et al., 1983; Doucette, 1991; Calof et al., 1996; reviewed by Chuah et al., 2010). Dendritic receptors of individual olfactory sensory neurons are partly exposed on the surface of the olfactory epithelium and their axons course through the cribriform plate into the CNS, where they synapse with second order neurons in the olfactory bulbs. The olfactory sensory neurons are regularly replaced by differentiation of neurons from stem cells in the olfactory epithelium necessitating axonal regrowth from the peripheral epithelium into the CNS (Doucette et al., 1983; Mackay-Sim and Kittel, 1991; Chuah et al., 2003). Olfactory sensory neuron axons will continue to grow from the olfactory epithelium into the brain after removal of an olfactory bulb and the bulbectomy strongly stimulates olfactory sensory neuron renewal (Graziadei and Graziadei, 1979; Hendricks et al., 1994; Bauer et al., 2003).

1.11 Olfactory ensheathing cells

1.11.0 Olfactory ensheathing cells ensheath olfactory sensory neuron axons

Olfactory sensory neurons are closely associated with equally remarkable glial cells, the olfactory ensheathing cells (OECs) (Doucette, 1984; Doucette, 1989; Chuah and Au, 1993; Li et al., 2005b). Unlike other glial cells, OECs are found in both the peripheral and CNS regions of the olfactory system (Figure 1.6). OECs are asymmetrical, spindle-shaped cells (Fig. 1.7A) that extend thin sheet-like cytoplasmic processes to ensheath the small fascicles of the unmyelinated olfactory neuron axons (Fig. 1.7B) along their entire trajectories from the peripheral lamina propria into the olfactory nerve layers of the olfactory bulbs in the brain (Doucette, 1990; Chuah and West, 2002). OECs, like the

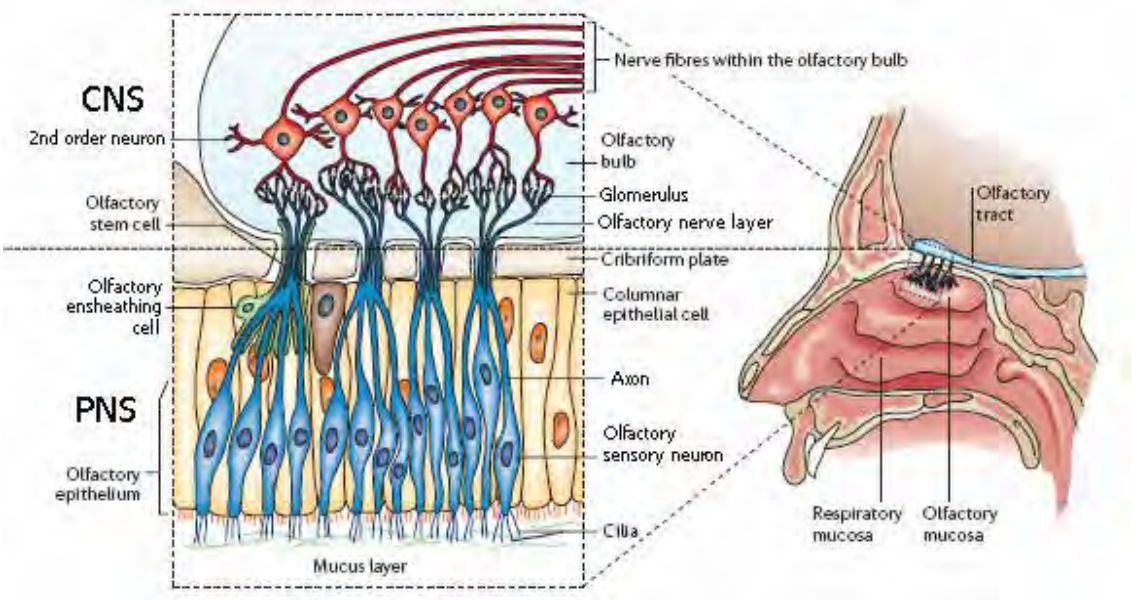

Figure 1.6 The olfactory nervous system. Schematic sagittal section through the human head, showing the olfactory nervous system (right), with a section of the olfactory nervous system depicted in greater detail (inset). Stem cells at the base of the olfactory epithelium generate new olfactory receptor neurons throughout life, which then extend *de novo* axons to the olfactory bulb. These axons are ensheathed by olfactory ensheathing cells throughout their entire trajectories from the lamina propria of the olfactory mucosa in the peripheral nervous system (PNS) and into the olfactory nerve layer of the olfactory bulbs in the central nervous system (CNS) via the cribriform plate. The axons emerge from the olfactory ensheathing cells to synapse with second order neurons in odorant-specific glomeruli in the bulbs, from where nerve fibres extend to the brain via the olfactory tract (adapted from Thuret, 2006).

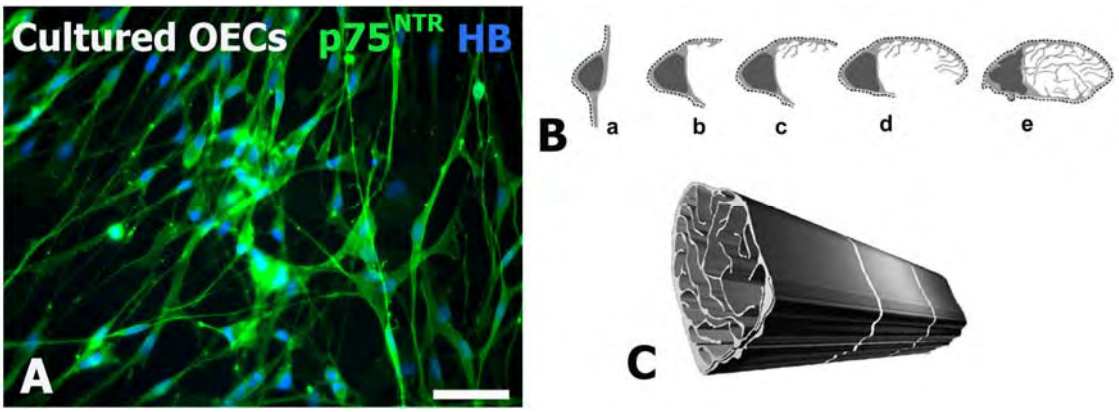

Figure 1.7 Olfactory ensheathing cells. A: Immunostaining of olfactory ensheathing cells (OECs) from an *in vitro* purified culture derived from neonatal rat olfactory bulbs. OECs are asymmetrical cells that show immunoreactivity for the low affinity neurotrophin receptor (green, $p75^{NTR}$) on the plasma membrane throughout the cell bodies and the long spindly processes. Nuclei have been counter-stained with Hoechst blue DNA dye (HB). Scale bar is 50μM. B: OEC folding for axon ensheathment. Morphologically, the OECs have an epithelial origin. A single OEC in represented (a) as an asymmetrical cell with a basal lamina-lined inner surface (left of the cell), which faces the mesenchymal fibroblasts and an outer, naked surface (to the right), which apposes the olfactory nerve fibres. Progressive curling over of the cell (b to e) shows the formation of an enclosed channel to ensheath the olfactory nerve axons, which are partially divided into interconnecting territories by thin cytoplasmic sheets arising from the inner, naked surface of the OECs. Overall cell diameter ~10μm (adapted from Li et al, 2005). C: Fascicular ensheathment. The end-to-end apposition of individual OECs forms long continuous channels that ensheath olfactory neuron axon fascicles. Overall diameter ~10μm (adapted from Li et al, 2005).

olfactory sensory neurons, originate from the olfactory placode on the ectodermal surface (Chuah and Au, 1993; Li et al., 2005b). As development proceeds, the OECs migrate inwards through the mesoderm and into the neuroectoderm of the neural tube in association with the sensory neuron axons as they grow from the peripheral epithelium to the olfactory bulbs in the CNS (Chuah and Au, 1991; Tennent and Chuah, 1996). A basal lamina covers the outer surface of OECs and is then encircled by layers formed by the thin processes of mesodermal fibroblasts (Doucette, 1990; Chuah, 2003; Li et al., 2005b). In the lamina propria single OECs form cylindrical sheaths around axon fascicles (Fig. 1.7B). The cylinders formed by individual OECs are arranged end to end creating a continuous passage for nerve fibre growth. Further along the olfactory nerve pathway, two or more OECS combine to form larger cylinders (Fig. 1.7C) surrounded by a common basal lamina. Surrounding fibroblasts interact with the OECs to generate basal laminae and collagen fibres which probably help maintain the integrity of the nerve fascicle passages during phases of olfactory neuron degeneration and regeneration. At the olfactory bulb the basal lamina and surrounding fibroblasts separate from the nerve fibre fascicles and OEC sheaths to form the pial surface of the bulb. OECs near the pial surface extend end-feet that interact with surrounding fibroblasts to form the glia limitans around the olfactory bulbs (Doucette, 1993b; Boyd et al., 2003; Li et al., 2005b). Similar astrocyte interactions with fibroblasts form the glia limitans elsewhere in the CNS (Berry et al., 1983; Abbott et al., 1992; Bundesen et al., 2003). Within the olfactory nerve layer of the olfactory bulb the ensheathed nerve fascicles separate and continue to their target glomeruli (Valverde et al., 1992; Doucette, 1993b; Dynes and Ngai, 1998; Treloar et al., 1999). OECs are present throughout the olfactory nerve layer of the bulb but are not found deeper in the bulbs, while astrocytes are present throughout the olfactory nerve layer and deeper layers. The ensheathing cylinders open at the glomerular layer to allow individual olfactory sensory neuron axons to synapse with the dendrites of second-order neurons. OEC processes intermingle with the processes of CNS astrocytes in the olfactory glomeruli and this association of OECs and astrocytes without any intervening basal laminae or fibroblasts may be crucial for directing regenerating olfactory sensory neuron axons to the correct synaptic targets. This pathway for regenerating olfactory

sensory neuron axons growing from the periphery into the CNS remains open throughout life (Doucette et al., 1983; Doucette, 1991; Li et al., 2005b).

1.11.1 OECs are specialised glial cells

OECs have morphological, protein expression and functional similarities with both peripheral Schwann cells and CNS astrocytes (Tennent and Chuah, 1996; Chuah and West, 2002; Fairless et al., 2005; Li et al., 2005b; Vincent et al., 2005b). All three glial cell types express neurotrophins and neuregulins which promote their proliferation, differentiation and survival (Thompson et al., 2000; Woodhall et al., 2001). Although OECs and astrocytes both express GFAP there are only sparse scattered filaments in OECs, whereas astrocytes have multiple dense bundles of the intermediate filaments (Chuah and West, 2002; Fairless et al., 2005; Li et al., 2005b; Vincent et al., 2005b). Genetic profiling and morphology indicate that OECs constitute a distinct cell type with more similarity to Schwann cells than astrocytes, although OEC morphology exhibits variability and plasticity (Vincent et al., 2003; Vincent et al., 2005b; Franssen et al., 2008). The different glia have separate developmental origins, with OECs arising from the olfactory placode, Schwann cells from the neural crest (Doucette, 1993a; Chuah and West, 2002; Richter et al., 2005; Leaver et al., 2006) and olfactory bulbar astrocytes from progenitors that migrate to the bulbs from the subventricular zone in the brain (Barnett et al., 1993; Li et al., 2005b; Vergara et al., 2005; Parent et al., 2006).

1.12 OECs and neuronal regeneration

In mammals, both the exceptionally high neuronal turnover rate and the regrowth of axons from the periphery into the brain are unique to the olfactory nervous system (Doucette et al., 1983; Doucette, 1990; Richter and Roskams, 2008). Axons fail to elongate from the periphery into the CNS and are therefore unable to re-establish appropriate synaptic connections following neuronal damage elsewhere in the nervous system (Li et al., 1997; Li et al., 2004; Ruitenberg et al., 2006). The close association of OECs with regenerating olfactory sensory neuron axons suggested that OECs may be important contributors to the capability for neuronal regeneration and axon regrowth in the olfactory system (Doucette, 1990, 1993b; Li et al., 2004; Richter and Roskams, 2008). Radial glia stimulate and guide

early neurite outgrowth in the developing CNS (Parnavelas and Nadarajah, 2001; Campbell, 2003). OECs and other specialised glia such as hypothalamic tanycytes and hypophyseal pituicytes have similar functions to radial glia in CNS regions where axon regeneration occurs throughout life (Gudino-Cabrera and Nieto-Sampedro, 1999; Boyd et al., 2003). These cells sometimes referred to as aldynoglia, have similar morphologies in culture and share immunological markers, including the p75 low affinity neurotrophin receptor, O4 antigen and insulin-like growth factor. Increased expression of the cytokine, leukaemia inhibitory factor (LIF), in the olfactory epithelium precedes olfactory sensory neuron renewal induced by bulbectomy (Bauer et al., 2003). LIF appears to be expressed by the degenerating olfactory neurons and glia-like sustentacular cells (Bauer et al., 2003), while OECs also upregulate their expression of the LIF receptor at 3 days post-bulbectomy (Nan et al., 2001). Exogenous LIF also stimulates cellular proliferation in the olfactory epithelium and LIF expression by astrocytes promotes neural stem cell renewal in the brain (Bauer et al., 2003; Bauer and Patterson, 2006; Dell'Albani, 2008). Furthermore, OECs express a variety of neurotrophins and other molecules that support axon growth and guidance, including NGF, BDNF, glial cell line-derived neurotrophic factor (GDNF), CNTF, neuregulins, integrins, cell adhesion molecules, cadherins and laminin (Kafitz and Greer, 1999; Wewetzer et al., 2001; Woodhall et al., 2001; Asan et al., 2003; Lipson et al., 2003; Franssen et al., 2008). The unique capacity for renewal of olfactory neurons and the substantial evidence for OECs providing trophic support for this neurogenesis and de novo axon growth (Kafitz and Greer, 1999; Christensen et al., 2001; Woodhall et al., 2001; Lipson et al., 2003; Schwob, 2005) has led to extensive research to determine whether transplanted OECs could similarly promote neuronal regeneration after spinal cord and brain injuries (reviewed by Chuah et al., 2010). A particular advantage of OECs for cellular transplantation therapy is the relative accessibility of OECs in the olfactory mucosa of live donors for autologous transplant into the CNS of the donors (Barnett and Chang, 2004; Feron et al., 2005; Dewar et al., 2007; Mackay-Sim et al., 2008). Autologous transplantation eliminates the need for immunosuppression and the attendant increased risk of pathogenic infection.

1.13 OEC transplantation therapy

1.13.0 Different CNS injury models have variable therapeutic outcomes

OEC transplantation into the injured CNS has been associated with decreased tissue and neuronal damage (Ruitenberg et al., 2003, 2005; Ramer et al., 2004b; Sasaki et al., 2006; Toft et al., 2007), improved axon sprouting and regrowth (Li et al., 1998b; Guntinas-Lichius et al., 2001; Deumens et al., 2006b), remyelination of spinal cord axons (Barnett et al., 2000; Akiyama et al., 2004), angiogenesis (Richter et al., 2003) and enhanced functional recovery (Imaizumi et al., 2000a; Lu et al., 2002; Keyvan-Fouladi et al., 2003; Li et al., 2003; Johansson et al., 2005; reviewed by Chuah et al., 2010) although some studies have not found therapeutic benefits (Gomez et al., 2003; Deumens et al., 2006a; Lu et al., 2006). Understandably, much of the research has focussed on the capacity of OECs to induce regeneration of injured axons (Bartolomei and Greer, 2000; Guntinas-Lichius et al., 2001; Deumens et al., 2006c). Spinal cord injury models to investigate the regenerative effects of OEC transplantation have included electrolytic lesions (Li and Raisman, 1995; Li et al., 1998b; Keyvan-Fouladi et al., 2003), photochemical lesions (Verdu et al., 2003), partial dorsal column (Chuah et al., 2004; Ramer et al., 2004b; Ruitenberg et al., 2005) or complete spinal cord transections (Ramon-Cueto et al., 2000; Lopez-Vales et al., 2006a; Toft et al., 2007) dorsal rhizotomy (Gomez et al., 2003; Li et al., 2004; Ramer et al., 2004a; Riddell et al, 2004) and contusion lesions (Takami et al., 2002; Plant et al., 2003; Collazos-Castro et al., 2005). Although the majority of studies report enhanced axon regrowth and some functional recovery there are also inconsistent results that can be partly attributed to marked variations in the extent and anatomical features of the injuries arising from the different injury models (reviewed by Bartolomei and Greer, 2000; Nieto-Sampedro, 2003; Barnett and Riddell, 2004; Ruitenberg et al., 2006; Ruitenberg and Vukovic, 2008; Chuah et al., 2010). There is also considerable variation in the severity and nature of clinical traumatic CNS injuries and the different injury models may provide insight into the type of injuries most likely to benefit from OEC transplantation. Discrepancies between the reported therapeutic outcomes of the injury models could also have arisen from differences in the experimental protocols affecting the timing and location of transplantation, the composition of the transplanted OEC cultures and the severity of inflammation and glial scarring. In comparison to brain

injuries, where severe injury is more likely to be fatal, spinal cord injuries are associated with stronger inflammatory responses and more extensive glial scarring, with large cavities often developing in the lesion. There is no unequivocal evidence for axon regrowth across these large spinal cord lesion cavities or of improvements in functional recovery due to axonal regeneration following complete transection of the spinal cord (Plant et al., 2003; Verdu et al., 2003; Deumens et al., 2006a, c; Sasaki et al., 2006; Barnett and Riddell, 2007; Toft et al., 2007; Ruitenberg and Vukovic, 2008). Any therapeutic benefits of OECs for these severe spinal cord injuries are probably mediated by neuroprotective effects that ameliorate secondary neuronal and axonal damage. However, there is evidence of transplanted OECs promoting limited axonal regeneration into spinal cord lesions, including the regrowth of severed dorsal roots into the spinal cord. OECs have also been reported to promote the regeneration of peripheral axons (Guntinas-Lichius et al., 2001; Radtke et al., 2009) and of transected nigrostriatal axons in the brain (Teng et al., 2008).

1.13.1 Do OECs remyelinate axons?

Transplants of Schwann cells (Richardson et al., 1980; Martin et al., 1996; Xu et al., 1997) and OECs (Franklin et al., 1996; Kato et al., 2000; Sasaki et al., 2006; Barnett and Riddell, 2007) have both been postulated to mediate repair of spinal cord lesions by promoting axon growth and re-myelination. Both cell types promote and guide axon growth and express similar neurotrophic factors, cell adhesion molecules and extracellular matrix proteins (Vincent et al., 2005b; Franssen et al., 2008). OECs only ensheath unmyelinated axons in the olfactory system and it may seem improbable that transplanted OECs could remyelinate damaged or regenerating axons after spinal cord injury, as suggested by some studies (Imaizumi et al., 2000b; Kato et al., 2000; Akiyama et al, 2004). However, Schwann cells ensheath small diameter unmyelinated axons in a similar manner to OECs and only form myelinated sheaths around larger diameter axons with longer nerve fibres where action potential conduction speed becomes more physiologically important. *In vitro* experiments and *in vivo* transplantation of OECs into demyelinated regions of the CNS suggest that OECs can also form myelin sheaths around axons of suitable diameter (Kato et al., 2000; Franklin, 2003; Lakatos et al., 2003b; Boyd

et al., 2004; Sasaki et al., 2007). However, remyelination by OECs could be restricted to demyelinating lesions and was not replicated in other injury models (Boyd et al., 2004; Ramer et al., 2004a; Richter et al., 2005). Schwann cell integrins binding to fibronectin secreted by fibroblasts promotes myelination (Mirsky and Jessen, 1999; Previtali et al., 2003). Similar interactions between OECs and fibronectin and other extracellular matrix proteins expressed by meningeal fibroblasts may enhance re-myelination by transplanted OECs (Lakatos et al., 2000; Lakatos et al., 2003b). The presence of meningeal fibroblasts in OEC cultures transplanted into demyelinated lesions increased both the remyelination of axons and the number of myelinating cells in the lesions. OECs appeared to form myelin sheaths around the large diameter axons in the demyelinated spinal cords, while surrounding fibronectin-expressing fibroblasts separated them into fascicles. Growth factors such as fibroblast growth factor 2 secreted by the fibroblasts may also have promoted OEC proliferation, survival and migration along axon tracts in the lesion (Hsu et al., 2001; Yan et al., 2001; Barraud et al., 2007; Santos-Silva et al., 2007). It is also possible that contaminating Schwann cells in the OEC or neuronal cultures were responsible for the *in vitro* remyelination (Plant et al., 2002; Li et al., 2005b). Schwann cells can often invade spinal cord lesions along with meningeal fibroblasts and may also have been responsible for the *in vivo* remyelination, with fibroblast growth factor 2 or other factors produced by the transplanted fibroblasts and OECs possibly promoting Schwann cell migration into the lesion (Boyd et al., 2004; Ramer et al., 2004a; Richter et al., 2005).

1.13.2 OEC migration in vitro and after transplantation

Other research shows that transplanted Schwann cells are less able than OECs to migrate and survive in the CNS and only remyelinate axons in astrocyte-free regions (Fairless et al., 2005; Santos-Silva et al., 2007). Schwann cells also fail to migrate among astrocytes *in vitro*, instead forming discrete boundaries and inducing a hypertrophic reactive phenotype characterised by increased expression of GFAP and axon growth inhibitory CSPGs, in the astrocytes. In contrast OECs intermingle and migrate amongst astrocytes *in vitro* without forming boundaries or inducing astrocyte activation (Lakatos et al., 2000; Li et al., 2005b; O'Toole et al., 2007). Although several studies have reported that OECs

are capable of migrating from the injection site, over white matter tracts and grey matter (Ramon-Cueto et al., 1998; Ramon-Cueto et al., 2000; Resnick et al., 2003), the possibility of dye leakage or the engulfment of dead pre-labelled OECs by macrophages have cast doubt on these claims. Labelling of OECs by viral vector-mediated expression of green fluorescent protein has revealed a more conservative migratory capability, while others have suggested that the eventual localization of OECs was more likely due to passive spreading rather than active migration (Ruitenberg et al., 2002; Lu et al., 2006). Recent *in vitro* experiments have revealed that TNF-α secreted by activated astrocytes stimulates OEC chemotaxis and a linear expression gradient of TNF-α has been detected in the glial scar after spinal hemisection that could conceivably regulate the migration of transplanted OECs (Su et al., 2009). TNF-α levels peaked at 7 days after injury and in studies that failed to show OEC migration, the timing or location of OEC transplantation may not have coincided with the TNF-α levels required for chemotaxis (Chuah et al., 2010).

1.13.3 Regulation of OEC migration

Comparative gene expression profiling (Vincent et al., 2005b; Franssen et al., 2008) indicates that OECs express distinct additional genes associated with tissue repair and angiogenesis, which may confer the reported advantages of OECs over Schwann cells as therapeutic transplants. The differences between Schwann cell and OEC migration amongst astrocytes may be due to stronger neuronal cadherin-mediated adhesion between Schwann cells and astrocytes than between OECs and astrocytes (Fairless et al., 2005). Suppression of neuronal cadherin activity enhances Schwann cell migration and reduces boundary formation in co-cultures with astrocytes but does not alter the intermingling of OECs and astrocytes in co-cultures. An additional possible component of the mechanism for these differences involves fibroblast growth factor 2, which is expressed by reactive astrocytes and invasive fibroblasts after CNS injury and heparan sulphate proteoglycans produced by Schwann cells (Santos-Silva et al., 2007). Soluble heparan sulphate proteoglycans may induce astrogliosis by enhancing binding of fibroblast growth factors to receptors on astrocytes and Schwann cells to promote boundary formation between the two cell types. Digestion of heparan sulphate proteoglycans inhibits this boundary

formation and promotes Schwann cell migration in co-cultures with astrocytes, while addition of fibroblast growth factor 2 and heparin induces boundary formation in OEC/astrocyte co-cultures. While the molecules mediating the superior spatial integration of OECs and astrocytes are unknown, the repertoire of cadherins (cadherin-3, cadherin-5 and MT-protocadherin) and integrins (alpha 1, alpha 6, alpha 7 and beta 4) expressed by OECs are likely candidates for future investigation (Franssen et al., 2008).

1.13.4 The 'pathway hypothesis'

The compatibility of OECs and astrocytes in co-culture has similarities with their interaction in the olfactory bulbs (Fairless et al., 2005; Li et al., 2005b; Santos-Silva et al., 2007). No discrete boundary forms between OECs in the outer layer of the olfactory bulb and astrocytes of the inner layers and there is no inhibition of olfactory sensory neuron axon growth at the transition between the OEC and astrocyte dominated regions. Following neuronal damage in peripheral regions where axons are ensheathed by Schwann cells there is no regeneration of nerve fibres into the CNS as occurs with the olfactory sensory axons (Carlstedt, 1997; Chong et al., 1999; Li et al., 2005b). Except in the olfactory system, astrocytes interact with invading fibroblasts and capillary endothelial cells to form basal laminae and a glia limitans around CNS sites of neuronal damage that are impenetrable to regenerating axons. If dorsal root axons are severed near their entry zone to the spinal cord (dorsal rhizotomy), reactive astrocytes reform a continuous glial-pial membrane with an outward facing basal lamina that excludes the peripheral Schwann cells and is impenetrable to regenerating axons (Liuzzi and Lasek, 1987; Wroblewski et al., 2000; Pascual et al., 2002; Li et al., 2005b). When OECs were transplanted into the entry zone after rhizotomy there was extensive outgrowth of astrocyte processes, which interwove with OEC and Schwann cell processes, forming bridges that allowed dorsal root axons to regenerate into the spinal cord (Li et al., 2004). This research led to the 'pathway hypothesis', which proposes that favourable interactions between astrocytes and transplanted OECs after injury in the CNS may inhibit the formation of an inhibitory glial scar boundary and establish a permissive pathway for regenerating axons similar to that existing in the olfactory system (Nieto-Sampedro, 2003; Li et al., 2005b; Teng et al., 2008). The inclusion of fibroblasts in the

transplants (Li et al., 1998b; Li et al., 2003; Teng et al., 2008) may further enhance the regenerative properties of OECs, possibly by producing growth factors and extracellular matrix proteins that regulate OEC migration (Raisman, 2001; Teng et al., 2008). Transplantation of mixed OEC and meningeal fibroblasts into electrolytic lesions in the adult rat corticospinal tract led to growth of neuronal sprouts across the lesion and into the spinal cord caudal of the lesion (Li et al., 1997, 1998b). Functional recovery in response to this treatment appears to depend on precise location of OECs that allows their interaction with the processes of reactive astrocytes (Keyvan-Fouladi et al., 2003). Restoration of axonal connectivity in the olfactory system does not involve regrowth from existing neurons as is required for the repair of spinal cord injuries. Instead, olfactory axon replacement depends on neurogenesis from globose basal progenitor cells in the olfactory epithelium and *de novo* axon growth to reconnect with the olfactory bulbs (Verhaagen et al., 1990; Christensen et al., 2002; Schwob, 2002). While normal innervation and function is restored by olfactory neuron renewal following peripheral deafferentation of the olfactory epithelium, reinnervation is abnormal and incomplete following transection of the olfactory nerve. Although unilateral bulbectomy strongly stimulates proliferation and differentiation of progenitor cells in the olfactory epithelium, in the absence of the target tissue, most of the newly formed olfactory neurons remain immature and die within a few weeks. Apoptosis and degradation of the olfactory sensory neurons and the subsequent axonal renewal appears to occur within intact ensheathment channels formed by OECs and the surrounding fibroblasts, supporting the view that OECs may have neurotrophic and axon guidance functions. However, the injury responses in the olfactory tract also imply that OECs may need to be transplanted at or be capable of migrating to suitable locations to induce regrowth of axons towards the required targets. These requirements may explain why other groups have found no benefit from OEC transplantation after rhizotomy (Gomez et al., 2003; Ramer et al., 2004a; Riddell et al., 2004) or that transplanted OECs suppressed astrogliosis and promoted neurite sprouting, but not in the required direction to repair the injury (Ramon-Cueto and Nieto-Sampedro, 1994; Nieto-Sampedro, 2003). Subsequently, it was proposed that OECs may only be able to promote regeneration when the preferred direction of OEC migration coincides with the alignment of new axonal sprouts. This

view is supported by experiments involving the implantation of encapsulated OECs into the injured spinal cord where regenerating corticospinal collateral nerve fibres were directed towards the capsules (Chuah et al., 2004). OECs that were free to migrate after direct injection into the injured spinal cord induced significantly more sprouting of collateral branches than the encapsulated OEC implants. Adenoviral transduction to increase neurotrophin expression in transplanted OECs augmented axonal sprouting but the associated improvements in functional recovery were attributed to enhanced neuroprotection leading to smaller lesion sizes and more axons spared from secondary damage rather than being a consequence of axonal regeneration (Ruitenberg et al., 2003, 2005). The failure of these and other therapies to promote substantial axonal regeneration has led to the view that some form of aligned substrate to support axon growth across large lesions is an essential requirement for the repair of spinal cord injuries (reviewed by Bunge, 2001; Ruitenberg et al., 2006; Ruitenberg and Vukovic, 2008). A combination treatment using OECs and olfactory nerve fibroblasts aligned on biomatrix bridges did increase axon growth into the lesion but the regrowth still did not extend across the lesion (Deumens et al., 2006). OEC implantation has also been associated with decreased astrogliosis and reduced glial scarring around the lesion in many CNS injury models (Ramon-Cueto et al., 2000; Takami et al., 2002; Nieto-Sampedro, 2003; Plant, 2003; Ramer et al., 2004b; Teng et al., 2008). Since OEC transplantation has been associated with neuroprotective effects (Toft et al., 2007; Ruitenberg and Vukovic, 2008) and decreased lesion size, it could be argued that the less severe astrogliosis was an indirect effect of a reduction in secondary neuronal damage. However, some of the studies reporting improved neuronal survival involved genetically-modified OECs (Ruitenberg et al., 2003, 2005) and it is also plausible that the moderation of astrogliosis could have initiated the neuroprotective effects. Some evidence suggests that glial scar transformation by transplanted OECs is crucial for promoting axonal sprouting (Ramer et al., 2004b; Teng et al., 2008) and transplants of OECs combined with Schwann cells to bridge the lesion and chondroitinase, to digest growth-inhibitory chondroitin sulphate proetoglycans in the glial scar, induced significantly more axonal sparing and functional recovery than a variety of other combination treatments (Bunge, 2008). However, other

studies have reported improved axonal regeneration independent of effects on astrogliosis (Lopez-Vales et al., 2006a; López-Vales et al., 2007).

1.2 Research rationale

Although the numerous studies on OEC transplantation therapy for CNS injury have produced considerable evidence for improved neuronal regeneration and some functional recovery, the results have been inconsistent and the mechanisms for the reported beneficial effects remain debatable (reviewed by Bunge, 2008; Ruitenberg and Vukovic, 2008; Chuah et al., 2010). While there is evidence for enhanced neuronal survival and decreased lesion size in response to OEC transplantation it is uncertain how OECs mediate these effects. Primary neuronal and glial cell death caused by the initial physical trauma and ischemia of CNS injury stimulates an inflammatory response that, when severe, can lead to extensive secondary neuronal damage (Lenzlinger et al., 2001; Morganti-Kossmann et al., 2002; Block et al., 2007; Doyle et al., 2008). Activated astrocytes make a major contribution to the inflammatory mediators that regulate the severity, duration and resolution of the CNS inflammation (Chen and Swanson, 2003; John et al., 2005; Fawcett, 2006b; Floyd and Lyeth, 2007; Fitch and Silver, 2008; Laird et al., 2008). Strongly activated astrocytes on the lesion perimeter form a glial scar that protects penumbral tissue from more severe inflammation in the lesion core but presents a barrier to axon regeneration. More severe inflammation is associated with increased neuronal damage, more severe glial scarring and worse functional deficits. Moderation of astrocyte activation could therefore enhance neuronal survival and axonal regeneration. Many studies report moderation of astrogliosis and glial scarring as a consequence of OEC implantation and OECs appear able to migrate freely amongst astrocytes in the olfactory bulbs, injured CNS tissue and *in vitro* (reviewed by Chuah et al., 2010). However, partly because of the different injury models used and the complexity of cellular interactions *in vivo*, the effects of OEC implantation have been inconsistent and inconclusive. There has been additional uncertainty related to possible contributions to the effects of OECs by Schwann cells and fibroblasts that either invade lesions or are introduced with the OEC transplants. *In vitro* research utilising purified cultures of OECs and other relevant cell types could provide some insight into the cellular interactions and

mechanisms that affect the success of OEC transplantation therapy. Hence, this PhD research is an *in vitro* study to investigate the possibility that OECs moderate astrocyte inflammatory activation and could thereby contribute to the beneficial effects of OEC implantation therapy. This hypothetical OEC moderation of astrocyte activation has not been the specific topic of previous research. In order to research this topic it is first necessary to establish a suitable *in vitro* model of astrocyte activation, which can then be utilised to investigate the effects of OECs. Strong inflammatory stimuli can lead to astrocyte apoptosis and astrocyte survival is essential for neuronal survival and axon regeneration (Swanson et al., 2004; Giffard and Swanson, 2005; Matute et al., 2006; Laird et al., 2008; Broughton et al., 2009). Consequently, it was considered advisable to also investigate whether the inflammatory stimuli used for the *in vitro* model induced astrocyte apoptosis and whether OECs could modulate any such apoptotic effect.

1.3 Specific aims

1. Establish an in vitro model of astrocyte inflammatory activation.

2. Determine whether OECs inhibit in vitro astrocyte inflammatory activation.

3. Determine whether the inflammatory activation induces astrocyte apoptosis.

4. Determine whether OECs modulate astrocyte apoptosis.

CHAPTER 2: Materials and Methods

2.0 Ethics

All animal procedures were approved by the Animal Experimentation Ethics Committee of the University of Tasmania and are consistent with the Australian Code of Practice for the Care and Use of Animals for Scientific Purposes. Hooded Wistar rats were used for all experimental procedures involving animals and all cell types were harvested from 2 day-old rats.

2.1 Cell culture

2.10 Culture media and incubation

Following harvesting from 2 day-old Hooded Wistar rats, all cell types were plated at densities of 2 x 10^4 cells/cm^2 and cultured in Dulbecco's Modified Eagle's Medium (DMEM; Invitrogen) supplemented with 10% foetal bovine serum (JRH Biosciences) and 1% penicillin-streptomycin-amphotericin B solution (Invitrogen). All media and reagents for use with cell cultures were made up with sterile distilled or milliQ water, filter sterilised and stored at 4^0C or -20^0C. The serum-supplemented culture medium (DMEM-10S) was replaced with serum-free DMEM (supplemented only with the 1% antibiotic/antimycotic) 24 hours prior to and throughout experiments. Medium conditioned by OECs, astrocytes, microglia or fibroblasts was collected from confluent cultures in culture flasks after 24 hours of culture in serum-free DMEM. All cultures were maintained in an incubator (Forma Scientific) at 37^0C in a humid atmosphere containing 5% carbon dioxide.

2.11 Astrocytes

Cortical astrocytes were cultured as previously described (McCarthy and De Vellis, 1980; Vincent et al., 2005b) with some modifications. Briefly, each rat pup was anaesthetized in ice for 10 minutes, the head removed, sterilized with 70% ethanol and transferred to a Petri dish, containing warm (37^0C) DMEM-10S, in a laminar flow hood to maintain sterile conditions. The skin and skull above the cerebral hemispheres was removed, the

cerebral hemispheres separated from the olfactory bulbs and hindbrain, removed into a separate Petri dish containing warm (37^0C) Modified Eagle's Medium with HEPES (MEM-H; Sigma), hemispheres separated down the midline and the remaining hindbrain removed from each cortical lobe. The meninges were carefully peeled from each cortical lobe and cortices then transferred to another Petri dish containing 2.5mL warm (37^0C) Hank's Balanced Salt Solution (HBSS; Sigma) and finely macerated with scissors. The macerated neocortical tissues from two rats were then digested in 0.25% trypsin (Gibco) at 37^0C for 20 minutes, excess trypsin removed and trypsinisation inhibited by re-suspension in DMEM-10S. The cell suspension was filtered through a 60μm pore mesh, plated and cells grown to confluence over ~6 days in 1:25 poly-L-lysine (PLL; Sigma)-coated 75 cm^2 flasks (TRP, Switzerland), purified by shaking at 250 rpm on an oscillating shaker for 24 hours (McCarthy and De Vellis, 1980) to remove microglia, oligodendrocytes and progenitor cells, followed by 4 days with a 20 μM addition to the culture medium of the mitotic inhibitor, cytosine-β-D-arabinofuranoside (AraC; Sigma) to remove rapidly dividing cells such as fibroblasts or remaining progenitor cells. Astrocyte cultures were then passaged twice and grown to confluence after each passage. Astrocytes were harvested from flasks by washing with 2mM ethylenediamine tetraacetate (EDTA; Sigma) in 0.1M PBS (Versene) to inhibit cell adherence by chelating calcium ions, followed by trypsinisation (0.25%) and re-plated onto PLL-coated 18-mm diameter acid-washed glass coverslips (Nunc) in 12-well culture plates or, for PCR samples, directly into PLL-coated 6-well culture plates. This method yielded cultures containing ~95% GFAP-positive astrocytes.

2.12 Olfactory ensheathing cells

2.12.0 OEC source tissue

Different researchers have cultured OECs from peripheral olfactory mucosal tissue (Barber and Lindsay, 1982; Chuah and Au, 1991; Pixley, 1992), the olfactory nerve layer of the olfactory bulbs in the CNS (Chuah and Au, 1993; Franceschini and Barnett, 1996; Li et al., 1998a) or pooled tissues from both locations (Chuah et al., 2004; Vincent et al., 2005b) using a variety of purification techniques and culture conditions. These different culture techniques may in part have led to the divergent views on the antigenic profile

and identity of OECs, as well as the variable efficacies reported for OECs as therapeutic transplants for CNS injury. OEC cultures are subject to contamination by Schwann cells that surround some peripheral axons in the olfactory mucosa, astrocytes from the deeper layers of the olfactory bulbs and by fibroblasts that surround the OECs of the olfactory nerve fascicles and the glia limitans of the olfactory bulbs. Initially, OECs were prepared following protocols from previous research that utilised pooled tissue dissected from the nasal septum and olfactory bulbs (Chuah and Teague, 1999; Vincent et al., 2003). Dissecting the tissue from both the nasal septum and olfactory bulbs was time-consuming and risked introducing contaminating Schwann cells (Kawaja et al., 2009), which are difficult to distinguish from OECs since they have similar morphology and immunoreactivity for $p75^{NTR}$ and S100 in culture (Boyd et al, 2003). In addition, inclusion of the peripheral olfactory tissue led to an increase in the percentage of contaminating fibroblasts to levels that prevented their elimination from the cultures. Sufficient OECs were obtained for later experiments and collection of conditioned medium by culturing entirely from olfactory bulb tissue with further modifications of the previous culturing protocols. Differences between cultures of mucosal and bulbar OECs appear to arise predominantly from the different proportions of contaminating cells, with purified mature OECs from either source tissue having similar antigenic profiles and abilities to promote neurite growth *in vitro* (Jani and Raisman, 2004; Kumar et al., 2005; Krudewig et al., 2006). Therefore, although bulbar OECs cannot be harvested from living donors for autologous transplantation, this choice of source tissue was not considered to be a serious impediment to the generalisability of this research. The research implications of the source tissues for OEC cultures are discussed further in Chapter 6.

2.12.1 OEC culture from olfactory bulbs

Briefly, following removal of cerebral hemispheres for astrocyte culture, the olfactory bulbs were carefully removed from rat pup skulls using fine forceps and transferred to a Petri dish containing warm (37^0C) MEM-H. The outer layer of each olfactory bulb was carefully peeled away and held using a hypodermic syringe with the needle bent at 90^0 while any adhering tissue from the inner layers was scraped free using a second hypodermic syringe with the needle bent at 45^0. The tissue harvested from the outer

layers of 6-8 olfactory bulbs were pooled and digested in 0.25% trypsin (Gibco) at 37^0C for 30 minutes, excess trypsin solution removed and trypsinisation inhibited by re-suspension in DMEM-10S. The tissue was then partially dissociated by syringing through a 23-gauge needle and pelleted by centrifugation at 500g for 10 minutes. Cells were then resuspended in DMEM-10S and plated without filtering onto 1:25 PLL-coated 18 mm acid-washed coverslips (Nunc) in 12-well culture plates, PLL-coated 25 cm^2 culture flasks (TRP, Switzerland) or Falcon™ cell culture inserts incorporating polyethylene terephthalate membranes with 400nm pores (Becton Dickinson). Cells were purified for 3 days with 100μM AraC and expanded for four days using 100 μg/ml bovine pituitary extract (Sigma). Cultures with ~95% low affinity neurotrophin receptor ($p75^{NTR}$)-positive OECs were obtained for experiments by this method.

2.13 Microglia

Microglia were cultured by plating the medium collected from astrocyte cultures after 30 minutes of shaking onto uncoated 25 cm^2 flasks or 18 mm coverslips in 12-well culture plates. Microglia tended to proliferate cyclically and detach spontaneously from cortical cell cultures. Higher yields were therefore obtained by monitoring cultures under phase contrast and commencing shaking when large numbers of microglia were visible on the upper surface of the cortical cell cultures. Shaking for less than 45 minutes minimised detachment of cell types other than microglia. The cultures were placed in the incubator for about 20 minutes to allow microglia to adhere and then the cultures were swirled and gently tapped to remove any oligodendrocytes or progenitor cells (which adhered less readily than microglia) before changing the medium and returning the purified microglia cultures to the incubator. Microglia are an abundant CNS cell type (Yang et al., 2010) and this procedure immediately yielded large numbers of microglia, which proliferated slowly over three to five days to produce dense cultures. These cultures contained ~95% CD11b-positive microglia with astrocytes as the predominant contaminating cells.

2.14 Meningeal fibroblasts

Fibroblasts were cultured from meningeal tissue separated from cerebral hemispheres during astrocyte culture preparation. The meningeal tissue was treated as for astrocyte

culture except that it was not filtered prior to plating into 75 cm^2 flasks. Cultures were grown to confluence and passaged several times in flasks before plating onto PLL-coated 18 mm coverslips in 12-well culture plates. These cultures contained ~95% fibronectin-positive/GFAP-negative fibroblasts. The meningeal fibroblast monocultures contained few contaminating cells without requiring any specific procedure for their elimination due to the rapid proliferation rate of the fibroblasts. Fibroblasts are present in most tissues and their rapid proliferation rate confers a propensity for contaminating cultures of other cells (Gibbons et al., 2007).

2.2 Immunocytochemistry

2.20 Immunostaining

Cultures on coverslips were fixed in 4% paraformaldehyde, washed with 0.1M PBS containing 0.3% Triton X-100 (Sigma) to permeabilise cell membranes and incubated with serum-free protein block (Dako) for 5 minutes to block non-specific binding of antibodies. Primary antibodies were applied for 1 hour at room temperature at the concentrations shown below (Table 2.0), in 0.1M PBS containing 0.3% Triton X-100. In most instances, a rabbit and mouse primary antibody were applied simultaneously in the same solution. A no primary antibody control sample was included for all experiments. Following washing with PBS, the secondary antibodies, goat anti-rabbit Alexa Fluor 594 and goat anti-mouse Alexa Fluor 488 (both Molecular Probes) were each diluted at 1:1000 in 0.1M PBS containing 0.3% Triton X-100, in the same solution, for simultaneous incubation, for 1 hour in the dark. When required cells, were delineated with Alexa Fluor 488 phalloidin staining (1:40 in 0.1M PBS for 20 minutes in the dark; Molecular Probes) of cytoskeletal actin filaments in place of a mouse primary antibody and the goat anti-mouse Alexa Fluor 488 secondary antibody. Nuclei were counter-stained by incubating with Hoechst blue DNA dye 33342 (200 ng/mL in 0.1M PBS; Molecular Probes) for 30 minutes in the dark. Coverslips were placed on wax-filled culture plate lids for antibody incubations to enable the use of small volumes of antibody solution (100µL/coverslip) and then returned to culture plate wells for PBS washes and Hoechst staining of nuclei. Coverslips were washed in 0.1M PBS, rinsed in distilled

water and mounted on glass slides using Permafluor™ aqueous mounting medium (Immunotech, France) and stored in the dark.

2.21 Fluorescence imaging

Specimens were viewed on an Olympus BX50 fluorescence microscope using Olympus UplanF1 10X, 20X and 40X lenses or a Leica 60X oil immersion lens for image capture with an Optronics Magnafire camera. Images were usually taken at the same magnification and location on the coverslip for the Hoechst nuclear stain and each antibody. Image locations on the coverslip were selected randomly, commencing with a central location and separated by two to three microscope fields. Where possible, images for the same primary antibody and magnification were taken at the same exposure. Sets of 3 images were merged using Adobe Photoshop 7.0 © (Adobe Systems, San Jose, CA, USA) when required, for example, to show immunoreactivity for NF-κB, a cell-specific protein (astrocytes: GFAP; OECs: $p75^{NTR}$; microglia: CD11b) and Hoechst blue nuclear staining.

Table 2.0 Primary antibodies for immunocytochemistry

Antibody	**Concentration**	**Host species/clonality**	**Manufacturer**
anti-p65 NF-κB	1:100	rabbit polyclonal	Santa Cruz
anti-c-Rel NF-κB	1:100	rabbit polyclonal	Santa Cruz
anti-GFAP	1:1000	rabbit polyclonal	Dako
anti-GFAP	1:1000	mouse monoclonal	Millipore
anti-fibronectin	1:100	rabbit polyclonal	Abcam
anti-ferritin	1:1000	rabbit polyclonal	Abcam
anti-S100	1:500	rabbit polyclonal	Dako
anti-$p75^{NTR}$	1:100	rabbit polyclonal	Upstate
anti-$p75^{NTR}$	1:100	mouse monoclonal	Millipore
anti-CD11b	1:500	mouse monoclonal	Sigma
anti-IGF-1	1:100	mouse monoclonal	Millipore
anti-Iba1	1:1000	rabbit polyclonal	Wako

2.3 Identification of cell types

2.30 Monitoring the cellular composition of live cultures

The progress, cellular composition and viability of cell cultures were monitored daily by observing the live cultures on an Olympus CK2 bifocal microscope under phase contrast and imaging, when required, with an Olympus DP10 camera (Figs. 2.0, 2.1). To enable identification of cells from the observed morphologies in the live cultures, sample cultures were compared after immunostaining for cell-specific marker proteins (Figs. 2.2-2.12). Live cultures of astrocytes (Fig. 2.0A-C), fibroblasts (Fig. 2.0D), OECs (Fig. 2.1A, B) and microglia (Fig. 2.1C, D) displayed distinctive morphologies under phase contrast.

2.30.0 Astrocyte morphology

Astrocytes in serum-supplemented medium (Fig. 2.0A) appeared as large flat cells that formed dense confluent monocultures. Astrocytes had large oval nuclei and variably shaped cell bodies from which long broad processes extended, typically arranged in a distinctive radial 'star-like' distribution (McCarthy and De Vellis, 1980). Ingredients of serum such as thrombin, lysophosphatidic acid and fibronectin promote attachment to culture substrates by activating the cytoskeletal regulator, RhoA leading to downstream assembly of actin stress fibres and their attachment at focal adhesions (Goldman and Abramson, 1990; Suidan et al., 1997; Ramakers and Moolenaar, 1998; Safavi-Abbasi et al., 2001; Peters et al., 2005). Consequently astrocytes in serum-supplemented media have focal adhesions linked to radially arranged actin stress fibres resulting in large flattened cell bodies (Fig. 2.0A) while those growing in serum-free conditions have smaller cell bodies and longer processes (Fig. 2.0B). Cyclic AMP analogues such as dibutyryl-cyclic AMP (db-cAMP) strongly inactivate RhoA resulting in rapid retraction of cytoplasm to produce stellate astrocyte morphologies with small cell bodies and long narrow radially distributed processes (Fig. 2.0C), independent of any synthesis of cytoskeletal proteins.

2.30.1 Meningeal fibroblast morphology

Meningeal fibroblasts (Fig. 2.0D) form dense confluent cultures that, although resembling astrocytes, are morphologically distinct (Hanson et al., 1982; Grumet and Edelman, 1988; Deloulme et al., 1997; Niclou et al., 2003). Fibroblasts are more uniform

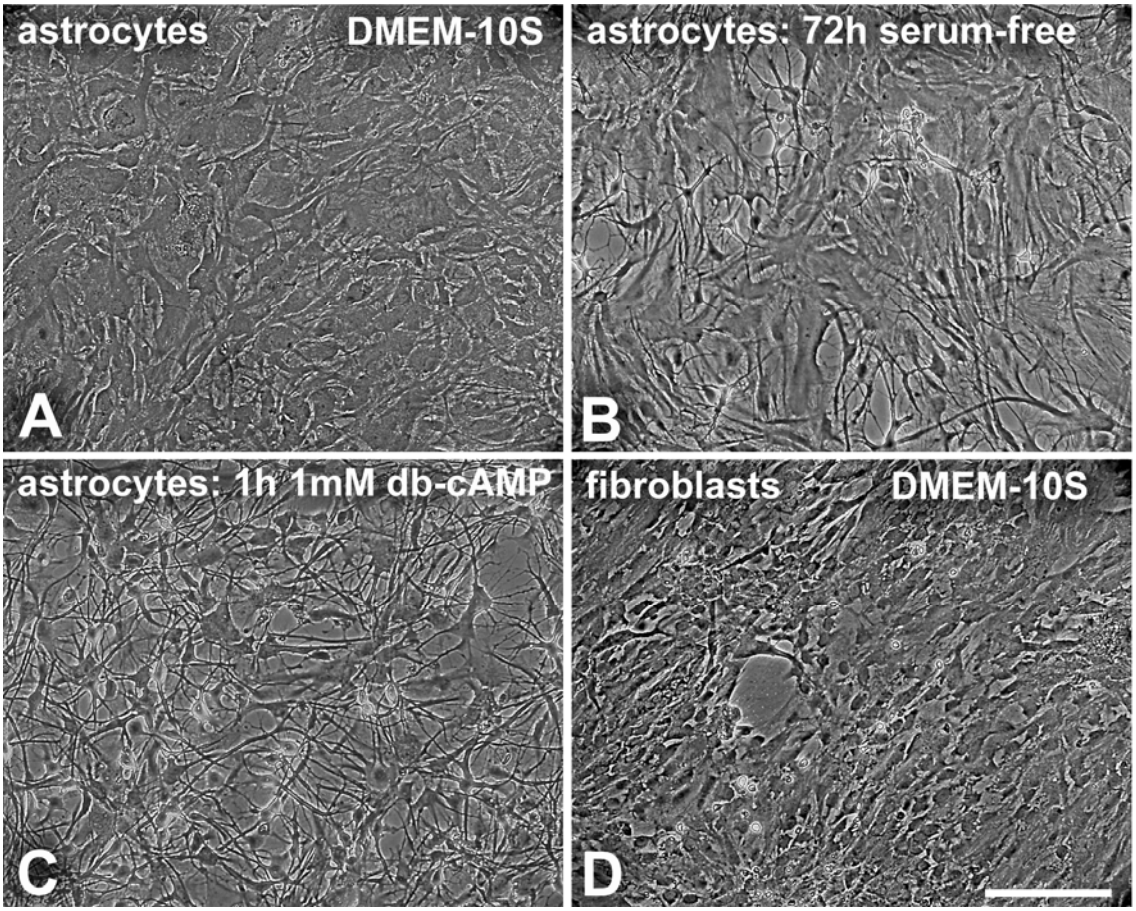

Figure 2.0 Phase contrast live images of astrocyte and fibroblast cultures. Astrocytes (A-C) and fibroblasts (D) cultured in 75cm^2 culture flasks were imaged live under phase contrast. Astrocytes formed dense confluent cultures and although displaying highly variable size and morphology, when cultured in DMEM supplemented with 10% foetal calf serum (DMEM-10S) they tended to have flattened, epitheloid cell bodies with long broad processes (A). Culture in serum-free conditions promoted a gradual change to more process-bearing stellate astrocyte morphologies (B) while treatment of astrocytes with the cyclic-AMP analogue dibutyryl-cyclic-AMP (db-cAMP) strongly and rapidly induced these stellate process-bearing morphologies (C). Fibroblasts also formed dense confluent cultures (D) with cells of variable size but with relatively uniform epitheloid morphologies usually having much shorter processes than astrocytes. Scale bar is 200μm.

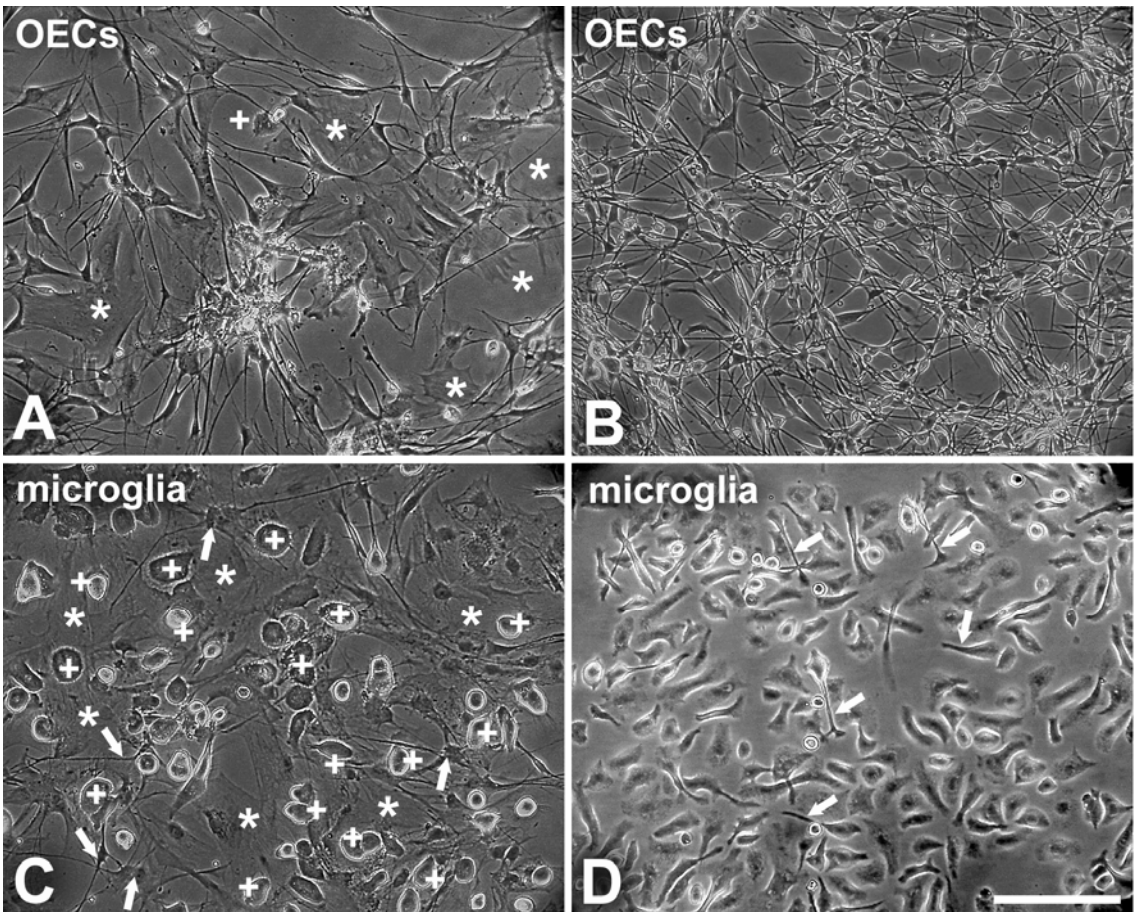

Figure 2.1 Phase contrast live images of OEC and microglia cultures. OECs (A, B) and microglia (C, D) cultured in 25cm^2 culture flasks were imaged live under phase contrast. Cultures of both OECs and microglia varied from cultures that appeared to contain a mixture of cell types (A, C) to those that were predominantly monocultures (B, D). In the OEC monocultures (B) dense clusters of small high-contrast cell bodies extended a dense network of long thin processes. In other OEC cultures (A) these high contrast cells and process networks were more sparse with an underlying layer of large, flat, low-contrast cells with short processes (asterisks in A) that resembled fibroblasts. Microglia monocultures (D) contained rounded high-contrast cells with mainly short processes, although there was often a single long process (arrows in D) sometimes terminating in a fan-shaped structure resembling an axonal growth cone. Microglia tended to occupy discrete domains in these cultures with relatively little overlapping of adjoining cells compared with cultures of the other cell types. In other microglia cultures (C) the high-contrast rounded microglia (plus signs in C) were on a basal layer of large flattened low-contrast cells (asterisks in C) while other cells had small dark cell bodies with long thin processes (arrows in C). Cells resembling microglia were also occasionally seen in the OEC cultures (plus sign in A). Scale bar is 200μm.

in shape than astrocytes, tend to align along parallel bipolar axes rather than having the random distribution of astrocytes and usually have shorter and fewer processes.

2.30.2 OEC morphology

OECs (Fig. 2.1B) appear as medium to dark grey, high-contrast, spindly bipolar cells with oval cell bodies that are smaller than most astrocyte cell bodies and long processes that are much thinner than astrocyte processes (Chuah and Au, 1993; Vincent, 2003; Vincent et al., 2005a). OECs often occurred in dense clusters of small high-contrast cell bodies that extended dense networks of long thin processes that tended to align in parallel. Some OECs had larger more polygonal cell bodies with a more radial distribution of processes. The OEC cultures (Fig. 2.1A) were subject to contamination by fibroblasts (asterisks in Fig. 2.1A) and occasionally microglia (plus sign in Fig. 2.1A).

2.30.3 Microglial morphology

Microglia (Fig. 2.1D) appeared as small medium to dark grey, high-contrast cells with irregular outlines having many short fine processes and sometimes one or several larger processes (arrows in Fig. 2.1D), that sometimes terminated in a fan-shaped structure resembling an axonal growth cone. Overall cell-shape varies remarkably (Dobrenis, 1998; Frank et al., 2006) including small rounded cells resembling the activated amoeboid in vivo phenotype, relatively large rounded flat cells, long irregular rod-shaped cells and very irregular cells resembling the ramified quiescent in vivo phenotype. Microglia tended to occupy discrete domains in these cultures with relatively little overlapping of adjoining cells compared with cultures of the other cell types. Cultures of microglia (plus signs in Fig. 2.1C) sometimes contained contaminating fibroblasts (asterisks in Fig. 2.1C) and progenitor cells (arrows in Fig. 2.1C) that appear as small, dark cells occupying separate domains with radially-distributed, highly-branched processes (McCarthy and De Vellis, 1980; Itoh, 2002).

2.31 Determination of cell type and culture purity by immunoreactivity

Cultures were imaged after immunostaining for protein markers of the intended culture cell type (Table 2.1) and probable contaminating cell types, together with Alexa Fluor 488 phalloidin staining of cytoskeletal actin filaments to delineate cell morphologies and

Hoechst blue counter-staining of nuclei. Unfortunately, it is rarely possible to find marker proteins that are expressed exclusively by a specific cell type. For this reason, cell type was identified using the expression of marker proteins in conjunction with the intracellular distribution of immunoreactivity for the marker proteins and cell morphology. The reliability of identification using this methodology is discussed below for each cell type.

Table 2.1 Marker proteins for identifying cell type

Cell type	**Marker protein**
astrocyte	GFAP
microglia	CD11b
fibroblast	fibronectin
OEC	$p75^{NTR}$

2.31.0 Astrocyte cultures

Astrocytes (Fig. 2.2) are commonly identified by their expression of the intermediate filament protein, glial fibrillary acidic protein (GFAP) (Reeves et al., 1989; Goldman and Abramson, 1990; De Groot et al., 1997; Reilly et al., 1998; Silva et al., 1998; Gomes et al., 1999; Brahmachari et al., 2006; Cebolla and Vallejo, 2006; Tramontina et al., 2007). Although other glial cells express some GFAP, only astrocytes have distinctive prominent cytoplasmic bundles of GFAP. In common with other glial cells, astrocytes also express S100, a cytoplasmic calcium-binding protein (Goncalves et al., 1997; Sorci et al., 1998; Raponi et al., 2007). GFAP immunoreactivity (Fig. 2.2A, D, G and green in Fig. 2.2C, F, I) revealed a dense network of the intermediate filaments throughout astrocyte cell bodies and processes while S100 (Fig. 2.2B and red in Fig. 2.2C) appeared as diffuse bright immunoreactivity throughout cell bodies and processes. Nuclei were large and oval-shaped (blue in Fig. 2.2C, F) while cytoskeletal actin filaments (Fig. 2.2E and red in Fig. 2.2F) were radially distributed around centres in the cell bodies (asterisks in Fig. 2.2D-F) away from nuclei and not obviously aligned with the processes delineated

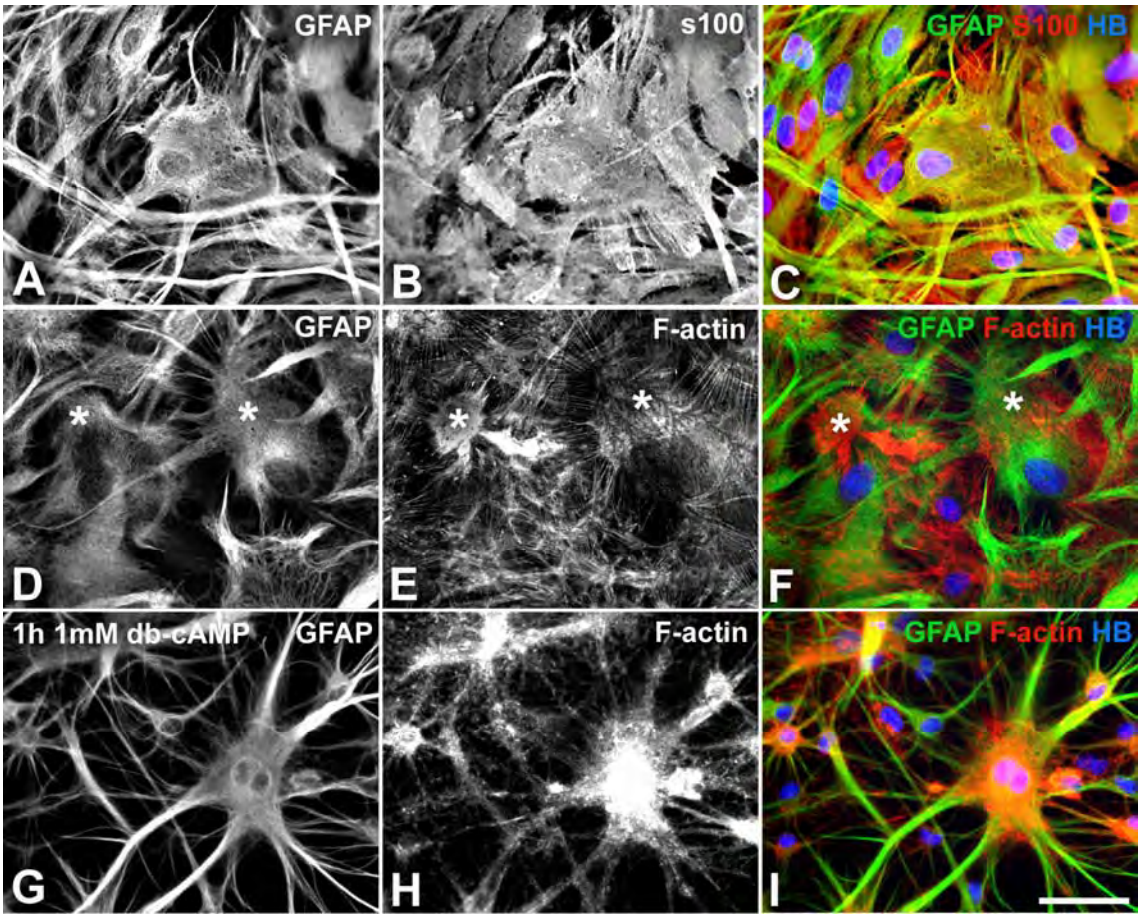

Figure 2.2 Immunostaining characterisation of astrocytes. Cultured astrocytes were maintained in serum-free DMEM for 24 hours prior to immunostaining for GFAP (A, D, G and green in C, F, I) and S100 (B and red in C). Cytoskeletal actin filaments (F-actin) were stained with Alexa fluor 488-conjugated phalloidin (E, H and red in F, I) and nuclei were stained with Hoechst blue (HB; blue in C, F, I). GFAP immunoreactivity is prominent in astrocytes as a dense network of the intermediate filaments throughout cell bodies and processes. Cultured astrocytes also showed diffuse bright immunoreactivity for S100 throughout cell bodies and processes. After 24 hours in serum-free conditions astrocytes tended to stellate morphologies with flattened epitheloid cell bodies and radially distributed processes. Nuclei were large and oval-shaped (blue in C, F) while cytoskeletal actin filaments (E and red in F) were radially distributed around centres in the cell bodies (asterisks in D-F) away from nuclei and not obviously aligned with the processes delineated by GFAP filaments (D and green in F). Treatment with 1mM db-cAMP induced strong stellation of astrocytes within 1 hour (G-I). The db-cAMP treated astrocytes had small cell bodies with radially distributed long thin processes that formed dense interwoven networks. The rapid compression of cytoplasm into cell bodies and narrow processes is associated with intensification of immunoreactivity. Substantial depolymerisation of actin filaments, which are radially distributed around nuclei and aligned with GFAP filaments in processes (H and red in I), accompanied the cytoplasmic compression. Nuclei were also compressed and became more rounded (blue in I). Scale bar is 50μm.

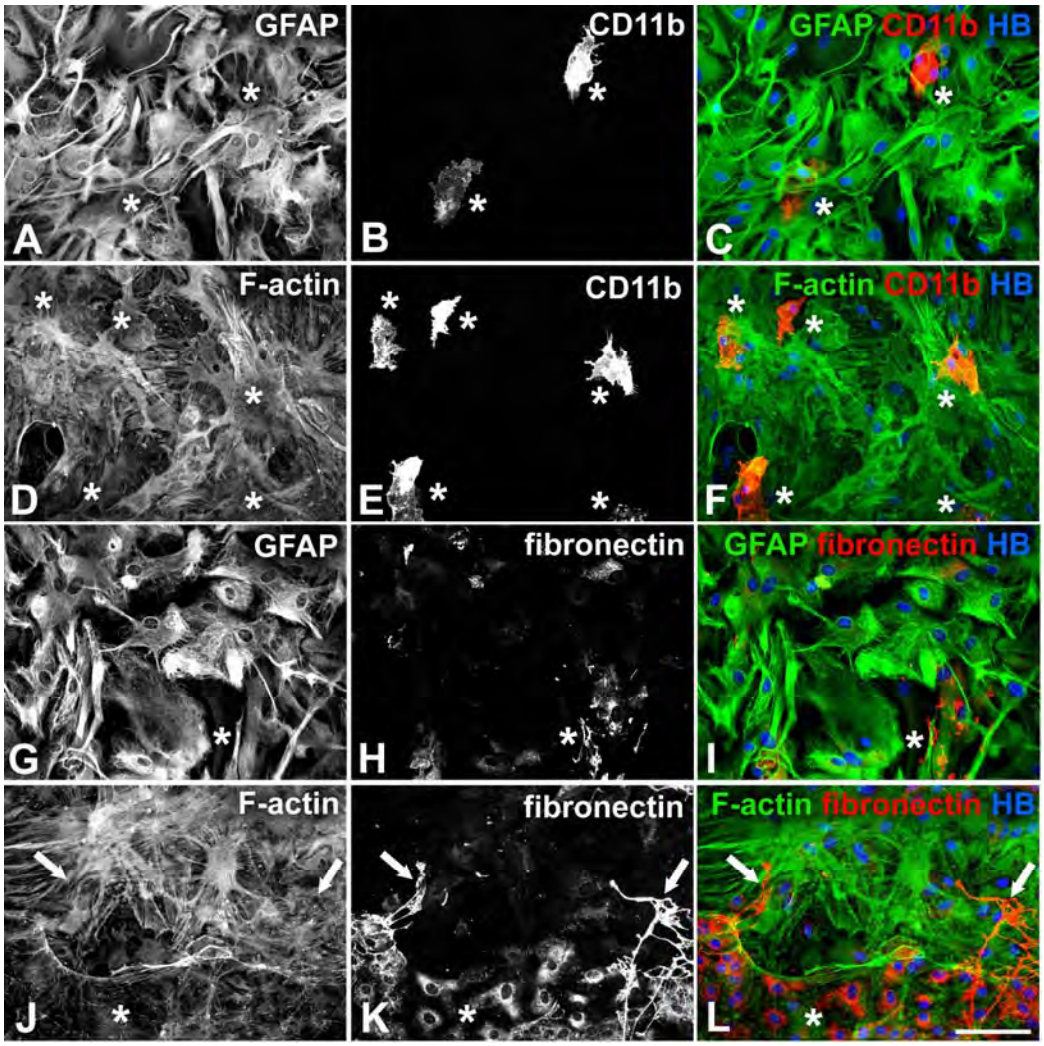

Figure 2.3 Contaminating cells in astrocyte cultures. Astrocytes were identified by immunoreactivity for GFAP (A, D and green in C, I). Contaminating microglia were identified by immunoreactivity for CD11b (B, E and red in C, F) and fibroblasts by immunoreactivity for fibronectin (H, K and red in I, L). Nuclei were stained with Hoechst blue (HB; blue in C, F, I, L). Cytoskeletal actin filaments (F-actin) were stained with Alexa fluor 488-conjugated phalloidin (D, J and green in F, L) to facilitate comparisons of cell morphologies with live cultures viewed under phase contrast (Fig. 3.0). CD11b-positive microglia (asterisks in A-F) were rarely found in the astrocyte cultures. Microglia had irregular morphologies with numerous short processes (B, E) and were negative for GFAP (asterisks in A). Actin filaments in microglia (asterisks in D) were not discernible against the dense background of radially arranged astrocyte actin filaments. Although astrocyte cultures appeared to usually be of high purity (G-I) there were occasionally dense patches of contaminating fibroblasts (lower section of J-L). Astrocytes and fibroblasts both expressed fibronectin in a perinuclear punctate distribution (H, K and red in I, L), but immunoreactivity was usually more intense in fibroblasts (lower section of K, L) and networks of secreted fibronectin (arrows in K, L) appeared to be associated only with fibroblasts. Actin filaments in fibroblasts were sparser and more randomly distributed (lower section of J) than in astrocytes (D, J). Some fibroblasts appeared to be growing on a basal layer of astrocytes (asterisk in J-L) with secreted fibronectin extending out from the boundary (arrows in J-L and asterisk in G-I). Scale bar is 100μm.

by GFAP filaments (Fig. 2.2D and green in Fig. 2.2F). The rapid compression of cytoplasm into cell bodies and narrow processes, associated with db-cAMP induced astrocyte stellation (Fig. 2.2G-I), resulted in intensification of immunoreactivity and depolymerisation of cytoskeletal actin filaments, which became radially distributed around nuclei and aligned with GFAP filaments in processes (Fig. 2.2H and red in Fig. 2.2I). Nuclei were also compressed and became more rounded (blue in Fig. 2.2I). Occasional contaminating microglia in astrocyte cultures (asterisks in Fig. 2.3A-F) were identified by positive immunoreactivity for the complement receptor, CD11b (Fig. 2.3B, E and red in Fig. 2.3C, F) and although negative for GFAP (asterisks in Fig. 2.3A), this would be difficult to discern within dense GFAP-positive astrocyte cultures without counter-staining for CD11b to locate the microglia. There were also occasionally dense patches of contaminating fibroblasts in the astrocyte cultures (Fig. 2.3J-L). Although immunoreactivity for the extracellular matrix protein, fibronectin, was usually more intense in fibroblasts (Fig. 2.3K, L) and networks of secreted fibronectin were associated only with fibroblasts (arrows in Fig. 2.3K, L), both astrocytes and fibroblasts expressed fibronectin in a perinuclear punctate distribution (Fig. 2.3H, K and red in Fig. 2.3I, L). Although fibroblasts were negative for GFAP, this would again be difficult to discern in dense astrocyte cultures, particularly where fibroblasts were growing on or under a layer of astrocytes (asterisk in Fig. 2.3J-L). Careful removal of meningeal tissue during cerebral hemisphere dissection helped to ensure that fibroblasts remained within the acceptable limits of 5% of cells in the astrocyte cultures.

2.31.1 Microglial cultures

Microglia were identified by immunostaining for the integrin, CD11b (Fig. 2.4B, D, K, M, green in Fig. 2.4C, L and red in Fig. 2.4F, O), a component of complement receptor 3 (Koguchi et al., 2003; Frank et al., 2006; Garcao et al., 2006; Haynes et al., 2006; Vincent et al., 2007). Peripheral macrophages also express CD11b (Haynes et al., 2006; Farber et al., 2009) but these are usually only present in very low numbers within healthy brain parenchyma (Dobrenis, 1998; Frank et al., 2006). Although outer meningeal tissue was removed during culture preparation, it is not possible to separate the pia mater, which has been reported to contain a large population of monocyte-derived macrophages in

adult rodents (Chinnery et al., 2010). These macrophages could represent a remaining source of contaminating cells in the microglia cultures. However, they would only be likely to make a minor contribution to the cultures because of the small volume of pial tissue relative to the cerebral hemispheres. In addition, large numbers of microglia could also be expected in the outer meninges and pia mater in the tissue from neonatal rats used for this current research, since circulating microglia precursors derived from mesodermal hematopoietic cells enter the developing brain through the meninges during perinatal stages and transform into microglia (Boya et al., 1987; Cuadros and Navascues, 1998; Dobrenis, 1998; Monier et al., 2006; Yang et al., 2010). In the perinatal brain, microglia predominantly adopt amoeboid phagocytic morphologies and transform into ramified resting microglia during development. These microglia cannot readily be distinguished from monocyte-derived macrophages on the basis of either morphology or immunology (Rolls et al., 2008; Yang et al., 2010; Schwartz et al., 2010). Chinnery et al., 2010 use major histocompatiblity complex Class II (MHCII) expression to distinguish pial macrophages from microglia, despite the known expression of MHCII by activated microglia (Sasaki and Nakazato, 1992; Longbrake et al., 2007; Yang et al. 2010). Furthermore, Chinnery et al., 2010 only present low resolution out-of-focus images of microglia that, as far as can be discerned, morphologically resemble the monocyte-derived macrophages. All microglia also showed positive immunostaining for the iron-storage protein, ferritin (Fig. 2.4A, G, J and red in Fig. 2.4C, I, L), which has been used to identify activated microglia and other immune cells in vivo after CNS injury (Huang and Ong, 2005). However, ferritin is the major intracellular iron storage protein in all animals and was not specific to microglia. Astrocytes, fibroblasts, OECs (data not shown) and progenitor cells (asterisks in Fig. 2.4G-O) were all positive for ferritin but negative for CD11b immunostaining. Contaminating astrocytes (Fig. 2.5A-F) and fibroblasts (Fig. 2.5G-I) could be identified by positive immunostaining for GFAP and fibronectin respectively and negative immunostaining for CD11b, although CD11b-positive microglia sometimes exhibited weak staining for both GFAP (plus sign Fig. 2.5D-F) and fibronectin (plus signs Fig. 2.5G-I). Microglia, astrocytes and fibroblasts could also be distinguished by their morphologies and distributions of cytoskeletal actin filaments (Fig. 2.5J-R).

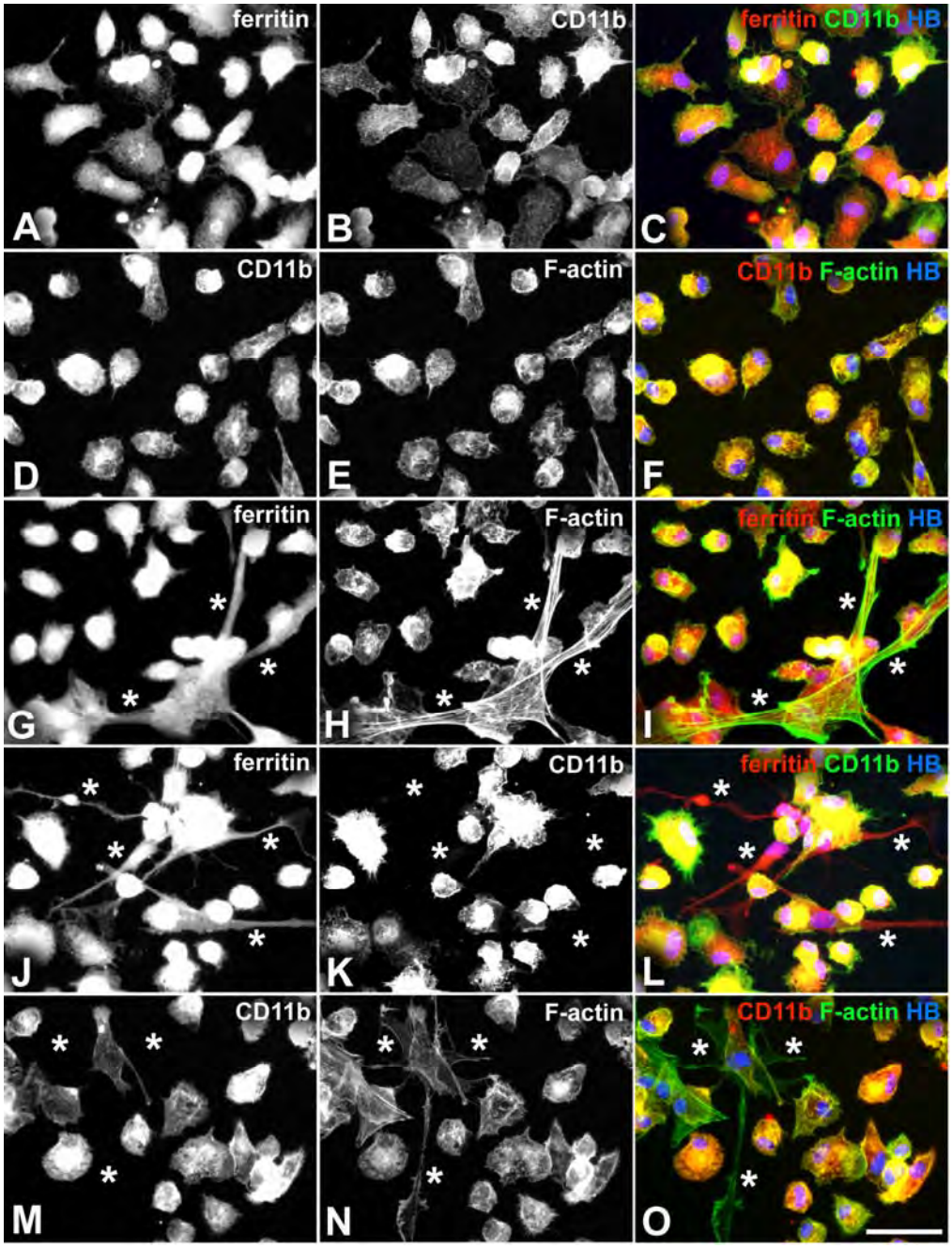

Figure 2.4 Immunostaining characterisation of microglia. Microglia were identified by immunoreactivity for CD11b (B, D, K, M, green in C, L and red in F, O) and ferritin (A, G, J and red in C, I, L). Nuclei were stained with Hoechst blue (HB; blue in C, F, I, L, O). Cytoskeletal actin filaments (F-actin) were stained with Alex fluor 488-conjugated phalloidin (E, H, N and green in F, I, O) to facilitate comparisons of cell morphologies with live cultures viewed under phase contrast (Fig. 3.1). Microglia were all positive for ferritin and CD11b and had rounded to irregular morphologies with numerous short processes. There was little difference in the appearance of microglial morphologies revealed by staining for ferritin, CD11b or actin filaments (D-I). Contaminating progenitor cells in the microglia cultures had small cell bodies and long thin processes (asterisks in G-O), and were positive for ferritin but negative for CD11b immunoreactivity. Scale bar is 100μm.

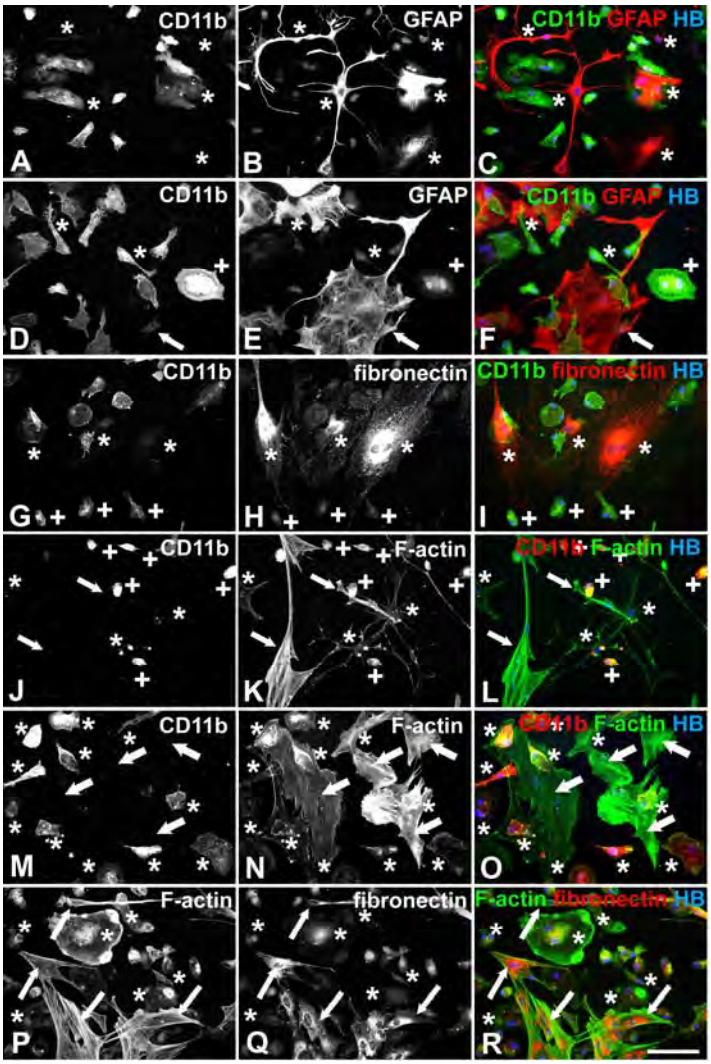

Figure 2.5 Contaminating cells in microglia cultures. Microglia were identified by immunoreactivity for CD11b (A, D, G, J, M, green in C, F, I and red in L, O). Contaminating astrocytes were identified by immunoreactivity for GFAP (B, E and red in C, F) and fibroblasts by immunoreactivity for fibronectin (H, Q and red in I, R). Nuclei were stained with Hoechst blue (HB; blue in C, F, I, L, O, R). Cytoskeletal actin filaments (F-actin) were stained with Alex fluor 488-conjugated phalloidin (K, N, P and green in L, O, R) for morphological comparisons with live cultures viewed under phase contrast (Figs. 3.0, 3.1). GFAP positive astrocytes varied from small cells with long thin processes (asterisks in A-C) to large flattened cells with shorter processes (E and red in F) and were all CD11b-negative (A, D). Large flattened astrocytes had stronger GFAP immunoreactivity. GFAP immunoreactivity was imaged at 2x exposure in B and was otherwise only very faint in these progenitor-like astrocytes (arrow in D-F; cell underlying the large astrocyte). There was some background nuclear and peri-nuclear immunoreactivity and occasionally bright (plus sign D-F) immunoreactivity in microglia with the polyclonal GFAP antibody (Dako). Most microglia had rounded to irregular morphologies with short processes and occasionally a larger process, terminating in a fan-shaped structure (asterisks D-F). There was also some background staining in microglia (plus signs G-I) with the fibronectin antibody but immunoreactivity was much stronger in the CD11b-negative contaminating fibroblasts (asterisks in G-I). Contaminating fibronectin-positive fibroblasts (arrows in Q-R) had sheet-like distributions of thick parallel actin filaments (arrows in J- R) whereas the irregularly-shaped microglia had a relatively diffuse distribution of actin filaments (asterisks M-R). Contaminating astrocytes had finer actin filaments that extended into radially arranged processes (asterisks J-L) and were distinguishable from actin filaments of fibroblasts (arrows in J-L) and CD11b-positive microglia (plus signs J-L). Scale bar is 100μm.

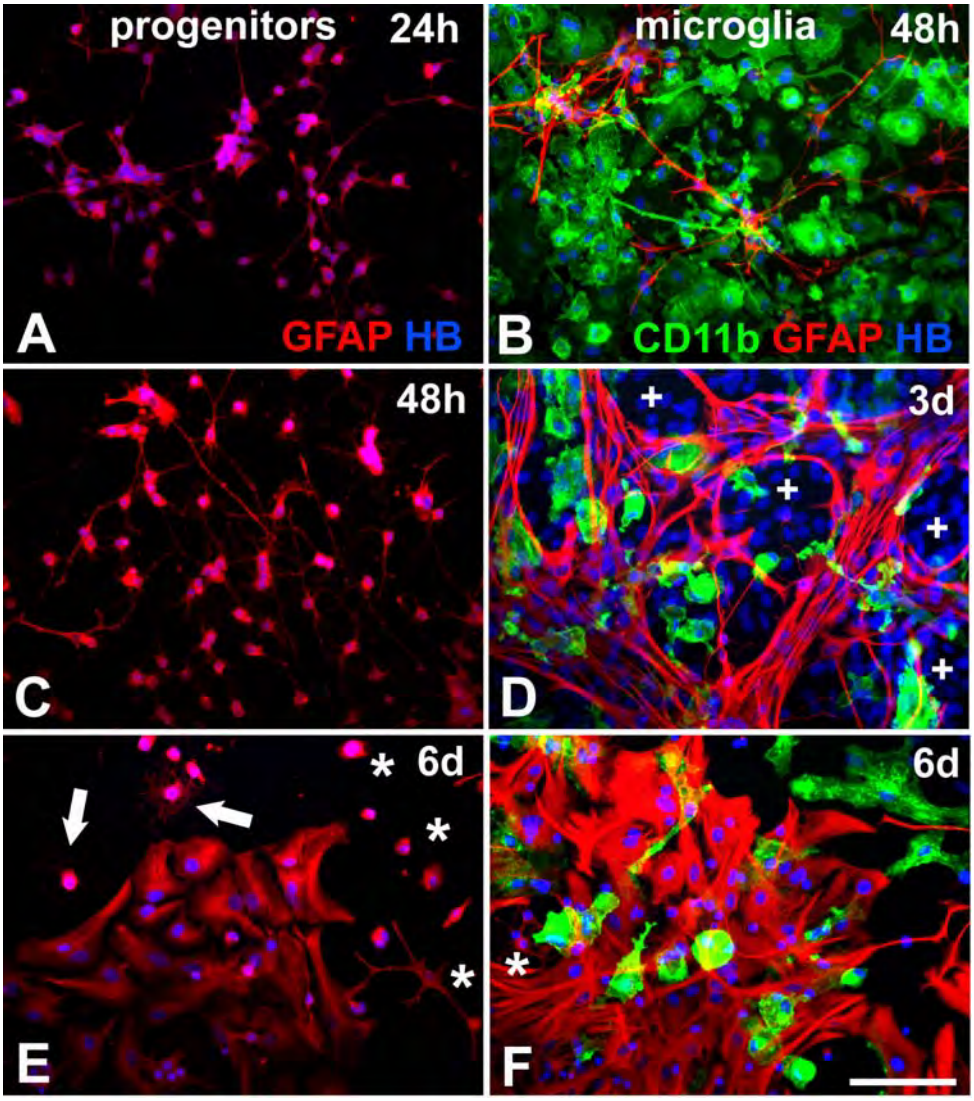

Figure 2.6 Contaminating progenitor cells in microglia cultures. Progenitor cells (A, C, E) were separated from astrocytes in confluent cortical cell cultures by 23 hours of shaking following earlier removal of microglia after 1 hour of shaking. Immunostaining for GFAP indicated that in monoculture the progenitor cells differentiated into astrocytes. After 24 hours most cells in these cultures had small cell bodies with two or three short branched processes. By 48 hours most cells had numerous longer, highly-branched processes. After 6 days the majority of cells were mature astrocytes with flattened epitheloid morphologies, although there were still numerous cells present similar to those seen in the earlier cultures (asterisks in E). Some progenitors with highly branched interwoven processes may have been differentiating into oligodendrocytes (arrows in E). Contaminating GFAP-positive progenitors (red in B, D, F) showed a similar progression of differentiation into astrocytes within cultures of CD11b-positive microglia (green in B, D, F). After 48 hours (B) the contaminating progenitors had long thin processes similar to those seen in monoculture after the same time in culture (C). By three days the GFAP-positive processes had thickened to form tract-like networks through the culture (D). Hoechst blue-stained nuclei (HB; blue in B, D, F) revealed there were some contaminating cells that were negative for GFAP and CD11b (plus signs in D). By 6 days (F) the contaminating cells were mainly mature astrocytes although there were also some still immature progenitors present (asterisk in F). Scale bar is 100μm.

2.31.2 Progenitor cells

Neural progenitor cells that express NG2, a chondroitin sulphate proteoglycan, generate oligodendrocytes during development (Nishiyama et al., 2005; Wigley et al., 2007) and can differentiate into astrocytes or oligodendrocytes, depending on the growth factor environment, in culture (Raff et al., 1983; Franklin et al., 1995; Parnavelas, 1999). Microglia and progenitor cells were both removed from cortical cell cultures by shaking during preparation of astrocyte cultures and therefore, progenitor cells were a likely contaminating cell in microglia cultures. Progenitor cells (Fig. 2.6) cultured in the presence of serum appear to rapidly differentiate into GFAP-positive astrocytes within 48 hours and then gradually develop more mature astrocyte morphologies over several days (Fawcett and Asher, 1999; Rhodes et al., 2006), whether cultured separately (Fig. 2.6A, C, E) or as contaminating cells (red in Fig. 2.6B, D, F) in the microglia (green in Fig. 2.6B, D, F) cultures. Hence, any progenitor cells remaining in astrocyte cultures would be unlikely to affect the purity of the astrocyte cultures by the time of experimentation. Although not observed, there may have been small numbers of quiescent progenitors in the astrocyte cultures (Crang and Blakemore, 1997) that could contribute to the continued proliferation of astrocytes in confluent cultures (Faijerson et al., 2006; Sergent-Tanguy et al., 2006). Gradual differentiation of progenitors into astrocytes could account for some of the observed morphological heterogeneity of astrocytes in the cultures. Rarely, progenitors may have been differentiating into oligodendrocytes (arrows in Fig. 2.6E) and there were also some contaminating cells negative for GFAP and CD11b (plus signs in Fig. 2.6D) that were most likely to have been fibroblasts.

2.31.3 Fibroblast cultures

Fibroblasts all showed positive immunostaining for the extracellular matrix protein, fibronectin (Hirsch et al., 1995; Lakatos et al., 2003b; Mulsow et al., 2005; Ito et al., 2006a; Gibbons et al., 2007; Ibanez et al., 2007) with stronger perinuclear staining in more isolated cells (Fig. 2.7D-F) and interlocking networks of secreted fibronectin forming over dense patches of fibroblasts (Fig. 2.7A-C, G-I). Fibroblasts had shorter processes that, unlike astrocyte processes, were not radially arranged and oval nuclei that tended to be larger than astrocyte nuclei. Fibroblasts were negative for GFAP showing

only faint background staining (Fig. 2.7B) with the monoclonal GFAP antibody (Chemicon). The coarse sheet-like parallel actin filaments of fibroblasts could be distinguished from the interwoven dense networks of fine radially distributed actin filaments in S100-positive astrocytes (Fig. 2.7). Fibroblasts showed only nuclear and faint perinuclear S100 immunoreactivity. Contaminating cells, which were identified as GFAP-positive astrocytes (asterisks in Fig. 2.8A) and CD11b-positive microglia (asterisks in Fig. 2.8B), were rare in the fibroblast cultures (Fig. 2.8) with the majority of Hoechst blue-stained nuclei belonging to GFAP/CD11b-negative fibroblasts.

2.31.4 OEC cultures

OECs were identified by immunostaining for the low affinity nerve growth factor receptor, $p75^{NTR}$ (Fig. 2.9A, D, G, green in Fig. 2.9C, F and red in Fig. 2.9I). All OECs also showed immunoreactivity for S100 (Fig. 2.9B, E and red in Fig. 2.9C, F). Schwann cells also express $p75^{NTR}$ and in culture are very similar in appearance to OECs (Lakatos et al., 2000; Vincent et al., 2005b; Franssen et al., 2008). Therefore, to exclude Schwann cells from the cultures, OECs were cultured from the only from olfactory bulb tissue for this research. The $p75^{NTR}$-positive OECs corresponded with those seen under phase contrast (Fig. 2.1) including both those with small cell bodies and long thin processes and more flattened cells. Consistent with previous research (Alexander et al., 2002; Chuah and West, 2002; Vincent et al., 2005b), immunostaining showed that the transition towards the more flattened, epitheloid, astrocyte-like morphologies with multiple radially-arranged processes was accompanied by a corresponding transition towards decreasing intensity of $p75^{NTR}$ immunoreactivity and increasing intensity of GFAP immunoreactivity (Fig. 2.10). GFAP immunoreactivity appeared as weak, diffuse staining in the more Schwann cell-like spindly bipolar OECs and as fibrous bundles of GFAP in astrocyte-like OECs. Neural stem cells and multipotent progenitor cells that can differentiate into neurons and astrocytes are present in large numbers in the olfactory bulbs during development and continue to migrate from the subventricular zone of the brain into the olfactory bulbs in the adult CNS (Barnett, 1993; Liu and Rao, 2003; Vergara et al., 2005; Parent et al., 2006; Maurer et al., 2008). The progenitor cells differentiate into granule cell and periglomerular second order neurons (Hack et al., 2005;

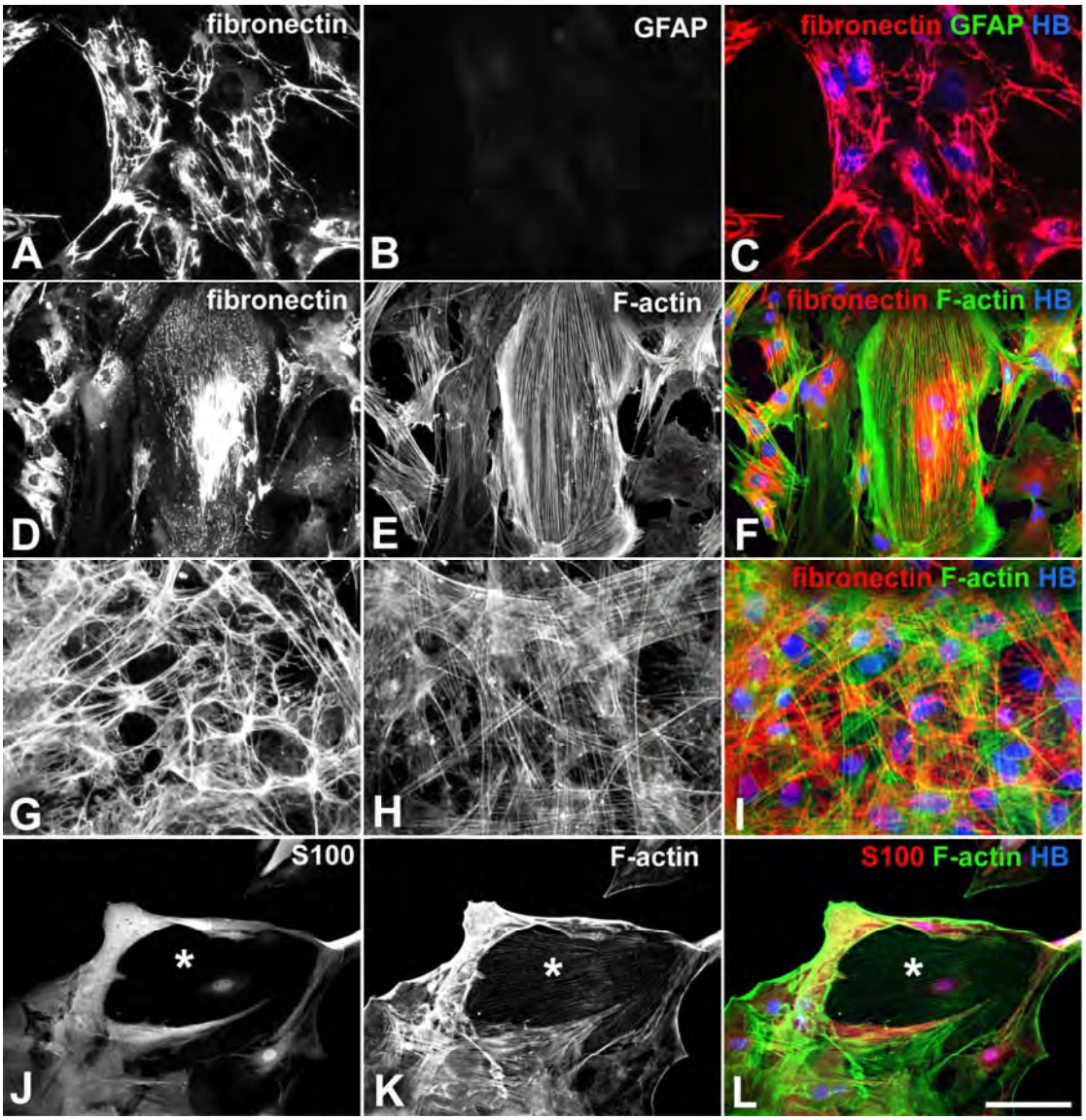

Figure 2.7 Immunostaining characterisation of fibroblasts. Fibroblasts were identified by immunoreactivity for fibronectin (A, D, G and red in C, F, I) and nuclei were stained with Hoechst blue (HB; blue in C, F, I, L). Cytoskeletal actin filaments (F-actin) were stained with Alex fluor 488-conjugated phalloidin (E, H, K and green in F, I, L) to facilitate comparisons of cell morphologies with live cultures viewed under phase contrast (Fig. 3.0). Fibroblasts were all fibronectin positive with stronger perinuclear staining in more isolated cells (D-F) and interlocking networks of secreted fibronectin forming over dense patches of fibroblasts (A-C, G-I). Fibroblasts were negative for GFAP showing only faint background staining (B) with the monoclonal GFAP antibody (Chemicon). Actin filaments in fibroblasts formed sheet-like structures with thick parallel fibres (D-F). In dense fibroblast cultures with secreted networks of fibronectin, the actin filaments formed a sparse criss-crossed network (G-I). The sheet-like parallel actin filaments of fibroblasts were distinct (asterisk in J-L) from the interwoven dense networks of fine radially distributed actin filaments in S100-positive (J, red in L) astrocytes. Fibroblasts showed only nuclear and faint perinuclear S100 immunoreactivity. Scale bar is 50μm (A-C, G-I) or 100μm (D-F, J-L).

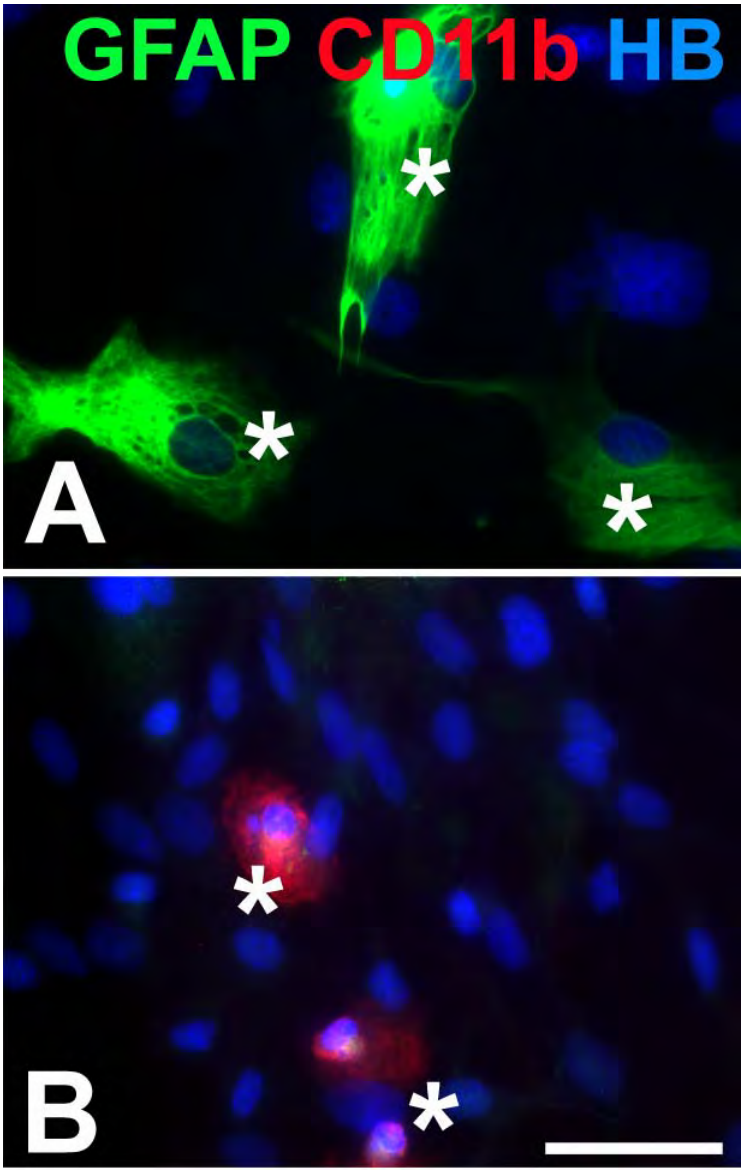

Figure 2.8 Contaminating cells in fibroblast cultures. Contaminating astrocytes (asterisks in A) and microglia (asterisks in B) in fibroblast cultures were identified by immunoreactivity for GFAP (green) and CD11b (red) respectively (A, B). Nuclei were stained with Hoechst blue (HB; blue). Contaminating cells were rare and the majority of nuclei belonged to GFAP/CD11b-negative fibroblasts. Scale bar is 50μm.

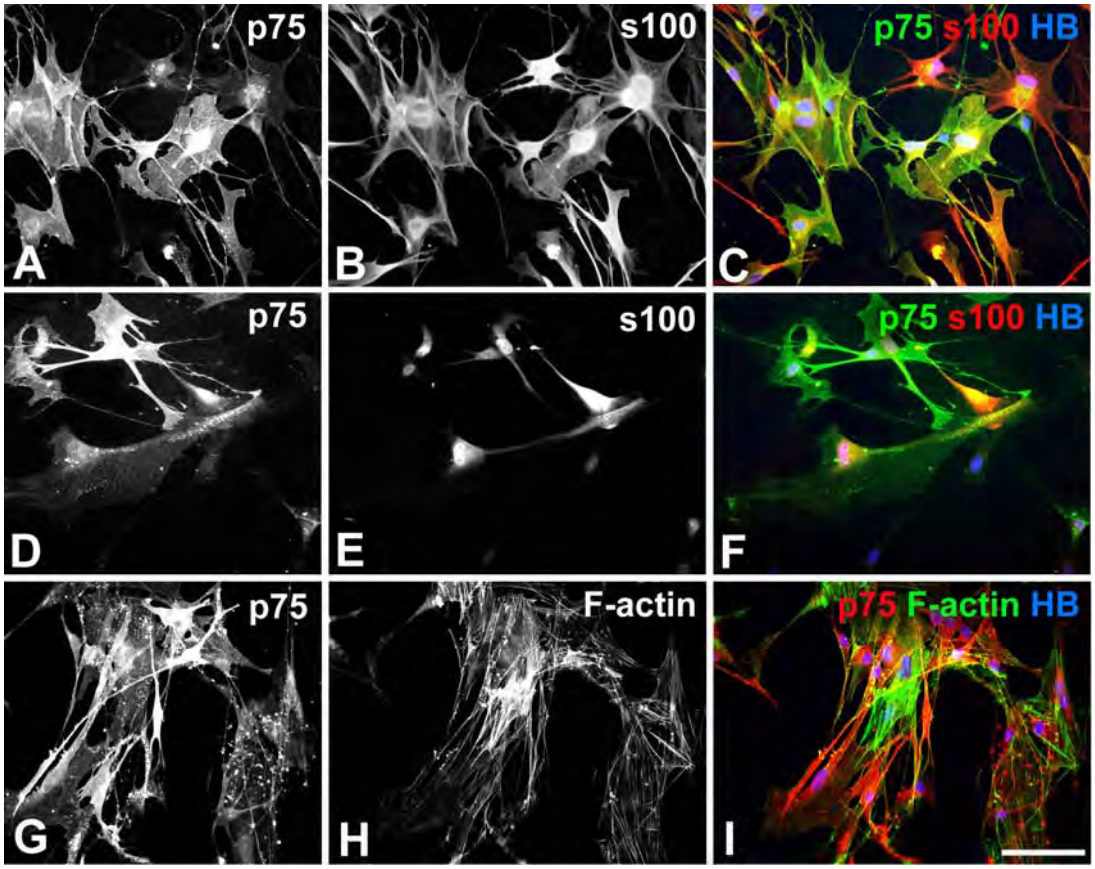

Figure 2.9 Immunostaining characterisation of OECs. OECs were identified by immunoreactivity for $p75^{NTR}$ (A, D, G, green in C, F and red in I) and S100 (B, E and red in C, F). Nuclei were stained with Hoechst blue (HB; blue in C, F, I). All OECs were $p75^{NTR}$ and S100-positive although staining intensity was more variable for S100. Cytoskeletal actin filaments (F-actin) were stained with Alex fluor 488-conjugated phalloidin (H and green in I) to facilitate comparisons of cell morphologies with live cultures viewed under phase contrast (Fig. 3.1). OECs had sheet-like arrangements of sparse fine actin filaments (G-I). Scale bar is 100μm.

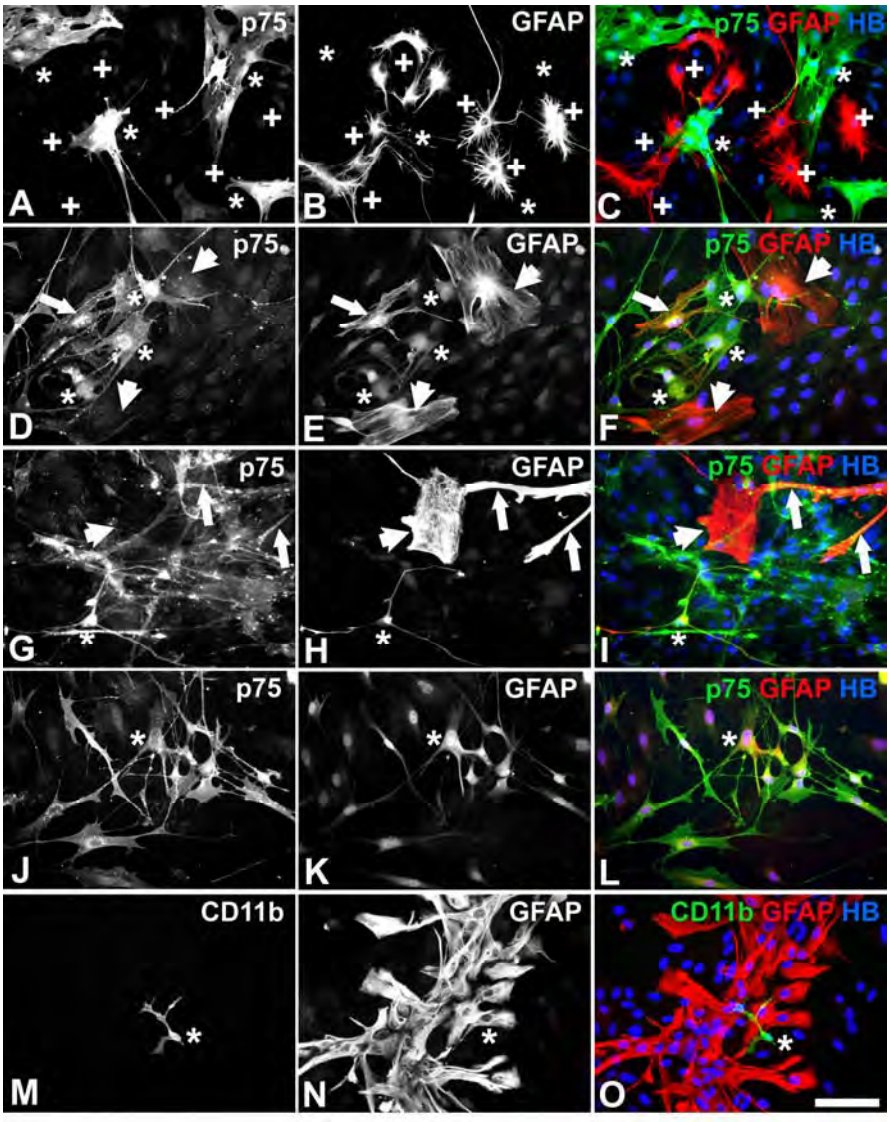

Figure 2.10 Contaminating cells in OEC cultures. OECs were identified by immunoreactivity for $p75^{NTR}$ (A, D, G, J and green in C, F, I, L) while contaminating astrocytes and microglia in OEC cultures were identified by immunoreactivity for GFAP (B, E, H, K, N and red in C, F, I, L, O) and CD11b (M and green in O) respectively. Nuclei were stained with Hoechst blue (HB; blue in C, F, I, L, O). There were some small astrocytes with fine processes (asterisks in A-C) resembling the astrocytes differentiating from progenitors in microglia cultures (Fig. 3.6). Occasional patches of mature astrocytes (M-O) had bright GFAP immunoreactivity and were $p75^{NTR}$-negative (A-C, M-O). Microglia were rare (asterisk in M-O). OECs were GFAP-negative (plus signs in A-C). unless imaged at 3x longer exposures (E, H, K), which revealed faint diffuse GFAP immunoreactivity in many $p75^{NTR}$-positive OECs (asterisks in D-L). There were also some $p75^{NTR}$-positive cells that showed fibrous GFAP immunoreactivity (arrows and arrowheads in D-I) that increased in intensity in larger more flattened cells with lower intensity $p75^{NTR}$ immunoreactivity (arrowheads in D-I). There were other contaminating cells identified by Hoechst stained nuclei (C, F, I, L, O) in cells that were negative for $p75^{NTR}$, GFAP and CD11b although they sometimes had faint perinuclear $p75^{NTR}$ immunoreactivity (A, D, G, J) and at longer exposures moderate nuclear and faint perinuclear GFAP immunoreactivity at similar levels to many OECs (E, H, K). Scale bar is 100μm.

Brill et al., 2008), and presumably astrocytes in the olfactory bulbs. Hence, it is possible that the variable OEC phenotypes observed in the cultures, derived from progenitor cells with the potential to differentiate into neurons, astrocytes or OECs, similar to the differentiation of neurons, astrocytes or oligodendrocytes from progenitors in the cortex. However, OECs are thought to originate from glial progenitors in the peripheral olfactory placode and migrate ahead of regenerating olfactory neuron axons into the olfactory bulbs (Doucette and Devon, 1993; Chuah and West, 2002; Li et al., 2005b; Richter et al., 2005). OEC differentiation in the cultures may instead have been affected by local biochemical environments before or after dissection. OECs had sheet-like arrangements of sparse fine actin filaments (Fig. 2.9G-I and Fig. 2.11G-I) similar to fibroblasts, although actin filaments in fibroblasts appeared thicker with more intense immunoreactivity (plus signs Fig. 2.11G-I). Rare contaminating microglia could be distinguished by their irregular morphologies and immunoreactivity for CD11b. The OEC cultures sometimes contained small astrocytes with numerous fine processes (asterisks in Fig. 2.10A-C) that resembled the astrocytes differentiating from progenitor cells seen in microglia cultures (Fig. 2.6). There were also occasional patches of mature astrocytes (Fig. 2.10M-O) that had bright GFAP immunoreactivity and were negative for $p75^{NTR}$ (Fig. 2.10A-C, Fig. 2.10M-O).

2.31.5 Contaminating fibroblasts in OEC cultures

Fibroblasts that presumably derived from the meningeal layers surrounding the olfactory bulbs and olfactory axon fascicles were the most prevalent contaminating cells in the OEC cultures (Fig. 2.10). Fibroblasts were best distinguished from OECs by the absence of $p75^{NTR}$ immunoreactivity in fibroblasts, although they sometimes had faint perinuclear $p75^{NTR}$ immunoreactivity (Fig. 2.11A, D, G, J and Os in Fig. 2.12D-F). OECs (arrows in Fig. 2.12A-C) and fibroblasts (Os in Fig. 2.12A-I) both expressed fibronectin although networks of secreted fibronectin only appeared to be associated with fibroblasts (Fig. 2.12D-F). The fibroblasts could proliferate rapidly, resulting in some cultures where OECs grew on dense layers of fibroblasts (Fig. 2.11D-F). This potential for contamination of OEC cultures by fibroblasts necessitated the confirmation of cell identity in experiments, by immunoreactivity for the cell-specific marker proteins. OEC

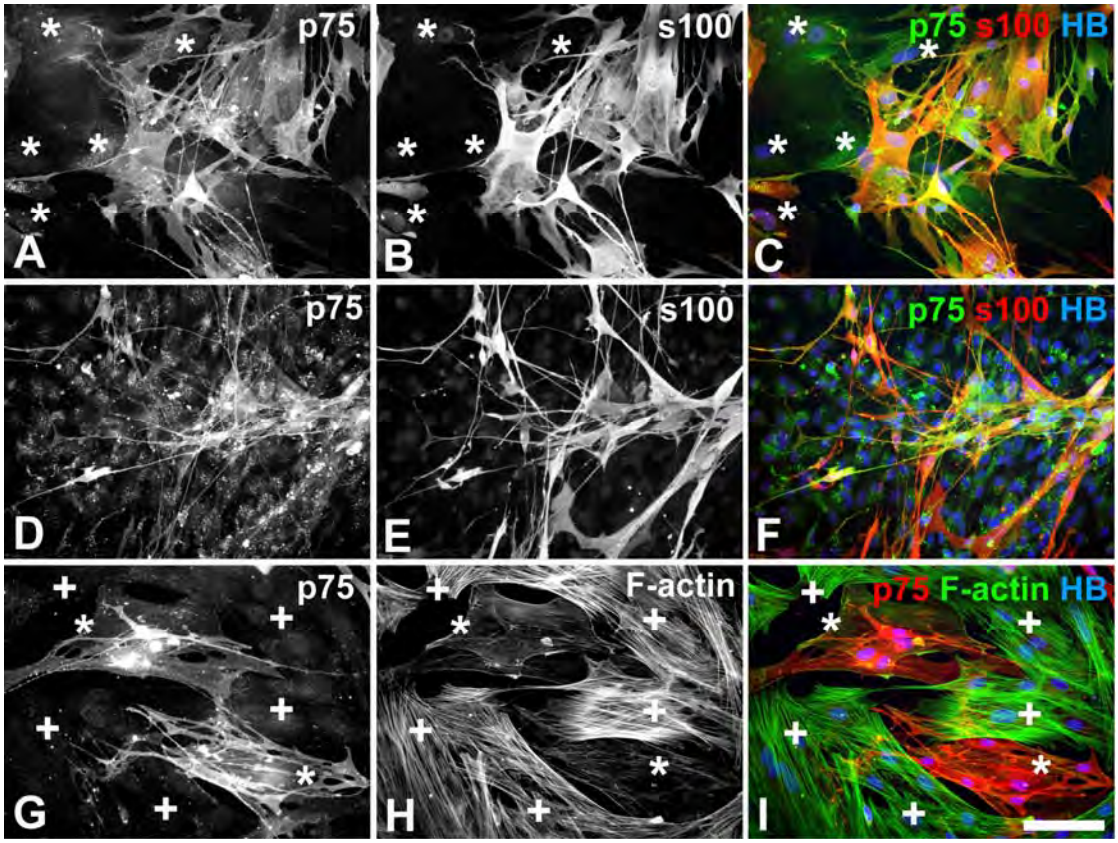

Figure 2.11 Contaminating fibroblasts in OEC cultures. OECs were identified by immunoreactivity for $p75^{NTR}$ (A, D, G, green in C, F and red in I) and S100 (B, E and red in C, F). Nuclei were stained with Hoechst blue (HB; blue in C, F, I). Cytoskeletal actin filaments (F-actin) were stained with Alex fluor 488-conjugated phalloidin (H and green in I) to facilitate comparisons of cell morphologies with live cultures viewed under phase contrast (Figs. 3.0, 3.1). Clusters of $p75^{NTR}$ and S100-positive OECs in cultures were often accompanied by fibroblasts showing faint nuclear and perinuclear background $p75^{NTR}$ and S100 immunoreactivity (asterisks A-C). The fibroblasts could proliferate rapidly, resulting in cultures where OECs grew on dense layers of fibroblasts (D-F). OECs had sheet-like distributions of fine parallel actin filaments (asterisks G-I). Actin filaments in fibroblasts had similar distributions but were thicker with more intense staining (plus signs G-I). Scale bar is 100μm.

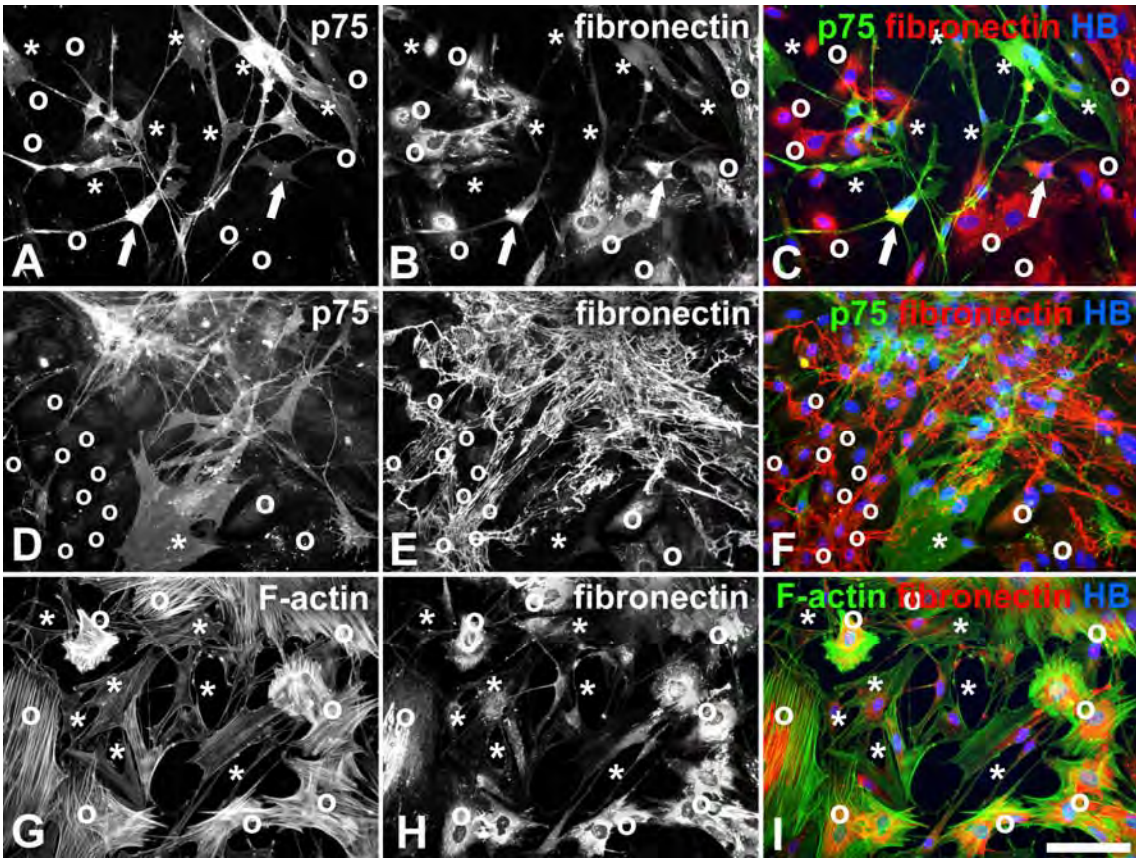

Figure 2.12 Fibronectin immunoreactivity in OEC cultures. OECs were identified by immunoreactivity for $p75^{NTR}$ (A, D, and green in C, F) and fibroblasts by immunoreactivity for fibronectin (B, E, H and red in C, F, I). Nuclei were stained with Hoechst blue (HB; blue in C, F, I). Cytoskeletal actin filaments (F-actin) were stained with Alexafluor 488-conjugated phalloidin (G and green in I) to facilitate comparisons of cell morphologies with live cultures viewed under phase contrast (Figs. 3.0, 3.1). $P75^{NTR}$-positive OECs (asterisks in A-I) also expressed fibronectin with immunoreactivity that was sometimes of similar intensity (arrows in A-C) to that in fibroblasts (Os in A-I) which had only faint background $p75^{NTR}$ immunoreactivity (Os in D-F). Networks of secreted fibronectin appeared to be associated with fibroblasts and not OECs (D-F). Fibronectin and actin filaments had similar distributions in OECs (asterisks in G-I) and fibroblasts (Os in G-I) but immunoreactivity was usually more intense in fibroblasts. Scale bar is 100μm.

cultures for later experiments were prepared using only olfactory bulb tissue, which consisted predominantly of Schwann-cell like OECs and had fewer contaminating fibroblasts and astrocytes.

2.4 Western blotting

2.40 Cell lysis

Lysis buffer:

20 mM Tris-HCl pH 7.5

150 mM NaCl

1 mM EDTA

0.5 % sodium deoxycholate

1 % Nonidet P-40

1:10 000 protease inhibitor cocktail (Sigma), added immediately before lysis.

Astrocytes were cultured in 12-well culture plates as previously described and treatments performed in triplicate on cultures in separate wells. Medium was removed from wells at the end of treatments and cultures were rinsed twice with ice-cold PBS. 200μL of ice-cold lysis buffer was added to each well, then cells were scraped and the cell suspension incubated for 30 minutes on ice. Lysate was collected into eppendorfs, centrifuged at 13 000 rpm for 30 minutes at 4^{O}C and the resulting supernatant lysate samples stored at minus 80^{O}C.

2.41 Lysis sample protein quantification

Total protein concentration of lysis samples was determined prior to storage of samples, to enable loading equal amounts of total protein from samples onto gels for electrophoresis and Western blotting. Protein concentration was determined using the BioRad protein assay, which is based on the Bradford protein assay whereby protein is quantified by comparison to a standard curve prepared using serial dilutions of bovine serum albumin. BioRad protein assay reagent was diluted 1:5 in MilliQ water. Bovine serum albumin (BSA; New England Biolabs) dilutions of 10μg/mL, 20μg/mL, 50μg/mL, 100μg/mL and 500μg/mL were prepared, 10μL of each dilution added to 990μL of the diluted BioRad assay reagent, mixed and incubated at room temperature for 5 minutes,

before absorbance was measured at 595nm with a SmartSpec 3000 spectrophotometer (BioRad). A standard curve was prepared from the measured absorbances of the BSA dilutions. 10μL of each sample (diluted 1:10 in MilliQ water for samples with high protein content) was added to 990μL of diluted assay reagent, mixed, incubated and absorbances read as for the BSA standards. The protein concentration of each sample was then determined from the standard curve.

2.42 SDS-PAGE

Samples for sodium dodecyl sulphate polyacrylamide gel electrophoresis (SDS-PAGE) were used undiluted or diluted with sufficient milliQ water for a total protein content of ~0.5 to 5mg/mL in a total volume of 18μL. Lower concentrations were used for Western blots for abundant proteins such as GFAP and higher concentrations for less abundant proteins such as metallothionein. Separate samples for each SDS-PAGE gel and subsequent Western blot were diluted according to the protein content of the sample such that the same amount of total protein was loaded into each sample lane of the gel. 7μL of 4x NuPAGE LDS sample buffer (Invitrogen), which contained SDS to denature and negatively charge proteins, and 3μL of sample reducing agent (Invitrogen) to reduce disulphide bonds between cysteine residues, was then added to the samples, which were then mixed by vortexing, pulse-centrifuged to consolidate, heated at 85-95^{O}C for 10 minutes to denature proteins, vortexed and again pulse-centrifuged. SDS-PAGE was performed using an Xcell *Surelock* Mini-cell (Invitrogen) with ~500mL of 1x NuPage MES SDS running buffer (Invitrogen) in the outer chamber and ~200mL of 1x MES buffer (Invitrogen) with 0.5mL of NuPAGE antioxidant (Invitrogen) to minimise sample oxidation, in the inner chamber. Samples were loaded into a NuPAGE 10% Bis-Tris gel (Invitrogen) and 10μL SeeBlue Plus2 protein markers (Invitrogen) were loaded adjacent to the sample lanes as a size reference for sample protein bands. A constant voltage of 200V was applied to the gel for 40 minutes to separate the denatured proteins in samples according to size by electrophoresis. Gels were then removed from cassettes and processed for Western blotting or Coomassie staining.

2.43 Coomassie blue staining of SDS-PAGE gels

Coomassie blue staining solution:

250mL methanol (Ajax Chemicals)

0.25g Coomassie brilliant blue R-250 (Sigma0

50mL glacial acetic acid (Ajax Chemicals)

Made to 500mL with dH_2O and filtered through filter paper

Destaining solution:

400mL methanol (Ajax Chemicals)

100mL acetic acid (Ajax Chemicals)

Made to 1L with dH_2O

Following separation of proteins by SDS-PAGE, the gel was submerged in Coomassie blue staining solution on an orbital shaker until stained protein bands were visible. The gel was then destained by covering with destaining solution on an orbital shaker until (usually overnight) protein bands could be clearly distinguished from background staining. The gel was then rehydrated, heat-sealed in plastic and imaged with a scanner (Epson Perfection 1650).

2.44 Protein assay by Western blotting

2.44.0 Protein transfer from SDS-PAGE gels to nitrocellulose membranes

Transfer buffer:

50mL 20x NuPAGE transfer buffer (Invitrogen)

100mL methanol

Made to 1L with dH_2O

Following separation of proteins by electrophoresis, proteins from the gel were transferred to a nitrocellulose membrane (Micro Filtration Systems) using an X-cell II blot module (Novagen), to allow later identification of protein bands by probing with antibodies. A nitrocellulose membrane (Micro Filtration Systems) pre-soaked in transfer buffer was placed on the gel containing electrophoresed samples while the gel was still on one side of the opened gel cassette. Two layers of pre-soaked blotting paper were then placed on the nitrocellulose, the gel carefully separated from the cassette and another two

layers of pre-soaked blotting paper placed on the underside of the gel. The gel/nitrocellulose/ blotting paper sandwich was then rolled with a glass rod to remove bubbles before placing in the blot module inner chamber with the nitrocellulose membrane closer to the module cathode (+) and two or three pre-soaked sponges on either side of the blotting paper layers to ensure a tight fit. The inner chamber was placed in the transfer module and filled with transfer buffer and the outer chamber was filled with dH_2O. A constant voltage of 30V was applied to the blot module overnight at $4^{O}C$ to transfer proteins to the nitrocellulose membrane.

2.44.1 Blocking and probing of the nitrocellulose membrane

PBS-T:

1mL Tween 20 (Ajax Chemicals)

999mL 0.01M PBS

X% blocking solution:

Xg skimmed milk powder (Diploma)

100mL PBS-T

Following transfer, the nitrocellulose membrane was removed from the module and washed for 5 minutes three times in PBS-T on an orbital shaker. Unbound regions of the membrane were then blocked by incubating with a 5% blocking solution for one hour on the shaker at room temperature, followed by another three 5 minute washes with PBS-T. The blot was then incubated with primary antibody at the required dilution (Table 2.2) in 10mL of 2.5% blocking solution in a heat-sealed plastic bag, on the shaker, for 1-2 hours at room temperature, followed by another three 5 minute washes in PBS-T. The membrane was then incubated with the appropriate secondary antibody, goat anti-rabbit IgG or goat anti-mouse IgG conjugated to horseradish peroxidase (Dako), diluted 1:1000-2000 in 2.5% blocking solution in a heat-sealed plastic bag for one hour at room temperature on the shaker, followed by three 5 minute washes in PBS-T. Primary antibodies were used at the concentrations shown below (Table 2.2).

Table 2.2 Primary antibody concentrations for Western blotting

Antibody	Concentration	Host species/clonality	Manufacturer
anti-GFAP	1:20 000	rabbit polyclonal	Dako
anti-GFAP	1:20 000	mouse monoclonal	Millipore
anti-GAPDH	1:5000	mouse monoclonal	Santa Cruz
anti-β-actin	1:10 000	mouse monoclonal	Abcam

2.44.2 Antibody detection

Detection solution:

5mL SuperSignal West Pico Stable Peroxide solution (Pierce)

5mL SuperSignal West Pico Luminol/Enhancer solution (Pierce)

After probing with antibodies the membrane was incubated with 10mL of detection solution in a heat-sealed plastic bag for 5 minutes on a shaker. Detection solution was then poured off and the excess rolled out of the plastic bag with a glass rod. The membrane was placed in a photographic cassette with fluorescent stickers to later enable correct alignment of detected protein bands. Photographic film (Hyperfilm, Amersham Pharmacia Biotech) was then exposed to the membrane for suitable time intervals for optimal visualisation of protein bands. The film was developed (Ilford) until protein bands were sufficiently visible, washed, fixed (Ilford) until the unexposed regions of the film were transparent, washed and dried, before imaging on a scanner (Epson Perfection 1650). The size of proteins in detected bands in the imaged blots could then be estimated from the known size of proteins in the SeeBlue Plus 2 marker protein bands. The size of the protein and the relevant primary antibody probe allowed identification of detected proteins and determination of the specificity of the antibody for the correct protein. Since the same amount of total protein was loaded into each lane of the SDS-PAGE gel, the relative strength of protein bands in the lanes corresponding to separate samples, provided an indication of the relative amount of the protein represented by the band, in each sample. Blots were washed and re-probed for multiple proteins, including GFAP to confirm that samples were from astrocytes and because GFAP is a commonly used indicator of astrogliosis. Blots were also probed for loading control proteins, β actin and

GAPDH that are not usually altered by physiological changes to confirm equal loading of total protein in each lane of the SDS-PAGE gels and consistent migration and transfer of protein bands during electrophoresis and blotting.

2.5 *In vivo* cortical needle-stick injury and OEC implantation

2.50 OEC culture and staining for implantation

OECs for implantation in cortical injury sites were cultured as described above in 25cm^2 tissue culture flasks. OECs were labelled with carboxy-fluorescein diacetate succinimidyl ester (CFDA-SE; Vybrant® CFDA SE Cell Tracer Kit, Molecular Probes) to enable identification and confirm viability of OECs after implantation. CFDA-SE passively diffuses into cells and remains non-fluorescent until its acetate groups are cleaved by intracellular esterases to yield highly fluorescent, amine-reactive carboxyfluorescein succinimidyl ester (Lyons and Parish, 1994; De Boer et al., 2006; Callard and Hodgkin, 2007; Wu et al., 2009). The succinimidyl ester group reacts with intracellular amines, forming fluorescent conjugates that are well-retained and can be fixed with paraformaldehyde. Excess unconjugated reagent and by-products passively diffuse to the extracellular medium, where they can be washed away. The dye-protein adducts that form in labelled cells are retained by the cells throughout development, meiosis and *in vivo* tracing (Fujioka et al., 1994; De Boer et al., 2006; Hawkins et al., 2007; Ishii et al., 2007; Hua et al., 2008). The label is inherited by daughter cells after cell division and is not transferred to adjacent cells in a population (Lyons and Parish, 1994; Bracher et al., 2007; Quah et al., 2007; Weischenfeldt and Porse, 2008). Lymphocytes labelled with CFDA-SE have been detected up to eight weeks after injection into mice (Quah et al., 2007) and CFDA-SE labelled hepatocytes were easily located by fluorescence microscopy up to 14 days after transplantation (Fujioka et al., 1994; Spinelli et al., 2002; Wu et al., 2009), while CFDA-SE labelled skin fibroblasts were detectable for at least 7 days after implantation into rats (Mian et al., 2001). A 10mM stock solution of CFDA-SE in dimethyl sulphoxide (DMSO; Sigma) was diluted to 10μM in PBS for labelling OECs. Culture medium was removed from flasks and OECs were incubated in the 10μM CFDA-SE solution for 15 minutes in the incubator at 37^{O}C for 15 minutes. The CFDA-SE solution was then removed and the OECs returned to the incubator in fresh culture

medium for at least 30 minutes. When required for implantation, OECs were removed from flasks by trypsinisation (using 0.25% trypsin in PBS) after removing medium and two washes with Versene. Trypsinisation was halted with the addition of DMEM-10FCS, OECs spun down at 2500 rpm for 10 minutes and re-suspended in 10μL of 0.9% sterile saline and kept on ice until implantation.

2.51 Surgery and cortical needle-stick injury

A cortical needle-stick injury model (King et al., 2000; Chung et al., 2003), involving surgery to produce a controlled mild brain injury, was used for *in vivo* investigation of the effects of OEC transplantation on brain injury in rats. 240-260g adult male rats were initially anaesthetised for surgery in a container filled with 95% oxygen / 5% isoflurane gas (Bomac, Australia), delivered through a Stinger anaesthetic system (AAS, Australia). To control post-operative pain, rats were injected subcutaneously with 3mg/kg of the analgesic, meloxicam (Boehringer Ingelheim) using an insulin syringe. Hair was shaved from the scalp from in front of the ears to just behind the eyes using electric clippers and the rat then secured in a stereotaxic device (Stoelting, USA) with clamped ear bars and a nose mask. A constant supply of 97% oxygen / 3% isoflurane gas at 0.8L/minute was delivered to the nose and mouth of the rat through the nose mask. The exposed scalp of the rat was wiped clean with isopropanol wipes and the rat's eyes kept moist throughout the procedure by periodically applying drops of 0.1M PBS. The scalp was incised with a sterile scalpel blade (No. 10, Swann-Morton) to expose the midline of the skull where the left and right parietal plates fuse. A drill with a 1mm bit (Dremel) attached to an adapter arm on the stereotax was aligned with the bit positioned above the skull reference point, lambda, where the left and right parietal plates fuse with the interparietal plate. A Vernier scale on the stereotax arm was then used to realign the drill and bit over a specific region of the right somatosensory cortical hemisphere by moving 5mm anterior and 4.5 mm to the right. The membrane over the skull was scraped away with a scalpel blade from the area below the position of the drill bit and the skin and membrane held clear with a haemostat while carefully lowering the drill, set on high speed, to drill through the skull without penetrating the underlying meninges. The drill was raised and a 1μL 22 gauge (outer diameter 0.711 mm) bevelled-end Hamilton syringe (Supelco, USA), containing

1μL of OECs suspended in sterile saline (0.9%) for transplantation treatments or saline only for controls, was fitted to the adapter arm and lowered 1.5mm into the brain. The syringe was left in the brain for 10 minutes and raised 1mm after 7 minutes for injection of the syringe contents into the injury site. After removing the syringe, a piece of gel foam (Upjohn, USA) was used to fill the hole in the skull and the wound was sutured with a single stitch. 1μL of saline alone or approximately 1000 OECs suspended in 1μL of saline was injected into the cortical injury site with the Hamilton syringe, which was sterilised with 70% ethanol, followed by several washes with milliQ water, between treatments on separate rats. This relatively low number of cells for injection was considered appropriate for the small lesion size, ease of injection and to possibly improve the low survivability found in previous research utilising implantation of ~100,000 to millions of cells (Richter et al., 2005; Hill et al., 2007; Vukovic et al., 2007). After surgery, each rat was placed in a warm cage, monitored until it regained consciousness and then kept in a cage with ample food and water until being euthanized 1, 4 or 7 days later for assessment of the cortical injury responses. A total of 14 rats were used for this preliminary *in vivo* study. 4 rats were used for each post-treatment euthanasia time-point; 2 receiving OEC implantations and 2 controls receiving saline injections, with another 2 rats used as uninjured controls. One brain from each pair of rats was used for injury assessment by immunocytochemistry with the other brain being used for protein assay by Western blotting.

2.52 Rat perfusion and brain dissection for immunocytochemistry

Rats were euthanized by intraperitoneal injection with 60mg/kg of sodium pentobarbitone (Boehinger Inglelheim) using an insulin syringe. A series of reflex tests were administered after rats became unconscious to ensure that rats were unresponsive to stimuli and therefore sufficiently anaesthetised before commencing surgery for perfusion. Surgery was then conducted efficiently to enable perfusion to commence while there was still a heartbeat. The abdominal cavity was opened with a lateral incision below the sternum using scissors. The chest cavity was entered by cutting through the diaphragm with scissors, parallel incisions made upwards through each ribcage on either side of the solar plexus and the heart fully exposed by lifting the ribcage towards the head with a

clamp attached to the sternum. The base of the heart was held with forceps, a small incision made into the lower left ventricle with fine scissors, a catheter inserted into the ventricle through the incision and the catheter clamped with a haemostat to seal the incision, ensuring that perfusate delivered through the catheter would travel through the circulatory system via the aorta. Ice-cold PBS was gravity fed through the catheter and the right atrium of the heart cut to allow circulation of the PBS (150-200mL/rat) to flush blood from the rat's circulatory system. When blood was sufficiently cleared as indicated by loss of liver colouration, perfusion was continued with ice-cold 4% paraformaldehyde solution (100-150mL/rat) to fix tissues until muscular twitching in response to the paraformaldehyde ceased and the rat was rigid. Following perfusion, rats were decapitated, skin and flesh removed with scissors and the skull carefully snapped away from the brain with bone scissors. The whole brain was carefully removed with a spatula and post-fixed in 4% paraformaldehyde for 1-2 days before storing in PBS containing 0.03% (w/v) sodium azide (PBS-azide) solution at 4ºC, until sectioning for immunocytochemistry.

2.53 Cortical sectioning for immunocytochemistry

Brains were removed from PBS-azide solution, washed twice with PBS, sagittally trimmed 2mm anterior and posterior of the injury site and embedded in 5% (w/v) agarose. The brains were squared off at the front and rear by making a sagittal incision 1mm anterior and 1mm posterior of the injury site with a flat blade. Multiple 50µm coronal sections were cut through the injury site across the whole brain, so that each section contained injured and uninjured cortical hemisphere portions. Sectioning commenced anterior to the injury site and 2-3 sections were stored in each well of 12-well culture plates in order of sectioning in PBS-azide at 4^{O}C.

2.54 Immunostaining of cortical sections

Brain sections were immunostained and imaged following the same procedures described above for immunostaining of cell cultures except that antibodies were applied to sections in 12-well culture plates. Primary antibodies were applied at the concentrations shown below (Table 2.3). For samples that had been implanted with OECs labelled with CFDA-

SE, only one primary antibody for conjugation to either goat anti-rabbit Alexa Fluor 594 or goat anti-mouse Alexa Fluor 594 (Molecular Probes) could be used, since the CFDA-SE had similar fluorescence to Alexa Fluor 488.

Table 2.3 Primary antibodies for immunostaining tissue sections

Antibody	Concentration	Host species/clonality	Manufacturer
anti-GFAP	1:1000	rabbit polyclonal	Dako
anti-GFAP	1:1000	mouse monoclonal	Millipore
anti-EphA4	1:250	rabbit polyclonal	Santa Cruz
anti-ferritin	1:1000	rabbit polyclonal	Santa Cruz
anti-metallothionein 1/2	1:500	mouse monoclonal	Abcam
anti-phosphorylated neurofilament (SMI312)	1:1000	mouse monoclonal	Sternberger

2.55 Rat brain dissection for Western blotting

For Western blot samples, rats were euthanized and whole brains removed as described above, without perfusion or fixation. The brain was placed on ice in a Petri dish lid and a 4mm sagittal section, 2mm either side of the injury site was made through the whole brain using a scalpel blade (No. 10, Swann-Morton). The cortex was separated from the hindbrain portion of the section, the injured cortical hemisphere separated from the uninjured hemisphere, the injured hemisphere portion trimmed to 2mm each side of the injury site at right angles to the initial sagittal section and the uninjured hemisphere similarly trimmed to provide an equivalent sample. The two samples were placed in separate eppendorfs and snap frozen in liquid nitrogen before storage at -80^{O}C.

2.56 Lysis of cortical samples and Western blotting

Frozen tissue samples were crushed under liquid nitrogen using a cold mortar and pestle, then diluted in 500µL of lysis buffer (recipe as described above for lysis of cultured cells) and transferred to a 15mL Falcon tube. Samples were homogenised on ice with several brief pulses using an Ultra-Turrax T25 (Janke & Kunkel, IKA® Labortechnik),

centrifuged for 20 minutes at 13 000 rpm at 4^{O}C and the supernatant samples stored at minus 80^{O}C. Western blotting was conducted on samples as described above for cell culture samples.

CHAPTER 3:

Nuclear factor-κB translocation and astrocyte activation

3.0 Introduction

3.00 Why measure astrocyte activation?

Brain tissue viability after injury depends on astrocyte survival because of their critical roles in the active uptake of glutamate and its conversion to glutamine, buffering of extracellular potassium ions (K^+) and calcium ions (Ca^{2+}), maintenance of extracellular pH and provision of lactate and pyruvate to neurons as alternative energy sources under the hypoxic and hyperglycaemic conditions (Swanson and Benington, 1996; Chen and Swanson, 2003; Swanson et al., 2004; Laird et al., 2008). In particular, the uptake of excess extracellular glutamate through the astrocyte excitatory amino acid transporters (EAAT) 1 and 2, (also known as the glutamate/aspartate transporter (GLAST) and glutamate transporter-1 (GLT-1) respectively) is essential for protecting neurons from glutamate-induced excitotoxicity and enabling their survival in the injury penumbra (Chen and Swanson, 2003; Vermeiren et al., 2005; Sullivan et al., 2007; Arranz et al., 2010). However, as described in Chapter 1 the inflammatory activation of astrocytes eventually leads to reactive astrogliosis and the development of the glial scar. Although the glial scar may protect penumbral tissue from cytotoxic conditions in the lesion core it also appears to be a barrier to axon regrowth across the lesion. Similarly, reactive astrocytes produce growth factors and cytokines that can promote wound-healing and the resolution of inflammation, while more severe astrogliosis is associated with increased tissue damage due to the production of factors that amplify and prolong inflammation. It follows that measurement of the severity of astrocyte inflammatory activation, within the context of an experimental model enabling equivalent initial injuries, could provide a useful indication of the likely efficacy of OEC implantation and other potential therapies for CNS injury. Although it could be argued that any moderation of astrocyte reactivity was a consequence rather than a cause of decreased neuronal damage, these are likely to be mutually complementary events. Reactive astrocytes are a major source of cytokines and chemokines that regulate the extent of immune cell recruitment and the consequent inflammation that causes secondary neuronal damage. Secondary neuronal death can then

initiate further inflammation and astrocyte activation. Furthermore, glutamate uptake, free radical scavenging and the production of metabolites by astrocytes can protect neurons against the cytotoxic conditions arising from injury and inflammation.

3.01 Glial fibrillary acidic protein (GFAP) and astrocyte activation

3.01.0 GFAP is upregulated in response to CNS inflammation

GFAP expression in astrocytes is sensitive to a wide variety of even mild CNS disturbances and consequently is frequently used as an indicator of the severity of astrogliosis that is assumed to correlate with the severity of inflammation and related CNS tissue damage (Oh et al., 1993; Yu et al., 1993; Krohn et al., 1999; Brahmachari et al., 2006; O'Toole et al., 2007; Tramontina et al., 2007; Wanner et al., 2008). This may be problematic, particularly for *in vitro* models, since GFAP expression varies with astrocyte type and brain region and may be differently regulated by a variety of inflammatory mediators (Wofchuk and Rodnight, 1994; Rodnight et al., 1997; Gomes et al., 1999; Kommers et al., 2002; Sousa Vde et al., 2004; Sullivan et al., 2010b).

3.01.1 Progenitor differentiation contributes to GFAP upregulation

The GFAP gene promoter region contains binding sites for nuclear factor-κB (NF-κB), nuclear factor (NF) 1, AP-1, STAT, Smad proteins and response elements for cAMP, transforming growth factor (TGF)β, glucocorticoids and hormones and many of these factors regulate GFAP expression during astrocyte development (Reeves et al., 1989; Gomes et al., 1999; Krohn et al., 1999; Cebolla and Vallejo, 2006). Many of these regulators of astrogliogenesis are upregulated following CNS injury, provoking research into their possible roles in promoting injury-induced GFAP upregulation and the associated astrogliosis. There have been some conflicting results from this research that may be partly because astrogliosis and glial scar formation involves both mature astrocytes and immature astrocytes that differentiate from progenitor cells at injury sites (Yang et al., 1997; Fawcett and Asher, 1999; Alonso, 2005; Panickar and Norenberg, 2005; Faijerson et al., 2006). For example, although IL-1β and TNF-α activate NF-κB and inflammatory gene expression leading to astrogliosis (Taupin et al., 1993; Feuerstein et al., 1994; Lee et al., 1995) they do not necessarily induce GFAP upregulation *in vitro*

(Oh et al., 1993). However, IL-1B and TNF-α induce NF-κB-dependent production of IL-6 (Meeuwsen et al., 2003a; Aronica et al., 2005; John et al., 2005; Fernandes et al., 2006), which has structural similarities with CNTF and activates the JAK/STAT1/3 and MAPK pathways to promote differentiation of neural progenitors into astrocytes (Rajan and McKay, 1998; Justicia et al., 2000; Fan et al., 2005; He et al., 2005; Nakanishi et al., 2007) and the transformation of astrocytes to a reactive phenotype (Korzus et al., 1997; Okada et al., 2004; Bolin et al., 2005; Na et al., 2007).

3.01.2 Astrocyte swelling induces GFAP upregulation

GFAP is normally expressed at only low levels in mature cortical astrocytes but following injury it is dramatically upregulated in mature astrocytes, particularly in the glial scar region (Fawcett and Asher, 1999; Panickar and Norenberg, 2005; Wilhelmsson et al., 2006). GFAP upregulation also occurs over a wide area in the injury penumbra and surrounding undamaged tissue (Fig. 1.4). The mature astrocytes away from the lesion border substantially retain their normal morphology and their increased GFAP expression may be associated with astrocyte swelling and upregulation of the aquaporin 4 (AQP4) water channel to facilitate the uptake of excess water, extracellular potassium ions and glutamate resulting from the vasogenic oedema that follows BBB damage during CNS injury (Wilhelmsson et al., 2006; Gunnarson et al., 2008; Nesic et al., 2008; Papadopoulos and Verkman, 2008). The upregulation of GFAP and astrocyte process growth after injury could provide additional binding sites and structural stability for additional membrane receptors, transport proteins and ion channels required for restoring homeostasis (Wilhelmsson et al., 2004; Lee et al., 2007; Sullivan et al., 2007; Saadoun and Papadopoulos, 2009; Wang and Hatton, 2009).

3.01.3 Depolymerisation may alter GFAP immunoreactivity

The variety of stimuli and the involvement of mature astrocytes and progenitor cells in GFAP upregulation after CNS injury make the interpretation of the pathological implications of GFAP expression levels difficult, especially for *in vitro* studies. Further ambiguities can arise from measuring expression levels by immunocytochemistry. GFAP may be less accessible to antibody binding when in the de-phosphorylated polymerised

form than when in phosphorylated monomeric form and glutamate-induced increases in intracellular Ca^{2+} following CNS injury can rapidly induce phosphorylation and depolymerisation of GFAP (Rodnight et al., 1997; Tramontina et al., 2007; Sullivan et al., 2010b). Ca^{2+} influx also activates the Ca^{2+}-dependent protease, calpain (Robles et al., 2003) resulting in depolymerisation and degradation of GFAP (Du et al., 1999; Stys, 2004). Furthermore, while GFAP levels may provide an indication of the severity of the astrogliosis that results from astrocyte inflammatory activation it would be useful to have an earlier measure of the intensity of astrocyte activation for assessing the efficacy of anti-inflammatory therapies.

3.02 NF-κB translocation as a measure of astrocyte inflammatory activation

3.02.0 NF-κB is a key early regulator of inflammation

NF-κB is a key regulator of inflammatory gene expression that has a major role in CNS injury responses (Wagner, 2007; Yang et al., 2007; Ridder and Schwaninger, 2009). Many of the factors elevated by CNS injury activate NF-κB, including cytokines, glutamate, ROS and increases in intracellular Ca^{2+}. Activated NF-κB then promotes the transcription of many genes involved in the pathogenesis of CNS injury and inflammation, including cytokines, chemokines, adhesion molecules, iNOS, which generates NO and inducible cyclooxygenase-2 (COX-2), which generates prostaglandins (Bethea et al., 1998; Schneider et al., 1999; Yamamoto and Gaynor, 2001). The cytokines IL-1β, TNF-α, IL-6 and IFN-γ have crucial roles in the inflammatory response to CNS injury (Ballestas and Benveniste, 1995; Tzeng et al., 1999; Lenzlinger et al., 2001; Meeuwsen et al., 2003a; John et al., 2005) and they all regulate gene expression via NF-κB (Baldwin, 1996; O'Neill and Kaltschmidt, 1997; Bethea et al., 1998; Tak and Firestein, 2001; Yamamoto and Gaynor, 2001). These NF-κB-activating cytokines are also induced by NF-κB and the resultant positive autoregulation can increase the amplitude and duration of inflammation (Yamamoto and Gaynor, 2001; Tian et al., 2005). The extent of the inflammatory response affects the progression of pathogenesis and secondary damage following the initial injury (Schneider et al., 1999; Bethea, 2000; Brambilla et al., 2009). Consequently, NF-κB activation could provide an effective early measure of the severity of inflammation relevant to CNS injury responses.

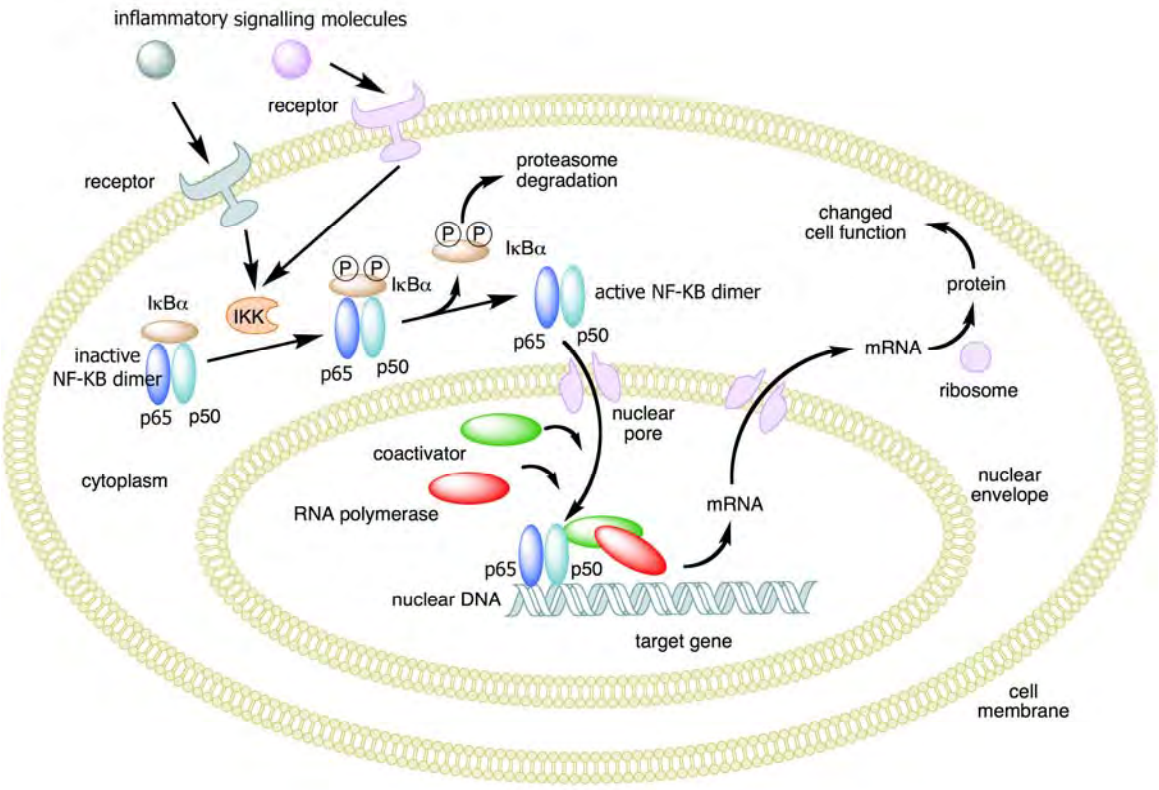

Figure 3.0 Activation of nuclear factor-κB. Nuclear factor-κB (NF-κB) dimers exist predominantly in the cytoplasm of unstimulated cells where they are bound to inhibitor of κB (IκB) family proteins. Translocation of dimers to the nucleus is essential for NF-κB promotion of gene transcription. Signal-mediated phosphorylation of IκBs by IκB kinase (IKK) leads to ubiquitination of IκB and subsequent degradation by the proteasome. Removal of IκBs promotes translocation of the free NF-κB dimers to the nucleus where they bind specific sequences in the promoter and enhancer regions of genes. NF-κB activation, mainly involving the p50/p65 dimers, regulates transcription of many genes involved in CNS inflammatory responses to injury and can thereby induce increased expression of cytokines, chemokines, adhesion molecules, iNOS, aquaporins, GFAP and growth factors.

3.02.1 Translocation to nuclei is essential for NF-κB activity

NF-κB is a ubiquitous dimeric transcription factor with five mammalian subunits, p65 (also known as RelA), Rel-B, c-Rel, p50 and p52 that are expressed in most cells (Baeuerle and Henkel, 1994; Baeuerle, 1998; Hayden and Ghosh, 2004). NF-κB homo- or heterodimers exist predominantly in the cytoplasm of unstimulated cells where they are bound to inhibitor of κB (IκB) family proteins (Fig. 3.0). Inflammatory stimuli induce phosphorylation of IκBs by IκB kinase (IKK) causing IκB to dissociate from NF-κB and marking IκB for polyubiquitination and proteosomal degradation. Removal of IκBs promotes translocation of the free NF-κB dimers to the nucleus where they bind specific DNA sequences in the promoter and enhancer regions of genes. NF-κB proteins share a 300–amino acid Rel homology domain that mediates the DNA binding, dimerisation, and nuclear transport of the proteins (Baeuerle, 1998; Yamamoto and Gaynor, 2001; Chen and Greene, 2004a; Hayden and Ghosh, 2004). In addition to the Rel homology domain, the NF-κB family members, c-Rel, RelB, and p65 (also known as RelA) contain transactivation domains, which interact with components of the basal transcription apparatus. Although the NF-κB subunits p50 and p52, which are derived from the inactive precursors, p105 and p100, respectively, possess DNA binding and dimerisation properties through their Rel domains, they do not have strong transactivation domains. In addition to the inflammatory gene targets, NF-κB also promotes transcription of its own primary regulators, the IκBs (Baeuerle, 1998; Ghosh et al, 1998; Hoffman et al., 2002; O'Dea et al., 2007). Newly formed IκBs translocate to the nucleus where they bind NF-κB and mask its nuclear localization signals. The NF-κB:IκB complex is then exported to the cytoplasm to complete a cycle of NF-κB activation and deactivation. Due to this autoregulatory mechanism, NF-κB transcriptional activity is usually transient, lasting only between 1 and 4 hours in most cells and deletion of IκB expression results in persistent NF-κB activation, leading to postnatal lethality (Hertlein et al., 2005). The synthesis and degradation rates of IκBs are critical controlling factors of NF-κB activity. NF-κB activation is Ca^{2+}- and PKC-dependent and resynthesis of IκBs is favoured by decreased concentrations of these factors either in the absence of activating stimuli or during prolonged exposure, which may deplete intracellular calcium stores and simultaneously inhibit the ATP production required for their replenishment (Carafoli,

2002; Fisher et al., 2006; Hoffman et al., 2002; Hertlein et al., 2005; Sorriento et al., 2008). The three isoforms of IκB have differing regulatory effects on NF-κB (Hoffman et al., 2002; O'Dea et al, 2007). IκBα synthesis is controlled by a highly NF-κB responsive promoter and consequently, provides strong negative feedback resulting in an oscillatory NF-κB response. The slower responses of IκBβ and IκBε can dampen the oscillations so that they gradually diminish in amplitude over about 6 hours as NF-κB activity returns to basal levels. However, in the absence of IκBα, IκBβ and IκBε can induce sustained NF-κB activation. Translocation of dimers is essential for NF-κB activation and promotion of gene transcription is associated with the subsequent binding of co-activators to the NF-κB transactivation domains. NF-κB activity, mainly involving the p50/p65 dimers (Schneider et al., 1999; Hang et al., 2006; Ridder and Schwaninger, 2009), is increased in neurons, microglia and astrocytes within hours of CNS injury and remains elevated for months (Bethea et al., 1998; Bethea, 2000; Domanska-Janik et al., 2001; Tak and Firestein, 2001; Zhang et al., 2007). Translocation of NF-κB from the cytoplasm to nuclei can be measured by relatively simple techniques including, immunostaining of intact cells, Western blotting of nuclear and cytoplasmic fractions, electrophoretic mobility shift assay (EMSA) and chromatin immunoprecipitation (CHIP) assay, thus providing a convenient measure of the inflammatory activation (Bethea et al., 1998; Brettingham-Moore et al., 2005a; Vincent et al., 2007; Zhang et al., 2007).

3.02.2 Regulation of the NF-κB signalling pathway is complex

NF-κB family subunit differences in expression, nuclear translocation, ability to heterodimerise with other subunits and interaction with components of the transcription apparatus contribute to the diverse effects of NF-κB pathway activation (Tak and Firestein, 2001; Chen and Greene, 2004a; Johansen et al., 2005; Brettingham-Moore et al., 2008; Pizzi et al., 2009). Transcription can be further enhanced by phosphorylation and acetylation of NF-κB subunits and interactions with the MAPK inflammatory signalling pathways (Fig. 1.2) and associated transcription factors (Chan and Riches, 2001; Hayden and Ghosh, 2004; Chen et al., 2007; Brettingham-Moore et al., 2008; Wolter et al., 2008). Genomic screening has identified 154 positive and 88 negative modulators of NF-κB signalling, with most of the positive modulators converging on

activation of the IκB kinases and a number of negative modulators providing an additional downstream layer of control (Halsey et al., 2007). The differential tissue distribution of these modulators together with the downstream negative regulation enables NF-κB to mediate different responses to different stimuli. The complexity of the NF-κB signalling pathway can result in either monophasic or oscillatory cycles of transcriptional activation and de-activation involving multiple activating stimuli, the recruitment of co-activators to gene promoter regions, interactions between NF-κB subunits and enhanced transcription of both NF-κB subunit and inhibitor of NF-κB (IκB) genes as well as other genes that promote or inhibit NF-κB activity (Baeuerle, 1998; Chen and Greene, 2004b; Hayden and Ghosh, 2004; Tian et al., 2005; Wietek and O'Neill, 2007; Hertlein et al., 2005). NF-κB also regulates transcription of the NF-κB subunit and IκB genes to respectively prolong or resolve inflammation. The modulation of NF-κB activation by these multiple factors allows the integration of signalling and feedback from the diversity of inflammatory mediators. NF-κB activation is thereby a sensitive and immediate indicator of the severity of inflammatory activation.

3.02.3 NF-κB activation promotes astrogliosis

Most of the protein expression changes that characterize astrogliosis are regulated by NF-κB, including the increased expression of cytokines and chemokines (Schwaninger et al., 1999; Meeuwsen et al., 2003a; Neary and Kang, 2005; Khorooshi et al., 2008), adhesion molecules (Ballestas and Benveniste, 1995; Ellison et al., 1999), iNOS (Zhang et al., 2007; Sinke et al., 2008), AQP4 (Ito et al., 2006b; Gunnarson et al., 2008), granulocyte macrophage-colony stimulating factor (GM-CSF) (Zaheer et al., 2002), GFAP (Bae et al., 2006), insulin-like growth factor (Ye et al., 2004), NGF, GDNF and BDNF (Meeuwsen et al., 2003a; Kuno et al., 2006). The NF-κB-dependent protein expression changes are associated with a change to a neurite growth inhibitory astrocyte phenotype accompanied by increased GFAP expression and the development of a glial scar around the lesion (Stichel and Muller, 1998; de Freitas et al., 2002; Sandvig et al., 2004; Fawcett, 2006a; Wilhelmsson et al., 2006). The chemokines, adhesion molecules and increased nitric oxide (NO) production promote recruitment of microglia and leukocytes to the lesion (Babcock et al., 2003; Meeuwsen et al., 2003a; Panickar and Norenberg, 2005;

Khorooshi et al., 2008). GM-CSF together with other growth factors and cytokines induce NF-κB-regulated proliferation and activation of the recruited microglia and leukocytes (Liva et al., 1999; Koguchi et al., 2003; Henze et al., 2005; Suh et al., 2005) resulting in enhanced secretion of inflammatory cytokines (Hanisch, 2002; Zaheer et al., 2002) and increases in the production of NO and ROS to potentially neurotoxic levels (Block et al., 2007; Hanisch and Kettenmann, 2007). Hence, NF-κB activation in astrocytes appears to be a highly relevant determinant of astrocyte inflammatory responses and consequently, the extent of neuronal damage and the potential for axonal regeneration after CNS injury.

3.02.4 Increased intracellular calcium activates NF-κB via PKC in astrocytes

An increase in intracellular Ca^{2+} levels in asytrocytes is an early event in the activation of inflammatory gene transcription through the NF-κB and MAPK pathways (Fig. 1.2) by the high levels of extracellular glutamate, ATP, Ca^{2+} following CNS injury (Neary and Kang, 2005; Smith et al., 2005; Weisman et al., 2005; O'Riordan et al., 2006; Zeng et al., 2008b). ATP can increase Ca^{2+} influx due to activation of ionotropic (P2X) or by release from internal stores due to activation of metabotropic (P2Y) purinergic receptors (Sun et al., 1999; Zeng et al., 2008b). Activation of G protein-linked receptors by glutamate and ATP (Fig. 1.2) can activate calcium-dependent protein kinase (PKC) (Norris et al., 1994; Haak et al., 1997), an important signalling molecule in the NF-κB and MAPK pathways (Akita et al., 1990; Ballestas and Benveniste, 1995; McCarthy et al., 1998; Silberman et al., 2005; Gonczi et al., 2008). PKC activates NF-κB by phosphorylation of IκB, allowing translocation of NF-κB dimers to the nucleus. The inflammatory cytokines, IL-1β and TNF-α, activate PKC in astrocytes to increase expression of IL-6 (Norris et al., 1994), ICAM-1 (Ballestas and Benveniste, 1995; Chen et al., 2001b) and COX-2 (Huang et al., 2003). Chemokine upregulation by reactive astrocytes in response to TNF-α and IFN-γ is also regulated by PKC activation (Ludwig et al., 2005). ROS generation by NADPH oxidase in astrocytes is regulated by PKC (Abramov et al., 2005) and the novel PKC isoform, PKCη activates NF-κB to upregulate iNOS and increase NO production in astrocytes (Chen et al., 1998). PKC has also been reported to both promote (Zhu et al., 2009) and inhibit (Tang et al., 2007) AQP4 expression by reactive astrocytes.

3.02.5 Other calcium signalling pathways modulate NF-κB activity in astrocytes

Increases in intracellular free Ca^{2+} also activate the Ca^{2+}-dependent phosphatase, calcineurin, which dephosphorylates inactive cytosolic NFAT promoting its translocation to the nucleus where it forms complexes with NF-κB and other transcription factors to regulate transcription of specific inflammatory genes (Canellada et al., 2008; Perez-Ortiz et al., 2008). In lymphocytes, simultaneous Ca^{2+}- and calcineurin-dependent activation of NF-κB and NFAT is required to achieve the high rate of proliferation necessary for inflammatory responses (Baldwin, 1996; Brettingham-Moore et al., 2005a; Winslow and Crabtree, 2005). Calcineurin also regulates the calcium-dependent initiation and resolution of inflammation through its activation of NF-κB and NFAT in astrocytes (Morita et al., 2003; Norris et al., 2005; Fernandez et al., 2007a; Perez-Ortiz et al., 2008; Sama et al., 2008). In astrocytes, calcium influx induced by glutamate stimulation of calcineurin via metabotropic glutamate receptors activates the NFATc3 isoform, while ATP activation of P2Y receptors promotes activation of NFATc1 by calcineurin (Canellada et al., 2008; Perez-Ortiz et al., 2008). Glutamate-induced increases in intracellular Ca^{2+} can also activate calcium/calmodulin-dependent protein kinase (CaMKII) and iNOS to upregulate the water channel, AQP4, and promote astrocyte swelling in response to oedema following CNS injury (Gunnarson et al., 2008).

3.03 PMA and ionophore activate NF-κB via calcium signals and PKC

3.03.0 PMA is an analogue of diacylglycerol

Phorbol esters, including phorbol myristate acetate (PMA), are analogues of diacylglycerol (DAG) and can therefore activate conventional and novel PKC isoforms (Zalewski et al., 1990; Obeid et al., 1992; Quest and Bell, 1994; Newton, 1997; Medkova and Cho, 1999). Unlike DAG, phorbol esters are not readily metabolised following binding to PKC and induce chronic PKC activation (Newton, 1997). This prolonged activation accounts for the tumorigenic effects of phorbol esters and led to the identification of PKC as the intracellular effector molecule (Marquez et al., 1992; Szallasi et al., 1996; Ventura and Maioli, 2001). Phorbol esters have consequently been used

extensively in research on PKC biochemistry (Zalewski et al., 1990; James and Olson, 1992; Obeid et al., 1992; Quest and Bell, 1994; Newton, 1997; Medkova and Cho, 1999), gene expression (Ventura and Maioli, 2001; Suh et al., 2004; Brettingham-Moore et al., 2005a) tumorigenesis (Correale et al., 1997; Gopalakrishna et al., 1997; Chen et al., 2000; Esteve et al., 2002), inflammation (Genot et al., 1995; Han et al., 2003; Abramov et al., 2005; Hull et al., 2006; Hashioka et al., 2007), cytoskeletal regulation (Wilms et al., 1997; Abe and Saito, 1999; Cheng et al., 2000; Kobayashi et al., 2001) and other effects (Kermorgant et al., 2003; Michel et al., 2005; Kheifets et al., 2006) mediated by PKC. The phorbol ester research includes numerous studies on the intracellular targets of PKC, including NF-κB (Baldwin, 1996; Schwaninger et al., 1999; Huang et al., 2003; Brettingham-Moore et al., 2005a), in a variety of cell types including astrocytes (Abe and Saito, 2000; Suh et al., 2004; Amos et al., 2005; Ludwig et al., 2005; Vermeiren et al., 2005; Hull et al., 2006) and microglia (Han et al., 2003; Hashioka et al., 2007; Moon-Sook et al., 2008; Woo et al., 2008).

3.03.1 Ionophores induce intracellular calcium ion influx

As described above, calcium ions are important second messengers in intracellular signalling pathways and increases in intracellular calcium ion concentration regulate many of the cellular responses to CNS injury. Ionophores, such as ionomycin or calcium ionophore (also known as calcimycin or A23187), can transport divalent cations across cell membranes down electrochemical gradients (Kolber and Haynes, 1981; Fasolato and Pozzan, 1989; Bergling et al., 1998). Since intracellular calcium ion (Ca^{2+}) concentration is actively maintained by cells at much lower levels than extracellular levels (Carafoli, 2002; Clapham, 2007), ionophores induce Ca^{2+} influx that can initiate calcium transients under normal physiological and cell culture conditions (Venance et al., 1997; Calegari et al., 1999). The increased intracellular Ca^{2+} can promote activation of NF-κB through conventional PKC isoform activation (Nishizuka, 1988; Ahmed et al., 1991; Li et al., 2005a) and other calcium signalling pathways (Tsuboi et al., 1994; Baldwin, 1996; Abramov et al., 2005; Belcheva et al., 2005; Brettingham-Moore et al., 2005a; Silberman et al., 2005). Smooth endoplasmic reticulum calcium (SERCA) pumps and other Ca^{2+}-ATPases actively transport calcium into intracellular calcium stores that are

predominantly located in the endoplasmic reticulum and mitochondria (Kannurpatti et al., 2000; Guerini et al., 2002; Beech et al., 2003; Paschen and Mengesdorf, 2003). Blocking these Ca^{2+}-ATPase transporters with thapsigargin, can also elevate intracellular calcium ion concentrations (Lampe et al., 1995; Bergling et al., 1998; Brunig et al., 2004) leading to PKC and NF-κB activation (Pahl and Baeuerle, 1996; Paria et al., 2003).

3.03.2 Combined PMA and ionophore activation of NF-κB

Full activation of inflammatory genes requires interactions between NF-κB and other transcription factors (Chan et al., 2001; Grassl et al., 2003; Hayden and Ghosh, 2004; Chen et al., 2007; Wolter et al., 2008). Consequently, combined treatment with PMA and calcium ionophore has commonly been used to stimulate expression of NF-κB-regulated inflammatory genes in lymphocytes (Tsuboi et al., 1994; Baldwin, 1996; Schwaninger et al., 1999; Brettingham-Moore et al., 2005a; Silberman et al., 2005). Combined PMA and calcium ionophore also stimulated PKC-dependent production of IL-6 (Norris et al., 1994) and ICAM-1 expression (Ballestas and Benveniste, 1995) in astrocytes in a similar manner to the inflammatory cytokines, IL-1β and TNF-α. Furthermore, PMA and ionomycin-induced calcium influx promoted ROS generation by NADPH oxidase in astrocytes (Abramov et al., 2005) and activated NF-κB to induce COX-2 and subsequent prostaglandin production in an astroglial cell line (Rael et al., 2004a). However, the effects of these reagents are not always synergistic, with nerve growth factor production in astrocytes being promoted by PMA and inhibited by calcium ionophore- or thapsigargin-induced intracellular Ca^{2+} elevation (Jehan et al., 1995). As described above, both PKC and calcium signalling are involved in activating NF-κB to promote production of inflammatory mediators in astrocytes. Therefore, since PMA stimulates PKC and ionophore stimulates calcium signalling, NF-κB translocation to astrocyte nuclei in response to combined PMA and ionophore treatment was investigated in this Chapter as an *in vitro* model of astrocyte inflammatory activation.

3.04 Research rationale

The aim of this Chapter was to establish a model of astrocyte inflammatory activation relevant to CNS injury, as required for the following research on the possible moderation

of this activation by OECs. To investigate activation, NF-κB translocation to astrocyte nuclei *in vitro* was measured by immunocytochemistry following stimulation with PMA and calcium ionophore. Translocation of NF-κB to astrocyte nuclei was chosen as a suitable relevant measure of astrocyte activation, since NF-κB is a key transcriptional regulator of inflammatory genes including many of the inflammatory genes involved in astrogliosis. Translocation of the p65 (or RelA) subunit was measured since it is the most potent transcriptional activator of the NF-κB family (Baeuerle and Henkel, 1994; Baldwin, 1996; Wang and Baldwin, 1998; Madrid et al., 2001; Ridder and Schwaninger, 2009) and most NF-κB activity in response to CNS injury involves the p50/p65 dimers (Schneider et al., 1999; Hang et al., 2006; Ridder and Schwaninger, 2009). The combined treatment with PMA and calcium ionophore is an established, well-characterised treatment that induces NF-κB translocation via activation of the PKC and calcium signalling pathways, both of which regulate astrocyte responses to CNS injury. GFAP expression was measured in response to stimulation with PMA and calcium ionophore since it is upregulated by reactive astrocytes following CNS injury.

3.05 Specific aims

1. Investigate PMA and calcium ionophore stimulation of p65 NF-κB translocation to astrocyte nuclei as a measure of inflammatory activation.

2. Investigate GFAP expression in astrocytes following stimulation with PMA and calcium ionophore.

3.1 Materials and Methods

3.10 Quantitative analysis of astrocyte activation using NF-κB immunoreactivity

Sets of 3 images showing immunostaining for p65 NF-κB (Fig. 3.1C), GFAP (Fig. 3.1E) and Hoechst blue nuclear staining (Fig. 3.1A) were taken at the same exposure (for each fluorophore) and magnification (200x). Image locations on the coverslip were selected randomly, commencing with a central location and separated by two to three microscope fields. Image sets were then merged using Adobe Photoshop© (Fig. 3.1F). Images containing any contaminating non-GFAP positive cells were excluded from analysis to

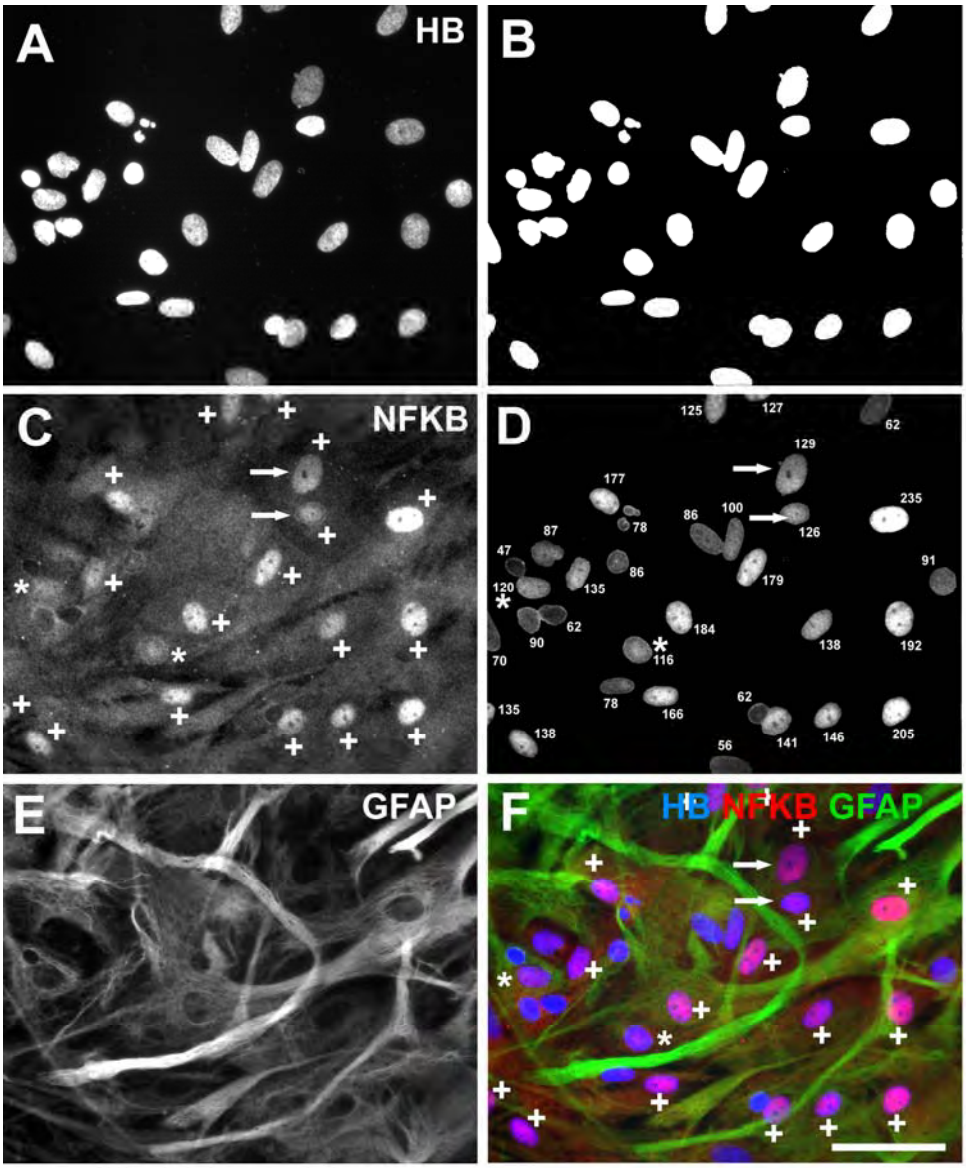

Figure 3.1 Quantitative analysis of astrocyte activation. GFAP immunoreactivity (E, green in F) identified astrocytes while NF-κB immunoreactivity (C, red in F) identified activated astrocytes. Nuclei were counterstained with Hoechst blue (HB; A, blue in F. Images of Hoechst blue-stained astrocyte nuclei (A) were batch processed with HCA-Vision© to generate images of nuclei that were thresholded using Adobe Photoshop© (B). The thresholded nuclear images (B) masked cytoplasmic immunoreactivity when blended with the corresponding image of astrocyte NF-κB immunoreactivity (C) in Adobe Photoshop©. This masking process resulted in images showing only nuclear NF-κB immunoreactivity (D), which were again batch processed with HCA-Vision© to generate result images with accompanying intensity measurements for each nucleus (numbers in D) and a count of total cells/image. Astrocytes having nuclei with mean intensity above an arbitrary level (>125) were deemed activated (plus signs in C and F) for calculating the mean percentage of activated astrocytes for each image. Asterisks and arrows (C, D and F) respectively indicate nuclei just below (intensity 120 and 116 in D) and above (intensity 126 and 129 in D) this arbitrary intensity level used to measure activation. Scale bar is 50 μm.

assure the homogeneity of cultures for treatment comparisons and to avoid any unknown confounding effects of interactions with other unidentified cell types. In addition, the automated quantitation method described below would not have distinguished between astrocytes and other cell types. The nuclear staining images were batch processed using HCA-Vision© software (CSIRO, North Ryde, Australia) to generate thresholded images of nuclear regions that were used as masks for merging with the NF-κB immunostaining images (Fig. 3.1). This produced images showing NF-κB staining only in the nuclear regions, which was not altered by the masking process, allowing them to be batch processed using HCA-Vision©. HCA-Vision© could not batch process the whole cell NF-κB images (Fig. 3.1C) prior to the masking process, because it could not identify individual cells or separate nuclear regions from cytoplasmic regions in these images. The batch processing allowed simultaneous processing of hundreds of images to generate Excel files listing nuclear NF-κB immunoreactivity intensity measurements for every astrocyte in the images. Astrocytes having nuclei with mean NF-κB immunoreactivity intensity above an arbitrary level (>125) were deemed activated and used to calculate the mean percentage of activated astrocytes for each image. This choice of minimum intensity level ensured that astrocytes were scored as activated only when their nuclear NF-κB immunoreactivity was visibly more intense than the cytoplasmic NF-κB immunoreactivity (plus signs in Fig. 3.1C, D and F), to preclude the possibility of false positives due to overlapping stronger cytoplasmic NF-κB immunoreactivity in quiescent astrocytes (e.g. arrows, Fig. 3.2A-H). This method may have resulted in some underestimation of activation due to false negatives. This possible underestimation was considered preferable to an overestimation, with some error being unavoidable due to the variability of both cytoplasmic and nuclear NF-κB immunoreactivity intensity. At least 8 images showing ~120 cells/image from 2-3 cell cultures from the pooled tissue of 2-4 neonatal rats on separate coverslips were analysed to generate means for each treatment group. Data were analysed for significant differences between treatment group means by ANOVA and post-hoc Tukey tests.

3.11 Comparisons of NF-κB translocation

Astrocytes were cultured on 18mm diameter coverslips in 12-well culture plates, as described previously. Fluorescence microscope images of immunostained astrocytes were used for comparisons of nuclear NF-κB immunoreactivity intensity in astrocytes that were untreated or stimulated with the following reagents:

1. phorbol-12-myristate-13-acetate (PMA; Calbiochem)

2. calcium ionophore (antibiotic A23187 or calcimycin, free acid from Streptomyces chartreusensis, Calbiochem)

3. thapsigargin (Alamone Labs)

Astrocytes were usually incubated in serum-free DMEM for 24 hours prior to and during experiments. Comparisons of astrocyte activation were also made using cultures incubated in serum- and calcium-free DMEM or serum- and calcium-free DMEM supplemented with 200μM EDTA.

3.12 Comparisons of GFAP expression

3.12.0 GFAP immunoreactivity and morphology

Following 24 hours of treatment of astrocyte cultures with 1μM ionophore, immunocytochemistry was conducted and the intensity of GFAP immunoreactivity was measured within astrocytes using the Adobe Photoshop© selection and histogram functions. The area of the same astrocytes revealed by the GFAP immunoreactivity was then measured using ImageJ to enable comparison of astrocyte area relative to the intensity of GFAP immunoreactivity.

3.12.1 Western blotting

Western blotting was used to compare GFAP expression in untreated astrocytes and astrocytes treated with PMA and ionophore for 48 hours, to allow time for protein expression changes in response to activation, in:

1. serum-free DMEM

2. serum- and calcium-free DMEM

3. serum- and calcium-free DMEM supplemented with 5mM calcium chloride.

3.2 Results

3.20 PMA and ionophore activate astrocytes

The relative effects of 20ng/mL PMA, 500nM ionophore and combined PMA/ionophore on astrocyte activation were compared by measuring the intensity of p65 NF-κB nuclear immunoreactivity. Combined PMA/ionophore was the most effective treatment for activating astrocytes as illustrated by the shift from cytoplasm to nucleus of the predominant location of the more intense NF-κB immunoreactivity (Fig. 3.2A-H). Prior to PMA and ionophore treatment (Fig. 3.2A, B) only about 5% of astrocytes were activated (Fig. 3.2E). PMA and ionophore both rapidly activated astrocytes with large significant increases in the percentage of activated astrocytes ($p < 0.001$) within 30 minutes of treatment. The maximum response to PMA occurred after 30 minutes of treatment with activation of 25.45±3.14% of astrocytes. Ionophore was a stronger activator than PMA, inducing activation of significantly more astrocytes at 30 minutes (37.21±3.09%; $p < 0.05$) and 1 hour (38.39±3.63%; $p < 0.001$). Combining the PMA and ionophore treatments induced an additional significant increase in activated astrocytes to a maximum by 1 hour (55.7±3.1 %; $p < 0.01$). By 2 hours, the percentage of activated astrocytes had diminished to near basal untreated levels ($p > 0.05$) and remained unchanged at 3, 4 and 24 hours (data not shown).

3.21 Optimisation of PMA/ionophore activation of astrocytes

3.21.0 Ionophore concentration

To determine the optimal ionophore concentration for astrocyte activation, NF-κB translocation was compared for 125nM, 250nM, 500nM and 1μM ionophore combined with 20ng/mL PMA (Fig. 3.3). The percentage of activated astrocytes was not significantly different across the range of tested ionophore concentrations ($p > 0.05$),

however after only 1 hour of treatment with 1μM ionophore (Fig. 3.3D) there appeared to be some apoptotic astrocytes with condensed nuclei (arrows in Fig. 3.3D) and condensed cytoplasm, resulting in more intense GFAP immunoreactivity. This increase in immunoreactivity was too soon for GFAP upregulation and was presumably due to the morphological alteration. After 24 hours at this 1μM dose of ionophore, about half the astrocytes appeared apoptotic, with blebby morphologies, partial detachment from the substrate and condensed nuclei (Fig. 3.3F-G). The astrocytes apparently displaying condensed cytoplasm had much higher intensity immunostaining than the astrocytes with flattened morphologies and normal nuclei. Comparison of the area of astrocytes displaying high (150.79±3.82) or low (68.63±7.07) intensity GFAP immunoreactivity showed that the more intense GFAP immunoreactivity was associated with astrocytes of significantly smaller mean area ($p < 0.001$), again implying that the increased intensity was due to the morphological alterations associated with apoptosis rather than an upregulation of GFAP expression. Ionophore was used at 500nM or less in later experiments on astrocyte activation to minimise possible confounding effects due to the induction of apoptosis.

3.21.1 PMA concentration

To determine the optimal PMA concentration for astrocyte activation, NF-κB translocation was compared for 20ng/mL, 100ng/mL and 200ng/mL PMA combined with 125nM ionophore (Fig. 3.4). The percentage of activated astrocytes was not significantly different across the range of tested PMA concentrations ($p > 0.05$). PMA had already been shown to contribute significantly less to astrocyte activation than ionophore and was therefore used at the minimum concentration tested of 20ng/mL for remaining experiments to minimise possible unknown confounding effects.

3.22 Calcium-dependence of NF-κB-mediated astrocyte activation

3.22.0 Astrocyte activation in calcium-free medium

Since ionophore was responsible for the major proportion of PMA/ionophore-induced astrocyte activation, NF-κB translocation in astrocytes was further investigated to determine whether the activation was dependent on calcium ions. Surprisingly, 1 hour

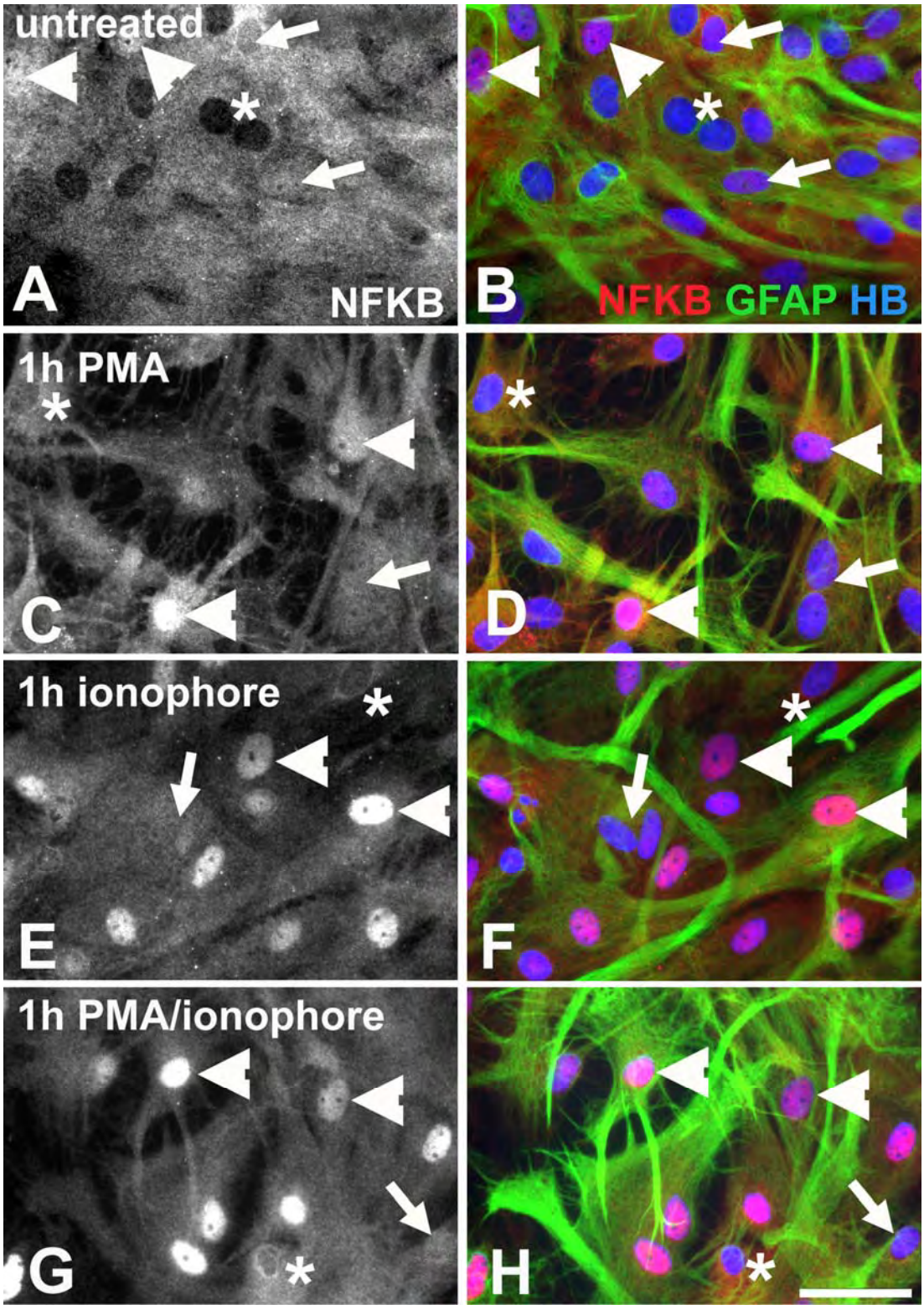
untreated
A
NFKB
B
NFKB GFAP HB
1h PMA
C
D
1h ionophore
E
F
1h PMA/ionophore
G
H

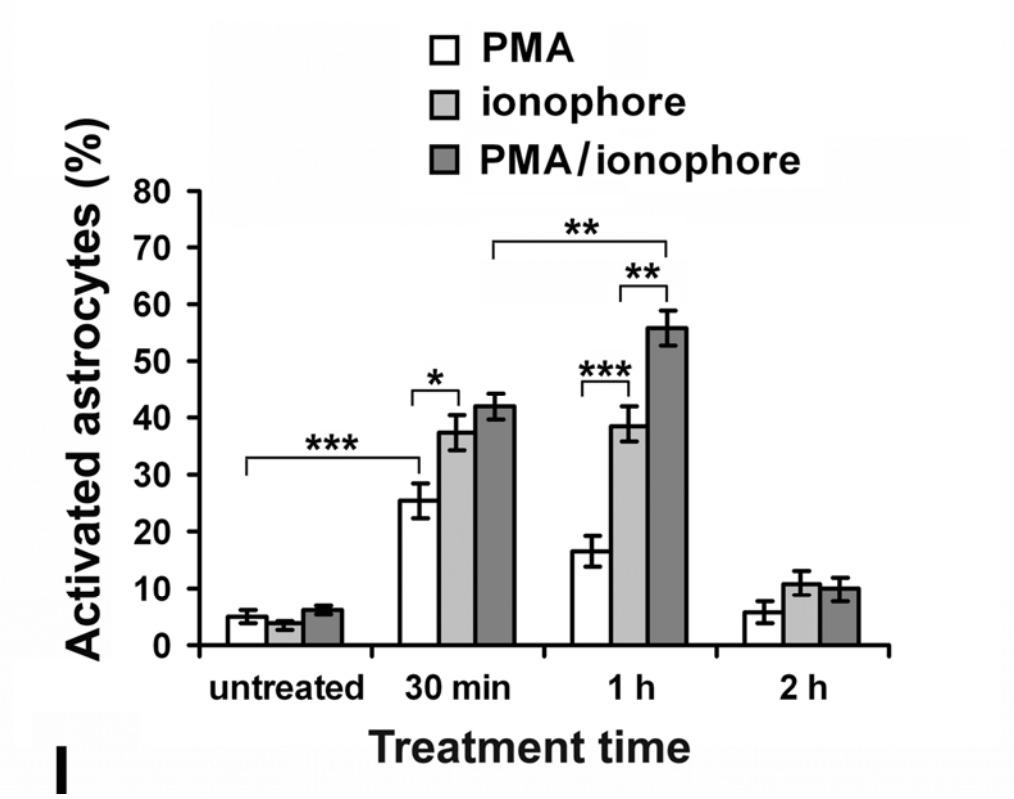

Figure 3.2 PMA and ionophore activation of astrocytes. Astrocytes were treated with either 20ng/mL PMA (C, D), 500nM ionophore (E, F) or both (PMA/ionophore; G, H) for 30 minutes, 1 hour or 2 hours, with untreated astrocytes (A, B) providing control comparisons. Immunostaining for GFAP (green) was used to identify astrocytes, NF-κB (red) to identify activated astrocytes and nuclei were counterstained with Hoechst blue (HB). Images show NF-κB (A, C, E, G) or combined immunoreactivity (B, D, F, H) after 1 hour. NF-κB immunoreactivity was predominantly cytoplasmic in untreated astrocytes (A, B) and translocated to nuclei following activation with PMA and ionophore (C-H). NF-κB translocation was apparent from the more intense nuclear than cytoplasmic NF-κB immunoreactivity in the activated astrocytes (C, E, G) compared with untreated astrocytes (A). Astrocytes scored as activated had mean nuclear NF-κB immunoreactivity intensity noticeably above the background cytoplasmic immunoreactivity (e.g. arrow-heads in A-H). Due to variations in the position of cells relative to the image plane of focus, astrocytes deemed quiescent included those with nuclei where NF-κB was clearly absent (e.g. asterisks in A-H) and others where nuclear regions (e.g. arrows in A-H) had staining intensity similar to cytoplasmic levels and may have represented overlapping cytoplasmic staining. Scale bar is 50 μm. I: Quantitative analysis of astrocyte activation by PMA and ionophore. Separate or combined treatment with PMA and ionophore induced significant increases in the percentage of activated astrocytes ($p < 0.001$) within 30 minutes. Activation was significantly greater in the presence of ionophore than for PMA alone at both 30 minutes ($p < 0.05$) and 1 hour ($p < 0.001$) after treatment. The maximum response to separate PMA or ionophore treatment occurred by 30 minutes whereas with combined PMA/ionophore there was a further significant increase ($p < 0.01$) by 1 hour. By 2 hours after treatments the percentage of activated astrocytes had diminished to near basal untreated levels ($p > 0.05$). Data were analysed by 2-way ANOVA and post-hoc Tukey's multiple comparison test. Results are means ± SEM, n = 15. Asterisks denote significant differences: * $p < 0.05$, ** $p < 0.01$, *** $p < 0.001$.

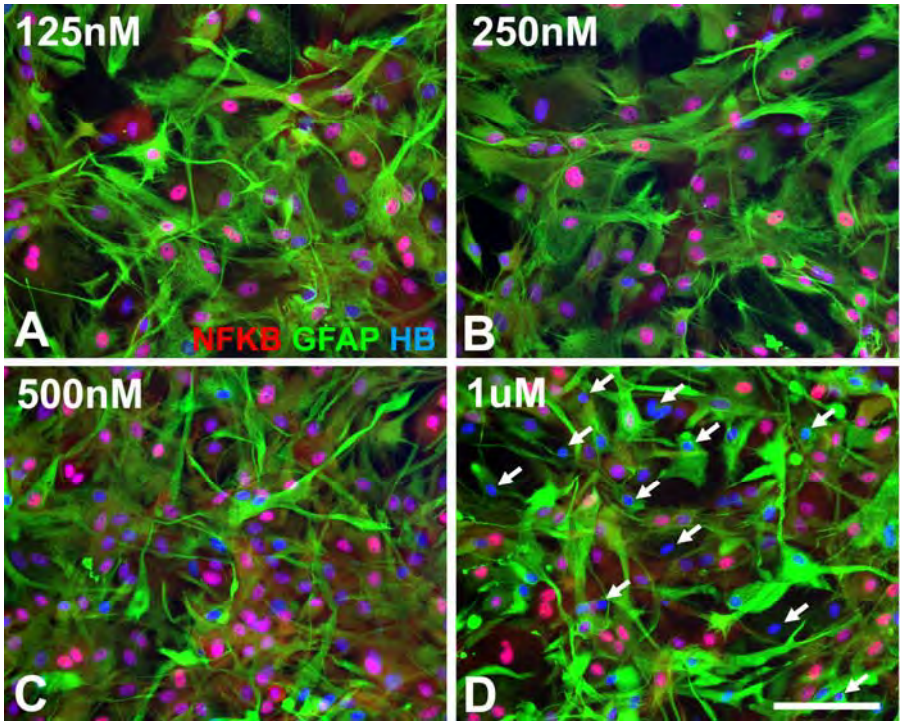
125nM
250nM
A
NFKB GFAP HB
B
500nM
1uM
C
D

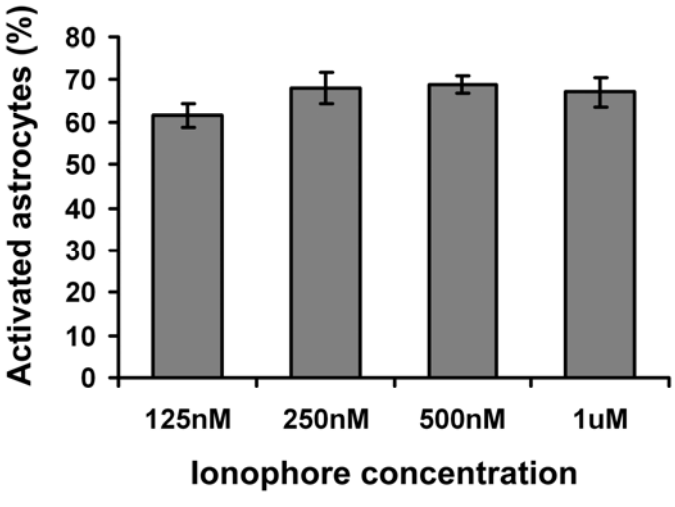
Activated astrocytes (%)
80
70
60
50
40
30
20
10
0
125nM
250nM
500nM
1uM
Ionophore concentration

E

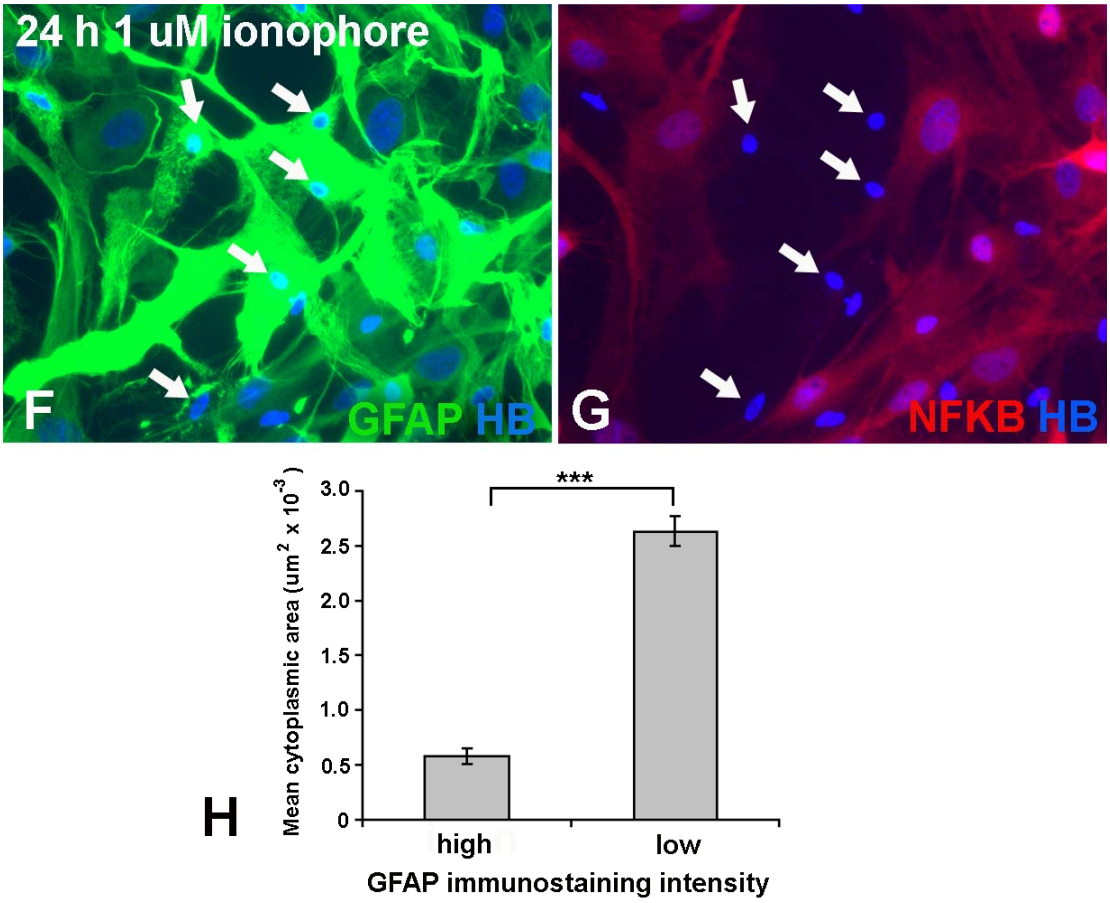

Figure 3.3 Ionophore dose and astrocyte activation. Astrocytes were treated for 1 hour with 20ng/mL PMA combined with 125nM (A), 250nM (B), 500nM (C) or 1μM (D) ionophore. A-D: Immunostaining for GFAP (green) was used to identify astrocytes and NF-κB (red) to identify activated astrocytes. Nuclei were counterstained with Hoechst blue (HB). Similar astrocyte activation appeared to be induced across the range of ionophore concentrations. 1μM ionophore appeared to induce some apoptosis as indicated by bright GFAP immunoreactivity suggesting cytoplasmic and nuclear condensation (arrows in D). Scale bar is 100 μm. E: Quantitative analysis of astrocyte activation. The percentage of astrocytes activated by PMA/ionophore was not significantly altered by varying the ionophore dose from 125nM to 1μM ($p > 0.05$). Data were analysed by ANOVA and post-hoc Tukey's multiple comparison test. Results are means ± SEM, n = 8. F-G: After 24 hours of treatment with 1μM ionophore about 50% of astrocytes appeared to be apoptotic, displaying condensed nuclei (arrows), intense GFAP immunostaining (A) and faint or absent NF-κB immunostaining (G). H: Quantitative comparison of cell area for astrocytes displaying high or low intensity GFAP immunostaining following 24 hours of treatment with 1μM ionophore. Astrocytes with high intensity GFAP immunostaining presented a significantly smaller mean area on the coverslip/image plane. Data were analysed by ANOVA. Results are means ± SEM, n = 50. Asterisks denote significant differences: *** $p < 0.001$.

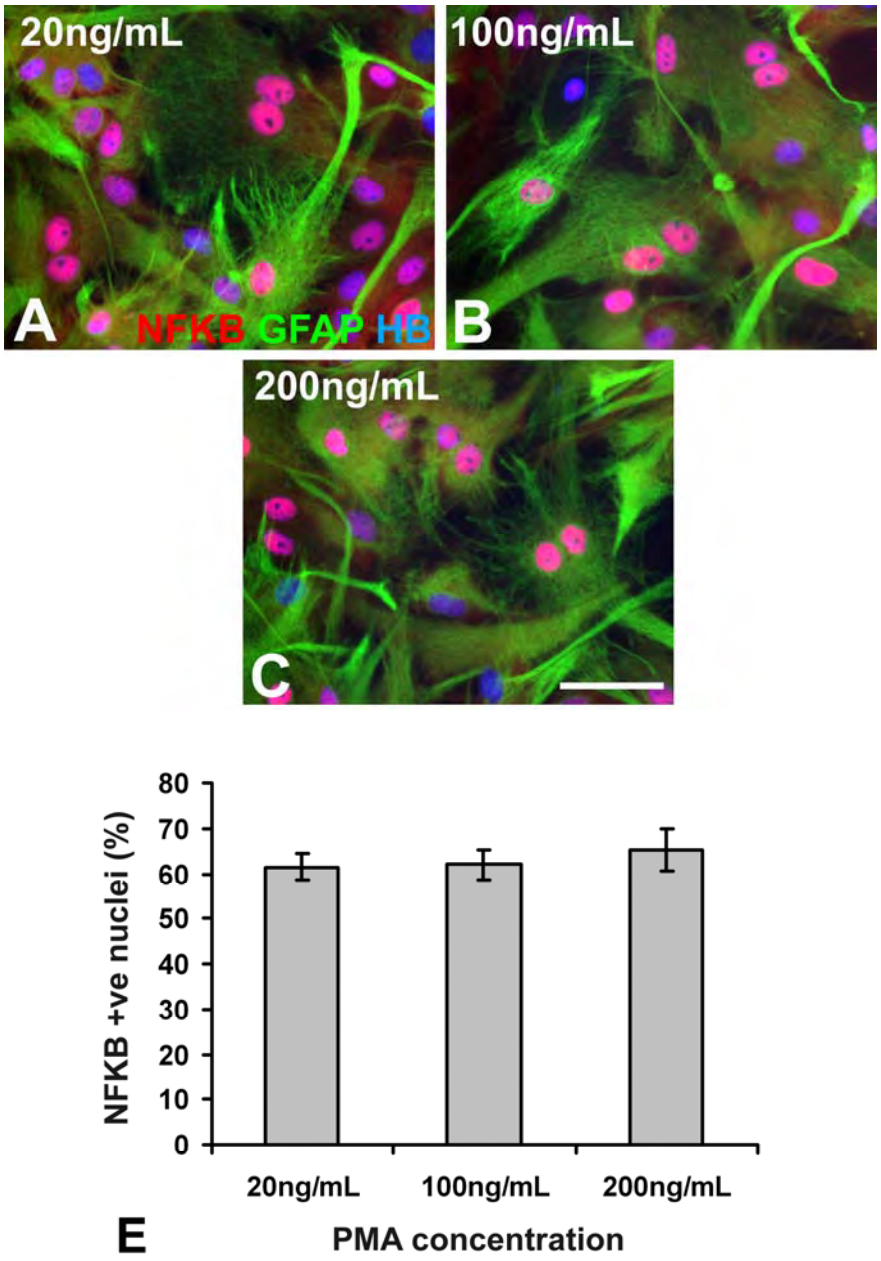

Figure 3.4 PMA dose and astrocyte activation. Astrocytes were treated for 1 hour with 125nM ionophore combined with 20ng/mL (A), 100ng/mL (B) or 200ng/mL (C) PMA. A-C: Immunostaining for GFAP (green) was used to identify astrocytes and NF-κB (red) to identify activated astrocytes. Nuclei were counterstained with Hoechst blue (HB). Similar astrocyte activation appeared to be induced across the range of PMA concentrations. Scale bar is 50 μm. E: Quantitative analysis of astrocyte activation. The percentage of astrocytes activated by PMA/ionophore was not significantly altered by varying the PMA dose from 20ng/mL to 200ng/mL ($p > 0.05$). Data were analysed by ANOVA and post-hoc Tukey's multiple comparison test. Results are means ± SEM, $n = 8$.

after a change of culture medium from DMEM to calcium-free DMEM (Fig. 3.5D, H), NF-κB had translocated to astrocyte nuclei indicating significant activation (62.10±4.78%; $p < 0.001$), similar to that induced by 1 hour of PMA/ionophore treatment in DMEM (Fig. 3.5C, H). Combining the change to calcium-free medium with PMA/ionophore treatment induced a further significant increase in astrocyte activation (72.86±2.94%; $p < 0.05$; Fig. 3.5E, H). However, when astrocytes were pre-incubated for 4 hours in calcium-free DMEM supplemented with 200μM EDTA, to chelate any calcium ions that may have been released from astrocyte intracellular stores, there was significantly less astrocyte activation 1 hour after a subsequent change of this EDTA-supplemented calcium-free DMEM (1.24±0.81%; $p < 0.05$; Fig. 3.5F, H) compared with a change of normal DMEM (6.28±0.92%; Fig. 3.5B, H), which contains 1.8mM calcium chloride. In addition, significantly less astrocyte activation was induced by PMA/ionophore when combined with the EDTA-supplemented calcium-free DMEM following the 4 hour pre-incubation (14.1±1.87%; $p < 0.001$; Fig. 3.5G, H). The total of 5 hours incubation in calcium-free conditions resulted in a noticeable change in astrocyte morphology to a more elongated bipolar form with sparse GFAP fibres (Fig. 3.5F, G).

3.22.1 Thapsigargin activates astrocytes

As described above, intracellular Ca^{2+} can also be increased by blocking intracellular storage calcium pumps with thapsigargin. Therefore, the effect of thapsigargin on activation was compared for astrocytes in DMEM and EDTA-supplemented calcium-free DMEM (Fig. 3.6). 1μM thapsigargin induced significant activation of astrocytes in DMEM (60.85±2.77%; $p < 0.001$; Fig. 3.6B, F) that was not significantly different from the activation induced by PMA/ionophore ($p > 0.05$; Fig. 3.6D, F). However, in calcium-free medium, thapsigargin only increased activation (6.48±1.04%; $p < 0.05$; Fig. 3.6C, F) to the basal levels of untreated astrocytes in DMEM. In the calcium-free conditions, PMA/ionophore activated significantly more astrocytes (14.1±1.87%) than thapsigargin ($p < 0.05$) and combining the treatments induced a further significant additive effect (22.66±2.11%; $p < 0.05$; Fig. 3.6E, F), however the activation in both cases remained significantly less than for similarly treated astrocytes in DMEM ($p < 0.001$; Fig. 3.6F). The elongated bipolar astrocyte morphology with sparse GFAP fibres induced by

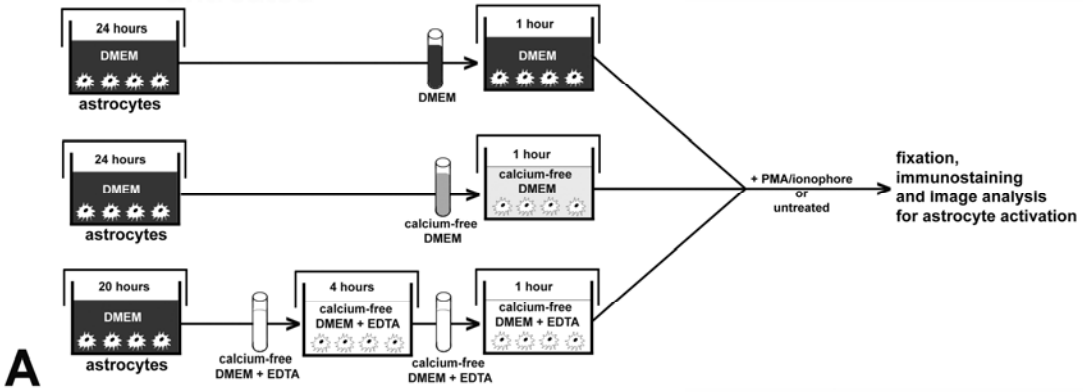
24 hours
DMEM
astrocytes
DMEM
1 hour
DMEM
24 hours
DMEM
astrocytes
calcium-free
DMEM
1 hour
calcium-free
DMEM
20 hours
DMEM
astrocytes
calcium-free
DMEM + EDTA
4 hours
calcium-free
DMEM + EDTA
calcium-free
DMEM + EDTA
1 hour
calcium-free
DMEM + EDTA
+ PMA/ionophore
or
untreated
fixation,
immunostaining
and image analysis
for astrocyte activation
A

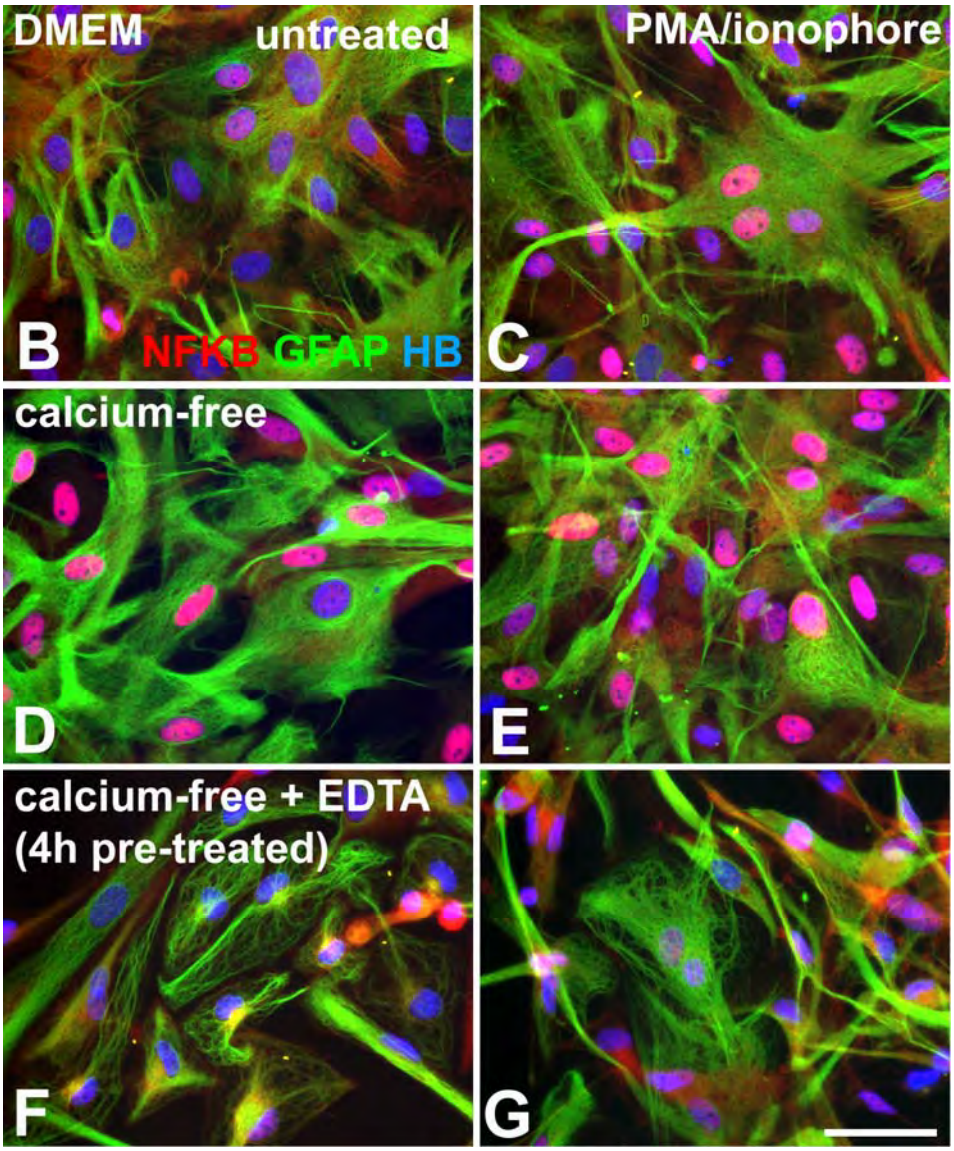
DMEM
untreated
B
NFKB GFAP HB
PMA/ionophore
C
calcium-free
D
E
calcium-free + EDTA
(4h pre-treated)
F
G

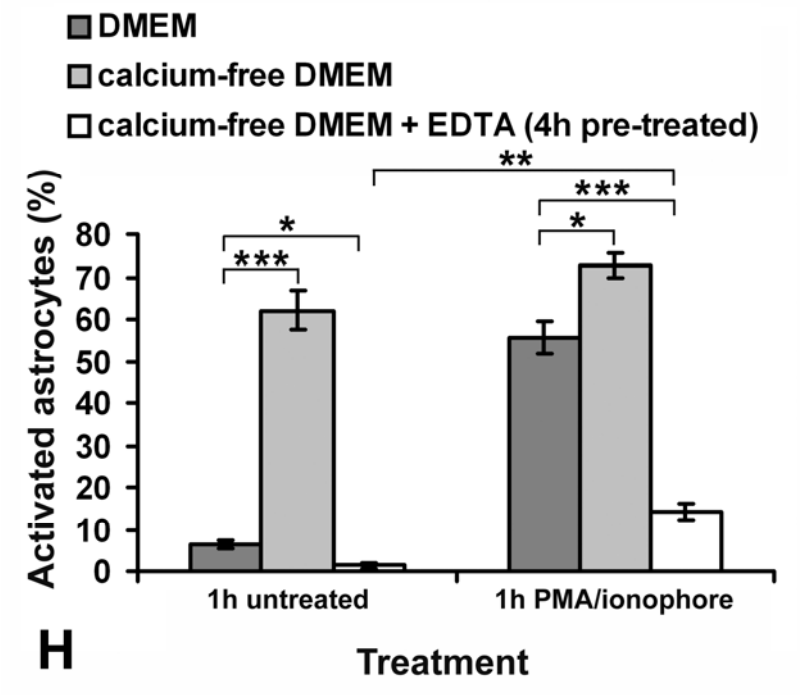

Figure 3.5 Calcium-dependence of NF-κB mediated astrocyte activation. A: Activation was compared for astrocytes treated for 1 hour with 20ng/mL PMA/500nM ionophore in DMEM, calcium-free DMEM or in calcium-free DMEM supplemented with 200μM EDTA after 4 hours pre-incubation in this medium, with untreated astrocytes 1 hour after a change of DMEM or calcium-free DMEM with EDTA or from DMEM to calcium-free DMEM for comparison controls. B-G: Immunostaining for GFAP (green) was used to identify astrocytes and NF-κB (red) to identify activated astrocytes. Nuclei were counterstained with Hoechst blue (HB). A change from DMEM (B) to calcium-free medium induced astrocyte activation (D) similarly to treatment with PMA/ionophore (C, E). Incubation of astrocytes in calcium-free medium supplemented with the chelating agent EDTA resulted in more elongated astrocyte morphologies with only sparse GFAP fibres (F, G). In these conditions astrocytes were not activated by medium change (F) and only a low percentage were activated by PMA/ionophore (G). Scale bar is 50 μm. H: Quantitative analysis of astrocyte activation. Incubation in calcium-free DMEM induced a significant increase in astrocyte activation ($p < 0.001$) that was not significantly different ($p > 0.05$) from the increase induced by PMA/ionophore for astrocytes in DMEM. However, compared to untreated astrocytes in DMEM, there were significantly less activated astrocytes 1 hour after a change to fresh calcium-free DMEM supplemented with EDTA following 4 hours pre-incubation in the same medium conditions ($p < 0.05$). Although PMA/ionophore induced a significant increase in activation for the pre-incubated astrocytes in EDTA-supplemented calcium-free DMEM ($p < 0.01$), the increase was significantly less than for astrocytes in DMEM ($p < 0.001$). In contrast there were significantly more activated astrocytes after PMA/ionophore treatment in calcium-free DMEM without pre-incubation than for astrocytes in DMEM ($p < 0.05$). Data were analysed by 2-way ANOVA and post-hoc Tukey's multiple comparison test. Results are means ± SEM, $n = 8$. Asterisks denote significant differences: * $p < 0.05$, ** $p < 0.01$, *** $p < 0.001$.

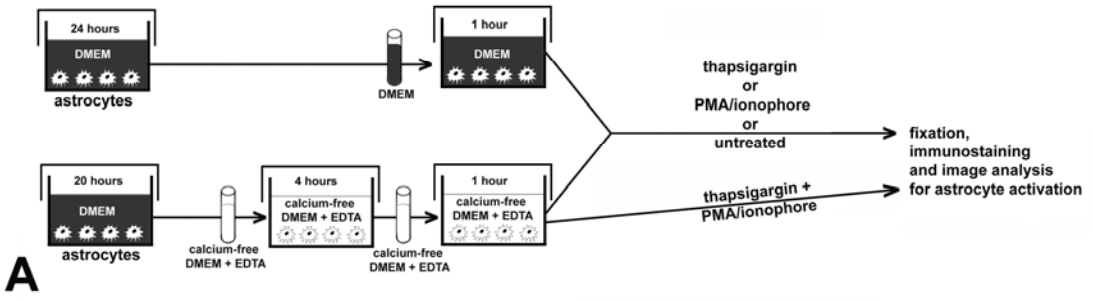
24 hours
DMEM
astrocytes
DMEM
1 hour
DMEM
20 hours
DMEM
astrocytes
calcium-free
DMEM + EDTA
4 hours
calcium-free
DMEM + EDTA
calcium-free
DMEM + EDTA
1 hour
calcium-free
DMEM + EDTA
thapsigargin
or
PMA/ionophore
or
untreated
thapsigargin +
PMA/ionophore
fixation,
immunostaining
and image analysis
for astrocyte activation
A

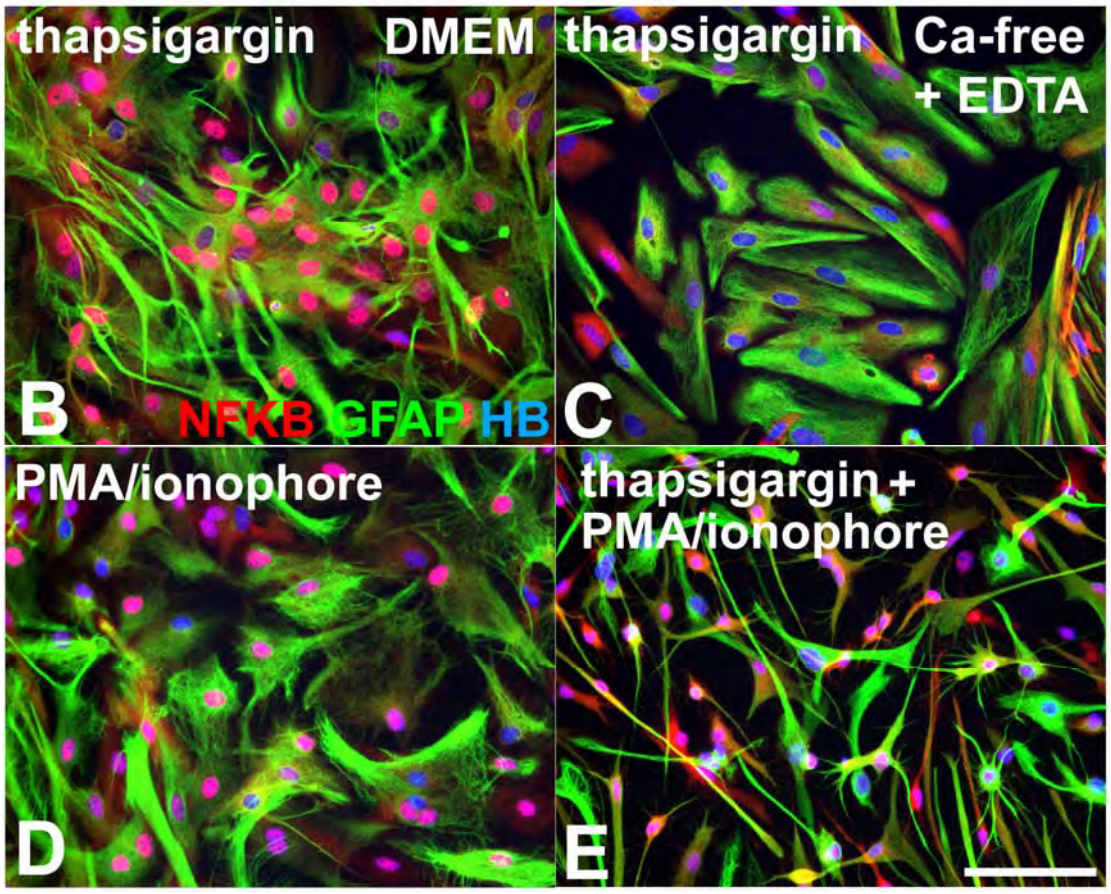
thapsigargin
DMEM
B
NFKB GFAP HB
thapsigargin
Ca-free
+ EDTA
C
PMA/ionophore
D
thapsigargin +
PMA/ionophore
E

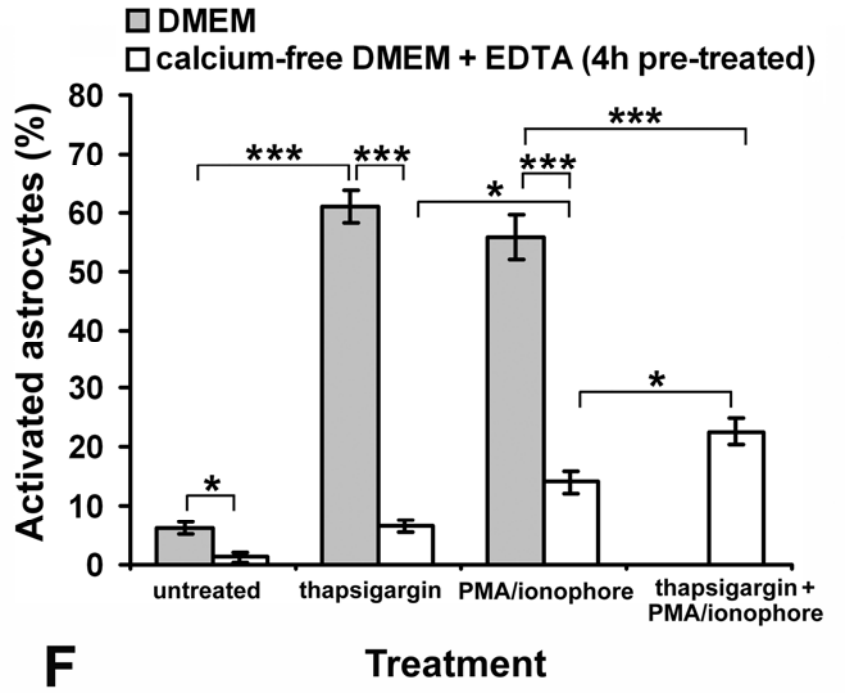

Figure 3.6 Thapsigargin activates astrocytes. A: Activation was compared for astrocytes treated for 1 hour with PMA/ionophore and/or the specific internal store Ca^{2+}-ATPase blocker, thapsigargin (1μM) in DMEM or calcium-free DMEM supplemented with 200μM EDTA (after 4 hours pre-incubation in this medium) with untreated astrocytes in the same media as comparison controls. B-E: Immunostaining for GFAP (green) was used to identify astrocytes and NF-κB (red) to identify activated astrocytes. Nuclei were counterstained with Hoechst blue (HB). Thapsigargin activated astrocytes in DMEM (B) to a similar extent as PMA/ionophore (D) but not when astrocytes were incubated in calcium-free conditions (C). Calcium-free medium induced an elongated astrocyte morphology with sparse GFAP fibres (Figs. 3.4F, 3.5A) that was not altered by thapsigargin treatment (C). However when thapsigargin was combined with PMA/ionophore, astrocytes adopted a spindly morphology with compressed GFAP fibres and some were activated (E). Scale bar is 50 μm. F: Quantitative analysis of astrocyte activation. Thapsigargin induced significant activation of astrocytes in DMEM ($p < 0.001$) that was not significantly different from the activation induced by PMA/ionophore ($p > 0.05$). However, for astrocytes in calcium-free medium, thapsigargin only increased activation ($p < 0.05$) to the basal levels of untreated astrocytes in DMEM. Although PMA/ionophore activated significantly more astrocytes than thapsigargin ($p < 0.05$) and combining the treatments induced a further significant additive effect ($p < 0.05$) in the calcium-free conditions, the activation remained significantly less than for similarly treated astrocytes in DMEM ($p < 0.001$). Data were analysed by 2-way ANOVA and post-hoc Tukey's multiple comparison test. Results are means ± SEM, n = 8. Asterisks denote significant differences: * $p < 0.05$, ** $p < 0.01$, *** $p < 0.001$.

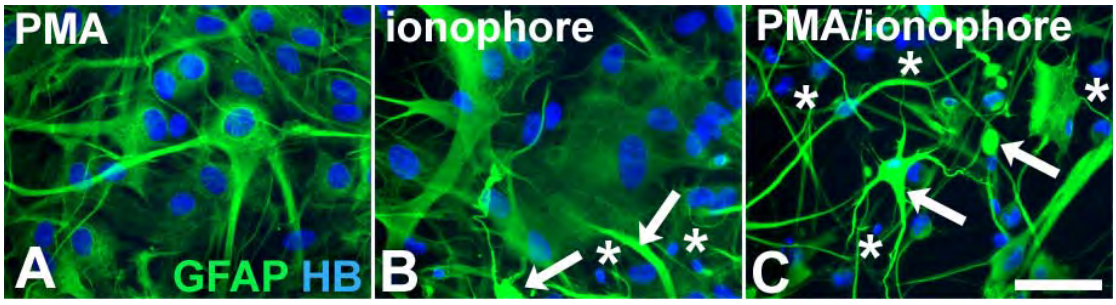
PMA
ionophore
PMA/ionophore
A
GFAP HB
B
C

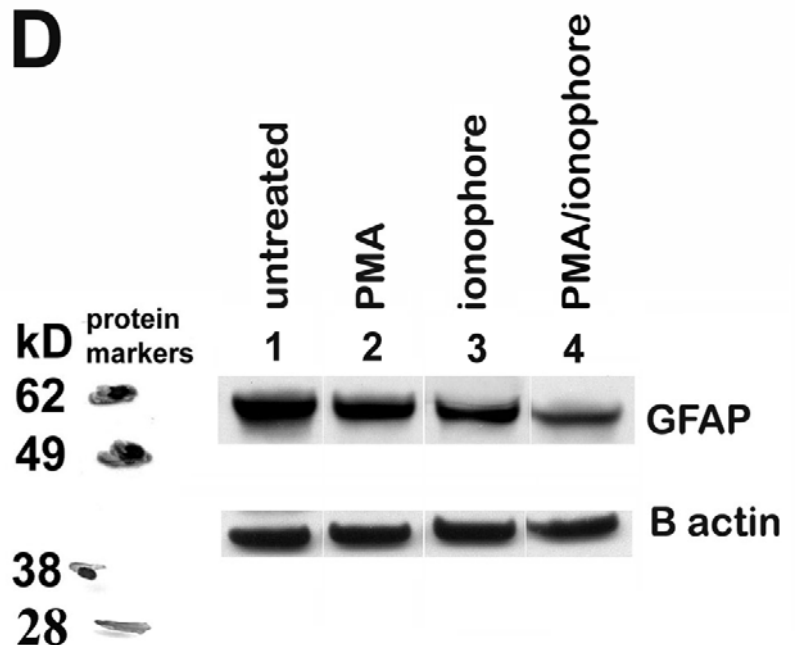
D
untreated
PMA
ionophore
PMA/ionophore
kD
protein markers
1
2
3
4
62
49
38
28
GFAP
B actin

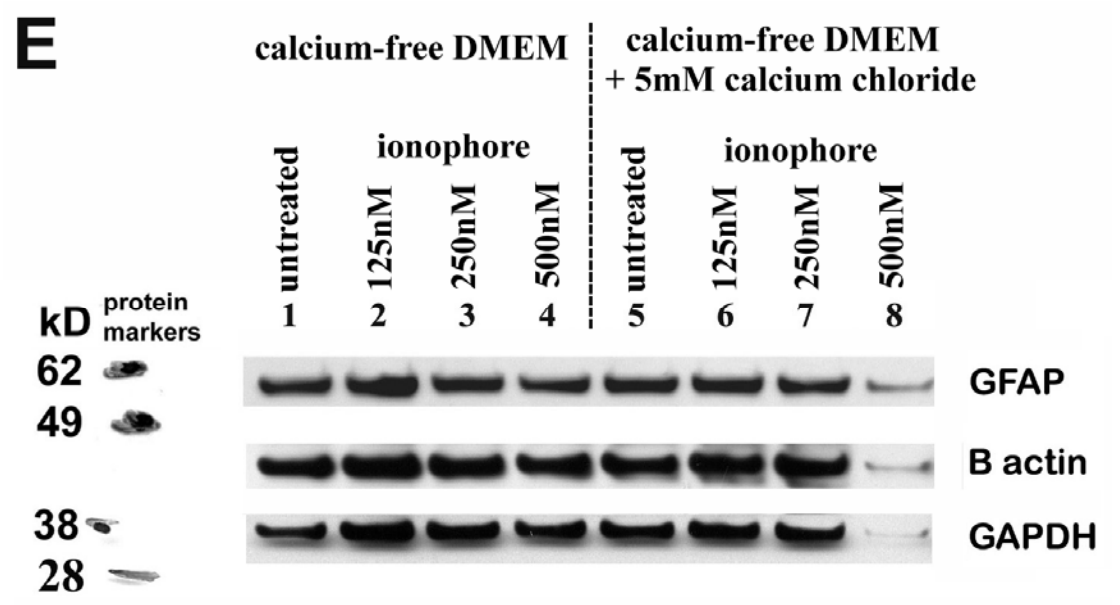

Figure 3.7 Calcium-dependent effects of PMA/ionophore on astrocyte morphology and GFAP expression. A: PMA induced some stellation of astrocytes but did not alter GFAP immunoreactivity. B: Ionophore induced some apoptosis of astrocytes that was associated with decreased intensity of GFAP immunoreactivity in relatively intact cells and more intense immunoreactivity in detached cells displaying GFAP depolymerisation (arrows) and cytoplasmic condensation (asterisks). C: The apoptosis and depolymerisation were accentuated by combined PMA/ionophore treatment. Scale bar is 50μm. D: GFAP expression was analysed by Western blot for untreated astrocytes (lane 1) and astrocytes treated for 48 hours with 20ng/mL PMA (lane 2), 500nM ionophore (lane 3) and combined PMA/ionophore (lane 4). Protein bands were obtained at about 55kDa with the anti-GFAP primary antibody. GFAP levels appeared to be highest for untreated astrocytes with slightly lower expression levels following PMA treatment. GFAP levels decreased a little further in ionophore-treated astrocytes and were noticeably much lower following combined PMA/ionophore treatment. Equal quantities of total protein were loaded for each lane as confirmed by similar intensity immunoreactivity in each lane for the β actin (~ 42kDa) loading control. E: Calcium and ionophore dose dependence of GFAP expression. GFAP expression was analysed by Western blot for untreated astrocytes in calcium-free DMEM (lane 1) or calcium-free DMEM with a 5mM addition of calcium chloride (lane 5), astrocytes treated with 250nM ionophore in calcium-free DMEM (lane 2) or calcium-free DMEM with 5mM calcium chloride (lane 6), astrocytes treated with 500nM ionophore in calcium-free DMEM (lane 3) or calcium-free DMEM with 5mM calcium chloride (lane 7) and astrocytes treated with 1μM ionophore in calcium-free DMEM (lane 4) or calcium-free DMEM with 5mM calcium chloride (lane 8). All treatments were for 48 hours. The blot image is representative of 4 blots performed on separate samples. There was little difference in GFAP expression for untreated astrocytes in DMEM with 5mM calcium chloride (lane 5) and astrocytes treated with 250nM or 500nM ionophore in either medium condition (lanes 2-3 and 6-7). There was possibly slightly lower GFAP expression for untreated astrocytes (lane 1) and 1μM ionophore treated astrocytes (lane 4) in calcium-free DMEM and noticeably much less GFAP expression for astrocytes treated with 1μM ionophore in calcium-free DMEM with 5mM calcium chloride (lane 8). All differences between lanes seen for the GFAP bands corresponded with similar differences for the bands for β actin and GAPDH loading controls.

calcium-free medium conditions (Figs. 3.5) was not altered by thapsigargin treatment (Fig. 3.6C), however combining thapsigargin with PMA/ionophore in calcium-free medium induced an even more elongated, spindly astrocyte morphology with compression of the sparse GFAP fibres (Fig. 3.6E).

3.23 PMA/ionophore decreases GFAP levels

PMA alone induced some stellation of astrocytes but did not appreciably affect GFAP immunoreactivity (Fig. 3.7A) or expression levels (Fig. 3.7D lane 2). Ionophore appeared to induce dose-dependent detachment from the substrate and apoptosis of astrocytes (Figs. 3.3 and 3.7B). This effect was accentuated by combined PMA/ionophore treatment (Fig. 3.7C). These results were supported by Western blotting, with lower GFAP expression being detected following treatment with 500nM ionophore (Fig. 3.7D lane 3). Following combined PMA/ionophore treatment (Fig. 3.7D lane 4) much lower levels of GFAP were detected, consistent with the appearance of apoptotic cells showing condensed nuclei and protein degradation indicated by patchy, faint or absent immunoreactivity for GFAP in the immunocytochemistry images (Fig. 3.7C). Western blotting showed that the decreased levels of GFAP were dependent on Ca^{2+} influx since it was inhibited in calcium-free medium (Fig. 3.7E lane 4) and augmented by high levels of extracellular Ca^{2+} (5mM) (Fig. 3.7E lane 8). Despite equal protein loading in all lanes, GFAP and the loading controls β actin and glyceraldehyde 3-phosphate dehydrogenase (GAPDH) were all detected at much lower levels, in the samples from astrocytes treated with 500nM ionophore in medium supplemented with 5mM calcium chloride (Fig. 3.7E lane 8), probably due to high numbers of apoptotic cells and the associated degradation of proteins.

3.24 Astrocyte morphology and NF-κB translocation

3.24.0 Are astrocyte morphology changes associated with NF-κB activation?

Results above show that PMA induces astrocyte stellation and moderate NF-κB activation while calcium ionophore strongly induces NF-κB activation without any noticeable astrocyte morphology change. To investigate the relationship between astrocyte morphology and activation further, dibutyryl cyclic AMP (db-cAMP),

lysophosphatidic acid (LPA), glutamate, metallothionein 2A were compared with PMA and ionophore for effects on astrocyte morphology and NF-κB translocation. As briefly described below, these reagents have all been previously reported to alter astrocyte morphology and induce astrogliosis. Cyclic-AMP analogues, such as db-cAMP, strongly inactivate the GTPase RhoA to induce actin depolymerisation and rapid rearrangements of focal adhesions that produce highly stellate morphologies (Goldman and Abramson, 1990; Ramakers and Moolenaar, 1998; Safavi-Abbasi et al., 2001; Cechin et al., 2002). After injury, ingredients of serum such as endothelin, thrombin and LPA can enter the CNS where they induce inflammatory responses (Manning and Sontheimer, 1997; Steiner et al., 2002; Sorensen et al., 2003; Koh et al., 2005). *In vitro* these factors inhibit the effects of cAMP and induce flattened epitheloid astrocyte morphologies by activating RhoA, leading to downstream assembly of actin stress fibres and their attachment at focal adhesions (Koyama et al., 1993; Suidan et al., 1997; Ramakers and Moolenaar, 1998; Safavi-Abbasi et al., 2001). Excitatory amino acids, including glutamate can also activate RhoA to induce flattened morphologies in astrocytes (Chen et al., 2006a; Lau et al., 2010). Metallothionein 1/2 is strongly upregulated by reactive astrocytes after CNS injury, prior to the peak in GFAP expression and glial scar development (Neal et al., 1996; Buniatian et al., 2001; Penkowa et al., 2002) and may have a role in regulating ROS-mediated astrocyte swelling and inflammation (Wakida et al., 2007; Li et al., 2008a; Vitellaro-Zuccarello et al., 2008). Exogenous metallothionein 2A promotes neuronal survival and neurite outgrowth (Chung et al., 2003; Chung and West, 2004; Ambjorn et al., 2008) and induces astrogliosis with more process-bearing astrocyte morphologies and increased GFAP expression through the JAK/STAT pathway (Leung et al., 2010), which is downstream from NF-κB activation via IL-6.

3.24.1 Rapid astrocyte morphology changes were independent of NF-κB translocation

Of the additional agents tested only metallothionein 2A induced significant NF-κB translocation in astrocytes (Fig. 3.8A) with the response being similar to that induced by PMA and significantly less than the activation induced by ionophore ($p < 0.01$ at 1 hour). As expected, db-cAMP strongly induced the stellate morphologies (Fig. 3.8B-D) associated with RhoA inactivation while LPA (Fig. 3.8H) and glutamate (Fig. 3.8I)

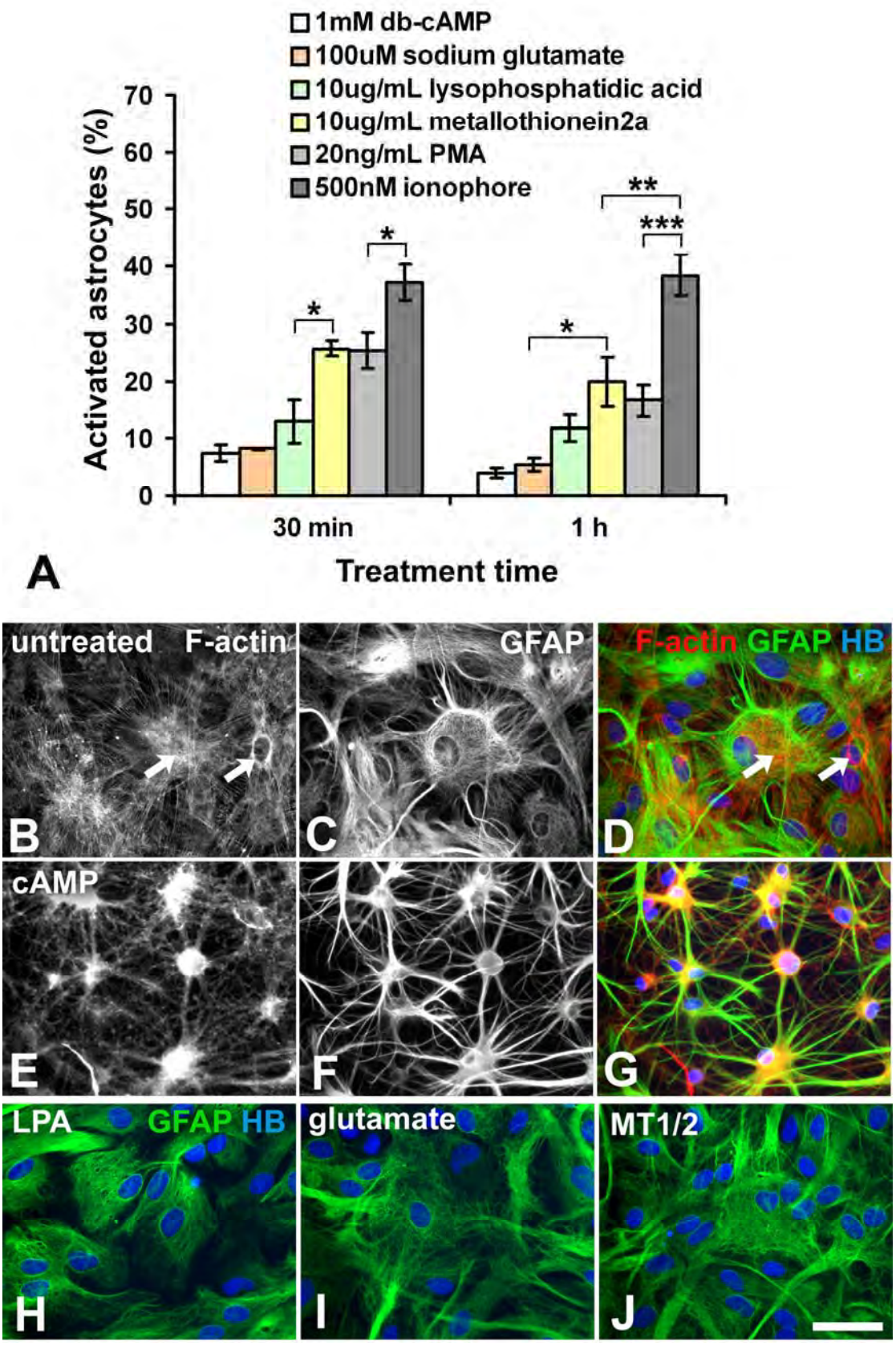
1mM db-cAMP
100uM sodium glutamate
10ug/mL lysophosphatidic acid
10ug/mL metallothionein2a
20ng/mL PMA
500nM ionophore
Activated astrocytes (%)
70
60
50
40
30
20
10
0
*
*
*
**
***
30 min
1 h
Treatment time
A
untreated
F-actin
B
GFAP
C
F-actin GFAP HB
D
cAMP
E
F
G
LPA
GFAP HB
H
glutamate
I
MT1/2
J

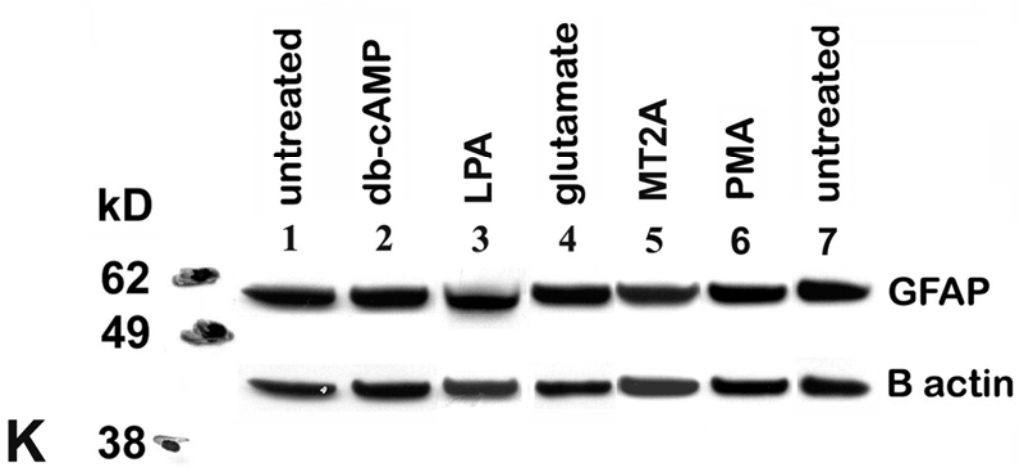

Figure 3.8 Comparative effects of reagents on astrocyte activation, morphology and GFAP expression. A: Activation was compared for astrocytes treated for 30 minutes or 1 hour with 1mM db-cAMP, 100μM sodium glutamate, 10μg/mL lysophosphatidic acid (LPA), 10μg/mL metallothionein 2A (MT2A) and for comparison controls, 20ng/mL PMA and 500nM ionophore (see Fig. 3.2). Db-cAMP, glutamate and LPA did not significantly activate astrocytes ($p > 0.05$) above basal untreated levels (Fig. 3.2). Metallothionein significantly activated astrocytes ($p < 0.05$) in a manner that was not significantly different from the activation induced by PMA ($p > 0.05$), reaching a maximum by 30 minutes and being significantly less than for ionophore at both 30 minutes ($p < 0.05$) and 1 hour ($p < 0.01$). Data were analysed by 2-way ANOVA and post-hoc Tukey's multiple comparison test. Results are means ± SEM, n = 8. Asterisks denote significant differences: * $p < 0.05$, ** $p < 0.01$, *** $p < 0.001$. B-J: Morphologies were compared for untreated astrocytes after 48 hours of treatment with the above reagents (A). Immunostaining for GFAP (C, F and green in D, G and H-J) identified astrocytes and actin filaments were stained with Alexa fluor 488 phalloidin (B, E and red in D, G). Nuclei were counterstained with Hoechst blue (HB, D, G and H-J). Untreated astrocytes (B-D) had flattened cell bodies and actin filaments that were radially distributed around rings (arrows in B, D) offset from nuclei. Db-cAMP (E-G) induced stellate morphologies characterised by compressed cell bodies, depolymerisation of actin filaments (E) and long, narrow, radially distributed processes. LPA (H) and glutamate (I) both induced broad flattened cell bodies with dense networks of GFAP and actin filaments (not shown) similar to those in the untreated astrocytes. Metallothionein induced flattened cell bodies with many long broad processes (J). Scale bar is 50 μm. K: Western blot of astrocyte samples after 48 hour reagent treatments shows no substantial differences in GFAP expression between untreated astrocytes (lanes 1 and 7) and db-cAMP (lane 2), LPA (lane 3), glutamate (lane 4), MT2A (lane 5) and PMA (lane 6) treated astrocytes. GFAP expression for the treated astrocytes is within the limits of variation indicated by the B actin loading control bands and the untreated sample GFAP bands. The blot image is representative of 6 blots performed on separate samples.

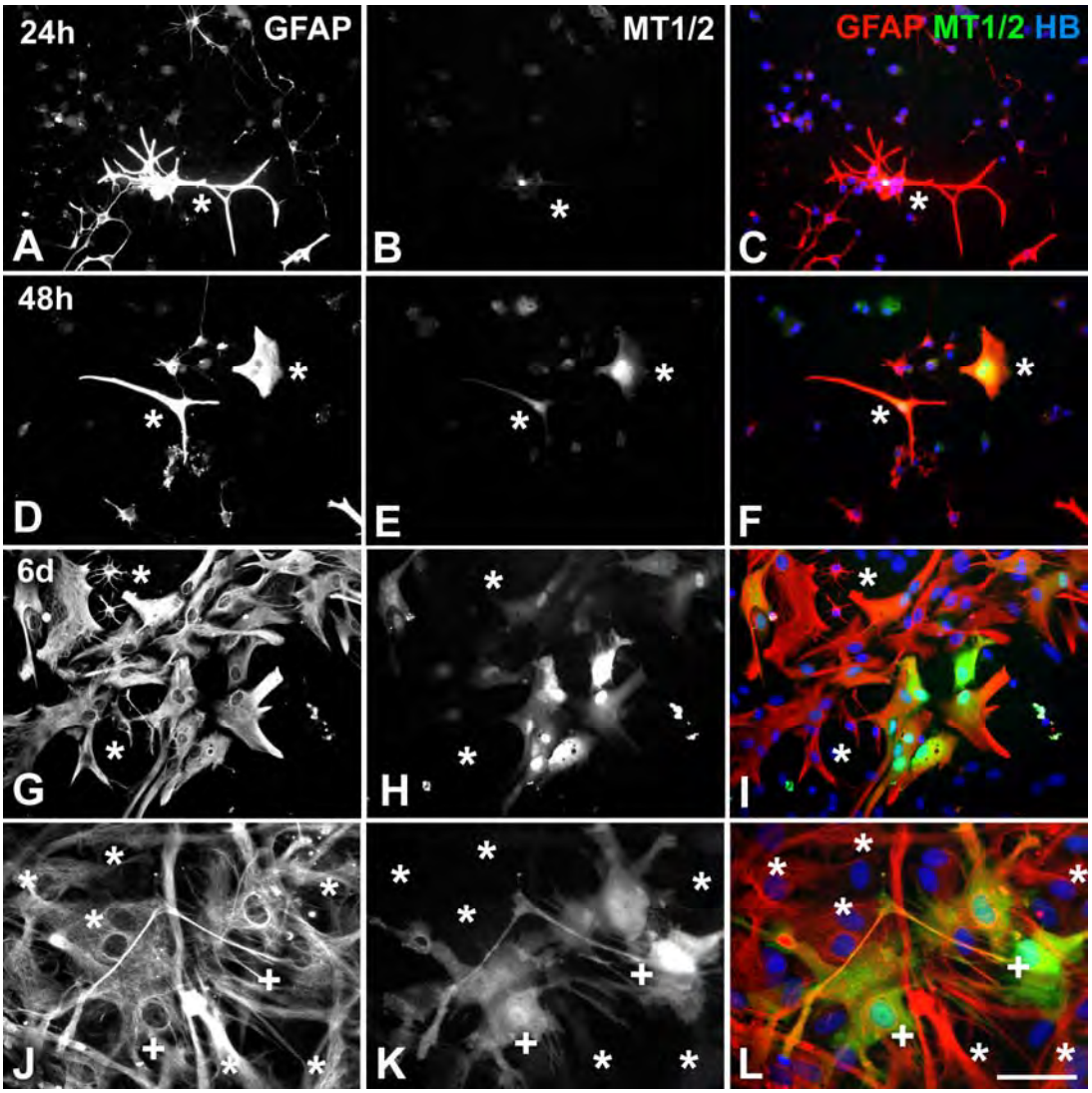

Figure 3.9 Metallothionein 1/2 immunoreactivity in astrocytes and progenitors. Progenitor cells after 24 hours, 48 hours or 6 days in culture and astrocyte cultures were immunostained for GFAP (A, D, G, J and red in C, F, I, L) to identify astrocytes and counter-stained for metallothionein 1/2 (B, E, H, K and green in C, F, I, L). Nuclei were stained with Hoechst blue (HB; blue in C, F, I, L). In 24- and 48-hour progenitor cell cultures metallothionein 1/2 immunoreactivity occurred in the nuclei and very faintly in the processes of cells that had begun to extend GFAP-positive processes (asterisk in A-C). More intense metallothionein 1/2 immunoreactivity occurred in astrocytes with more flattened morphologies (D-F). After 6 days most cells had differentiated into astrocytes with flattened morphologies and many exhibited metallothionein 1/2 immunoreactivity that was most intense in the nuclear region (G-I). Metallothionein 1/2 immunoreactivity was not detected in GFAP expressing cells with progenitor-like morphologies in the 6 day cultures (asterisks in G-I). Metallothionein 1/2 expression was highly variable in mature astrocyte cultures (J-L). Some astrocytes had strong metallothionein 1/2 immunoreactivity while in others immunoreactivity was very faint or absent (asterisks in J-L). The metallothionein 1/2 immunoreactivity was more intense in the nuclear region of some astrocytes (plus signs in J-L) but was usually evenly distributed throughout cells. Scale bar is 100μm (A-I) or 50μm (J-L).

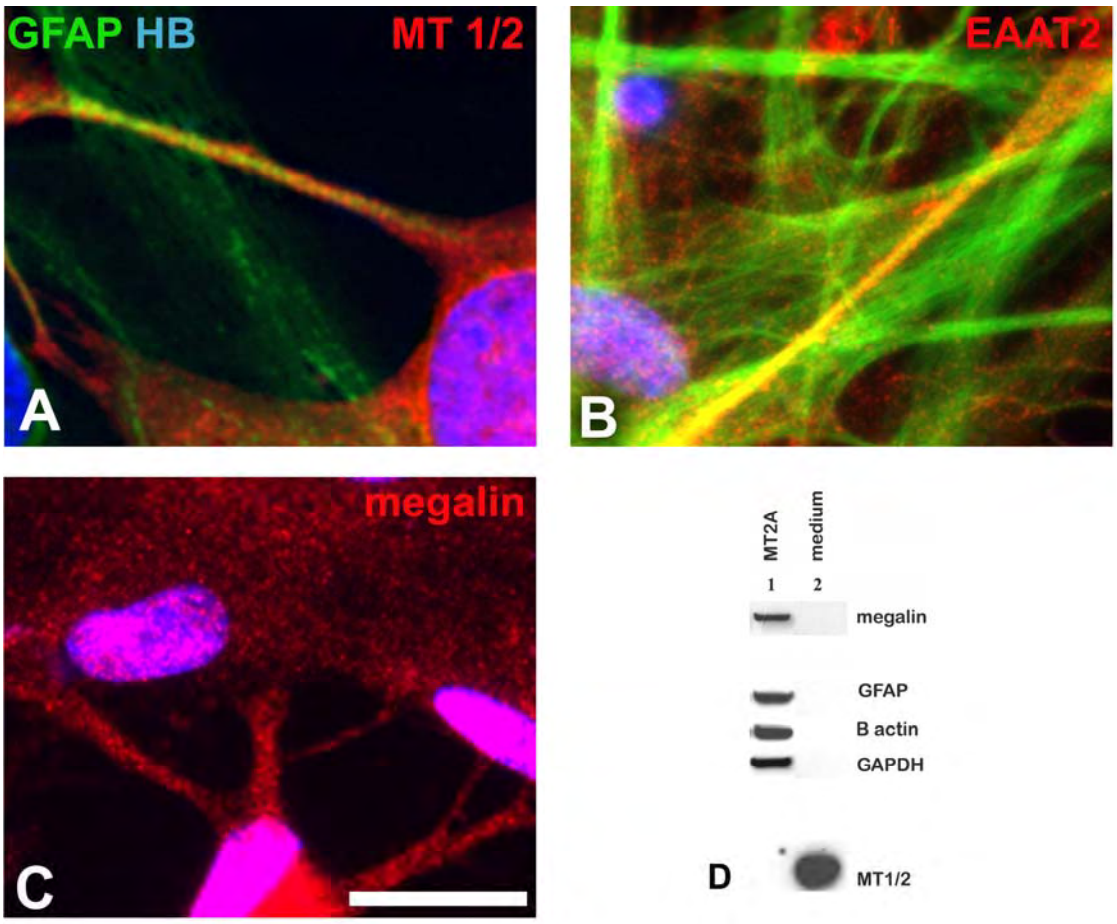

Figure 3.10 Metallothionein 1/2, excitatory amino acid transporter 2 and megalin immunoreactivity in astrocytes. Detail of merged images of immunostaining for metallothionein (MT) 1/2 (red in A), EAAT2 (red in B), megalin (red in C), GFAP (green in A and B) and Hoechst blue nuclear stain (blue in A-C) showed that punctate immunoreactivity for metallothionein 1/2 and excitatory amino acid transporter 2 (EAAT2; also known as glutamate/aspartate transporter) surrounded fibrous immunoreactivity for GFAP in astrocyte processes and cell bodies. Megalin immunoreactivity showed a similar punctate distribution, did not vary markedly between cells and occurred throughout astrocyte cell bodies, nuclear regions and processes. Scale bar is 15µm (A) or 40µm (B and C). D: Western blot analysis of megalin and metallothionein 1/2 (MT1/2) expression by astrocytes. Astrocytes were treated for 48 hours with 10µg/mL metallothionein (MT)2A (lane 1) and medium was collected from the MT2A-treated astrocytes and run as a control (lane 2) for the anti-metallothionein 1/2 primary antibody. Probing with the anti-megalin primary antibody detected protein bands at about 80kDa. Bands for GFAP, B actin and GAPDH were detected as controls. No bands were detected for metallothionein 1/2 from the astrocyte samples for exposures up to 10 minutes. However, a strong band at ~10kDa was detected for metallothionein 1/2 for the control medium sample after only a short exposure (~10 seconds).

induced the flattened morphologies associated with RhoA activation. Metallothionein 2A (Fig. 3.8J) induced morphologies intermediate between the extremes of RhoA activation and inactivation. It is possible that this intermediate state presents suitable conditions for growth, which requires co-ordinated activity of the various Rho family GTPases that regulate attachment, process extension and spreading of cell membranes (Weber et al., 1998; Kuhn et al., 2000; Guan and Rao, 2003; Hall, 2005; Holtje et al., 2005). These morphological effects occurred within 30 minutes to one hour of treatment (data not shown) and were maintained 48 hours later (Fig. 3.8B-J). Western blotting (Fig. 3.8K) indicated that after 48 hours there no substantial change in GFAP expression resulted from the treatments and associated differences in astrocyte morphologies.

3.24.2 Metallothionein 1/2 and megalin localised at astrocyte cell membranes

Metallothionein 1/2 immunoreactivity occurred only in astrocytes and not in OECs, microglia or fibroblasts (data not shown). Progenitor cells did not appear to express metallothionein 1/2 before differentiating into astrocytes (asterisk in Fig. 3.9A-C) and expression increased with astrocyte maturation (Fig. 3.9D-F). Metallothionein expression was highly variable in mature astrocyte cultures (Fig. 3.9J-L). Some astrocytes had strong metallothionein immunoreactivity while in others immunoreactivity was very faint or absent (asterisks in Fig. 3.9J-L). The metallothionein immunoreactivity was more intense in the nuclear region of some astrocytes (plus signs in Fig. 3.9J-L) but usually expression was evenly distributed throughout cells and was not altered by reagent treatments (data not shown). Extracellular metallothionein 1/2 interacts with the low-density lipoprotein scavenger receptor, megalin, to facilitate zinc and cadmium transport in the kidney (Klassen et al., 2004; Wolff et al., 2006). Neurons and astrocytes also express megalin and it may be involved in a mechanism for the promotion of neurite outgrowth by astrocytic secretion of metallothionein 1/2 (Chung et al., 2003; Chung et al., 2008). Interestingly, metallothionein 1/2 and megalin immunoreactivity in astrocytes both showed a punctate distribution similar to that for the glutamate/aspartate transporter (also known as excitatory amino acid transporter 2), appearing to be located at astrocyte plasma membranes (Fig. 3.10A-C). Western blotting (Fig. 3.10D) and immunocytochemistry indicated that reagent treatments did not alter megalin expression

and distribution (data not shown). Metallothionein 1/2 could not be detected in the cultured astrocytes by Western blotting (Fig. 3.10D) even following exogenous metallothionein 2A treatment, although it was readily detectable in the culture medium from the treated astrocytes. This result implies that there was no substantial uptake of metallothionein 2A by astrocytes or that it was rapidly altered following uptake.

3.3 Discussion

3.30 PMA/ionophore induced NF-κB translocation to astrocyte nuclei

3.30.0 Ionophore activated astrocytes more strongly than PMA

PMA and ionophore both rapidly induced NF-κB translocation from the cytoplasm to nuclei in astrocytes that was readily detectable by immunocytochemistry. Utilising immunocytochemistry to detect p65 NF-κB translocation provided simple, direct, unambiguous evidence of these rapid robust activation responses in astrocytes and simultaneously enabled positive confirmation that the activated cells were astrocytes by counter-staining for GFAP. Consistent with the central role of increased intracellular calcium in glial responses to CNS injury, NF-κB translocation in astrocytes was induced more strongly by ionophore, with only a relatively small additive effect attributable to PMA, when astrocytes were treated simultaneously with PMA and ionophore. This result differs from PMA/ionophore stimulation of T cells, where NF-κB-mediated activation is more strongly induced (although still relatively weakly) through PMA activation of PKC and there is a strong synergistic increase in activation by combined PMA/ionophore treatment or other stimuli, such as TNF-α, that activate both calcium signalling and PKC (Baeuerle and Henkel, 1994; Brettingham-Moore et al., 2005a).

3.30.1 NF-κB translocation was rapid and transient

In the cultured astrocytes, NF-κB translocation was both rapid and transient reaching a peak by 1 hour after stimulation, followed by a significant decrease within the following hour. Although the time-course of this response was not atypical for NF-κB (Hertlein et al., 2005), a more sustained activation could have been expected in response to the reagent treatments, since ionophore promotes sustained elevation of intracellular calcium levels (Kolber and Haynes, 1981), while PMA induces chronic activation of PKC

(Newton, 1997). Both of these effects are likely to inhibit resynthesis of IκBs for subsequent binding and inactivation of NF-κB, which is favoured by lower intracellular concentrations of Ca^{2+} and PKC (Fisher et al., 2006). Cells are rapidly depleted of IκB in response to activating stimuli because they induce the required removal and proteolysis of IκB for activation of NF-κB (Baeuerle and Henkel, 1994; Hertlein et al., 2005; Fisher et al, 2006). Consequently, the autoregulatory upregulation of IκB transcription by NF-κB can dramatically decrease the time required for inhibition of NF-κB by IκB in response to subsequent stimuli (Brown et al., 1993; Sun et al., 1993; Zabel et al., 1993; Baeuerle and Henkel, 1994). Hence, the relatively rapid transient activation of NF-κB by PMA/ionophore treatment suggests that IκB transcription may have already been upregulated in the astrocytes, possibly due to earlier NF-κB activation during culture preparation. This may have provided sufficient inhibition of NF-κB until the synthesis of more IκB was induced following stimulation by PMA/ionophore, thereby preventing an oscillatory NF-κB response. Although it is uncertain how long higher levels of IκB transcription and synthesis would persist after a phase of NF-κB activation, IκB levels appear to be dynamically regulated even in quiescent cells (O'Dea et al, 2007). IκBs still undergo constitutive degradation and synthesis in the absence of stimuli that induce proteasomal degradation of IκBs following their release from NF-κB dimers. The majority of newly synthesised IκB is probably degraded before ever binding to NF-κB dimers, because free IκB is degraded much more rapidly than IκB bound to NF-κB. This implies that constitutive synthesis of IκB would be required at a higher rate than would otherwise be predicted based on the relative stability of the IκB:NF-κB complex in unstimulated cells. Hence, the free IκB degradation pathway appears to be an important determinant of constitutive NF-κB activity and responsiveness to stimuli. Therefore, it could be informative to investigate IκB expression and localisation, in addition to NF-κB in the astrocytes, both in response to reagent treatments and at different stages of tissue dissection and astrocyte culture.

3.30.2 Astrocyte activation may have been asynchronous

Although no significant difference was detected in NF-κB translocation for ionophore doses from 125nM to 1μM and PMA doses from 20ng/mL to 200ng/mL, the protocol for

measuring NF-κB translocation did not take into account any differences in NF-κB immunoreactivity intensity in nuclei above an arbitrary threshold. Although it is uncertain whether there would be any functional importance to such differences, it is probable that more intense immunoreactivity would indicate more NF-κB had translocated to the nucleus and this could result in greater enhancement of transcription. For similar reasons, although nuclear NF-κB immunoreactivity intensity was lower than the arbitrary detection threshold at time-points following the peak response, nuclear NF-κB could have remained higher than levels prior to treatment and could have been sufficient to maintain increased gene transcription. Western blotting of nuclear and cytoplasmic fractions of astrocytes and/or chromatin immuno-precipitation assay for NF-κB subunits (Butler et al., 2002; Hoffman et al., 2002; Brettingham-Moore et al., 2005a; Fan and Cooper, 2009) in conjunction with the immunocytochemistry could have provided a more accurate indication of relative activation levels in the cultures. If these alternative techniques using samples from whole culture lysates had been utilised it may have been assumed that NF-κB activation was equally distributed in astrocytes throughout the cultures. This assumption could also arise from modeling of NF-κB activation, based on the dissociation rates of the most relevant molecular interactions, which predicts the maximum percentage of activated NF-κB dimers for different treatment conditions (Hoffman et al., 2002; Halsey et al., 2007). Furthermore, it could have been expected that subjecting the cultured astrocytes to soluble activating factors in the culture media would have simultaneously activated all astrocytes to the same extent within each culture. However, the differences in NF-κB activation between treatments, measured with the immunocytochemical method in this study, clearly represented differences in the percentages of synchronously-activated astrocytes in the cultures. It is likely that measured differences in NF-κB activity are also unequally distributed between cells in research using other methodologies and this has implications for explanations of NF-κB regulation and the related physiological effects. The observed effects in this study could have arisen from different rates of NF-κB activation in response to different treatments with higher activation rates resulting in more astrocytes simultaneously reaching the activation threshold at earlier time-points. Alternatively, the more inflammatory treatments may have been able to activate a greater percentage of astrocytes in the

cultures. It is also possible that the effects on the percentage of activated astrocytes were accompanied by corresponding unmeasured effects on the maximum percentage of activated NF-κB dimers in individual astrocytes. All of these explanations imply that there must have been uneven distributions of IκBs and/or other NF-κB signalling modulators between individual astrocytes in the cultures, possibly due to differences in maturity, cell cycle and growth phases between astrocytes or contact inhibition effects related to variations in cell density. These variables could be assumed to be equally distributed between cultures and would therefore not affect the validity or physiological relevance of the measured effects. However, a more detailed investigation of the sequence of events regulating NF-κB activation in individual astrocytes could provide valuable insight into the mechanisms that modulate inflammation and how they could limit the spread of secondary damage to neighbouring tissue. Fluorescence imaging of live astrocyte cultures could reveal the time-course of activation and deactivation of individual astrocytes within the cultures. 1μM ionophore did appear to induce apoptosis of astrocytes and ionophore was therefore used at lower doses in later experiments. High levels of intracellular calcium are known to induce apoptosis (Stys, 2004) and although NF-κB is considered to usually have growth-promoting and anti-apoptotic effects, it has been linked to apoptosis, particularly in neurons. Apoptosis in response to PMA and ionophore treatments are further investigated in Chapter 5.

3.31 NF-κB translocation involved a calcium-dependent mechanism

3.31.0 NF-κB translocation was sensitive to extracellular calcium levels

The induction of NF-κB translocation by ionophore inferred a Ca^{2+}-dependent mechanism. This result was as expected since many inflammatory stimuli activate NF-κB via PKC and other calcium dependent protein kinases (Fan and Cooper, 2009; Fisher et al., 2006; Gonczi et al., 2008). Interactions between calcium receptors, transporters and channels coordinate influx of extracellular Ca^{2+} with release from intracellular stores to create oscillations of intracellular Ca^{2+} concentration that act as a second messenger for intracellular signalling through a variety of calcium binding proteins (Gomez and Spitzer, 1999; Carafoli, 2002; Robles et al., 2003; Clapham, 2007). Variations in the frequency of the Ca^{2+} concentration oscillations favour different protein interactions dependent on the

affinity of Ca^{2+} for the different calcium binding proteins and the binding dissociation rates of the subsequent protein interactions. Dissociation from NF-κB and degradation of IκB is favoured by high Ca^{2+} levels and modeling based on dissociation rates predicts that NF-κB is inactive at intracellular Ca^{2+} concentrations below 0.1μM with activity rising rapidly as intracellular Ca^{2+} increases across the physiological range from 0.1 to 0.5μM (Fisher et al., 2006). This model of NF-κB activation by calcium signalling was consistent with the rapid activation of NF-κB by ionophore in astrocytes, which reached a maximum within 30 minutes, as is predicted by the modeling, in response to low frequency Ca^{2+} oscillations across the physiological range. It was unlikely that the ionophore-induced translocation was PKC-dependent since there was not a synergistic increase in translocation when PMA was combined with ionophore treatment. However, the activation by PMA may have involved conventional Ca^{2+}-dependent PKC or Ca^{2+}-independent novel PKC isoforms (Nishizuka, 1988; Deacon et al., 1997; Bright and Mochly-Rosen, 2005), which have both been implicated in astrogliosis (Ballestas and Benveniste, 1995; Pascale et al., 2004; Amos et al., 2005; Hung et al., 2005; Burgos et al., 2007a). In T-cells, novel PKCε activated NFAT, AP-1 and NF-κB while conventional PKCα only activated NFAT and AP-1 and less effectively than PKCε (Genot et al., 1995). The translocation response in the cultured astrocytes was very sensitive to extracellular Ca^{2+} levels since a change to calcium-free medium induced NF-κB translocation as effectively as PMA/ionophore. Cells require a large gradient between intracellular and extracellular Ca^{2+} levels to maintain suitable ionic homeostasis for cellular functions (Carafoli, 2002; Clapham, 2007). Low extracellular Ca^{2+} would therefore lead to efflux of intracellular Ca^{2+} from astrocytes in an attempt to restore normal ionic gradients and simultaneous release of Ca^{2+} from internal stores to maintain normal intracellular levels. This perturbation of intracellular Ca^{2+} levels was apparently sufficient to stimulate calcium signalling leading to NF-κB translocation.

3.31.1 Astrocyte attachment may affect activation

There may also have been some cytoskeletal contribution to the stimulation of NF-κB translocation, since attachment of cells to substrates via integrins, adhesion molecules and cytoskeletal focal adhesions is Ca^{2+}-dependent (Woods and Couchman, 1992;

Gottfried et al., 2003; Hall, 2005; Clapham, 2007). Astrocytes adopted spindly bipolar morphologies in the calcium-free conditions and this morphology change could have been associated with signalling through Rho GTPases that can lead to NF-κB activation (John et al., 2004; Kettritz et al., 2004; Hall, 2005). A cytoskeletal contribution to the induction of NF-κB translocation could provide an explanation for the significantly greater NF-κB translocation when astrocytes were treated with PMA/ionophore simultaneously with the change to calcium-free medium compared with PMA/ionophore or the medium change alone. Decreased cell to cell and cell to substrate attachment associated with the altered astrocyte morphologies in the calcium-free conditions could have limited a cytoskeleton-mediated inhibitory effect on astrocyte activation. Although cell density effects on NF-κB translocation were not specifically investigated, relatively less translocation did appear to occur among astrocytes in locally dense regions of the cultures under all treatment conditions. NF-κB translocation was not induced by a change of medium after astrocytes were pre-incubated for 4 hours in calcium-free DMEM supplemented with EDTA to chelate any free Ca^{2+} and the basal level of NF-κB activation was significantly less in these conditions than in DMEM, confirming the Ca^{2+}-dependence of the response to medium change. However, treatment with PMA/ionophore did still induce significant NF-κB translocation in these conditions, although the effect was significantly less than for ionophore or PMA treatment in normal DMEM, suggesting that there may have been a novel PKC component to the induction of translocation by PMA. Testing separate treatments with PMA and ionophore in the calcium-free conditions may help reveal the involvement of a novel PKC isoform, although conclusive evidence would require the use of inhibitors of specific PKC isoforms or experimental models involving knock-down or blocking of PKC isoforms.

3.31.2 Thapsigargin confirmed the calcium-dependence of astrocyte activation

Thapsigargin, which elevates intracellular Ca^{2+} levels by blocking active transport into intracellular stores (Pahl and Baeuerle, 1996; Araque et al., 1998; Chen et al., 2001a), induced similar levels of NF-κB translocation as PMA/ionophore, confirming that this translocation response in astrocytes was predominantly Ca^{2+}-dependent. In addition, thapsigargin induced significantly less NF-κB translocation than PMA/ionophore in

astrocytes that had been pre-incubated in EDTA-supplemented calcium-free medium, providing further support for the possibility that a component of the translocation induced by PMA was mediated by a novel PKC isoform. Again, it could have been informative to test the effects of PMA and ionophore separately in combination with thapsigargin. Combining PMA/ionophore and thapsigargin treatments in the calcium-free conditions induced significantly more NF-κB translocation than PMA/ionophore alone in these conditions. Since ionophore transports Ca^{2+} down concentration gradients it could have induced some elevation of intracellular Ca^{2+}, by transporting Ca^{2+} out of intracellular stores in the calcium-free medium conditions, when active transport back into the intracellular stores was blocked by thapsigargin. The resultant elevation of intracellular Ca^{2+} could have induced increased NF-κB translocation by augmenting a component of the translocation response mediated by a conventional PKC isoform or other calcium signalling pathways but significantly less so than for the same treatments in the presence of normal extracellular Ca^{2+} levels. A more sophisticated investigation of calcium signalling involvement in the NF-κB translocation response, utilising specific activators and inhibitors of the variety of Ca^{2+} channels and pumps together with the measurement of Ca^{2+} transients with Ca^{2+}-sensitive fluorophores, could provide valuable information on the mechanisms of NF-κB translocation and the related inflammatory gene transcription responses in astrocytes.

3.32 PMA and ionophore altered astrocyte morphology

3.32.0 Astrocyte morphology and astrogliosis

The NF-κB translocation induced by PMA, ionophore, thapsigargin and the change to calcium-free medium were all accompanied by morphological changes that were evident within 2 hours of stimulation. Changes in astrocyte morphology and motility associated with CNS injury and glial scar formation are often cited as characteristics of astrogliosis (Hou et al., 1995; Pindon et al., 1998; Rabchevsky et al., 1998; Panickar and Norenberg, 2005). It has been proposed that Rho GTPase (Hall, 1998; Safavi-Abbasi et al., 2001) and calcium signalling (Gu and Spitzer, 1997; Doherty et al., 2000; Chierzi et al., 2005; Takenaga and Kozlova, 2006) stimulation of astrocyte cytoskeletal dynamics (Goldman and Abramson, 1990; Manning and Sontheimer, 1997; Suidan et al., 1997) in response to

CNS injury initiates activation of NF-κB and other inflammatory pathways (Steiner et al., 2002; Sorensen et al., 2003; Hall, 2005; Koh et al., 2005) to stimulate the required ATP production (Carafoli, 2002; Cogswell et al., 2003; Clapham, 2007) and protein synthesis for growth (Ellison et al., 1999; Jacques-Silva et al., 2004; Hall, 2005) and differentiation to a reactive phenotype (Eddleston and Mucke, 1993; O'Neill and Kaltschmidt, 1997; Meeuwsen et al., 2003a; Sofroniew, 2005).

3.32.1 Calcium-dependent alteration of astrocyte morphology

While it was possible that alterations in cytoskeletal dynamics associated with the morphology changes may have contributed to the NF-κB activation in response to some or all of the stimuli, it appeared unlikely that activation was predominantly initiated via the cytoskeleton. NF-κB translocation occurred within 30 minutes in response to activating stimuli, before morphological changes were apparent, except in calcium-free medium conditions, which induced almost immediate morphological changes. However, addition of 500μM-1mM calcium chloride prevented the morphology changes but did not eliminate the NF-κB translocation that was rapidly induced by briefly washing astrocytes with calcium-free medium. Furthermore, the morphological changes induced by ionophore were dose-dependent, with alteration to spindly bipolar morphologies only occurring at higher doses, while NF-κB activation was not dose-dependent, with similar levels of NF-κB translocation being induced across the 125nM to 1μm range of ionophore concentrations. The morphological changes induced by ionophore, thapsigargin and calcium-free medium were consistent with the disruption of Ca^{2+}-regulated cell-cell and cell-substrate attachment. Detachment of astrocytes was most evident in calcium-free conditions where blebby astrocytes with retracted, sinusoidal and coiled processes suggested a loss of tension due to disrupted cell-cell and cell-substrate attachment. At higher doses of ionophore, particularly in combination with PMA, astrocyte apoptosis appeared to contribute to the disruption of attachment and associated morphological changes. Although the morphological effects of ionophore and thapsigargin were accentuated by calcium-free conditions, NF-κB translocation in response to the reagents was moderated, again suggesting the morphological effects of disrupted calcium signalling were substantially independent of astrocyte activation. More

conclusively, pre-incubation in EDTA-supplemented calcium-free medium eliminated translocation of NF-κB in response to medium change, while the morphological effects were accentuated by the longer incubation in calcium-free conditions.

3.32.2 Morphological effects were independent of NF-κB translocation

The results were consistent with previous research that has revealed the role of RhoA in regulating astrocyte morphology. The flattened polygonal morphologies of the untreated astrocytes were accentuated by LPA and glutamate treatment and were accompanied by cytoplasmic networks of GFAP and radially arranged actin fibres that have been associated with RhoA activation (Suidan et al., 1997). Db-cAMP and PMA induced depolymerisation of actin fibres and the compression of cytoplasm and GFAP fibres into stellate morphologies that have been associated with inhibition of RhoA and disassembly of focal adhesions (Safavi-Abbasi et al., 2001). However, there was no evidence of a relationship between the inferred RhoA effects on astrocyte morphology and NF-κB activation or GFAP expression. There was no evidence of altered GFAP expression with any of the tested reagents. Untreated, LPA-treated and glutamate-treated astrocytes all had flattened polygonal morphologies consistent with RhoA activation and low levels of NF-κB activation. Flattened polygonal astrocyte morphologies were also maintained at the lower 125-250nM ionophore doses that induced NF-κB translocation as strongly as the higher ionophore doses that altered astrocyte morphology, probably by disrupting cell-cell and cell-substrate attachment and inducing apoptosis. The moderately more stellate process-bearing astrocyte morphologies induced by PMA and metallothionein 2A were associated with only moderate levels of NF-κB translocation, while the strong stellation induced by db-cAMP was not accompanied by any evidence of NF-κB translocation. Process extension by immature astrocytes differentiating from progenitors on the boundaries of CNS lesions may have led to the association of a process-bearing morphology with the reactive astrocyte phenotype. However, GFAP expression increases as the progenitors differentiate into astrocytes and develop broader processes. Consequently, the flattening of morphologies in response to inflammatory mediators such as LPA and thrombin from blood has also been cited as evidence for astrogliosis (Manning and Sontheimer, 1997; Steiner et al., 2002; Sorensen et al., 2003; Koh et al.,

2005). In addition, analysis of the morphology changes are based mainly on immunostaining for GFAP and recent evidence shows that mature astrocytes substantially remain in their exclusive domains following injury (Wilhelmsson et al., 2006). The observed 'hypertrophy' and 'stellation' appears to be merely due to a thickening of the cytoplasmic GFAP bundles that already have a stellate distribution in mature astrocytes in normal tissue prior to injury. Mature astrocytes on the border of the lesion may extend GFAP-rich processes into the void created by cell death and progenitors that migrate into the lesion differentiate into astrocytes, grow and retain a highly process-bearing morphology that contributes to glial scar development (Fawcett and Asher, 1999; Alonso, 2005; Sofroniew, 2008). Cytoskeleton-regulated morphology changes are essential (Hall, 2005; Holtje et al., 2005) for the required cell migration, proliferation, growth and differentiation during inflammatory responses and wound-healing (Ellison et al., 1999; Emsley et al., 2005; John et al., 2005; Fawcett, 2006a). However, the results suggest that morphological evidence alone for the induction of astrogliosis has even more questionable validity than evidence based solely on GFAP expression. This study and previous research show that rapid changes between stellate and epitheloid extremes of astrocyte morphology can be induced in culture independent of any synthesis or degradation of cytoskeletal proteins (Safavi-Abbasi et al., 2001). Consequently, the implications of these morphology changes for astrogliosis remain uncertain (Goldman and Abramson, 1990; Pinto et al., 2000; Safavi-Abbasi et al., 2001; Koh et al., 2005; Chan et al., 2007).

3.33 PMA/ionophore induced depolymerisation and decreased levels of GFAP

3.33.0 Depolymerisation may have increased GFAP immunoreactivity

It could have been expected that induction of inflammatory gene expression by NF-κB in the cultured astrocytes would have led to a detectable increase in GFAP expression, consistent with the development of astrogliosis. However, no apparent increase in GFAP expression was detected by immunohistochemistry or Western blot, within 48 hours of any of the investigated treatments, independent of whether they induced NF-κB translocation. Immunoreactivity was already relatively intense in the cultured astrocytes in comparison to cortical astrocytes in healthy tissue *in vivo* and it may be that in these

circumstances any changes in GFAP expression were not sufficient to be detectable. The possibility that the cultured astrocytes had already undergone activation and astrogliosis during dissection and culture preparation is discussed further in Chapter 4. A consistent decrease in GFAP levels was detected by Western blot in response to prolonged treatments with higher doses of ionophore or combined PMA/ionophore. Immunocytochemistry on astrocyte cultures subjected to the same treatments revealed that these ionophore and PMA/ionophore treated cultures contained some astrocytes where GFAP appeared to be depolymerised, as evidenced by diffuse high intensity immunoreactivity, and other astrocytes that appeared to be apoptotic, with condensed nuclei and patchy, faint or absent immunoreactivity for GFAP. The much higher intensity GFAP immunoreactivity within 1 hour of treatment in astrocytes where GFAP appeared to be depolymerised, together with unchanged or decreased GFAP levels, after 48 hours, indicated by the corresponding Western blots, supported previous research showing that depolymerisation of GFAP increases accessibility to some antibodies resulting in rapid increases in immunoreactivity independent of increases in GFAP expression (Tramontina et al., 2007). The higher intensity GFAP immunoreactivity was demonstrated to be associated with the change to a blebby morphology in apoptotic astrocytes in cultures treated with 1μM ionophore for 24 hours. As could be expected for a cytoplasmic protein, NF-κB immunoreactivity appeared to be lost at an earlier time-point than immunoreactivity for the fibrous cytoskeletal GFAP, in these apoptotic astrocytes. The apparent GFAP depolymerisation in response to ionophore is consistent with the phosphorylation and depolymerisation of GFAP due to calcium influx following CNS injury (Rodnight et al., 1997; Robles et al., 2003; Sullivan et al., 2010b). The Ca^{2+}-dependence of the apoptotic effect of ionophore was demonstrated by moderation of the decrease in GFAP levels by incubation in calcium-free medium and a marked exacerbation of the decrease in GFAP levels, accompanied by similar decreases in β actin and GAPDH levels, by high extracellular Ca^{2+} levels. PMA activation of PKC could have enhanced depolymerisation of GFAP but it is uncertain why PMA appeared to augment the apoptotic effects of ionophore-induced Ca^{2+} influx. PMA directly activates PKC by binding the DAG activation site without inducing intracellular Ca^{2+} release by generating IP_3, as occurs following activation of mGluRs by glutamate (Akita et al., 1990; Chen et

al., 2000; Cheng et al., 2000; Shindo et al., 2001). PMA may have activated PKC-regulated growth and metabolic pathways (Huang et al., 1989; Chen et al., 2001c; Chattopadhyay et al., 2002; Nakashima, 2002) that possibly rendered astrocytes more susceptible to mitochondrial damage and consequent apoptosis in response to the ionophore-induced Ca^{2+} influx.

3.33.1 Depolymerisation is necessary for redistribution of cytoskeletal proteins

The NF-κB-regulated cytokines, TNF-α and IL-1β are rapidly upregulated after CNS injury and can inhibit GFAP transcription and expression (Selmaj et al., 1991; Oh et al., 1993; Murphy et al., 1995; Krohn et al., 1999). In regions of severe cellular damage and decreased GFAP immunostaining 72 hours after hypoxic injury in pig brain, surviving astrocytes had abnormal morphologies, characterised by retraction of processes and bulbous swellings (Sullivan et al., 2010b, a), resembling the detached and apoptotic astrocytes following PMA/ionophore treatment in this study. GFAP immunoreactivity was increased in less damaged regions of the hypoxic pig brains and similar increases in GFAP following CNS injuries have been correlated with a thickening of cytoplasmic GFAP bundles and processes without any growth beyond the normal exclusive astrocyte domains (Wilhelmsson et al., 2006). The changes in cell morphology that accompany growth and motility require rapid redistribution of cytoskeletal proteins that is achieved by cycles of depolymerisation and polymerisation (Lin et al., 1994; Dickson, 2002). Mobilisation of cytoskeletal proteins by depolymerisation could therefore be expected following CNS injury, to allow cell growth and motility for inflammatory responses, tissue remodelling and wound healing. The large increase in immunoreactivity to an antibody specific for the phosphorylated depolymerised form of GFAP following hypoxic injury (Sullivan et al., 2010a) could have been a manifestation of a requirement for redistribution of GFAP to maintain or alter astrocyte morphologies following tissue damage. Since depolymerisation of GFAP can increase accessibility to other antibodies and thereby increase immunoreactivity intensity it may be that increased immunoreactivity for GFAP, particularly when they occur rapidly in response to treatments, may often represent depolymerisation and/or redistribution of GFAP within cells to allow cytoskeletal remodelling for morphology changes, separate from any

increased synthesis of new protein that would be required for cell growth. It would therefore be interesting to compare immunoreactivity using the anti-phosphorylated GFAP antibody and the anti-GFAP antibodies used for immunocytochemistry and Western blotting in this research, in response to PMA/ionophore and the other reagent treatments.

3.33.2 Loss of GFAP immunoreactivity may be an initial effect of CNS injury

IL-1β and TNF-α are the predominant cytokines promoting transcription of other pro-inflammatory cytokines, chemokines and growth factors in the early response to CNS injury (Taupin et al., 1993; Chao et al., 1995; Meeuwsen et al., 2003a; John et al., 2005; Gosselin and Rivest, 2007; Clausen et al., 2008) and during this period of severe inflammation there may be a loss of GFAP due to death of astrocytes and transcriptional inhibition. The transcriptional effects of IL-1β and TNF-α are regulated by NF-κB and the strong activation of astrocytic NF-κB by PMA/ionophore and the associated apoptosis and decreased GFAP expression had similarities with the effects of these cytokines. However, the cytokines induced by IL-1β and TNF-α include TGFβ1 and IL-6, which activate the JAK/STAT pathway in astrocytes leading to astrogliosis and GFAP up-regulation. GFAP up-regulation develops gradually following CNS injury and reaches a peak after about 7 days in the glial scar (Yang et al., 1997; Fawcett and Asher, 1999; Alonso, 2005; Sofroniew, 2008). Perhaps the balance between the inhibition of GFAP transcription by IL-1β and TNF-α and its promotion by TGFβ1 and IL-6 determines the location and timing of GFAP expression by reactive astrocytes during inflammatory responses. The widespread up-regulation of GFAP by mature astrocytes, in undamaged tissue away from the region of severe inflammation, may be related to astrocyte swelling in response to oedema (Wilhelmsson et al., 2006; Gunnarson et al., 2008; Laird et al., 2008). Progenitor cells attracted to the lesion by chemokines may initially be stimulated to proliferate and then, over several days following injury, differentiate into GFAP-expressing astrocytes that make a major contribution to development of the glial scar (Alonso, 2005; Tan et al., 2005). Surviving mature astrocytes in the injury penumbra may also extend GFAP-rich processes towards and around the lesion as inflammation subsides and wound healing progresses. Comparing NF-κB activation and GFAP expression in

response to PMA/ionophore and other reagents in cultures of constitutively active AQP4 mutant astrocytes and AQP4 null astrocytes or with AQP4 knock-down could provide useful information on the relationship between astrocyte swelling and GFAP in astrogliosis.

3.34 Metallothionein 1/2 and astrocyte activation

There are some intriguing parallels and interactions between PKC and metallothionein that may be related to them having similar activating effects on astrocytes. PMA, which is known to activate PKC, and metallothionein 2A induced similar moderate levels of NF-κB translocation in the cultured astrocytes. If this response translated to a moderate level of inflammation and astrogliosis *in vivo*, it could provide suitable conditions for neuroprotection, neurogenesis and enhanced wound healing. Although metallothionein 1/2 has been reported to strongly induce astrogliosis, this has been inferred from the upregulation of GFAP and related factors that may reflect an emphasis on the growth-related wound healing components of astrogliosis (Chung et al., 2008; Leung et al, 2010). PKC activity is calcium and zinc dependent (Huang et al., 1989; Ahmed et al., 1991), while metallothionein 1/2 regulates zinc homeostasis (Maret, 2000; Coyle et al., 2002). Metallothionein 1/2 upregulation by astrocytes can be regulated by IL-6 and TNF-α (Carrasco et al., 1998; Penkowa and Hidalgo, 2000; Penkowa et al., 2001) and is dependent on a factor released by injured neurons, possibly glutamate (Chung et al., 2004; Chung and West, 2004) or zinc (McCormick et al., 1981; Coyle et al., 1993; Kruczek et al., 2009). Vesicular zinc is released during normal glutaminergic signalling and in massive amounts, together with protein-bound zinc after injury (Frederickson and Bush, 2001; Kauppinen et al., 2008). The high levels of extracellular zinc can exacerbate neuronal damage by promoting inflammation and ROS production (Choi et al., 1988; Frederickson and Bush, 2001; Hellmich et al., 2004). ROS activation of PKC can then increase metallothionein 1/2 expression via NF-κB and increased transcription of metal transcription factor-1 (MTF-1) (Saydam et al., 2002; Rao et al., 2003; Spahl et al., 2003; Hara and Aizenman, 2004; Nakano et al., 2006). Metallothionein 1/2 can then bind the excess zinc to protect neurons. Astrocyte swelling following CNS injury also promotes ROS formation leading to cell damage, the release of zinc ions from protein zinc-sulphur

complexes (Katakai et al., 2001; Kruczek et al., 2009) and increased aquaporin expression via NF-κB (Gunnarson et al., 2008). The elevation in extracellular zinc ions again leads to increased expression of metallothionein 1/2, which binds the excess zinc ions and scavenges ROS to provide protection against the oxidative stress (Dalton et al., 1994; Kumari et al., 2000; Maret, 2003; Ebadi et al., 2005; Hashimoto et al., 2009). Zinc can also block Ca^{2+} entry into astrocytes in response to stimulation of metabotropic receptors by ATP and glutamate (Kresse et al., 2005). Ca^{2+} influx can promote glutamate uptake by astrocytes (Duan et al., 1999; Vermeiren et al., 2005; Verkhratsky, 2006) and induce astrogliosis via PKC and NF-κB activation (Ballestas and Benveniste, 1995; Ciccarelli et al., 2004; Abramov et al., 2005; Norris et al., 2005; Perez-Ortiz et al., 2008). The inhibition of Ca^{2+} influx by zinc could lead to increased neuronal damage due to higher extracellular and glutamate levels. Metallothionein 1/2 could protect neurons by binding the zinc and allowing Ca^{2+} and glutamate uptake by astrocytes, which could simultaneously lead to increased astrogliosis. This may explain why metallothionein 1/2 null transgenic mice exhibit decreased gliosis but suffer more severe neuronal damage in response to kainic acid (Carrasco et al., 2000a). A further cyto-protective function of metallothionein 1/2 involves the regulation of mitochondrial zinc levels to maintain oxidative phosphorylation through alterations in metallothionein zinc-binding affinity resulting from interaction between ATP and metallothionein (Maret et al., 2002). Intracellular calcium ion levels similarly co-ordinate the mitochondrial production of ATP with the protein synthesis demands of growth and inflammatory responses stimulated through PKC, NF-κB and other calcium-dependent signalling pathways (Fig. 1.1). Signalling complexes containing glutamate receptors and transporters, aquaporins, calcium channels and regulatory molecules, such as PKC are located at astrocyte cell membranes (Iadecola and Nedergaard, 2007; Sullivan et al., 2007; Gunnarson et al., 2008; Zeng et al., 2008a). Determining whether metallothionein 1/2 and megalin co-localise with these signalling complexes using confocal microscopy and co-immunoprecipitation could provide insight into the mechanisms for the effects of metallothionein 1/2 on astrogliosis and axon growth.

3.35 Conclusions

The consistent rapid robust activation of NF-κB in astrocytes by PMA/ionophore established this treatment as a useful valid model for research on astrocyte inflammatory activation. Utilising immunocytochemistry to detect p65 NF-κB translocation provided simple, direct, unambiguous evidence of these rapid robust activation responses in astrocytes together with confirmation that the activated cells were astrocytes by counter-staining for GFAP. The decreased GFAP levels and the apoptosis induced by high concentrations of ionophore and Ca^{2+} were consistent with previous research on the early responses of astrocytes to CNS injury, indicating that the PMA/ionophore treatment model was relevant for CNS injury research. Ionophore most potently activated NF-κB in astrocytes, with PMA inducing only moderate activation.

CHAPTER 4:

OECs moderate astrocyte inflammatory activation

4.0 Introduction

4.00 Moderation of inflammation may be therapeutic for CNS injury

4.00.0 Methylprednisolone is the recommended treatment for acute spinal cord injury

The association of more severe and prolonged inflammation with increased secondary neuronal damage has motivated research into adrenal and gonadal steroid hormones as anti-inflammatory treatments for CNS injury (for reviews see Garcia-Segura and Balthazart, 2009; Sorrels and Sapolsky, 2008). Glucocorticoids are adrenal steroid hormones that exert anti-inflammatory actions by inhibiting the adaptive immune activity of lymphocytes, T-cells and dendritic cells and at the molecular level, by directly inhibiting the transcriptional activity of NF-κB and activating protein 1 (AP-1) (reviewed by Sorrels and Sapolsky, 2008; Chen et al., 2007; MacNevin, et al., 2009). This inhibition of NF-κB and AP-1 results in decreased expression of chemoattractants for immune cells and of pro-inflammatory cytokines, including IL-1β, TNF-α and IL-6, while enhancing expression of anti-inflammatory cytokines such as IL-10 and TGF-β. In addition, there is decreased expression of other pro-inflammatory molecules, such as inducible COX-2 and prostaglandins. However, research into the therapeutic use of glucocorticoids in CNS injury and other conditions has shown that the anti-inflammatory effects are dose-dependent. While basal levels of glucocorticoids can have anti-inflammatory, protective effects, higher levels, either administered therapeutically or due to chronic stress, can exacerbate inflammation and increase neuronal damage following injury. This is partly because glucocorticoids inhibit glucose uptake so that less energy is available to neurons and astrocytes to counter the effects of ischemia and excitotoxicity. Methylprednisolone is a synthetic glucocorticoid steroid that was developed for its enhanced anti-inflammatory activity relative to the other effects of glucocorticoids (Donnelly and Popovich, 2008; Hall, 1992; Hall et al., 2010; Nash et al., 2002). In contrast to endogenous glucocorticoids, methylprednisolone has only been demonstrated to improve recovery from spinal cord injury when used at high doses. This is consistent with

evidence that, rather than the anti-inflammatory action, it is the anti-oxidant activity of methylprednisolone, particularly the amelioration of lipid peroxidation that is responsible for the therapeutic effects (Werner, 1997; Hall et al., 2010; Wu et al., 2010). Treatment is only considered effective if commenced within 8 hours of injury and is usually continued for 48 hours, covering the period of glucocorticoid receptor upregulation, strong excitotoxicity and high oxidative stress at injury sites. Methylprednisolone is the only drug treatment advocated for acute spinal cord injury (O'Connor et al., 2003; Molloy et al, 2002; Lee et al., 2007) and remains in widespread use, despite uncertainty about its efficacy and safety (Bracken and Holford, 2002; Kronvall et al., 2005; Aalborg et al, 2008). High methylprednisolone doses have only provided modest improvements in neurological outcomes for some spinal cord injuries, while the systemic immunosuppression resulting from the treatment can result in worse patient outcomes due to infections. Subsequently, non-glucocorticoid steroids with enhanced antioxidant and less anti-inflammatory activity, such as tirilazad, have been found to have similar beneficial effects as methylprednisolone, without the adverse immunosuppressive effects (Werner, 1997; Nash et al., 2002; Hall et al., 2010). The endogenous adrenal steroids, progesterone, testosterone, oestrogen and estradiol, have also been reported to provide neuroprotection after traumatic brain injury and stroke by a variety of related mechanisms, including regulating astrocytic AQP4 expression to attenuate cerebral oedema, anti-inflammatory effects and the reduction of lipid peroxidation, oxidative stress and apoptosis (Garcia-Segura and Balthazart, 2009; MacNevin et al., 2009; Samantaray et al., 2010). These steroids and their metabolites can also be produced from cholesterol by neurons and glial cells and may thereby exert paracrine neuroprotective effects within the brain and spinal cord. Steroids are lipophilic and can therefore cross the BBB when administered systemically. However, their lipophilicity confers low aqueous solubility, which is problematic for intravenous delivery. Consequently water-soluble analogues of progesterone have been developed that reproduce some of its neuroprotective effects (MacNevin et al., 2009), while methylprednisolone is delivered as a succinated ester, which releases the free steroid following injection (Nash et al, 2002).

4.00.1 Inhibition of NF-κB moderates CNS injury damage

Earlier Chapters explain how more severe inflammation following CNS injury typically leads to increased tissue damage, larger infarct area and more secondary post-ischemic neuronal damage. Since NF-κB is a key regulator of inflammation (Kracht and Saklatvala, 2002; Chen and Greene, 2004a) that is robustly activated within 15 minutes of CNS injury (Yenari and Han, 2006; Zhao, 2007), limiting NF-κB activation has moderated inflammation with beneficial effects in a variety of CNS injury models (Schneider et al., 1999; Fernandez et al., 2007a; Khorooshi et al., 2008). Furthermore, the moderation of post-CNS injury damage by diverse anti-inflammatory treatments appears to be dependent on the inhibition of NF-κB activation (Blondeau et al., 2001). For example, the attenuation of apoptotic cell death after cortical contusion in rats by progesterone administration was associated with down-regulation of toll-like receptor expression and the moderation of NF-κB activation that resulted in decreased expression of intercellular adhesion molecule-1 (ICAM-1) and the inflammatory cytokines IL-1β, TNF-α and IL-6 (Chen et al., 2008). Similarly, NF-κB activation, neutrophil infiltration and astrogliosis were suppressed following cerebral artery occlusion in scavenger receptor CD36-null mice (Kunz et al., 2008). The neuroprotective effect of prostaglandin A after cerebral ischemia in rats also involved NF-κB inhibition (Zhang et al., 2008). In addition, the neuroprotection and suppression of post-ischemic inflammation by hypothermia (Yenari and Han, 2006), the inhibition of 5-lipoxygenase production of inflammatory leukotrienes (Jatana et al., 2006) and chelation of extracellular zinc released from damaged neurons (Kauppinen et al., 2008) all involved NF-κB inhibition. Finally, the development of tolerance to ischemia in cultured neurons and astrocytes following pre-conditioning with TNF-α treatment was dependent on inhibition of p65 NF-κB phosphorylation, thereby preventing binding to an adaptor protein, p300 that was required for ICAM-1 transcription (Ginis et al., 2002).

4.01 Inhibition of NF-κB in astrocytes as a therapy for CNS injury

As described in the previous Chapters, more severe astrogliosis has been associated with increased secondary neuronal damage and more extensive axon-growth inhibitory glial scarring. This association between the severity of the astrocytic inflammatory response

and tissue damage has led to research on NF-κB inhibition targeted specifically to astrocytes as a therapy for CNS injury. Inhibition of NF-κB in transgenic mice, bearing a dominant negative form of IκBα under the control of an astrocyte-specific GFAP promoter, resulted in decreased white matter damage and lesion size, followed by improved functional recovery after contusive spinal cord injury (Brambilla et al., 2005b; Brambilla et al., 2009). Decreased astrocytic expression of the pro-inflammatory chemokines, CXCL10 and CCL2, transforming growth factor-β2 and the chondroitin sulphate proteoglycans (CSPGs), neurocan and phosphacan accompanied the improvements in the injury response. Transforming growth factor-β2 regulates glial scar formation (Lagord et al., 2002), while secretion of neurocan and phosphacan and other CSPGs into the extracellular matrix is considered to contribute to the axon growth inhibitory environment of the glial scar (Properzi et al., 2005; Carter et al., 2008; Shen et al., 2008). In addition, transgenic mice with astrocyte-specific inhibition of NF-κB had less STAT2 upregulation in astrocytes, CCL2 expression and leukocyte infiltration in response to injury than wild-type mice (Khorooshi et al., 2008). Similarly, transgenic mice expressing an astrocyte-specific constitutively active form of the calcium-dependent phosphatase, calcineurin, exhibited less p65 NF-κB-dependent glial inflammation and neuronal death following penetrating brain injuries (Fernandez et al., 2007a). TNF-α activated the calcium-dependent phosphatase, calcineurin to induce inflammatory gene transcription in astrocytes through the NF-κB and NFAT pathways. However, at the later stages of injury responses, IGF-1 also recruited calcineurin in reactive astrocytes to inhibit NF-κB/NFAT activation. Calcineurin-dependent dephosphorylation of IκB by IGF-1 protected IκB against TNF-α initiated phosphorylation and subsequent translocation of NF-κB to astrocyte nuclei, suggesting a probable mechanism for the therapeutic anti-inflammatory effects of IGF-1 (Pons and Torres-Aleman, 2000). Three different inhibitors, SC-514, BAY 11-7082 and caffeic acid phenyl ester, which block distinct steps in the NF-κB pathway, attenuated the release of NO, TNF-α and chemokine receptor CXCL2 respectively from activated astrocytes and NO production was diminished in TNF-α knockout astrocytes (Phulwani et al., 2008). Inhibition of NF-κB by BAY 11-7082 and SN-50 also blocked the iNOS upregulation and subsequent NO production responsible for astrocyte swelling (Sinke et al., 2008). It therefore appears that

targeted inactivation of NF-κB in astrocytes may prevent the initiation of processes involved in the progression of inflammation and secondary cellular damage after injury.

4.02 OEC transplants and astrogliosis

Although as described in Chapter 1, there has been extensive research on OEC transplantation therapy for CNS injury, the molecular, cellular and tissue repair consequences of this therapy remain uncertain (reviewed by Chuah et al., 2010). It has been suggested that transplanted OECs could promote neuronal repair by their production of growth factors, by re-myelinating axons or by forming a permissive tract for axon growth across lesions. Another possibility is that transplanted OECs could moderate astrogliosis to provide a more permissive environment for axon regeneration at injury sites. The lack of boundary formation between astrocytes and co-cultured or transplanted OECs suggest that OECs may have a moderating effect on astrogliosis and glial scar formation (Lakatos et al., 2000; Lakatos et al., 2003a; Li et al., 2005b). Although there is divergent evidence concerning the behaviour and therapeutic efficacy of transplanted OECs, many studies report the amelioration of astrogliosis and glial scarring (Ramon-Cueto et al., 2000; Takami et al., 2002; Nieto-Sampedro, 2003; Plant, 2003; Ramer et al., 2004b). Since the severity of astrocytic inflammatory activation and glial scarring are key determinants of the extent of secondary neuronal damage and subsequently, the capacity for axon regeneration, this amelioration of astrogliosis by transplanted OECs could be an important component of any therapeutic effects. Improved axon regrowth in response to co-cultured or transplanted OECs has been associated with decreased GFAP upregulation by reactive astrocytes (Lopez-Vales et al., 2004; Li et al., 2005b; Richter et al., 2005; Lopez-Vales et al., 2006a), decreased astrocytic production of axon growth-inhibitory CSPGs (Leaver et al., 2006; Lopez-Vales et al., 2006a), prevention of the formation of a GFAP and CSPG enriched glial scar boundary (Ramer et al., 2004b) and prevention of the development of a fibrotic scar with basal laminae (Li et al., 2005b; Teng et al., 2008). Further evidence suggests that transplanted OECs may modulate the IL-1β, COX-2 and iNOS expression components of the inflammatory response at CNS injury sites to induce an initially more intense but shorter duration inflammation that moderates glial scarring and improves tissue repair (Lopez-Vales et al., 2004; Lopez-Vales et al., 2006b).

4.03 Research rationale

4.03.0 Do OECs moderate the inflammatory activation of astrocytes?

Although previous research provides some evidence that transplanted OECs may moderate astrogliosis and improve the permissiveness of the glial scar to axon growth, the evidence has been somewhat variable and inconsistent. This study was intended to further investigate the possibility that OECs could moderate the inflammatory responses of astrocytes with potentially beneficial consequences for recovery from CNS injury. NF-κB activation is a key early event in CNS injury responses leading to astrogliosis and as shown in Chapter 3, PMA/ionophore robustly induces rapid translocation of p65 NF-κB to astrocyte nuclei. This treatment model was therefore utilised to determine whether OECs could directly moderate astrocyte inflammatory activation. There has been no previous investigation into the direct effects of OECs on the initiation of astrocyte activation. The effects of OECs on astrocyte activation were compared with the effects of microglia and meningeal fibroblasts because both cell types interact with astrocytes during CNS injury responses. CNS injury rapidly activates microglia, stimulating their production of IL-1β, TNF-α, IL-6 and other inflammatory mediators (Davalos et al., 2005; Haynes et al., 2006; Hanisch and Kettenmann, 2007) that can promote astrogliosis and the development of the glial scar (Meeuwsen et al., 2003a; Bolin et al., 2005; John et al., 2005). Invading meningeal fibroblasts can interact with reactive astrocytes to exacerbate glial scarring by enhancing extracellular matrix protein deposition and forming axon-growth inhibitory basal laminae layers (Sandvig et al., 2004; Laabs et al., 2005; Teng et al., 2008). In addition, olfactory meningeal fibroblasts in OEC cultures may promote OEC migration and modulate interactions between OECs and astrocytes to, perhaps paradoxically, prevent the formation of inhibitory basal laminae in glial scars (Li et al., 2005b; Teng et al., 2008). Comparisons were also made between the effects of PMA/ionophore on NF-κB translocation in astrocytes, OECs, microglia and meningeal fibroblasts, since this treatment model has not previously been used to investigate NF-κB translocation in these cell types and their activation would be relevant to responses at CNS injury sites.

4.03.1 Do OECs moderate inflammatory gene transcription by astrocytes?

If OECs were found to moderate NF-κB translocation in astrocytes it was considered important to demonstrate that there was a corresponding moderating effect on the astrocytic transcription of NF-κB-regulated inflammatory genes relevant to CNS injury. NF-κB regulates transcription of granulocyte-macrophage colony-stimulating factor (GM-CSF) (Schreck and Baeuerle, 1990; Tsuboi et al., 1994; Brettingham-Moore et al., 2005a), which is rapidly upregulated following CNS injury together with other pro-inflammatory cytokines (Kaltschmidt et al., 1993; Franzen et al., 2004; Frugier et al., 2009). GM-CSF produced by astrocytes and microglia can promote proliferation and differentiation of microglia and recruited peripheral immune cells to phagocytic and antigen-presenting phenotypes (Hayashi et al., 1993; Re et al., 2002; Schermer and Humpel, 2002; Koguchi et al., 2003) with beneficial effects on wound-healing (Ellison et al., 1999; Schwartz, 2003; Jones et al., 2005; Kurpius et al., 2007). However, high levels of GM-CSF released by astrocytes can stimulate microglia to produce cytotoxic levels of TNF-α, IL-1β and IL-6 (Zaheer et al., 2007) that can exacerbate inflammation and astrogliosis (Guillemin et al., 1996; Lenzlinger et al., 2001; Meeuwsen et al., 2003a; John et al., 2005). Moderation of astrocytic GM-CSF production could therefore limit neuronal damage and improve tissue repair after CNS injury. GM-CSF regulates the production, differentiation and function of myeloid cells (Schreck and Baeuerle, 1990; Tsuboi et al., 1994; Brettingham-Moore et al., 2008) and has been well-characterised as a target gene for NF-κB following activation by PMA/ionophore in lymphocytes (Holloway et al., 2003; Brettingham-Moore et al., 2005a; Brettingham-Moore et al., 2008). However, PMA/ionophore stimulation of NF-κB translocation and induction of GM-CSF transcription have not previously been investigated in astrocytes. Therefore, to determine whether OECs could moderate NF-κB-dependent inflammatory gene expression in astrocytes, the effects of OECs and microglia on GM-CSF transcription in astrocytes were investigated following stimulation of astrocytic NF-κB translocation with PMA/ionophore.

4.04 Specific aims

1. Determine whether PMA/ionophore induces NF-κB translocation in OECs, microglia and meningeal fibroblasts.

2. Compare the effects of OECs, microglia and meningeal fibroblasts on NF-κB translocation in astrocytes.

3. Determine whether OECs moderate NF-κB translocation in astrocytes in vitro.

4. Determine whether OECs moderate GM-CSF transcription in astrocytes.

5. Compare the effects of OECs and microglia on GM-CSF transcription in astrocytes.

4.1 Materials and Methods

4.10 Cell culture

Astrocytes, OECs, microglia and meningeal fibroblasts were cultured on 18mm coverslips in 12-well culture plates, as described in Chapter 2. Direct co-cultures of astrocytes and OECs, astrocytes and microglia or astrocytes and fibroblasts were obtained by harvesting cells from flasks by trypsinisation and re-plating onto 18 mm coverslips in 12-well plates at approximately equal densities (10^4/cell type). After growth to confluence, this procedure typically resulted in co-cultures containing about 70% astrocytes. Astrocyte/OEC co-cultures were also prepared by establishing OEC cultures on cell culture inserts incorporating polyethylene terephthalate membranes with 400 nm pores (Becton Dickinson) and later transferring these to culture plate wells containing previously established astrocyte cultures on coverslips.

4.11 Immunocytochemistry

Following experimental treatments, monocultures were immunostained following the previously described protocols for p65 NF-κB and a cell marker protein: GFAP for astrocytes, $p75^{NTR}$ for OECs and CD11b for microglia. The purity of sample fibroblast cultures was verified by immunostaining for fibronectin and GFAP to show that cells were predominantly fibronectin positive/GFAP negative fibroblasts. However, fibroblast

cultures used in experiments were delineated with phalloidin staining of actin filaments rather than immunostaining for fibronectin, which is secreted and often formed an adherent layer on the PLL-coated coverslips (Fig. 2.7). All co-cultures were immunostained for NF-κB and GFAP to identify activated astrocytes. The identity of OECs, microglia and fibroblasts in the co-cultures with astrocytes was inferred from immunostaining of the monocultures from which they were derived and from the morphology revealed by NF-κB immunoreactivity in cells that did not express GFAP in each type of co-culture. Nuclei in all cells were counter-stained with Hoechst blue.

4.12 Comparisons of NF-κB translocation

Immunostained cultures were imaged as described in Chapter 2 and the resulting fluorescence microscope images were used for comparisons of nuclear relative to cytoplasmic NF-κB immunoreactivity intensity between:

1. astrocyte/OEC, astrocyte/fibroblast and astrocyte/microglia co-cultures stimulated with PMA/ionophore (Fig. 4.0)

2. cultures of astrocytes, OECs, microglia and fibroblasts stimulated with PMA/ionophore (Fig. 4.1)

3. astrocytes in astrocyte-, OEC- or microglia-conditioned medium (Fig. 4.3)

4. astrocytes in DMEM, OEC- or microglia-conditioned medium stimulated with PMA/ionophore (Fig. 4.4)

5. astrocytes pre-incubated for 24 hours with OECs on tissue culture inserts or astrocytes alone, with both culture types then stimulated by incubation in microglia-conditioned medium in the presence or absence of PMA/ionophore (Figs. 4.5, 4.6)

6. astrocytes stimulated with PMA/ionophore or microglia-conditioned medium in the presence or absence of insulin-like growth factor-1 (Millipore) (Fig. 4.7).

4.13 Quantitative analysis of cell activation

Astrocyte activation in monocultures was quantified using HCA-Vision© software as described in Chapter 3. Astrocyte activation in co-cultures, in comparisons between co-cultures and other treatments and activation of other cell types were scored manually because of differences in the NF-κB immunoreactivity intensity between the different cell types. By either method, cells were scored as activated only when their nuclear NF-κB immunoreactivity was visibly more intense than the cytoplasmic NF-κB immunoreactivity. At least eight images (selected randomly as described previously) showing ~120 cells/image from 2-3 separate cell cultures were analysed to generate means for each treatment group. Data were analysed for significant differences between treatment group means by ANOVA and post-hoc Tukey tests.

4.14 Quantitative RNA analysis by real-time PCR

4.14.0 RNA isolation from treatment samples

Astrocyte cultures in 6-well culture plates were treated with 20ng/mL PMA/ 250nM ionophore in DMEM, OEC CM or microglia CM for 4, 8, 12, 18 or 24 h with untreated cultures in DMEM as comparison controls. Total RNA was isolated using Tri-Reagent (Sigma) according to the manufacturer's protocol. Briefly, culture wells were washed with PBS after removal of culture medium was removed from culture wells and cells lysed with the addition of 1 mL Tri-Reagent to each well. Wells were scraped to remove any remaining adherent material and after 5-10 minutes samples were removed into eppendorfs and stored at -80^{o}C. Samples were thawed at room temperature and 200 μL chloroform added to each sample tube with vigorous shaking for 15 seconds. After 15 minutes incubation at room temperature, samples were centrifuged at 13000rpm for 20 minutes and the upper clear aqueous phase containing the RNA transferred to new eppendorfs. 500μl of isopropanol was added to each sample, mixed by inversion, RNA precipitated by overnight incubation at -20^{o}C (or -80^{o}C for 30 minutes), centrifuged at 13000rpm for 20 minutes at room temperature, the supernatant removed, 1mL 75% ethanol added to each pellet and mixed by vortexing followed by centrifugation at 13000rpm for 20 minutes at room temperature. The supernatant was then removed, the pelleted RNA air-dried at room temperature over several minutes and re-suspended in

50µL MilliQ water with vortexing followed by incubation at 65^{o}C for 5 minutes. Samples were then consolidated by brief centrifugation at 13000 rpm and the purity and RNA content of each sample measured on a Nanodrop Spectrophotometer (ND-1000). 2µL undiluted aliquots of each sample were used for the measurements and RNA content was quantified by measuring the optical density at 260nm. Optical density was measured to preclude protein contamination of RNA samples with a 260nm:280nm fluorescence ratio of $\geq$ 1.8 indicating sufficient RNA purity. The RNA sample solutions were then snap frozen in liquid nitrogen and stored at –80^{o}C.

4.14.1 cDNA synthesis

1µg of each RNA sample was used to synthesise cDNA by reverse transcription using Superscript II Reverse Transcriptase (Life Technologies). All samples for each experiment were processed simultaneously with each sample reaction in a separate eppendorf tube. Any remaining genomic DNA was degraded by incubation with DNase prior to reverse transcription. Sufficient RNA solution to provide 1µg of RNA for each sample was added to 2µl of 5x first strand buffer (Invitrogen), 1µl of DNase (Sigma) and sufficient MilliQ water for a total volume of 10µL. The solution was incubated at 37^{o}C for 30 minutes and the DNase then inactivated by heating to 75^{o}C for 5 minutes. 1µl of 1µg/ml oligodT primer (Invitrogen) and 3.5µl of water were added, reactions incubated at 70^{o}C for 10 minutes and then chilled on ice to promote oligodT binding to RNA poly-A tails. 2µL of 5x first strand buffer, 2µl of 0.1M DTT (Invitrogen), 1µl of 10mM dNTPs (Promega) and 0.5µl of Superscript reverse transcriptase (Invitrogen) was then added, each reaction incubated at 42^{o}C for 50 minutes for transcription and the transcriptase then inactivated by heating to 70^{o}C for 15 minutes. Master mixes of sufficient volume were prepared for each of the above incubation steps and equally aliquotted to each sample tube, to minimise cross-contamination between samples. The resulting cDNA samples were stored at –80^{o}C.

4.14.2 Real time PCR

Primers were designed using Primer 3 **(http://frodo.wit.mit.edu/cgi-bin/primer3/)** and sequences obtained from the NCBI website (http://www.ncbi.nlm.nih.gov/). Primers were

designed to have melt temperatures of about 60ºC and to generate product sizes of about 100 base pairs. The lypophilised oligonucleotide primers (Sigma) were diluted to 100μM with sterile MilliQ water and then, in separate tubes, 5μM for working stocks. Real time quantification of DNA amplification was achieved using a QuantiTect SYBR Green PCR kit (Qiagen) on a Rotor-Gene 2000 real-time cycler (Corbett Research), as described previously (Brettingham-Moore et al, 2005). PCR was conducted using the rattus norvegicus (rat) GM-CSF primers, sense: 5'-CCCGCCTGAAGCTATACAAG-3' and antisense: 5'-AGTGGCTGGCTATCATGGTC-3' in parallel with the rat GAPDH primers, sense: 5'-TGCCACTCAGAAGACTGTGG-3' and antisense: 5'-GGATGCAGGGATGA-TGTTCT-3', to normalize for differences in cDNA synthesis and RNA input. GAPDH was used as a loading control for Western blotting of astrocyte samples in Chapter 3 and did not appear to be regulated by the treatment conditions. The cDNA was diluted 1:5 for real time PCR and a 5μl aliquot used in each reaction. The other reagents were prepared as a master mix to minimise cross contamination, in the following proportions: 12.5 μL SYBR green, 1.5μL forward primer (5μM), 1.5μL reverse primer (5μM) and 4.5μL RNase-free water, for a total reaction volume of 25μL. A no template control, where the 5μl of sample cDNA was replaced with 5μl of RNase free water, was prepared for each run to detect any contaminating DNA. The PCR cycling conditions were as follows for all samples: melt at 95^{o}C held for 15 minutes, 40 cycles of 95^{o}C hold for 15 seconds followed by 60^{o}C hold for 60 seconds with data acquired to cycling channel 1, melt from 60-95^{o}C holding for 5 seconds after each 1^{o}C increase with data acquired to melt channel 1. Analysis of PCR product melt curves for a single peak and product visualization by agarose (2%) gel electrophoresis with ethidium bromide staining indicated that PCR generated single products of the expected size (81 base pairs for GM-CSF, 85 base pairs for GAPDH). Threshold values from the amplification plots derived from the acquired cycling data were converted to copy number by generating a standard curve using purified GM-CSF and GAPDH PCR products. Three separate culture samples analysed in separate PCR amplifications were used for each culture condition and time-point. Data were analysed for significant differences between treatment group means by ANOVA and post-hoc Tukey tests.

4.14.3 DNA purification and standard curves

Real time PCR DNA products were purified by ethanol precipitation to remove other reaction components. Each PCR reaction solution (25µl) was added to a microcentrifuge tube containing 3µl of 3M sodium acetate (pH~6, Ajax chemicals) and 75µl of 100% ice cold ethanol (Sigma), incubated for 24 hours at -20ºC to precipitate DNA, centrifuged at 13,000 rpm for 5 minutes at 4ºC and the DNA pellet washed in 70% ice cold ethanol. The DNA was then vacuum dried for 5-10 minutes and resuspended in 30µL of MilliQ water by vortexing after heating to 65ºC. The DNA concentration of sample solutions was determined from their measured optical density at 260nm, known product size and the calculated number of DNA product copies. Solutions were serially diluted to produce 8 standard solutions containing 10^9-10^2 copies/µl of PCR product. These standards of known copy number were then quantified by real time PCR as described above to generate standard curves of copy number plotted against threshold value.

4.2 Results

4.20 OECs moderate activation of co-cultured astrocytes both in the absence and presence of PMA/ionophore

One-hour combined PMA/ionophore treatment was used to compare the activation responses of astrocytes that were co-cultured with OECs, fibroblasts or microglia and astrocyte monocultures (Fig. 4.0A). PMA/ionophore treatment induced significant increases in the percentages of activated astrocytes in all cultures ($p < 0.001$) (Fig. 4.0) similar to those previously seen in astrocyte monocultures (Fig. 3.1). The results suggested a moderating effect of OECs on astrocyte inflammation with significantly fewer activated astrocytes occurring in astrocyte/OEC co-cultures (Fig. 4.0B, C, H) than in co-cultures of astrocytes with fibroblasts (Fig. 4.0D, E, H) or microglia (Fig. 4.0F, G, H) and astrocyte monocultures for both untreated (astrocyte/OEC, 0.7±0.3%; astrocyte/fibroblasts, 9.8±3.63 %; astrocyte/microglia, 30.9±2.3%; astrocytes, 7.3±1.8%; $p < 0.001$) and PMA/ionophore-treated cultures (astrocytes/OECs, 34.6±4.4%; astrocytes/fibroblasts, 55.3±5.3%; astrocytes/microglia, 53.0±4.7%; $p < 0.01$; astrocyte monocultures, 62.1±1.8%; $p < 0.001$). There were significantly more activated astrocytes

in the untreated astrocyte/microglia co-cultures than for untreated astrocyte/fibroblast, astrocyte/OEC co-cultures or astrocyte monocultures (Fig. 4.0H) ($p < 0.001$). However, percentages of activated astrocytes were not significantly different between untreated astrocyte monocultures and astrocyte/fibroblast co-cultures or between astrocyte monocultures and astrocyte/microglia or astrocyte/fibroblast co-cultures after the increase in activation induced by PMA/ionophore. PMA/ionophore also appeared to activate some microglia (asterisks, Fig. 4.0F, G) and fibroblasts (asterisks, Fig. 4.0D, E) in the co-cultures. However, OECs in the co-cultures did not appear to be activated by PMA/ionophore despite displaying strong cytoplasmic immunoreactivity for NF-κB (asterisks and arrows, Fig. 4.0B, C).

4.21 PMA/ionophore activates all cell types except OECs

The apparent differences in activation of the different cell types in the co-cultures were further investigated by comparing their NF-κB translocation responses to PMA/ionophore using monocultures of astrocytes, microglia, meningeal fibroblasts and OECs. Microglia had a higher basal level of activity, there being significantly more activated cells in the untreated cultures of microglia (Fig. 4.1C, I) than for the other cell types ($p < 0.001$) (Fig. 4.1A, E, G, I). PMA/ionophore induced significant increases in activation for astrocytes ($p < 0.001$) (Fig. 4.1B, I), microglia ($p < 0.05$) (Fig. 4.1D, I) and meningeal fibroblasts ($p < 0.001$) (Fig. 4.1F, I) to levels that were not significantly different for these three cell types ($p > 0.05$) (Fig. 4.1I). In contrast, PMA/ionophore did not activate OECs (Fig. 4.1H). Although OECs displayed bright cytoplasmic NF-κB immunoreactivity in the untreated (Fig. 4.1G) and treated (Fig. 4.1H) cultures, OEC nuclear immunoreactivity was never observed to be brighter than the cytoplasmic immunoreactivity. Apparent faint NF-κB immunoreactivity within the nuclear regions of OECs (asterisks, Fig. 4.1G, H) was probably due to overlying cytoplasmic immunoreactivity because it was not distributed evenly throughout the nuclear region, was absent when nuclei could be distinguished without overlying cytoplasm (arrows, Fig. 4.1G, H) and was not altered by PMA/ionophore treatment (Fig. 4.1H). Consequently, OECs were deemed to be not activated by PMA/ionophore.

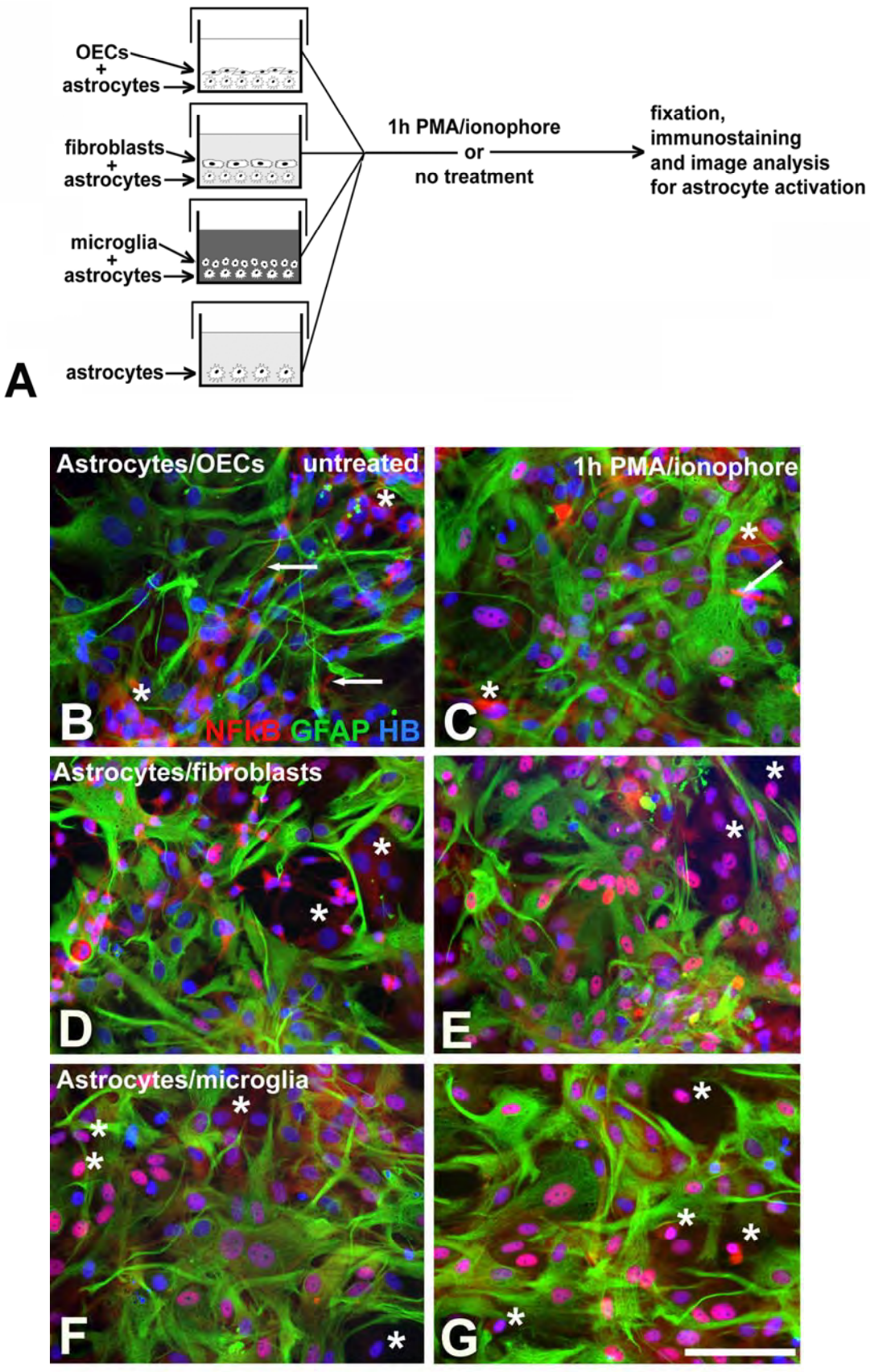
OECs
+
astrocytes
fibroblasts
+
astrocytes
microglia
+
astrocytes
astrocytes
1h PMA/ionophore
or
no treatment
fixation,
immunostaining
and image analysis
for astrocyte activation
A
Astrocytes/OECs
untreated
B
NFkB GFAP HB
1h PMA/ionophore
C
Astrocytes/fibroblasts
D
E
Astrocytes/microglia
F
G

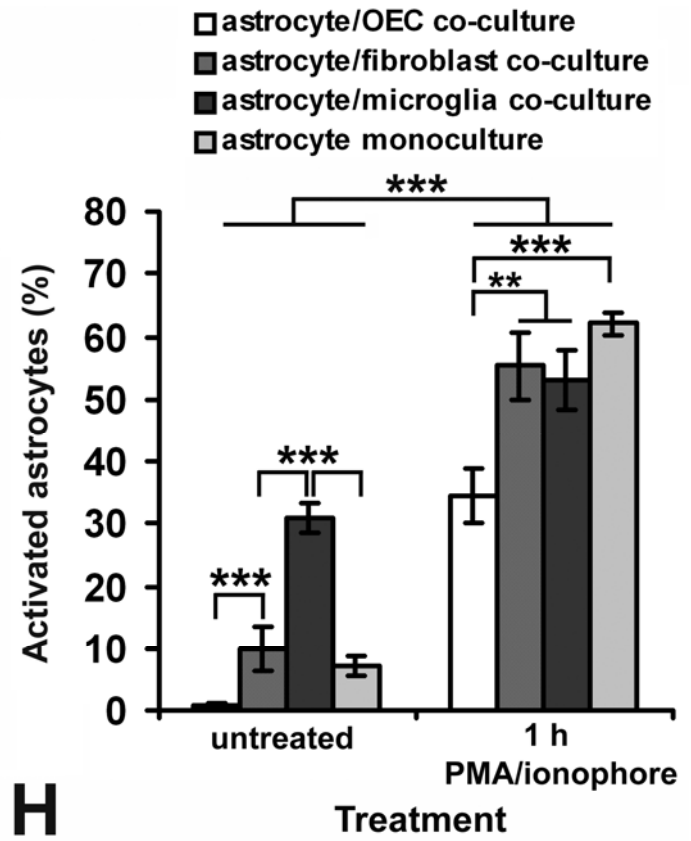

Figure 4.0 Comparison of astrocyte activation in co-cultures with OECs, microglia or meningeal fibroblasts. A: Co-cultures of astrocytes with OECs, astrocytes with meningeal fibroblasts or astrocytes with microglia and for control comparison, astrocyte monocultures, were treated with PMA/ionophore or were untreated. B-G: Cultures were immunostained for NF-κB (red) and GFAP (green), with nuclei counterstained using Hoechst blue. The majority of nuclei in the images belong to GFAP positive astrocytes except in B where there are some dense clusters of OECs (asterisks). There appeared to be more NF-κB positive astrocyte nuclei in the untreated astrocyte/microglia co-cultures (F) than for the other untreated co-cultures (B, D). Although PMA/ionophore increased astrocyte activation in all cultures (C, E, G), there was fewer activated astrocytes in the astrocyte/OEC co-cultures (C). Bright cytoplasmic NF-κB staining occurred in OEC cell bodies (asterisks in B, C) and processes (arrows in B, C). NF-κB immunoreactivity in OEC nuclei in the co-cultures appeared to be of low intensity before (asterisks in B) and after treatment (asterisks in C) while PMA/ionophore increased nuclear NF-κB immunoreactivity for fibroblasts (asterisks in D, E) and microglia (asterisks in F, G). Scale bar is 100 μm. H: Quantitative analysis of astrocyte activation in co-cultures with OECs, microglia or meningeal fibroblasts and astrocyte monocultures. PMA/ionophore (P/I) induced significant increases in astrocyte activation in all cultures ($p < 0.001$). There were significantly fewer activated astrocytes in astrocyte/OEC co-cultures than in astrocyte/microglia or astrocyte/fibroblast co-cultures either in the absence ($p < 0.001$) or presence of PMA/ionophore treatment ($p<0.01$ or $p<0.001$ for astrocyte monocultures). There were also significantly more activated astrocytes in the untreated astrocyte/microglia co-cultures than in the other untreated cultures ($p<0.001$). Percentages are means ± SEM, n = 15; ** $p<0.01$, *** $p<0.001$.

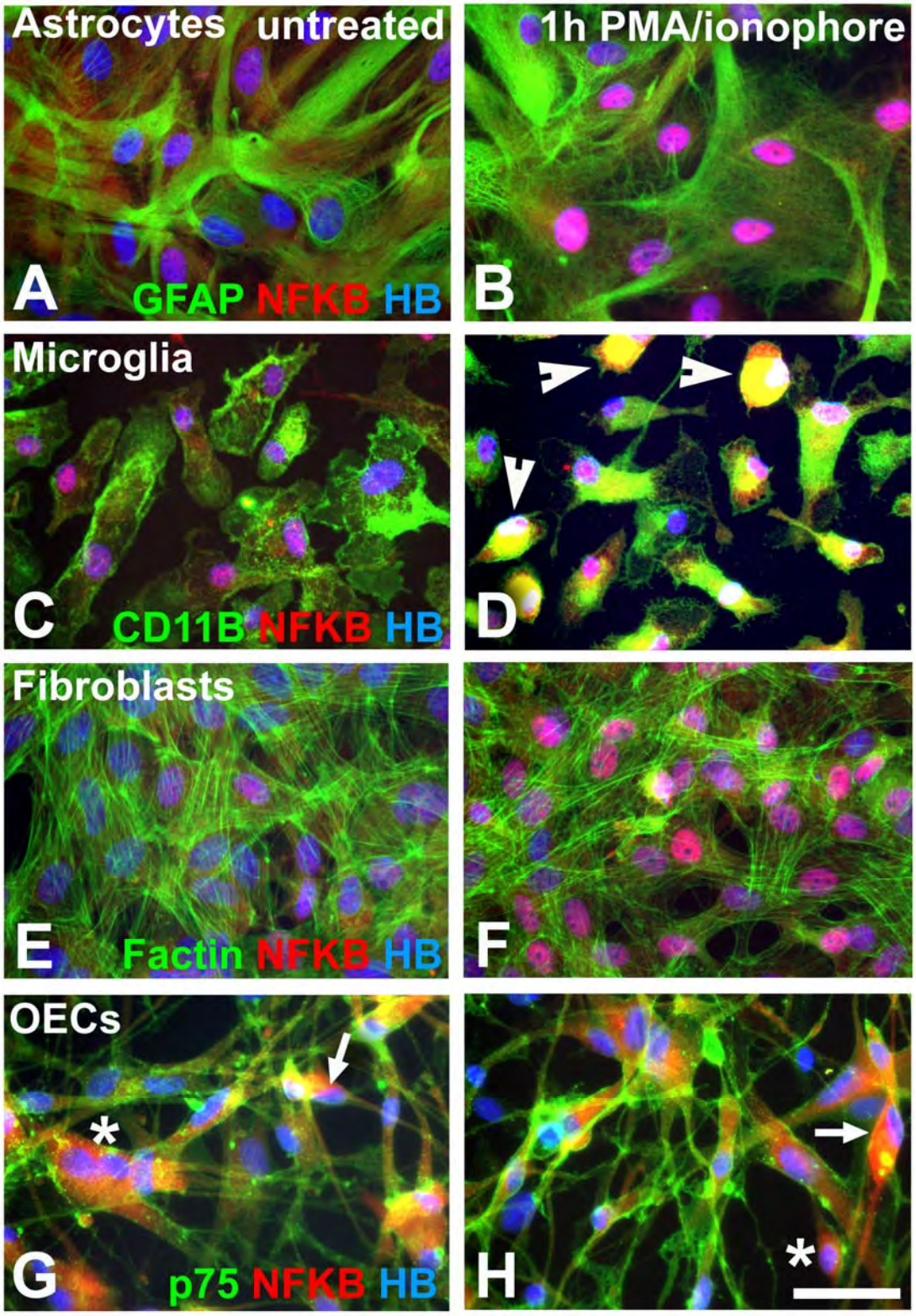
Astrocytes untreated
A
GFAP NFKB HB
1h PMA/ionophore
B
Microglia
C
CD11B NFKB HB
D
Fibroblasts
E
Factin NFKB HB
F
OECs
G
p75 NFKB HB
H

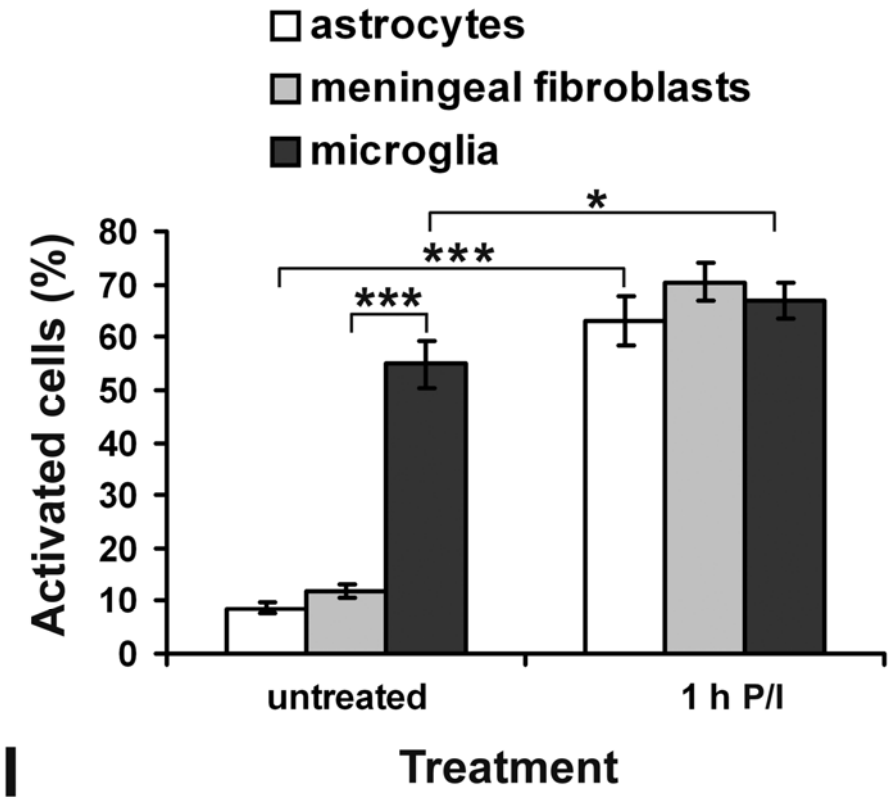

Figure 4.1 PMA/ionophore activates all cell types except OECs. Cultures of each cell type were treated with PMA/ionophore and untreated cultures provided comparison controls. Cultures were immunostained for NF-κB (red), and cell specific proteins (green); GFAP for astrocytes (A, B), CD11B for microglia (C, D) and $p75^{NTR}$ for OECs (G, H). Meningeal fibroblasts (E, F) were delineated with phalloidin staining of cytoskeletal actin filaments (green). Nuclei were stained with Hoechst blue (HB). More intense nuclear immunoreactivity for NF-κB following activation by PMA/ionophore occurred for astrocytes (B), microglia (D) and meningeal fibroblasts (F) but not for OECs (H). After PMA/ionophore treatment, some microglia appeared to be highly activated, displaying rounded morphologies with intense NF-κB and CD11B immunoreactivity (arrowheads in D). OECs displayed bright to moderate intensity cytoplasmic NF-κB immunoreactivity in cell bodies and processes with no difference in the NF-κB immunoreactivity between untreated (G) and PMA/ionophore treated (H) cultures. Where cytoplasmic NF-κB immunoreactivity was intense there was faint nuclear immunoreactivity (asterisks in G and H) probably due to overlying cytoplasmic immunoreactivity. This was confirmed by fortuitously orientated OECs that allowed Hoechst blue-stained nuclei, devoid of NF-κB, to be distinguished from adjacent bright cytoplasmic NF-κB immunoreactivity (arrows in G and H). Scale bar is 50 μm. I: Quantitative analysis of PMA/ionophore (P/I) activation of astrocytes, microglia and meningeal fibroblasts. There were significantly more activated microglia than astrocytes or fibroblasts in the untreated cultures ($p < 0.001$). PMA/ionophore induced significant increases in activation of the three cell types ($p < 0.05$ for microglia; $p < 0.001$ for astrocytes and fibroblasts). Results for OECs were not graphed since they had no NF-κB positive nuclei. Data were analysed by 2-way ANOVA and post-hoc Tukey's multiple comparison test. Percentages are means ± SEM, n = 15. Asterisks denote significant differences: * $p < 0.05$, *** $p < 0.001$.

Contaminating fibroblasts in some OEC cultures were also activated by PMA/ionophore (Fig. 4.2) and if counter-staining with $p75^{NTR}$ had not been used to identify OECs (Fig. 4.1G, H; Fig. 4.2B, green in D) it would have been possible for activated $p75^{NTR}$-negative fibroblasts (Fig. 4.2A, B, D) to have been misinterpreted as activated OECs.

4.22 Microglia release soluble factors that activate astrocytes

Microglia had a relatively high level of basal activity in the culture conditions (Fig. 4.1C, I) and when co-cultured with microglia, about 31% of astrocytes were already activated before PMA/ionophore treatment (Fig. 4.0F, H). Astrocyte cultures were therefore incubated with microglia-conditioned medium (CM) (Fig. 4.3E, F) for 30 minutes, 1 hour, 2 hours or 3 hours to test whether soluble factors released by activated microglia could have been responsible for the previously observed activation of co-cultured astrocytes. Astrocytes were also incubated with media conditioned by OECs and astrocytes for comparisons (Fig. 4.3A-D). Incubation with astrocyte CM and OEC CM induced small significant increases in astrocyte activation within 30 minutes (10.2±1.3 % and 9.9±2.1 % respectively; $p < 0.05$ which represented increases of about 5% from levels prior to the medium change. However these responses were significantly much less than the increase induced by microglia CM (38.4±4.1 %; $p < 0.001$) (Fig. 4.3G). Activation remained significantly higher in the presence of microglia CM at 1 hour (59.3±4.5 %; $p < 0.001$) and 2 hours (20.4±2.4 %; $p < 0.01$) after the medium changes. Significantly more astrocytes were activated following the 1 hour of incubation with microglia CM than after about 4 days of co-culture with microglia ($p < 0.01$) (Figs. 4.1H, 4.3G). Activation had returned to basal levels for all cultures by 3 hours after the medium changes. Therefore, the data indicated that microglia-derived soluble factors activated astrocytes in a similar manner to PMA/ionophore with NF-κB translocation induced mainly within the first hour of exposure to either treatment. Since these results indicated that medium change alone could induce some activation, astrocytes were pre-incubated in media for 24 hours prior to reagent treatments to eliminate any possible confounding effect.

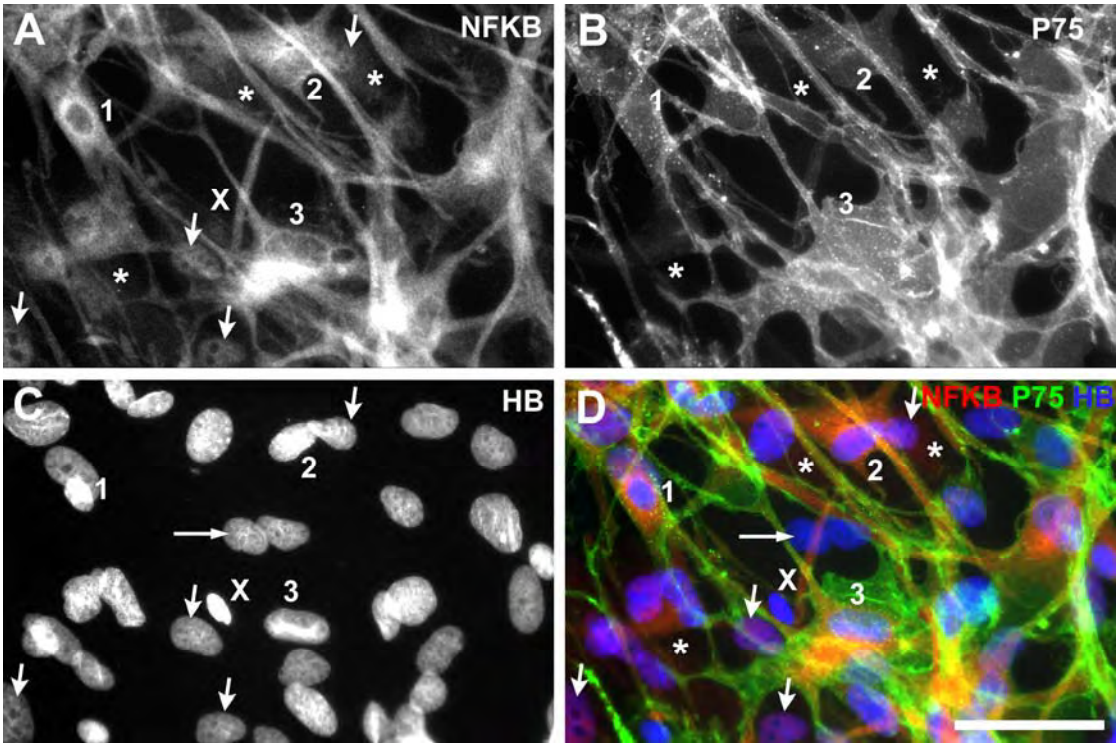

Figure 4.2 Contaminating fibroblasts in OEC cultures. The images represent an OEC culture with contaminating fibroblasts after 1 hour of PMA/ionophore treatment. Cells were immunostained for NF-κB (A and red in D) and counterstained for $P75^{NTR}$ (B and green in D) to identify OECs. Nuclei were stained with Hoechst blue (C and blue in D). Bright cytoplasmic NF-κB immunoreactivity in OEC cell bodies and processes (A) co-localised with $p75^{NTR}$ (B and D). Faint cytoplasmic immunoreactivity in fibroblasts (asterisks in A) occurred in $p75^{NTR}$ negative regions (asterisks in B and D). OEC nuclei occupy regions of low intensity NF-κB immunoreactivity (e.g. 1, 2, and 3 in A-D) ringed by brighter cytoplasmic immunoreactivity. OEC nuclei and cytoplasm sometimes overlapped with fibroblasts (e.g. 1 and 2) or with other OECs (e.g. 3). Fibroblast nuclei were usually larger than OEC nuclei and the majority were NF-κB positive (vertical arrows in A, C and D). Two NF-κB negative fibroblast nuclei are in the centre of the images (long horizontal arrow in C and D). A small nucleus with intense Hoechst blue staining (X in C and D) and low NF-κB immunoreactivity (X in A) probably represents an apoptotic fibroblast. Scale bar is 50 μm.

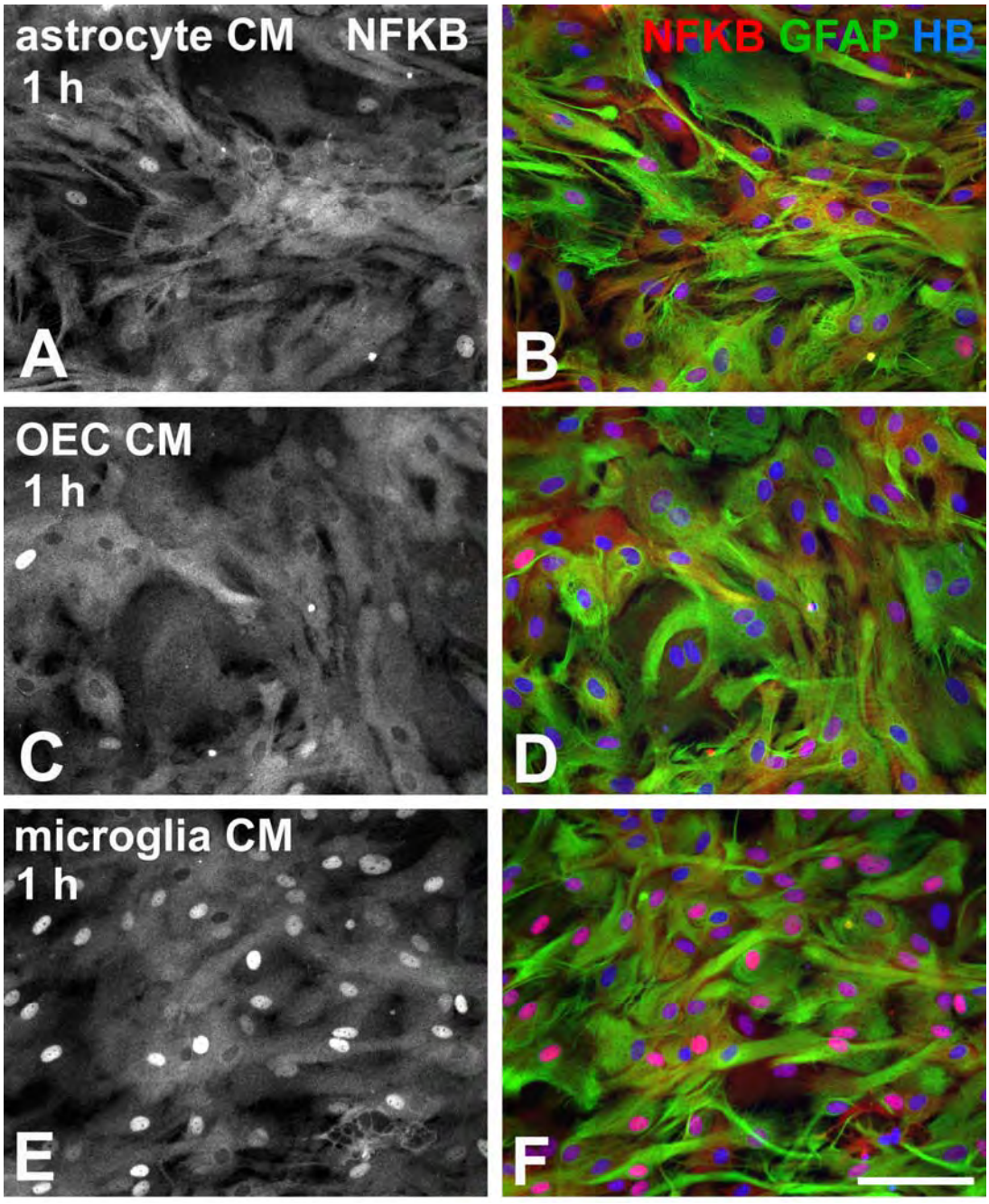
astrocyte CM NFKB
1 h
A
NFKB GFAP HB
B
OEC CM
1 h
C
D
microglia CM
1 h
E
F

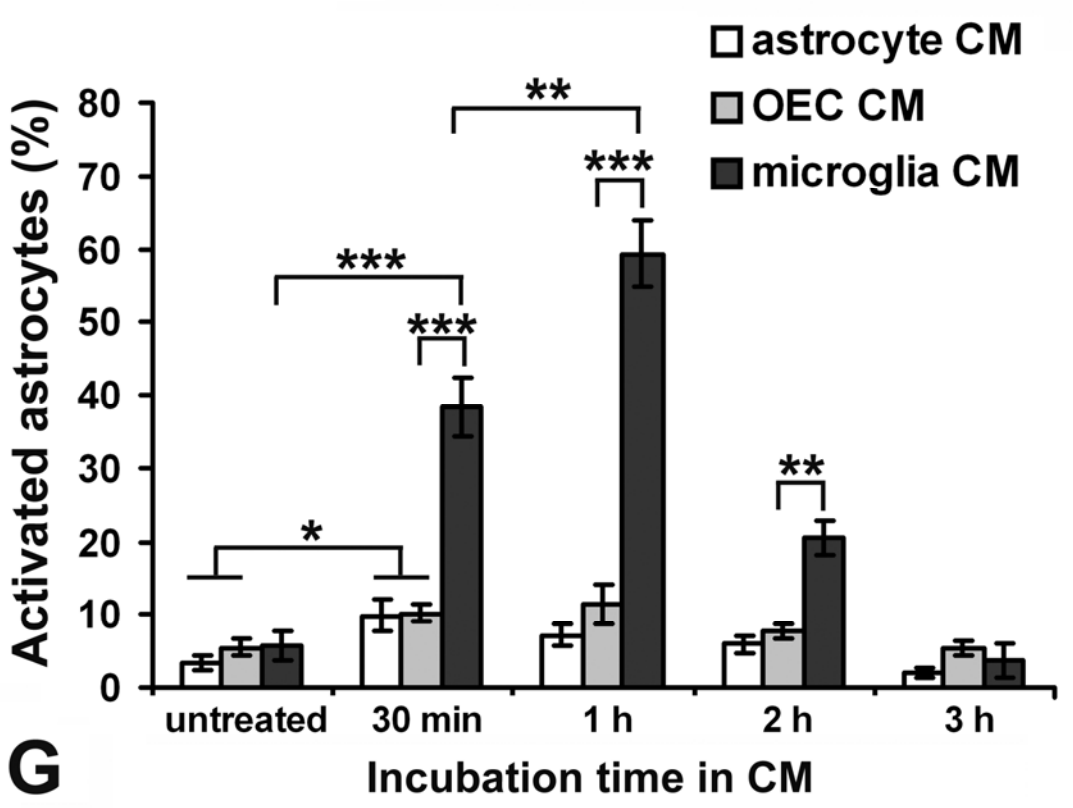

Figure 4.3 Microglia CM activates astrocytes. Astrocytes were incubated for 30 minutes, 1 hour, 2 hours or 3 hours in medium conditioned for 24 hours by astrocyte (A, B), OEC (C, D) or microglia cultures (E, F). Cultures were immunostained for NF-κB (A, C, E and red in B, D, F) and GFAP (green in B, D, F). Nuclei were counterstained with Hoechst blue (B, D, F). Only astrocytes incubated in microglia-conditioned medium (CM) had noticeably increased activation as indicated by high levels of nuclear NF-κB immunoreactivity (E, F). Scale bar is 100 μm. G: Quantitative analysis of astrocyte activation by CM. Incubation with microglia CM induced a highly significant increase in astrocyte activation within 30 minutes ($p < 0.001$). Although 30 minutes and 1 hour of incubation with astrocyte CM and OEC CM induced small significant increases in astrocyte activation ($p < 0.05$) these were significantly less than the large increase in activation induced by microglia CM ($p < 0.001$). After 2 hours of incubation, astrocyte activation had returned to basal levels except for astrocytes incubated with microglia CM where activation remained significantly higher ($p < 0.01$) until 3 hours after the medium change. Data were analysed by 2-way ANOVA and post-hoc Tukey's multiple comparison test. Percentages are means ± SEM, n = 12. Asterisks denote significant differences: * $p < 0.05$, ** $p < 0.01$, *** $p < 0.001$.

4.23 OECs release soluble factors that moderate astrocyte activation

4.23.0 OEC CM moderates astrocyte activation by PMA/ionophore

The effects of media conditioned by OECs or microglia on astrocyte activation were then compared to investigate whether soluble factors released by the OECs could have mediated the moderation of astrocyte activation by the co-cultured OECs. Astrocyte cultures were incubated in OEC CM, microglia CM or DMEM for 24 hours and then activated with PMA/ionophore (Fig. 4.4A). The OEC- and microglia-conditioned media had similar effects on PMA/ionophore-induced astrocyte activation as occurred when astrocytes were co-cultured with these same cell types. There were significantly fewer astrocytes activated by PMA/ionophore for cultures incubated in OEC CM (31.3±2.5 %; Fig. 4.4B, C, F) than for cultures incubated in microglia CM (58.6±1.6 %; Fig. 4.4D, E, F) or DMEM (56.4±2.6 %; Fig. 4.4F) ($p < 0.001$). There was no significant difference in PMA/ionophore induced astrocyte activation between cultures pre-incubated 24 hours with microglia CM and those pre-incubated with DMEM ($p > 0.05$). Comparisons revealed that the moderating effects of OEC CM on astrocyte activation were similar to those resulting from co-culture of astrocytes with OECs (Figs. 4.1H, 4.4F), suggesting that the effects of the co-cultured OECs were mediated substantially by soluble factors released by the OECs.

4.23.1 Soluble factors released by OECs moderate astrocyte activation by PMA/ionophore and microglia CM

Results in Fig 4.3G showed that like PMA/ionophore, soluble activating factors derived from microglia had most effect on astrocytes within the first hour of exposure. Therefore, perhaps due to the rapid depletion or de-activation of the microglia-derived factors, pre-incubation for 24 hours with microglia CM did not enhance PMA/ionophore induction of NF-κB translocation in astrocytes. It is also possible that PMA/ionophore and the microglia-derived factors exerted their effects through similar intracellular pathways and that the observed ~55-60 % of astrocytes activated was the maximum possible for these stimuli. Astrocytes proliferate and differentiate in culture and may not all be synchronously responsive to activating stimuli. To differentiate between these two alternatives and because astrocytes can be activated by multiple stimuli following CNS

injury, we wanted to determine whether soluble factors derived from OECs were able to moderate activation of astrocytes by microglia in both the presence and absence of PMA/calcium ionophore (Fig. 4.5). OEC cultures were established on permeable nitrocellulose membranes that were later inserted into culture wells above astrocyte cultures, 24 hours prior to the cultures being treated with microglia CM, PMA/ionophore or simultaneously with both stimuli (Fig. 4.5A). Pre-incubation with OECs on inserts resulted in significant decreases from about 58% to 22% of astrocytes being activated by microglia CM, PMA/ionophore or simultaneously by both treatments ($p<0.001$) (Fig. 4.5F). These results confirmed that a soluble factor released by OECs moderated the astrocyte activation induced by either PMA/ionophore or by microglia CM and that there was no additional activation of astrocytes when stimulation with microglia CM was combined with PMA/calcium ionophore. Therefore the percentage of synchronously activated astrocytes approximated the maximum measurable for these stimuli under the culture conditions. Most importantly, under all the treatment conditions tested, OECs were able to attenuate the activation of astrocytes. The observed small differences in the apparent OEC-mediated moderation of astrocyte activation could have been related to the different duration of exposure of astrocytes to soluble factors released by OECs and possible interactions between astrocytes and OECs allowed by the different treatment models. In the OEC/astrocyte co-cultures, astrocytes were exposed to soluble factors released by the OECs for several days prior to treatment and these untreated co-cultures had fewer activated astrocytes than any other cultures. However, following PMA/ionophore treatment there were significantly fewer activated astrocytes for astrocytes co-cultured with OECs on tissue culture inserts (Fig. 4.5F), which separated the two cell types by about 4mm, than for either astrocytes in direct co-culture with astrocytes (Fig. 4.0H) or astrocytes incubated in OEC CM (Fig. 4.4F) ($p < 0.05$).

4.23.2 Combined treatment with PMA/ionophore and microglia CM activated some OECs

Immunostaining of OEC cultures on inserts (Fig. 4.6) used during astrocyte treatments confirmed that as found previously (Fig. 4.1G, H) PMA/ionophore (Fig. 4.6C, D and, in addition, microglia CM (Fig. 4.6A, B) did not induce NF-κB translocation in OECs.

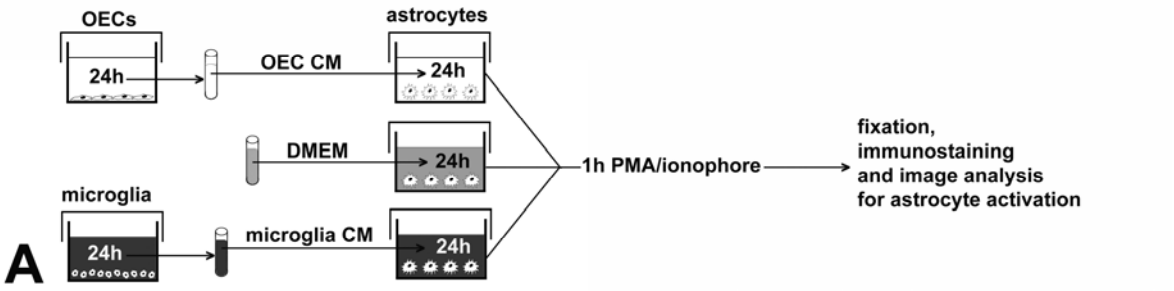
OECs
24h
OEC CM
astrocytes
24h
DMEM
24h
microglia
24h
microglia CM
24h
1h PMA/ionophore
fixation,
immunostaining
and image analysis
for astrocyte activation
A

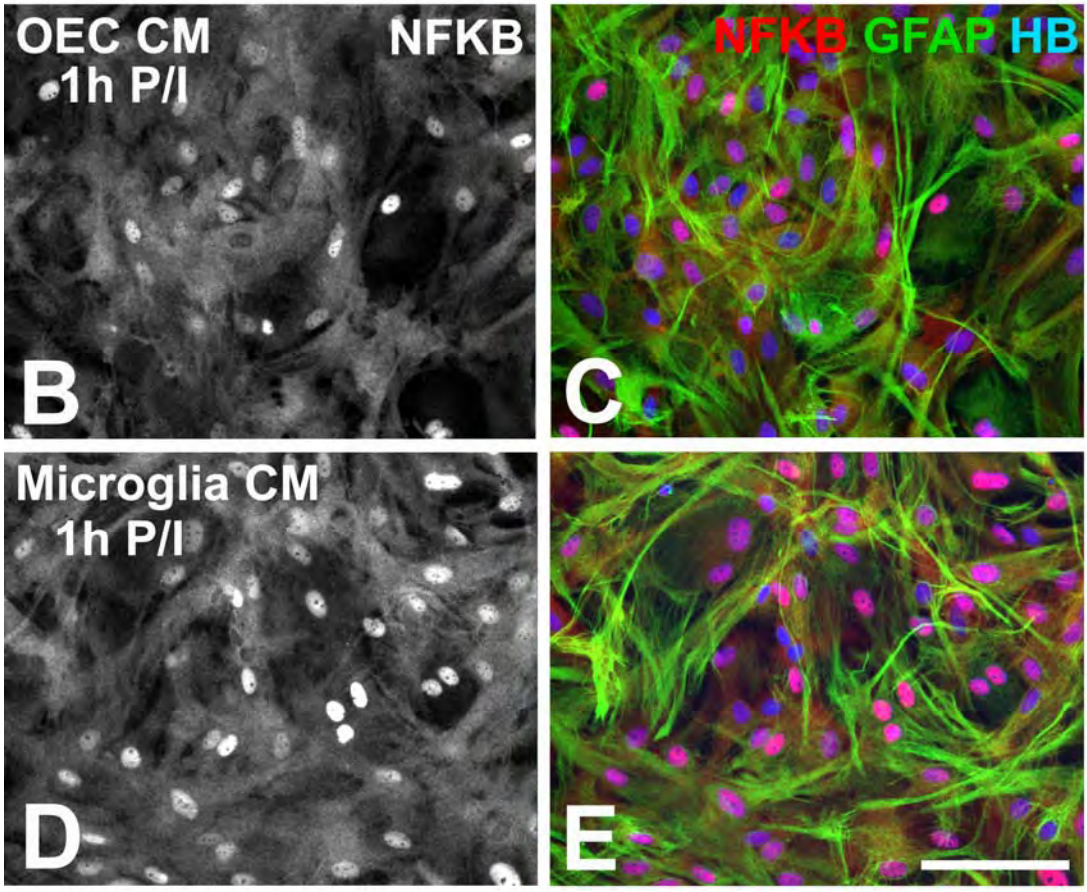
OEC CM
1h P/I
NFKB
B
NFKB GFAP HB
C
Microglia CM
1h P/I
D
E

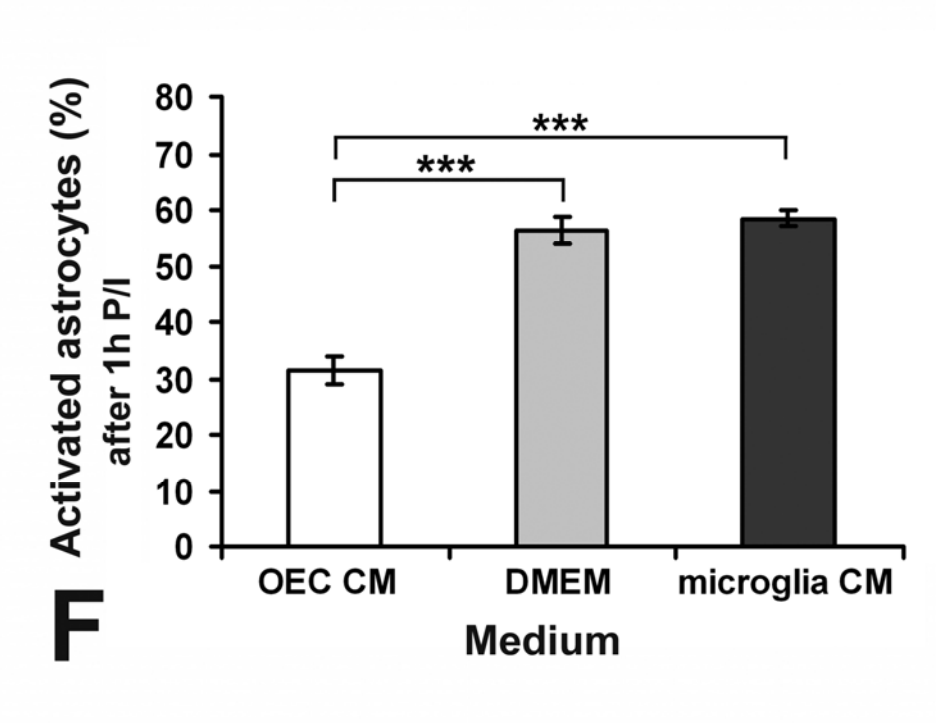

Figure 4.4 OEC CM moderates activation of astrocytes by PMA/ionophore. Astrocytes in DMEM and astrocytes pre-incubated in medium conditioned by OECs or microglia were stimulated with PMA/ionophore (A). Cultures were immunostained for NF-κB (B, D and red in C, E) and GFAP (green in C, E). Nuclei were counterstained with Hoechst blue (C, E). Following treatment with PMA/ionophore more astrocytes in microglia-conditioned medium (CM) (D, E) had intense nuclear NF-κB immunoreactivity than astrocytes in OEC CM (B, C). Scale bar is 100 μm. F: Quantitative analysis of astrocyte activation after 1 hour incubation with PMA/ionophore in OEC CM, microglia CM or DMEM. There was significantly less astrocyte activation induced by PMA/ionophore in OEC CM than when in microglia CM or DMEM ($p < 0.001$). There was no significant difference in activation of astrocytes by PMA/ionophore in DMEM or microglia CM ($p > 0.05$). Data were analysed by ANOVA and post-hoc Tukey's multiple comparison test. Percentages are means ± SEM, n = 24. Asterisks denote significant differences: *** $p < 0.001$.

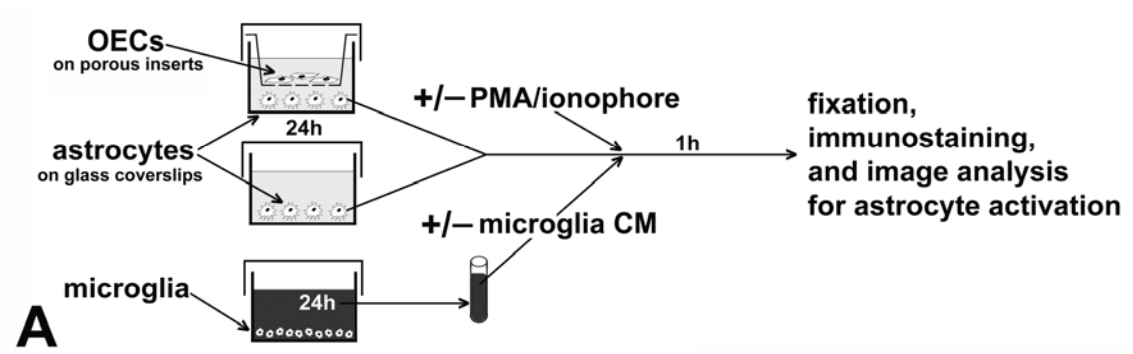
OECs
on porous inserts
24h
astrocytes
on glass coverslips
+/– PMA/ionophore
1h
fixation,
immunostaining,
and image analysis
for astrocyte activation
+/– microglia CM
microglia
24h
A

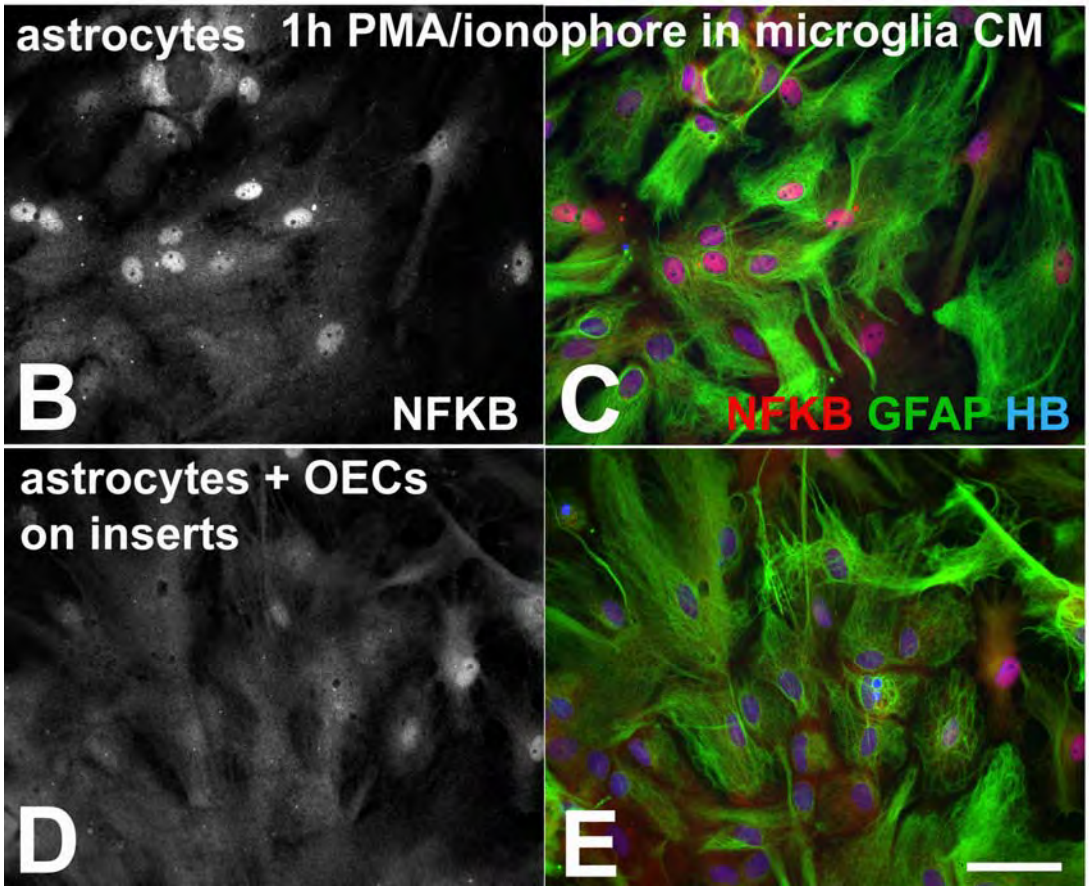
astrocytes
1h PMA/ionophore in microglia CM
B
NFKB
C
NFKB GFAP HB
astrocytes + OECs
on inserts
D
E

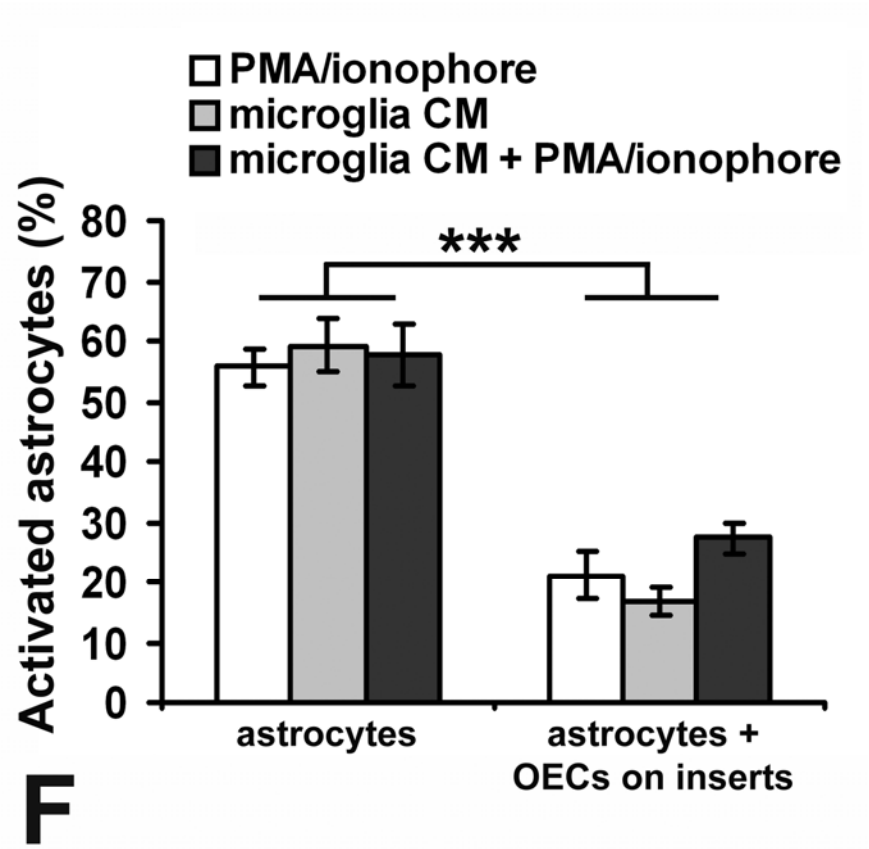

Figure 4.5 OECs moderate astrocyte activation by incubation in microglia CM and/or PMA/ionophore. A: Astrocytes pre-incubated for 24 hours with OECs on inserts and astrocyte monocultures were treated for 1 hour with PMA/ionophore, microglia-conditioned medium (CM) or simultaneously with PMA/calcium ionophore and microglia CM. Astrocytes from monocultures (B, C) and astrocytes from co-cultures with OECs on inserts (D, E) were immunostained for NF-κB (B, D, and red in C, E) and GFAP (green in C, E). Nuclei were counterstained with Hoechst blue (C, E). Less PMA/ionophore-treated astrocytes had bright nuclear NF-κB immunoreactivity in the presence of OECs (D, E). Scale bar is 50 μm. F: Quantitative analysis of astrocyte activation for astrocyte/OEC co-cultures and astrocyte monocultures. In the presence of co-cultured OECs on inserts, significantly fewer astrocytes ($p<0.001$) were activated by either separate or combined treatments with PMA/ionophore and microglia CM. Percentages are means ± SEM, n = 24; *** $p<0.001$.

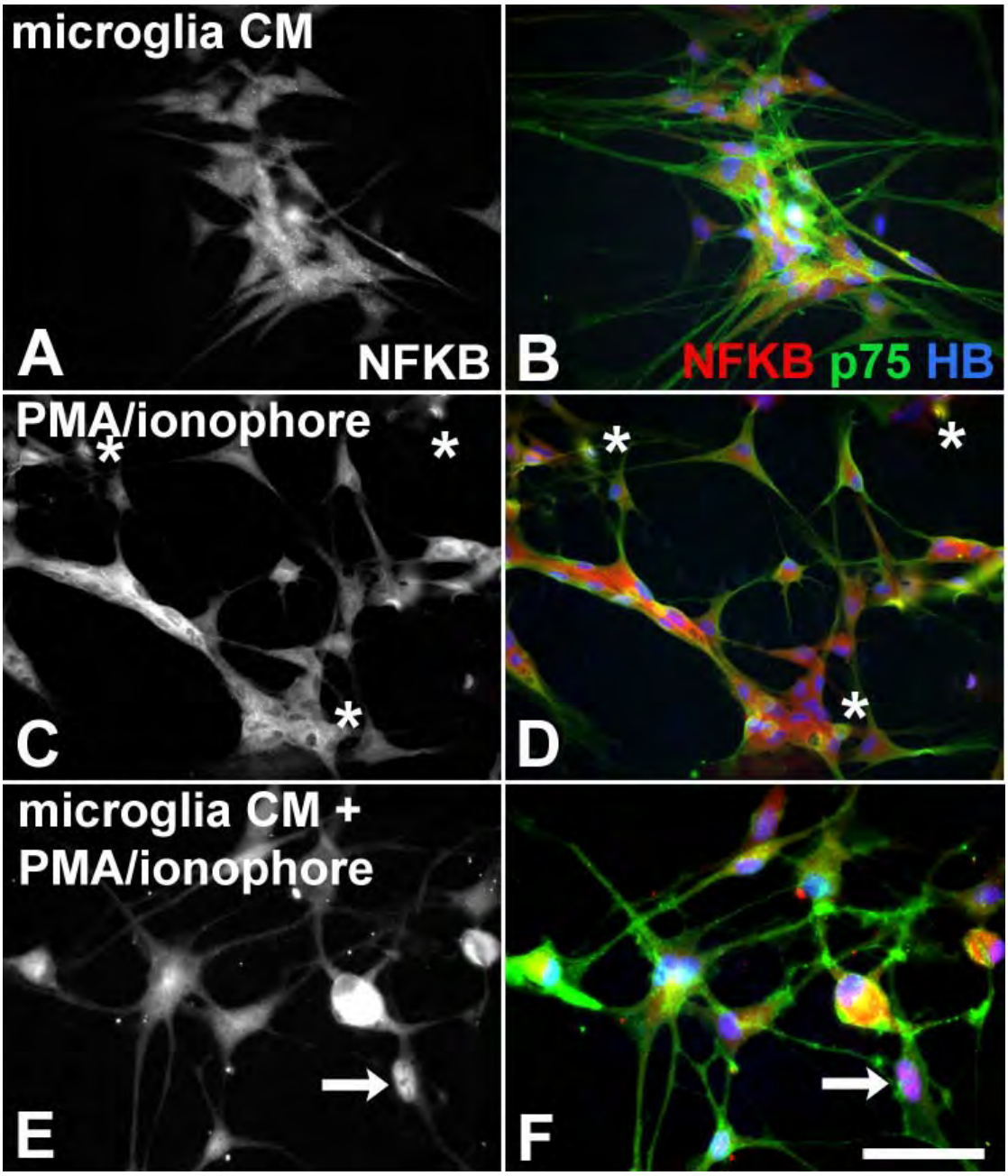

Figure 4.6 NF-κB is not activated in OECs. OECs on inserts used for incubation with astrocytes cultures were immunostained for NF-κB (A, C, E and red in B, D, F), and $p75^{NTR}$ (green in B, D, F), with nuclei counterstained with Hoechst blue (B, D, F). OEC nuclei remained devoid of NF-κB immunoreactivity following separate treatments with microglia CM (A, B) and PMA/ionophore (C, D). A small percentage of OECs (4.2±1.4%, n = 12) had predominantly nuclear localisation of NF-κB immunoreactivity (arrow in E, F) after simultaneous treatment with microglia CM and PMA/ionophore. Pores in the insert membranes can be seen in some images (asterisks C, D). Scale bar is 50 μm.

Interestingly however, a small percentage (4.2±1.4%) of the co-cultured OECs on inserts were activated after 1 hour of the combined treatment with PMA/ionophore and microglia CM, as indicated by more intense nuclear than cytoplasmic NF-κB immunoreactivity (arrow, Fig. 4.6E, F).

4.23.3 Insulin-like growth factor-1 may contribute to the moderation of astrocyte activation by OECs

OECs express a number of growth factors including insulin-like growth factor-1 (IGF-1) (Gudino-Cabrera and Nieto-Sampedro, 2000), which has been shown to inhibit the NF-κB dependent production of inflammatory mediators in astrocytes (Fernandez et al., 2007a). Immunoreactivity for IGF-1 occurred throughout the cell bodies and processes of the cultured OECs (Fig. 4.7 A, B). Addition of 500ng/mL IGF-1 in the culture medium resulted in significant decreases ($p<0.05$) in the percentage of astrocytes activated by PMA/calcium ionophore (43.8±3.3) or microglia CM (45.0±3.0). Therefore, IGF-1 is a probable component of the OEC-derived soluble factors that could contribute to their moderating effect on astrocyte activation. Significantly more astrocytes ($p<0.01$) were activated by both PMA/ionophore and microglia in the presence of IGF-1 (Fig. 4.7C) than in the presence of co-cultured OECs on inserts (Fig. 4.6F), implying that IGF-1 alone is not sufficient to account for the moderating effect of OECs on astrocyte activation.

4.24 OECs moderate GM-CSF transcription by activated astrocytes

Real-time PCR was used to compare transcription of mRNA for the NF-κB-dependent pro-inflammatory cytokine, GM-CSF, in astrocytes incubated for 4, 8, 12, 18 and 24 hours with PMA/ionophore in OEC CM**,** microglia CM or unconditioned medium (DMEM), to determine whether the moderation of astrocyte activation by OECs was associated with decreased GM-CSF production (Fig. 4.8). GM-CSF mRNA transcripts increased for 8 hours of PMA/ionophore treatment in astrocytes cultured in OEC CM or DMEM to a maximum (~5 fold) that was significantly less than for astrocytes in microglia CM (~7 fold; $p < 0.05$) where transcripts continued to increase until 12 hours (Fig. 4.8). GM-CSF transcripts had decreased substantially for astrocytes in OEC CM by

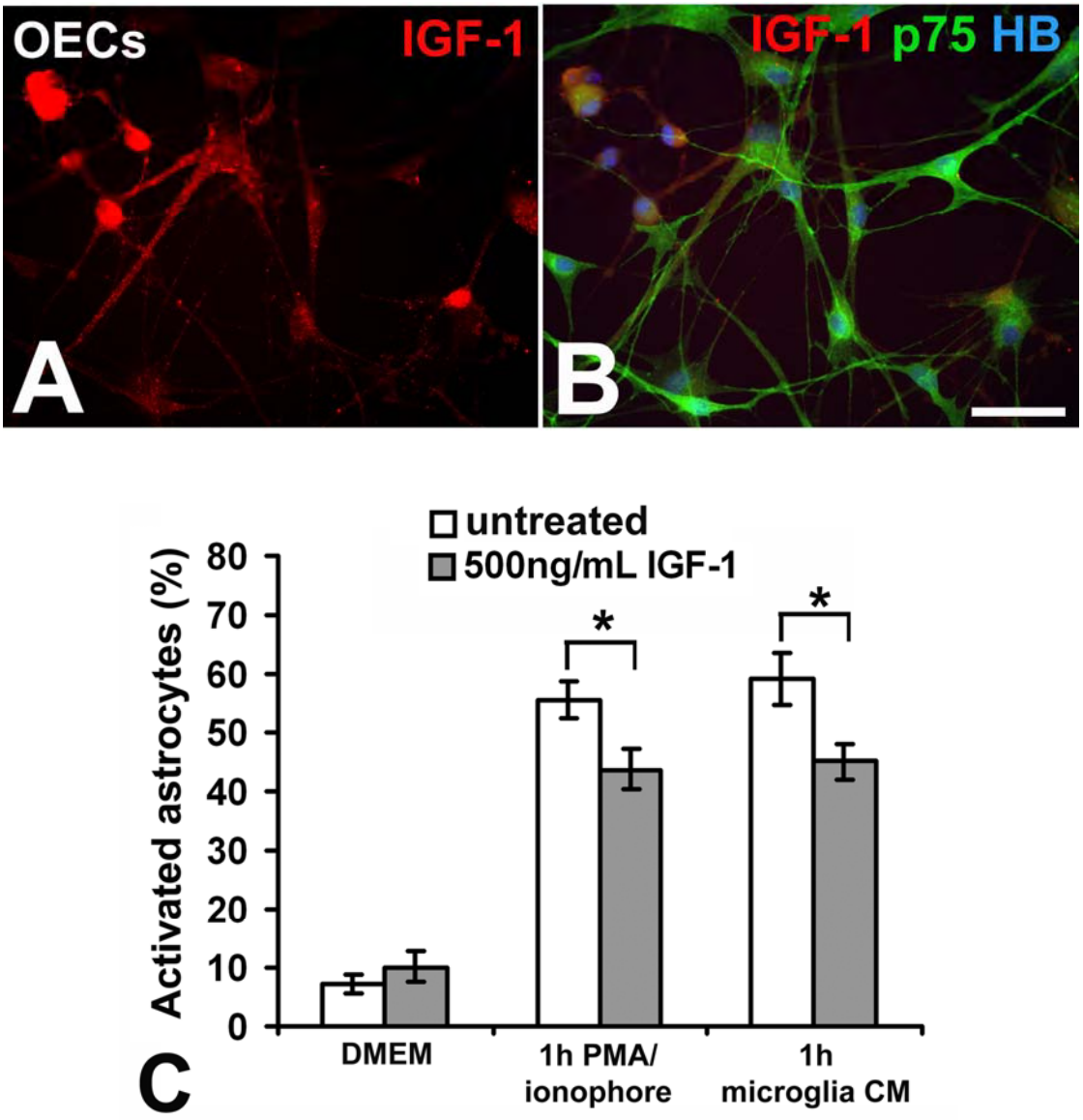

Figure 4.7 IGF-1 moderates astrocyte activation. A: Immunoreactivity for insulin-like growth factor-1 (IGF-1) occurs in the perikaryon and processes of OECs. B: Merged immunoreactivity image shows IGF-1 (red), $p75^{NTR}$ to identify OECs and Hoechst blue nuclear counterstaining. Scale bar is 50 μm. C: Astrocyte activation was compared, with and without the addition of 500ng/mL IGF-1, for astrocytes in DMEM and astrocytes incubated for 1h with PMA/ionophore or microglia CM. Addition of IGF-1 resulted in significantly fewer astrocytes ($p<0.05$) being activated by incubation with either PMA/ionophore or microglia CM. Percentages are means ± SEM, n = 18; * $p<0.05$.

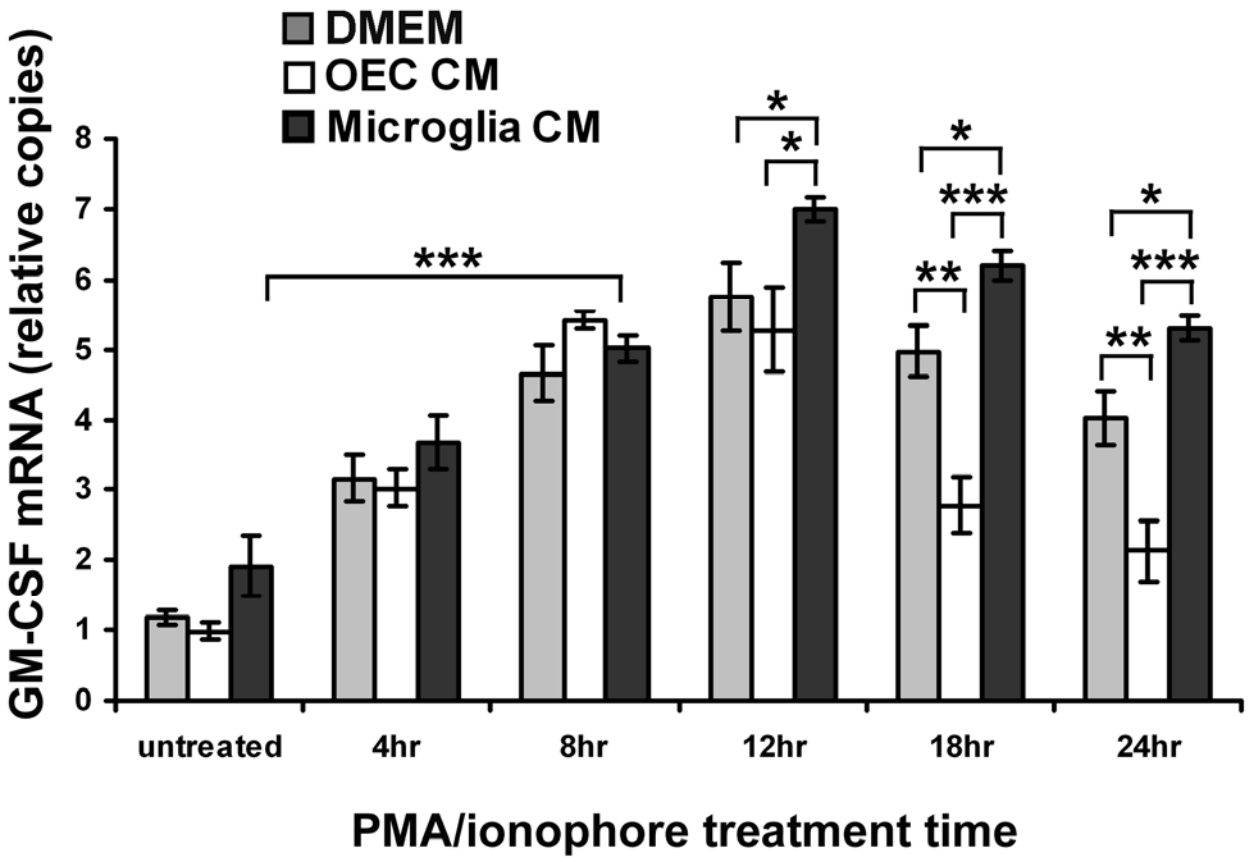

Figure 4.8 Quantitative real time PCR comparison of GM-CSF mRNA transcription in response to PMA/ionophore for astrocytes cultured in OEC CM, microglia CM or DMEM. Data were graphed as GM-CSF mRNA copies relative to copies of GAPDH mRNA for each sample. PMA/ionophore induced significant increases in GM-CSF transcription to a maximum at 8h ($p < 0.001$) for astrocytes in OEC CM or DMEM, while for astrocytes in microglia CM there was a further increase in GM-CSF transcription to significantly higher levels at 12 hours ($p < 0.05$). After 18-24 hours of incubation, GM-CSF transcription in astrocytes cultured in OEC CM had diminished to significantly lower levels than for astrocytes in microglia CM ($p < 0.001$) or DMEM ($p < 0.01$). Data were analysed by 2-way ANOVA and post-hoc Tukey's multiple comparison test. Results are means ± SEM, n = 3. Asterisks denote significant differences: * $p < 0.05$, ** $p < 0.01$, *** $p < 0.001$.

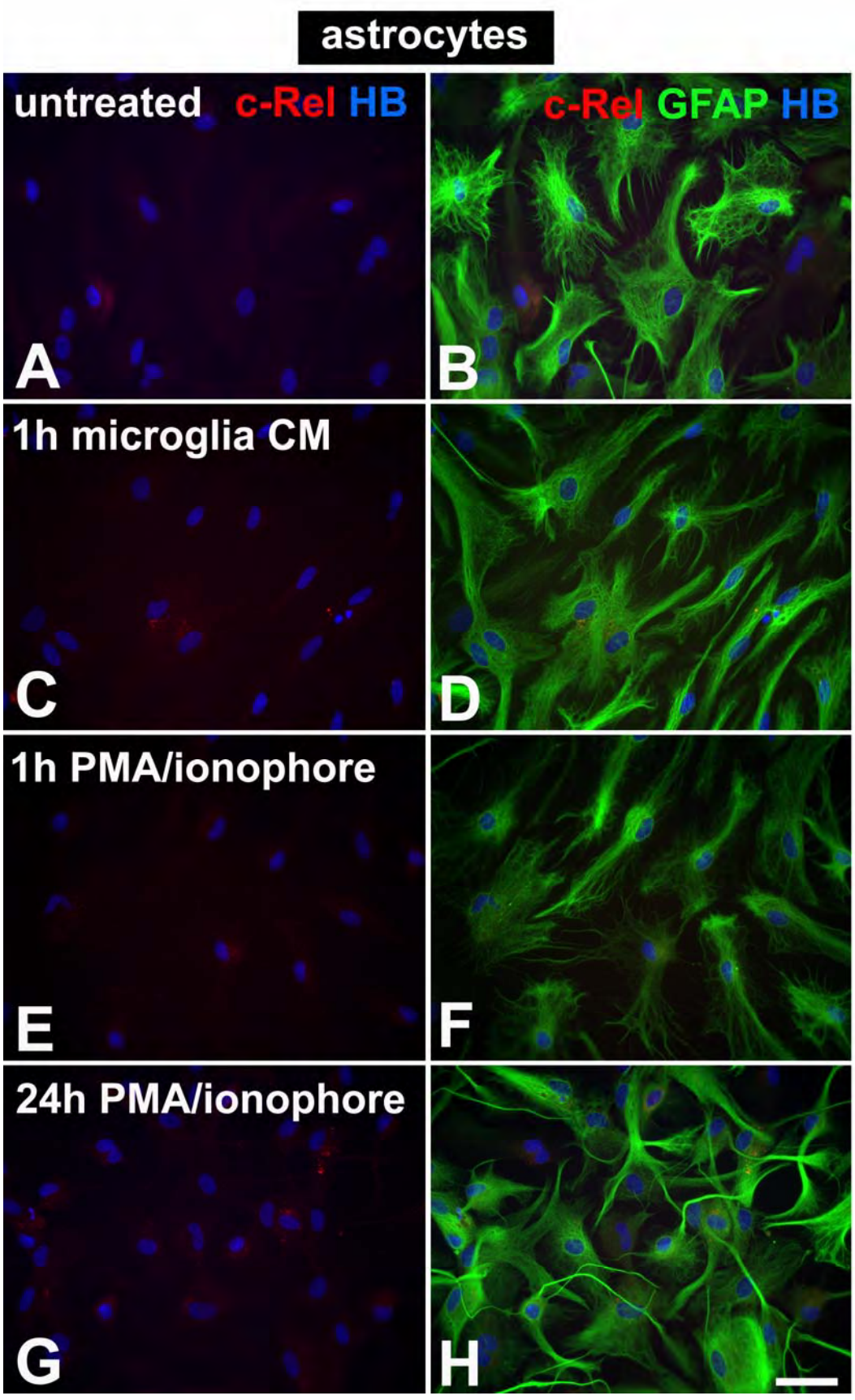
astrocytes
untreated c-Rel HB
A
c-Rel GFAP HB
B
1h microglia CM
C
D
1h PMA/ionophore
E
F
24h PMA/ionophore
G
H

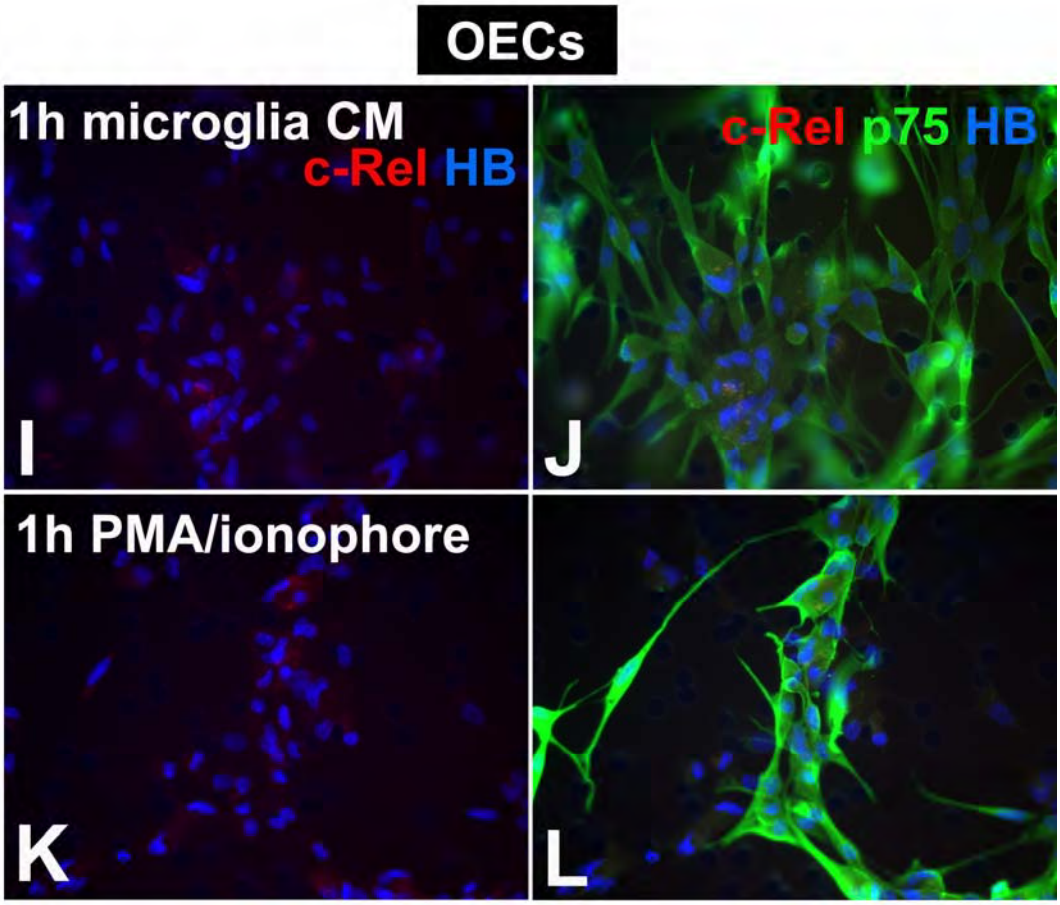

Figure 4.9 C-Rel immunoreactivity in astrocytes and OECs. Untreated astrocytes (A, B) and astrocytes stimulated with microglia CM for 1 hour (C, D) or PMA/ionophore for 1 hour (E, F) or 24 hours (G, H) were immunostained for c-Rel NF-κB (red in A-H) and GFAP (green in B, D, F, H), with nuclei counter-stained with Hoechst blue (A-L). OECs on inserts used for co-culture with astrocytes during stimulation with microglia CM (I, J) and PMA/ionophore (K, L) were immunostained for c-Rel (red in I-L) and $p75^{NTR}$ (green in J, L). C-Rel immunoreactivity was of low intensity and predominantly cytoplasmic in astrocytes and OECs under all conditions. Note: c-Rel immunoreactivity was imaged at ~4x the exposures used for imaging p65 NF-κB immunoreactivity in astrocytes. Scale bar is 50 μm.

the later time-points of 18 and 24 hours of treatment and were significantly less than for astrocytes in microglia CM ($p < 0.001$) or DMEM ($p < 0.01$). After 24 hours of treatment GM-CSF transcripts for astrocytes in OEC CM were not significantly different from untreated astrocytes whereas GM-CSF transcripts remained significantly elevated for astrocytes in microglia CM ($p < 0.001$) or DMEM ($p < 0.01$). There were also significantly more transcripts for astrocytes in microglia CM than in DMEM at 18 and 24 hours ($p < 0.05$).

4.25 Astrocyte activation by PMA/ionophore or microglia did not involve c-Rel

Full activation of the GM-CSF gene in T-cells requires translocation to nuclei of both the c-Rel and p65 NF-κB isoforms (Brettingham-Moore et al., 2005a). Immunoreactivity for c-Rel was only observed at very low levels in the cultured astrocytes and occurred predominantly in the cytoplasm (Fig. 4.9). The intensity and distribution of c-Rel immunoreactivity was not altered following 1 hour of incubation with microglia CM (Fig. 4.9C, D) or PMA/ionophore (Fig,. 4.9E, F), or 24 hours incubation with PMA/ionophore (Fig. 4.9G, H). Combining these stimuli with co-cultured OECs on inserts or IGF-1 also had no effect on c-Rel immunoreactivity in astrocytes (data not shown). C-Rel immunoreactivity in the OECs on inserts used for co-culture experiments was also of low intensity and unaffected by treatments (Fig. 4.9I-L).

4.26 Microglial activation of NF-κB and pre-conditioning of astrocyte cultures

The activation of astrocytes by microglia implied that, if not already activated during dissection and trypsinisation, astrocytes would become activated during the preparation of the cortical cultures due to the presence of microglia in the un-purified cultures. Immunostaining of the un-purified cortical cultures for NF-κB confirmed that strong activation of astrocytes, progenitor cells, microglia and fibroblasts occurred in these cultures (Fig. 4.10), possibly implying that the later responses to activating stimuli were more representative of astrocytes that have been pre-conditioned to injury than astrocytes in normal adult cortical tissue. However, it is uncertain whether any such pre-conditioning effect would persist through the later passaging and within the purified astrocyte monocultures. Although the cultured cortical astrocytes do have strong GFAP

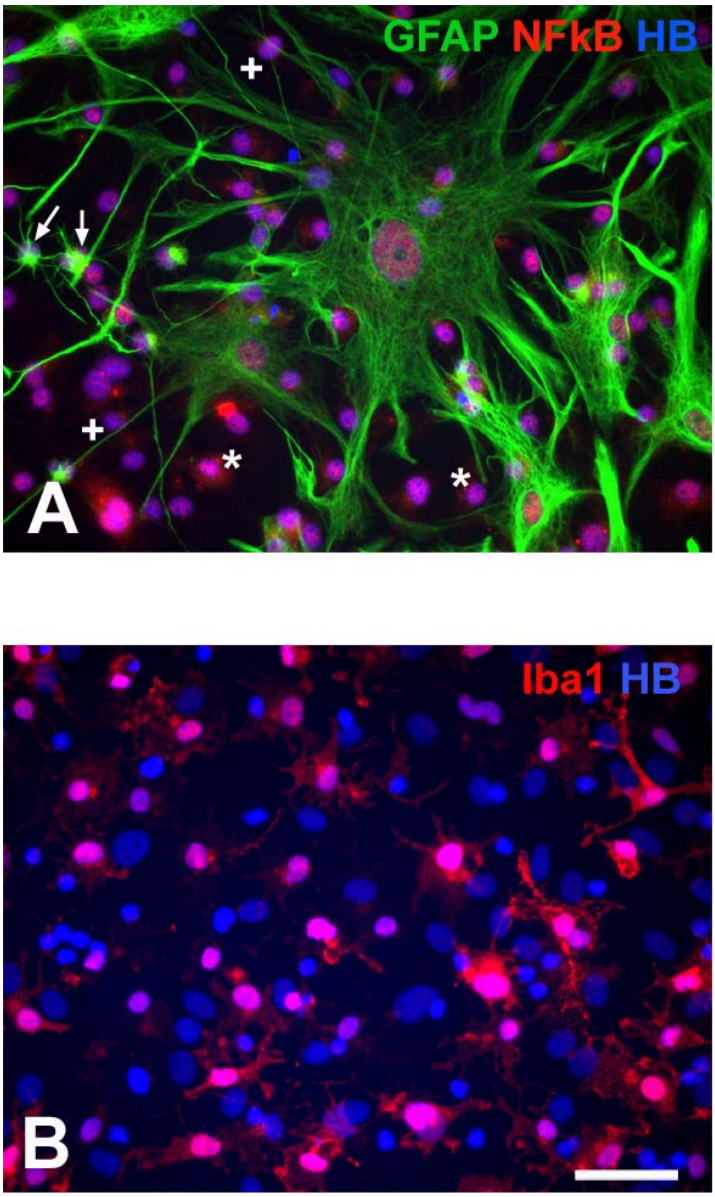

Figure 4.10 Inflammatory activation during cortical cell culture. A: Nuclear immunoreactivity for NF-κB (red) indicates that the majority of cells are activated in primary cortical cell cultures. Mature astrocytes have networks of cytoplasmic GFAP (green) while immature astrocytes (arrows) have thin radial GFAP-positive processes. The morphology revealed by cytoplasmic NF-κB immunoreactivity sometimes identified GFAP-negative cells as microglia (asterisks) or progenitor cells (plus signs). GFAP-negative cells with larger nuclei are probably fibroblasts. B: Ionized calcium binding adapter molecule 1 (Iba1) immunoreactivity (red; pink nuclei) identifies numerous activated microglia (Ito et al, 1998) in the cortical cultures. Counter-staining of nuclei with Hoechst blue (HB) identifies Iba1-negative cells, comprising astrocytes, progenitors and fibroblasts. Scale bar is 50μm.

immunoreactivity that is more similar to reactive astrocytes than adult cortical astrocytes *in vivo* this could be due to the absence of the usual cellular interactions and the different mode of cell-substrate attachment *in vitro*, rather than being an indication of astrocyte inflammation. However, the quiescence of astrocytes in the untreated cultures is not inconsistent with the possibility of earlier pre-conditioning, because transient NF-κB activation can directly and indirectly activate gene transcription that leads to permanently altered phenotypes. Pre-conditioning can confer resistance to later inflammatory stimulation due to the upregulation of anti-inflammatory factors in response to a moderate pre-conditioning stimulus (Ginis et al., 2002; Bright and Mochly-Rosen, 2005; Lehotsky et al., 2009; Lu et al., 2009; Ridder and Schwaninger, 2009). This response acts, at least in part, as a negative feedback mechanism to limit inflammatory activation and includes the upregulation of IκB proteins that bind and inactivate NF-κB dimers.

4.3 Discussion

4.30 OECs release a soluble factor that moderated astrocyte inflammatory activation

The regulation of inflammatory genes in astrocytes, microglia and fibroblasts by NF-κB is a key determinant of CNS injury responses (Baeuerle and Henkel, 1994; Schneider et al., 1999; Kracht and Saklatvala, 2002; Chen and Greene, 2004b). PMA/ionophore stimulation appeared to be a relevant treatment model for investigating these inflammatory responses since it strongly induced translocation of NF-κB to nuclei of astrocytes, microglia and meningeal fibroblasts and increased astrocytic transcription of the pro-inflammatory cytokine, GM-CSF. Interestingly, PMA/ionophore did not appear to induce NF-κB translocation in OECs and this may have implications for the efficacy of OECs in CNS injury therapy. Importantly, a soluble factor released by OECs moderated both the NF-κB translocation and GM-CSF transcription components of astrocyte activation. PMA/ionophore and soluble factors released by microglia stimulated NF-κB translocation in a similar manner in astrocytes and OECs moderated the translocation induced by either stimulus. Furthermore, prior to PMA/ionophore treatment, astrocytes co-cultured with OECs remained quiescent while monocultures and co-cultures with microglia and fibroblasts had significantly more astrocytes exhibiting predominantly nuclear localisation of NF-κB. This moderation of astrocyte reactivity represents a

possible mechanism whereby transplanted OECs could facilitate neural repair after CNS injury. The mediation of these potentially beneficial effects by a soluble factor released from OECs is of particular relevance to the therapeutic potential of OEC transplants. If the therapeutic effects are principally mediated by a soluble factor then debate concerning the migratory capacity of transplanted OECs within the injured CNS (Ramon-Cueto et al., 1998; Ramon-Cueto et al., 2000; Resnick et al., 2003, Ruitenberg et al., 2002; Lu et al., 2006) may be less relevant. A soluble anti-inflammatory factor released by the transplanted OECs could potentially ameliorate injury responses at a distance from the transplant site, dependent on the concentration gradient generated and the distance the soluble factor could diffuse before inactivation *in vivo.* Furthermore the release of anti-inflammatory factors by transplanted OECs near the lesion could avoid the systemic immune suppression problems associated with intravenous methylprednisolone treatment (Bracken and Holford, 2002; Kronvall et al., 2005; Sorensen, 2008). Isolation of the relevant soluble factors released by the OECs would assist research into these possibilities.

4.31 Restriction of NF-κB activation in OECs may confer therapeutic benefits

4.31.0 OEC activation and innate immunity

Surprisingly, OECs, unlike astrocytes, microglia and fibroblasts were not activated by PMA/ionophore or microglia-conditioned medium. Although this result was unexpected it suggests the possibility that OECs transplanted into CNS lesions may at least remain inactivated and not have pro-inflammatory actions. It may be that the soluble anti-inflammatory factor released by OECs that ameliorated inflammatory NF-κB translocation in astrocytes had the even stronger effect of eliminating NF-κB translocation in the OECs. This could be a consequence of stoichiometric factors such as the diffusion rate of the soluble factor or its intracellular rate of inactivation. OECs may also have high constitutive expression levels of IκBs, the primary negative regulators of NF-κB, which could explain the lack of response to a variety of stimuli, possibly including multiple inflammatory cytokines in the microglia-conditioned media. Another possible explanation is that OECs exert additional paracrine or contact-mediated anti-inflammatory effects on adjoining cells in confluent cultures. Similar mechanisms could

serve to maintain a supportive environment for neuronal survival within OEC ensheathments in the olfactory tract. OECs do express fractalkine, which could have imparted a contact-dependent component to the anti-inflammatory activity (Ruitenberg et al., 2008), since it is a membrane-bound chemokine that has been shown to exert neuroprotective anti-inflammatory effects (Cardona et al., 2006; Held-Feindt et al., 2010; Lauro et al., 2010). Although PMA/ionophore stimulation of OECs has not previously been studied, Escherichia coli (E. coli) induced NF-κB translocation to nuclei in a subset of $p75^{NTR}$-positive OECs in cultures derived from peripheral olfactory mucosal and CNS olfactory bulb tissue (Vincent et al., 2007). Bacterial activation of OECs has been associated with nitric oxide production, inflammatory cytokine secretion, toll-like receptor (TLR) expression and phagocytic behaviour, supporting a postulated innate immune function of OECs that could prevent the spread of infections along the peripheral olfactory tract into the CNS (Vincent et al., 2007; Harris, 2008; Leung et al., 2008; Harris et al., 2009). The constitutive periodic replacement of olfactory neurons throughout life and the acceleration of this replacement following pathogenic invasion provides a primary defence mechanism against pathogenic invasion of the CNS through the olfactory tract (Carr and Farbman, 1993; Bauer et al., 2003; Chen et al., 2005a; Borders et al., 2007a; Leung et al., 2007). TLR activation can induce innate immune responses of variable intensity within the CNS, involving interactions between complement cascades, reactive oxygen species, NF-κB activation, chemokines expression and the recruitment of leukocytes and activation of macrophages (Lee and Lee, 2002; Akira and Sato, 2003; Konat et al., 2006; Frangogiannis, 2007). The absence of NF-κB translocation in OECs following PMA/ionophore treatment in this study allows the possibility that OECs could have evolved a specific moderate innate immune response to pathogens. Moderate inflammatory responses have been associated with increased expression of growth factors that promote axon growth (Lenzlinger et al., 2001; Laird et al., 2008). A moderate inflammatory response by OECs in response to residual pathogens could both stimulate axon regrowth from regenerating olfactory neurons (Borders et al., 2007b) and provide an additional targeted defence against pathogens being carried into the CNS by the regrowing axons.

4.31.2 Toll-like receptors and innate immunity

The unresponsiveness of OECs to PMA/ionophore is not inconsistent with a role in innate immune responses involving TLR activation by pathogens. Unlike PMA/ionophore treatment, TLR stimulation of inflammatory gene expression via NF-κB activation does not involve PKC- and calcium-dependent intracellular signalling pathways (Lee and Lee, 2002; Akira and Sato, 2003; Takeda et al., 2003; Konat et al., 2006). TLRs are expressed by most cells including astrocytes, microglia, oligodendrocytes and neurons and they play an important role in CNS innate and adaptive immune responses to pathogens and injury (Lee and Lee, 2002; Bowman et al., 2003; Janssens and Beyaert, 2003; Carpentier et al., 2005; Konat et al., 2006; Hanisch et al., 2008). TLRs are responsive to bacteria and viruses and their activation induces increased expression of IL-1β, TNF-α, IFN-γ, IL-6 and other inflammatory cytokines and chemokines (Bsibsi et al., 2002; Lee and Lee, 2002; Konat et al., 2006; Hanisch et al., 2008), which can then induce immune and glial cell differentiation leading to adaptive immune responses (Carpentier et al., 2005; Town et al., 2005; Glezer et al., 2007; Voskuhl et al., 2009). Pre-conditioning of astrocytes through activation of NF-κB by TNF-α or bacterial lipopolysaccharide (LPS) stimulation of TLRs can result in neuroprotective tolerance to ischemia and the pre-conditioning with TNF-α induces tolerance to subsequent LPS exposure (Phulwani et al., 2008). However, TLR activation has also been associated with chronic immune activation and neurodegeneration (Maslinska et al., 2004; Chakravarty and Herkenham, 2005; Lehnardt et al., 2008). It is conceivable that TLR activation in transplanted OECs could also induce a tolerance to ischemia. Whether this would be more beneficial than TLR activation in resident astrocytes and microglia could depend on the timing of OEC transplantation and the inflammatory conditions in the lesion. It would therefore be interesting to extend this research to compare the effects of OECs on PMA/ionophore and bacterial stimulation of NF-κB translocation in astrocytes.

4.31.1 OEC cultural differences

It is also possible that NF-κB is less readily activated in the CNS olfactory bulb OECs used in this study than in peripheral mucosal OECs. Robust immune responses can cause

detrimental secondary neuronal damage within the CNS and perhaps for this reason, olfactory bulb OECs are not readily activated by either E. coli or PMA/ionophore. The subset of OECs where NF-κB was activated in the previous study (Vincent et al, 2007) may have represented the mucosal OECs in the mixed mucosal and bulbar OEC cultures. However, select groups of OECs along specific olfactory nerve tracts from the lamina propria into the outer layers of the olfactory nerve layer in the olfactory bulb express TLR4, which is activated by gram-negative bacteria (Vincent et al, 2007). It is also possible that the subset of activated cells in these cultures were contaminating Schwann cells since these occur in the peripheral olfactory tract, express p75NTR and have similar morphologies to OECs. It would therefore be interesting to compare the responses to bacterial and PMA/ionophore stimulation of separate cultures of lamina propria OECs, olfactory bulb OECs and Schwann cells. Functional differences have been reported between peripheral and CNS OECs used in transplants (Kumar et al., 2005; Richter et al., 2005), although these differences may primarily have been due to different proportions of contaminating fibroblasts in the cultures (Lakatos et al., 2003b; Kumar et al., 2005; Ibanez et al., 2007; Teng et al., 2008). The fascicles of olfactory sensory axons and their surrounding OECs are enclosed by basal laminae and overlying fibroblasts along the trajectories of the nerve fascicles through the peripheral olfactory system to the olfactory bulb where the fibroblasts separate from the fascicles to form a meningeal glia limitans around the bulb (Boyd et al., 2003; Li et al., 2005b). Fibroblasts are therefore a common contaminating cell in OEC cultures (Ito et al., 2006a), with the propensity to proliferate more rapidly than OECs (Gibbons et al., 2007). Hence, it is essential that behaviours ascribed to OECs be correlated with positive identification using a distinguishing marker protein to identify OECs as demonstrated in this study, where PMA/ionophore activated contaminating $p75^{NTR}$-negative fibroblasts and not $p75^{NTR}$-positive OECs.

4.31.2 Are multiple stimuli required for OEC activation?

Rather than peripheral and CNS OECs representing different cell populations, it may be that any immune function of OECs specifically targets invasive pathogens. Co-culture with microglia significantly enhanced the activation of OECs by E. coli, presumably due to the release of inflammatory cytokines resulting from simultaneous activation of the co-

cultured microglia by E. coli (Vincent et al, 2007). It was therefore interesting, in this study, that although OECs were not activated by separate stimulation with PMA/ionophore or microglia-conditioned medium, a small percentage of the OECs on culture inserts were activated by simultaneous application of these stimuli. TNF-α promotes oligodendrocyte apoptosis in multiple sclerosis (Penkowa and Hidalgo, 2001; Espejo et al., 2002) by strongly activating NF-κB via oligodendrial $p75^{NTR}$ (Ladiwala et al., 1998). TNF-α released by activated microglia could induce NF-κB translocation in OECs by a similar mechanism. Bacteria could activate OECs both directly and through stimulation of TNF-α release by microglia. In this study, astrocytes were activated by microglia-conditioned medium possibly due to the presence of IL-1β or other cytokines released by the microglia, to which OECs may have been unresponsive. If OECs were insensitive to these inflammatory cytokines it could confer benefits for OEC transplant therapies. This possibility warrants a thorough investigation of the effects of IL-1β, TNF-α and other pro-inflammatory factors on NF-κB translocation and the expression of anti-inflammatory factors by OECs. The anti-inflammatory actions of OECs that were identified in this study through their moderating effects on astrocyte activation could also have direct neuroprotective effects both in the context of OEC transplant therapy for CNS injury and during the normal development and regeneration of olfactory neurons.

4.32 Microglia and PMA/ionophore similarly activated astrocytes

Microglia in monocultures had a high basal level of activation in the culture conditions consistent with their postulated surveillance role in normal CNS tissue and rapid inflammatory responses to a variety of abnormal extracellular conditions. Presumably and not surprisingly, conditions in the cell cultures were sufficiently abnormal to induce the observed microglial activation. Consequently, culture medium conditioned by microglia or co-culture with microglia rapidly activated astrocytes, probably because of pro-inflammatory cytokines secreted by the activated microglia. This similarity of astrocyte activation by PMA/ionophore and microglia further substantiated the physiological relevance of the reagent treatment. Activated microglia are known to secrete IL-1β, IL-6, TNF-α and other pro-inflammatory cytokines, which stimulate further activation of NF-κB in astrocytes and immune cells, thereby increasing the

amplitude and duration of inflammation (Yamamoto and Gaynor, 2001; Saklatvala, 2007; Block et al, 2007). Astrocyte activation was significantly lower in untreated astrocyte/microglia co-cultures than in astrocyte monocultures after 1 hour of incubation in microglia-conditioned medium, possibly because, in the several days prior to reagent treatment, astrocytes in the co-cultures could have released factors that inhibited activation of microglia (Wilms et al, 1997; Schilling et al, 2001) in the unstimulated co-cultures. Furthermore, PMA/ionophore directly increased NF-κB translocation to nuclei in both astrocytes and microglia, presumably leading to increased expression of pro-inflammatory factors by both microglia and astrocytes in the co-cultures.

4.33 OECs could moderate astrocyte activation induced by multiple stimuli

Following CNS injury, NF-κB-regulated astrocyte inflammation can be induced directly by factors such as glutamate (Abe and Saito, 2001; Matute et al., 2006) and ATP (Neary and Kang, 2005; Weisman et al., 2005; Chen et al., 2006b) released from damaged cells, or indirectly in response to cytokines, such as IL-1β and TNF-α, secreted by activated microglia and other immune cells (Norris et al., 1994; Meeuwsen et al., 2003a; Brahmachari et al., 2006; Kim et al., 2006). Importantly, in addition to being unresponsive to PMA/calcium ionophore, OECs substantially moderated astrocyte activation whether induced by PMA/calcium ionophore and/or microglia-derived factors. This represents a plausible mechanism for the promotion of neural repair by OEC transplants since astrocyte-specific NF-κB inhibition results in decreased axonal damage, smaller lesion size, decreased inhibitory CSPG deposition in glial scars and improved functional recovery after spinal cord injury (Brambilla et al., 2005a).

4.34 Insulin-like growth factor-1 may have contributed to the moderation of astrocyte activation

Astrocyte activation was similarly moderated by direct co-culture with OECs, co-culture with OECs separated by tissue culture inserts or incubation in culture medium conditioned by OECs, indicating that the moderating effect was due to a soluble factor released by the OECs. There are many soluble cellular products in the CNS, including N-acetyl aspartate (Rael et al., 2004b), proliferation-related acidic leucine-rich protein

(Shen et al., 2009), IL-10 (Cheng et al., 2009), insulin-like growth factor-1 (IGF-1) (Butovsky et al., 2005), prostaglandins (Zhang et al., 2008) and glucocorticoids (Sorrells and Sapolsky, 2007), with NF-κB-inhibiting and anti-inflammatory actions. IGF-1 is one possible candidate for mediating the moderating effect of OECs on NF-κB translocation, since it is a secreted soluble factor expressed by OECs (Gudino-Cabrera and Nieto-Sampedro, 2000; Rojas-Mayorquín et al., 2010) and it has been shown to inhibit the NF-κB-dependent production of the inflammatory mediators, inducible nitric oxide synthase and cyclo-oxygenase in astrocytes (Fernandez et al., 2007a). IGF-1 exerts neuroprotective effects in both white and gray matter under different detrimental conditions, including ischemic stroke (Guan and Gluckman, 2009; Kooijman et al., 2009). The anti-inflammatory action of IGF-1 is highly relevant to this study since it has been shown to prevent the translocation of NF-κB to astrocyte nuclei by inhibiting the degradation of IκB induced by TNF-α (Pons and Torres-Aleman, 2000). In addition, IGF-1 promotes the differentiation of neuronal precursors into olfactory sensory neurons (Mason et al., 2003) and OEC-conditioned medium induced increased expression of IGF-binding protein in neural precursor cells (Rojas-Mayorquin et al., 2008). This research confirmed the expression of IGF-1 by OECs and indicated that while IGF-1 may be a contributing factor, it was insufficient to account in full for the inhibition of NF-κB translocation in astrocytes by the OEC-derived soluble factors. It is not improbable that multiple factors released by OECs could differentially regulate NF-κB by interacting with different molecules in the inflammatory pathway. Identification of these factors and their specific roles could allow anti-inflammatory therapies targeted at specific molecules. The involvement of IGF-1 or other soluble factors released by OECs in the moderation of astrocyte activation could be further investigated using transgenic knockout or gene knockdown models, by blocking the effects of soluble factors with specific reagents or with antibodies against the soluble factors and their specific receptors. Commercially available cytokine and growth factor assays or micro-arrays could be used to screen for possible mediating factors by comparing the expression profiles of cells and medium from unstimulated and PMA/ionophore-stimulated astrocyte and OEC mono- and co-cultures.

4.35 OECs did not eliminate astrocyte activation

4.35.0 Moderate activation of astrocytes has beneficial effects

OECs moderated, but did not eliminate, NF-κB-mediated astrocyte activation and this may present an advantage for neural repair. Drastic suppression of astrocytic activation leading to abolition of astrogliosis has been associated with increased neural damage (Bush et al., 1999; Faulkner et al., 2004). Although presenting barriers to axon regrowth, glial scars may also serve to protect perilesional tissue from the cytotoxic conditions ensuing from strong immune responses in the lesion (Sofroniew, 2005; Fitch and Silver, 2008; Sofroniew, 2008; Voskuhl et al., 2009). Similarly, while reactive astrocytes and fibroblasts may inhibit axon regrowth by depositing CSPGs and interacting to form basal laminae at glial scars, they also secrete neurotrophic factors (Meeuwsen et al., 2003b; Laird et al., 2008). Moderation of astrocyte activation by transplanted OECs could therefore inhibit CSPG deposition and basal laminae formation to improve the axon growth-permissiveness of the glial scar while maintaining and contributing (Woodhall et al., 2001) to neurotrophin production.

4.35.1 OEC moderation of astrocyte activation could prevent excessive cytokine and ROS production

A previous study has suggested that transplanted OECs may have a biphasic effect, initially promoting and later inhibiting inflammatory responses (Lopez-Vales et al., 2004). This biphasic effect could be related to a requirement for specific pathogens or microglia-derived cytokines to induce the inflammatory activation of OECs. High levels of TNF-α and IL-1β can have neurotoxic consequences while at lower levels both cytokines can also exert neuroprotective and neurotrophic effects (Feuerstein et al., 1994; John et al., 2005; Gosselin and Rivest, 2007; Lambertsen et al., 2009; Whitney et al., 2009). Microglia are a major source of TNF-α (Meme et al., 2006; Clausen et al., 2008; Kaushal and Schlichter, 2008; Tuttolomondo et al., 2008; Lambertsen et al., 2009) and astrocytic NF-κB inhibition did not alter levels of this cytokine (Brambilla et al, 2005). However, IL-1β is another key cytokine regulating CNS injury responses (John et al, 2005) and OEC transplantation into injured spinal cords was associated with initial increases and later decreases in the post-injury levels of IL-1β, iNOS and astrocyte activation (Lopez-

Vales et al, 2004). Although OEC survival was not monitored after transplantation, the transplanted OECs could possibly have limited lesion size and the spread of secondary damage by at first contributing to strong acute immune responses initiated by microglia in the lesion and later moderating the inflammatory responses of perilesional reactive astrocytes. OEC moderation of astrocyte activation could also have the therapeutic effect of inhibiting the production of cytotoxic ROS. Both PMA activation of PKC and calcium influx induced by ionophore or ATP activated NF-κB-dependent generation of ROS by NADPH oxidase in cultured astrocytes (Abramov et al., 2005). If not detoxified by superoxide dismutase, excess superoxide generated by NADPH oxidase may combine with NO generated by iNOS to generate highly cytotoxic peroxynitrite (Forman and Torres, 2001). Moderation of astrocyte activation by transplanted OECs could therefore enhance neuronal survival and axon regrowth by moderating peroxynitrite production in perilesional reactive astrocytes, following resolution of the initial acute immune cell response.

4.36 Meningeal fibroblasts did not moderate astrocyte activation

In this study, co-culture with OECs inhibited activation of astrocytes, supporting the notion that interactions between astrocytes and transplanted OECs may prevent the development of axon growth-inhibitory boundaries as occurs in response to invading meningeal fibroblasts (Teng et al, 2008) or transplanted Schwann cells (Fairless et al, 2004; Nieto-Sampedro, 2003). In addition, while PMA/ionophore strongly activated meningeal fibroblasts, co-culture of astrocytes with fibroblasts did not alter PMA/ionophore-induced activation of astrocytes. The similarity of PMA/ionophore-induced astrocyte and fibroblast activation is consistent with the interaction between reactive astrocytes and activated meningeal fibroblasts that leads to the formation of axon growth-inhibitory basal laminae in the glial scar (Logan et al., 1999; Bundesen et al., 2003; Sandvig et al., 2004). However, some studies have indicated that OEC/fibroblast co-cultures are more beneficial than OEC monocultures as therapeutic transplants after CNS injury, possibly because the fibroblasts promote the migration of OECs to form axon-growth permissive conduits across lesions (Li et al., 2005b; Teng et al., 2008). Alternatively, fibroblasts could promote the migration of peripheral Schwann cells into

lesions, leading to the promotion of axon-growth and remyelination (Lakatos et al., 2003b; Boyd et al., 2004). Testing the effects of OECs on NF-κB translocation and inflammatory gene transcription in fibroblasts using the experimental model employed in this study could shed further light on interactions between fibroblasts and therapeutically transplanted OECs.

4.37 OECs moderated pro- inflammatory GM-CSF transcription in astrocytes

4.37.0 PMA/ionophore stimulated GM-CSF transcription in astrocytes

Although increases in nuclear levels of NF-κB are associated with increased production of pro-inflammatory cytokines and more severe inflammation, it remained uncertain whether the significant moderation of NF-κB translocation to astrocyte nuclei by OECs had functional significance. The PMA/ionophore-induced astrocytic NF-κB translocation was associated with increased transcription of the pro-inflammatory cytokine, GM-CSF, as found in T cells (Schreck and Baeuerle, 1990; Brettingham-Moore et al., 2005a), where the increased transcription has been conclusively demonstrated to involve translocation to nuclei and DNA-binding of p65 NF-κB (Schreck and Baeuerle, 1990; Tsuboi et al., 1994; Holloway et al., 2003; Brettingham-Moore et al., 2008). There was only a transient peak in NF-κB transcription that occurred from 30 minutes to 1 hour after stimulation of astrocytes with PMA/ionophore whereas GM-CSF transcription was not significantly activated until 4 to 8 hours after stimulation, by which time NF-κB was inactive. However, this delay between NF-κB translocation and gene transcription is not unusual (Hoffman et al., 2002; Holloway et al., 2003; Brettingham-Moore et al., 2008). Even transient NF-κB activation for 15 to 30 minutes following stimulation by a brief pulse of the inflammatory cytokine, TNF-α, has been demonstrated to induce increased transcription of the chemokines, RANTES and IP-10, 4 to 8 hours later (Hoffman et al., 2002). The 5- to 7-fold increase in astrocytes was not as dramatic as that induced by PMA/calcium ionophore (~200-fold) in T cells (Brettingham-Moore et al., 2005b). However, the abundance and location of astrocytes in the injury penumbra, facilitates their major contribution to the inflammatory mediators at CNS lesions (Swanson et al., 2004; Panickar and Norenberg, 2005) including GM-CSF, which regulates the proliferation and immune activation of microglia (Xiao et al., 2002; Koguchi et al., 2003).

4.37.1 The comparative activating effects of ionophore and PMA differ between astrocytes and lymphocytes

In T cells, PMA alone induced GM-CSF transcription more strongly (20-fold) than ionophore alone (~4-fold), with the increased transcription in response to both reagents being dependent on PKC. Only PMA induced translocation of NF-κB to nuclei in T cells, whereas ionophore induced calcineurin-dependent translocation of NFAT (Brettingham-Moore et al., 2005a). Although the separate effects of PMA and ionophore on GM-CSF transcription were not investigated in this study, ionophore alone induced NF-κB translocation to astrocyte nuclei more strongly than PMA alone. Interestingly, the 4-fold increase in T cell GM-CSF transcription induced by ionophore was just below the 5 to 7-fold range of the increase in GM-CSF transcription induced by combined PMA/ionophore in astrocytes, where PMA had only a relatively small effect on NF-κB translocation. There are differences in NF-κB activity between immune cells involved in adaptive and innate immune responses (Baeuerle and Henkel, 1994) and it would be interesting to investigate whether the divergent responses of T cells and astrocytes to PMA/calcium ionophore are more generally indicative of differences in the activation of immune and non-immune cells.

4.37.2 C-Rel was not involved in GM-CSF transcription in astrocytes

The large synergistic increase in GM-CSF transcription induced 4-6 hours after PMA/ionophore treatment in T cells was associated with chromatin remodelling to improve access of transcription machinery to the gene promoter region (Brettingham-Moore et al, 2005). The chromatin remodelling was dependent on *de novo* synthesis and translocation of c-Rel NF-κB and to a lesser extent, NFATc, to T cell nuclei, following the earlier translocation of p65 NF-κB. The weak immunoreactivity for c-Rel in astrocytes under all treatment conditions suggested that it was probably not involved in the activation of astrocytes by PMA/ionophore or microglia. However, this result requires confirmation with immunostaining and ideally CHIP assays at the later time-points of 4 to 8 hours after treatments, when transcription peaked in lymphocytes. The absence of c-

Rel activity may explain the short duration of the activation mediated by p65 NF-κB and the relatively modest increase in GM-CSF transcription in astrocytes.

4.37.3 Moderation of GM-CSF production by OECs could attenuate inflammation

Importantly, the moderation of PMA/ionophore-induced NF-κB translocation to astrocyte nuclei by soluble factors released from OECs was accompanied by significantly moderated GM-CSF transcription in the cultured astrocytes. This result was consistent with the view that OEC transplants could act to moderate the severity and duration of inflammation, since high levels of GM-CSF have been associated with more severe inflammation and cytotoxic levels of pro-inflammatory cytokines and ROS (Zaheer et al., 2007). The NF-κB-regulated cytokines and ROS can also stimulate further NF-κB activation in astrocytes and immune cells to exacerbate and prolong inflammation (Pawate et al., 2004; Jia-Yi et al., 2006; Ridder and Schwaninger, 2009). While NF-κB translocation is necessary for robust inflammatory responses, full activation of inflammatory genes also requires the recruitment of co-activators and may involve interactions between NF-κB subunits, inhibitor of κB proteins, inflammatory gene products and other signalling pathways (Baeuerle and Henkel, 1994; Chen and Greene, 2004; Hayden and Ghosh, 2004). The lower peak in astrocytic GM-CSF transcription at 8-12 hours after stimulation in OEC-conditioned medium compared to microglia-conditioned medium and the attenuation of transcription at later time-points in comparison with both microglia-conditioned medium and unconditioned medium was consistent with OECs having ameliorated a sustained increase in GM-CSF transcription that has been associated with the recruitment of co-activators to the gene promoter region in T cells (Brettingham-Moore et al., 2005a). GM-CSF transcription was significantly elevated from 12 to 24 hours for astrocytes exposed to microglia-conditioned medium compared to astrocytes in OEC-conditioned or unconditioned medium. This suggested that cytokines or other factors released by microglia may have had an additional effect on transcription through a pathway independent of NF-κB, since microglia did not have a measurable additive effect on PMA/ionophore stimulation of NF-κB translocation. However, there may have been a stronger mean activation of NF-κB in individual astrocytes, not detectable as a difference in the percentage of activated astrocytes, which

led to the stronger and more sustained effects of PMA/ionophore on transcription in microglia-conditioned medium.

4.38 Were the cultured astrocytes pre-conditioned to injury?

A variety of pre-conditioning treatments have been shown to moderate inflammatory responses and tissue damage to subsequent CNS injuries (Liu et al., 2000; Carmel et al., 2004; Drozdz et al., 2006; Ambros et al., 2007; Bigdeli et al., 2009; Lehotsky et al., 2009) and the tolerance to ischemia is dependent on PKC and NF-κB activation during the pre-conditioning in many treatment models (Ginis et al., 2002; Bright and Mochly-Rosen, 2005; Lu et al., 2009; Ridder and Schwaninger, 2009). The Chapter 4 results show that the cultured astrocytes in this research were activated in the presence of co-cultured microglia and by soluble factors that microglia released into conditioned medium. Astrocytes were found to be similarly activated in the presence of activated microglia in the unpurified cortical cultures during the preparation of cultures for later experimentation. Even changes of media were demonstrated to significantly activate astrocytes and activation of immediate early genes in response to media changes has been previously demonstrated in epithelial cells (Yang et al., 2006). Consequently, cultured astrocytes may represent a pre-conditioned cell population that are resistant to further inflammatory activation except in response to strong stimuli, such as PMA and ionophore. Pre-conditioning could explain why there was only relatively modest upregulation of the cytokine, GM-CSF, associated with the PMA/ionophore stimulation of NF-κB in the cultured astrocytes. Unlike mature cortical astrocytes *in vivo*, cultured cortical astrocytes express high levels of GFAP, consistent with their having undergone activation during culture, leading to the development of a reactive phenotype. Any stimuli strong enough to induce re-activation of the cultured astrocytes may also induce apoptosis and accompanying degradation of GFAP and other proteins. In addition, high levels of nuclear IκB in the cultured astrocytes due to earlier activation of NF-κB could explain the rapid cycle of NF-κB activation and deactivation (Brown et al., 1993; Sun et al., 1993; Zabel et al., 1993; Baeuerle and Henkel, 1994) in response to PMA and ionophore stimulation.

4.39 Conclusions

This research provided evidence that a soluble factor released by OECs moderated both the NF-κB translocation and GM-CSF transcription components of astrocyte activation. This moderation of astrocyte reactivity represents a plausible mechanism whereby transplanted OECs enhance neuronal survival and increase the likelihood of neural repair after CNS injury. Investigation of the direct effects of OECs on neuronal responses using the *in vitro* model of inflammatory activation established by this research could provide further insight into these possibilities. PMA/ionophore stimulated translocation of NF-κB to nuclei of microglia and meningeal fibroblasts, in addition to astrocytes and increased astrocytic transcription of the pro-inflammatory cytokine, GM-CSF, providing further evidence of the relevance of the treatment model to the investigation of inflammatory responses following CNS injury. Furthermore, stimulation with PMA/ionophore and by soluble factors released from microglia induced NF-κB translocation to a similar extent in astrocytes and OECs moderated the translocation induced by either stimulus. The similarity of the activating effects of microglia and PMA/ionophore supports the physiological relevance of the *in vitro* activation model, since activated microglia participate and interact with astrocytes during the inflammatory response to CNS injury. Co-culture with OECs also appeared to maintain astrocytes in a more quiescent state prior to PMA/ionophore treatment than found in astrocyte monocultures or co-cultures with microglia and fibroblasts. In addition, the NF-κB translocation response in OECs displayed apparent insensitivity to PMA/ionophore and microglia-conditioned medium. Insensitivity to these stimuli may indicate a resistance to injury-induced pro-inflammatory signals that could be an advantage for therapeutic transplants of OECs after CNS injury. Although the moderation of GM-CSF transcription by OECs supported the physiological relevance of the moderation of astrocytic NF-κB translocation, testing the effects of OECs on astrocytic transcription of other NF-κB-dependent pro-inflammatory mediators, particularly IL-1β, TNF-α, IL-6, iNOS, COX-2 and chemokines, could provide stronger evidence. Assays for cytokines and ROS, and Western blots or real-time quantitative RNA analysis for expression of proteins associated with astrogliosis, such as GFAP and CSPGs, could also provide useful evidence concerning the possible

therapeutic efficacy and mechanisms for the observed moderation of astrocytic NF-κB translocation by OECs.

CHAPTER 5:
OECs and astrocyte apoptosis

5.0 Introduction

5.00 Apoptosis and CNS injury

Ischemia following the disruption of blood supply by CNS injury results in insufficient oxygen and glucose delivery to maintain cellular homeostasis and consequently leads to necrotic or apoptotic cell death through multiple mechanisms including excitotoxicity, acidosis, ionic dysregulation and oxidative stress (Bright and Mochly-Rosen, 2005; Doyle et al., 2008; Harting et al., 2008; Broughton et al., 2009; Candelario-Jalil, 2009). Rapid energy depletion, mitochondrial collapse and ion pump failure result in large increases in intracellular calcium and extracellular potassium (Swanson et al., 1997; Hansson and Ronnback, 2004; Doyle et al., 2008; Broughton et al., 2009; Candelario-Jalil, 2009). Cell swelling, lysis and extensive necrotic cell death follow within minutes in the lesion core where the restriction of blood flow and associated ischemia is most severe. Collateral blood supply can help maintain tissue viability in the injury penumbra where the severity of ischemia and the timing of reperfusion are major determinants of cell survival. Cell death occurs less rapidly in the penumbra and is more likely to be through regulated apoptosis than necrosis. Waves of peri-infarct depolarisation emanating from excitotoxicity in the lesion core, diffusion of glutamate and potassium, and the production of reactive oxygen species, particularly in response to reperfusion, can increase penumbral damage by promoting apoptosis. Further regulation of apoptosis occurs through interaction between the inflammatory responses of neurons, glia and migratory immune cells involving intracellular signalling pathways and secreted inflammatory mediators. Inflammation following CNS injury can lead to increased apoptotic cell death that may continue for months. This temporally delayed second wave of programmed cell death in the ischemic penumbra can cause tissue damage that exceeds the initial injury and contributes significantly to functional deficits (Swanson et al., 1997; Doyle et al., 2008; Rami et al., 2008). The delayed nature of the penumbral

apoptotic cell death and its regulation by multiple intracellular and extracellular factors provides an attractive feasible target for therapeutic strategies (Broughton et al., 2009).

5.01 Excessive intracellular calcium levels induce apoptosis

The failure of mitochondrial ATP production in the hypoxic conditions following CNS injury prevents the plasma membrane Ca^{2+} ATPase from maintaining the usual low intracellular calcium ion concentrations necessary for normal cell functions (Pivovarova et al., 2004; Jemmerson et al., 2005; Nguyen and Jafri, 2005; Christophe and Nicolas, 2006). Excitoxicity resulting from elevated extracellular glutamate levels allows further influx of calcium into neurons through activation of N-methyl-D-aspartate (NMDA) receptors and increased calcium permeability of alpha-amino-3-hydroxy-5-methylisoxazole-4-propionic acid (AMPA) receptors. The rise in intracellular calcium levels during ischemia activates numerous calcium-dependent proteases, lipases and DNases resulting in damage to essential cell structures and cell death by necrosis or apoptosis. Activated caspases directly promote apoptosis (Beer et al., 2001; Faubel and Edelstein, 2005; Verkhratsky, 2007; Nakka et al., 2008; Broughton et al., 2009) and can also cleave and inactivate the plasma membrane Ca^{2+} ATPase to exacerbate the elevation of intracellular calcium levels (Schwab et al., 2002). Activation of the calpain family of calcium-dependent cysteine proteases can induce apoptosis by cleavage of caspases, cleavage and release of apoptosis inducing factor from mitochondria or, less directly, by cleavage of metabotropic glutamate receptors, ion channels, calcineurin and other intracellular targets (Du et al., 1999; Ray, 2006; Zhu et al., 2007; Bevers et al., 2009; Leon et al., 2009). While the uptake of calcium ions by mitochondria provides an important buffering mechanism to maintain normal intracellular calcium levels (Kannurpatti et al., 2000; Carafoli, 2002; Clapham, 2007), excessive accumulation of calcium by mitochondria plays a crucial role in delayed neuronal death after CNS injury (Liu, 1997; Brustovetsky et al., 2002; Pivovarova et al., 2004; Jemmerson et al., 2005; Wang and Youle, 2009). Mitochondrial calcium overload leads to increased permeability of the inner mitochondrial membrane, swelling of the matrix and outer membrane rupture, releasing respiratory chain cytochrome c into the cytosol where it initiates apoptosis by activating caspases. Cytochrome c can also be released by the formation of a permeability

transition pore in the mitochondrial outer membrane, an event that is regulated by the Bcl-2 family of proteins (Brustovetsky et al., 2002; Soane et al., 2007; Leon et al., 2009; Robertson et al., 2009; Wang et al., 2009a). Oxidative phosphorylation is calcium-dependent and increases in mitochondrial calcium levels of viable cells in the injury penumbra can increase oxidative phosphorylation and the associated ROS production (Perez-Pinzon et al., 2005; Loh et al., 2006; Szeto, 2006; Busija et al., 2008; Niizuma et al., 2009; Wang et al., 2009a). The resultant high levels of nitric oxide, superoxide and peroxynitrite can damage mitochondrial and cellular molecules triggering signalling mechanisms that culminate in apoptosis.

5.02 Does NF-κB promote apoptosis?

5.02.0 NF-κB promotes growth and differentiation

As a key regulator of inflammatory responses, NF-κB controls transcription of genes that promote immune cell survival, proliferation and differentiation (Baeuerle and Henkel, 1994; Baldwin, 1996; Yamamoto and Gaynor, 2001; Ridder and Schwaninger, 2009). Activation of NF-κB is therefore generally considered to be anti-apoptotic with p65-deficient cells being more susceptible to apoptosis and constitutive NF-κB activation being involved in the abnormal growth and proliferation of tumour cells (Wang et al., 1996; Ridder and Schwaninger, 2009). NF-κB directly activates anti-apoptotic genes including TNF receptor-associated factors, inhibitors of apoptosis and Bcl-2 proteins, which inhibit TNFα-induced apoptosis, block the activation of caspases and prevent cytochrome c release from mitochondria respectively (Wang et al., 1996; Wang et al., 1999; Weaver et al., 2003; Groesdonk et al., 2007; Plesnila et al., 2007; Rami et al., 2008). NF-κB also promotes transcription of cyclin D1, which promotes cell cycle progression (Guttridge et al., 1999). Despite these known anti-apoptotic effects, NF-κB activation associated with the severe ischemia following CNS injury contributes to cell death and increases tissue damage (Ridder and Schwaninger, 2009) and the NF-κB-dependent cytokines, IL-1β and TNF-α can induce apoptosis (Chao et al., 1995; Yokota et al., 2000; Li et al., 2001; Ortis et al., 2006; Gosselin and Rivest, 2007). These conflicting effects may to some extent be related to variations in the sensitivity of different cell types to various inflammatory stimuli and NF-κB activation (Baeuerle and

Henkel, 1994; Ridder and Schwaninger, 2009). However, suppression of NF-κB in both neurons and astrocytes has been demonstrated to decrease tissue damage and enhance recovery after CNS injury (Schneider et al., 1999; Brambilla et al., 2005b; Zhang et al., 2008; Brambilla et al., 2009). In contrast, delayed neuronal apoptosis after brain injury has been shown to involve inhibition of NF-κB by the pro-apoptotic transcription factor, p53 (Plesnila et al., 2007) and NF-κB activation during TNFα-induced inflammation promotes astrocyte survival (Ginis et al., 2002; Quinones et al., 2008).

5.02.1 NF-κB transcriptional effects depend on the severity and duration of activation

It appears likely that the variable effects of NF-κB on apoptosis relate to the strength and duration of activation and interactions with other inflammatory signalling molecules (Baichwal and Baeuerle, 1997; Yamamoto and Gaynor, 2001; Ridder and Schwaninger, 2009). Preconditioning by inducing a brief period of sublethal ischemia protects against a subsequent severe ischemic insult (Blondeau et al., 2001; Ginis et al., 2002; Carmel et al., 2004; Dhodda et al., 2004; Noguchi et al., 2007; Bigdeli et al., 2009; Lehotsky et al., 2009). The neuroprotection conferred by preconditioning is dependent on NF-κB and can be induced by treatment with the NF-κB-regulated pro-inflammatory cytokine, TNFα (Ginis et al., 2002; Bigdeli et al., 2009; Guo et al., 2009; Ridder and Schwaninger, 2009). The moderate transient activation of NF-κB during preconditioning apparently favours the transcription of anti-apoptotic and neuroprotective factors that can then moderate the effects of the strong sustained activation of NF-κB that occurs during severe ischemia. Sustained NF-κB activation induces production of ROS and inflammatory cytokines that can induce apoptosis through intrinsic and extrinsic pathways (Clemens et al., 1998; Ginis et al., 2002; Hoffman et al., 2002; Dhodda et al., 2004; Loh et al., 2006; Ortis et al., 2006). High levels of pro-inflammatory mediators increase blood flow and disrupt the BBB resulting in increased oedema, ionic imbalance and recruitment of leukocytes (Lopez-Neblina et al., 2005; Harukuni and Bhardwaj, 2006; Nakka et al., 2008). The consequent amplification of inflammation prolongs NF-κB activation and increases delayed apoptotic cell death. Interestingly, the transcription factor, CEBP homologous protein, which can synergise with NF-κB to promote inflammatory gene expression, is upregulated in cultured astrocytes in response to hypoxia and hypoglycaemia but only

induces apoptosis when the upregulation is sustained and not when the upregulation is transient (Benavides et al., 2005).

5.02.2 NF-κB family members have differing transcriptional effects

Differential expression and activation of NF-κB family members may also contribute to the variable effects on neuronal apoptosis with p65 activation promoting apoptosis and c-Rel activation protecting neurons against ischemia by inducing anti-apoptotic gene expression (Pizzi et al., 2009; Sarnico et al., 2009; Valerio et al., 2009). However, the transcriptional effects of NF-κB family members vary with cell type and c-Rel activation can also promote apoptosis and is required for sustained activation of inflammatory gene transcription in lymphocytes (Baldwin, 1996; Cogswell et al., 2003; Brettingham-Moore et al., 2005a; Bednarski et al., 2009).

5.03 Neurons are more susceptible to ischemic apoptosis than astrocytes

Neurons are more susceptible to ischemia-induced apoptosis than astrocytes because they are subject to excitotoxicity, have exceptionally high energy demands and are particularly vulnerable to oxidative stress (Pivovarova et al., 2004; Doyle et al., 2008; Broughton et al., 2009; Forder and Tymianski, 2009; Guo et al., 2009; Niizuma et al., 2009). The much greater resistance of astrocytes to ischemic damage substantially relates to their neuronal metabolic support role (Takuma et al., 2004; Panickar and Norenberg, 2005; Laird et al., 2008; Wang and Bordey, 2008). Astrocytes have large stores of the metabolic substrates, glycogen, glutamate and glutamine that enable the maintenance of metabolic activity for 1-2 hours in the absence of glucose and a greater capacity than neurons to utilise fatty acids and ketone bodies for metabolism. Elevated extracellular glutamate and calcium levels ensue from cell death and damage during CNS injury and the consequent excitotoxic stimulation of neurons leads to uptake of excessive calcium and consequently apoptotic or necrotic neuronal death (Kannurpatti et al., 2000; Johnston, 2005; Verkhratsky, 2007; Villmann and Becker, 2007; Candelario-Jalil, 2009). Astrocytes protect neurons against excitotoxicity by taking up the excess calcium and glutamate both following CNS injury and as a normal physiological function (Kim et al., 1994; Verkhratsky and Steinhauser, 2000; Simard and Nedergaard, 2004; Panickar and

Norenberg, 2005; Girouard and Iadecola, 2006; Iadecola and Nedergaard, 2007; Wang and Bordey, 2008). Commensurate with their physiological role in maintaining extracellular ionic homeostasis, astrocytes have superior calcium buffering capacity to neurons and are accordingly less susceptible to apoptosis (Cornell-Bell et al., 1992; Venance et al., 1997; Verkhratsky et al., 1998; Lee et al., 2000; Verkhratsky, 2006; Burgos et al., 2007b).Compared to neurons, astrocytes have higher levels of glutathione, ascorbic acid, anti-apoptotic proteins, such as Bcl-2, and the anti-oxidant enzymes, catalase, superoxide dismutase (SOD) and glutathione peroxidase to protect against free radical damage (Eddleston and Mucke, 1993; Penkowa and Hidalgo, 2000; Swanson et al., 2004; Acarin et al., 2005; Chen et al., 2006b; Jia-Yi et al., 2006). TNF family ligands are important inducers of apoptosis in the CNS from which astrocytes are protected by their constitutive calcium/calmodulin kinase II activity (Song et al., 2006). Furthermore, TNFα induces expression of the calcium-binding protein, calbindin-D, which protects astrocytes against apoptosis induced by elevated intracellular calcium in response to calcium ionophore or amyloid β-peptide (Wernyj et al., 1999).

5.04 Astrocyte apoptosis can be induced in vitro

Despite their protective mechanisms, apoptosis can been readily induced in cultured astrocytes (reviewed by Takuma et al., 2004; Giffard and Swanson, 2005) using a variety of in vitro models of ischemia (Yu et al., 2001; Xu et al., 2004; Benavides et al., 2005; Chen et al., 2005c; Chu et al., 2008) and other treatments related to CNS injury including acidosis (Swanson et al., 1997; Giffard and Swanson, 2005), oxidative stress (Takuma et al., 1999; Bonini et al., 2004) inflammatory cytokines (Song et al., 2006) and elevation of intracellular calcium levels induced by hypoxia (Kintner et al., 2007), calcium ionophore (Wernyj et al., 1999) or thapsigargin (Takuma et al., 1999). Astrocyte apoptosis has also been identified following ischemic (Li et al., 1995; Beer et al., 2001) or contusive (Kaya et al., 1999; Moroni, 2008) brain injury. Apoptosis is more difficult to confirm *in vivo* (Giffard and Swanson, 2005) because of the high cell density of the tissue together with variable cell morphologies and nuclear sizes. In addition, apoptotic cells and fragments are removed by macrophages in the lesion and surrounding tissue. Identification of astrocytes by their expression of GFAP may have led to an underestimation of astrocyte

apoptosis following CNS injury. GFAP is normally only expressed at low levels in grey matter astrocytes preventing the correct identification of apoptotic astrocytes in the early stages of injury responses. The upregulation of GFAP by reactive astrocytes does not become pronounced until several days after injury and is probably accompanied by the induction of anti-apoptotic factors (Swanson et al., 2004; Takuma et al., 2004; Giffard and Swanson, 2005).

5.05 Astrocytes are essential for neuronal survival after CNS injury

The normal physiological functions of astrocytes, including the clearance of extracellular glutamate and its conversion to glutamine, maintenance of extracellular ionic and pH homeostasis, coupling of cerebral blood flow to neuronal activity, provision of metabolic substrates for neurons and ROS scavenging are obviously crucial to neuronal function and survival (Swanson et al., 2004; Takuma et al., 2004; Panickar and Norenberg, 2005; Iadecola and Nedergaard, 2007; Kintner et al., 2007; Wang and Bordey, 2008). After CNS injury astrocyte survival is a critical determinant of neuronal survival and the maintenance of tissue viability in the lesion penumbra. Enhanced glutamate uptake due to upregulation of glutamate transporters by reactive astrocytes may limit neuronal excitotoxic damage. Production of antioxidants such as ascorbate, glutathione and metallothionein by reactive astrocytes can detoxify high levels of ROS that could otherwise damage neurons and induce apoptosis (Neal et al., 1996; Penkowa et al., 1997; Swanson et al., 2004; Wakida et al., 2007). Reactive astrocytes also secrete neuroprotective factors, such as erythropoietin (Diaz et al., 2005; Wakida et al., 2007) and glial cell line-derived growth factor (Choi-Lundberg and Bohn, 1995; Widenfalk et al., 2001; Lin et al., 2006; Chu et al., 2008) that can activate neuronal NF-κB to induce transcription of anti-apoptotic proteins. However, strongly activated astrocytes release high levels of nitric oxide, chemokines, matrix metalloproteases and the pro-inflammatory cytokines, TNFα and IL-1β that can contribute to neuronal death and promote recruitment of leukocytes, which may further intensify the inflammatory response (Feuerstein et al., 1994; Chen et al., 2001b; Domanska-Janik et al., 2001; Meeuwsen et al., 2003a; Swanson et al., 2004; John et al., 2005; Gosselin and Rivest, 2007).

5.06 Research rationale

Since astrocyte survival and reactivity following CNS injury are crucial determinants of neuronal survival, OEC-mediated protection of astrocytes against apoptosis is a possible mechanism for the beneficial effects of OEC transplant therapy. Conditioned medium from OECs has been previously reported to protect PC12 cells from 6-OHDA induced apoptosis in an in vitro model of Parkinson's disease (Feng et al., 2008), although the identity of the cultured OECs was not confirmed in this research. Furthermore, the described OEC culture method involved passaging to remove fibroblasts, which is likely to have had the opposite effect, since fibroblasts survive passaging better than OECs. In Chapter 3, PMA and ionophore induced NF-κB activation in astrocytes and at high doses, ionophore appeared to induce apoptosis. In Chapter 4, OECs moderated PMA and ionophore-induced NF-κB activation in astrocytes. Moderate transient activation of NF-κB appears to be protective against ischemia-induced neuronal apoptosis, while strong sustained activation of NF-κB appears to promote apoptosis (Ridder and Schwaninger, 2009). Therefore, the moderation of NF-κB activation by OECs could inhibit the astrocyte apoptosis associated with ionophore treatment. OEC moderation of ionophore-induced apoptosis would be highly relevant for CNS injury therapy, since ionophore induces elevation of intracellular calcium, a key factor in CNS injury responses and the initiation of apoptosis (Gwag et al., 1999; Clapham, 2007; Doyle et al., 2008; Guo et al., 2009). Hence, this component of the research investigates ionophore-induced astrocyte apoptosis and its potential moderation by soluble factors released from OECs. OEC effects on apoptosis were compared with the effects of microglia and fibroblasts for additional controls and because soluble factors from microglia activated astrocytic NF-κB similarly to PMA and ionophore. The apoptotic effects of ionophore on OECs and astrocytes were also compared because transplanted OECs *in vivo* would be subject to the same post-injury conditions as astrocytes and PMA/ionophore did not activate NF-κB in OECs.

5.07 Specific aims

1. Investigate astrocyte apoptosis in response to ionophore.

2. Determine whether OECs moderate ionophore-induced astrocyte apoptosis.

3. Compare the effects of microglia, meningeal fibroblasts and OECs on astrocyte apoptosis.

4. Compare the apoptotic effects of ionophore on OECs and astrocytes.

5.1 Method

5.10 Comparisons of apoptosis by nuclear condensation

Apoptosis was assayed by measuring the percentage of cells with condensed nuclei in the following experiments:

1. untreated astrocytes and astrocytes stimulated with 20ng/mL PMA combined with 500nM ionophore for 1, 3, 6 or 24 hours (Fig. 5.1)
2. astrocytes stimulated with 20ng/mL PMA combined with 500nM or 1μM ionophore for 8 hours (Fig. 5.2)
3. astrocytes stimulated with 20ng/mL PMA, 1μM ionophore or combined 20ng/mL PMA and 1μM ionophore for 8 hours (Fig. 5.3)
4. astrocytes incubated in OEC CM, microglia CM or DMEM for 30 hours with and without 1μM ionophore for the final 6 hours (Fig. 5.3)
5. OECs that were untreated or stimulated for 3 hours with 60nM, 125nM, 500nM or 1μM ionophore (Fig. 5.9)

5.11 Measurement of nuclear condensation in astrocytes and OECs

Astrocytes or OECs were cultured on 18mm coverslips in 12-well culture plates as described in Chapter 2. Following treatments, cells were fixed, immunostained for GFAP (astrocytes) or $p75^{NTR}$ (OECs) and NF-κB, with Hoechst blue 33342 (Molecular Probes) counterstaining of nuclei and imaged as described for immunocytochemistry in Chapter 2. The images of Hoechst blue stained astrocyte nuclei were used to assess apoptosis by

nuclear condensation. Cells with relatively small, brightly stained nuclei were scored as apoptotic (plus signs in Figs. 5.2, 5.3 and 5.4). Merged immunoreactivity images confirmed that condensed nuclei were associated with apoptotic cells displaying cytoplasmic condensation and degradation of cytoplasmic protein. 8 images were used to generate group means and data were analysed by Student's t-test or, where possible, ANOVA and post hoc Tukey tests.

5.12 Comparisons of astrocyte apoptosis by TUNEL assay

Initially TUNEL assays were conducted using fluorescence microscopy to optimise treatment conditions prior to assays using flow cytometry. Astrocytes were cultured and treated on 18mm coverslips in 12-well culture plates for comparisons using fluorescence microscopy and in 25cm^2 culture flasks for comparisons using flow cytometry. Astrocyte apoptosis was compared by TUNEL assay after the following treatments, using fluorescence microscopy:

1. 500nM ionophore for 4, 6 or 8 hours (Fig. 5.5).
2. 125nM, 250nM, 500nM or 1μM ionophore for 8 hours (Fig. 5.6).

and using flow cytometry:

3. 1μM ionophore for 8 hours and untreated astrocytes (Fig. 5.7).
4. incubation for 32 hours in astrocyte CM, OEC CM, fibroblast CM microglia CM and all treated with 1μM ionophore for the final 8 hours (Fig. 5.8).

5.13 TUNEL assay for detection of apoptotic astrocytes

The Apo-BrdU™ kit (Calbiochem®), a two colour terminal deoxynucleotide transferase dUTP nick end labelling (TUNEL) assay, labelled DNA breaks in apoptotic nuclei with fluorescein and total cellular DNA in all nuclei with propidium iodide. The labelling procedure illustrated in the flow diagram (Fig. 5.0) followed the kit protocol with minor modifications, as follows:

Astrocytes for flow cytometry analysis were detached from 25cm^2 culture flasks by washing with 2mL warm Versene to inhibit cell-substrate binding by chelating calcium

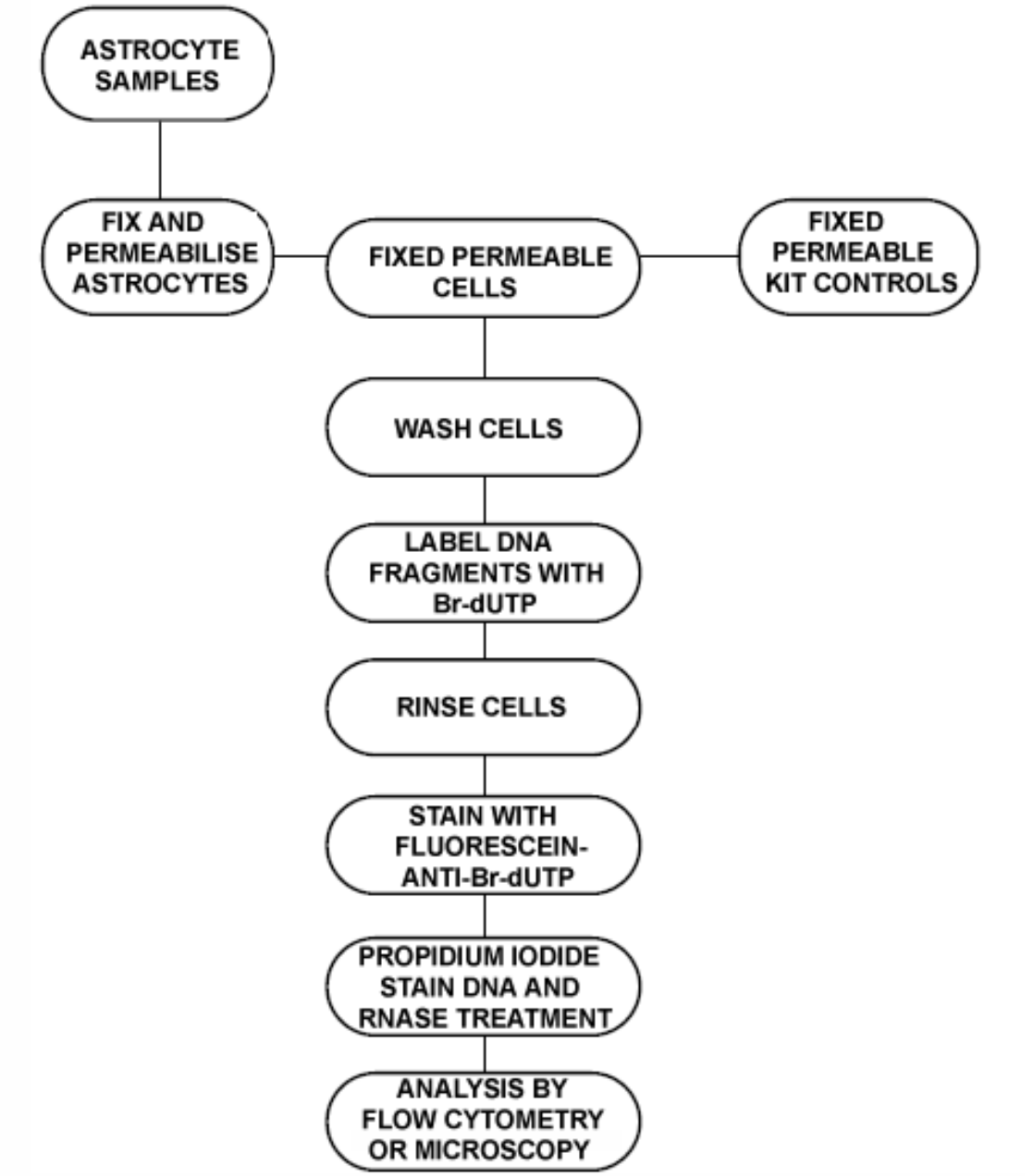

Figure 5.0 Flow chart for Apo-BrdU™ kit TUNEL staining protocol. The Apo-BrdU™ kit (Calbiochem®), a two colour Terminal deoxynucleotide transferase dUTP Nick End Labelling (TUNEL) assay, labelled DNA breaks with fluorescein and total cellular DNA with propidium iodide. Astrocytes and kit control lymphocytes were stained for detection of apoptotic cells by flow cytometry and fluorescence microscopy.

ions followed by treatment with 1mL 0.75% trypsin in HBSS. Detached astrocytes were resuspended in 2mL DMEM-10S to halt trypsinisation, combined with the medium removed from the flask before trypsinisation that may have contained previously detached apoptotic cells, centrifuged at 300g for 5 minutes and resuspended in 2% (w/v) paraformaldehyde in pH 7.4 PBS at a concentration of ~10^6 cells/mL for 30-60 minutes on ice to cross-link DNA. Samples were centrifuged at 300g for 5 minutes and washed with PBS twice, cells resuspended in the residual PBS by gentle vortexing, diluted to ~10^6 cells/mL with ice-cold 70% (v/v) ethanol to permeabilise cell membranes and stored overnight at -20^{O}C. Normal lymphocytes and apoptotic lymphocytes that had been fixed and permeabilised using the above protocol were provided with the kit as negative and positive controls respectively. Kit control and astrocyte cell suspensions were swirled to resuspend cells and 1 mL aliquots containing ~10^6 cells/mL were transferred to 15mL centrifuge tubes (Becton Dickinson) and centrifuged at 300g for 5 minutes and the ethanol removed carefully by aspiration. Samples were resuspended in 1 mL wash buffer and centrifuged at 300g for 5 minutes twice before resuspending in 50 μL of DNA fragment (TUNEL) labelling solution that to ensure equal concentrations of reagents for each sample was prepared as a master mix, as follows:

DNA LABELLING SOLUTION	1 Sample	10 Samples
Reaction Buffer	10 μL	100 μL
Terminal deoxynucleotide transferase	0.75 μL	7.5 μL
Br-dUTP	8 μL	80 μL
Distilled H_2O	32.25 μL	322.5 μL
Total Volume	51 μL	510 μL

Samples were incubated with the DNA labelling solution for 3 hours at 37^{O}C on a shaker to keep cells in suspension. Labelling solution was then removed by twice adding 1 mL of rinse buffer, centrifuging at 300g for 5 minutes and removing the supernatant by

aspiration. To stain Br-dUTP labelled DNA fragments, cells were then resuspended in 100 μL of fluorescein isothiocyanate (FITC)-conjugated anti-BR-dUTP solution that was also prepared as a master mix, as follows:

ANTIBODY SOLUTION	1 Sample	10 Samples
FITC-anti-Br-dUTP	5 μL	50 μL
Rinse Buffer	95 μL	950 μL
Total Volume	100 μL	1000 μL

The samples were incubated with the antibody solution for 1 hour, at room temperature on a shaker, in the dark (by wrapping sample tubes in aluminium foil). For the final 30 minutes of the antibody incubation 500 μL of buffer containing propidium iodide to label all DNA in the samples and RNase A to degrade any mRNA in the samples was added to each sample. Samples were kept in the dark and analysed within 3 hours by flow cytometry. Astrocytes for analysis by fluorescence microscopy were fixed, permeabilised and stained while remaining adherent to 18 mm glass coverslips in 12-well culture plates. Coverslips were removed from culture plates and placed on wax-filled culture plate lids for the DNA labelling and antibody incubation steps and only required 100 μL/sample additions of the propidium iodide/RNase buffer. Coverslips were then rinsed in distilled water, mounted on glass slides using Permafluor™ aqueous mounting medium (Immunotech, France), stored in the dark and imaged within 6 hours.

5.14 Fluorescence microscopy analysis of TUNEL stained samples

Specimens were viewed on a fluorescence microscope (Olympus BX50) for image capture with an Optronics Magnafire camera. Adobe Photoshop© was used to merge sets of 2 images showing propidium iodide (red) and TUNEL staining with fluorescein isothiocyanate (FITC; green) (Fig. 5.5). Nuclei that stained with both propidium iodide and FITC appeared yellow in the merged images and were scored as apoptotic. Eight

images were used to generate group means and data were analysed by ANOVA and post hoc Tukey tests.

5.15 Flow cytometry analysis of TUNEL stained samples

Samples were run on a Coulter Elite EST flow cytometer (Miami, USA) and excited with a 488 nm argon laser that induced propidium iodide to fluoresce at 623 nm and fluorescein at 520 nm without any requirement for fluorescence compensation. The intensity of fluorescence at each wavelength was simultaneously acquired by the flow cytometer software as stained nuclei passed the detector. Each detected event was plotted on a log FITC fluorescence intensity versus log propidium iodide fluorescence intensity graph (Figs. 5.7 and 5.8) for each sample using Windows Multiple Document Interface (WinMDI©) for flow cytometry analysis, Version 2.9 (Copyright© Joseph Trotter, available free online at (http://facs.scripps.edu/software.html). DNA in apoptotic cells was expected to be stained by both propidium iodide and fluorescein. Therefore events plotting in the upper right quadrant of each graph were deemed to represent apoptotic nuclei. Using the positive and negative control graphs (Fig. 5.7), quadrant grids (x = 488, y = 232) were selected to provide the best separation of the dual-stained apoptotic nuclei and were applied to graphs of each sample to enable calculation of the percentages of apoptotic astrocytes. 6 samples from separate cultures were used for each treatment in the comparison between ionophore-treated and untreated astrocytes in DMEM (Fig. 5.7) and 3 samples from separate cultures for comparisons between ionophore-treated astrocytes in the conditioned media (Fig. 5.8). Kit negative and positive controls were included in each TUNEL assay experiment to verify that the staining protocol had been effective. Data were analysed by ANOVA and post hoc Tukey tests.

5.2 Results

5.20 PMA/ionophore induced time-dependent astrocyte apoptosis

NF-κB activation may lead to apoptosis of neurons and glia contributing to the pathogenesis of CNS injury. Since PMA/ionophore activated NF-κB in astrocytes, this treatment was further investigated for possible effects on astrocyte apoptosis. The images of Hoechst blue staining of nuclei and immunostaining for GFAP and NF-κB revealed

that from 3 to 24 hours following treatment with 20ng/mL PMA combined with 500nM ionophore, increasing numbers of astrocytes displayed morphology changes consistent with apoptosis (Fig. 5.1). As previously described, NF-κB translocated to astrocyte nuclei after 1 hour of treatment without any obvious changes in cytoplasmic or nuclear size or morphology (Xs in Fig. 5.1E-H). However after 3 hours or more of treatment many astrocytes showed signs of apoptosis, including irregular, condensed nuclei with intense Hoechst staining (e.g. plus signs in Fig. 5.1I-P) together with cytoplasmic condensation and depolymerisation of GFAP. Many nuclei also had punctate Hoechst staining (e.g. asterisks in Fig. 5.1Q-T; enlarged in Fig. 6.1V) indicating fragmentation of nuclear DNA, an unambiguous marker of apoptosis. The morphology changes that accompanied cytoplasmic condensation progressed from stellate to blebby as processes appeared to become detached from the substrate. Astrocytes with the most condensed nuclei appeared to revert to a flattened morphology delineated by fragmented GFAP immunoreactivity while NF-κB immunoreactivity was lost from the cytoplasm, although there was often a faint remnant in the nuclear region (e.g. Xs in Fig. 5.1R). Quantitative analysis of the percentage of apoptotic astrocytes, as indicated by nuclear condensation, (Fig. 5.1U) showed that the 3% of untreated astrocytes were apoptotic and there was no significant change after 1 hour of PMA/ionophore treatment ($p > 0.05$). The percentage of apoptotic astrocytes had increased significantly after 3 hours (18.66±0.95%; $p < 0.001$), with further significant increases after 6 and 24 hours of treatment ($p < 0.001$), by which time the large majority of astrocytes were apoptotic (78.67±3.39%).

5.21 PMA/ionophore-induced astrocyte apoptosis depended on ionophore concentration

Different PMA and ionophore doses were used during the investigation of astrocyte activation and although there was no measurable increase in the induction of NF-κB translocation, there did appear to be increased apoptosis with higher ionophore concentrations (Fig. 5.2). Comparisons of Hoechst-stained astrocyte nuclei (Fig. 5.2I) showed that there were significantly more apoptotic astrocytes (plus signs in A-H) with 1μM ionophore (74.56±6.35%) than with 500nM ionophore (41.82±5.41%) in 8 hour combined PMA/ionophore treatments ($p < 0.001$). Similar alterations of normal astrocyte

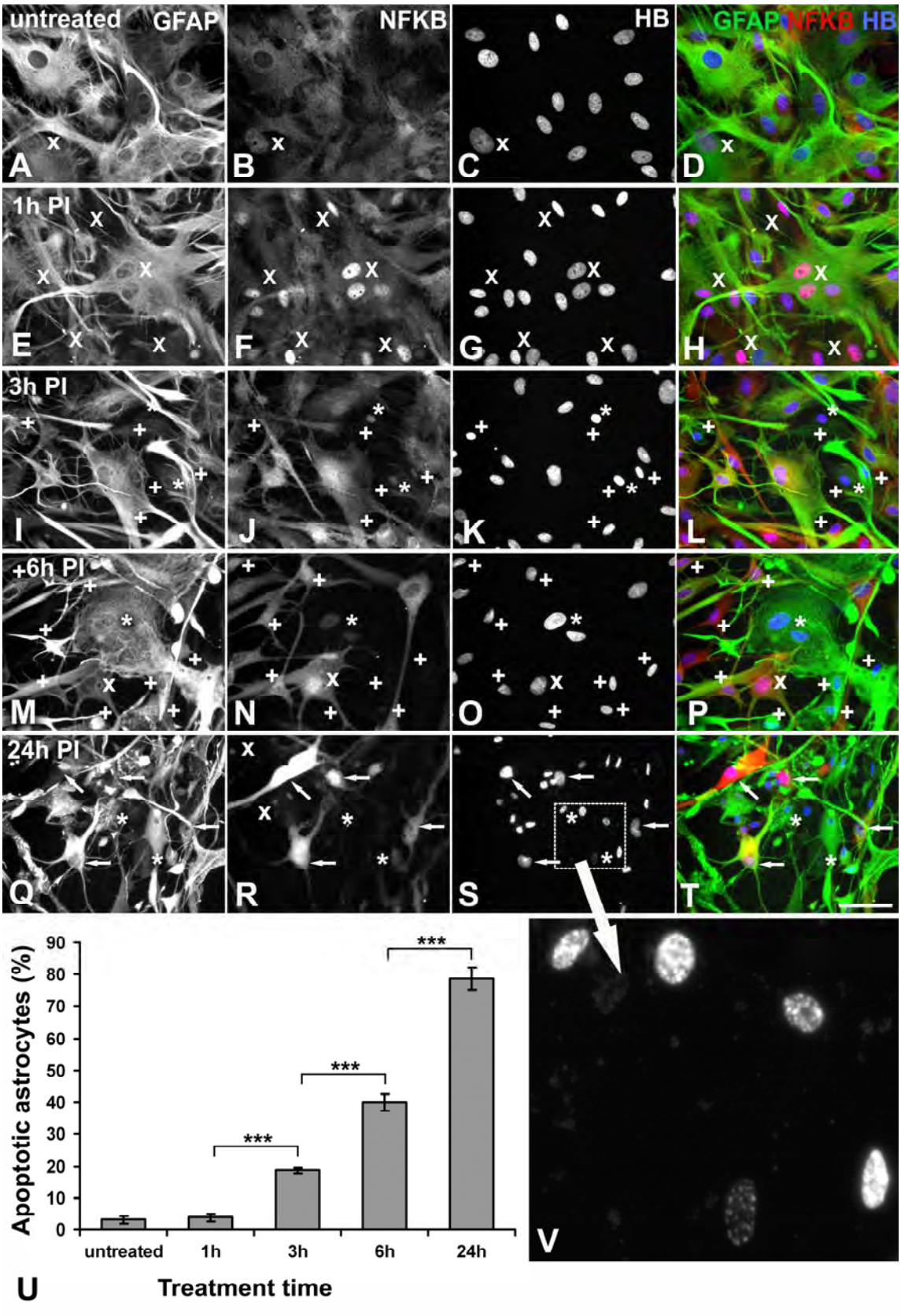
untreated
GFAP
NFKB
HB
GFAP NFKB HB
A
B
C
D
1h PI
E
F
G
H
3h PI
I
J
K
L
+6h PI
M
N
O
P
24h PI
Q
R
S
T
Apoptotic astrocytes (%)
90
80
70
60
50
40
30
20
10
0
***
***
***
untreated
1h
3h
6h
24h
Treatment time
U
V

Figure 5.1 PMA/ionophore induces time-dependent astrocyte apoptosis. Apoptosis was compared for untreated astrocytes (A-D) and astrocytes treated with 20ng/mL PMA combined with 500nM ionophore (PI) for one (E-H), three (I-L), six (M-P) or 24 hours (Q-T). Immunostaining for GFAP (A, E, I, M, Q and green in D, H, L, P, T) was used to identify astrocytes and NF-κB (B, F, J, N, R and red in D, H, L, P, T) to identify activated astrocytes. Nuclei were counterstained with Hoechst blue (HB) (C, G, K, O, S and blue in D, H, L, P, T). Only a few astrocytes had nuclei with NF-κB immunoreactivity more intense than in the cytoplasm in untreated (Xs in A-D) and 6 hour PMA/ionophore-treated cultures (Xs in M-P). In the untreated astrocytes, GFAP and NF-κB immunoreactivity was uniformly distributed in the cytoplasm and nuclei were large and ovoid, with uniform Hoechst staining of nuclear DNA. Following 1 hour of PMA/ionophore treatment there was intense NF-κB immunoreactivity in many nuclei (Xs in E-H) without any noticeable change in cytoplasmic or nuclear morphology and Hoechst staining. After 3 and 6 hours of treatment, many astrocytes appeared apoptotic (plus signs I-P) with condensed nuclei and cytoplasm, accompanied by depolymerisation of GFAP. Astrocytes with cytoplasmic NF-κB immunoreactivity have stellate morphologies but in cells with more condensed nuclei, cytoplasmic NF-κB is absent, there is sometimes faint nuclear NF-κB immunoreactivity (asterisks in I-L) and morphologies are flattened or blebby. Two large nuclei near the centre of images M-P (asterisks) with punctate Hoechst staining belong to astrocytes in the early stages of apoptosis. The flattened astrocytes exhibited detachment and condensation of processes with only faint nuclear NF-κB immunoreactivity. After 24 hours of treatment, most astrocytes are apoptotic with depolymerised GFAP and blebby or flattened morphologies. Nuclei are either condensed or irregularly-shaped and many have punctate Hoechst staining of DNA (e.g. asterisks in Q-T) clearly illustrated in the enlargement (V) of the indicated area in S. Astrocytes with the least condensed nuclei (arrows in Q-T) retain some cytoplasmic NF-κB immunoreactivity while in others there are faint remnants of NF-κB staining in nuclei (e.g. Xs in R). U: Quantitative analysis of astrocyte apoptosis. Astrocytes with condensed nuclei were scored as apoptotic. There was a significant increase in the percentage of apoptotic astrocytes following PMA/ionophore treatment for 3 hours ($p < 0.001$) with further significant increases after 6 and 24 hours of treatment ($p < 0.001$). Data were analysed by ANOVA with post-hoc Tukey's multiple comparison tests. Percentages are means ± SEM, $n = 8$. Asterisks denote significant differences: *** $p < 0.001$.

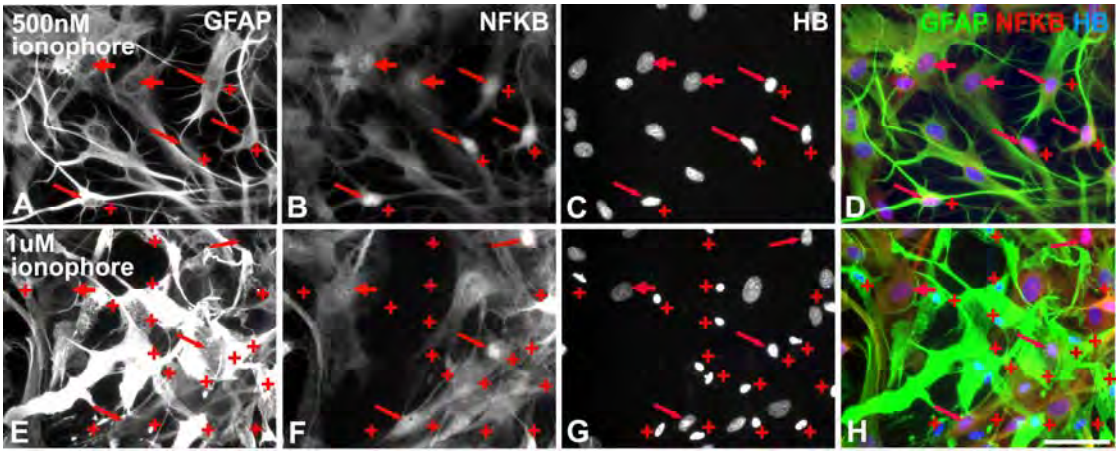

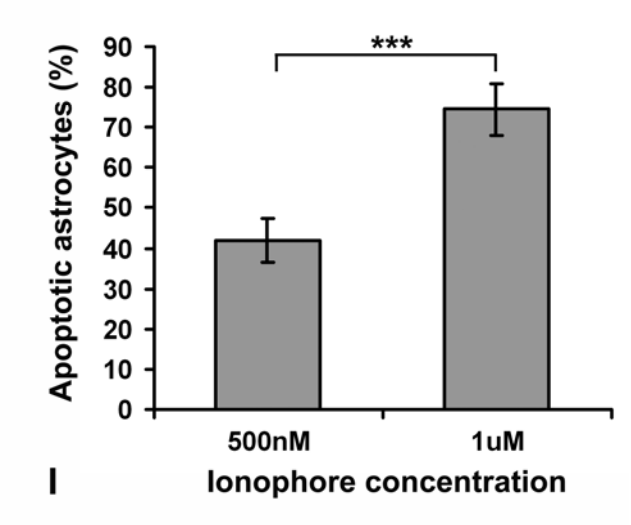

Figure 5.2 Astrocyte apoptosis induced by PMA/ionophore depends on ionophore concentration. Astrocytes were treated with 20ng/mL PMA combined with 500nM or 1μM ionophore for 8 hours. Immunostaining for GFAP (A, E and green in D, H) was used to identify astrocytes and NF-κB (B, F and red in D, H) to identify activated astrocytes. Nuclei were counterstained with Hoechst blue (HB) (C, G and blue in D, H). A few activated astrocytes with intense nuclear NF-κB immunoreactivity retained normal nuclear and cytoplasmic morphologies (broad arrows in A-H) while others had condensed nuclei and cytoplasm (long arrows in A-H). Apoptotic astrocytes were more frequent following treatment with 1μM ionophore (D-H) and were characterised by condensed nuclei (plus signs in A-H) accompanied by condensed cytoplasm as revealed by intense GFAP immunoreactivity (A, D, E, H). Initially cytoplasmic NF-κB immunoreactivity increased as cytoplasm condensed in apoptotic cells but with increasing nuclear condensation there was a loss of NF-κB immunoreactivity (B, F). Scale bar is 50 μm. I: Quantitative analysis of astrocyte apoptosis. Astrocytes with condensed nuclei were scored as apoptotic. There were significantly more apoptotic astrocytes following treatment with PMA combined with 1μM ionophore than for PMA combined with 500nM ionophore ($p < 0.001$). Data were analysed by Student's t-test. Percentages are means ± SEM, n = 8. Asterisks denote significant differences: *** $p < 0.001$.

(broad arrows in A-H) morphology and immunostaining to those seen previously (Fig. 5.1) accompanied apoptosis. Apoptotic astrocytes had condensed cytoplasm (long arrows in Fig. 5.2A-H) resulting in intense GFAP and, initially, NF-κB immunoreactivity while at later stages cytoplasmic NF-κB immunoreactivity was absent (Fig. 5.2A-H).

5.22 Ionophore alone induced astrocyte apoptosis

The relative effects of separate and combined treatments with PMA and ionophore on astrocyte apoptosis were then investigated (Fig. 5.3), since NF-κB translocation preceded apoptosis and was induced more strongly by ionophore than PMA. Comparisons of astrocyte apoptosis using Hoechst staining of nuclei (Fig. 5.3G) revealed that after 8 hours of treatment with 20ng/mL PMA there was no significant difference from the low levels of apoptosis in untreated cultures ($p > 0.05$). However, there were large significant increases in the percentage of apoptotic astrocytes (plus signs in Fig. 5.3B, C, E and F) after treatment for 8 hours with 1μM ionophore or combined PMA/ionophore ($p < 0.001$). Although there was more apoptosis with the combined treatment (76.19±8.43%) than for ionophore alone (58.48±4.94%), the difference was not quite significant ($p = 0.054$).

5.23 OECs and microglia did not modulate ionophore-induced astrocyte apoptosis

The effects of media conditioned by OECs or microglia on the ionophore-induced astrocyte apoptosis were then investigated (Fig. 5.4) since OECs had moderated PMA/ionophore-induced NF-κB translocation in astrocytes and microglia had induced NF-κB translocation in a similar manner to PMA/ionophore. Again using Hoechst staining of nuclei for comparisons of astrocyte apoptosis (Fig. 5.4E), no significant effect on astrocyte apoptosis was found in response to 6 hour incubations with OEC or microglia CM ($p > 0.05$). Although treatment for 6 hours with 500nM ionophore did significantly increase apoptosis ($p < 0.001$), there was again no effect attributable to OECs or microglia, since no significant difference was found in the percentage of apoptotic astrocytes ($p > 0.05$) whether treated with ionophore in DMEM (35.93±2.10%), OEC CM (34.83±1.73%) or microglia CM (35.84±1.50%).

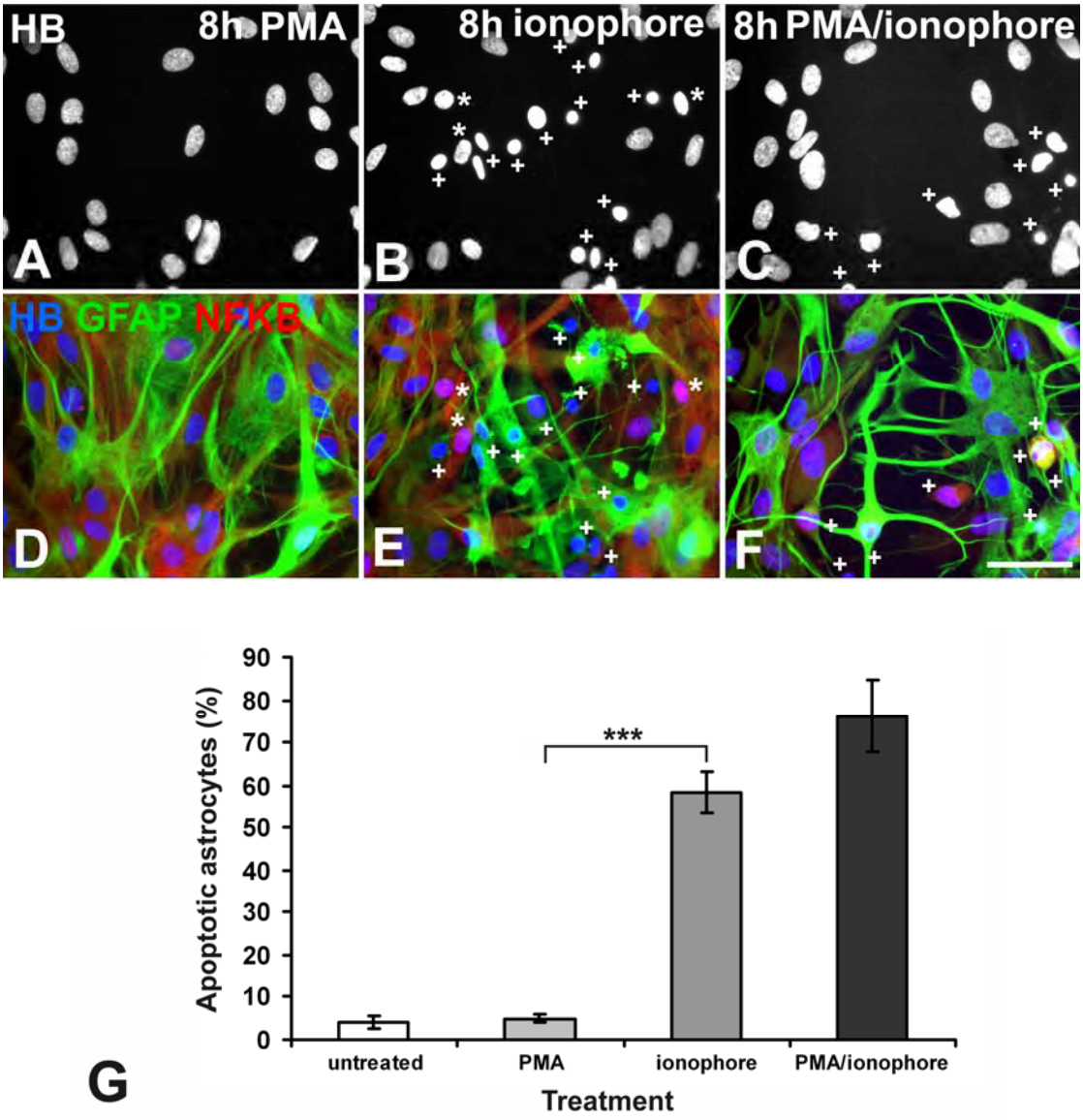

Figure 5.3 Ionophore induces astrocyte apoptosis. Astrocytes were treated for 8 hours with 20ng/mL PMA (A, D), 1μM ionophore (B, E), combined PMA/ionophore (C, F) or were untreated. Immunostaining for GFAP (green) identified astrocytes and NF-κB (red) indicated astrocyte activation (D-F). Nuclei were counterstained with Hoechst blue (HB) (A-C and blue in D-F). Few astrocytes had high levels of nuclear NF-κB immunoreactivity (asterisks in B, E) after 8 hours of PMA treatment. Many ionophore and PMA/ionophore treated astrocytes appeared apoptotic with condensed nuclei (plus signs in B, C, E, F) and cytoplasm as revealed by GFAP immunoreactivity (E, F). Scale bar is 50 μm. G: Quantitative analysis of astrocyte apoptosis. Astrocytes with condensed nuclei were scored as apoptotic. There were significantly more apoptotic astrocytes following ionophore or PMA/ionophore treatment than for PMA-treated or untreated astrocytes ($p < 0.001$). Data were analysed by ANOVA and post-hoc Tukey's multiple comparison test. Percentages are means ± SEM, n = 12. Asterisks denote significant differences: *** $p < 0.001$.

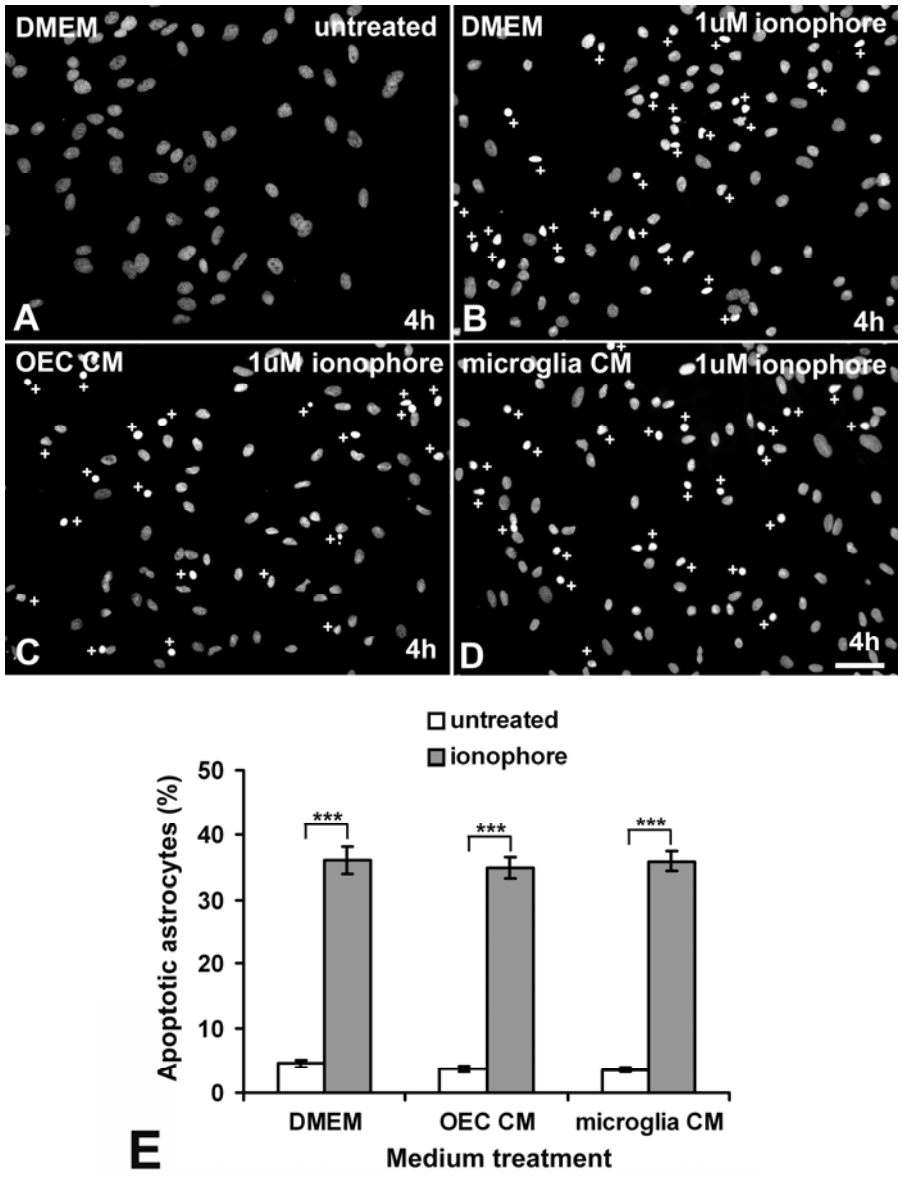

Figure 5.4 Comparison of ionophore-induced apoptosis for astrocytes incubated in OEC CM, microglia CM or DMEM. Astrocytes were treated with 1μM ionophore in DMEM (B), OEC CM (C) or microglia CM (D), or incubated in DMEM (A), OEC CM or microglia CM without ionophore. Cultures were fixed and immunostained for GFAP and NF-κB, 6 hours after ionophore stimulation. Nuclei were counter-stained with Hoechst blue (A-D). Apoptotic cells had condensed nuclei with bright Hoechst staining (plus signs) and were far more frequent following ionophore treatment in all media. Scale bar is 100 μm. E: Quantitative analysis of astrocyte apoptosis. Astrocytes with condensed nuclei were scored as apoptotic. There were significantly more apoptotic astrocytes following ionophore treatment than for untreated astrocytes in all media ($p < 0.001$). There was no significant difference in the percentage of apoptotic astrocytes in DMEM, OEC CM or microglia CM before or after ionophore treatment ($p > 0.05$). Data were analysed by ANOVA and post-hoc Tukey's multiple comparison test. Percentages are means ± SEM, n = 18. Asterisks denote significant differences: *** $p < 0.001$.

5.24 TUNEL staining reveals time-dependent ionophore-induced DNA fragmentation in astrocytes.

Nuclear size can increase as cells grow, varies at different stages of cell cycles and nuclear condensation occurs during both necrotic and apoptotic cell death. Therefore, further experiments were conducted using a Terminal deoxynucleotide transferase dUTP Nick End Labelling (TUNEL) assay to confirm that the ionophore-induced nuclear condensation was a consequence of astrocyte apoptosis. The TUNEL assay could also potentially allow a less subjective and more efficient analysis of apoptotic cells using flow cytometry. Initial assay optimisation experiments (Figs. 5.5 and 5.6) were analysed by fluorescence microscopy before proceeding to flow cytometry analysis. The Apo-BrdU™ TUNEL assay kit labelled DNA in all nuclei with propidium iodide (Fig. 5.5A, D and G) and DNA fragments in apoptotic nuclei with FITC (Fig. 5.5B, E and H). Therefore normal nuclei appeared red and apoptotic nuclei appeared yellow in the merged fluorescence images (Fig. 5.5C, F, I and Fig. 5.6A-D). Although some apoptosis was detected by nuclear condensation in untreated cultures and at significantly higher levels after 3 hours of PMA/ionophore treatment, no nuclei with FITC-labelled DNA fragments were detected using the TUNEL assay after 2 or 4 hours of treatment with 500nM ionophore (Fig. 5.5J). However, many FITC-labelled nuclei, indicative of apoptosis, were clearly identifiable by 6 hours after treatment (33.5±4.82% of astrocytes) and this was similar to the percentage of apoptotic astrocytes detected by nuclear condensation using Hoechst staining for the same treatment (Fig. 5.4; 35.93±2.10%). By 8 hours after treatment, the percentage of apoptotic astrocytes detected by the TUNEL assay was 44.48±6.80%, although this increase was not significant ($p > 0.05$), reflecting the considerable variation in the results between different cultures for similar treatments. The result at 8 hours was similar to the percentage of apoptotic astrocytes detected by Hoechst staining for treatment for the same time period with 500nM ionophore combined with PMA (Fig. 5.2; 41.82±5.41%) and less than for 1μM ionophore alone (Fig. 5.3; 58.48±4.94%).

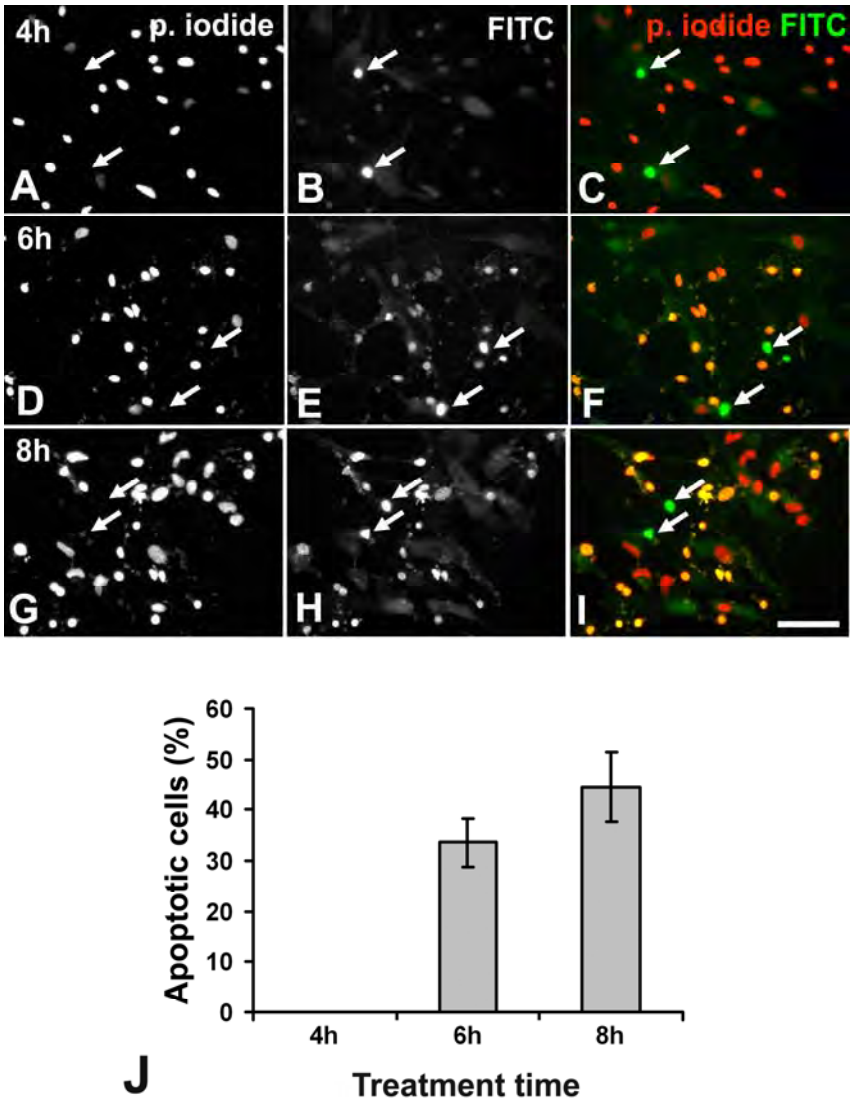

Figure 5.5 Time-dependent DNA fragmentation in ionophore-treated astrocytes. Astrocytes were treated with 500nM ionophore for two (data not shown), four (A-C), six (D-F) or eight (G-I) hours and then stained using an Apo-BrdU™ kit (Calbiochem). The kit provided dual labelling of nuclei with propidium iodide (A, D, G and red in C, F, I) and FITC (B, E, H and green in C, F, I) after permeabilising cell membranes with 70% (v/v) ethanol. Propidium iodide stained DNA in all cells while DNA fragments in nuclei of apoptotic cells were also labelled using Br-dUTP followed by incubation with FITC conjugated anti-Br-dUTP. Therefore nuclei of normal cells appeared red and nuclei of apoptotic cells appeared yellow in the merged images (C, F, I). There was some non-specific FITC staining (green; arrows in A-I) that was not associated with nuclei or incubation time. Apoptotic nuclei were detected only after 6 or 8 hours of incubation with only background levels of FITC immunoreactivity after 4 hours of incubation (B). Scale bar is 50 μm. J: Quantitative analysis of astrocyte apoptosis. Astrocytes with nuclei that appeared yellow in the merged images were scored as apoptotic. No astrocytes were apoptotic after 4 hours incubation and therefore significantly more astrocytes were apoptotic after longer incubations ($p < 0.001$). There was no significant difference in the percentage of apoptotic astrocytes for 6 and 8 hour incubations ($p > 0.05$). Data were analysed by ANOVA and post-hoc Tukey's multiple comparison test. Percentages are means ± SEM, n = 8.

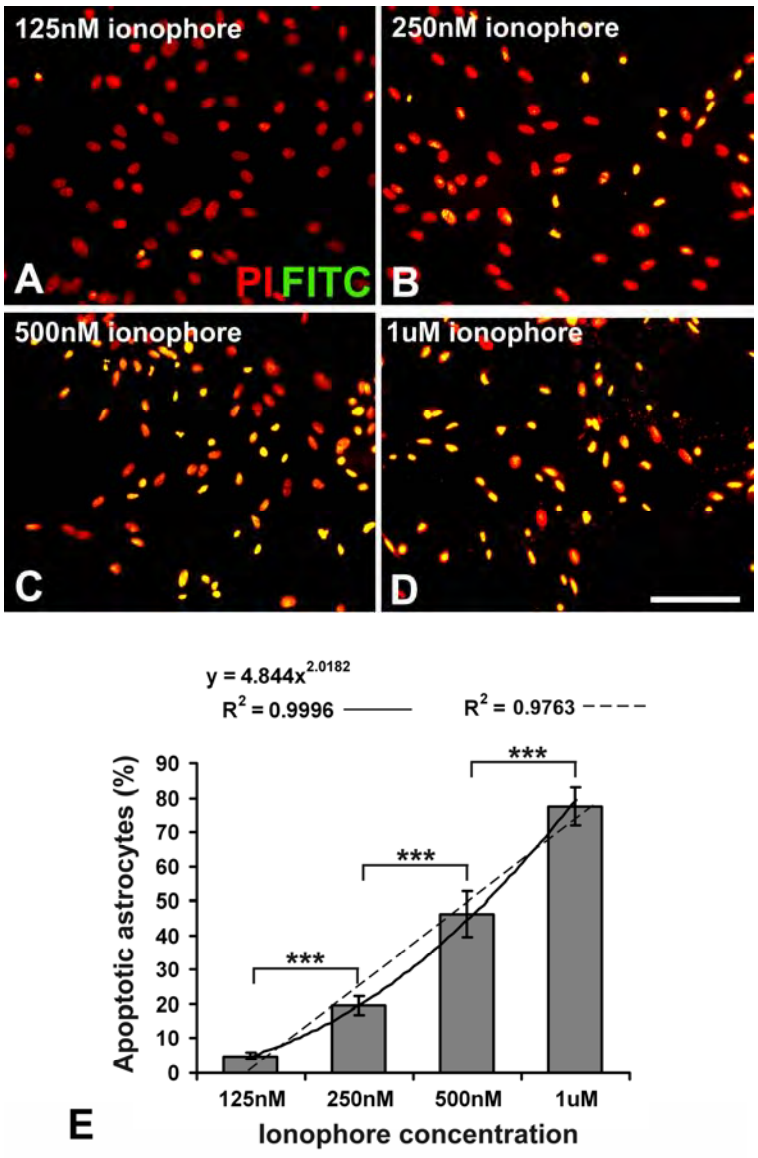

Figure 5.6 Ionophore-induced astrocyte apoptosis is concentration-dependent. Astrocytes were treated with 125nM (A), 250nM (B), 500nM (C) or 1μM (D) ionophore for 8 hours and stained with propidium iodide (PI; red) and TUNEL labelled with FITC (green) using the Apo-BrdU™ kit. A-D: In the merged images, normal nuclei were stained only with propidium iodide and appeared red while apoptotic nuclei were condensed and appeared yellow due to TUNEL/FITC labelling of DNA fragments. Apoptotic nuclei increased in frequency with increasing ionophore concentration. Scale bar is 100 μm. E: Quantitative analysis of astrocyte apoptosis. Astrocytes with nuclei that appeared yellow in the merged images were scored as apoptotic. The percentage of apoptotic astrocytes increased significantly and exponentially with each increase in ionophore concentration ($p < 0.001$, $y = 4.8x^{2.02}$, $R^2 = 0.9996$). The data could also have represented a linear increase in apoptosis with ionophore concentration ($R^2 = 0.9763$). Data were analysed by ANOVA, linear and polynomial regressions and post-hoc Tukey's multiple comparison test. Percentages are means ± SEM, n = 8. Asterisks denote significant differences: *** $p < 0.001$.

5.25 Astrocyte apoptosis was ionophore concentration-dependent

Apoptosis was then compared by TUNEL assay for astrocytes treated with a 125nM (Fig. 5.6A), 250nM (Fig. 5.6B), 500nM (Fig. 5.6C) and 1μM (Fig. 5.6D) ionophore for 8 hours. Only 4.82±0.88% of astrocytes were apoptotic with 125nM ionophore (Fig. 5.6E), similar to the levels identified in untreated cultures by nuclear condensation (Figs. 5.1, 5.3 and 5.4; 3.05±1.26% to 4.64±0.59%). The percentage of apoptotic astrocytes increased significantly ($p < 0.001$) in an exponential manner ($y = 4.8x^{2.02}$, $R^2 = 0.9996$) with each increase in ionophore concentration (19.49±2.81% for 250nM, 46.11±6.68% for 500nM and 77.51±5.33% for 1μM), although the data also fitted well with a linear increase ($R^2 = 0.9763$).

5.26 Flow cytometry assay of apoptosis in ionophore-treated astrocytes

Untreated astrocytes and astrocytes treated with 1μM ionophore were then TUNEL assayed using flow cytometry, together with the kit negative control normal lymphocytes and positive control apoptotic lymphocytes (Fig. 5.7). Particles detected by the flow cytometer were plotted on log FITC fluorescence (520nm) intensity against log propidium iodide fluorescence (623nm) intensity graphs and the graphs divided into quadrants using the same co-ordinates ($x = 488$, $y = 232$) for each graph (Fig. 5.7A-D). The graphs confirmed that dual propidium iodide/FITC labelled apoptotic nuclei from the positive control plotted in the upper right quadrants of the graphs, indicating both high propidium iodide and high FITC fluorescence. Normal nuclei from the positive and negative controls plotted in the upper left quadrant, indicating high propidium iodide fluorescence but low FITC fluorescence. As expected there were significantly more apoptotic nuclei detected by this method for the positive control lymphocyte samples (46.60±4.05%; $p < 0.001$; Fig. 5.7E). Applying the same quadrants selected for the kit control graphs to the graphs for astrocytes indicated that significantly more apoptotic nuclei were detected for the ionophore-treated astrocyte cultures (53.20±4.11%) than for the untreated astrocytes ($p < 0.01$). The percentage of apoptotic nuclei detected was similar for the kit positive controls and ionophore-treated astrocytes. The low percentage of apoptotic nuclei detected in the kit negative controls (3.89±0.94%) was similar to that detected using fluorescence microscope imaging of the untreated astrocytes with either

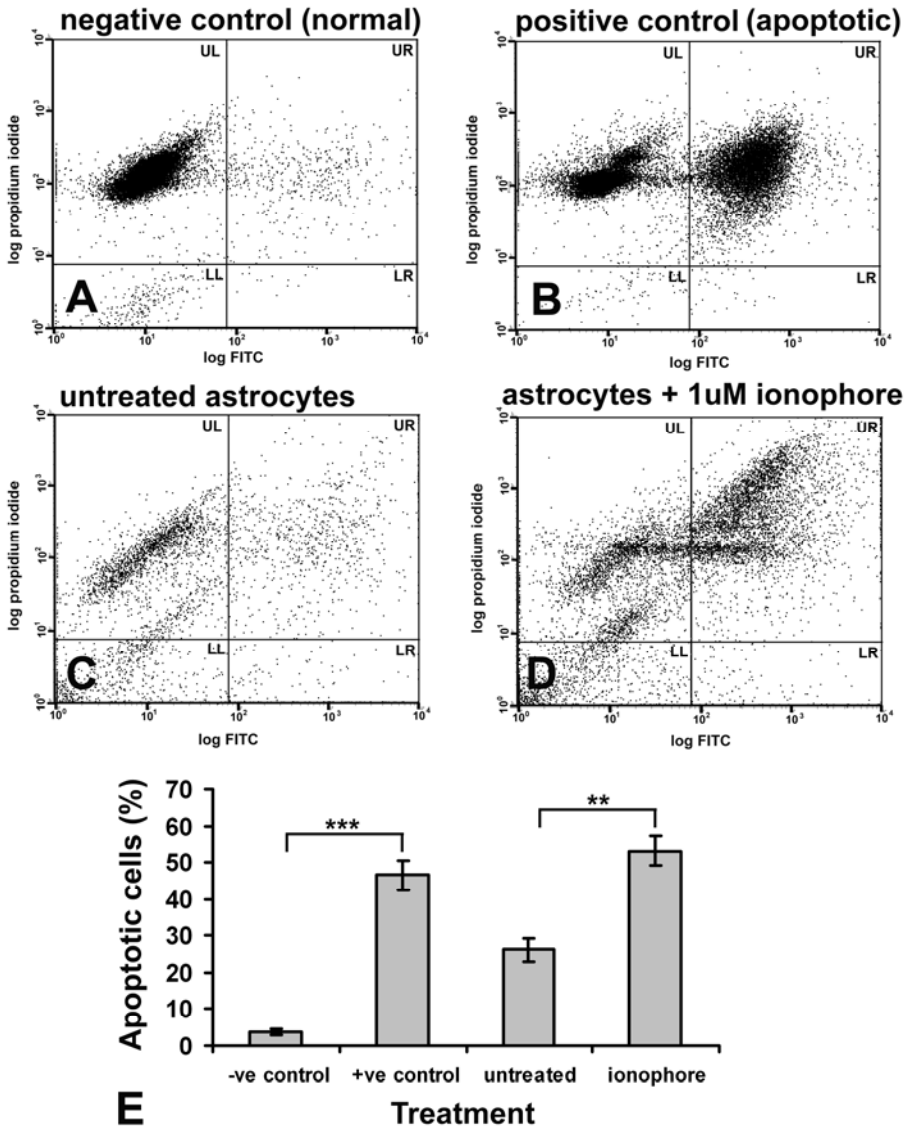

Figure 5.7 Analysis of astrocyte apoptosis by flow cytometry. Apoptosis was compared for Apo-BrdU™ kit lymphocyte negative (A) and positive (B) controls and astrocytes that were untreated (C) or treated for 8 hours with 1μM ionophore (D). All samples including the kit controls were TUNEL labelled with FITC and propidium iodide stained using the Apo-BrdU™ kit and analysed by flow cytometry with excitation at 488 nm. Each detected event was plotted on a scale of log FITC fluorescence (520 nm) intensity against log propidium iodide fluorescence (623 nm) intensity (A-D) and the graphs divided into quadrants using the same co-ordinates (x = 488, y = 232) for each graph. The kit controls confirmed that, as predicted, apoptotic nuclei plotted in the upper right quadrant of the graphs (A, B). More astrocyte nuclei plotted in the upper right quadrant following ionophore treatment (C, D). E: Quantitative analysis of astrocyte apoptosis. Detected events plotting in the upper right quadrants of the log FITC/log propidium iodide graphs were scored as apoptotic cells. There were significantly more apoptotic lymphocytes in the kit positive control samples than in the negative controls ($p < 0.001$). Similarly, there were significantly more apoptotic astrocytes in the ionophore-treated samples than in the untreated astrocyte samples ($p < 0.01$). Data were analysed by ANOVA and post-hoc Tukey's multiple comparison test. Percentages are means ± SEM, n = 4.

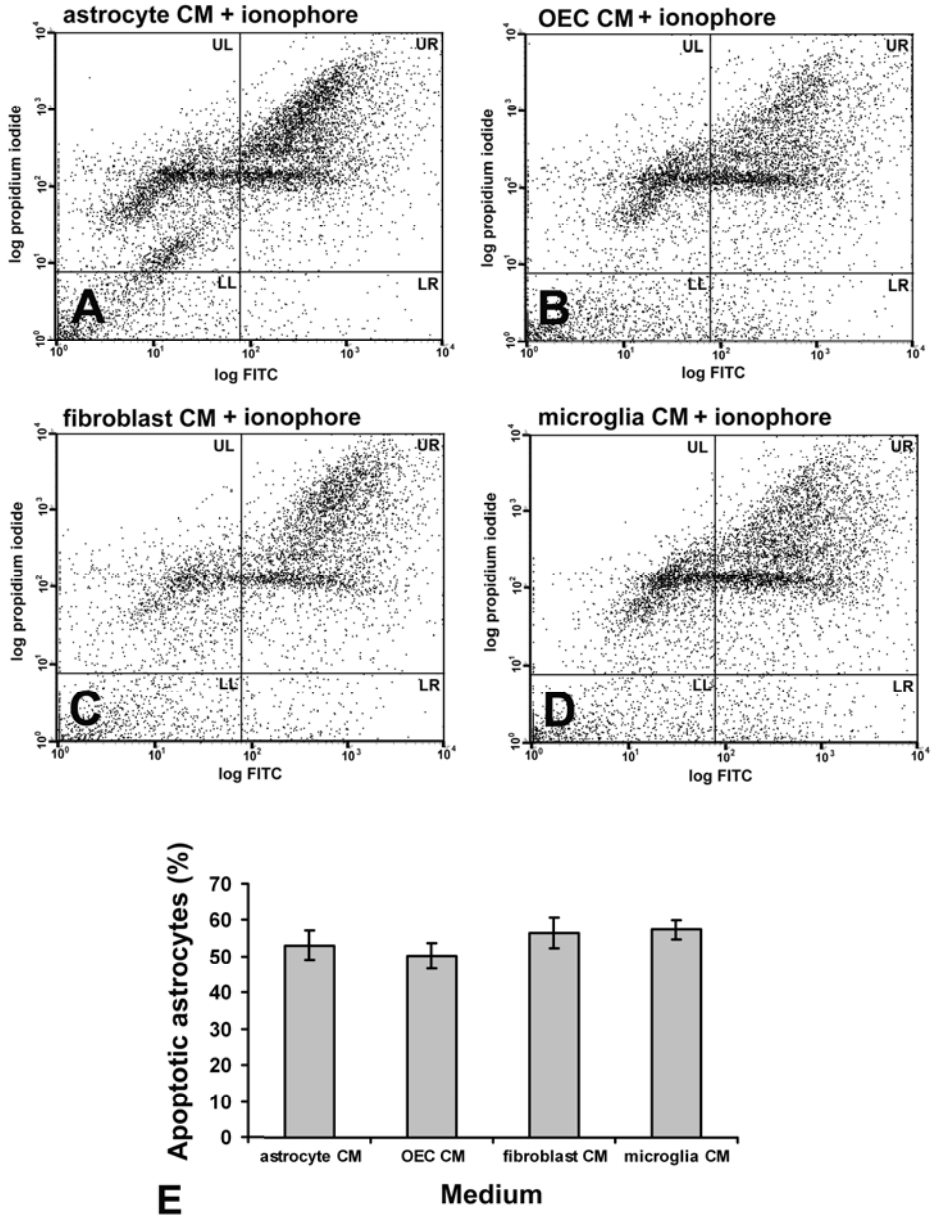

Figure 5.8 Flow cytometric comparison of ionophore-induced apoptosis in astrocytes incubated in astrocyte CM, OEC CM, fibroblast CM or microglia CM. Apoptosis was compared for astrocytes incubated in astrocyte CM (A), OEC CM (B), fibroblast CM (C) or microglia CM (D) after treatment for 8 hours with 1μM ionophore. Samples were TUNEL labelled with FITC and propidium iodide stained using the Apo-BrdU™ kit and analysed by flow cytometry with excitation at 488 nm. Detected events were plotted on log FITC intensity/ log propidium iodide intensity graphs for each sample and as previously (Fig. 6.7), divided into quadrants (A-D). E: Quantitative analysis of astrocyte apoptosis. Detected events plotting in the upper right quadrants of the log FITC/log propidium iodide graphs were scored as apoptotic cells. There was no significant difference in the percentage of apoptotic astrocytes in the different media following ionophore treatment ($p > 0.05$). Data were analysed by ANOVA and post-hoc Tukey's multiple comparison test. Percentages are means ± SEM, n = 4.

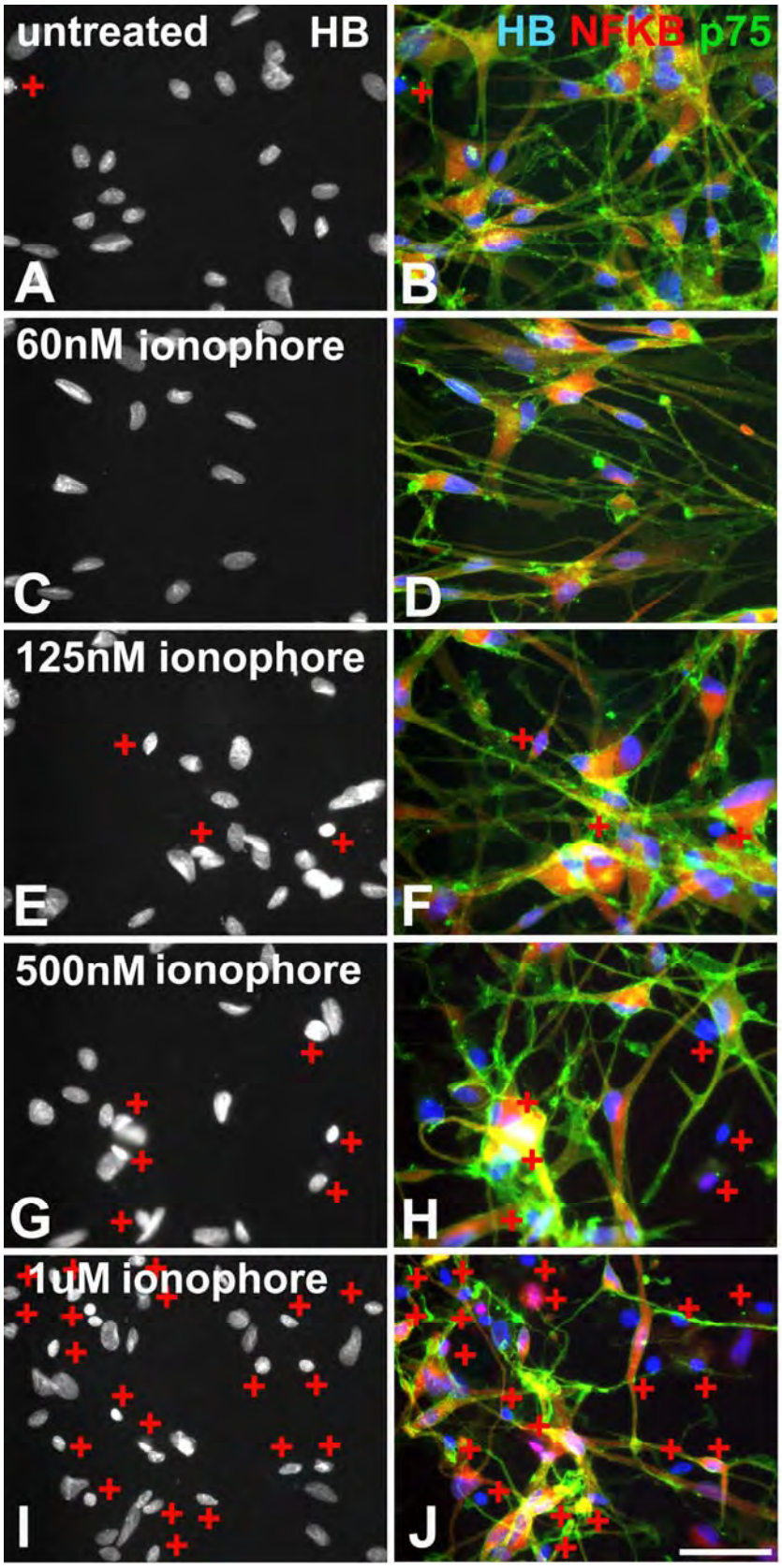
untreated
HB
HB NFKB p75
A
B
60nM ionophore
C
D
125nM ionophore
E
F
500nM ionophore
G
H
1uM ionophore
I
J

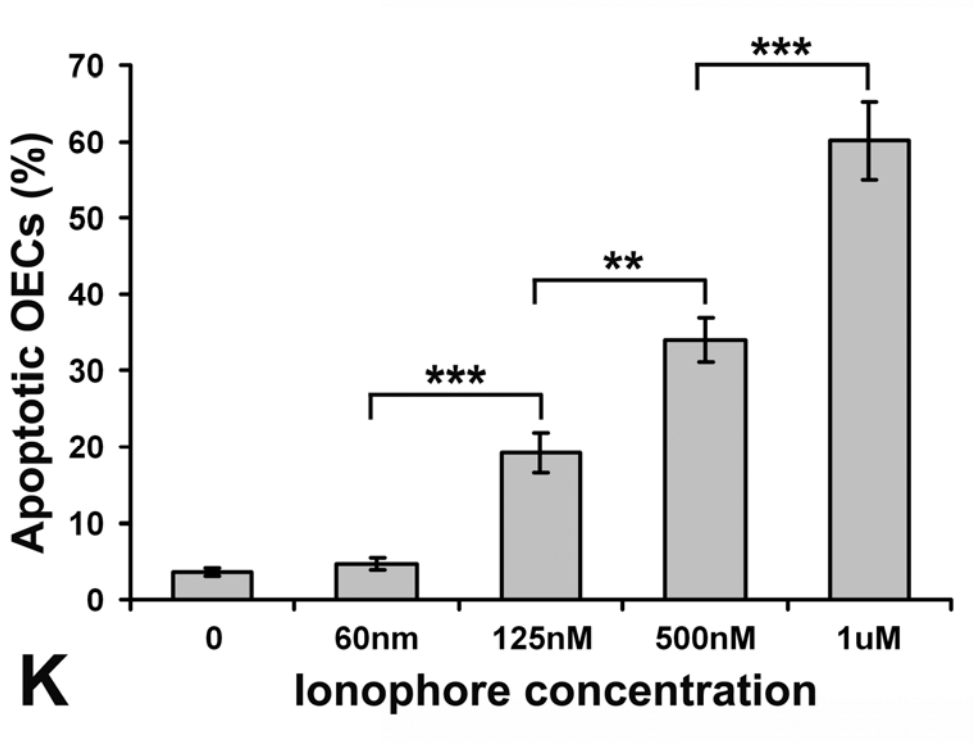

Figure 5.9 Ionophore rapidly induces OEC apoptosis. Apoptosis was compared for OECs that were untreated (A, B) or stimulated for 3 hours with 60nM (C, D), 125nM (E, F), 500nM (G, H) or 1μM (I, J) ionophore. OECs were immunostained for $p75^{NTR}$ (green in B, D, F, H, J) and NF-κB (red in B, D, F, H, J), and nuclei were counterstained with Hoechst blue (A, C, E, G, I and blue in B, D, F, H, J). Apoptotic cells were identified by condensed nuclei (red plus signs in A-J) and were associated with condensed cytoplasm, detachment from the substrate and loss of $p75^{NTR}$ and NF-κB immunoreactivity (B, F, H, J). Few OECs appeared apoptotic in untreated or 60nM ionophore treated cultures but apoptosis increased with increasing ionophore concentration until the majority of OECs appeared apoptotic with 1μM ionophore. Scale bar is 50μm. K: Quantitative analysis of OEC apoptosis. OECs with condensed nuclei were scored as apoptotic. Less than 5% of OECs were apoptotic in untreated or 60nM ionophore treated cultures. With each following increase in ionophore concentration, there was a significant increase in the percentage of apoptotic OECs ($p < 0.001$, 60nM to125nM; $p < 0.01$, 125nM to 500nM; $p < 0.001$, 500nM to 1μM). Data were analysed by ANOVA and post-hoc Tukey's multiple comparison test. Percentages are means ± SEM, n = 8. Asterisks denote significant differences: ** $p < 0.01$, *** $p < 0.001$.

the TUNEL assay or Hoechst staining of nuclei. However, TUNEL assay by flow cytometry detected a significantly much higher percentage of apoptotic nuclei for untreated astrocytes (26.18±3.20%; $p < 0.001$). For the 1μM ionophore-treated astrocytes, similar levels of apoptosis were detected by flow cytometric TUNEL assay (53.20±4.11%) and fluorescence microscopy of Hoechst staining (58.48±4.94%) but higher levels were detected by fluorescence microscopic analysis of the TUNEL assays (77.51±5.33%).

5.27 Flow cytometry did not detect any modulation of ionophore-induced astrocyte apoptosis by OECs, fibroblasts or microglia

Apoptosis was then compared by flow cytometric TUNEL assay for astrocytes treated for 8 hours with 1μM ionophore in medium conditioned by astrocytes, OECs, fibroblasts or microglia (Fig. 5.8). Rather than fresh DMEM, astrocyte CM was the control for comparison with the media conditioned by the other cell types, as it was possible that depletion of nutrients from media by cells during conditioning could contribute to the induction of apoptosis. Detected events were plotted on log FITC fluorescence (520nm) intensity against log propidium iodide fluorescence (623nm) intensity graphs (Fig. 5.8A-D) and using the same co-ordinates as previously (Fig. 5.7), events in the upper right quadrant were scored as apoptotic astrocytes. The detected events graphed as in Figs. 5.7 and 5.8 reached the preset recordable maximum of 20,000 for all the kit control samples whereas for the astrocyte samples, detected events varied between 1278 and 9728 and averaged 4745. Significantly more apoptotic astrocytes were detected after ionophore treatment ($p < 0.001$) independent of the medium conditions, there being no significant differences ($p > 0.05$) in the percentages of apoptotic astrocytes that ranged from 50.35±3.49% for astrocytes in OEC CM to 57.55±2.57% for astrocytes in microglia CM (Fig. 5.8E). This result agreed with the results from Hoechst staining of 500nM ionophore-treated astrocytes in OEC CM and microglia CM (Fig. 5.4), where there was also no significant effect attributable to the conditioned media.

5.28 Ionophore rapidly induced apoptosis of OECs

Although PMA/ionophore did not induce NF-κB translocation in OECs, apoptosis appeared to be occurring much sooner after treatment in OEC cultures than in astrocyte

cultures for the same ionophore dose. Consequently, ionophore concentration-dependent OEC apoptosis was investigated using the images of immunostaining from OEC activation experiments. Apoptosis was compared in OEC cultures that were untreated or treated for 3 hours with 60nM, 125nM, 500nM or 1μM ionophore (Fig. 5.9). Apoptotic cells were identified by condensed nuclei and were associated with condensed cytoplasm, detachment from the substrate and loss of $p75^{NTR}$ and NF-κB immunoreactivity (Fig. 5.9A-J). Less than 5% of OECs were apoptotic in untreated or 60nM ionophore treated cultures (Fig. 5.9K) but thereafter with each increase in ionophore concentration there was a significant increase in the percentage of apoptotic OECs to 19.31±2.62% at 125nM ($p < 0.001$), 33.91±2.80% at 500nM ($p < 0.01$) and 60.16±5.20% at 1μM ($p < 0.001$). At the higher ionophore concentrations, as apoptosis increased, many OECs appeared to have detached from the substrate displaying sinusoidal processes and a tendency to form clumps (Fig. 5.9H, J). Few OECs remained attached to coverslips preventing any analysis following treatment with 125nM to 1μM ionophore for 6 to 8 hours. Similar levels of apoptosis were found in astrocyte cultures at these longer treatment durations (Figs. 5.4, 5.6) as found after only 3 hours of treatment for OECs.

5.3 Discussion

5.30 Ionophore induced astrocyte apoptosis

In addition to activating astrocytes by inducing NF-κB translocation, PMA/ionophore robustly induced astrocyte apoptosis within 6 to 8 hours of treatment. Ionophore more strongly induced NF-κB translocation than PMA and appeared to be entirely responsible for the induction of apoptosis, with the usual stimulus dose of 20ng/mL PMA alone not inducing any increase in astrocyte apoptosis. There was a trend towards increased apoptosis with combined PMA/ionophore compared with ionophore alone, although this was not investigated over a range of PMA and ionophore doses. It is possible that stimulation of oxidative phosphorylation and metabolism through stimulation of protein kinase C and calcium signalling pathways by combined PMA/ionophore could promote ROS production and increase the susceptibility of astrocytes to the apoptotic effects of ionophore-induced increases in intracellular calcium levels.

5.31 Hoechst nuclear staining and TUNEL assays detected similar levels of astrocyte apoptosis

Similar results were obtained using Hoechst staining of nuclei and TUNEL staining with microscopy or flow cytometry. However, flow cytometry detected far fewer cells in astrocyte samples than in the control lymphocyte samples from the TUNEL kit. This was presumably due to loss of astrocytes by disintegration or adherence to plastic tubes during sample preparation and suggested that flow cytometry may not be a suitable method for adherent cells, such as astrocytes. A further problem with the flow cytometric method was the necessity for removing the adherent cells from culture flasks by trypsinisation, which itself induces some apoptosis. This probably explains the significantly higher level of apoptosis found in untreated astrocyte cultures by flow cytometry compared with microscopy and could have obscured any treatment differences in apoptosis. While TUNEL staining provided less ambiguous detection of apoptotic cells than Hoechst staining, both methods yielded similar results and only detected apoptosis at a relatively late stage in the process. Apoptosis assays that detect cytochrome c release from mitochondria or alterations of the plasma membrane could detect apoptosis at earlier stages. These methods could possibly provide results that are more accurate by avoiding the loss of detached cells that occurs at later stages of apoptosis *in vitro*.

5.32 Ionophore-induced astrocyte apoptosis may be independent of NF-κB translocation

The apoptotic effect of ionophore was dose-dependent with large increases in the percentage of apoptotic astrocytes from basal levels of apoptosis with 125nM ionophore to the large majority of astrocytes becoming apoptotic with 1μM ionophore after 8 hours of treatment. To some extent, these results were consistent with the view that stronger activation of NF-κB can promote apoptosis. Although there was no significant difference in astrocyte activation across the range of ionophore concentrations tested there did appear to be more intense nuclear NF-κB immunoreactivity at higher ionophore concentrations. Elevation of intracellular calcium by ionophore treatment induces apoptosis and this mechanism may have induced astrocyte apoptosis independent of ionophore stimulation of NF-κB translocation. The apoptotic effects of ionophore

occurred within 8 hours of treatment, too soon for any substantial protein expression changes deriving from the NF-κB activation, implying that the induction of apoptosis and NF-κB translocation were most probably independent effects. Furthermore, although there was no systematic investigation of the apoptotic time-course, morphological indications of apoptosis did occur at much earlier time-points.

5.33 OECs, microglia and fibroblasts did not modulate astrocyte apoptosis

There was no evidence for the modulation of astrocyte apoptosis by medium conditioned by microglia, OECs or fibroblasts. Microglia-conditioned medium induced NF-κB translocation in astrocytes in a similar manner to PMA/ionophore but did not induce apoptosis in astrocytes or modulate the ionophore-induced apoptosis. This result provided strong evidence that the activation of NF-κB and induction of apoptosis in astrocytes were independent processes within the experimental conditions utilised in this research. Pro-inflammatory cytokines released by activated microglia, particularly Il-1β and TNF-α, are the probable components of the microglia-conditioned medium that activate NF-κB in astrocytes. Unlike ionophore, these cytokines do not directly promote increased intracellular calcium levels and the microglia-conditioned medium did not promote apoptosis, inferring that the initiating factor for astrocyte apoptosis was elevated intracellular calcium levels rather than NF-κB translocation. It is also possible that microglia-conditioned medium preferentially stimulated the expression of anti-apoptotic NF-κB-dependent genes in astrocytes, since TNF-α can promote the expression of anti-apoptotic factors that protect against ionophore-induced calcium influx (Wernyj et al., 1999) and NF-κB activation can promote the expression of factors that protect against TNF-α-induced apoptosis (Groesdonk et al., 2007; Rami et al., 2008). However, the composition of the microglia-conditioned medium is unknown and it did not inhibit the ionophore-induced apoptosis. Excessive intracellular calcium resulting from ischemia is a crucial determinant of neuronal apoptosis following CNS injury (Verkhratsky, 2006, 2007; Doyle et al., 2008; Nakka et al., 2008; Broughton et al., 2009) and this research suggests that the same probably applies to astrocytes. Modification of the PMA/ionophore treatment model by varying the ionophore dose and extracellular

calcium levels could possibly mimic injuries of different severity or different regions in the injury penumbra.

5.34 OECs are more susceptible to ionophore-induced apoptosis than astrocytes

The moderation of NF-κB translocation by OECs was not accompanied by any corresponding evidence of the moderation of ionophore-induced astrocyte apoptosis by OEC-conditioned medium. This result was again consistent with separate pathways regulating ionophore-induced NF-κB translocation and ionophore-induced apoptosis in astrocytes. In addition to not protecting astrocytes from the ionophore-induced apoptosis, OECs were themselves significantly more susceptible to the apoptotic effects of ionophore than astrocytes. Apoptosis was induced more rapidly and at lower ionophore doses in OECs than in astrocytes. This susceptibility to apoptosis in response to calcium influx may have implications for the use of OECs as therapeutic implants because extracellular calcium levels are elevated following cellular and vascular damage by CNS injury. Although microglia-conditioned medium did not induce apoptosis in astrocytes, it would be informative to determine whether OECs were also susceptible to apoptosis in response to factors released by microglia. In addition to testing the effects of microglia-conditioned medium, it would be relevant to test the effects of pro-inflammatory cytokines, such as TNF-α and IL-1β, on OEC apoptosis, since these are produced by activated microglia, astrocytes and peripheral macrophages at CNS injury sites. For similar reasons, comparisons between the responses of OECs and astrocytes to reactive oxygen species could provide further insight into the responses of transplanted OECs at injury sites.

5.35 Conclusions

Astrocytes are less susceptible than neurons to apoptosis following CNS injury partly due to their superior glutamate and calcium buffering capacity (Cornell-Bell et al., 1990; Kim et al., 1994; Verkhratsky et al., 1998; Verkhratsky, 2006; Iadecola and Nedergaard, 2007; Wang and Bordey, 2008). However, the severe disruption of extracellular homeostasis following CNS injury can overcome even the calcium buffering capacity of astrocytes,

leading to disruption of mitochondrial membranes and the initiation of apoptosis (Swanson et al., 1997; Takuma et al., 1999; Matute et al., 2002). Thus, ionophore-induced astrocyte apoptosis represents a useful model of astrocyte apoptosis ensuing from CNS injury. The greater resistance of astrocytes to the ionophore-induced apoptosis suggests that they have superior calcium buffering to OECs. Consequently, OECs transplanted into ischemic regions of CNS lesions, where there are high levels of extracellular calcium ions, glutamate and ATP could become apoptotic due to excessive calcium influx. Disruption of the surviving vasculature during OEC transplantation could re-initiate ischemia and *in vivo* research may be required to determine the optimal timing and location for transplanting OECs. It may be preferable to introduce therapeutic OEC transplants away from the ischemic core of injuries and, as far as possible, without disrupting the surviving vasculature. However, correct location of OEC transplants to allow interaction with astrocytes and possibly migration of OECs in a suitable direction for axon regeneration may also be necessary to promote axon regrowth (Raisman, 2000; Li et al., 2005b; Teng et al., 2008). Once inflammation subsides, any remnant lesion cavity may be the ideal location for OEC transplantation and moderate inflammation induced by the transplant procedure may stimulate cellular mobilisation and neurite sprouting. It is perhaps relevant to these observations that OECs transplanted directly into corticospinal cord lesion cavities, 8 weeks after injury, promoted spinal cord repair and some recovery of motor function but had no beneficial effect when misplaced a few hundred microns dorsal to cavities (Keyvan-Fouladi et al., 2003). However, ionophore directly transports calcium ions across membranes down the concentration gradient (Mitani and Otake, 1978; Fasolato and Pozzan, 1989; Dedkova et al., 2000) and in the absence of this reagent, the relationship between extracellular calcium levels and excessive calcium influx would depend on the expression and function of calcium channels and pumps in OECs.

ATP and glutamate released from olfactory neurons can evoke calcium signalling in OECs with similarities to the calcium signalling that occurs in astrocytes in response to neural activity (Rieger et al., 2007). Other evidence based on measurements of intracellular calcium ion concentrations suggest that OECs have unusual calcium

dynamics, including high resting intracellular calcium ion levels and the absence of voltage-gated calcium channels (Hayat et al., 2003). These features of OEC biology may explain their vulnerability to ionophore-induced calcium influx and in this regard, it would be informative to investigate the comparative expression of calcium channels and pumps in OECs and astrocytes using immunocytochemistry. OEC susceptibility to apoptosis may relate to a normal physiological role during the turnover and replacement of olfactory neurons. Rather than becoming activated by physiological challenges, OECs surrounding olfactory nerve fascicles could undergo apoptosis, thus initiating apoptosis and replacement of the olfactory neurons. This could represent a defence mechanism against the spread of infections along the olfactory tract into the CNS, when an inflammatory challenge is too severe for any protective anti-inflammatory or innate immune functions of OECs. However, it is uncertain whether OECs are replaced or, instead, axons regrow within channels formed by surviving OECs, during olfactory neuron turnover. Further investigation of OEC responses to other inflammatory and apoptotic stimuli could shed light on the physiological and therapeutic importance of the susceptibility of OECs to ionophore-induced apoptosis.

CHAPTER 6:
Summary and further research

6.0 A mechanism for the therapeutic effects of OEC transplants

The unique regenerative capacity of olfactory neurons has led to research related to the use of olfactory ensheathing cell (OEC) transplantation as a therapy for CNS injury, including this study. While there is considerable evidence for improved CNS tissue repair in response to OEC transplants, some evidence is inconsistent and debate continues regarding the possible mechanisms for the reported therapeutic effects. Chapter 4 of this thesis shows that OECs can moderate the inflammatory activation of astrocytes *in vitro* and explains how this represents a plausible mechanism that could contribute to improved neuroprotection and tissue regeneration in response to OEC transplantation after CNS injury. Briefly, strong inflammatory activation of astrocytes in response to CNS injury increases production of pro-inflammatory mediators leading to increased neuronal damage and the formation of a glial scar, which presents a major impediment to axonal regeneration. NF-κB is a key regulator of inflammatory genes and is essential for these robust inflammatory responses. Chapter 4 shows that soluble factors released from OECs moderated NF-κB translocation in astrocytes *in vitro.* OECs also moderated astrocytic transcription of the NF-κB-dependent pro-inflammatory cytokine, GM-CSF, confirming the physiological relevance of the moderation in NF-κB translocation. Hence, if transplanted OECs had a similar moderating effect on astrocyte inflammatory activation *in vivo,* this mechanism could both enhance both neuronal survival and axon regrowth following CNS injury. In addition to this major research finding, the study:

- identified insulin-like growth factor 1 (IGF-1) as a possible component of the OEC-derived factors that could contribute to the anti-inflammatory effects
- identified a resistance of OECs to inflammatory stimuli
- optimised a protocol for growing highly purified OEC cultures that can be used for transplantation and related research
- established an effective *in vitro* model of astrocyte inflammatory activation

- identified a susceptibility of OECs to apoptosis induced by calcium ion influx, which may have implications for the timing and location of therapeutic OEC implants in the injured CNS.

6.1 Was the *in vitro* research with cultured OECs relevant?

6.10 The in vitro research paradigm

Chapter 2 of this thesis established protocols for the preparation of high purity OEC monocultures from olfactory bulbs suitable for research into OEC biology and OEC transplantation therapy for CNS injury. *In vitro* cell culture provides a simplified research paradigm that may help to identify useful therapeutic targets by revealing relevant underlying components of the complex responses to injury in CNS tissue. This justification of the cell-culture research paradigm self-evidently requires the capability for preparing cultures that are demonstrably monocultures of specific cell types relevant to the intended research (Crang and Blakemore, 1997; Szabo et al., 1997; Silva et al., 1998; Yang and Hernandez, 2003). However, it is difficult to prepare 100% homogeneous primary cell monocultures from live tissue and in addition, definitions and identification of specific cell types may be uncertain (McCarthy and De Vellis, 1980; Morrison and de Vellis, 1981; Crang and Blakemore, 1997). Although pure monocultures can be prepared using clonal cell lines, they do not have identical phenotypes to the primary cells from which they derive (Kikuchi et al., 1993; Gendron et al., 2003; Kim et al., 2006). Therefore, research findings relating to tissue responses based on cell line cultures may be of questionable relevance.

6.11 Are there important differences between olfactory bulb and lamina propria OECs?

6.11.0 Mucosal and bulbar OEC cultures

OEC cultures for experiments were prepared using only olfactory bulb tissue since these cultures consisted predominantly of Schwann cell-like OECs, were less likely to contain contaminating Schwann cells (Kawaja et al., 2009) and had fewer contaminating fibroblasts (Ruitenberg et al., 2005). Sourcing OECs from the more accessible peripheral lamina propria tissue would obviously be preferable for autologous transplantation (Ramer et al., 2004b; Feron et al., 2005; Mackay-Sim et al., 2008). However, this

research using OECs from the olfactory bulbs remains relevant, since bulbar and laminar propria OECs are believed to represent a single population of cells with a common origin in the olfactory placode (Doucette, 1993; Chuah and West, 2002; Au and Roskams, 2003). A subpopulation of horizontal basal cells in the epithelium of the olfactory mucosa appears to be the source of OEC progenitors (Carter et al., 2004). During development, the immature OECs probably migrate along the peripheral olfactory tract and into the olfactory bulbs as they ensheath bundles of olfactory neuron axons along this entire tract (Doucette, 1990, 1993b). The different mode of ensheathment of olfactory neurons in the peripheral olfactory tract and the olfactory bulbs, together with the possibility of immature OECs in cultures from the mucosa, led to research comparing therapeutic transplants of OECs cultured from mucosal and bulbar tissue (Richter et al., 2005). However, differences between cultures of mucosal and bulbar OECs appear to arise predominantly from the different proportions of contaminating cells (Au and Roskams, 2003; Jani and Raisman, 2004; Kumar et al., 2005; Krudewig et al., 2006; Smith et al. 2002). Mucosal OEC cultures contain more fibroblasts while bulbar OEC cultures contain more astrocytes. The mucosal cultures are reported to continue proliferating for longer than the bulbar cultures possibly due to the presence of OEC progenitors or the influence of fibroblast-derived growth factors. However, purified mature OECs from either source tissue have similar antigenic profiles and abilities to promote neurite growth *in vitro*. Recent comparative gene expression profiling of OECs from olfactory bulb and olfactory mucosa identified more genes associated with neurogenesis, angiogenesis, inflammation and hematopoiesis in the olfactory bulb OECs and more extracellular matrix and tissue repair related genes in the olfactory mucosal OECs (Guerout et al., 2010). This result is consistent with the identification of potentially neuroprotective anti-inflammatory factors expressed by olfactory bulb-derived OECs in this research and allows for the possibility that OECs from each source could have therapeutic effects through somewhat different mechanisms. However, these differences may again have been due to more contamination of mucosal cultures by fibroblasts and of bulbar cultures by astrocytes, since fibroblast growth factor was more prominent in the mucosal OEC profile and GFAP was more prominent in the bulbar OEC samples. Unfortunately, none of the genetic profiling studies on OECs (Vincent et al., 2005; Pastrana et al., 2006;

Franssen et al., 2008; Guerout et al., 2010) make comparisons with fibroblasts, which this and other studies (Smith et al. 2002; Jani and Raisman, 2004; Kumar et al., 2005; Krudewig et al., 2006) identify as the most frequent contaminating cell type in OEC cultures. If the differently expressed genes in mucosal relative to bulbar OEC cultures were also more highly expressed by fibroblasts, it would imply that relatively greater fibroblast contamination of the mucosal cultures could account for the differences. Further research is clearly required to determine the most effective method for obtaining purified cultures and comparative phenotyping of OECs from either source tissue, and of the relative efficacy of these cells as therapeutic transplants. A culture method based on the differential adhesion of OECs and contaminating cell types (Nash et al., 2002; Smith et al. 2002; Jani and Raisman, 2004; Kumar et al., 2005; Krudewig et al., 2006; Sasaki et al., 2006) combined with the mitotic inhibitor, cytosine-β-D-arabinofuranoside, used to deplete contaminating cells in this study, could possibly enable the reliable production of highly purified OECs from either of the source tissues.

6.11.1 Therapeutic transplantation of mucosal and bulbar OECs

Furthermore, transplants of OECs cultured from CNS olfactory bulbs (Lakatos et al., 2003a; Sasaki et al., 2006; Lopez-Vales et al., 2007; Mackay-Sim et al., 2008), peripheral lamina propria (Ramer et al., 2004b; Mackay-Sim, 2005; Richter et al., 2005) or pooled tissue from both sources (Chuah et al., 2004; Teng et al., 2008) have all been reported to improve recovery from CNS injury. Some of the conflicting results in studies using either mucosal or bulbar OEC transplants have been attributed to possible phenotypic differences between the OECs (Ramer et al., 2004a) and there is some evidence that mucosal OECs are more beneficial when transplanted after CNS injury (Richter et al., 2005). However, other studies could not replicate this finding (Ramer et al., 2004a; Lu et al., 2006) and the reported differences between peripheral and bulbar OECs may have been due to the presence of contaminating fibroblasts in the mucosal cultures (Jani and Raisman, 2004; Kumar et al., 2005; Mackay-Sim, 2005). Ramer et al., 2004 used Thy1.1 mediated lysis to remove fibroblasts from the mucosal cultures and a p75NTR immunopanning method to purify the bulbar cultures and the different methods could have resulted in different proportions of contaminating cells in the cultures. Schwann

cells are present in the peripheral olfactory tract and, in common with OECs, express p75NTR, while both cell types also express Thy1.1, albeit at lower levels than fibroblasts (Smith et al. 2002; Jani and Raisman, 2004; Kumar et al., 2005; Krudewig et al., 2006). Thy1.1 mediated lysis and p75NTR or O4 antigen immunopanning have been found to be ineffective methods for eliminating contaminating cells from OEC or Schwann cell cultures (Smith et al. 2002; Jani and Raisman, 2004; Ratner et al., 2006; Kawaja et al., 2009) and other researchers have reported the difficulty of eliminating fibroblasts from mucosal OEC cultures (Ruitenberg et al., 2006; Teng et al., 2008). Therefore, variable numbers of fibroblasts, Schwann cells and astrocytes could have been transplanted along with OECs in the many studies whether using these purification methods (Barnett et al., 1993; Ramon-Cueto and Nieto-Sampedro, 1994; Ramon-Cueto et al., 1998, 2000; Plant et al., 2002, 2003; Ruitenberg et al., 2003; Ramer et al., 2004a, b; Lu et al, 2006), no specific purification procedure (Feron et al, 2005; Deng et al., 2006) or intentionally unpurified OEC cultures (Li et al., 1998, 2003; Sonigra et al., 1999; Lakatos et al., 2003; Teng et al., 2008). The possible therapeutic contribution of fibroblasts inadvertently introduced during OEC transplantation has led to research suggesting that transplants of OECs combined with meningeal fibroblasts are reportedly more beneficial in axonal repair and regeneration than transplants of OECs alone (Lakatos et al., 2003b; Li et al., 2005; Teng et al., 2008) and this current research project suggests that lamina propria cultures may be more susceptible to fibroblast contamination. Therefore, reported differences in the therapeutic efficacy of OECs from the lamina propria and olfactory bulbs may have arisen merely from the different contributions of contaminating cells to the cultures from each tissue source. This question regarding the cellular composition of cultures used for transplants underlines the importance of directly identifying the cell types responsible for measured effects. The immunohistochemical method for measuring cellular inflammatory activation utilised in this research had the advantage of enabling simultaneous identification of cell type by counterstaining with antibodies against specific marker proteins. Even if OECs from the olfactory bulbs represent a separate population, this research project could provide important evidence concerning this cell population for comparison with other studies using OECs cultured from the olfactory mucosa. Similarly, any lingering uncertainty about whether OECs constitute a separate

cell type or are a variant of non-myelinating Schwann cells may ultimately have little relevance for their therapeutic value. The constant turnover and regeneration of olfactory neurons and progenitors in the olfactory epithelium implies a probable role for OECs in the regeneration and allows their harvesting from the olfactory system for autologous transplant without causing undue trauma or disruption of normal function. Identification of the proteins responsible for the therapeutic effects of OECs may eventually lead to the development of OEC-based transgenic cell lines expressing a variety of beneficial molecules for CNS injury transplantation therapy.

6.2 The *in vitro* astrocyte activation model

6.20 Further investigation of the effects of NF-κB translocation in astrocytes

Phorbol myristate acetate (PMA) and calcium ionophore (PMA/ionophore) consistently induced rapid robust translocation of p65 NF-κB from the cytoplasm to the nucleus in astrocytes, providing an effective in vitro model of astrocyte inflammatory activation that is highly relevant for CNS injury research. Immunocytochemistry allowed simultaneous detection of NF-κB subcellular localisation with counterstaining for GFAP to identify astrocytes, thus providing simple, direct, unambiguous detection of the astrocyte activation. The treatment model is highly relevant for CNS injury research because the PMA/ionophore activation of NF-κB, through the PKC and calcium signaling pathways, simulates inflammatory activation during CNS injury responses. Specific inhibitors and activators of signaling molecules, genetically modified cells and protein constructs could be utilised in this treatment model to help decipher the mechanisms for the anti-inflammatory effects of OECs. Microglia-conditioned medium promoted NF-κB translocation similarly to PMA/ionophore in astrocytes, supporting the physiological relevance of the reagent treatment, since cytokines and other factors released by microglia contribute to inflammatory responses after CNS injury. However, the composition of the conditioned medium was unknown and may have varied between cultures. Specific inflammatory cytokines, particularly IL-1β and TNF-α, and other known microglia-derived factors would be more informative treatments for further investigation of the mechanisms of NF-κB activation in astrocytes and the anti-inflammatory effects of OECs. Although there was no significant difference in NF-κB

translocation for ionophore doses from 125nM to 1μM and PMA doses from 20ng/mL to 200ng/mL, the protocol for measuring NF-κB translocation did not take into account any differences in NF-κB immunoreactivity intensity in nuclei above an arbitrary threshold. While it is uncertain whether there would be any functional importance to such differences, it is plausible that more intense immunostaining would indicate more NF-κB had translocated to the nucleus and this could result in greater enhancement of transcription. For similar reasons, although nuclear NF-κB immunoreactivity intensity was lower than the arbitrary detection threshold at time-points following the peak response, nuclear NF-κB could have remained higher than levels prior to treatment and may have been sufficient to maintain increased gene transcription. This could explain why combining PMA/ionophore with microglia-conditioned medium had an additive effect only on GM-CSF transcription and not on the measured NF-κB activation. However, it is also plausible that factors in the microglia-conditioned medium promoted transcription through pathways independent of NF-κB activation. Western blotting of nuclear and cytoplasmic fractions of astrocytes and/or chromatin immunoprecipitation assay for NF-κB subunits (Butler et al., 2002; Brettingham-Moore et al., 2005a) in conjunction with the immunocytochemistry could provide a more accurate indication of relative activation levels in the cultures. While, the stimulation of GM-CSF transcription in astrocytes by PMA/ionophore supported the physiological relevance of the NF-κB translocation, a causal relationship between these effects should ideally be confirmed using specific inhibition of NF-κB. Stronger evidence of the physiological relevance of the NF-κB translocation could be gained by measuring transcription of the numerous other NF-κB-dependent pro-inflammatory mediators produced by astrocytes, particularly IL-1β, TNF-α, IL-6, iNOS, COX-2 and chemokines. Assays for cytokines, nitric oxide and reactive oxygen species, together with Western blots for expression of proteins associated with astrogliosis, such as GFAP and CSPGs, could provide further relevant corroborative evidence. Testing the effects of OECs on these additional parameters could reveal more detail relevant to the therapeutic effects of OEC transplants that may assist in isolating therapeutic molecules.

6.21 Implications for the timing and location of therapeutic OEC implants

Most importantly, Chapter 4 showed that soluble factors released by OECs significantly moderated NF-κB translocation in astrocytes, whether it was induced by PMA/ionophore or microglia. Chapter 5 shows that in addition to activating NF-κB, calcium influx induced by ionophore treatment promoted apoptosis in a dose-dependent manner. The apoptotic effect of ionophore appeared to be independent of NF-κB activation, since unlike NF-κB translocation, the astrocyte apoptosis was unaffected by soluble factors from either OECs or microglia. Interestingly, although PMA/ionophore and microglia did not activate NF-κB in OECs, they were more susceptible to ionophore-induced apoptosis than astrocytes. This finding further supports the independence of ionophore-induced NF-κB activation and apoptosis, and implies that the therapeutic success of OEC implants may depend on the severity of inflammation at the implantation site. For the *in vitro* experiments, astrocytes were exposed to co-cultured OECs or OEC-conditioned medium for at least 24 hours before activation to allow establishment of the cultures and to avoid any confounding effects of abrupt media changes. This pre-incubation could be interpreted as a caveat against the anti-inflammatory effects of OECs being replicated when transplanted directly into inflamed CNS tissue. However, establishment of the OEC cultures, particularly in co-culture with astrocytes, could be likened to implantation of OECs into the CNS. The experimental findings suggest that as long as the OECs survived transplantation they could, once established, exert the same anti-inflammatory influence seen *in vitro*. The transient and asynchronous pattern of NF-κB activation in the cultured astrocytes is particularly relevant to this question, since it implies that not all astrocytes would be equally activated at the time of implantation. Whether OECs could moderate the responses of astrocytes where NF-κB was pre-activated or could only prevent the spread of inflammation to quiescent astrocytes would depend on the mechanism for their anti-inflammatory effects. The lack of response to PMA/ionophore and microglia implies that is unlikely implanted OECs would be activated by inflammatory mediators released by microglia or by other factors evoked by CNS injury that stimulate PKC or calcium ion influx. Therefore, implanted OECs would probably be able to maintain the quiescent *in vitro* phenotype to enable the moderation of astrocyte inflammatory activation surrounding the implantation site. However, OECs were more susceptible to ionophore-

induced apoptosis and could become apoptotic due to excessive calcium influx if transplanted into ischemic regions of CNS lesions where there are high levels of extracellular calcium ions, glutamate and ATP. Previous research showing that tissue repair and functional recovery required precise transplantation of OECs into corticospinal tract lesion cavities (Keyvan-Fouladi et al., 2003) may have been partly related to this susceptibility of OECs to calcium influx-induced apoptosis. Furthermore, disruption of the surviving vasculature during OEC transplantation could re-initiate ischemia and *in vivo* research may be required to determine the optimal timing and location for transplanting OECs. Both the OEC moderation of astrocyte activation and the absence of OEC inflammatory activation imply that if transplanted OECs survive, they are likely to enhance neuronal survival by moderating inflammation. Once the initial severe ischemia due to a CNS injury has subsided, any remnant lesion cavity may present the ideal location for OEC implantation. OEC implantation could fill the cavity with non-inflammatory, axon growth-promoting cells without disrupting the blood supply. Transplanted OECs could release IGF-1 and other soluble factors to moderate inflammation in the surrounding reactive astrocytes. The anti-inflammatory effects could protect neurons, promote neurogenesis and may also promote infiltration of the scar tissue by the OECs, to possibly form a permissive conduit for axon-growth through the glial scar and across the lesion. It may be that the inclusion of fibroblasts and/or Schwann cells with the transplanted OECs would be required to create the necessary aligned substrate for substantial axon regrowth (Ruitenberg et al., 2006; Bunge, 2008; Ruitenberg and Vukovic, 2008; Teng et al., 2008). With regard to the anti-inflammatory effects of OECs identified by this research, it is interesting that a combination treatment of methylprednisolone and OECs for corticospinal tract lesion in rats was shown to be significantly more effective than methylprednisolone alone and OECs alone were almost as effective as the combined treatment in improving axonal regeneration and improved neurological outcomes (Nash et al, 2002). This result is not inconsistent with the possibility that the anti-inflammatory effect of OECs identified in this study is replicated by transplanted OECs and confers a therapeutic effect of similar magnitude to that of methylprednisolone. While the therapeutic effects of methylprednisolone are probably due to its anti-oxidant activity, transplanted OECs could indirectly moderate the

production of reactive oxygen species, through their anti-inflammatory effects on astrocytes, to achieve similarly beneficial effects. If so, utilising these anti-inflammatory properties by transplanting OECs near the lesion, could avoid the systemic immune suppression problems (Bracken and Holford, 2002; Kronvall et al., 2005; Sorensen, 2008) associated with intravenous treatments, such as methylprednisolone. Dependent on the survival time of transplanted OECs, they could also provide a physiological dose of the therapeutic factors, targeted precisely to the injury site for an extended period. While the *in vitro* research showed that OECs could moderate astrocyte activation induced by microglia-derived factors, there was no investigation of direct OEC effects on the activation of microglia. Further investigation of NF-κB activation during interactions between neurons, astrocytes, OECs, activated microglia and peripheral macrophages, which all participate in CNS injury responses and coexist in the olfactory system, could provide additional evidence on the therapeutic potential of OECs and their normal physiological role in the olfactory system.

6.22 Identification of active components of the OEC-derived soluble factors

Identification of the active components responsible for the OEC moderation of astrocyte activation could allow the development of molecular therapies that would avoid the potential complications of apoptosis and the re-initiation of ischemia associated with cell transplantation. However, the physical interaction between OECs, astrocytes and axonal growth cones may be an important component of the therapeutic mechanism of transplanted OECs. In addition, there may be a range of protective factors produced by OECs, with some possibly limited to paracrine effects requiring close proximity to the target tissues. OECs do express fractalkine, the only known membrane-bound chemokine, which mediates its effects by binding to the specific CX3CR1 receptor that is expressed by microglia, macrophages and other peripheral leukocytes (Cardona et al., 2006; Ruitenberg et al., 2008). Constitutive neuronal fractalkine expression has been shown to exert neuroprotective anti-inflammatory effects on microglia (Cardona et al., 2006; Held-Feindt et al., 2010; Lauro et al., 2010). OEC and olfactory neuronal expression of fractalkine could have similar constitutive anti-inflammatory actions on microglia and macrophages in the olfactory tract (Ruitenberg et al., 2008). Fractalkine expression could

therefore contribute a contact-dependent component to the anti-inflammatory activity of transplanted OECs. Although the effect of the soluble anti-inflammatory factor inferred by this research was maintained in conditioned medium it could be rapidly inactivated by other factors following *in vivo* OEC transplantation. Insulin-like growth factor 1 (IGF-1) was identified as a factor expressed by OECs that could contribute to the anti-inflammatory effects. IGF-1 is expressed by macrophages, reactive astrocytes, neurons and microglia in damaged tissue following traumatic brain injury in rats and appears to regulate gliosis and axonal sprouting in both an autocrine and paracrine manner (Walter et al., 1997). Interestingly, some of the neuroprotective effects of estradiol may be mediated by its promotion of IGF-1 production by astrocytes (Kipp and Beyer, 2009). Previous research indicates that IGF-1 recruitment of calcineurin can inhibit NF-κB and nuclear factor of activated T-cells (NFAT) activity resulting in the moderation of the inflammatory activation of astrocytes by TNF-α (Fernandez et al., 2007a; Perez-Ortiz et al., 2008). IGF-1 may similarly have moderated a calcium signalling-dependent component of the astrocyte activation induced by PMA/ionophore and microglia in this research. It would therefore be interesting to investigate the involvement of calcineurin and NFAT using the *in vitro* astrocyte activation model. In the olfactory system, IGF-1 induces neuronal precursors to differentiate into olfactory sensory neurons and has similar effects in the developing CNS (Drago et al., 1991; McCurdy et al., 2005). IGF-1 also promotes remyelination by regulating the proliferation and differentiation of oligodendrocyte progenitors (Drago et al., 1991; Mason et al., 2003), has neuroprotective effects in CNS white and grey matter under different detrimental conditions and improves long-term function after focal brain injury following cerebroventricular, intravenous or intranasal administration (Guan and Gluckman, 2009; Kooijman et al., 2009). Although in Chapter 4, the effect of IGF-1 was insufficient to fully account for the anti-inflammatory effects of OECs, these previously reported effects are similar to those reported for OECs. It is also interesting to note that the lipoprotein receptor, megalin is involved in some of the neuroprotective effects of exogenous IGF-1 and its transport into the brain (Carro et al., 2005). Antioxidant production by OECs could also have contributed to the anti-inflammatory effects. High levels of antioxidants, including superoxide dismutase, glutathione peroxidase, catalase, ascorbate and alpha-tocopherol

are present in the rat nasal cavity presumably to protect cells against oxidative stress during immune responses to pathogens (Reed et al., 2003) and may be produced by OECs. Treatment with an agent that upregulated glutathione production was recently shown to protect against oxidative stress and peryoxynitrite-mediated protein nitration after traumatic brain injury (Reed et al., 2009). Understanding the biological actions and intracellular pathways involved in the effects of identified therapeutic molecules will be important for identifying targets, optimising treatments and for recognising probable side-effects and limitations. The development of clonal cell lines based on the OEC phenotype that express a range of therapeutic molecules could provide any required physical interaction for tissue repair in addition to enhanced production of factors that moderate inflammation and promote tissue repair.

6.23 NF-κB dimer activity and transcription

Astrocyte activation was measured using localisation of p65 NF-κB in this research because activity during CNS injury responses has been reported to involve mainly p65/p50 NF-κB dimers (Schneider et al., 1999; Hang et al., 2006; Ridder and Schwaninger, 2009). There was only low cytoplasmic immunoreactivity for c-Rel NF-κB in the cultured astrocytes and no translocation occurred in response to treatments, supporting the relevance of using p65 immunoreactivity for measuring activation. In T cells, PMA alone induced GM-CSF transcription more strongly (20-fold) than ionophore alone (~4-fold), with the increased transcription in response to both reagents being dependent on PKC (Brettingham-Moore et al, 2005). Only PMA induced translocation of NF-κB to nuclei in T cells, whereas ionophore induced calcineurin-dependent translocation of NFAT. Although the separate effects of PMA and ionophore on GM-CSF transcription were not investigated in this study, ionophore alone induced NF-κB translocation to astrocyte nuclei more strongly than PMA alone. Interestingly, the 4-fold increase in T cell GM-CSF transcription induced by ionophore was just below the 5- to 7-fold range of the increase in GM-CSF transcription induced by combined PMA/ionophore in astrocytes, where PMA had only a relatively small effect on NF-κB translocation. The synergistic increase in GM-CSF transcription evoked by combined PMA and ionophore stimulation of T cells involved *de novo* synthesis and translocation

of c-Rel NF-κB to nuclei following the earlier translocation of p65 NF-κB (Brettingham-Moore et al, 2005). Somewhat contrary to these findings, a weaker but more prolonged inflammatory activation has more generally been associated with c-Rel translocation in comparison to p65 NF-κB, which may relate to a less effective dissociation of c-Rel-DNA complexes by IκB than for p65 or c-Rel promotion of the transcription of genes that suppress IκB activity (Baeuerle and Henkel, 1994). During adaptive immune responses, antigens induce NF-κB activation in T lymphocytes leading to the production of pro-inflammatory cytokines and cytotoxic levels of ROS to assist the clearance of pathogens by macrophages. NF-κB is a constitutively active nuclear protein in mature B cells, which produce antibodies and also secrete IL-1β and TNF-α (Sen and Baltimore, 1986; Baeuerle and Henkel, 1994; Kaltschmidt et al., 1994; Wietek and O'Neill, 2007) but, unlike T cells, do not produce GM-CSF. Nuclear NF-κB in B cells mainly consists of c-Rel/p50 dimers while the p50/p65 dimers are mainly cytoplasmic (Baeuerle and Henkel, 1994; Baldwin, 1996; Chen and Greene, 2004a), consistent with the requirement for nuclear localisation of both p65 and c-Rel for enhanced GM-CSF transcription in T cells (Brettingham-Moore et al., 2008). Astrocytes have been implicated in both the cytokine production and antigen-presenting components of innate immune responses (Sasaki and Nakazato, 1992; Dong and Benveniste, 2001; Carpentier et al., 2005; Bsibsi et al., 2006) and macrophages produce similar inflammatory mediators to astrocytes, including M-CSF, G-CSF, GM-CSF, TNF-α, IL-1β, IL-6, chemokines and iNOS, in response to NF-κB activation during innate and adaptive immune responses (Muller et al., 1993; Baeuerle and Henkel, 1994; Muller et al., 1997). The relatively modest increase in GM-CSF transcription in astrocytes is consistent with the absence of c-Rel involvement and the moderation of transcription by OECs was possibly due to the direct inhibition of p65 NF-κB translocation. It would therefore be informative to investigate whether OECs moderate the separate effects of PMA and ionophore on NF-κB translocation and GM-CSF transcription in astrocytes and the possible involvement of protein synthesis, calcineurin, NFAT and chromatin remodelling in these events.

6.24 Does NF-κB activity reveal a hierarchy of immune functions?

The different activity of NF-κB family members in the different cell types suggests there may be a related hierarchy of immune activity, with c-Rel constitutively active in mature B-cells for continuous antibody production, inducible c-Rel and p65 activity in T-cells for antigen-specific adaptive immune responses and only inducible p65 activity in astrocytes for their innate immune responses. These responses are probably at least partially regulated by variable expression levels of the IκB isoforms, which are the primary regulators of NF-κB activity (Suyang et al., 1996; Hoffman et al., 2007; Rao et al., 2010). IκBβ is degraded more slowly than IκBα in response to inflammatory stimuli and is re-synthesised in a hypophosphorylated form that stably binds to p65:c-Rel NF-κB heterodimers that cannot be inhibited by free IκBα. Unlike phosphorylated IκBβ or IκBα, hypophosphorylated IκBβ does not mask the nuclear localization signal or DNA binding domain of NF-κB. Hence, in response to persistent stimuli the newly synthesized hypophosphorylated IκBβ can form stable IκBβ:NF-κB complexes that enter the nucleus where they can bind to DNA and maintain prolonged expression of inflammatory genes. The results of this and previous studies suggest that OECs have only a relatively muted innate immune response (Vincent et al., 2007; Harris et al., 2008; Harris et al., 2009). Separate treatments with PMA/ionophore or microglia did not activate NF-κB in OECs. Even when the treatments were combined less than 5% of OECs showed nuclear localisation of p65 immunoreactivity. Therefore, it could prove informative to investigate IκB isoform expression in OECs. Perhaps OECs have high levels of constitutive IκBα expression and low levels of IκBβ expression, which could impart a resistance to NF-κB activation. This could be mediated by OEC expression of factors, such as G-protein-coupled receptor kinases, which can promote nuclear accumulation of IκBα (Sorriento et al., 2008). The resultant high levels of nuclear IκBα impaired protection against apoptosis in endothelial cells and inhibited NF-κB activation, TNF-α production and inflammation, consistent with the lack of NF-κB activation and susceptibility to apoptosis in OECs. IGF-1 has been previously shown to inhibit TNF-α stimulation of NF-κB translocation in astrocytes by activating the calcium-dependent phosphatase, calcineurin, to dephosphorylate IκBα (Pons and Torres-Aleman, 2000). The enhanced

dephosphorylation of IκBα protects it against TNF-α-induced phosphorylation and removal from the inactivated NF-κB dimers, thus inhibiting NF-κB translocation to nuclei for gene transcription. IGF-1 probably inhibited NF-κB translocation in response to PMA/ionophore and microglia-conditioned medium by the same mechanism, especially considering that ionophore and thapsigargin strongly induced NF-κB translocation in the cultured astrocytes in a similar manner to microglia-conditioned medium and TNF-α is a likely component of the conditioned medium. IGF-1 expression was detected in OECs and could have exerted a stronger inhibitory effect on OECs than astrocytes because of higher expression levels of IGF-1 receptors or other factors in the NF-κB signalling pathway, including IκBα. Interestingly, the synthetic glucocorticoid dexamethasone also inhibits TNF-α stimulation of NF-κB activation via IκB, in this case by upregulating IκB gene transcription (Scheinman et al., 1995). If OEC moderation of NF-κB activation in astrocytes is also mediated by effects on IκB it would lend some support to the possibility that OECs could provide a targeted anti-inflammatory treatment that is as effective as systemic glucocorticoid treatment, without the risks of systemic immunosuppression.

6.25 Is OEC innate immunity targeted at invasive pathogens?

OECs may have an innate immune response targeted specifically at pathogens migrating along the olfactory tract from the mucosa into the CNS (Harris et al., 2008; Leung et al., 2008; Harris et al., 2009). However, fewer OECs showed nuclear localisation of p65 NF-κB in response to Escherichia coli (E. coli) than astrocytes or microglia, although similar to the finding in this study, there was more activation by E. coli when OECs were in co-culture with microglia (Vincent et al., 2007). OECs also had a muted inflammatory response to Staphylococcus aureus (S. aureus) with only minimal upregulation of iNOS associated with weak nuclear p65 immunoreactivity, which could have been partly due to growth factors in the culture medium, contaminating cells in the culture and overlapping cytoplasmic immunoreactivity (Harris et al., 2009). This lesser response to S. aureus may represent a greater tolerance to these Gram-positive bacteria that are more commonly present on the facial skin and olfactory mucosa than E. coli. A muted innate immune response in OECs could serve to protect olfactory neurons against the neurotoxic effects

of severe inflammation. OECs produce the chemokines Gro1 and MCP-1 in culture (Vincent et al., 2005b) and these could attract macrophages to sites of pathogen accumulation. Fractalkine is another chemokine that is produced by OECs, as well as by olfactory sensory neurons in the olfactory tract, that is known to have an important role in recruiting macrophages (Ruitenberg et al., 2008). The moderation of inflammatory responses by IGF-1 and other factors released by OECs could protect olfactory neurons and restrict inflammation to the macrophage-occupied region outside the ensheathed olfactory neuron fascicles. However, if the infection progressed, dual stimulation by pro-inflammatory cytokines released from activated macrophages and binding of pathogens to TLRs could activate OECs to initiate an inflammatory response within the axon fascicles. Apoptosis of neurons could then occur due to their susceptibility to inflammation preventing spread of the infection into the CNS. Neuronal death would release calcium ions, glutamate and ATP, which could induce OEC apoptosis because of their susceptibility to calcium influx. Release of Gro1, IGF-1 and other factors from surviving or apoptotic OECs could then initiate progenitor proliferation and differentiation in the olfactory epithelium for olfactory neuron renewal. It is possible that the immune behaviour of OECs alters as they mature after differentiating from progenitors in the olfactory epithelium while accompanying and then ensheathing developing or regenerating olfactory axons. Previous studies on immune function in OECs have utilised cultures from combined lamina propria and olfactory bulb tissue (Vincent et al., 2007; Harris, 2008; Leung et al., 2008; Harris et al., 2009). A sub-population of more motile immature OECs derived from progenitor cells in the lamina propria epithelial tissue during culture could have been principally responsible for the immune responses observed in these studies. OECs have been observed migrating together with developing olfactory neuron axons (Doucette, 1989; Tennent and Chuah, 1996). Although there is no evidence of increased OEC motility or proliferation following zinc sulphate irrigation injury, with olfactory neuron regeneration and axon regrowth apparently occurring within the existing channels formed by the intact OEC ensheathments (Williams et al., 2004), this experimental treatment may not accurately replicate the response to pathogens. In addition, signaling through olfactory neuronal CX3CL1 (fractalkine) to recruit monocyte-derived macrophages and possibly to promote

progenitor cell proliferation and differentiation in the olfactory epithelium, appears to be an important process in olfactory sensory neuron renewal (Ruitenberg et al., 2008). Another possibility is that the sub-population of activated cells were contaminating Schwann cells from the peripheral olfactory tract tissue used for the cultures. Comparison of NF-κB activation in OECs and Schwann cells could help to clarify this possibility. Research on immune responses in mixed cultures containing OECs and olfactory neurons at different stages of maturity and related *in vivo* research on the olfactory system could help to further elucidate the immune functions of OECs.

6.26 Correlating astrocyte activation levels with the potential for CNS repair

As discussed throughout this thesis, moderate inflammatory astrocyte activation probably leads to conditions that are conducive to axonal regeneration and CNS tissue repair, whereas both severe inflammation and complete inhibition of astrogliosis have detrimental effects. It is therefore noteworthy that the moderate levels of astrocyte activation following the moderation of PMA/ionophore-induced activation by OECs were similar to those following treatment with either metallothionein 2A or PMA. Exogenous metallothionein 2A strongly promotes axonal regeneration lending support to the view that these moderate levels of astrocyte activation are favourable for CNS repair. Phorbol esters, such as PMA were first identified as tumour promoters that induce excessive growth and inhibit apoptosis by chronically activating calcium-dependent protein kinase (PKC) (Jaken, 1990; Marquez et al., 1992; Szallasi et al., 1996; Ventura and Maioli, 2001; Papp et al., 2003). PKC activates NF-κB via phosphorylation of IKK (Fig. 1.1) (Baeuerle, 1998; Huang et al., 2003; Amos et al., 2005; Hull et al., 2006) and the moderate levels of NF-κB translocation induced by PMA, metallothionein 2A and by PMA/ionophore in the presence of OECs may represent activation through this PKC pathway that could lead to the transcription of neuroprotective and growth-promoting genes. In contrast, excessive calcium ion influx following CNS injury has detrimental effects on cells as illustrated by the dose-dependent calcium ionophore-induced apoptosis described in Chapter 5. The stronger activation of astrocytes by ionophore or combined PMA/ionophore may stimulate calcium signalling pathways that combine with the PKC pathway to more strongly induce NF-κB translocation. Simultaneously activated MAPK pathways could

synergise with NF-κB to promote increased transcription of pro-inflammatory factors that can increase CNS tissue damage. These possibilities reinforce the need to compare the transcriptional effects of the different levels of astrocyte activation in response to these treatments and the moderating effects of OECs.

6.3 *In vivo* OEC implantation research

6.30 Implanted OECs survive in the lesion

The research in this thesis aimed to provide insight into possible mechanisms that may contribute to improved tissue repair in response to OEC transplantation following CNS injury. Any findings of the research ultimately require testing *in vivo* and some progress has been made towards this goal using a focal cortical needle-stick injury model (Fig. 6.0) (King et al., 1997; Chung et al., 2003). This preliminary *in vivo* research, outlined below, has produced some promising results as well as revealing some potential sources of error that should be considered for future research. Carboxy-fluorescein diacetate succinimidyl ester (CFDA-SE) staining of implanted OECs confirmed that many remained viable 7 days after implantation in the lesion, since the fluorescent label is only inherited by daughter cells after cell division, is not transferred to adjacent cells in a population and is rapidly degraded in dead cells (Lyons and Parish, 1994; Bracher et al., 2007; Quah et al., 2007; Weischenfeldt and Porse, 2008). Some of the implanted cells infiltrated the reactive astrocytes surrounding the lesion, although the majority remained in the lesion within the boundary formed by the GFAP-positive astrocyte processes aligned along the border of the lesion (Fig. 6.0 B-D). Some weak GFAP immunostaining could have been expected in the implanted OECs, although it may not have been visible at the exposures used for these images. Additional high magnification, longer exposure images of the cells in the lesion, together with a nuclear stain, could help to positively identify, delineate and demonstrate the viability of these cells. There are always some fibroblasts in the OEC cultures and it is possible that these preferentially survived and proliferated during the 7 days after implantation. For this reason, it would be desirable to conduct immunostaining against, for example, $p75^{NTR}$ and S100, for which OECs immunostain more intensely than for GFAP, in conjunction with the CFDA-SE staining, to confirm the presence of surviving OECs in the implants.

6.31 Measuring the injury response

This needle-stick injury was ~0.5mm deeper than intended and cavities formed at the base of the lesion (Fig. 6.0B-C) probably due to blood vessel damage and consequent severe local ischemia. Despite this relatively severe injury, the GFAP immunoreactivity around the lesion was not as intense or extensive as following a 1.5mm deep lesion in a control saline-injected lesion, where there was no apparent blood vessel damage or lesion cavity (Fig. 6.1A). This promising result could be due to the moderation of astrocyte inflammatory activation by the implanted OECs as found in the *in vitro* model. Obviously, this requires confirmation with additional animals and ideally immunostaining, Western blotting and real-time PCR evidence for the moderation of NF-κB activation, inflammatory gene expression, astrogliosis and glial scarring. It is possible that any cellular implant is preferable to an open injury cavity and the implantation of other cell types such as astrocytes, fibroblasts and microglia could provide useful comparisons with the OEC transplants. Small variations in the position and orientation of the needle-stick injury can result in large variations in the extent of injury due to blood vessel damage (Fig. 6.1B) independent of any intentional treatment effects. This variation would obviously be a confounding effect with seriously detrimental consequences for the validity of the research if the initial injuries were assumed to be equivalent for comparisons between controls and/or treatment groups. Consequently, animals should all be of the same age and size. Furthermore, great care and skill is required in positioning animals correctly in the surgical stereotax, location of the injury site, drilling through the skull, performing the needle-stick injury (Fig. 6.1) and suturing the wound. Metallothionein 1/2 upregulation reaches a peak at 2 to 4 days post-injury (Fig. 6.2) and is another potential indicator of astrocyte inflammatory activation (Penkowa et al., 1997; Campagne et al., 2000; Trendelenburg et al., 2002; Chung et al., 2008) and the severity of injury. Immunoreactivity for ferritin identifies activated macrophages (King et al., 2001; Huang and Ong, 2005) in the lesion and penumbra (Fig. 6.2). Western blotting of cortical samples revealed increased GFAP expression in the samples from injured compared to

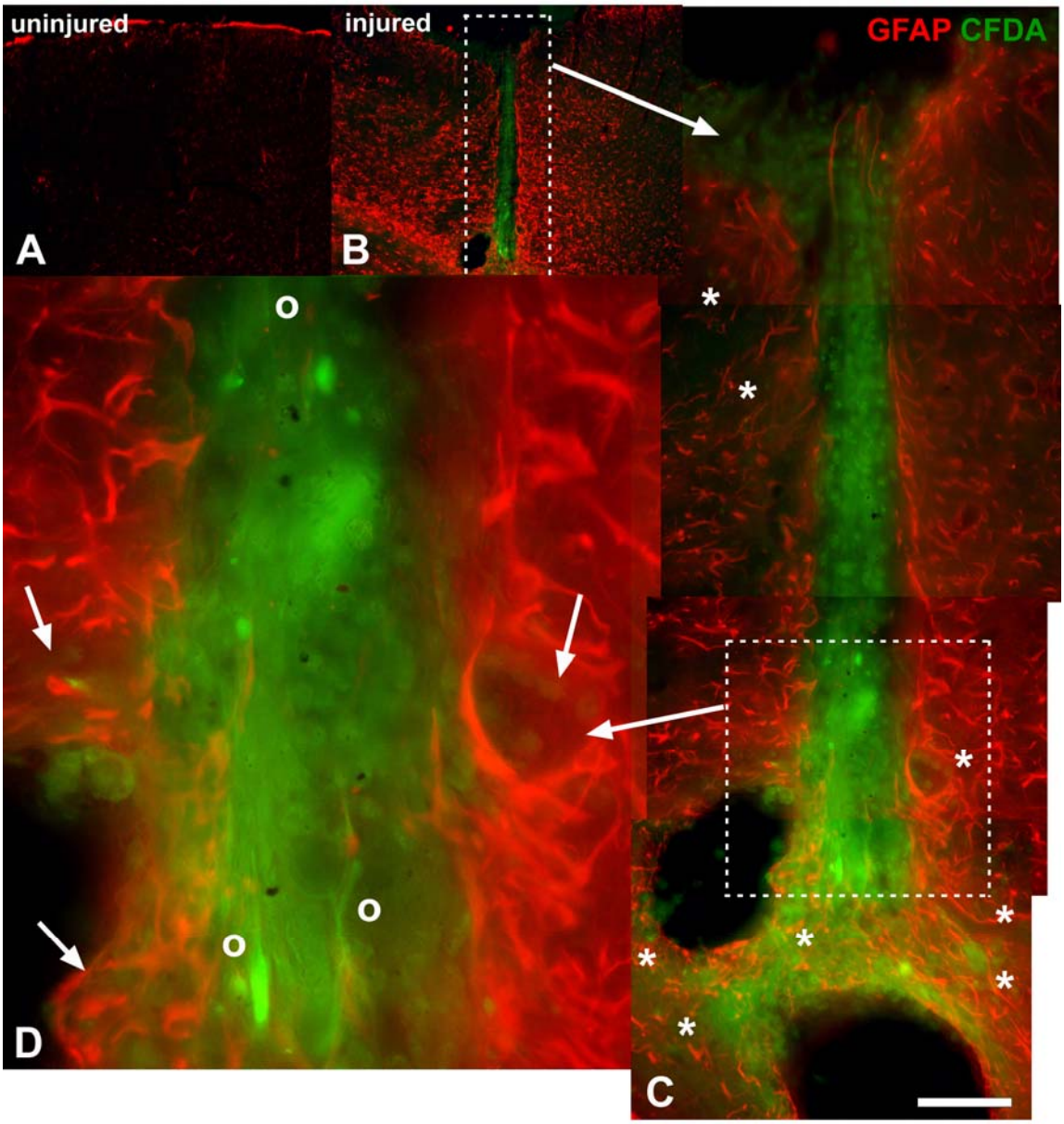

Figure 6.0 A focal cortical injury with implanted OECs. Carboxyfluorescein diacetate succinimidyl ester-stained (CFDA, green in B-D) OECs were implanted at the time of injury into a 2mm deep cortical needle-stick injury in an adult male rat. Markedly increased GFAP immunoreactivity occurred around the injury (B-D) contrasting with the low immunoreactivity throughout the uninjured hemisphere (A). GFAP-expressing astrocyte processes align with the lesion border (C and D). There are two large cavities at the base of the lesion (C) probably due to blood vessel damage. The majority of the implanted OECs occupy the lesion but some have infiltrated the reactive astrocytes in the lesion penumbra (asterisks in C and arrows in D). Some CFDA-stained cells have elongated morphologies that resemble *in vitro* OEC morphologies (Os in D). Scale bar is 200μm.

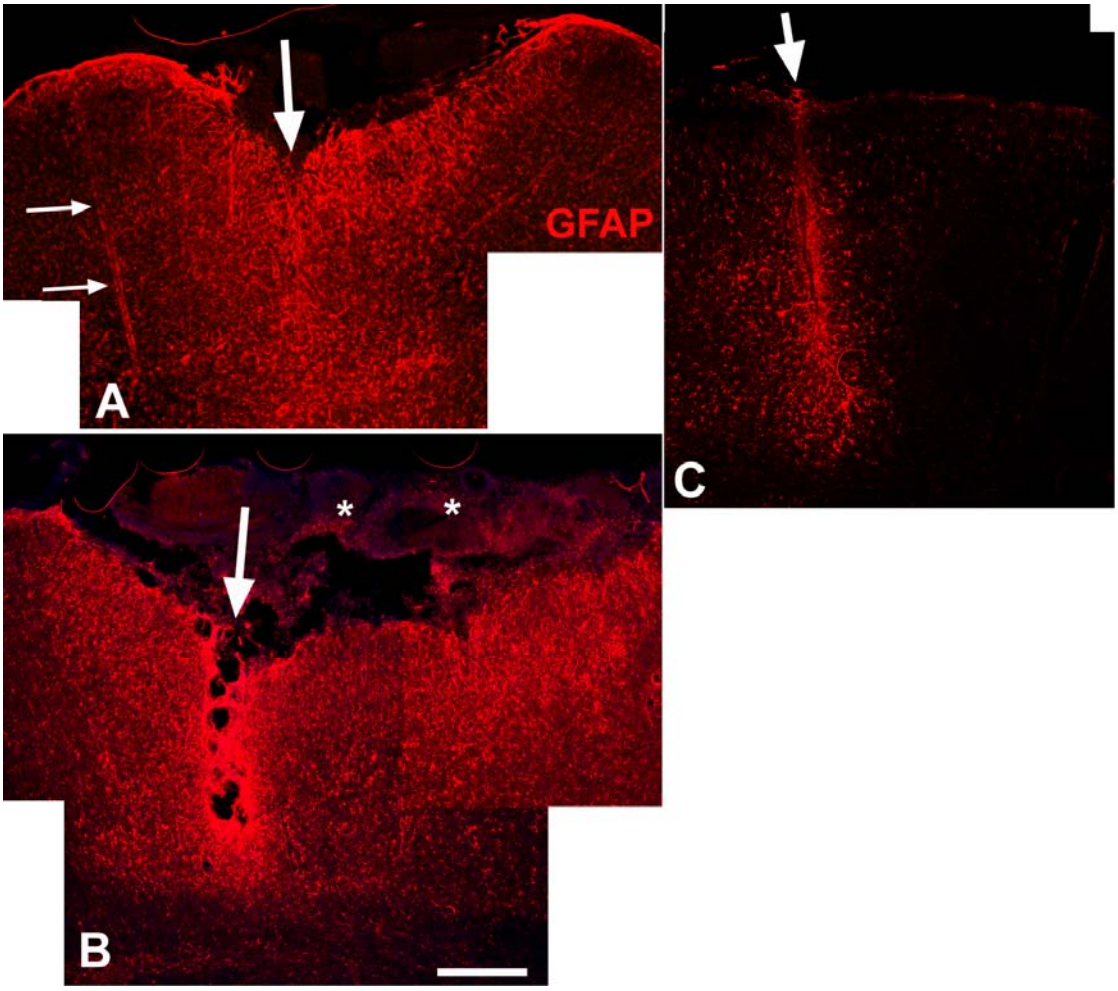

Figure 6.1 Vascular damage increases lesion size. All three cortical needle-stick injuries (location shown by large arrows in A, B and C) received control saline injections at the time of injury. Tissue was dissected and fixed 7 days after injury, then sectioned and immunostained for GFAP (red). A small variation in the location of the injuries caused vascular damage and a large lesion cavity 7 days after injury (B). A descending arteriole is to the left of the lesion in A (small arrows). Large concave lesions on the cortical surface can be caused by heat and abrasion while drilling through the skull and become filled with coagulated blood and immune cells (asterisks in B), which are often lost from the section during processing (A). This unintentional drill damage can cause more damage than the needle-stick and is potentially a major confounding factor in this injury model. Improvements in the drilling technique enabled needle-stick injuries with little surface injury (C) and consequently a much more restricted region of increased GFAP immunoreactivity around the lesion. Scale bar is 500μm.

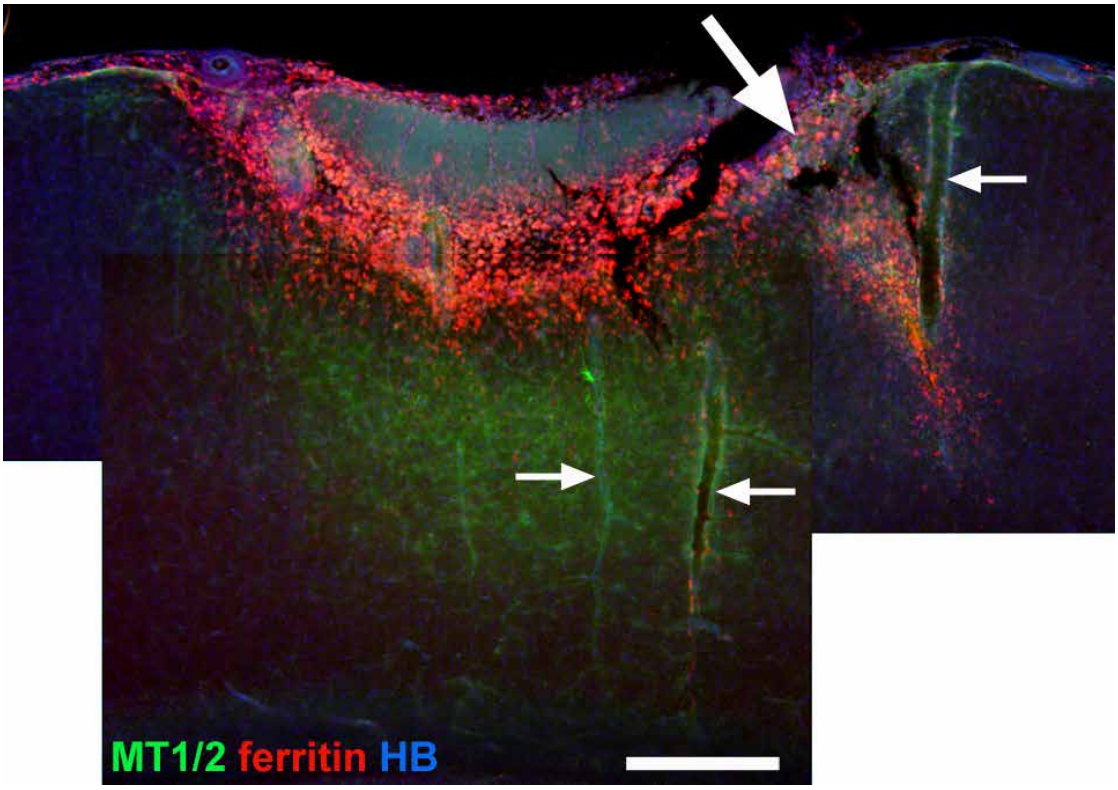

Figure 6.2 Metallothionein 1/2 and ferritin expression at 4 days post-injury. Immunoreactivity for metallothionein 1/2 (MT1/2, green) is increased in astrocytes in the lesion penumbra, 4 days after a cortical needle-stick injury (large arrow). Ferritin immunoreactivity (red) identifies activated macrophages, which occupy the needle-stick lesion and a large concave lesion caused by drilling through the skull. More sparsely distributed activated macrophages also occur in the penumbral tissue. These may represent both activated microglia migrating towards the lesion and macrophages from blood migrating into the injured CNS tissue from the lesion. Nuclei are counter-stained with Hoechst blue DNA stain (HB). Several descending blood vessels can be clearly distinguished in the section (small arrows) and the needle-stick lesion intersects the largest of these. Scale bar is 500μm.

uninjured hemispheres (Fig. 6.3). The relative differences in GFAP expression are also dependent on the size of the tissue sample relative to the region of altered protein expression and the extent to which increased GFAP immunoreactivity represents increased expression rather than merely changes in phosphorylation and polymerisation status. Changes in protein expression may also refect changes in cellular composition within the sample region and immunostaining of equivalent regions would help to clarify this possibility.

6.32 Measuring CNS tissue repair and functional recovery

The measures described above can provide valuable information regarding the likelihood of beneficial effects from OEC implantation and the mechanisms for any such effects. However, the therapeutic goal of this research is to demonstrate improvements in neuronal regeneration and functional recovery. Immunoreactivity for phosphorylated neurofilaments has been used as an indicator of neurite sprouting (King et al., 1997; Maxwell et al., 1997; Dickson et al., 2000). The most intense immunoreactivity (Fig. 6.4) for phosphorylated neurofilaments co-localises with microtubule-associated protein 2 (MAP2) immunoreactivity (Fig. 6.4G and H) in damaged axons on the lesion border (Fig. 6.4F). If this intense SMI312 staining does unequivocally represent neurite sprouting, it implies there must be massive sprouting of abortive neurites into the lesion. A less marked increase in phosphorylated neurofilament immunoreactivity occurs in the lesion penumbra and injuries where the lesion appears to be due primarily to the needle-stick (Fig. 6.4A-C). This phosphorylated neurofilament immunoreactivity in relatively intact tissue may represent neurite sprouting or axonal restructuring, although immunoreactivity is also increased in regions that were damaged during sectioning of the fixed tissue (Fig. 6.4D and E). Higher resolution confocal microscopy and axonal growth cone markers, such as GAP 43 (Dickson et al., 2000; King et al., 2001; Cafferty et al., 2004), may be required to demonstrate improvements in axonal regeneration. Spinal cord and brain injury models where distinct axonal tracts are lesioned may be more amenable to assessing both axon regeneration and any functional improvements in motor or cognitive behaviour resulting from OEC implantation.

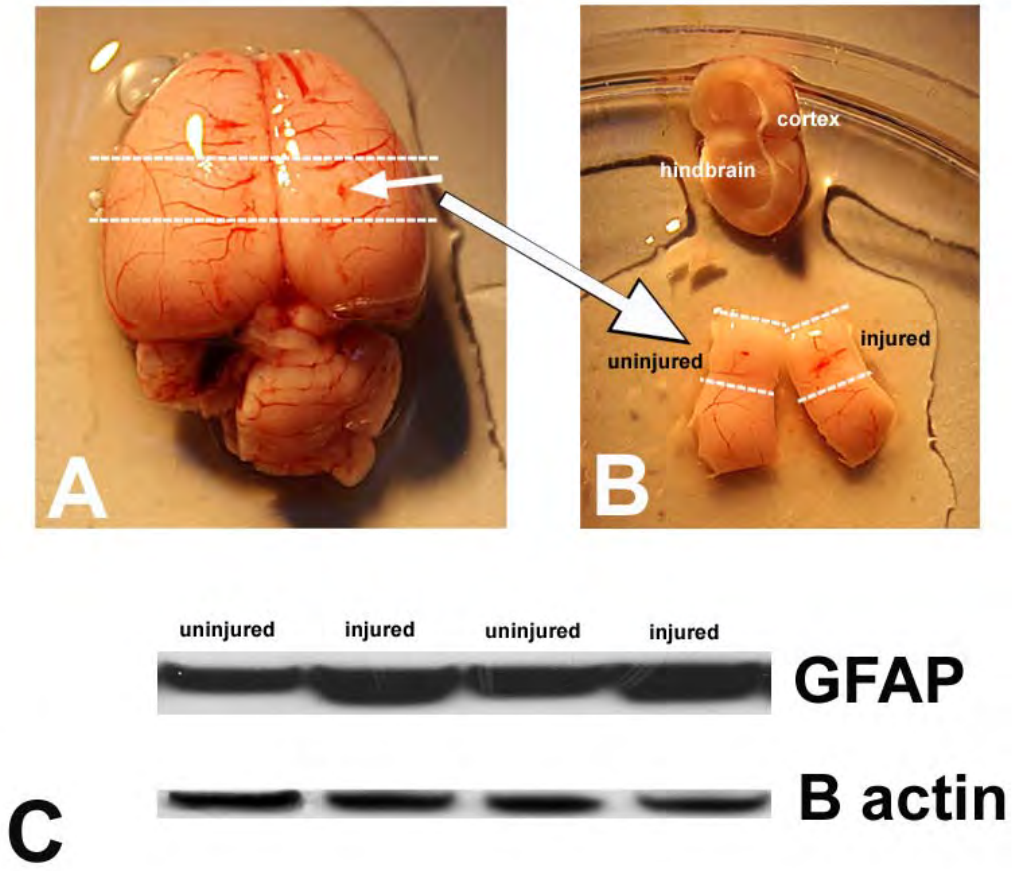

Figure 6.3 Cortical injury increases GFAP expression. Rats were euthanised 7 days post-injury, brains removed and a 4mm section that included the lesion (small arrow in A) cut (dashed lines in A) through the entire brain. The injured and uninjured hemisphere portions of the section were separated and the cortical portions peeled from the hindbrain (B). A 4x4mm section of the cortex centred on the injury site and an equivalent section from the uninjured hemisphere (dashed lines in B) were cut and processed for Western blotting (C). All samples are from the same control saline-injected, cortical needle-stick injured rat. Blot lanes alternate between uninjured and injured hemisphere samples. Stronger protein bands indicate increased GFAP expression in injured hemispheres relative to uninjured hemispheres. B actin loading control lanes indicated similar amounts of total protein were loaded in each lane.

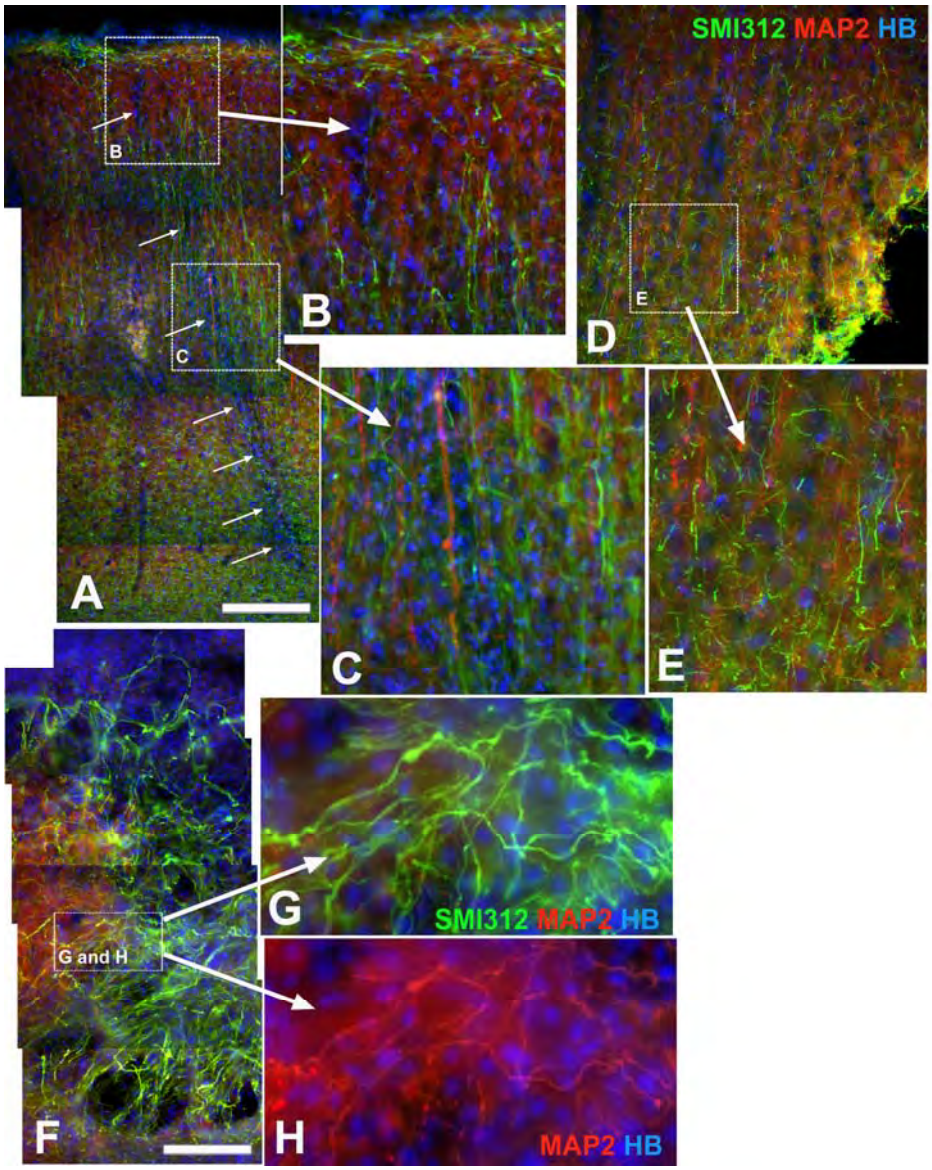

Figure 6.4 Phosphorylated neurofilament and MAP 2 immunoreactivity in injured neurons. Cortical sections were immunostained using antibodies against phosphorylated neurofilaments (SMI312, green) and microtubule-associated protein 2 (MAP2, red) 7 days after needle-stick injuries. Nuclei are counter-stained with Hoechst blue (HB). In injuries where the lesion corresponds closely to the needle-stick (A) neuronal death in the lesion results in a loss of MAP2 immunoreactivity and the lesion appears as a dark region in the image (small arrows in A). The section is on the border of the lesion and there is overlying increased MAP2 and SMI312 immunoreactivity in neurites in the lesion border more clearly seen in the enlarged images (B and C). The phosphorylated neurofilaments appear to commence around layer 3 of the cortex (C) and extend towards layer 1 and the dorsal surface (B). The phosphorylated neurofilament immunoreactivity within the relatively intact tissue does not coincide with the MAP2 immunoreactivity. A similar pattern and increase in immunoreactivity occurs in cortical tissue damaged after fixation during sectioning (D and E). Where there is more extensive tissue damage (F) intense immunoreactivity for phosphorylated neurofilaments (F and G) co-localises with MAP2 immunoreactivity (F, G and H) in a tangled mass of neurites. Scale bar is 250μm.

6.4 Conclusion

This thesis provides evidence for a moderating effect of OECs on astrocyte inflammatory activation that could contribute to improved tissue repair following CNS injury in response to transplanted OECs. An apparent resistance of OECs to inflammatory activation and a susceptibility to apoptosis in response to inflammation-related calcium influx have implications for OEC interaction with neurons and other cells in their normal olfactory neuron support role and for transplanted OECs. Continuing research utilising the *in vitro* model established by this research complemented by the additional *in vitro* and *in vivo* research described above will further elucidate OEC biology and the mechanisms for their therapeutic effects.

REFERENCES

Abbott NJ (2002) Astrocyte-endothelial interactions and blood-brain barrier permeability. J Anat 200:629-638.

Abbott NJ, Hughes CC, Revest PA, Greenwood J (1992) Development and characterisation of a rat brain capillary endothelial culture: towards an in vitro blood-brain barrier. J Cell Sci 103 (Pt 1):23-37.

Abe K, Saito H (1999) Effect of ATP on astrocyte stellation is switched from suppressive to stimulatory during development. Brain Res 850:150-157.

Abe K, Saito H (2000) The p44/42 mitogen-activated protein kinase cascade is involved in the induction and maintenance of astrocyte stellation mediated by protein kinase C. Neurosci Res 36:251-257.

Abe K, Saito H (2001) Possible linkage between glutamate transporter and mitogen-activated protein kinase cascade in cultured rat cortical astrocytes. J Neurochem 76:217-223.

Abramov AY, Jacobson J, Wientjes F, Hothersall J, Canevari L, Duchen MR (2005) Expression and modulation of an NADPH oxidase in mammalian astrocytes. J Neurosci 25:9176-9184.

Acarin L, Peluffo H, Barbeito L, Castellano B, Gonzalez B (2005) Astroglial nitration after postnatal excitotoxic damage: correlation with nitric oxide sources, cytoskeletal, apoptotic and antioxidant proteins. J Neurotrauma 22:189-200.

Ahmed S, Kozma R, Lee J, Monfries C, Harden N, Lim L (1991) The cysteine-rich domain of human proteins, neuronal chimaerin, protein kinase C and diacylglycerol kinase binds zinc. Evidence for the involvement of a zinc-dependent structure in phorbol ester binding. Biochem J 280 (Pt 1):233-241.

Akira S, Sato S (2003) Toll-like receptors and their signaling mechanisms. Scand J Infect Dis 35:555-562.

Akita Y, Ohno S, Konno Y, Yano A, Suzuki K (1990) Expression and properties of two distinct classes of the phorbol ester receptor family, four conventional protein kinase C types, and a novel protein kinase C. J Biol Chem 265:354-362.

Akiyama Y, Lankford K, Radtke C, Greer CA, Kocsis JD (2004) Remyelination of spinal cord axons by olfactory ensheathing cells and Schwann cells derived from a transgenic rat expressing alkaline phosphatase marker gene. Neuron Glia Biol 1:47-55.

Albrecht PJ, Dahl JP, Stoltzfus OK, Levenson R, Levison SW (2002) Ciliary neurotrophic factor activates spinal cord astrocytes, stimulating their production and release of fibroblast growth factor-2, to increase motor neuron survival. Exp Neurol 173:46-62.

Alexander CL, Fitzgerald UF, Barnett SC (2002) Identification of growth factors that promote long-term proliferation of olfactory ensheathing cells and modulate their antigenic phenotype. Glia 37:349-364.

Aloisi F (2001) Immune function of microglia. Glia 36:165-179.

Alonso G (2005) NG2 proteoglycan-expressing cells of the adult rat brain: possible involvement in the formation of glial scar astrocytes following stab wound. Glia 49:318-338.

Ambjorn M, Asmussen JW, Lindstam M, Gotfryd K, Jacobsen C, Kiselyov VV, Moestrup SK, Penkowa M, Bock E, Berezin V (2008) Metallothionein and a peptide modeled after metallothionein, EmtinB, induce neuronal differentiation and survival through binding to receptors of the low-density lipoprotein receptor family. J Neurochem 104:21-37.

Ambros JT, Herrero-Fresneda I, Borau OG, Boira JM (2007) Ischemic preconditioning in solid organ transplantation: from experimental to clinics. Transpl Int 20:219-229.

Amos S, Martin PM, Polar GA, Parsons SJ, Hussaini IM (2005) Phorbol 12-myristate 13-acetate induces epidermal growth factor receptor transactivation via protein kinase Cdelta/c-Src pathways in glioblastoma cells. J Biol Chem 280:7729-7738.

Ankeny DP, Popovich PG (2009) Mechanisms and implications of adaptive immune responses after traumatic spinal cord injury. Neuroscience 158:1112-1121.

Ankeny DP, Guan Z, Popovich PG (2009) B cells produce pathogenic antibodies and impair recovery after spinal cord injury in mice. J. Clin. Invest. 119:2990-2999.
Araque A, Sanzgiri RP, Parpura V, Haydon PG (1998) Calcium elevation in astrocytes causes an NMDA receptor-dependent increase in the frequency of miniature synaptic currents in cultured hippocampal neurons. J Neurosci 18:6822-6829.
Aronica E, Gorter JA, Rozemuller AJ, Yankaya B, Troost D (2005) Activation of metabotropic glutamate receptor 3 enhances interleukin (IL)-1beta-stimulated release of IL-6 in cultured human astrocytes. Neuroscience 130:927-933.
Arranz AM, Gottlieb M, Perez-Cerda F, Matute C (2010) Increased expression of glutamate transporters in subcortical white matter after transient focal cerebral ischemia. Neurobiol Dis 37:156-165.
Asan E, Langenhan T, Holtmann B, Bock H, Sendtner M, Carroll P (2003) Ciliary neurotrophic factor in the olfactory bulb of rats and mice. Neuroscience 120:99-112.
Aschner M (1998) Metallothionein (MT) isoforms in the central nervous system (CNS): regional and cell-specific distribution and potential functions as an antioxidant. Neurotoxicology 19:653-660.
Au E, Roskams AJ (2003) Olfactory ensheathing cells of the lamina propria in vivo and in vitro. Glia 41:224-236.
Ayer RE, Zhang JH (2008) The clinical significance of acute brain injury in subarachnoid hemorrhage and opportunity for intervention. Acta Neurochir Suppl 105:179-184.
Babcock AA, Kuziel WA, Rivest S, Owens T (2003) Chemokine Expression by Glial Cells Directs Leukocytes to Sites of Axonal Injury in the CNS. J Neurosci 23:7922-7930.
Bae MK, Kim SR, Lee HJ, Wee HJ, Yoo MA, Ock Oh S, Baek SY, Kim BS, Kim JB, Sik Y, Bae SK (2006) Aspirin-induced blockade of NF-kappaB activity restrains up-regulation of glial fibrillary acidic protein in human astroglial cells. Biochim Biophys Acta 1763:282-289.
Baeuerle PA (1998) IkappaB-NF-kappaB structures: at the interface of inflammation control. Cell 95:729-731.
Baeuerle PA, Henkel T (1994) Function and activation of NF-kappa B in the immune system. Annu Rev Immunol 12:141-179.
Baichwal VR, Baeuerle PA (1997) Activate NF-kappa B or die? Curr Biol 7:R94-96.
Baldwin AS, Jr. (1996) The NF-kappa B and I kappa B proteins: new discoveries and insights. Annu Rev Immunol 14:649-683.
Ballestas ME, Benveniste EN (1995) Interleukin 1-beta- and tumor necrosis factor-alpha-mediated regulation of ICAM-1 gene expression in astrocytes requires protein kinase C activity. Glia 14:267-278.
Barber PC, Lindsay RM (1982) Schwann cells of the olfactory nerves contain glial fibrillary acidic protein and resemble astrocytes. Neuroscience 7:3077-3090.
Barnett SC, Chang L (2004) Olfactory ensheathing cells and CNS repair: going solo or in need of a friend? Trends Neurosci 27:54-60.
Barnett SC, Riddell JS (2004) Olfactory ensheathing cells (OECs) and the treatment of CNS injury: advantages and possible caveats. J Anat 204:57-67.
Barnett SC, Riddell JS (2007) Olfactory ensheathing cell transplantation as a strategy for spinal cord repair--what can it achieve? Nat Clin Pract Neurol 3:152-161.
Barnett SC, Hutchins AM, Noble M (1993) Purification of olfactory nerve ensheathing cells from the olfactory bulb. Dev Biol 155:337-350.
Barnett SC, Alexander CL, Iwashita Y, Gilson JM, Crowther J, Clark L, Dunn LT, Papanastassiou V, Kennedy PG, Franklin RJ (2000) Identification of a human olfactory ensheathing cell that can effect transplant-mediated remyelination of demyelinated CNS axons. Brain 123:1581-1588.
Barraud P, He X, Zhao C, Ibanez C, Raha-Chowdhury R, Caldwell MA, Franklin RJ (2007) Contrasting effects of basic fibroblast growth factor and epidermal growth factor on mouse neonatal olfactory mucosa cells. Eur J Neurosci 26:3345-3357.
Bartolomei JC, Greer CA (2000) Olfactory ensheathing cells: bridging the gap in spinal cord injury. Neurosurgery 47:1057-1069.

Bauer S, Patterson PH (2006) Leukemia inhibitory factor promotes neural stem cell self-renewal in the adult brain. J Neurosci 26:12089-12099.

Bauer S, Rasika S, Han J, Mauduit C, Raccurt M, Morel G, Jourdan F, Benahmed M, Moyse E, Patterson PH (2003) Leukemia inhibitory factor is a key signal for injury-induced neurogenesis in the adult mouse olfactory epithelium. J Neurosci 23:1792-1803.

Bednarski BK, Baldwin AS, Jr., Kim HJ (2009) Addressing reported pro-apoptotic functions of NF-kappaB: targeted inhibition of canonical NF-kappaB enhances the apoptotic effects of doxorubicin. PLoS One 4:e6992.

Beech DJ, Xu SZ, McHugh D, Flemming R (2003) TRPC1 store-operated cationic channel subunit. Cell Calcium 33:433-440.

Beer R, Franz G, Krajewski S, Pike BR, Hayes RL, Reed JC, Wang KK, Klimmer C, Schmutzhard E, Poewe W, Kampfl A (2001) Temporal and spatial profile of caspase 8 expression and proteolysis after experimental traumatic brain injury. J Neurochem 78:862-873.

Bekku Y, Rauch U, Ninomiya Y, Oohashi T (2009) Brevican distinctively assembles extracellular components at the large diameter nodes of Ranvier in the CNS. J Neurochem 108:1266-1276.

Belcheva MM, Clark AL, Haas PD, Serna JS, Hahn JW, Kiss A, Coscia CJ (2005) Mu and kappa opioid receptors activate ERK/MAPK via different protein kinase C isoforms and secondary messengers in astrocytes. J Biol Chem 280:27662-27669.

Benavides A, Pastor D, Santos P, Tranque P, Calvo S (2005) CHOP plays a pivotal role in the astrocyte death induced by oxygen and glucose deprivation. Glia 52:261-275.

Bergling S, Dolmetsch R, Lewis RS, Keizer J (1998) A fluorometric method for estimating the calcium content of internal stores. Cell Calcium 23:251-259.

Berry M, Maxwell WL, Logan A, Mathewson A, McConnell P, Ashhurst DE, Thomas GH (1983) Deposition of scar tissue in the central nervous system. Acta Neurochir Suppl (Wien) 32:31-53.

Beschorner R, Dietz K, Schauer N, Mittelbronn M, Schluesener HJ, Trautmann K, Meyermann R, Simon P (2007) Expression of EAAT1 reflects a possible neuroprotective function of reactive astrocytes and activated microglia following human traumatic brain injury. Histol Histopathol 22:515-526.

Bethea JR (2000) Spinal cord injury-induced inflammation: a dual edged sword. Prog Brain Res 128:33-42.

Bethea JR, Castro M, Keane RW, Lee TT, Dietrich WD, Yezierski RP (1998) Traumatic spinal cord injury induces nuclear factor-kappaB activation. J Neurosci 18:3251-3260.

Bevers MB, Lawrence E, Maronski M, Starr N, Amesquita M, Neumar RW (2009) Knockdown of m-calpain increases survival of primary hippocampal neurons following NMDA excitotoxicity. J Neurochem 108:1237-1250.

Bigdeli MR, Rahnema M, Khoshbaten A (2009) Preconditioning with sublethal ischemia or intermittent normobaric hyperoxia up-regulates glutamate transporters and tumor necrosis factor-alpha converting enzyme in the rat brain. J Stroke Cerebrovasc Dis 18:336-342.

Bjornsen LP, Eid T, Holmseth S, Danbolt NC, Spencer DD, de Lanerolle NC (2007) Changes in glial glutamate transporters in human epileptogenic hippocampus: inadequate explanation for high extracellular glutamate during seizures. Neurobiol Dis 25:319-330.

Block ML, Zecca L, Hong JS (2007) Microglia-mediated neurotoxicity: uncovering the molecular mechanisms. Nat Rev Neurosci 8:57-69.

Blomgren K, Hagberg H (2006) Free radicals, mitochondria, and hypoxia-ischemia in the developing brain. Free Radic Biol Med 40:388-397.

Blondeau N, Widmann C, Lazdunski M, Heurteaux C (2001) Activation of the nuclear factor-kappaB is a key event in brain tolerance. J Neurosci 21:4668-4677.

Bolin LM, Zhaung A, Strychkarska-Orczyk I, Nelson E, Huang I, Malit M, Nguyen Q (2005) Differential inflammatory activation of IL-6 (-/-) astrocytes. Cytokine 30:47-55.

Bonini P, Cicconi S, Cardinale A, Vitale C, Serafino AL, Ciotti MT, Marlier LN (2004) Oxidative stress induces p53-mediated apoptosis in glia: p53 transcription-independent way to die. J Neurosci Res 75:83-95.

Borders AS, Getchell ML, Etscheidt JT, van Rooijen N, Cohen DA, Getchell TV (2007a) Macrophage depletion in the murine olfactory epithelium leads to increased neuronal death and decreased neurogenesis. The Journal of Comparative Neurology 501:206-218.

Borders AS, Hersh MA, Getchell ML, van Rooijen N, Cohen DA, Stromberg AJ, Getchell TV (2007b) Macrophage-mediated neuroprotection and neurogenesis in the olfactory epithelium. Physiol Genomics 31:531-543.

Boya J, Carbonell AL, Calvo J, Borregon A (1987) Ultrastructural study on the origin of rat microglia cells. Acta Anat. (Basel) 130:329-335.

Bowman CC, Rasley A, Tranguch SL, Marriott I (2003) Cultured astrocytes express toll-like receptors for bacterial products. Glia 43:281-291.

Boyd JG, Skihar V, Kawaja M, Doucette R (2003) Olfactory ensheathing cells: Historical perspective and therapeutic potential. Anat Rec 271B:49-60.

Boyd JG, Lee J, Skihar V, Doucette R, Kawaja MD (2004) LacZ-expressing olfactory ensheathing cells do not associate with myelinated axons after implantation into the compressed spinal cord. PNAS 101:2162-2166.

Bracher M, Gould HJ, Sutton BJ, Dombrowicz D, Karagiannis SN (2007) Three-colour flow cytometric method to measure antibody-dependent tumour cell killing by cytotoxicity and phagocytosis. J Immunol Methods 323:160-171.

Bracken MB, Holford TR (2002) Neurological and functional status 1 year after acute spinal cord injury: estimates of functional recovery in National Acute Spinal Cord Injury Study II from results modeled in National Acute Spinal Cord Injury Study III. J. Neurosurg. 96:259-266.

Brahmachari S, Fung YK, Pahan K (2006) Induction of glial fibrillary acidic protein expression in astrocytes by nitric oxide. J Neurosci 26:4930-4939.

Brambilla R, Hurtado A, Persaud T, Esham K, Pearse DD, Oudega M, Bethea JR (2009) Transgenic inhibition of astroglial NF-kappa B leads to increased axonal sparing and sprouting following spinal cord injury. Journal of Neurochemistry 110:765-778.

Brambilla R, Bracchi-Ricard V, Hu WH, Frydel B, Bramwell A, Karmally S, Green EJ, Bethea JR (2005) Inhibition of astroglial nuclear factor kappaB reduces inflammation and improves functional recovery after spinal cord injury. J Exp Med 202:145-156.

Bregman BS, McAtee M, Dai HN, Kuhn PL (1997) Neurotrophic factors increase axonal growth after spinal cord injury and transplantation in the adult rat. Exp Neurol 148:475-494.

Brettingham-Moore KH, Rao S, Juelich T, Shannon MF, Holloway AF (2005) GM-CSF promoter chromatin remodelling and gene transcription display distinct signal and transcription factor requirements. Nucleic Acids Res 33:225-234.

Brettingham-Moore KH, Sprod OR, Chen X, Oakford P, Shannon MF, Holloway AF (2008) Determinants of a transcriptionally competent environment at the GM-CSF promoter. Nucleic Acids Res 36:2639-2653.

Bright R, Mochly-Rosen D (2005) The role of protein kinase C in cerebral ischemic and reperfusion injury. Stroke 36:2781-2790.

Brill MS, Snapyan M, Wohlfrom H, Ninkovic J, Jawerka M, Mastick GS, Ashery-Padan R, Saghatelyan A, Berninger B, Gotz M (2008) A dlx2- and pax6-dependent transcriptional code for periglomerular neuron specification in the adult olfactory bulb. J Neurosci 28:6439-6452.

Broughton BR, Reutens DC, Sobey CG (2009) Apoptotic mechanisms after cerebral ischemia. Stroke 40:e331-339.

Brown K, Park S, Kanno T, Franzoso G, Siebenlist U (1993) Mutual regulation of the transcriptional activator NF-kappa B and its inhibitor, I kappa B-alpha. Proc Natl Acad Sci U S A 90:2532-2536.

Brunig I, Kaech S, Brinkhaus H, Oertner TG, Matus A (2004) Influx of extracellular calcium regulates actin-dependent morphological plasticity in dendritic spines. Neuropharmacology 47:669-676.

Brustovetsky N, Brustovetsky T, Jernmerson R, Dubinsky JM (2002) Calcium-induced Cytochrome c release from CNS mitochondria is associated with the permeability transition and rupture of the outer membrane. J Neurochem 80:207-218.

Bsibsi M, Ravid R, Gveric D, van Noort JM (2002) Broad expression of Toll-like receptors in the human central nervous system. J Neuropathol Exp Neurol 61:1013-1021.
Bsibsi M, Persoon-Deen C, Verwer RW, Meeuwsen S, Ravid R, Van Noort JM (2006) Toll-like receptor 3 on adult human astrocytes triggers production of neuroprotective mediators. Glia 53:688-695.
Bundesen LQ, Scheel TA, Bregman BS, Kromer LF (2003) Ephrin-B2 and EphB2 regulation of astrocyte-meningeal fibroblast interactions in response to spinal cord lesions in adult rats. J Neurosci 23:7789-7800.
Bunge MB (2001) Bridging areas of injury in the spinal cord. Neuroscientist 7:325-339.
Bunge MB (2008) Novel combination strategies to repair the injured mammalian spinal cord. J Spinal Cord Med 31:262-269.
Buniatian GH, Hartmann H, Traub P, Weser U, Wiesinger H, Gebhardt R (2001) Acquisition of blood-tissue barrier-supporting features by hepatic stellate cells and astrocytes of myofibroblastic phenotype. Inverse dynamics of metallothionein and glial fibrillary acidic protein expression. Neurochem Int 38:373-383.
Burgos M, Calvo S, Molina F, Vaquero CF, Samarel A, Llopis J, Tranque P (2007a) PKCepsilon induces astrocyte stellation by modulating multiple cytoskeletal proteins and interacting with Rho A signalling pathways: implications for neuroinflammation. Eur J Neurosci 25:1069-1078.
Burgos M, Pastor MD, Gonzalez JC, Martinez-Galan JR, Vaquero CF, Fradejas N, Benavides A, Hernandez-Guijo JM, Tranque P, Calvo S (2007b) PKCepsilon upregulates voltage-dependent calcium channels in cultured astrocytes. Glia 55:1437-1448.
Bush TG, Puvanachandra N, Horner CH, Polito A, Ostenfeld T, Svendsen CN, Mucke L, Johnson MH, Sofroniew MV (1999) Leukocyte infiltration, neuronal degeneration, and neurite outgrowth after ablation of scar-forming, reactive astrocytes in adult transgenic mice. Neuron 23:297-308.
Busija DW, Gaspar T, Domoki F, Katakam PV, Bari F (2008) Mitochondrial-mediated suppression of ROS production upon exposure of neurons to lethal stress: mitochondrial targeted preconditioning. Adv Drug Deliv Rev 60:1471-1477.
Butler MP, Moynagh PN, O'Connor JJ (2002) Methods of detection of the transcription factor NF-kappa B in rat hippocampal slices. J Neurosci Methods 119:185-190.
Butovsky O, Talpalar AE, Ben-Yaakov K, Schwartz M (2005) Activation of microglia by aggregated beta-amyloid or lipopolysaccharide impairs MHC-II expression and renders them cytotoxic whereas IFN-gamma and IL-4 render them protective. Mol Cell Neurosci 29:381-393.
Cafferty WB, Gardiner NJ, Das P, Qiu J, McMahon SB, Thompson SW (2004) Conditioning injury-induced spinal axon regeneration fails in interleukin-6 knock-out mice. J Neurosci 24:4432-4443.
Calegari F, Coco S, Taverna E, Bassetti M, Verderio C, Corradi N, Matteoli M, Rosa P (1999) A regulated secretory pathway in cultured hippocampal astrocytes. J Biol Chem 274:22539-22547.
Callard R, Hodgkin P (2007) Modeling T- and B-cell growth and differentiation. Immunol Rev 216:119-129.
Calof AL, Hagiwara N, Holcomb JD, Mumm JS, Shou J (1996) Neurogenesis and cell death in olfactory epithelium. J Neurobiol 30:67-81.
Campagne MV, Thibodeaux H, van Bruggen N, Cairns B, Lowe DG (2000) Increased binding activity at an antioxidant-responsive element in the metallothionein-1 promoter and rapid induction of metallothionein-1 and -2 in response to cerebral ischemia and reperfusion. J Neurosci 20:5200-5207.
Campbell K (2003) Signaling to and from radial glia. Glia 43:44-46.
Candelario-Jalil E (2009) Injury and repair mechanisms in ischemic stroke: considerations for the development of novel neurotherapeutics. Curr Opin Investig Drugs 10:644-654.

Canellada A, Ramirez BG, Minami T, Redondo JM, Cano E (2008) Calcium/calcineurin signaling in primary cortical astrocyte cultures: Rcan1-4 and cyclooxygenase-2 as NFAT target genes. Glia 56:709-722.

Carafoli E (2002) Calcium signaling: a tale for all seasons. Proc Natl Acad Sci U S A 99:1115-1122.

Cardona AE, Pioro EP, Sasse ME, Kostenko V, Cardona SM, Dijkstra IM, Huang D, Kidd G, Dombrowski S, Dutta R, Lee JC, Cook DN, Jung S, Lira SA, Littman DR, Ransohoff RM (2006) Control of microglial neurotoxicity by the fractalkine receptor. Nat. Neurosci. 9:917-924.

Carlstedt T (1997) Nerve fibre regeneration across the peripheral-central transitional zone. J Anat 190 (Pt 1):51-56.

Carmel JB, Kakinohana O, Mestril R, Young W, Marsala M, Hart RP (2004) Mediators of ischemic preconditioning identified by microarray analysis of rat spinal cord. Experimental Neurology 185:81-96.

Carpentier PA, Begolka WS, Olson JK, Elhofy A, Karpus WJ, Miller SD (2005) Differential activation of astrocytes by innate and adaptive immune stimuli. Glia 49:360-374.

Carr VM, Farbman AI (1993) The dynamics of cell death in the olfactory epithelium. Exp Neurol 124:308-314.

Carrasco J, Hernandez J, Bluethmann H, Hidalgo J (1998) Interleukin-6 and tumor necrosis factor-alpha type 1 receptor deficient mice reveal a role of IL-6 and TNF-alpha on brain metallothionein-I and -III regulation. Brain Res Mol Brain Res 57:221-234.

Carrasco J, Penkowa M, Hadberg H, Molinero A, Hidalgo J (2000a) Enhanced seizures and hippocampal neurodegeneration following kainic acid-induced seizures in metallothionein-I + II-deficient mice. Eur J Neurosci 12:2311-2322.

Carrasco J, Giralt M, Penkowa M, Stalder AK, Campbell IL, Hidalgo J (2000b) Metallothioneins are upregulated in symptomatic mice with astrocyte- targeted expression of tumor necrosis factor-alpha. Exp Neurol 163:46-54.

Carro E, Spuch C, Trejo JL, Antequera D, Torres-Aleman I (2005) Choroid plexus megalin is involved in neuroprotection by serum insulin-like growth factor I. J Neurosci 25:10884-10893.

Carter LA, MacDonald JL, Roskams AJ (2004) Olfactory horizontal basal cells demonstrate a conserved multipotent progenitor phenotype. J. Neurosci. 24:5670-5683.

Carter LM, Starkey ML, Akrimi SF, Davies M, McMahon SB, Bradbury EJ (2008) The yellow fluorescent protein (YFP-H) mouse reveals neuroprotection as a novel mechanism underlying chondroitinase ABC-mediated repair after spinal cord injury. J Neurosci 28:14107-14120.

Casetta I, Govoni V, Granieri E (2005) Oxidative Stress, Antioxidants and Neurodegenerative Diseases. Current Pharmaceutical Design 11:2033.

Cebolla B, Vallejo M (2006) Nuclear factor-I regulates glial fibrillary acidic protein gene expression in astrocytes differentiated from cortical precursor cells. J Neurochem 97:1057-1070.

Cechin SR, Gottfried C, Prestes CC, Andrighetti L, Wofchuk ST, Rodnight R (2002) Astrocyte stellation in saline media lacking bicarbonate: possible relation to intracellular pH and tyrosine phosphorylation. Brain Res 946:12-23.

Chakravarty S, Herkenham M (2005) Toll-like receptor 4 on nonhematopoietic cells sustains CNS inflammation during endotoxemia, independent of systemic cytokines. J Neurosci 25:1788-1796.

Chan CC, Wong AK, Liu J, Steeves JD, Tetzlaff W (2007) ROCK inhibition with Y27632 activates astrocytes and increases their expression of neurite growth-inhibitory chondroitin sulfate proteoglycans. Glia 55:369-384.

Chan ED, Riches DW (2001) IFN-gamma + LPS induction of iNOS is modulated by ERK, JNK/SAPK, and p38(mapk) in a mouse macrophage cell line. Am J Physiol Cell Physiol 280:C441-450.

Chan ED, Morris KR, Belisle JT, Hill P, Remigio LK, Brennan PJ, Riches DW (2001) Induction of inducible nitric oxide synthase-NO* by lipoarabinomannan of Mycobacterium tuberculosis is

mediated by MEK1-ERK, MKK7-JNK, and NF-kappaB signaling pathways. Infect Immun 69:2001-2010.
Chao CC, Hu S, Ehrlich L, Peterson PK (1995) Interleukin-1 and tumor necrosis factor-alpha synergistically mediate neurotoxicity: involvement of nitric oxide and of N-methyl-D-aspartate receptors. Brain Behav Immun 9:355-365.
Chattopadhyay N, Tfelt-Hansen J, Brown EM (2002) PKC, p42/44 MAPK and p38 MAPK regulate hepatocyte growth factor secretion from human astrocytoma cells. Brain Res Mol Brain Res 102:73-82.
Chau CH, Shum DK, Li H, Pei J, Lui YY, Wirthlin L, Chan YS, Xu XM (2004) Chondroitinase ABC enhances axonal regrowth through Schwann cell-seeded guidance channels after spinal cord injury. FASEB J 18:194-196.
Chen BC, Hsieh SL, Lin WW (2001a) Involvement of protein kinases in the potentiation of lipopolysaccharide-induced inflammatory mediator formation by thapsigargin in peritoneal macrophages. J Leukoc Biol 69:280-288.
Chen C, Chou C, Sun Y, Huang W (2001b) Tumor necrosis factor alpha-induced activation of downstream NF-kappaB site of the promoter mediates epithelial ICAM-1 expression and monocyte adhesion. Involvement of PKCalpha, tyrosine kinase, and IKK2, but not MAPKs, pathway. Cell Signal 13:543-553.
Chen CC, Wang JK, Chen WC, Lin SB (1998) Protein kinase C eta mediates lipopolysaccharide-induced nitric-oxide synthase expression in primary astrocytes. J Biol Chem 273:19424-19430.
Chen CJ, Ou YC, Lin SY, Liao SL, Huang YS, Chiang AN (2006a) L-glutamate activates RhoA GTPase leading to suppression of astrocyte stellation. Eur J Neurosci 23:1977-1987.
Chen CY, Peng WH, Tsai KD, Hsu SL (2007) Luteolin suppresses inflammation-associated gene expression by blocking NF-kappaB and AP-1 activation pathway in mouse alveolar macrophages. Life Sci 81:1602-1614.
Chen G, Shi J, Jin W, Wang L, Xie W, Sun J, Hang C (2008) Progesterone administration modulates TLRs/NF-kappaB signaling pathway in rat brain after cortical contusion. Ann Clin Lab Sci 38:65-74.
Chen H, Kohno K, Gong Q (2005a) Conditional ablation of mature olfactory sensory neurons mediated by diphtheria toxin receptor. J Neurocytol 34:37-47.
Chen HB, Chan YT, Hung AC, Tsai YC, Sun SH (2006b) Elucidation of ATP-stimulated stress protein expression of RBA-2 type-2 astrocytes: ATP potentiate HSP60 and Cu/Zn SOD expression and stimulates pI shift of peroxiredoxin II. J Cell Biochem 97:314-326.
Chen JS, Chai MQ, Song JG (2000) Regulation of Protein Kinase C in A-549 Cells by Phorbol Ester. Sheng Wu Hua Xue Yu Sheng Wu Wu Li Xue Bao (Shanghai) 32:645-648.
Chen L, Hahn H, Wu G, Chen CH, Liron T, Schechtman D, Cavallaro G, Banci L, Guo Y, Bolli R, Dorn GW, 2nd, Mochly-Rosen D (2001c) Opposing cardioprotective actions and parallel hypertrophic effects of delta PKC and epsilon PKC. Proc Natl Acad Sci U S A 98:11114-11119.
Chen LF, Greene WC (2004) Shaping the nuclear action of NF-kappaB. Nat Rev Mol Cell Biol 5:392-401.
Chen XQ, Fung YW, Yu AC (2005b) Association of 14-3-3gamma and phosphorylated bad attenuates injury in ischemic astrocytes. J Cereb Blood Flow Metab 25:338-347.
Chen XQ, Qin LY, Zhang CG, Yang LT, Gao Z, Liu S, Lau LT, Fung YW, Greenberg DA, Yu AC (2005c) Presence of neuroglobin in cultured astrocytes. Glia 50:182-186.
Chen Y, Swanson RA (2003) Astrocytes and brain injury. J Cereb Blood Flow Metab 23:137-149.
Chen Z, Palmer TD (2008) Cellular repair of CNS disorders: an immunological perspective. Hum Mol Genet 17:R84-92.
Cheng S, Mao J, Rehder V (2000) Filopodial behavior is dependent on the phosphorylation state of neuronal growth cones. Cell Motil Cytoskeleton 47:337-350.

Cheng YL, Wang CY, Huang WC, Tsai CC, Chen CL, Shen CF, Chi CY, Lin CF (2009) Staphylococcus aureus induces microglial inflammation via a glycogen synthase kinase 3beta-regulated pathway. Infect Immun 77:4002-4008.

Chierzi S, Ratto GM, Verma P, Fawcett JW (2005) The ability of axons to regenerate their growth cones depends on axonal type and age, and is regulated by calcium, cAMP and ERK. Eur J Neurosci 21:2051-2062.

Chinnery HR, Ruitenberg MJ, McMenamin PG (2010) Novel characterization of monocyte-derived cell populations in the meninges and choroid plexus and their rates of replenishment in bone marrow chimeric mice. J. Neuropathol. Exp. Neurol. 69:896-909.

Choi-Lundberg DL, Bohn MC (1995) Ontogeny and distribution of glial cell line-derived neurotrophic factor (GDNF) mRNA in rat. Brain Res Dev Brain Res 85:80-88.

Choi DW, Yokoyama M, Koh J (1988) Zinc neurotoxicity in cortical cell culture. Neuroscience 24:67-79.

Choi SH, Lee da Y, Kim SU, Jin BK (2005) Thrombin-induced oxidative stress contributes to the death of hippocampal neurons in vivo: role of microglial NADPH oxidase. J Neurosci 25:4082-4090.

Chong MS, Woolf CJ, Haque NS, Anderson PN (1999) Axonal regeneration from injured dorsal roots into the spinal cord of adult rats. J Comp Neurol 410:42-54.

Christensen MD, Holbrook EH, Costanzo RM, Schwob JE (2001) Rhinotopy is disrupted during the re-innervation of the olfactory bulb that follows transection of the olfactory nerve. Chem. Senses 26:359-369.

Christophe M, Nicolas S (2006) Mitochondria: a target for neuroprotective interventions in cerebral ischemia-reperfusion. Curr Pharm Des 12:739-757.

Chu LF, Wang WT, Ghanta VK, Lin CH, Chiang YY, Hsueh CM (2008) Ischemic brain cell-derived conditioned medium protects astrocytes against ischemia through GDNF/ERK/NF-kB signaling pathway. Brain Res 1239:24-35.

Chuah MI, Au C (1991) Olfactory Schwann cells are derived from precursor cells in the olfactory epithelium. J Neurosci Res 29:172-180.

Chuah MI, Au C (1993) Cultures of ensheathing cells from neonatal rat olfactory bulbs. Brain Res 601:213-220.

Chuah MI, Teague R (1999) Basic fibroblast growth factor in the primary olfactory pathway: mitogenic effect on ensheathing cells. Neuroscience 88:1043-1050.

Chuah MI, West AK (2002) Cellular and molecular biology of ensheathing cells. Microsc Res Tech 58:216-227.

Chuah MI, Schwob JE, Farbman AI (2003) Developmental Anatomy of the Olfactory System. In: Handbook of Olfaction and Gustation, Second Edition Edition (Dory RL, ed), pp 115-138. NY: Marcel Dekker, Inc.

Chuah MI, Hale DM, West AK (2010) Interaction of olfactory ensheathing cells with other cell types in vitro and after transplantation: Glial scars and inflammation. Exp Neurol.

Chuah MI, Choi-Lundberg D, Weston S, Vincent AJ, Chung RS, Vickers JC, West AK (2004) Olfactory ensheathing cells promote collateral axonal branching in the injured adult rat spinal cord. Exp Neurol 185:15-25.

Chung RS, West AK (2004) A role for extracellular metallothioneins in CNS injury and repair. Neuroscience 123:595-599.

Chung RS, Vickers JC, Chuah MI, West AK (2003) Metallothionein-IIA Promotes Initial Neurite Elongation and Postinjury Reactive Neurite Growth and Facilitates Healing after Focal Cortical Brain Injury. J Neurosci 23:3336-3342.

Chung RS, Adlard PA, Dittmann J, Vickers JC, Chuah MI, West AK (2004) Neuron-glia communication: metallothionein expression is specifically up-regulated by astrocytes in response to neuronal injury. J Neurochem 88:454-461.

Chung RS, Penkowa M, Dittmann J, King CE, Bartlett C, Asmussen JW, Hidalgo J, Carrasco J, Leung YK, Walker AK, Fung SJ, Dunlop SA, Fitzgerald M, Beazley LD, Chuah MI, Vickers JC, West AK (2008) Redefining the role of metallothionein within the injured brain: extracellular

metallothioneins play an important role in the astrocyte-neuron response to injury. J Biol Chem 283:15349-15358.
Ciccarelli R, D'Alimonte I, Santavenere C, D'Auro M, Ballerini P, Nargi E, Buccella S, NicosiaFolco S, Caciagli F, Di Iorio P (2004) Cysteinyl-leukotrienes are released from astrocytes and increase astrocyte proliferation and glial fibrillary acidic protein via cys-LT1 receptors and mitogen-activated protein kinase pathway. Eur J Neurosci 20:1514-1524.
Clapham DE (2007) Calcium signaling. Cell 131:1047-1058.
Clausen BH, Lambertsen KL, Babcock AA, Holm TH, Dagnaes-Hansen F, Finsen B (2008) Interleukin-1beta and tumor necrosis factor-alpha are expressed by different subsets of microglia and macrophages after ischemic stroke in mice. J Neuroinflammation 5:46.
Clemens MJ, Bushell M, Morley SJ (1998) Degradation of eukaryotic polypeptide chain initiation factor (eIF) 4G in response to induction of apoptosis in human lymphoma cell lines. Oncogene 17:2921-2931.
Cogswell PC, Kashatus DF, Keifer JA, Guttridge DC, Reuther JY, Bristow C, Roy S, Nicholson DW, Baldwin AS, Jr. (2003) NF-kappa B and I kappa B alpha are found in the mitochondria. Evidence for regulation of mitochondrial gene expression by NF-kappa B. J Biol Chem 278:2963-2968.
Collazos-Castro JE, Muneton-Gomez VC, Nieto-Sampedro M (2005) Olfactory glia transplantation into cervical spinal cord contusion injuries. J Neurosurg Spine 3:308-317.
Cornell-Bell AH, Thomas PG, Caffrey JM (1992) Ca2+ and filopodial responses to glutamate in cultured astrocytes and neurons. Can J Physiol Pharmacol 70 Suppl:S206-218.
Cornell-Bell AH, Finkbeiner SM, Cooper MS, Smith SJ (1990) Glutamate induces calcium waves in cultured astrocytes: long-range glial signaling. Science 247:470-473.
Correale P, Tagliaferri P, Guarrasi R, Caraglia M, Giuliano M, Marinetti MR, Bianco AR, Procopio A (1997) Extracellular adenosine 5' triphosphate involvement in the death of LAK-engaged human tumor cells via P2X-receptor activation. Immunol Lett 55:69-78.
Coyle JT, Puttfarcken P (1993) Oxidative stress, glutamate, and neurodegenerative disorders. Science 262:689-695.
Coyle P, Philcox JC, Rofe AM (1993) Corticosterone enhances the zinc and interleukin-6-mediated induction of metallothionein in cultured rat hepatocytes. J Nutr 123:1464-1470.
Coyle P, Philcox JC, Carey LC, Rofe AM (2002) Metallothionein: the multipurpose protein. Cell Mol Life Sci 59:627-647.
Crang AJ, Blakemore WF (1997) Attempts to produce astrocyte cultures devoid of oligodendrocyte generating potential by the use of antimitotic treatment reveal the presence of quiescent oligodendrocyte precursors. J Neurosci Res 49:64-71.
Cuadros MA, Navascues J (1998) The origin and differentiation of microglial cells during development. Prog. Neurobiol. 56:173-189.
Curin Y, Ritz MF, Andriantsitohaina R (2006) Cellular mechanisms of the protective effect of polyphenols on the neurovascular unit in strokes. Cardiovasc Hematol Agents Med Chem 4:277-288.
Dalton T, Palmiter RD, Andrews GK (1994) Transcriptional induction of the mouse metallothionein-I gene in hydrogen peroxide-treated Hepa cells involves a composite major late transcription factor/antioxidant response element and metal response promoter elements. Nucleic Acids Res 22:5016-5023.
Das S, Basu A (2008) Inflammation: a new candidate in modulating adult neurogenesis. J Neurosci Res 86:1199-1208.
Davalos D, Grutzendler J, Yang G, Kim JV, Zuo Y, Jung S, Littman DR, Dustin ML, Gan WB (2005) ATP mediates rapid microglial response to local brain injury in vivo. Nat Neurosci 8:752-758.
De Boer RJ, Ganusov VV, Milutinovic D, Hodgkin PD, Perelson AS (2006) Estimating lymphocyte division and death rates from CFSE data. Bull Math Biol 68:1011-1031.
Deng C, Gorrie C, Hayward I, Elston B, Venn M, Mackay-Sim A, Waite P (2006) Survival and migration of human and rat olfactory ensheathing cells in intact and injured spinal cord. J. Neurosci. Res. 83:1201-1212.

de Freitas MS, Spohr TC, Benedito AB, Caetano MS, Margulis B, Lopes UG, Moura-Neto V (2002) Neurite outgrowth is impaired on HSP70-positive astrocytes through a mechanism that requires NF-kappaB activation. Brain Res 958:359-370.

De Groot CJ, Langeveld CH, Jongenelen CA, Montagne L, Van Der Valk P, Dijkstra CD (1997) Establishment of human adult astrocyte cultures derived from postmortem multiple sclerosis and control brain and spinal cord regions: immunophenotypical and functional characterization. J Neurosci Res 49:342-354.

Deacon EM, Pongracz J, Griffiths G, Lord JM (1997) Isoenzymes of protein kinase C: differential involvement in apoptosis and pathogenesis. Mol Pathol 50:124-131.

Dedkova EN, Sigova AA, Zinchenko VP (2000) Mechanism of action of calcium ionophores on intact cells: ionophore-resistant cells. Membr Cell Biol 13:357-368.

Del Rio JA, Soriano E (2007) Overcoming chondroitin sulphate proteoglycan inhibition of axon growth in the injured brain: lessons from chondroitinase ABC. Curr Pharm Des 13:2485-2492.

del Zoppo GJ (2010) The neurovascular unit in the setting of stroke. J Intern Med 267:156-171.

Dell'Albani P (2008) Stem cell markers in gliomas. Neurochem Res 33:2407-2415.

Deloulme JC, Helies A, Ledig M, Lucas M, Sensenbrenner M (1997) A comparative study of the distribution of alpha- and gamma-enolase subunits in cultured rat neural cells and fibroblasts. Int J Dev Neurosci 15:183-194.

Deumens R, Koopmans GC, Honig WM, Maquet V, Jerome R, Steinbusch HW, Joosten EA (2006a) Chronically injured corticospinal axons do not cross large spinal lesion gaps after a multifactorial transplantation strategy using olfactory ensheathing cell/olfactory nerve fibroblast-biomatrix bridges. J Neurosci Res 83:811-820.

Deumens R, Koopmans GC, Lemmens M, Mollers S, Honig WM, Steinbusch HW, Brook G, Joosten EA (2006b) Neurite outgrowth promoting effects of enriched and mixed OEC/ONF cultures. Neurosci Lett 397:20-24.

Deumens R, Koopmans GC, Honig WM, Hamers FP, Maquet V, Jerome R, Steinbusch HW, Joosten EA (2006c) Olfactory ensheathing cells, olfactory nerve fibroblasts and biomatrices to promote long-distance axon regrowth and functional recovery in the dorsally hemisected adult rat spinal cord. Exp Neurol 200:89-103.

Dewar D, Bentley D, Barnett SC (2007) Implantation of pure cultured olfactory ensheathing cells in an animal model of parkinsonism. Acta Neurochir (Wien) 149:407-414.

Dhodda VK, Sailor KA, Bowen KK, Vemuganti R (2004) Putative endogenous mediators of preconditioning-induced ischemic tolerance in rat brain identified by genomic and proteomic analysis. J Neurochem 89:73-89.

Diaz Z, Assaraf MI, Miller WH, Jr., Schipper HM (2005) Astroglial cytoprotection by erythropoietin pre-conditioning: implications for ischemic and degenerative CNS disorders. J Neurochem 93:392-402.

Dickson BJ (2002) Molecular mechanisms of axon guidance. Science 298:1959-1964.

Dickson TC, Adlard PA, Vickers JC (2000) Sequence of cellular changes following localized axotomy to cortical neurons in glia-free culture. J Neurotrauma 17:1095-1103.

Dobrenis K (1998) Microglia in cell culture and in transplantation therapy for central nervous system disease. Methods 16:320-344.

Doherty P, Williams G, Williams EJ (2000) CAMs and axonal growth: A critical evaluation of the role of calcium and the MAPK cascade. Mol Cell Neurosci 16:283-295.

Domanska-Janik K, Bronisz-Kowalczyk A, Zajac H, Zablocka B (2001) Interrelations between nuclear-factor kappa B activation, glial response and neuronal apoptosis in gerbil hippocampus after ischemia. Acta Neurobiol Exp (Wars) 61:45-51.

Dong Y, Benveniste EN (2001) Immune function of astrocytes. Glia 36:180-190.

Donnelly DJ, Popovich PG (2008) Inflammation and its role in neuroprotection, axonal regeneration and functional recovery after spinal cord injury. Exp. Neurol. 209:378-388.

Doucette JR (1984) The glial cells in the nerve fiber layer of the rat olfactory bulb. Anat Rec 210:385-391.

Doucette JR, Devon R (1993) Olfactory ensheathing cells: factors influencing the phenotype of these glial cells. In: Biology and Pathology of Astrocyte-Neuron Interactions (al Fe, ed), pp 117-124. New York: Plenum Press.
Doucette JR, Kiernan JA, Flumerfelt BA (1983) The re-innervation of olfactory glomeruli following transection of primary olfactory axons in the central or peripheral nervous system. J Anat 137:1-19.
Doucette R (1989) Development of the nerve fiber layer in the olfactory bulb of mouse embryos. J Comp Neurol 285:514-527.
Doucette R (1990) Glial influences on axonal growth in the primary olfactory system. Glia 3:433-449.
Doucette R (1991) PNS-CNS transitional zone of the first cranial nerve. J Comp Neurol 312:451-466.
Doucette R (1993a) Glial progenitor cells of the nerve fiber layer of the olfactory bulb: effect of astrocyte growth media. J Neurosci Res 35:274-287.
Doucette R (1993b) Glial cells in the nerve fiber layer of the main olfactory bulb of embryonic and adult mammals. Microsc Res Tech 24:113-130.
Doyle KP, Simon RP, Stenzel-Poore MP (2008) Mechanisms of ischemic brain damage. Neuropharmacology 55:310-318.
Drago J, Murphy M, Carroll SM, Harvey RP, Bartlett PF (1991) Fibroblast growth factor-mediated proliferation of central nervous system precursors depends on endogenous production of insulin-like growth factor I. Proc Natl Acad Sci U S A 88:2199-2203.
Drozdz W, Sarwa A, Labza H (2006) [Clinical implication of ischemic preconditioning in protection of reperfused tissues]. Przegl Lek 63:271-277.
Du S, Rubin A, Klepper S, Barrett C, Kim YC, Rhim HW, Lee EB, Park CW, Markelonis GJ, Oh TH (1999) Calcium influx and activation of calpain I mediate acute reactive gliosis in injured spinal cord. Exp Neurol 157:96-105.
Duan S, Anderson CM, Stein BA, Swanson RA (1999) Glutamate induces rapid upregulation of astrocyte glutamate transport and cell-surface expression of GLAST. J Neurosci 19:10193-10200.
Dugan LL, Sensi SL, Canzoniero LM, Handran SD, Rothman SM, Lin TS, Goldberg MP, Choi DW (1995) Mitochondrial production of reactive oxygen species in cortical neurons following exposure to N-methyl-D-aspartate. J Neurosci 15:6377-6388.
Dynes JL, Ngai J (1998) Pathfinding of olfactory neuron axons to stereotyped glomerular targets revealed by dynamic imaging in living zebrafish embryos. Neuron 20:1081-1091.
Ebadi M, Brown-Borg H, El Refaey H, Singh BB, Garrett S, Shavali S, Sharma SK (2005) Metallothionein-mediated neuroprotection in genetically engineered mouse models of Parkinson's disease. Brain Res Mol Brain Res 134:67-75.
Eddleston M, Mucke L (1993) Molecular profile of reactive astrocytes--implications for their role in neurologic disease. Neuroscience 54:15-36.
Edvinsson L (2006) Neuropeptide Y and the cerebral circulation. EXS:105-112.
Ellison JA, Barone FC, Feuerstein GZ (1999) Matrix remodeling after stroke. De novo expression of matrix proteins and integrin receptors. Ann N Y Acad Sci 890:204-222.
Emsley JG, Mitchell BD, Kempermann G, Macklis JD (2005) Adult neurogenesis and repair of the adult CNS with neural progenitors, precursors, and stem cells. Prog Neurobiol 75:321-341.
Ennis SR, Keep RF (2006) Forebrain ischemia and the blood-cerebrospinal fluid barrier. Acta Neurochir Suppl 96:276-278.
Espejo C, Penkowa M, Saez-Torres I, Hidalgo J, Garcia A, Montalban X, Martinez-Caceres EM (2002) Interferon-gamma regulates oxidative stress during experimental autoimmune encephalomyelitis. Exp Neurol 177:21-31.
Esteve PO, Chicoine E, Robledo O, Aoudjit F, Descoteaux A, Potworowski EF, St-Pierre Y (2002) Protein kinase C-zeta regulates transcription of the matrix metalloproteinase-9 gene induced by IL-1 and TNF-alpha in glioma cells via NF-kappa B. J Biol Chem 277:35150-35155.
Faijerson J, Tinsley RB, Aprico K, Thorsell A, Nodin C, Nilsson M, Blomstrand F, Eriksson PS (2006) Reactive astrogliosis induces astrocytic differentiation of adult neural stem/progenitor cells in vitro. J Neurosci Res 84:1415-1424.

Fairless R, Frame MC, Barnett SC (2005) N-cadherin differentially determines Schwann cell and olfactory ensheathing cell adhesion and migration responses upon contact with astrocytes. Mol Cell Neurosci 28:253-263.
Fan G, Martinowich K, Chin MH, He F, Fouse SD, Hutnick L, Hattori D, Ge W, Shen Y, Wu H, Ten Hoeve J, Shuai K, Sun YE (2005) DNA methylation controls the timing of astrogliogenesis through regulation of JAK-STAT signaling. Development 132:3345-3356.
Fan W, Cooper NG (2009) Glutamate-induced NFkappaB activation in the retina. Invest. Ophthalmol. Vis. Sci. 50:917-925.
Farber K, Cheung G, Mitchell D, Wallis R, Weihe E, Schwaeble W, Kettenmann H (2009) C1q, the recognition subcomponent of the classical pathway of complement, drives microglial activation. J Neurosci Res 87:644-652.
Farooqui AA, Horrocks LA, Farooqui T (2007) Modulation of inflammation in brain: a matter of fat. J Neurochem 101:577-599.
Fasolato C, Pozzan T (1989) Effect of membrane potential on divalent cation transport catalyzed by the "electroneutral" ionophores A23187 and ionomycin. J Biol Chem 264:19630-19636.
Faubel S, Edelstein CL (2005) Caspases as drug targets in ischemic organ injury. Curr Drug Targets Immune Endocr Metabol Disord 5:269-287.
Faulkner JR, Herrmann JE, Woo MJ, Tansey KE, Doan NB, Sofroniew MV (2004) Reactive Astrocytes Protect Tissue and Preserve Function after Spinal Cord Injury. J Neurosci 24:2143-2155.
Fawcett JW (2006a) The glial response to injury and its role in the inhibition of CNS repair. Adv Exp Med Biol 557:11-24.
Fawcett JW (2006b) Overcoming inhibition in the damaged spinal cord. J Neurotrauma 23:371-383.
Fawcett JW, Asher RA (1999) The glial scar and central nervous system repair. Brain Res Bull 49:377-391.
Feng L, Meng H, Wu F, Cheng B, He X, Wang X, Li Z, Liu S (2008) Olfactory ensheathing cells conditioned medium prevented apoptosis induced by 6-OHDA in PC12 cells through modulation of intrinsic apoptotic pathways. Int J Dev Neurosci 26:323-329.
Fernandes A, Falcao AS, Silva RF, Gordo AC, Gama MJ, Brito MA, Brites D (2006) Inflammatory signalling pathways involved in astroglial activation by unconjugated bilirubin. J Neurochem 96:1667-1679.
Fernandez-Gomez FJ, Hernandez F, Argandona L, Galindo MF, Segura T, Jordan J (2008) [Pharmacology of neuroprotection in acute ischemic stroke]. Rev Neurol 47:253-260.
Fernandez AM, Gonzalez de la Vega AG, Planas B, Torres-Aleman I (1999) Neuroprotective actions of peripherally administered insulin-like growth factor I in the injured olivo-cerebellar pathway. Eur J Neurosci 11:2019-2030.
Fernandez AM, Fernandez S, Carrero P, Garcia-Garcia M, Torres-Aleman I (2007a) Calcineurin in reactive astrocytes plays a key role in the interplay between proinflammatory and anti-inflammatory signals. J Neurosci 27:8745-8756.
Fernandez S, Fernandez AM, Lopez-Lopez C, Torres-Aleman I (2007b) Emerging roles of insulin-like growth factor-I in the adult brain. Growth Horm IGF Res 17:89-95.
Feron F, Perry C, Cochrane J, Licina P, Nowitzke A, Urquhart S, Geraghty T, Mackay-Sim A (2005) Autologous olfactory ensheathing cell transplantation in human spinal cord injury. Brain 128:2951-2960.
Feuerstein GZ, Liu T, Barone FC (1994) Cytokines, inflammation, and brain injury: role of tumor necrosis factor-alpha. Cerebrovasc Brain Metab Rev 6:341-360.
Fisher WG, Yang PC, Medikonduri RK, Jafri MS (2006) NFAT and NFkappaB activation in T lymphocytes: a model of differential activation of gene expression. Ann. Biomed. Eng. 34:1712-1728.
Fitch MT, Silver J (2008) CNS injury, glial scars, and inflammation: Inhibitory extracellular matrices and regeneration failure. Exp Neurol 209:294-301.
Floyd CL, Lyeth BG (2007) Astroglia: important mediators of traumatic brain injury. Prog Brain Res 161:61-79.

Forder JP, Tymianski M (2009) Postsynaptic mechanisms of excitotoxicity: Involvement of postsynaptic density proteins, radicals, and oxidant molecules. Neuroscience 158:293-300.
Forman HJ, Torres M (2001) Redox signaling in macrophages. Mol Aspects Med 22:189-216.
Forman LJ, Liu P, Nagele RG, Yin K, Wong PY (1998) Augmentation of nitric oxide, superoxide, and peroxynitrite production during cerebral ischemia and reperfusion in the rat. Neurochem Res 23:141-148.
Franceschini IA, Barnett SC (1996) Low-affinity NGF-receptor and E-N-CAM expression define two types of olfactory nerve ensheathing cells that share a common lineage. Dev Biol 173:327-343.
Frangogiannis NG (2007) Chemokines in ischemia and reperfusion. Thromb Haemost 97:738-747.
Frank MG, Wieseler-Frank JL, Watkins LR, Maier SF (2006) Rapid isolation of highly enriched and quiescent microglia from adult rat hippocampus: immunophenotypic and functional characteristics. J Neurosci Methods 151:121-130.
Franklin RJ (2003) Remyelination by transplanted olfactory ensheathing cells. Anat Rec 271B:71-76.
Franklin RJ, Gilson JM, Franceschini IA, Barnett SC (1996) Schwann cell-like myelination following transplantation of an olfactory bulb-ensheathing cell line into areas of demyelination in the adult CNS. Glia 17:217-224.
Franklin RJ, Bayley SA, Milner R, Ffrench-Constant C, Blakemore WF (1995) Differentiation of the O-2A progenitor cell line CG-4 into oligodendrocytes and astrocytes following transplantation into glia-deficient areas of CNS white matter. Glia 13:39-44.
Franssen EH, De Bree FM, Essing AH, Ramon-Cueto A, Verhaagen J (2008) Comparative gene expression profiling of olfactory ensheathing glia and Schwann cells indicates distinct tissue repair characteristics of olfactory ensheathing glia. Glia 56:1285-1298.
Franzen R, Bouhy D, Schoenen J (2004) Nervous system injury: focus on the inflammatory cytokine 'granulocyte-macrophage colony stimulating factor'. Neurosci Lett 361:76-78.
Frederickson CJ, Bush AI (2001) Synaptically released zinc: physiological functions and pathological effects. Biometals 14:353-366.
Frederickson CJ, Maret W, Cuajungco MP (2004) Zinc and excitotoxic brain injury: a new model. Neuroscientist 10:18-25.
Frugier T, Morganti-Kossmann C, O'Reilly D, McLean C (2009) In situ detection of inflammatory mediators in post-mortem human brain tissue following traumatic injury. J Neurotrauma.
Fujioka H, Hunt PJ, Rozga J, Wu GD, Cramer DV, Demetriou AA, Moscioni AD (1994) Carboxyfluorescein (CFSE) labelling of hepatocytes for short-term localization following intraportal transplantation. Cell Transplant 3:397-408.
Fujita H, Tanaka J, Toku K, Tateishi N, Suzuki Y, Matsuda S, Sakanaka M, Maeda N (1996) Effects of GM-CSF and ordinary supplements on the ramification of microglia in culture: a morphometrical study. Glia 18:269-281.
Furukawa S, Furukawa Y (2007) [FGF-2-treatment improves locomotor function via axonal regeneration in the transected rat spinal cord]. Brain Nerve 59:1333-1339.
Gallo G, Letourneau PC (2004) Regulation of growth cone actin filaments by guidance cues. J Neurobiol 58:92-102.
Galtrey CM, Fawcett JW (2007) The role of chondroitin sulfate proteoglycans in regeneration and plasticity in the central nervous system. Brain Res Rev 54:1-18.
Garcao P, Oliveira CR, Agostinho P (2006) Comparative study of microglia activation induced by amyloid-beta and prion peptides: role in neurodegeneration. J Neurosci Res 84:182-193.
Garcia-Segura LM, Balthazart J (2009) Steroids and neuroprotection: New advances. Front Neuroendocrinol 30:v-ix.
Gasque P, Singhrao SK, Neal JW, Gotze O, Morgan BP (1997) Expression of the receptor for complement C5a (CD88) is up-regulated on reactive astrocytes, microglia, and endothelial cells in the inflamed human central nervous system. Am J Pathol 150:31-41.
Gee JM, Kalil A, Shea C, Becker KJ (2007) Lymphocytes: potential mediators of postischemic injury and neuroprotection. Stroke 38:783-788.

Gendron FP, Neary JT, Theiss PM, Sun GY, Gonzalez FA, Weisman GA (2003) Mechanisms of P2X7 receptor-mediated ERK1/2 phosphorylation in human astrocytoma cells. Am J Physiol Cell Physiol 284:C571-581.

Genot EM, Parker PJ, Cantrell DA (1995) Analysis of the role of protein kinase C-alpha, -epsilon, and -zeta in T cell activation. J Biol Chem 270:9833-9839.

Getchell TV, Subhedar NK, Shah DS, Hackley G, Partin JV, Sen G, Getchell ML (2002) Chemokine regulation of macrophage recruitment into the olfactory epithelium following target ablation: involvement of macrophage inflammatory protein-1alpha and monocyte chemoattractant protein-1. J. Neurosci. Res. 70:784-793.

Gibbons HM, Hughes SM, Van Roon-Mom W, Greenwood JM, Narayan PJ, Teoh HH, Bergin PM, Mee EW, Wood PC, Faull RL, Dragunow M (2007) Cellular composition of human glial cultures from adult biopsy brain tissue. J Neurosci Methods 166:89-98.

Giehl KM, Tetzlaff W (1996) BDNF and NT-3, but not NGF, prevent axotomy-induced death of rat corticospinal neurons in vivo. Eur J Neurosci 8:1167-1175.

Giffard RG, Swanson RA (2005) Ischemia-induced programmed cell death in astrocytes. Glia 50:299-306.

Gilbert RJ, McKeon RJ, Darr A, Calabro A, Hascall VC, Bellamkonda RV (2005) CS-4,6 is differentially upregulated in glial scar and is a potent inhibitor of neurite extension. Mol Cell Neurosci 29:545-558.

Gilmore TD (1999) The Rel/NF-kappaB signal transduction pathway: introduction. Oncogene 18:6842-6844.

Ginis I, Jaiswal R, Klimanis D, Liu J, Greenspon J, Hallenbeck JM (2002) TNF-alpha-induced tolerance to ischemic injury involves differential control of NF-kappaB transactivation: the role of NF-kappaB association with p300 adaptor. J Cereb Blood Flow Metab 22:142-152.

Girouard H, Iadecola C (2006) Neurovascular coupling in the normal brain and in hypertension, stroke, and Alzheimer disease. J Appl Physiol 100:328-335.

Giulian D, Li J, Li X, George J, Rutecki PA (1994) The impact of microglia-derived cytokines upon gliosis in the CNS. Dev Neurosci 16:128-136.

Glezer I, Simard AR, Rivest S (2007) Neuroprotective role of the innate immune system by microglia. Neuroscience 147:867-883.

Go KG (1997) The normal and pathological physiology of brain water. Adv. Tech. Stand. Neurosurg. 23:47-142.

Goldman JE, Abramson B (1990) Cyclic AMP-induced shape changes of astrocytes are accompanied by rapid depolymerization of actin. Brain Res 528:189-196.

Goldshmit Y, McLenachan S, Turnley A (2006) Roles of Eph receptors and ephrins in the normal and damaged adult CNS. Brain Res Brain Res Rev.

Goldshmit Y, Munro K, Leong SY, Pebay A, Turnley AM (2010) LPA receptor expression in the central nervous system in health and following injury. Cell Tissue Res 341:23-32.

Gomes FC, Paulin D, Moura Neto V (1999) Glial fibrillary acidic protein (GFAP): modulation by growth factors and its implication in astrocyte differentiation. Braz J Med Biol Res 32:619-631.

Gomes FC, Sousa Vde O, Romao L (2005) Emerging roles for TGF-beta1 in nervous system development. Int J Dev Neurosci 23:413-424.

Gomez-Nicola D, Valle-Argos B, Nieto-Sampedro M (2010) Blockade of IL-15 activity inhibits microglial activation through the NFkappaB, p38, and ERK1/2 pathways, reducing cytokine and chemokine release. Glia 58:264-276.

Gomez-Nicola D, Valle-Argos B, Pita-Thomas DW, Nieto-Sampedro M (2008) Interleukin 15 expression in the CNS: blockade of its activity prevents glial activation after an inflammatory injury. Glia 56:494-505.

Gomez TM, Spitzer NC (1999) In vivo regulation of axon extension and pathfinding by growth-cone calcium transients. Nature 397:350-355.

Gomez VM, Averill S, King V, Yang Q, Doncel Perez E, Chacon SC, Ward R, Nieto-Sampedro M, Priestley J, Taylor J (2003) Transplantation of olfactory ensheathing cells fails to promote

significant axonal regeneration from dorsal roots into the rat cervical cord. J Neurocytol 32:53-70.
Goncalves CA, Gottfried C, Kommers T, Rodnight R (1997) Calcium-modulated proteins change their immunoreactivity in the presence of Ca2+: a study of antibody recognition in a dot immunoassay for calmodulin, calcineurin (beta-subunit), and S100B. Anal Biochem 253:127-130.
Gonczi M, Telek A, Czifra G, Balogh A, Blumberg PM, Biro T, Csernoch L (2008) Altered calcium handling following the recombinant overexpression of protein kinase C isoforms in HaCaT cells. Exp Dermatol 17:584-591.
Gopalakrishna R, Gundimeda U, Chen ZH (1997) Cancer-preventive selenocompounds induce a specific redox modification of cysteine-rich regions in Ca(2+)-dependent isoenzymes of protein kinase C. Arch Biochem Biophys 348:25-36.
Gosselin D, Rivest S (2007) Role of IL-1 and TNF in the brain: twenty years of progress on a Dr. Jekyll/Mr. Hyde duality of the innate immune system. Brain Behav Immun 21:281-289.
Gottfried C, Cechin SR, Gonzalez MA, Vaccaro TS, Rodnight R (2003) The influence of the extracellular matrix on the morphology and intracellular pH of cultured astrocytes exposed to media lacking bicarbonate. Neuroscience 121:553-562.
Graef IA, Wang F, Charron F, Chen L, Neilson J, Tessier-Lavigne M, Crabtree GR (2003) Neurotrophins and netrins require calcineurin/NFAT signaling to stimulate outgrowth of embryonic axons. Cell 113:657-670.
Grassl GA, Kracht M, Wiedemann A, Hoffmann E, Aepfelbacher M, von Eichel-Streiber C, Bohn E, Autenrieth IB (2003) Activation of NF-kappaB and IL-8 by Yersinia enterocolitica invasin protein is conferred by engagement of Rac1 and MAP kinase cascades. Cell Microbiol 5:957-971.
Graziadei PP, Graziadei GA (1979) Neurogenesis and neuron regeneration in the olfactory system of mammals. I. Morphological aspects of differentiation and structural organization of the olfactory sensory neurons. J Neurocytol 8:1-18.
Gris P, Tighe A, Levin D, Sharma R, Brown A (2007) Transcriptional regulation of scar gene expression in primary astrocytes. Glia 55:1145-1155.
Groesdonk HV, Wagner F, Hoffarth B, Georgieff M, Senftleben U (2007) Enhancement of NF-kappaB activation in lymphocytes prevents T cell apoptosis and improves survival in murine sepsis. J Immunol 179:8083-8089.
Gross RE, Mei Q, Gutekunst CA, Torre E (2007) The pivotal role of RhoA GTPase in the molecular signaling of axon growth inhibition after CNS injury and targeted therapeutic strategies. Cell Transplant 16:245-262.
Grumet M, Edelman GM (1988) Neuron-glia cell adhesion molecule interacts with neurons and astroglia via different binding mechanisms. J Cell Biol 106:487-503.
Gu X, Spitzer NC (1997) Breaking the code: regulation of neuronal differentiation by spontaneous calcium transients. Dev Neurosci 19:33-41.
Guan J, Gluckman PD (2009) IGF-1 derived small neuropeptides and analogues: a novel strategy for the development of pharmaceuticals for neurological conditions. Br J Pharmacol 157:881-891.
Guan KL, Rao Y (2003) Signalling mechanisms mediating neuronal responses to guidance cues. Nat Rev Neurosci 4:941-956.
Gudino-Cabrera G, Nieto-Sampedro M (1999) Estrogen receptor immunoreactivity in Schwann-like brain macroglia. J Neurobiol 40:458-470.
Gudino-Cabrera G, Nieto-Sampedro M (2000) Schwann-like macroglia in adult rat brain. Glia 30:49-63.
Guerini D, Guidi F, Carafoli E (2002) Differential membrane targeting of the SERCA and PMCA calcium pumps: experiments with recombinant chimeras. FASEB J 16:519-528.
Guerout N, Derambure C, Drouot L, Bon-Mardion N, Duclos C, Boyer O, Marie JP (2010) Comparative gene expression profiling of olfactory ensheathing cells from olfactory bulb and olfactory mucosa. Glia 58:1570-1580.

Guillemin G, Boussin FD, Le Grand R, Croitoru J, Coffigny H, Dormont D (1996) Granulocyte macrophage colony stimulating factor stimulates in vitro proliferation of astrocytes derived from simian mature brains. Glia 16:71-80.
Gulbenkian S, Uddman R, Edvinsson L (2001) Neuronal messengers in the human cerebral circulation. Peptides 22:995-1007.
Gunnarson E, Zelenina M, Axehult G, Song Y, Bondar A, Krieger P, Brismar H, Zelenin S, Aperia A (2008) Identification of a molecular target for glutamate regulation of astrocyte water permeability. Glia 56:587-596.
Guntinas-Lichius O, Angelov DN, Tomov TL, Dramiga J, Neiss WF, Wewetzer K (2001) Transplantation of olfactory ensheathing cells stimulates the collateral sprouting from axotomized adult rat facial motoneurons. Exp Neurol 172:70-80.
Guo ZH, Li F, Wang WZ (2009) The mechanisms of brain ischemic insult and potential protective interventions. Neurosci Bull 25:139-152.
Guttridge DC, Albanese C, Reuther JY, Pestell RG, Baldwin AS, Jr. (1999) NF-kappaB controls cell growth and differentiation through transcriptional regulation of cyclin D1. Mol Cell Biol 19:5785-5799.
Gwag BJ, Canzoniero LM, Sensi SL, Demaro JA, Koh JY, Goldberg MP, Jacquin M, Choi DW (1999) Calcium ionophores can induce either apoptosis or necrosis in cultured cortical neurons. Neuroscience 90:1339-1348.
Haak LL, Heller HC, van den Pol AN (1997) Metabotropic glutamate receptor activation modulates kainate and serotonin calcium response in astrocytes. J Neurosci 17:1825-1837.
Hack MA, Saghatelyan A, de Chevigny A, Pfeifer A, Ashery-Padan R, Lledo PM, Gotz M (2005) Neuronal fate determinants of adult olfactory bulb neurogenesis. Nat Neurosci 8:865-872.
Hall A (1998) Rho GTPases and the actin cytoskeleton. Science 279:509-514.
Hall A (2005) Rho GTPases and the control of cell behaviour. Biochem Soc Trans 33:891-895.
Hall ED (1992) The neuroprotective pharmacology of methylprednisolone. J Neurosurg 76:13-22.
Hall ED, Vaishnav RA, Mustafa AG (2010) Antioxidant therapies for traumatic brain injury. Neurotherapeutics 7:51-61.
Han I-O, Hee-Sun K, Hyoung-Chun K, Eun-Hye J, Won-Ki K (2003) Synergistic expression of inducible nitric oxide synthase by phorbol ester and interferon-gamma is mediated through NF-kappaB and ERK in microglial cells. J Neurosci Res 73:659-669.
Hang CH, Chen G, Shi JX, Zhang X, Li JS (2006) Cortical expression of nuclear factor kappa B after human brain contusion. Brain Res 1109:14-21.
Hanisch U-K, Johnson TV, Kipnis J (2008) Toll-like receptors: roles in neuroprotection? Trends in Neurosciences 31:176-182.
Hanisch UK (2002) Microglia as a source and target of cytokines. Glia 40:140-155.
Hanisch UK, Kettenmann H (2007) Microglia: active sensor and versatile effector cells in the normal and pathologic brain. Nat Neurosci 10:1387-1394.
Hanson GR, Partlow LM, Iversen PL (1982) Neuronal stimulation of non-neuronal (glial) cell proliferation: lack of specificity between different regions of the nervous system. Brain Res 255:547-555.
Hansson E, Ronnback L (2004) Glial-neuronal signaling and astroglial swelling in physiology and pathology. Adv Exp Med Biol 559:313-323.
Hara H, Aizenman E (2004) A molecular technique for detecting the liberation of intracellular zinc in cultured neurons. J Neurosci Methods 137:175-180.
Harris JA, West AK, Chuah MI (2009) Olfactory ensheathing cells: Nitric oxide production and innate immunity. Glia:in press.
Harris JA, Ruitenberg, M.J., West, A.K., Chuah, M.I. (2008) Inducible production of nitric oxide by olfactory ensheathing cells in response to bacteria. Proc Aus Neurosci Soc 18:64.
Harting MT, Jimenez F, Adams SD, Mercer DW, Cox CS, Jr. (2008) Acute, regional inflammatory response after traumatic brain injury: Implications for cellular therapy. Surgery 144:803-813.
Harukuni I, Bhardwaj A (2006) Mechanisms of brain injury after global cerebral ischemia. Neurol Clin 24:1-21.

Hashimoto K, Hayashi Y, Inuzuka T, Hozumi I (2009) Exercise induces metallothioneins in mouse spinal cord. Neuroscience epub DOI: S0306-4522(09)00981-6 [pii]

Hashioka S, Han Y-H, Fujii S, Kato T, Monji A, Utsumi H, Sawada M, Nakanishi H, Kanba S (2007) Phospholipids modulate superoxide and nitric oxide production by lipopolysaccharide and phorbol 12-myristate-13-acetate-activated microglia. Neurochemistry International 50:499-506.

Hawkins ED, Hommel M, Turner ML, Battye FL, Markham JF, Hodgkin PD (2007) Measuring lymphocyte proliferation, survival and differentiation using CFSE time-series data. Nat Protoc 2:2057-2067.

Hayashi M, Dorf ME, Abromson-Leeman S (1993) Granulocyte-macrophage colony stimulating factor inhibits class II major histocompatibility complex expression and antigen presentation by microglia. J Neuroimmunol 48:23-32.

Hayat S, Wigley CB, Robbins J (2003) Intracellular calcium handling in rat olfactory ensheathing cells and its role in axonal regeneration. Mol Cell Neurosci 22:259-270.

Hayden MS, Ghosh S (2004) Signaling to NF-κB. Genes and Dev 18:2195-2224.

Haynes SE, Hollopeter G, Yang G, Kurpius D, Dailey ME, Gan WB, Julius D (2006) The P2Y12 receptor regulates microglial activation by extracellular nucleotides. Nat Neurosci 9:1512-1519.

He F, Ge W, Martinowich K, Becker-Catania S, Coskun V, Zhu W, Wu H, Castro D, Guillemot F, Fan G, de Vellis J, Sun YE (2005) A positive autoregulatory loop of Jak-STAT signaling controls the onset of astrogliogenesis. Nat Neurosci 8:616-625.

Held-Feindt J, Hattermann K, Muerkoster SS, Wedderkopp H, Knerlich-Lukoschus F, Ungefroren H, Mehdorn HM, Mentlein R (2010) CX3CR1 promotes recruitment of human glioma-infiltrating microglia/macrophages (GIMs). Exp. Cell Res. 316:1553-1566.

Hellmich HL, Frederickson CJ, DeWitt DS, Saban R, Parsley MO, Stephenson R, Velasco M, Uchida T, Shimamura M, Prough DS (2004) Protective effects of zinc chelation in traumatic brain injury correlate with upregulation of neuroprotective genes in rat brain. Neurosci Lett 355:221-225.

Hendricks KR, Kott JN, Lee ME, Gooden MD, Evers SM, Westrum LE (1994) Recovery of olfactory behavior. I. Recovery after a complete olfactory bulb lesion correlates with patterns of olfactory nerve penetration. Brain Res 648:121-133.

Henze C, Hartmann A, Lescot T, Hirsch EC, Michel PP (2005) Proliferation of microglial cells induced by 1-methyl-4-phenylpyridinium in mesencephalic cultures results from an astrocyte-dependent mechanism: role of granulocyte macrophage colony-stimulating factor. J Neurochem 95:1069-1077.

Hermanns S, Klapka N, Gasis M, Muller HW (2006) The collagenous wound healing scar in the injured central nervous system inhibits axonal regeneration. Adv Exp Med Biol 557:177-190.

Hernandez MR, Agapova OA, Yang P, Salvador-Silva M, Ricard CS, Aoi S (2002) Differential gene expression in astrocytes from human normal and glaucomatous optic nerve head analyzed by cDNA microarray. Glia 38:45-64.

Hertel M, Tretter Y, Alzheimer C, Werner S (2000) Connective tissue growth factor: a novel player in tissue reorganization after brain injury? Eur J Neurosci 12:376-380.

Hertlein E, Wang J, Ladner KJ, Bakkar N, Guttridge DC (2005) RelA/p65 regulation of IkappaBbeta. Mol. Cell. Biol. 25:4956-4968.

Hidalgo J, Gasull T, Giralt M, Armario A (1994) Brain metallothionein in stress. Biol Signals 3:198-210.

Hill CE, Hurtado A, Blits B, Bahr BA, Wood PM, Bartlett Bunge M, Oudega M (2007) Early necrosis and apoptosis of Schwann cells transplanted into the injured rat spinal cord. Eur J Neurosci 26:1433-1445.

Hirsch S, Cahill MA, Stuermer CA (1995) Fibroblasts at the transection site of the injured goldfish optic nerve and their potential role during retinal axonal regeneration. J Comp Neurol 360:599-611.

Hoffman RA, Mahidhara RS, Wolf-Johnston AS, Lu L, Thomson AW, Simmons RL (2002) Differential modulation of CD4 and CD8 T-cell proliferation by induction of nitric oxide synthesis in antigen presenting cells. Transplantation 74:836-845.

Holloway AF, Rao S, Chen X, Shannon MF (2003) Changes in chromatin accessibility across the GM-CSF promoter upon T cell activation are dependent on nuclear factor kappaB proteins. J Exp Med 197:413-423.

Holtje M, Hoffmann A, Hofmann F, Mucke C, Grosse G, Van Rooijen N, Kettenmann H, Just I, Ahnert-Hilger G (2005) Role of Rho GTPase in astrocyte morphology and migratory response during in vitro wound healing. J Neurochem 95:1237-1248.

Horner PJ, Gage FH (2000) Regenerating the damaged central nervous system. Nature 407:963-970.

Hou YJ, Yu AC, Garcia JM, Aotaki-Keen A, Lee YL, Eng LF, Hjelmeland LJ, Menon VK (1995) Astrogliosis in culture. IV. Effects of basic fibroblast growth factor. J Neurosci Res 40:359-370.

Hsu P, Yu F, Feron F, Pickles JO, Sneesby K, Mackay-Sim A (2001) Basic fibroblast growth factor and fibroblast growth factor receptors in adult olfactory epithelium. Brain Res 896:188-197.

Hua R, Doucette R, Walz W (2008) Doublecortin-expressing cells in the ischemic penumbra of a small-vessel stroke. J Neurosci Res 86:883-893.

Huang E, Ong WY (2005) Distribution of ferritin in the rat hippocampus after kainate-induced neuronal injury. Exp Brain Res 161:502-511.

Huang KP, Huang FL, Nakabayashi H, Yoshida Y (1989) Roles of protein kinase C isozymes in cellular regulation. Adv Exp Med Biol 255:21-28.

Huang WC, Chen JJ, Inoue H, Chen CC (2003) Tyrosine phosphorylation of I-kappa B kinase alpha/beta by protein kinase C-dependent c-Src activation is involved in TNF-alpha-induced cyclooxygenase-2 expression. J Immunol 170:4767-4775.

Hughes PM, Botham MS, Frentzel S, Mir A, Perry VH (2002) Expression of fractalkine (CX3CL1) and its receptor, CX3CR1, during acute and chronic inflammation in the rodent CNS. Glia 37:314-327.

Hull M, Muksch B, Akundi RS, Waschbisch A, Hoozemans JJ, Veerhuis R, Fiebich BL (2006) Amyloid beta peptide (25-35) activates protein kinase C leading to cyclooxygenase-2 induction and prostaglandin E(2) release in primary midbrain astrocytes. Neurochem Int 48:663-672.

Hung AC, Chu YJ, Lin YH, Weng JY, Chen HB, Au YC, Sun SH (2005) Roles of protein kinase C in regulation of P2X7 receptor-mediated calcium signalling of cultured type-2 astrocyte cell line, RBA-2. Cell Signal 17:1384-1396.

Iadecola C, Nedergaard M (2007) Glial regulation of the cerebral microvasculature. Nat Neurosci 10:1369-1376.

Ibanez C, Ito D, Zawadzka M, Jeffery ND, Franklin RJ (2007) Calponin is expressed by fibroblasts and meningeal cells but not olfactory ensheathing cells in the adult peripheral olfactory system. Glia 55:144-151.

Iles KE, Forman HJ (2002) Macrophage signaling and respiratory burst. Immunol Res 26:95-105.

Imaizumi T, Lankford KL, Kocsis JD (2000a) Transplantation of olfactory ensheathing cells or Schwann cells restores rapid and secure conduction across the transected spinal cord. Brain Res 854:70-78.

Imaizumi T, Lankford KL, Kocsis JD, Sasaki M, Akiyama Y, Hashi K (2000b) [Comparison of myelin-forming cells as candidates for therapeutic transplantation in demyelinated CNS axons]. No To Shinkei 52:609-615.

Ishida H, Takemori K, Dote K, Ito H (2006) Expression of glucose transporter-1 and aquaporin-4 in the cerebral cortex of stroke-prone spontaneously hypertensive rats in relation to the blood-brain barrier function. Am J Hypertens 19:33-39.

Ishii G, Ito TK, Aoyagi K, Fujimoto H, Chiba H, Hasebe T, Fujii S, Nagai K, Sasaki H, Ochiai A (2007) Presence of human circulating progenitor cells for cancer stromal fibroblasts in the blood of lung cancer patients. Stem Cells 25:1469-1477.

Ito D, Imai Y, Ohsawa K, Nakajima K, Fukuuchi Y, Kohsaka S (1998) Microglia-specific localisation of a novel calcium binding protein, Iba1. Brain Res Mol Brain Res 57:1-9.

Ito D, Ibanez C, Ogawa H, Franklin RJ, Jeffery ND (2006a) Comparison of cell populations derived from canine olfactory bulb and olfactory mucosal cultures. Am J Vet Res 67:1050-1056.

Ito H, Yamamoto N, Arima H, Hirate H, Morishima T, Umenishi F, Tada T, Asai K, Katsuya H, Sobue K (2006b) Interleukin-1beta induces the expression of aquaporin-4 through a nuclear factor-kappaB pathway in rat astrocytes. J Neurochem 99:107-118.

Ito U, Kawakami E, Nagasao J, Kuroiwa T, Nakano I, Oyanagi K (2006c) Restitution of ischemic injuries in penumbra of cerebral cortex after temporary ischemia. Acta Neurochir Suppl 96:239-243.

Itoh K (2002) Culture of oligodendrocyte precursor cells (NG2(+)/O1(-)) and oligodendrocytes (NG2(-)/O1(+)) from embryonic rat cerebrum. Brain Res Brain Res Protoc 10:23-30.

Jacques-Silva MC, Rodnight R, Lenz G, Liao Z, Kong Q, Tran M, Kang Y, Gonzalez FA, Weisman GA, Neary JT (2004) P2X7 receptors stimulate AKT phosphorylation in astrocytes. Br J Pharmacol 141:1106-1117.

Jaeger CB, Blight AR (1997) Spinal cord compression injury in guinea pigs: structural changes of endothelium and its perivascular cell associations after blood-brain barrier breakdown and repair. Exp Neurol 144:381-399.

Jaken S (1990) Protein kinase C and tumor promoters. Curr Opin Cell Biol 2:192-197.

James G, Olson E (1992) Deletion of the regulatory domain of protein kinase C alpha exposes regions in the hinge and catalytic domains that mediate nuclear targeting. J Cell Biol 116:863-874.

Jani HR, Raisman G (2004) Ensheathing cell cultures from the olfactory bulb and mucosa. Glia 47:130-137.

Janssens S, Beyaert R (2003) Role of Toll-like receptors in pathogen recognition. Clin Microbiol Rev 16:637-646.

Jatana M, Giri S, Ansari MA, Elango C, Singh AK, Singh I, Khan M (2006) Inhibition of NF-kappaB activation by 5-lipoxygenase inhibitors protects brain against injury in a rat model of focal cerebral ischemia. J Neuroinflammation 3:12.

Jehan F, Neveu I, Naveilhan P, Wion D, Brachet P (1995) Interactions between second messenger pathways influence NGF synthesis in mouse primary astrocytes. Brain Res 672:128-136.

Jemmerson R, Dubinsky JM, Brustovetsky N (2005) Cytochrome C release from CNS mitochondria and potential for clinical intervention in apoptosis-mediated CNS diseases. Antioxid Redox Signal 7:1158-1172.

Jia-Yi W, Li- Li W, Ya-Ni H, Yen-Tsun C, Min-Chi K (2006) Dual Effects of Antioxidants in Neurodegeneration: Direct Neuroprotection against Oxidative Stress and Indirect Protection via Suppression of Gliamediated Inflammation. Current Pharmaceutical Design 12:3521.

Jiang H, Tian S, Zeng Y, Shi J (2008) Nerve growth factor inhibits Gd(3+)-sensitive calcium influx and reduces chemical anoxic neuronal death. J Huazhong Univ Sci Technolog Med Sci 28:379-382.

Johansen C, Flindt E, Kragballe K, Henningsen J, Westergaard M, Kristiansen K, Iversen L (2005) Inverse regulation of the nuclear factor-kappaB binding to the p53 and interleukin-8 kappaB response elements in lesional psoriatic skin. J Invest Dermatol 124:1284-1292.

Johansson S, Lee IH, Olson L, Spenger C (2005) Olfactory ensheathing glial co-grafts improve functional recovery in rats with 6-OHDA lesions. Brain 128:2961-2976.

John GR, Lee SC, Song X, Rivieccio M, Brosnan CF (2005) IL-1-regulated responses in astrocytes: relevance to injury and recovery. Glia 49:161-176.

John GR, Chen L, Rivieccio MA, Melendez-Vasquez CV, Hartley A, Brosnan CF (2004) Interleukin-1beta induces a reactive astroglial phenotype via deactivation of the Rho GTPase-Rock axis. J Neurosci 24:2837-2845.

Johnston MV (2005) Excitotoxicity in perinatal brain injury. Brain Pathol 15:234-240.

Jones TB, McDaniel EE, Popovich PG (2005) Inflammatory-mediated injury and repair in the traumatically injured spinal cord. Curr Pharm Des 11:1223-1236.

Jung KH, Chu K, Lee ST, Kim SJ, Sinn DI, Kim SU, Kim M, Roh JK (2006) Granulocyte colony-stimulating factor stimulates neurogenesis via vascular endothelial growth factor with STAT activation. Brain Res 1073-1074:190-201.
Justicia C, Gabriel C, Planas AM (2000) Activation of the JAK/STAT pathway following transient focal cerebral ischemia: signaling through Jak1 and Stat3 in astrocytes. Glia 30:253-270.
Kafitz KW, Greer CA (1999) Olfactory ensheathing cells promote neurite extension from embryonic olfactory receptor cells in vitro. Glia 25:99-110.
Kalaria RN, Cohen DL, Premkumar DR, Nag S, LaManna JC, Lust WD (1998) Vascular endothelial growth factor in Alzheimer's disease and experimental cerebral ischemia. Brain Res Mol Brain Res 62:101-105.
Kaltschmidt B, Baeuerle PA, Kaltschmidt C (1993) Potential involvement of the transcription factor NF-kappa B in neurological disorders. Mol Aspects Med 14:171-190.
Kaltschmidt C, Kaltschmidt B, Neumann H, Wekerle H, Baeuerle PA (1994) Constitutive NF-kappa B activity in neurons. Mol Cell Biol 14:3981-3992.
Kannurpatti SS, Joshi PG, Joshi NB (2000) Calcium sequestering ability of mitochondria modulates influx of calcium through glutamate receptor channel. Neurochem Res 25:1527-1536.
Katakai K, Liu J, Nakajima K, Keefer LK, Waalkes MP (2001) Nitric oxide induces metallothionein (MT) gene expression apparently by displacing zinc bound to MT. Toxicol Lett 119:103-108.
Kataoka A, Tozaki-Saitoh H, Koga Y, Tsuda M, Inoue K (2009) Activation of P2X7 receptors induces CCL3 production in microglial cells through transcription factor NFAT. J Neurochem 108:115-125.
Kato T, Honmou O, Uede T, Hashi K, Kocsis JD (2000) Transplantation of human olfactory ensheathing cells elicits remyelination of demyelinated rat spinal cord. Glia 30:209-218.
Kauppinen TM, Higashi Y, Suh SW, Escartin C, Nagasawa K, Swanson RA (2008) Zinc triggers microglial activation. J Neurosci 28:5827-5835.
Kaushal V, Schlichter LC (2008) Mechanisms of microglia-mediated neurotoxicity in a new model of the stroke penumbra. J Neurosci 28:2221-2230.
Kawaja MD, Boyd JG, Smithson LJ, Jahed A, Doucette R (2009) Technical strategies to isolate olfactory ensheathing cells for intraspinal implantation. J Neurotrauma 26:155-177.
Kaya N, Tanaka S, Koike T (2002) ATP selectively suppresses the synthesis of the inflammatory protein microglial response factor (MRF)-1 through Ca(2+) influx via P2X(7) receptors in cultured microglia. Brain Res 952:86-97.
Kaya SS, Mahmood A, Li Y, Yavuz E, Goksel M, Chopp M (1999) Apoptosis and expression of p53 response proteins and cyclin D1 after cortical impact in rat brain. Brain Res 818:23-33.
Kermorgant S, Zicha D, Parker PJ (2003) Protein kinase C controls microtubule-based traffic but not proteasomal degradation of c-Met. J Biol Chem 278:28921-28929.
Kernie SG, Erwin TM, Parada LF (2001) Brain remodeling due to neuronal and astrocytic proliferation after controlled cortical injury in mice. J Neurosci Res 66:317-326.
Kettritz R, Choi M, Rolle S, Wellner M, Luft FC (2004) Integrins and cytokines activate nuclear transcription factor-kappaB in human neutrophils. J Biol Chem 279:2657-2665.
Keyvan-Fouladi N, Raisman G, Li Y (2003) Functional repair of the corticospinal tract by delayed transplantation of olfactory ensheathing cells in adult rats. J Neurosci 23:9428-9434.
Kheifets V, Bright R, Inagaki K, Schechtman D, Mochly-Rosen D (2006) Protein kinase C delta (deltaPKC)-annexin V interaction: a required step in deltaPKC translocation and function. J Biol Chem 281:23218-23226.
Khorooshi R, Babcock AA, Owens T (2008) NF-kappaB-driven STAT2 and CCL2 expression in astrocytes in response to brain injury. J Immunol 181:7284-7291.
Kida S, Steart PV, Zhang ET, Weller RO (1993) Perivascular cells act as scavengers in the cerebral perivascular spaces and remain distinct from pericytes, microglia and macrophages. Acta Neuropathol 85:646-652.
Kigerl KA, Gensel JC, Ankeny DP, Alexander JK, Donnelly DJ, Popovich PG (2009) Identification of two distinct macrophage subsets with divergent effects causing either neurotoxicity or regeneration in the injured mouse spinal cord. J Neurosci 29:13435-13444.

Kikuchi Y, Irie M, Kasahara T, Sawada J, Terao T (1993) Induction of metallothionein in a human astrocytoma cell line by interleukin-1 and heavy metals. FEBS Lett 317:22-26.
Kim JV, Dustin ML (2006) Innate response to focal necrotic injury inside the blood-brain barrier. J Immunol 177:5269-5277.
Kim SU, de Vellis J (2005) Microglia in health and disease. J Neurosci Res 81:302-313.
Kim WT, Rioult MG, Cornell-Bell AH (1994) Glutamate-induced calcium signaling in astrocytes. Glia 11:173-184.
Kim YJ, Hwang SY, Oh ES, Oh S, Han IO (2006) IL-1beta, an immediate early protein secreted by activated microglia, induces iNOS/NO in C6 astrocytoma cells through p38 MAPK and NF-kappaB pathways. J Neurosci Res 84:1037-1046.
Kimelberg HK (2005) Astrocytic swelling in cerebral ischemia as a possible cause of injury and target for therapy. Glia 50:389-397.
King CE, Canty AJ, Vickers JC (2001) Alterations in neurofilaments associated with reactive brain changes and axonal sprouting following acute physical injury to the rat neocortex. Neuropathol Appl Neurobiol 27:115-126.
King CE, Jacobs I, Dickson TC, Vickers JC (1997) Physical damage to rat cortical axons mimics early Alzheimer's neuronal pathology. Neuroreport 8:1663-1665.
King CE, Dickson TC, Jacobs I, McCormack GH, Riederer BM, Vickers JC (2000) Acute CNS axonal injury models a subtype of dystrophic neurite in Alzheimer's disease. Alzheimer's Reports 3:31-40.
Kintner DB, Luo J, Gerdts J, Ballard AJ, Shull GE, Sun D (2007) Role of Na+-K+-Cl- cotransport and Na+/Ca2+ exchange in mitochondrial dysfunction in astrocytes following in vitro ischemia. Am J Physiol Cell Physiol 292:C1113-1122.
Kipp M, Beyer C (2009) Impact of sex steroids on neuroinflammatory processes and experimental multiple sclerosis. Front Neuroendocrinol 30:188-200.
Klassen RB, Crenshaw K, Kozyraki R, Verroust PJ, Tio L, Atrian S, Allen PL, Hammond TG (2004) Megalin mediates renal uptake of heavy metal metallothionein complexes. Am J Physiol Renal Physiol 287:F393-403.
Kloss CU, Kreutzberg GW, Raivich G (1997) Proliferation of ramified microglia on an astrocyte monolayer: characterization of stimulatory and inhibitory cytokines. J Neurosci Res 49:248-254.
Kobayashi M, Kidd D, Hutson E, Grafton J, McNulty S, Rumsby M (2001) Protein kinase C activation by 12-0-tetradecanoylphorbol 13-acetate in CG-4 line oligodendrocytes stimulates turnover of choline and ethanolamine phospholipids by phospholipase D and induces rapid process contraction. J Neurochem 76:361-371.
Koguchi K, Nakatsuji Y, Okuno T, Sawada M, Sakoda S (2003) Microglial cell cycle-associated proteins control microglial proliferation in vivo and in vitro and are regulated by GM-CSF and density-dependent inhibition. J Neurosci Res 74:898-905.
Koh PO, Kang BI, Kim GS, Oh YS, Won CK (2005) The effect of thrombin on astrocyte stellation with regional specificity. J Vet Med Sci 67:1047-1050.
Kolber MA, Haynes DH (1981) Fluorescence study of the divalent cation-transport mechanism of ionophore A23187 in phospholipid membranes. Biophys J 36:369-391.
Kommers T, Rodnight R, Boeck C, Vendite D, Oliveira D, Horn J, Oppelt D, Wofchuk S (2002) Phosphorylation of glial fibrillary acidic protein is stimulated by glutamate via NMDA receptors in cortical microslices and in mixed neuronal/glial cell cultures prepared from the cerebellum. Brain Res Dev Brain Res 137:139-148.
Konat GW, Kielian T, Marriott I (2006) The role of Toll-like receptors in CNS response to microbial challenge. J Neurochem 99:1-12.
Kooijman R, Sarre S, Michotte Y, De Keyser J (2009) Insulin-like growth factor I: a potential neuroprotective compound for the treatment of acute ischemic stroke? Stroke 40:e83-88.
Korzus E, Nagase H, Rydell R, Travis J (1997) The mitogen-activated protein kinase and JAK-STAT signaling pathways are required for an oncostatin M-responsive element-mediated activation of matrix metalloproteinase 1 gene expression. J Biol Chem 272:1188-1196.

Koyama Y, Ishibashi T, Hayata K, Baba A (1993) Endothelins modulate dibutyryl cAMP-induced stellation of cultured astrocytes. Brain Res 600:81-88.
Kracht M, Saklatvala J (2002) Transcriptional and post-transcriptional control of gene expression in inflammation. Cytokine 20:91-106.
Kresse W, Sekler I, Hoffmann A, Peters O, Nolte C, Moran A, Kettenmann H (2005) Zinc ions are endogenous modulators of neurotransmitter-stimulated capacitative Ca2+ entry in both cultured and in situ mouse astrocytes. Eur J Neurosci 21:1626-1634.
Kretz A, Happold CJ, Marticke JK, Isenmann S (2005) Erythropoietin promotes regeneration of adult CNS neurons via Jak2/Stat3 and PI3K/AKT pathway activation. Mol Cell Neurosci 29:569-579.
Krohn K, Rozovsky I, Wals P, Teter B, Anderson CP, Finch CE (1999) Glial fibrillary acidic protein transcription responses to transforming growth factor-beta 1 and interleukin-1 beta are mediated by a nuclear factor-1-like site in the near-upstream promoter. Journal of Neurochemistry 72:1353-1361.
Kronvall E, Sayer FT, Nilsson OG (2005) [Methylprednisolone in the treatment of acute spinal cord injury has become more and more questioned]. Lakartidningen 102:1887-1888, 1890.
Kruczek C, Gorg B, Keitel V, Pirev E, Kroncke KD, Schliess F, Haussinger D (2009) Hypoosmotic swelling affects zinc homeostasis in cultured rat astrocytes. Glia 57:79-92.
Krudewig C, Deschl U, Wewetzer K (2006) Purification and in vitro characterization of adult canine olfactory ensheathing cells. Cell Tissue Res. 326:687-696.
Kuhn TB, Meberg PJ, Brown MD, Bernstein BW, Minamide LS, Jensen JR, Okada K, Soda EA, Bamburg JR (2000) Regulating actin dynamics in neuronal growth cones by ADF/cofilin and rho family GTPases. J Neurobiol 44:126-144.
Kumar R, Hayat S, Felts P, Bunting S, Wigley C (2005) Functional differences and interactions between phenotypic subpopulations of olfactory ensheathing cells in promoting CNS axonal regeneration. Glia 50:12-20.
Kumari MV, Hiramatsu M, Ebadi M (2000) Free radical scavenging actions of hippocampal metallothionein isoforms and of antimetallothioneins: an electron spin resonance spectroscopic study. Cell Mol Biol (Noisy-le-grand) 46:627-636.
Kuno R, Yoshida Y, Nitta A, Nabeshima T, Wang J, Sonobe Y, Kawanokuchi J, Takeuchi H, Mizuno T, Suzumura A (2006) The role of TNF-alpha and its receptors in the production of NGF and GDNF by astrocytes. Brain Res 1116:12-18.
Kunz A, Abe T, Hochrainer K, Shimamura M, Anrather J, Racchumi G, Zhou P, Iadecola C (2008) Nuclear factor-kappaB activation and postischemic inflammation are suppressed in CD36-null mice after middle cerebral artery occlusion. J Neurosci 28:1649-1658.
Kurpius D, Nolley EP, Dailey ME (2007) Purines induce directed migration and rapid homing of microglia to injured pyramidal neurons in developing hippocampus. Glia 55:873-884.
Kwon I, Kim EH, del Zoppo GJ, Heo JH (2009) Ultrastructural and temporal changes of the microvascular basement membrane and astrocyte interface following focal cerebral ischemia. J Neurosci Res 87:668-676.
Kyriakis JM, Avruch J (2001) Mammalian mitogen-activated protein kinase signal transduction pathways activated by stress and inflammation. Physiol Rev 81:807-869.
Laabs T, Carulli D, Geller HM, Fawcett JW (2005) Chondroitin sulfate proteoglycans in neural development and regeneration. Curr Opin Neurobiol 15:116-120.
Ladiwala U, Lachance C, Simoneau SJ, Bhakar A, Barker PA, Antel JP (1998) p75 neurotrophin receptor expression on adult human oligodendrocytes: signaling without cell death in response to NGF. J Neurosci 18:1297-1304.
Lagord C, Berry M, Logan A (2002) Expression of TGFbeta2 but not TGFbeta1 correlates with the deposition of scar tissue in the lesioned spinal cord. Mol Cell Neurosci 20:69-92.
Lai AY, Todd KG (2006) Microglia in cerebral ischemia: molecular actions and interactions. Can J Physiol Pharmacol 84:49-59.
Lai AY, Todd KG (2008) Differential regulation of trophic and proinflammatory microglial effectors is dependent on severity of neuronal injury. Glia 56:259-270.

Lai WW, Yang JS, Lai KC, Kuo CL, Hsu CK, Wang CK, Chang CY, Lin JJ, Tang NY, Chen PY, Huang WW, Chung JG (2009) Rhein induced apoptosis through the endoplasmic reticulum stress, caspase- and mitochondria-dependent pathways in SCC-4 human tongue squamous cancer cells. In Vivo 23:309-316.

Laird MD, Vender JR, Dhandapani KM (2008) Opposing roles for reactive astrocytes following traumatic brain injury. Neurosignals 16:154-164.

Lakatos A, Franklin RJ, Barnett SC (2000) Olfactory ensheathing cells and Schwann cells differ in their in vitro interactions with astrocytes. Glia 32:214-225.

Lakatos A, Barnett SC, Franklin RJ (2003a) Olfactory ensheathing cells induce less host astrocyte response and chondroitin sulphate proteoglycan expression than Schwann cells following transplantation into adult CNS white matter. Exp Neurol 184:237-246.

Lakatos A, Smith PM, Barnett SC, Franklin RJ (2003b) Meningeal cells enhance limited CNS remyelination by transplanted olfactory ensheathing cells. Brain 126:598-609.

Lambertsen KL, Clausen BH, Babcock AA, Gregersen R, Fenger C, Nielsen HH, Haugaard LS, Wirenfeldt M, Nielsen M, Dagnaes-Hansen F, Bluethmann H, Faergeman NJ, Meldgaard M, Deierborg T, Finsen B (2009) Microglia protect neurons against ischemia by synthesis of tumor necrosis factor. J Neurosci 29:1319-1330.

Lampe PA, Cornbrooks EB, Juhasz A, Johnson EM, Jr., Franklin JL (1995) Suppression of programmed neuronal death by a thapsigargin-induced Ca2+ influx. J Neurobiol 26:205-212.

Lau CL, Beart PM, O'Shea RD (2010) Transportable and Non-transportable Inhibitors of L: -glutamate Uptake Produce Astrocytic Stellation and Increase EAAT2 Cell Surface Expression. Neurochem Res.

Lauro C, Cipriani R, Catalano M, Trettel F, Chece G, Brusadin V, Antonilli L, van Rooijen N, Eusebi F, Fredholm BB, Limatola C (2010) Adenosine A1 receptors and microglial cells mediate CX3CL1-induced protection of hippocampal neurons against Glu-induced death. Neuropsychopharmacology 35:1550-1559.

Le R, Esquenazi S (2002) Astrocytes mediate cerebral cortical neuronal axon and dendrite growth, in part, by release of fibroblast growth factor. Neurol Res 24:81-92.

Leaver SG, Harvey AR, Plant GW (2006) Adult olfactory ensheathing glia promote the long-distance growth of adult retinal ganglion cell neurites in vitro. Glia 53:467-476.

Lee A, Rayfield A, Hryciw DH, Ma TA, Wang D, Pow D, Broer S, Yun C, Poronnik P (2007) Na+-H+ exchanger regulatory factor 1 is a PDZ scaffold for the astroglial glutamate transporter GLAST. Glia 55:119-129.

Lee HC, Cho DY, Lee WY, Chuang HC (2007) Pitfalls in treatment of acute cervical spinal cord injury using high-dose methylprednisolone: a retrospect audit of 111 patients. Surg Neurol 68 Suppl 1:S37-41; discussion S41-32.

Lee SC, Dickson DW, Brosnan CF (1995) Interleukin-1, nitric oxide and reactive astrocytes. Brain Behav Immun 9:345-354.

Lee SJ, Lee S (2002) Toll-like receptors and inflammation in the CNS. Curr Drug Targets Inflamm Allergy 1:181-191.

Lee YB, Du S, Rhim H, Lee EB, Markelonis GJ, Oh TH (2000) Rapid increase in immunoreactivity to GFAP in astrocytes in vitro induced by acidic pH is mediated by calcium influx and calpain I. Brain Res 864:220-229.

Lehnardt S, Schott E, Trimbuch T, Laubisch D, Krueger C, Wulczyn G, Nitsch R, Weber JR (2008) A vicious cycle involving release of heat shock protein 60 from injured cells and activation of toll-like receptor 4 mediates neurodegeneration in the CNS. J Neurosci 28:2320-2331.

Lehotsky J, Burda J, Danielisova V, Gottlieb M, Kaplan P, Saniova B (2009) Ischemic tolerance: the mechanisms of neuroprotective strategy. Anat Rec (Hoboken) 292:2002-2012.

Lemons ML, Howland DR, Anderson DK (1999) Chondroitin sulfate proteoglycan immunoreactivity increases following spinal cord injury and transplantation. Exp Neurol 160:51-65.

Lenzlinger PM, Morganti-Kossmann MC, Laurer HL, McIntosh TK (2001) The duality of the inflammatory response to traumatic brain injury. Mol Neurobiol 24:169-181.

Leon R, Wu H, Jin Y, Wei J, Buddhala C, Prentice H, Wu JY (2009) Protective function of taurine in glutamate-induced apoptosis in cultured neurons. J Neurosci Res 87:1185-1194.
Leung CT, Coulombe PA, Reed RR (2007) Contribution of olfactory neural stem cells to tissue maintenance and regeneration. Nat Neurosci 10:720-726.
Leung JY, Chapman JA, Harris JA, Hale D, Chung RS, West AK, Chuah MI (2008) Olfactory ensheathing cells are attracted to, and can endocytose, bacteria. Cell Mol Life Sci 65:2732-2739.
Leung YK, Pankhurst M, Dunlop SA, Ray S, Dittmann J, Eaton ED, Palumaa P, Sillard R, Chuah MI, West AK, Chung RS (2010) Metallothionein induces a regenerative reactive astrocyte phenotype via JAK/STAT and RhoA signalling pathways. Exp Neurol 221:98-106.
Li G, Lucas JJ, Gelfand EW (2005a) Protein kinase C alpha, betaI, and betaII isozymes regulate cytokine production in mast cells through MEKK2/ERK5-dependent and -independent pathways. Cell Immunol 238:10-18.
Li J, Zheng R, Wang Z (2001) Mechanisms of the induction of apoptosis in human hepatoma cells by tumour necrosis factor-alpha. Cell Biol Int 25:1213-1219.
Li L et al. (2008a) Protective role of reactive astrocytes in brain ischemia. J Cereb Blood Flow Metab 28:468-481.
Li Y, Raisman G (1995) Sprouts from cut corticospinal axons persist in the presence of astrocytic scarring in long-term lesions of the adult rat spinal cord. Exp Neurol 134:102-111.
Li Y, Field PM, Raisman G (1997) Repair of adult rat corticospinal tract by transplants of olfactory ensheathing cells. Science 277:2000-2002.
Li Y, Field PM, Raisman G (1998) Regeneration of adult rat corticospinal axons induced by transplanted olfactory ensheathing cells. J Neurosci 18:10514-10524.
Li Y, Decherchi P, Raisman G (2003) Transplantation of olfactory ensheathing cells into spinal cord lesions restores breathing and climbing. J Neurosci 23:727-731.
Li Y, Field PM, Raisman G (2005) Olfactory ensheathing cells and olfactory nerve fibroblasts maintain continuous open channels for regrowth of olfactory nerve fibres. Glia 52:245-251.
Li Y, Chopp M, Jiang N, Zaloga C (1995) In situ detection of DNA fragmentation after focal cerebral ischemia in mice. Brain Res Mol Brain Res 28:164-168.
Li Y, Carlstedt T, Berthold CH, Raisman G (2004) Interaction of transplanted olfactory-ensheathing cells and host astrocytic processes provides a bridge for axons to regenerate across the dorsal root entry zone. Exp Neurol 188:300-308.
Li Y, Ogle ME, Wallace GCt, Lu ZY, Yu SP, Wei L (2008) Erythropoietin attenuates intracerebral hemorrhage by diminishing matrix metalloproteinases and maintaining blood-brain barrier integrity in mice. Acta Neurochir Suppl 105:105-112.
Lie DC, Song H, Colamarino SA, Ming GL, Gage FH (2004) Neurogenesis in the adult brain: new strategies for central nervous system diseases. Annu Rev Pharmacol Toxicol 44:399-421.
Lin CH, Thompson CA, Forscher P (1994) Cytoskeletal reorganization underlying growth cone motility. Curr Opin Neurobiol 4:640-647.
Lin CH, Cheng FC, Lu YZ, Chu LF, Wang CH, Hsueh CM (2006) Protection of ischemic brain cells is dependent on astrocyte-derived growth factors and their receptors. Exp Neurol.
Lipson AC, Widenfalk J, Lindqvist E, Ebendal T, Olson L (2003) Neurotrophic properties of olfactory ensheathing glia. Exp Neurol 180:167-171.
Lipton SA (2001) Physiology. Nitric oxide and respiration. Nature 413:118-119, 121.
Liu G, Rao Y (2003) Neuronal migration from the forebrain to the olfactory bulb requires a new attractant persistent in the olfactory bulb. J Neurosci 23:6651-6659.
Liu JS, John GR, Sikora A, Lee SC, Brosnan CF (2000) Modulation of interleukin-1beta and tumor necrosis factor alpha signaling by P2 purinergic receptors in human fetal astrocytes. J Neurosci 20:5292-5299.
Liu T, Clark RK, McDonnell PC, Young PR, White RF, Barone FC, Feuerstein GZ (1994) Tumor necrosis factor-alpha expression in ischemic neurons. Stroke 25:1481-1488.

Liu XZ, Xu, X.M., Hu, R., Du, C., Zhang, S.Z., McDonald, J.W., Dong, H.X., Wu, Y.J., Fan, G.S., Jacquin, M.F., Hsu, C.Y., Choi, D.W. (1997) Neuronal and glial apoptosis after traumatic spinal cord injury. J Neurosci 17:5395-5406.

Liuzzi FJ, Lasek RJ (1987) Astrocytes block axonal regeneration in mammals by activating the physiological stop pathway. Science 237:642-645.

Liva SM, Kahn MA, Dopp JM, de Vellis J (1999) Signal transduction pathways induced by GM-CSF in microglia: significance in the control of proliferation. Glia 26:344-352.

Logan A, Green J, Hunter A, Jackson R, Berry M (1999) Inhibition of glial scarring in the injured rat brain by a recombinant human monoclonal antibody to transforming growth factor-beta2. Eur J Neurosci 11:2367-2374.

Loh KP, Huang SH, De Silva R, Tan BK, Zhu YZ (2006) Oxidative stress: apoptosis in neuronal injury. Curr Alzheimer Res 3:327-337.

Lodhia KR, Shakui P, Keep RF (2006) Hydrocephalus in a rat model of intraventricular hemorrhage. Acta Neurochir. Suppl. 96:207-211.

Longbrake EE, Lai W, Ankeny DP, Popovich PG (2007) Characterization and modeling of monocyte-derived macrophages after spinal cord injury. J. Neurochem. 102:1083-1094.

Lopez-Neblina F, Toledo AH, Toledo-Pereyra LH (2005) Molecular biology of apoptosis in ischemia and reperfusion. J Invest Surg 18:335-350.

Lopez-Vales R, Fores J, Verdu E, Navarro X (2006a) Acute and delayed transplantation of olfactory ensheathing cells promote partial recovery after complete transection of the spinal cord. Neurobiol Dis 21:57-68.

Lopez-Vales R, Fores J, Navarro X, Verdu E (2007) Chronic transplantation of olfactory ensheathing cells promotes partial recovery after complete spinal cord transection in the rat. Glia 55:303-311.

Lopez-Vales R, Garcia-Alias G, Fores J, Vela JM, Navarro X, Verdu E (2004) Transplanted olfactory ensheathing cells modulate the inflammatory response in the injured spinal cord. Neuron Glia Biol 1:201-209.

Lopez-Vales R, Garcia-Alias G, Guzman-Lenis MS, Fores J, Casas C, Navarro X, Verdu E (2006b) Effects of COX-2 and iNOS inhibitors alone or in combination with olfactory ensheathing cell grafts after spinal cord injury. Spine 31:1100-1106.

López-Vales R, Forés J, Navarro X, Verdú E (2007) Chronic transplantation of olfactory ensheathing cells promotes partial recovery after complete spinal cord transection in the rat. Glia 55:303-311.

Lu J, Feron F, Mackay-Sim A, Waite PM (2002) Olfactory ensheathing cells promote locomotor recovery after delayed transplantation into transected spinal cord. Brain 125:14-21.

Lu P, Yang H, Jones LL, Filbin MT, Tuszynski MH (2004) Combinatorial therapy with neurotrophins and cAMP promotes axonal regeneration beyond sites of spinal cord injury. J Neurosci 24:6402-6409.

Lu P, Yang H, Culbertson M, Graham L, Roskams AJ, Tuszynski MH (2006) Olfactory ensheathing cells do not exhibit unique migratory or axonal growth-promoting properties after spinal cord injury. J Neurosci 26:11120-11130.

Lu X, Liu H, Wang L, Schaefer S (2009) Activation of NF-kappaB is a critical element in the antiapoptotic effect of anesthetic preconditioning. Am J Physiol Heart Circ Physiol 296:H1296-1304.

Lucas SM, Rothwell NJ, Gibson RM (2006) The role of inflammation in CNS injury and disease. Br J Pharmacol 147 Suppl 1:S232-240.

Ludwig A, Schulte A, Schnack C, Hundhausen C, Reiss K, Brodway N, Held-Feindt J, Mentlein R (2005) Enhanced expression and shedding of the transmembrane chemokine CXCL16 by reactive astrocytes and glioma cells. J Neurochem 93:1293-1303.

Lynch JR, Pineda JA, Morgan D, Zhang L, Warner DS, Benveniste H, Laskowitz DT (2002) Apolipoprotein E affects the central nervous system response to injury and the development of cerebral edema. Ann Neurol 51:113-117.

Lyons AB, Parish CR (1994) Determination of lymphocyte division by flow cytometry. J Immunol Methods 171:131-137.
Mackay-Sim A (2005) Olfactory ensheathing cells and spinal cord repair. Keio J Med 54:8-14.
Mackay-Sim A, Kittel P (1991) Cell dynamics in the adult mouse olfactory epithelium: a quantitative autoradiographic study. J Neurosci 11:979-984.
Mackay-Sim A, Feron F, Cochrane J, Bassingthwaighte L, Bayliss C, Davies W, Fronek P, Gray C, Kerr G, Licina P, Nowitzke A, Perry C, Silburn PA, Urquhart S, Geraghty T (2008) Autologous olfactory ensheathing cell transplantation in human paraplegia: a 3-year clinical trial. Brain.
MacNevin CJ, Atif F, Sayeed I, Stein DG, Liotta DC (2009) Development and screening of water-soluble analogues of progesterone and allopregnanolone in models of brain injury. J Med Chem 52:6012-6023.
Madrid LV, Mayo MW, Reuther JY, Baldwin AS, Jr. (2001) Akt stimulates the transactivation potential of the RelA/p65 Subunit of NF-kappa B through utilization of the Ikappa B kinase and activation of the mitogen-activated protein kinase p38. J Biol Chem 276:18934-18940.
Manning TJ, Jr., Sontheimer H (1997) Bovine serum albumin and lysophosphatidic acid stimulate calcium mobilization and reversal of cAMP-induced stellation in rat spinal cord astrocytes. Glia 20:163-172.
Maret W (2000) The function of zinc metallothionein: a link between cellular zinc and redox state. J Nutr 130:1455S-1458S.
Maret W (2003) Cellular zinc and redox states converge in the metallothionein/thionein pair. Journal of Nutrition 133:1460S-1462S.
Maret W, Heffron G, Hill HA, Djuricic D, Jiang LJ, Vallee BL (2002) The ATP/metallothionein interaction: NMR and STM. Biochemistry 41:1689-1694.
Marquez C, Martinez C, Kroemer G, Bosca L (1992) Protein kinase C isoenzymes display differential affinity for phorbol esters. Analysis of phorbol ester receptors in B cell differentiation. J Immunol 149:2560-2568.
Martin D, Robe P, Franzen R, Delree P, Schoenen J, Stevenaert A, Moonen G (1996) Effects of Schwann cell transplantation in a contusion model of rat spinal cord injury. J Neurosci Res 45:588-597.
Maslinska D, Laure-Kamionowska M, Maslinski S (2004) Toll-like receptors in rat brains injured by hypoxic-ischaemia or exposed to staphylococcal alpha-toxin. Folia Neuropathol 42:125-132.
Mason JL, Xuan S, Dragatsis I, Efstratiadis A, Goldman JE (2003) Insulin-like growth factor (IGF) signaling through type 1 IGF receptor plays an important role in remyelination. J Neurosci 23:7710-7718.
Matsumoto H, Kumon Y, Watanabe H, Ohnishi T, Shudou M, Ii C, Takahashi H, Imai Y, Tanaka J (2007) Antibodies to CD11b, CD68, and lectin label neutrophils rather than microglia in traumatic and ischemic brain lesions. J Neurosci Res 85:994-1009.
Matsumoto H, Kumon Y, Watanabe H, Ohnishi T, Shudou M, Chuai M, Imai Y, Takahashi H, Tanaka J (2008) Accumulation of macrophage-like cells expressing NG2 proteoglycan and Iba1 in ischemic core of rat brain after transient middle cerebral artery occlusion. J Cereb Blood Flow Metab 28:149-163.
Matute C, Domercq M, Sanchez-Gomez MV (2006) Glutamate-mediated glial injury: mechanisms and clinical importance. Glia 53:212-224.
Matute C, Alberdi E, Ibarretxe G, Sanchez-Gomez MV (2002) Excitotoxicity in glial cells. Eur J Pharmacol 447:239-246.
Maurer MH, Feldmann RE, Jr., Burgers HF, Kuschinsky W (2008) Protein expression differs between neural progenitor cells from the adult rat brain subventricular zone and olfactory bulb. BMC Neurosci 9:7.
Maxwell WL, Povlishock JT, Graham DL (1997) A mechanistic analysis of nondisruptive axonal injury: a review. J Neurotrauma 14:419-440.
McCarthy GM, Augustine JA, Baldwin AS, Christopherson PA, Cheung HS, Westfall PR, Scheinman RI (1998) Molecular mechanism of basic calcium phosphate crystal-induced activation of

human fibroblasts. Role of nuclear factor kappab, activator protein 1, and protein kinase c. J Biol Chem 273:35161-35169.
McCarthy KD, De Vellis J (1980) Preparation of separate astroglial and oligodendroglial cell cultures from rat cerebral tissue. J Cell Bio 85:890-902.
McCormick CC, Menard MP, Cousins RJ (1981) Induction of hepatic metallothionein by feeding zinc to rats of depleted zinc status. Am J Physiol 240:E414-421.
McCurdy RD, Feron F, McGrath JJ, Mackay-Sim A (2005) Regulation of adult olfactory neurogenesis by insulin-like growth factor-I. Eur J Neurosci 22:1581-1588.
Medkova M, Cho W (1999) Interplay of C1 and C2 domains of protein kinase C-alpha in its membrane binding and activation. J Biol Chem 274:19852-19861.
Meeuwsen S, Persoon-Deen C, Bsibsi M, Ravid R, van Noort JM (2003) Cytokine, chemokine and growth factor gene profiling of cultured human astrocytes after exposure to proinflammatory stimuli. Glia 43:243-253.
Mehta SL, Manhas N, Raghubir R (2007) Molecular targets in cerebral ischemia for developing novel therapeutics. Brain Res Rev 54:34-66.
Meme W, Calvo CF, Froger N, Ezan P, Amigou E, Koulakoff A, Giaume C (2006) Proinflammatory cytokines released from microglia inhibit gap junctions in astrocytes: potentiation by beta-amyloid. FASEB J 20:494-496.
Mian RA, Knight KR, Penington AJ, Hurley JV, Messina A, Romeo R, Morrison WA (2001) Stimulating effect of an arteriovenous shunt on the in vivo growth of isografted fibroblasts: a preliminary report. Tissue Eng 7:73-80.
Michel FJ, Fortin GD, Martel P, Yeomans J, Trudeau LE (2005) M3-like muscarinic receptors mediate Ca2+ influx in rat mesencephalic GABAergic neurones through a protein kinase C-dependent mechanism. Neuropharmacology 48:796-809.
Mirsky R, Jessen KR (1999) The neurobiology of Schwann cells. Brain Pathol 9:293-311.
Mitani M, Otake N (1978) Studies on the ionophorous antibiotics. XVI. The ionophore-mediated calcium transport and concomitant osmotic swelling of mitochondria. J Antibiot (Tokyo) 31:888-893.
Mizuno T, Kawanokuchi J, Numata K, Suzumura A (2003) Production and neuroprotective functions of fractalkine in the central nervous system. Brain Res. 979:65-70.
Molloy S, Middleton F, Casey AT (2002) Failure to administer methylprednisolone for acute traumatic spinal cord injury-a prospective audit of 100 patients from a regional spinal injuries unit. Injury 33:575-578.
Monier A, Evrard P, Gressens P, Verney C (2006) Distribution and differentiation of microglia in the human encephalon during the first two trimesters of gestation. J. Comp. Neurol. 499:565-582.
Moon-Sook W, Jin-Sun P, In-Young C, Won-Ki K, Hee-Sun K (2008) Inhibition of MMP-3 or -9 suppresses lipopolysaccharide-induced expression of proinflammatory cytokines and iNOS in microglia. Journal of Neurochemistry 106:770-780.
Morganti-Kossmann MC, Rancan M, Stahel PF, Kossmann T (2002) Inflammatory response in acute traumatic brain injury: a double-edged sword. Curr Opin Crit Care 8:101-105.
Morita M, Higuchi C, Moto T, Kozuka N, Susuki J, Itofusa R, Yamashita J, Kudo Y (2003) Dual regulation of calcium oscillation in astrocytes by growth factors and pro-inflammatory cytokines via the mitogen-activated protein kinase cascade. J Neurosci 23:10944-10952.
Moroni F (2008) Poly(ADP-ribose)polymerase 1 (PARP-1) and postischemic brain damage. Curr Opin Pharmacol 8:96-103.
Morrison RS, de Vellis J (1981) Growth of purified astrocytes in a chemically defined medium. Proc Natl Acad Sci U S A 78:7205-7209.
Muir EM, Adcock KH, Morgenstern DA, Clayton R, von Stillfried N, Rhodes K, Ellis C, Fawcett JW, Rogers JH (2002) Matrix metalloproteases and their inhibitors are produced by overlapping populations of activated astrocytes. Brain Res Mol Brain Res 100:103-117.
Muller JM, Ziegler-Heitbrock HW, Baeuerle PA (1993) Nuclear factor kappa B, a mediator of lipopolysaccharide effects. Immunobiology 187:233-256.

Muller JM, Rupec RA, Baeuerle PA (1997) Study of gene regulation by NF-kappa B and AP-1 in response to reactive oxygen intermediates. Methods 11:301-312.
Mulsow JJ, Watson RW, Fitzpatrick JM, O'Connell PR (2005) Transforming growth factor-beta promotes pro-fibrotic behavior by serosal fibroblasts via PKC and ERK1/2 mitogen activated protein kinase cell signaling. Ann Surg 242:880-887, discussion 887-889.
Murphy GM, Jr., Lee YL, Jia XC, Yu AC, Majewska A, Song Y, Schmidt K, Eng LF (1995) Tumor necrosis factor-alpha and basic fibroblast growth factor decrease glial fibrillary acidic protein and its encoding mRNA in astrocyte cultures and glioblastoma cells. J Neurochem 65:2716-2724.
Na YJ, Jin JK, Kim JI, Choi EK, Carp RI, Kim YS (2007) JAK-STAT signaling pathway mediates astrogliosis in brains of scrapie-infected mice. J Neurochem 103:637-649.
Nakanishi M, Niidome T, Matsuda S, Akaike A, Kihara T, Sugimoto H (2007) Microglia-derived interleukin-6 and leukaemia inhibitory factor promote astrocytic differentiation of neural stem/progenitor cells. Eur J Neurosci 25:649-658.
Nakano H, Ikenaga S, Aizu T, Kaneko T, Matsuzaki Y, Tsuchida S, Hanada K, Arima Y (2006) Human metallothionein gene expression is upregulated by beta-thujaplicin: possible involvement of protein kinase C and reactive oxygen species. Biol Pharm Bull 29:55-59.
Nakashima S (2002) Protein kinase C alpha (PKC alpha): regulation and biological function. J Biochem (Tokyo) 132:669-675.
Nakka VP, Gusain A, Mehta SL, Raghubir R (2008) Molecular mechanisms of apoptosis in cerebral ischemia: multiple neuroprotective opportunities. Mol Neurobiol 37:7-38.
Namiki J, Kojima A, Tator CH (2000) Effect of brain-derived neurotrophic factor, nerve growth factor, and neurotrophin-3 on functional recovery and regeneration after spinal cord injury in adult rats. J Neurotrauma 17:1219-1231.
Nan B, Getchell ML, Partin JV, Getchell TV (2001) Leukemia inhibitory factor, interleukin-6, and their receptors are expressed transiently in the olfactory mucosa after target ablation. J Comp Neurol 435:60-77.
Nash HH, Borke RC, Anders JJ (2002) Ensheathing cells and methylprednisolone promote axonal regeneration and functional recovery in the lesioned adult rat spinal cord. J. Neurosci. 22:7111-7120.
Neal JW, Singhrao SK, Jasani B, Newman GR, Vergun O, Sobolevsky AI, Yelshansky MV, Keelan J, Khodorov BI, Duchen MR (1996) Immunocytochemically detectable metallothionein is expressed by astrocytes in the ischaemic human brain: exploration of the role of reactive oxygen species in glutamate neurotoxicity in rat hippocampal neurones in culture. Neuropathol Appl Neurobiol 22:243-247.
Neary JT, Kang Y (2005) Signaling from P2 nucleotide receptors to protein kinase cascades induced by CNS injury: implications for reactive gliosis and neurodegeneration. Mol Neurobiol 31:95-103.
Nesic O, Lee J, Unabia GC, Johnson K, Ye Z, Vergara L, Hulsebosch CE, Perez-Polo JR (2008) Aquaporin 1 - a novel player in spinal cord injury. J Neurochem 105:628-640.
Newton AC (1997) Regulation of protein kinase C. Curr Opin Cell Biol 9:161-167.
Nguyen MH, Jafri MS (2005) Mitochondrial calcium signaling and energy metabolism. Ann N Y Acad Sci 1047:127-137.
Niclou SP, Franssen EH, Ehlert EM, Taniguchi M, Verhaagen J (2003) Meningeal cell-derived semaphorin 3A inhibits neurite outgrowth. Mol Cell Neurosci 24:902-912.
Nieto-Sampedro M (2003) Central nervous system lesions that can and those that cannot be repaired with the help of olfactory bulb ensheathing cell transplants. Neurochem Res 28:1659-1676.
Niizuma K, Endo H, Chan PH (2009) Oxidative stress and mitochondrial dysfunction as determinants of ischemic neuronal death and survival. J Neurochem 109 Suppl 1:133-138.
Nishiyama A, Yang Z, Butt A (2005) Astrocytes and NG2-glia: what's in a name? J Anat 207:687-693.
Nishizuka Y (1988) The molecular heterogeneity of protein kinase C and its implications for cellular regulation. Nature 334:661-665.

Noguchi CT, Asavaritikrai P, Teng R, Jia Y (2007) Role of erythropoietin in the brain. Crit Rev Oncol Hematol 64:159-171.
Norris CM, Kadish I, Blalock EM, Chen KC, Thibault V, Porter NM, Landfield PW, Kraner SD (2005) Calcineurin triggers reactive/inflammatory processes in astrocytes and is upregulated in aging and Alzheimer's models. J Neurosci 25:4649-4658.
Norris JG, Tang LP, Sparacio SM, Benveniste EN (1994) Signal transduction pathways mediating astrocyte IL-6 induction by IL-1 beta and tumor necrosis factor-alpha. J Immunol 152:841-850.
O'Connor PA, McCormack O, Gavin C, Dungan R, Kirke C, McCormack D, O'Byrne J, Stephens M, McManus F, Walsh M (2003) Methylprednisolone in acute spinal cord injuries. Ir J Med Sci 172:24-26.
O'Dea EL, Barken D, Peralta RQ, Tran KT, Werner SL, Kearns JD, Levchenko A, Hoffmann A (2007) A homeostatic model of IkappaB metabolism to control constitutive NF-kappaB activity. Mol. Syst. Biol. 3:111.
O'Neill LA, Kaltschmidt C (1997) NF-kappa B: a crucial transcription factor for glial and neuronal cell function. Trends Neurosci 20:252-258.
O'Riordan KJ, Huang IC, Pizzi M, Spano P, Boroni F, Egli R, Desai P, Fitch O, Malone L, Ahn HJ, Liou HC, Sweatt JD, Levenson JM (2006) Regulation of nuclear factor kappaB in the hippocampus by group I metabotropic glutamate receptors. J Neurosci 26:4870-4879.
O'Toole DA, West AK, Chuah MI (2007) Effect of olfactory ensheathing cells on reactive astrocytes in vitro. Cell Mol Life Sci 64:1303-1309.
Obeid LM, Blobe GC, Karolak LA, Hannun YA (1992) Cloning and characterization of the major promoter of the human protein kinase C beta gene. Regulation by phorbol esters. J Biol Chem 267:20804-20810.
Oechmichen M, Meissner C (2006) Cerebral hypoxia and ischemia: the forensic point of view: a review. J Forensic Sci 51:880-887.
Oh YJ, Markelonis GJ, Oh TH (1993) Effects of interleukin-1 beta and tumor necrosis factor-alpha on the expression of glial fibrillary acidic protein and transferrin in cultured astrocytes. Glia 8:77-86.
Okada S, Nakamura M, Mikami Y, Shimazaki T, Mihara M, Ohsugi Y, Iwamoto Y, Yoshizaki K, Kishimoto T, Toyama Y, Okano H (2004) Blockade of interleukin-6 receptor suppresses reactive astrogliosis and ameliorates functional recovery in experimental spinal cord injury. J Neurosci Res 76:265-276.
Ortis F, Cardozo AK, Crispim D, Storling J, Mandrup-Poulsen T, Eizirik DL (2006) Cytokine-induced pro-apoptotic gene expression in insulin-producing cells is related to rapid, sustained and non-oscillatory NF-kappaB activation. Mol Endocrinol.
Ostrowski RP, Colohan AR, Zhang JH (2006) Molecular mechanisms of early brain injury after subarachnoid hemorrhage. Neurol Res 28:399-414.
Oudega M, Hagg T (1996) Nerve growth factor promotes regeneration of sensory axons into adult rat spinal cord. Exp Neurol 140:218-229.
Pahl HL, Baeuerle PA (1996) Activation of NF-kappa B by ER stress requires both Ca2+ and reactive oxygen intermediates as messengers. FEBS Lett 392:129-136.
Panenka W, Jijon H, Herx LM, Armstrong JN, Feighan D, Wei T, Yong VW, Ransohoff RM, MacVicar BA (2001) P2X7-like receptor activation in astrocytes increases chemokine monocyte chemoattractant protein-1 expression via mitogen-activated protein kinase. J Neurosci 21:7135-7142.
Panickar KS, Norenberg MD (2005) Astrocytes in cerebral ischemic injury: morphological and general considerations. Glia 50:287-298.
Panickar KS, Jayakumar AR, Rao KV, Norenberg MD (2009) Ammonia-induced activation of p53 in cultured astrocytes: role in cell swelling and glutamate uptake. Neurochem Int 55:98-105.
Papadopoulos MC, Verkman AS (2008) Potential utility of aquaporin modulators for therapy of brain disorders. Prog Brain Res 170:589-601.

Papp H, Czifra G, Lazar J, Gonczi M, Csernoch L, Kovacs L, Biro T (2003) Protein kinase C isozymes regulate proliferation and high cell density-mediated differentiation in HaCaT keratinocytes. Exp Dermatol 12:811-824.

Parent JM, von dem Bussche N, Lowenstein DH (2006) Prolonged seizures recruit caudal subventricular zone glial progenitors into the injured hippocampus. Hippocampus 16:321-328.

Paria BC, Malik AB, Kwiatek AM, Rahman A, May MJ, Ghosh S, Tiruppathi C (2003) Tumor necrosis factor-alpha induces nuclear factor-kappaB-dependent TRPC1 expression in endothelial cells. J Biol Chem 278:37195-37203.

Parnavelas JG (1999) Glial cell lineages in the rat cerebral cortex. Exp Neurol 156:418-429.

Parnavelas JG, Nadarajah B (2001) Radial glial cells. are they really glia? Neuron 31:881-884.

Pascale A, Alkon DL, Grimaldi M (2004) Translocation of protein kinase C-betaII in astrocytes requires organized actin cytoskeleton and is not accompanied by synchronous RACK1 relocation. Glia 46:169-182.

Paschen W, Mengesdorf T (2003) Conditions associated with ER dysfunction activate homer 1a expression. J Neurochem 86:1108-1115.

Pastrana E, Moreno-Flores MT, Gurzov EN, Avila J, Wandosell F, Diaz-Nido J (2006) Genes associated with adult axon regeneration promoted by olfactory ensheathing cells: a new role for matrix metalloproteinase 2. J. Neurosci. 26:5347-5359.

Pascual JI, Gudino-Cabrera G, Insausti R, Nieto-Sampedro M (2002) Spinal implants of olfactory ensheathing cells promote axon regeneration and bladder activity after bilateral lumbosacral dorsal rhizotomy in the adult rat. J Urol 167:1522-1526.

Pawate S, Shen Q, Fan F, Bhat NR (2004) Redox regulation of glial inflammatory response to lipopolysaccharide and interferongamma. J Neurosci Res 77:540-551.

Penkowa M, Hidalgo J (2000) IL-6 deficiency leads to reduced metallothionein-I+II expression and increased oxidative stress in the brain stem after 6-aminonicotinamide treatment. Exp Neurol 163:72-84.

Penkowa M, Hidalgo J (2001) Metallothionein treatment reduces proinflammatory cytokines IL-6 and TNF-alpha and apoptotic cell death during experimental autoimmune encephalomyelitis (EAE). Exp Neurol 170:1-14.

Penkowa M, Hidalgo J, Moos T (1997) Increased astrocytic expression of metallothioneins I + II in brainstem of adult rats treated with 6-aminonicotinamide. Brain Res 774:256-259.

Penkowa M, Molinero A, Carrasco J, Hidalgo J (2001) Interleukin-6 deficiency reduces the brain inflammatory response and increases oxidative stress and neurodegeneration after kainic acid-induced seizures. Neuroscience 102:805-818.

Penkowa M, Giralt M, Camats J, Hidalgo J (2002) Metallothionein 1+2 protect the CNS during neuroglial degeneration induced by 6-aminonicotinamide. J Comp Neurol 444:174-189.

Penkowa M, Giralt M, Lago N, Camats J, Carrasco J, Hernandez J, Molinero A, Campbell IL, Hidalgo J (2003) Astrocyte-targeted expression of IL-6 protects the CNS against a focal brain injury. Exp Neurol 181:130-148.

Perez-Ortiz JM, Serrano-Perez MC, Pastor MD, Martin ED, Calvo S, Rincon M, Tranque P (2008) Mechanical lesion activates newly identified NFATc1 in primary astrocytes: implication of ATP and purinergic receptors. Eur J Neurosci 27:2453-2465.

Perez-Pinzon MA, Dave KR, Raval AP (2005) Role of reactive oxygen species and protein kinase C in ischemic tolerance in the brain. Antioxid Redox Signal 7:1150-1157.

Peters DM, Herbert K, Biddick B, Peterson JA (2005) Myocilin binding to Hep II domain of fibronectin inhibits cell spreading and incorporation of paxillin into focal adhesions. Exp Cell Res 303:218-228.

Phulwani NK, Esen N, Syed MM, Kielian T (2008) TLR2 expression in astrocytes is induced by TNF-alpha- and NF-kappa B-dependent pathways. J Immunol 181:3841-3849.

Pindon A, Festoff BW, Hantai D (1998) Thrombin-induced reversal of astrocyte stellation is mediated by activation of protein kinase C beta-1. Eur J Biochem 255:766-774.

Pineau I, Lacroix S (2009) Endogenous signals initiating inflammation in the injured nervous system. Glia 57:351-361.

Pinto SS, Gottfried C, Mendez A, Goncalves D, Karl J, Goncalves CA, Wofchuk S, Rodnight R (2000) Immunocontent and secretion of S100B in astrocyte cultures from different brain regions in relation to morphology. FEBS Lett 486:203-207.

Pivovarova NB, Nguyen HV, Winters CA, Brantner CA, Smith CL, Andrews SB (2004) Excitotoxic calcium overload in a subpopulation of mitochondria triggers delayed death in hippocampal neurons. J Neurosci 24:5611-5622.

Pixley SK (1992) The olfactory nerve contains two populations of glia, identified both in vivo and in vitro. Glia 5:269-284.

Pizzi M, Sarnico I, Lanzillotta A, Battistin L, Spano P (2009) Post-ischemic brain damage: NF-kappaB dimer heterogeneity as a molecular determinant of neuron vulnerability. FEBS J 276:27-35.

Plant GW, Christensen CL, Oudega M, Bunge MB (2003) Delayed transplantation of olfactory ensheathing glia promotes sparing/regeneration of supraspinal axons in the contused adult rat spinal cord. J Neurotrauma 20:1-16.

Plant GW, Currier PF, Cuervo EP, Bates ML, Pressman Y, Bunge MB, Wood PM (2002) Purified adult ensheathing glia fail to myelinate axons under culture conditions that enable Schwann cells to form myelin. J Neurosci 22:6083-6091.

Plesnila N, von Baumgarten L, Retiounskaia M, Engel D, Ardeshiri A, Zimmermann R, Hoffmann F, Landshamer S, Wagner E, Culmsee C (2007) Delayed neuronal death after brain trauma involves p53-dependent inhibition of NF-kappaB transcriptional activity. Cell Death Differ 14:1529-1541.

Pons S, Torres-Aleman I (2000) Insulin-like growth factor-I stimulates dephosphorylation of ikappa B through the serine phosphatase calcineurin (protein phosphatase 2B). J Biol Chem 275:38620-38625.

Popovich PG, van Rooijen N, Hickey WF, Preidis G, McGaughy V (2003) Hematogenous macrophages express CD8 and distribute to regions of lesion cavitation after spinal cord injury. Exp Neurol 182:275-287.

Previtali SC, Nodari A, Taveggia C, Pardini C, Dina G, Villa A, Wrabetz L, Quattrini A, Feltri ML (2003) Expression of laminin receptors in schwann cell differentiation: evidence for distinct roles. J Neurosci 23:5520-5530.

Proescholdt MG, Chakravarty S, Foster JA, Foti SB, Briley EM, Herkenham M (2002) Intracerebroventricular but not intravenous interleukin-1beta induces widespread vascular-mediated leukocyte infiltration and immune signal mRNA expression followed by brain-wide glial activation. Neuroscience 112:731-749.

Profyris C, Cheema SS, Zang D, Azari MF, Boyle K, Petratos S (2004) Degenerative and regenerative mechanisms governing spinal cord injury. Neurobiol Dis 15:415-436.

Properzi F, Carulli D, Asher RA, Muir E, Camargo LM, van Kuppevelt TH, ten Dam GB, Furukawa Y, Mikami T, Sugahara K, Toida T, Geller HM, Fawcett JW (2005) Chondroitin 6-sulphate synthesis is up-regulated in injured CNS, induced by injury-related cytokines and enhanced in axon-growth inhibitory glia. Eur J Neurosci 21:378-390.

Qiu J, Cai D, Filbin MT (2000) Glial inhibition of nerve regeneration in the mature mammalian CNS. Glia 29:166-174.

Quah BJ, Warren HS, Parish CR (2007) Monitoring lymphocyte proliferation in vitro and in vivo with the intracellular fluorescent dye carboxyfluorescein diacetate succinimidyl ester. Nat Protoc 2:2049-2056.

Quest AF, Bell RM (1994) The regulatory region of protein kinase C gamma. Studies of phorbol ester binding to individual and combined functional segments expressed as glutathione S-transferase fusion proteins indicate a complex mechanism of regulation by phospholipids, phorbol esters, and divalent cations. J Biol Chem 269:20000-20012.

Quinones MP, Kalkonde Y, Estrada CA, Jimenez F, Ramirez R, Mahimainathan L, Mummidi S, Choudhury GG, Martinez H, Adams L, Mack M, Reddick RL, Maffi S, Haralambous S, Probert L, Ahuja SK, Ahuja SS (2008) Role of astrocytes and chemokine systems in acute

TNFalpha induced demyelinating syndrome: CCR2-dependent signals promote astrocyte activation and survival via NF-kappaB and Akt. Mol Cell Neurosci 37:96-109.
Rabchevsky AG, Weinitz JM, Coulpier M, Fages C, Tinel M, Junier MP (1998) A role for transforming growth factor alpha as an inducer of astrogliosis. J Neurosci 18:10541-10552.
Rael LT, Thomas GW, Bar-Or R, Craun ML, Bar-Or D (2004) An anti-inflammatory role for N-acetyl aspartate in stimulated human astroglial cells. Biochem Biophys Res Commun 319:847-853.
Raff MC, Miller RH, Noble M (1983) A glial progenitor cell that develops in vitro into an astrocyte or an oligodendrocyte depending on culture medium. Nature 303:390-396.
Raghavendra Rao VL, Dhodda VK, Song G, Bowen KK, Dempsey RJ (2003) Traumatic brain injury-induced acute gene expression changes in rat cerebral cortex identified by GeneChip analysis. J Neurosci Res 71:208-219.
Raineteau O, Schwab ME (2001) Plasticity of motor systems after incomplete spinal cord injury. Nat Rev Neurosci 2:263-273.
Raisman G (2000) Repair of corticospinal axons by transplantation of olfactory ensheathing cells. Novartis Found Symp 231:94-97; discussion 97-109.
Raisman G (2001) Olfactory ensheathing cells - another miracle cure for spinal cord injury? Nat Rev Neurosci 2:369-375.
Rajan P, McKay RD (1998) Multiple routes to astrocytic differentiation in the CNS. J Neurosci 18:3620-3629.
Ramakers GJ, Moolenaar WH (1998) Regulation of astrocyte morphology by RhoA and lysophosphatidic acid. Exp Cell Res 245:252-262.
Ramer LM, Richter MW, Roskams AJ, Tetzlaff W, Ramer MS (2004a) Peripherally-derived olfactory ensheathing cells do not promote primary afferent regeneration following dorsal root injury. Glia 47:189-206.
Ramer LM, Au E, Richter MW, Liu J, Tetzlaff W, Roskams AJ (2004b) Peripheral olfactory ensheathing cells reduce scar and cavity formation and promote regeneration after spinal cord injury. J Comp Neurol 473:1-15.
Rami A, Bechmann I, Stehle JH (2008) Exploiting endogenous anti-apoptotic proteins for novel therapeutic strategies in cerebral ischemia. Prog Neurobiol 85:273-296.
Ramon-Cueto A, Nieto-Sampedro M (1994) Regeneration into the spinal cord of transected dorsal root axons is promoted by ensheathing glia transplants. Exp Neurol 127:232-244.
Ramon-Cueto A, Plant GW, Avila J, Bunge MB (1998) Long-distance axonal regeneration in the transected adult rat spinal cord is promoted by olfactory ensheathing glia transplants. J Neurosci 18:3803-3815.
Ramon-Cueto A, Cordero MI, Santos-Benito FF, Avila J (2000) Functional recovery of paraplegic rats and motor axon regeneration in their spinal cords by olfactory ensheathing glia. Neuron 25:425-435.
Rao P, Hayden MS, Long M, Scott ML, West AP, Zhang D, Oeckinghaus A, Lynch C, Hoffmann A, Baltimore D, Ghosh S (2010) IkappaBbeta acts to inhibit and activate gene expression during the inflammatory response. Nature 466:1115-1119.
Rao PS, Jaggi M, Smith DJ, Hemstreet GP, Balaji KC (2003) Metallothionein 2A interacts with the kinase domain of PKCmu in prostate cancer. Biochem Biophys Res Commun 310:1032-1038.
Raponi E, Agenes F, Delphin C, Assard N, Baudier J, Legraverend C, Deloulme JC (2007) S100B expression defines a state in which GFAP-expressing cells lose their neural stem cell potential and acquire a more mature developmental stage. Glia 55:165-177.
Ray SK (2006) Currently evaluated calpain and caspase inhibitors for neuroprotection in experimental brain ischemia. Curr Med Chem 13:3425-3440.
Re F, Belyanskaya SL, Riese RJ, Cipriani B, Fischer FR, Granucci F, Ricciardi-Castagnoli P, Brosnan C, Stern LJ, Strominger JL, Santambrogio L (2002) Granulocyte-macrophage colony-stimulating factor induces an expression program in neonatal microglia that primes them for antigen presentation. J Immunol 169:2264-2273.
Reed CJ, Robinson DA, Lock EA (2003) Antioxidant status of the rat nasal cavity. Free Radic Biol Med 34:607-615.

Reed TT, Owen J, Pierce WM, Sebastian A, Sullivan PG, Butterfield DA (2009) Proteomic identification of nitrated brain proteins in traumatic brain-injured rats treated postinjury with gamma-glutamylcysteine ethyl ester: insights into the role of elevation of glutathione as a potential therapeutic strategy for traumatic brain injury. J Neurosci Res 87:408-417.

Reeves SA, Helman LJ, Allison A, Israel MA (1989) Molecular cloning and primary structure of human glial fibrillary acidic protein. Proc Natl Acad Sci U S A 86:5178-5182.

Reilly JF, Maher PA, Kumari VG (1998) Regulation of astrocyte GFAP expression by TGF-beta1 and FGF-2. Glia 22:202-210.

Resnick DK, Cechvala CF, Yan Y, Witwer BP, Sun D, Zhang S (2003) Adult olfactory ensheathing cell transplantation for acute spinal cord injury. J Neurotrauma 20:279-285.

Rhodes KE, Raivich G, Fawcett JW (2006) The injury response of oligodendrocyte precursor cells is induced by platelets, macrophages and inflammation-associated cytokines. Neuroscience 140:87-100.

Richardson PM, McGuinness UM, Aguayo AJ (1980) Axons from CNS neurons regenerate into PNS grafts. Nature 284:264-265.

Richter M, Au E, Liu J, Kwon B, Tetzlaff W, Roskams AJ (2003) Neoangiogenesis in an ensheathing cell matrix: a trinity of mechanisms to promote spinal cord regeneration. In. Washington, DC: Society for Neuroscience: Abstract Viewer/Itinerary Planner.

Richter MW, Roskams AJ (2008) Olfactory ensheathing cell transplantation following spinal cord injury: hype or hope? Exp Neurol 209:353-367.

Richter MW, Fletcher PA, Liu J, Tetzlaff W, Roskams AJ (2005) Lamina propria and olfactory bulb ensheathing cells exhibit differential integration and migration and promote differential axon sprouting in the lesioned spinal cord. J Neurosci 25:10700-10711.

Riddell JS, Enriquez-Denton M, Toft A, Fairless R, Barnett SC (2004) Olfactory ensheathing cell grafts have minimal influence on regeneration at the dorsal root entry zone following rhizotomy. Glia 47:150-167.

Ridder DA, Schwaninger M (2009) NF-kappa B signaling in cerebral ischemia. Neurosci 158:995-1006.

Rieger A, Deitmer JW, Lohr C (2007) Axon-glia communication evokes calcium signaling in olfactory ensheathing cells of the developing olfactory bulb. Glia 55:352-359.

Risher WC, Andrew RD, Kirov SA (2009) Real-time passive volume responses of astrocytes to acute osmotic and ischemic stress in cortical slices and in vivo revealed by two-photon microscopy. Glia 57:207-221.

Robertson CL, Scafidi S, McKenna MC, Fiskum G (2009) Mitochondrial mechanisms of cell death and neuroprotection in pediatric ischemic and traumatic brain injury. Exp Neurol 218:371-380.

Robles E, Huttenlocher A, Gomez TM (2003) Filopodial calcium transients regulate growth cone motility and guidance through local activation of calpain. Neuron 38:597-609.

Rodnight R, Goncalves CA, Wofchuk ST, Leal R (1997) Control of the phosphorylation of the astrocyte marker glial fibrillary acidic protein (GFAP) in the immature rat hippocampus by glutamate and calcium ions: possible key factor in astrocytic plasticity. Braz J Med Biol Res 30:325-338.

Rojas-Mayorquin AE, Torres-Ruiz NM, Ortuno-Sahagun D, Gudino-Cabrera G (2008) Microarray analysis of striatal embryonic stem cells induced to differentiate by ensheathing cell conditioned media. Dev Dyn 237:979-994.

Rojas-Mayorquín AE, Torres-Ruiz NM, Gudiño-Cabrera G, Ortuño-Sahagún D (2010) Subtractive hybridization identifies genes differentially expressed by olfactory ensheathing cells and neural stem cells. International Journal of Developmental Neuroscience In Press, Accepted Manuscript.

Rolls A, Shechter R, London A, Segev Y, Jacob-Hirsch J, Amariglio N, Rechavi G, Schwartz M (2008) Two faces of chondroitin sulfate proteoglycan in spinal cord repair: a role in microglia/macrophage activation. PLoS Med 5:e171.

Ruitenberg MJ, Levison DB, Lee SV, Verhaagen J, Harvey AR, Plant GW (2005) NT-3 expression from engineered olfactory ensheathing glia promotes spinal sparing and regeneration. Brain 128:839-853.

Ruitenberg MJ, Plant GW, Christensen CL, Blits B, Niclou SP, Harvey AR, Boer GJ, Verhaagen J (2002) Viral vector-mediated gene expression in olfactory ensheathing glia implants in the lesioned rat spinal cord. Gene Ther 9:135-146.

Ruitenberg MJ, Plant GW, Hamers FP, Wortel J, Blits B, Dijkhuizen PA, Gispen WH, Boer GJ, Verhaagen J (2003) Ex vivo adenoviral vector-mediated neurotrophin gene transfer to olfactory ensheathing glia: effects on rubrospinal tract regeneration, lesion size, and functional recovery after implantation in the injured rat spinal cord. J. Neurosci. 23:7045-7058.

Ruitenberg MJ, Vukovic J (2008) Promoting central nervous system regeneration: lessons from cranial nerve I. Restor Neurol Neurosci 26:183-196.

Ruitenberg MJ, Vukovic J, Blomster L, Hall JM, Jung S, Filgueira L, McMenamin PG, Plant GW (2008) CX3CL1/fractalkine regulates branching and migration of monocyte-derived cells in the mouse olfactory epithelium. J. Neuroimmunol. 205:80-85.

Ruitenberg MJ, Vukovic J, Sarich J, Busfield SJ, Plant GW (2006) Olfactory ensheathing cells: characteristics, genetic engineering, and therapeutic potential. J Neurotrauma 23:468-478.

Saadoun S, Papadopoulos MC (2009) Aquaporin-4 in brain and spinal cord oedema. Neuroscience.

Safavi-Abbasi S, Wolff JR, Missler M (2001) Rapid morphological changes in astrocytes are accompanied by redistribution but not by quantitative changes of cytoskeletal proteins. Glia 36:102-115.

Saklatvala J (2007) Inflammatory signaling in cartilage: MAPK and NF-kappaB pathways in chondrocytes and the use of inhibitors for research into pathogenesis and therapy of osteoarthritis. Curr Drug Targets 8:305-313.

Sama MA, Mathis DM, Furman JL, Abdul HM, Artiushin IA, Kraner SD, Norris CM (2008) Interleukin-1beta-dependent signaling between astrocytes and neurons depends critically on astrocytic calcineurin/NFAT activity. J Biol Chem 283:21953-21964.

Samantaray S, Sribnick EA, Das A, Thakore NP, Matzelle D, Yu SP, Ray SK, Wei L, Banik NL (2010) Neuroprotective efficacy of estrogen in experimental spinal cord injury in rats. Ann N Y Acad Sci 1199:90-94.

Sandvig A, Berry M, Barrett LB, Butt A, Logan A (2004) Myelin-, reactive glia-, and scar-derived CNS axon growth inhibitors: expression, receptor signaling, and correlation with axon regeneration. Glia 46:225-251.

Santos-Silva A, Fairless R, Frame MC, Montague P, Smith GM, Toft A, Riddell JS, Barnett SC (2007) FGF/heparin differentially regulates Schwann cell and olfactory ensheathing cell interactions with astrocytes: a role in astrocytosis. J Neurosci 27:7154-7167.

Sarnico I, Lanzillotta A, Boroni F, Benarese M, Alghisi M, Schwaninger M, Inta I, Battistin L, Spano P, Pizzi M (2009) NF-kappaB p50/RelA and c-Rel-containing dimers: opposite regulators of neuron vulnerability to ischaemia. J Neurochem 108:475-485.

Sasaki A, Nakazato Y (1992) The identity of cells expressing MHC class II antigens in normal and pathological human brain. Neuropathol Appl Neurobiol 18:13-26.

Sasaki M, Hains BC, Lankford KL, Waxman SG, Kocsis JD (2006) Protection of corticospinal tract neurons after dorsal spinal cord transection and engraftment of olfactory ensheathing cells. Glia 53:352-359.

Sasaki M, Li B, Lankford KL, Radtke C, Kocsis JD (2007) Remyelination of the injured spinal cord. Prog Brain Res 161:419-433.

Satriotomo I, Bowen KK, Vemuganti R (2006) JAK2 and STAT3 activation contributes to neuronal damage following transient focal cerebral ischemia. J Neurochem 98:1353-1368.

Saydam N, Adams TK, Steiner F, Schaffner W, Freedman JH (2002) Regulation of metallothionein transcription by the metal-responsive transcription factor MTF-1: identification of signal transduction cascades that control metal-inducible transcription. J Biol Chem 277:20438-20445.

Scheinman RI, Cogswell PC, Lofquist AK, Baldwin AS, Jr. (1995) Role of transcriptional activation of I kappa B alpha in mediation of immunosuppression by glucocorticoids. Science 270:283-286.
Schermer C, Humpel C (2002) Granulocyte macrophage-colony stimulating factor activates microglia in rat cortex organotypic brain slices. Neurosci Lett 328:180-184.
Schilling T, Nitsch R, Heinemann U, Haas D, Eder C (2001) Astrocyte-released cytokines induce ramification and outward K+ channel expression in microglia via distinct signalling pathways. Eur J Neurosci 14:463-473.
Schneider A, Martin-Villalba A, Weih F, Vogel J, Wirth T, Schwaninger M (1999) NF-kappaB is activated and promotes cell death in focal cerebral ischemia. Nat Med 5:554-559.
Schnell L, Fearn S, Klassen H, Schwab ME, Perry VH (1999) Acute inflammatory responses to mechanical lesions in the CNS: differences between brain and spinal cord. Eur J Neurosci 11:3648-3658.
Schreck R, Baeuerle PA (1990) NF-kappa B as inducible transcriptional activator of the granulocyte-macrophage colony-stimulating factor gene. Mol Cell Biol 10:1281-1286.
Schwab BL, Guerini D, Didszun C, Bano D, Ferrando-May E, Fava E, Tam J, Xu D, Xanthoudakis S, Nicholson DW, Carafoli E, Nicotera P (2002) Cleavage of plasma membrane calcium pumps by caspases: a link between apoptosis and necrosis. Cell Death Differ 9:818-831.
Schwab ME (2002) Repairing the injured spinal cord. Science 295:1029-1031.
Schwaninger M, Sallmann S, Petersen N, Schneider A, Prinz S, Libermann TA, Spranger M (1999) Bradykinin induces interleukin-6 expression in astrocytes through activation of nuclear factor-kappaB. J Neurochem 73:1461-1466.
Schwartz M (2001a) Protective autoimmunity as a T-cell response to central nervous system trauma: prospects for therapeutic vaccines. Prog Neurobiol 65:489-496.
Schwartz M (2001b) Harnessing the immune system for neuroprotection: therapeutic vaccines for acute and chronic neurodegenerative disorders. Cell Mol Neurobiol 21:617-627.
Schwartz M (2003) Macrophages and microglia in central nervous system injury: are they helpful or harmful? J Cereb Blood Flow Metab 23:385-394.
Schwartz M (2010) "Tissue-repairing" blood-derived macrophages are essential for healing of the injured spinal cord: from skin-activated macrophages to infiltrating blood-derived cells? Brain Behav Immun 24:1054-1057.
Schwartz M, Cohen A, Stein-Izsak C, Belkin M (1989) Dichotomy of the glial cell response to axonal injury and regeneration. FASEB J 3:2371-2378.
Schwartz M, Butovsky O, Bruck W, Hanisch UK (2006) Microglial phenotype: is the commitment reversible? Trends Neurosci 29:68-74.
Schwartz M, London A, Shechter R (2009) Boosting T-cell immunity as a therapeutic approach for neurodegenerative conditions: the role of innate immunity. Neuroscience 158:1133-1142.
Schwob JE (2002) Neural regeneration and the peripheral olfactory system. Anat. Rec. 269:33-49.
Schwob JE (2005) Restoring olfaction: a view from the olfactory epithelium. Chem. Senses 30 Suppl 1:i131-132.
Segura T, Calleja S, Jordan J (2008) Recommendations and treatment strategies for the management of acute ischemic stroke. Expert Opin Pharmacother 9:1071-1085.
Selmaj K, Shafit-Zagardo B, Aquino DA, Farooq M, Raine CS, Norton WT, Brosnan CF (1991) Tumor necrosis factor-induced proliferation of astrocytes from mature brain is associated with down-regulation of glial fibrillary acidic protein mRNA. J Neurochem 57:823-830.
Sen R, Baltimore D (1986) Inducibility of kappa immunoglobulin enhancer-binding protein Nf-kappa B by a posttranslational mechanism. Cell 47:921-928.
Shechter R, London A, Varol C, Raposo C, Cusimano M, Yovel G, Rolls A, Mack M, Pluchino S, Martino G, Jung S, Schwartz M (2009) Infiltrating blood-derived macrophages are vital cells playing an anti-inflammatory role in recovery from spinal cord injury in mice. PLoS Med 6:e1000113.
Shen CC, Yang YC, Chiao MT, Cheng WY, Ko JL, Tsuei YS (2010) Characterization of Endogenous Neural Progenitor Cells after Experimental Ischemic Stroke. Curr Neurovasc Res.

Shen LF, Cheng H, Tsai MC, Kuo HS, Chak KF (2009) PAL31 may play an important role as inflammatory modulator in the repair process of the spinal cord injury rat. J Neurochem 108:1187-1197.
Shen LH, Li Y, Gao Q, Savant-Bhonsale S, Chopp M (2008) Down-regulation of neurocan expression in reactive astrocytes promotes axonal regeneration and facilitates the neurorestorative effects of bone marrow stromal cells in the ischemic rat brain. Glia 56:1747-1754.
Shih AY, Johnson DA, Wong G, Kraft AD, Jiang L, Erb H, Johnson JA, Murphy TH (2003) Coordinate regulation of glutathione biosynthesis and release by Nrf2-expressing glia potently protects neurons from oxidative stress. J Neurosci 23:3394-3406.
Shih AY, Fernandes HB, Choi FY, Kozoriz MG, Liu Y, Li P, Cowan CM, Klegeris A (2006) Policing the police: astrocytes modulate microglial activation. J Neurosci 26:3887-3888.
Shindo M, Irie K, Nakahara A, Ohigashi H, Konishi H, Kikkawa U, Fukuda H, Wender PA (2001) Toward the identification of selective modulators of protein kinase C (PKC) isozymes: establishment of a binding assay for PKC isozymes using synthetic C1 peptide receptors and identification of the critical residues involved in the phorbol ester binding. Bioorg Med Chem 9:2073-2081.
Si QS, Nakamura Y, Kataoka K (1997) Hypothermic suppression of microglial activation in culture: inhibition of cell proliferation and production of nitric oxide and superoxide. Neuroscience 81:223-229.
Silberman DM, Zorrilla-Zubilete M, Cremaschi GA, Genaro AM (2005) Protein kinase C-dependent NF-kappa B activation is altered in T cells by chronic stress. Cell Mol Life Sci 62:1744-1754.
Silva GA, Feeney C, Mills LR, Theriault E (1998) A novel and rapid method for culturing pure rat spinal cord astrocytes on untreated glass. J Neurosci Methods 80:75-79.
Silver J (1994) Inhibitory molecules in development and regeneration. J Neurol 242:S22-24.
Silver J, Miller JH (2004) Regeneration beyond the glial scar. Nat Rev Neurosci 5:146-156.
Simard M, Nedergaard M (2004) The neurobiology of glia in the context of water and ion homeostasis. Neuroscience 129:877-896.
Singleton RH, Povlishock JT (2004) Identification and Characterization of Heterogeneous Neuronal Injury and Death in Regions of Diffuse Brain Injury: Evidence for Multiple Independent Injury Phenotypes. J Neurosci 24:3543-3553.
Sinke AP, Jayakumar AR, Panickar KS, Moriyama M, Reddy PV, Norenberg MD (2008) NFkappaB in the mechanism of ammonia-induced astrocyte swelling in culture. J Neurochem 106:2302-2311.
Siren AL, McCarron R, Wang L, Garcia-Pinto P, Ruetzler C, Martin D, Hallenbeck JM (2001a) Proinflammatory cytokine expression contributes to brain injury provoked by chronic monocyte activation. Mol Med 7:219-229.
Siren AL, Fratelli M, Brines M, Goemans C, Casagrande S, Lewczuk P, Keenan S, Gleiter C, Pasquali C, Capobianco A, Mennini T, Heumann R, Cerami A, Ehrenreich H, Ghezzi P (2001b) Erythropoietin prevents neuronal apoptosis after cerebral ischemia and metabolic stress. Proc Natl Acad Sci U S A 98:4044-4049.
Smith GM, Strunz C (2005) Growth factor and cytokine regulation of chondroitin sulfate proteoglycans by astrocytes. Glia 52:209-218.
Smith IF, Boyle JP, Kang P, Rome S, Pearson HA, Peers C (2005) Hypoxic regulation of Ca2+ signaling in cultured rat astrocytes. Glia 49:153-157.
Smith PM, Lakatos A, Barnett SC, Jeffery ND, Franklin RJ (2002) Cryopreserved cells isolated from the adult canine olfactory bulb are capable of extensive remyelination following transplantation into the adult rat CNS. Exp. Neurol. 176:402-406.
Soane L, Kahraman S, Kristian T, Fiskum G (2007) Mechanisms of impaired mitochondrial energy metabolism in acute and chronic neurodegenerative disorders. J Neurosci Res 85:3407-3415.
Sofroniew MV (2005) Reactive astrocytes in neural repair and protection. Neuroscientist 11:400-407.
Sofroniew MV (2008) Molecular dissection of reactive astrogliosis and glial scar formation. Trends in Neurosciences In Press, Corrected Proof.

Song JH, Bellail A, Tse MC, Yong VW, Hao C (2006) Human astrocytes are resistant to Fas ligand and tumor necrosis factor-related apoptosis-inducing ligand-induced apoptosis. J Neurosci 26:3299-3308.
Sonigra RJ, Brighton PC, Jacoby J, Hall S, Wigley CB (1999) Adult rat olfactory nerve ensheathing cells are effective promoters of adult central nervous system neurite outgrowth in coculture. Glia 25:256-269.
Sorci G, Agneletti AL, Bianchi R, Donato R (1998) Association of S100B with intermediate filaments and microtubules in glial cells. Biochim Biophys Acta 1448:277-289.
Sorensen P (2008) [High-dose methylprednisolone in acute spinal injury]. Ugeskr Laeger 170:315-317.
Sorensen SD, Nicole O, Peavy RD, Montoya LM, Lee CJ, Murphy TJ, Traynelis SF, Hepler JR (2003) Common signaling pathways link activation of murine PAR-1, LPA, and S1P receptors to proliferation of astrocytes. Mol Pharmacol 64:1199-1209.
Sorrells SF, Sapolsky RM (2007) An inflammatory review of glucocorticoid actions in the CNS. Brain Behav Immun 21:259-272.
Sousa Vde O, Romao L, Neto VM, Gomes FC (2004) Glial fibrillary acidic protein gene promoter is differently modulated by transforming growth factor-beta 1 in astrocytes from distinct brain regions. Eur J Neurosci 19:1721-1730.
Spahl DU, Berendji-Grun D, Suschek CV, Kolb-Bachofen V, Kroncke KD (2003) Regulation of zinc homeostasis by inducible NO synthase-derived NO: Nuclear translocation and intranuclear metallothionein Zn2+ release. Proceedings of the National Academy of Sciences of the United States of America 100:13952-13957.
Spinelli SV, Rodriguez JV, Quintana AB, Mediavilla MG, Guibert EE (2002) Engraftment and function of intrasplenically transplanted cold stored rat hepatocytes. Cell Transplant 11:161-168.
Steiner MR, Urso JR, Klein J, Steiner SM (2002) Multiple astrocyte responses to lysophosphatidic acids. Biochim Biophys Acta 1582:154-160.
Stichel CC, Muller HW (1998) Experimental strategies to promote axonal regeneration after traumatic central nervous system injury. Prog Neurobiol 56:119-148.
Stipursky J, Gomes FC (2007) TGF-beta1/SMAD signaling induces astrocyte fate commitment in vitro: implications for radial glia development. Glia 55:1023-1033.
Stoll G, Jander S (1999) The role of microglia and macrophages in the pathophysiology of the CNS. Prog Neurobiol 58:233-247.
Streit WJ (2000) Microglial response to brain injury: a brief synopsis. Toxicol Pathol 28:28-30.
Stys PK (2004) White matter injury mechanisms. Curr Mol Med 4:113-130.
Su Z, Yuan Y, Chen J, Cao L, Zhu Y, Gao L, Qiu Y, He C (2009) Reactive astrocytes in glial scar attract olfactory ensheathing cells migration by secreted TNF-alpha in spinal cord lesion of rat. PLoS One 4.
Suh HS, Kim MO, Lee SC (2005) Inhibition of granulocyte-macrophage colony-stimulating factor signaling and microglial proliferation by anti-CD45RO: role of Hck tyrosine kinase and phosphatidylinositol 3-kinase/Akt. J Immunol 174:2712-2719.
Suh HW, Choi SS, Lee JK, Lee HK, Han EJ, Lee J (2004) Regulation of c-fos and c-jun gene expression by lipopolysaccharide and cytokines in primary cultured astrocytes: effect of PKA and PKC pathways. Arch Pharm Res 27:396-401.
Suidan HS, Nobes CD, Hall A, Monard D (1997) Astrocyte spreading in response to thrombin and lysophosphatidic acid is dependent on the Rho GTPase. Glia 21:244-252.
Sullivan SM, Bjorkman ST, Miller SM, Colditz PB, Pow DV (2010a) Morphological changes in white matter astrocytes in response to hypoxia/ischemia in the neonatal pig. Brain Res.
Sullivan SM, Bjorkman ST, Miller SM, Colditz PB, Pow DV (2010b) Structural remodeling of gray matter astrocytes in the neonatal pig brain after hypoxia/ischemia. Glia 58:181-194.
Sullivan SM, Lee A, Bjorkman ST, Miller SM, Sullivan RK, Poronnik P, Colditz PB, Pow DV (2007) Cytoskeletal anchoring of GLAST determines susceptibility to brain damage: an identified role for GFAP. J Biol Chem 282:29414-29423.

Sun GY, Horrocks LA, Farooqui AA (2007) The roles of NADPH oxidase and phospholipases A2 in oxidative and inflammatory responses in neurodegenerative diseases. J Neurochem 103:1-16.
Sun SC, Ganchi PA, Ballard DW, Greene WC (1993) NF-kappa B controls expression of inhibitor I kappa B alpha: evidence for an inducible autoregulatory pathway. Science 259:1912-1915.
Sun SH, Lin LB, Hung AC, Kuo JS (1999) ATP-stimulated Ca2+ influx and phospholipase D activities of a rat brain-derived type-2 astrocyte cell line, RBA-2, are mediated through P2X7 receptors. J Neurochem 73:334-343.
Suter DM, Forscher P (2000) Substrate-cytoskeletal coupling as a mechanism for the regulation of growth cone motility and guidance. J Neurobiol 44:97-113.
Suyang H, Phillips R, Douglas I, Ghosh S (1996) Role of unphosphorylated, newly synthesized I kappa B beta in persistent activation of NF-kappa B. Mol. Cell Biol. 16:5444-5449.
Swanson RA, Benington JH (1996) Astrocyte glucose metabolism under normal and pathological conditions in vitro. Dev Neurosci 18:515-521.
Swanson RA, Farrell K, Stein BA (1997) Astrocyte energetics, function, and death under conditions of incomplete ischemia: a mechanism of glial death in the penumbra. Glia 21:142-153.
Swanson RA, Ying W, Kauppinen TM (2004) Astrocyte influences on ischemic neuronal death. Curr Mol Med 4:193-205.
Szabo CA, Deli MA, Ngo TK, Joo F (1997) Production of pure primary rat cerebral endothelial cell culture: a comparison of different methods. Neurobiology (Bp) 5:1-16.
Szallasi Z, Bogi K, Gohari S, Biro T, Acs P, Blumberg PM (1996) Non-equivalent roles for the first and second zinc fingers of protein kinase Cdelta. Effect of their mutation on phorbol ester-induced translocation in NIH 3T3 cells. J Biol Chem 271:18299-18301.
Szeto HH (2006) Mitochondria-targeted peptide antioxidants: novel neuroprotective agents. AAPS J 8:E521-531.
Tak PP, Firestein GS (2001) NF-kappaB: a key role in inflammatory diseases. J Clin Invest 107:7-11.
Takami T, Oudega M, Bates ML, Wood PM, Kleitman N, Bunge MB (2002) Schwann cell but not olfactory ensheathing glia transplants improve hindlimb locomotor performance in the moderately contused adult rat thoracic spinal cord. J Neurosci 22:6670-6681.
Takeda K, Kaisho T, Akira S (2003) Toll-like receptors. Annu Rev Immunol 21:335-376.
Takenaga K, Kozlova EN (2006) Role of intracellular S100A4 for migration of rat astrocytes. Glia 53:313-321.
Takuma K, Baba A, Matsuda T (2004) Astrocyte apoptosis: implications for neuroprotection. Prog Neurobiol 72:111-127.
Takuma K, Lee E, Kidawara M, Mori K, Kimura Y, Baba A, Matsuda T (1999) Apoptosis in Ca2 + reperfusion injury of cultured astrocytes: roles of reactive oxygen species and NF-kappaB activation. Eur J Neurosci 11:4204-4212.
Tan AM, Zhang W, Levine JM (2005) NG2: a component of the glial scar that inhibits axon growth. J Anat 207:717-725.
Tang Y, Cai D, Chen Y (2007) Thrombin inhibits aquaporin 4 expression through protein kinase C-dependent pathway in cultured astrocytes. J Mol Neurosci 31:83-93.
Tatsumi K, Takebayashi H, Manabe T, Tanaka KF, Makinodan M, Yamauchi T, Makinodan E, Matsuyoshi H, Okuda H, Ikenaka K, Wanaka A (2008) Genetic fate mapping of Olig2 progenitors in the injured adult cerebral cortex reveals preferential differentiation into astrocytes. J Neurosci Res 86:3494-3502.
Taupin V, Toulmond S, Serrano A, Benavides J, Zavala F (1993) Increase in IL-6, IL-1 and TNF levels in rat brain following traumatic lesion. Influence of pre- and post-traumatic treatment with Ro5 4864, a peripheral-type (p site) benzodiazepine ligand. J Neuroimmunol 42:177-185.
Teng X, Nagata I, Li HP, Kimura-Kuroda J, Sango K, Kawamura K, Raisman G, Kawano H (2008) Regeneration of nigrostriatal dopaminergic axons after transplantation of olfactory ensheathing cells and fibroblasts prevents fibrotic scar formation at the lesion site. J Neurosci Res 86:3140-3150.
Tennent R, Chuah MI (1996) Ultrastructural study of ensheathing cells in early development of olfactory axons. Brain Res Dev Brain Res 95:135-139.

Thompson RJ, Roberts B, Alexander CL, Williams SK, Barnett SC (2000) Comparison of neuregulin-1 expression in olfactory ensheathing cells, Schwann cells and astrocytes. J Neurosci Res 61:172-185.

Thuret S, Moon LD, Gage FH (2006) Therapeutic interventions after spinal cord injury. Nat Rev Neurosci 7:628-643.

Tian B, Nowak DE, Brasier AR (2005) A TNF-induced gene expression program under oscillatory NF-kappaB control. BMC Genomics 6:137.

Toews AD, Barrett C, Morell P (1998) Monocyte chemoattractant protein 1 is responsible for macrophage recruitment following injury to sciatic nerve. J Neurosci Res 53:260-267.

Toft A, Scott DT, Barnett SC, Riddell JS (2007) Electrophysiological evidence that olfactory cell transplants improve function after spinal cord injury. Brain 130:970-984.

Town T, Nikolic V, Tan J (2005) The microglial "activation" continuum: from innate to adaptive responses. J Neuroinflammation 2:24.

Tramontina F, Leite MC, Cereser K, de Souza DF, Tramontina AC, Nardin P, Andreazza AC, Gottfried C, Kapczinski F, Goncalves CA (2007) Immunoassay for glial fibrillary acidic protein: antigen recognition is affected by its phosphorylation state. J Neurosci Methods 162:282-286.

Treloar HB, Purcell AL, Greer CA (1999) Glomerular formation in the developing rat olfactory bulb. J Comp Neurol 413:289-304.

Trendelenburg G, Prass K, Priller J, Kapinya K, Polley A, Muselmann C, Ruscher K, Kannbley U, Schmitt AO, Castell S, Wiegand F, Meisel A, Rosenthal A, Dirnagl U (2002) Serial analysis of gene expression identifies metallothionein-II as major neuroprotective gene in mouse focal cerebral ischemia. J Neurosci 22:5879-5888.

Tsuboi A, Muramatsu M, Tsutsumi A, Arai K, Arai N (1994) Calcineurin activates transcription from the GM-CSF promoter in synergy with either protein-kinase-C or NF-kappa-B/AP-1 in T-cells. Biochem Biophys Res Comm 199:1064-1072.

Tuttolomondo A, Di Raimondo D, di Sciacca R, Pinto A, Licata G (2008) Inflammatory cytokines in acute ischemic stroke. Curr Pharm Des 14:3574-3589.

Tzeng SF, Kahn M, Liva S, De Vellis J (1999) Tumor necrosis factor-alpha regulation of the Id gene family in astrocytes and microglia during CNS inflammatory injury. Glia 26:139-152.

Valerio A, Dossena M, Bertolotti P, Boroni F, Sarnico I, Faraco G, Chiarugi A, Frontini A, Giordano A, Liou HC, De Simoni MG, Spano P, Carruba MO, Pizzi M, Nisoli E (2009) Leptin is induced in the ischemic cerebral cortex and exerts neuroprotection through NF-kappaB/c-Rel-dependent transcription. Stroke 40:610-617.

Valko M, Leibfritz D, Moncol J, Cronin MT, Mazur M, Telser J (2007) Free radicals and antioxidants in normal physiological functions and human disease. Int J Biochem Cell Biol 39:44-84.

Valverde F, Santacana M, Heredia M (1992) Formation of an olfactory glomerulus: morphological aspects of development and organization. Neuroscience 49:255-275.

van Landeghem FK, Weiss T, Oehmichen M, von Deimling A (2006) Decreased expression of glutamate transporters in astrocytes after human traumatic brain injury. J Neurotrauma 23:1518-1528.

Vargas MR, Pehar M, Cassina P, Estevez AG, Beckman JS, Barbeito L (2004) Stimulation of nerve growth factor expression in astrocytes by peroxynitrite. In Vivo 18:269-274.

Venance L, Stella N, Glowinski J, Giaume C (1997) Mechanism involved in initiation and propagation of receptor-induced intercellular calcium signaling in cultured rat astrocytes. J Neurosci 17:1981-1992.

Ventura C, Maioli M (2001) Protein kinase C control of gene expression. Crit Rev Eukaryot Gene Expr 11:243-267.

Verdu E, Garcia-Alias G, Fores J, Lopez-Vales R, Navarro X (2003) Olfactory ensheathing cells transplanted in lesioned spinal cord prevent loss of spinal cord parenchyma and promote functional recovery. Glia 42:275-286.

Vergara MN, Arsenijevic Y, Del Rio-Tsonis K (2005) CNS regeneration: a morphogen's tale. J Neurobiol 64:491-507.

Verhaagen J, Oestreicher AB, Grillo M, Khew-Goodall YS, Gispen WH, Margolis FL (1990) Neuroplasticity in the olfactory system: differential effects of central and peripheral lesions of the primary olfactory pathway on the expression of B-50/GAP43 and the olfactory marker protein. J. Neurosci. Res. 26:31-44.

Verkhratsky A (2006) Glial calcium signaling in physiology and pathophysiology. Acta Pharmacol Sin 27:773-780.

Verkhratsky A (2007) Calcium and cell death. Subcell Biochem 45:465-480.

Verkhratsky A, Steinhauser C (2000) Ion channels in glial cells. Brain Res Brain Res Rev 32:380-412.

Verkhratsky A, Orkand RK, Kettenmann H (1998) Glial calcium: homeostasis and signaling function. Physiol Rev 78:99-141.

Vermeiren C, Najimi M, Vanhoutte N, Tilleux S, de Hemptinne I, Maloteaux JM, Hermans E (2005) Acute up-regulation of glutamate uptake mediated by mGluR5a in reactive astrocytes. J Neurochem 94:405-416.

Villmann C, Becker CM (2007) On the hypes and falls in neuroprotection: targeting the NMDA receptor. Neuroscientist 13:594-615.

Vinals F, Pouyssegur J (2001) Transforming growth factor beta1 (TGF-beta1) promotes endothelial cell survival during in vitro angiogenesis via an autocrine mechanism implicating TGF-alpha signaling. Mol Cell Biol 21:7218-7230.

Vincent AJ, West AK, Chuah MI (2003) Morphological plasticity of olfactory ensheathing cells is regulated by cAMP and endothelin-1. Glia 41:393-403.

Vincent AJ, West AK, Chuah MI (2005a) Morphological and functional plasticity of olfactory ensheathing cells. J Neurocytol 34:65-80.

Vincent AJ, Taylor JM, Choi-Lundberg DL, West AK, Chuah MI (2005b) Genetic expression profile of olfactory ensheathing cells is distinct from that of Schwann cells and astrocytes. Glia:Epub 23 March.

Vincent AJ, Choi-Lundberg DL, Harris JA, West AK, Chuah MI (2007) Bacteria and PAMPs activate nuclear factor kappaB and Gro production in a subset of olfactory ensheathing cells and astrocytes but not in Schwann cells. Glia 55:905-916.

Vitellaro-Zuccarello L, Mazzetti S, Madaschi L, Bosisio P, Fontana E, Gorio A, De Biasi S (2008) Chronic erythropoietin-mediated effects on the expression of astrocyte markers in a rat model of contusive spinal cord injury. Neuroscience 151:452-466.

Voskuhl RR, Peterson RS, Song B, Ao Y, Morales LBJ, Tiwari-Woodruff S, Sofroniew MV (2009) Reactive Astrocytes Form Scar-Like Perivascular Barriers to Leukocytes during Adaptive Immune Inflammation of the CNS. J Neurosci 29:11511-11522.

Vukovic J, Plant GW, Ruitenberg MJ, Harvey AR (2007) Influence of adult Schwann cells and olfactory ensheathing glia on axon--target cell interactions in the CNS: a comparative analysis using a retinotectal co-graft model. Neuron Glia Biol. 3:105-117.

Wagner KR (2007) Modeling intracerebral hemorrhage: glutamate, nuclear factor-kappa B signaling and cytokines. Stroke 38:753-758.

Wakida K, Shimazawa M, Hozumi I, Satoh M, Nagase H, Inuzuka T, Hara H (2007) Neuroprotective effect of erythropoietin, and role of metallothionein-1 and -2, in permanent focal cerebral ischemia. Neuroscience 148:105-114.

Walter HJ, Berry M, Hill DJ, Logan A (1997) Spatial and temporal changes in the insulin-like growth factor (IGF) axis indicate autocrine/paracrine actions of IGF-I within wounds of the rat brain. Endocrinology 138:3024-3034.

Wang C, Youle RJ (2009) The role of mitochondria in apoptosis*. Annu Rev Genet 43:95-118.

Wang CC, Fang KM, Yang CS, Tzeng SF (2009a) Reactive oxygen species-induced cell death of rat primary astrocytes through mitochondria-mediated mechanism. J Cell Biochem 107:933-943.

Wang CY, Mayo MW, Baldwin AS, Jr. (1996) TNF- and cancer therapy-induced apoptosis: potentiation by inhibition of NF-kappaB. Science 274:784-787.

Wang CY, Guttridge DC, Mayo MW, Baldwin AS, Jr. (1999) NF-kappaB induces expression of the Bcl-2 homologue A1/Bfl-1 to preferentially suppress chemotherapy-induced apoptosis. Mol Cell Biol 19:5923-5929.

Wang D, Baldwin AS, Jr. (1998) Activation of nuclear factor-kappaB-dependent transcription by tumor necrosis factor-alpha is mediated through phosphorylation of RelA/p65 on serine 529. J Biol Chem 273:29411-29416.

Wang DD, Bordey A (2008) The astrocyte odyssey. Prog Neurobiol 86:342-367.

Wang L, Luo QY, Zhang L, Wu M, Zhang ZZ (2009b) [Effect of metabolism activation on the oxidative cell damage induced by cigarette smoking]. Sichuan Da Xue Xue Bao Yi Xue Ban 40:807-811.

Wang XT, Liu PY, Tang JB (2006) PDGF gene therapy enhances expression of VEGF and bFGF genes and activates the NF-kappaB gene in signal pathways in ischemic flaps. Plast Reconstr Surg 117:129-137; discussion 138-129.

Wang YF, Hatton GI (2009) Astrocytic plasticity and patterned oxytocin neuronal activity: dynamic interactions. J Neurosci 29:1743-1754.

Wanner IB, Deik A, Torres M, Rosendahl A, Neary JT, Lemmon VP, Bixby JL (2008) A new in vitro model of the glial scar inhibits axon growth. Glia 56:1691-1709.

Weaver KD, Yeyeodu S, Cusack JC, Jr., Baldwin AS, Jr., Ewend MG (2003) Potentiation of chemotherapeutic agents following antagonism of nuclear factor kappa B in human gliomas. J Neurooncol 61:187-196.

Weber KS, Klickstein LB, Weber PC, Weber C (1998) Chemokine-induced monocyte transmigration requires cdc42-mediated cytoskeletal changes. Eur J Immunol 28:2245-2251.

Weischenfeldt J, Porse B (2008) Bone Marrow-Derived Macrophages (BMM): Isolation and Applications. Cold Spring Harbor Protocols 2008:pdb.prot5080-.

Weisman GA, Wang M, Kong Q, Chorna NE, Neary JT, Sun GY, Gonzalez FA, Seye CI, Erb L (2005) Molecular determinants of P2Y(2) nucleotide receptor function - Implications for proliferative and inflammatory pathways in astrocytes. Mol Neurobiol 31:169-183.

Werner PC (1997) New drugs for improving injury outcome in spinal cord injuries. West J Med 166:271-272.

Wernyj RP, Mattson MP, Christakos S (1999) Expression of calbindin-D28k in C6 glial cells stabilizes intracellular calcium levels and protects against apoptosis induced by calcium ionophore and amyloid beta-peptide. Brain Res Mol Brain Res 64:69-79.

Wewetzer K, Grothe C, Claus P (2001) In vitro expression and regulation of ciliary neurotrophic factor and its alpha receptor subunit in neonatal rat olfactory ensheathing cells. Neurosci Lett 306:165-168.

Whitney NP, Eidem TM, Peng H, Huang Y, Zheng JC (2009) Inflammation mediates varying effects in neurogenesis: relevance to the pathogenesis of brain injury and neurodegenerative disorders. J Neurochem 108:1343-1359.

Widenfalk J, Lundstromer K, Jubran M, Brene S, Olson L (2001) Neurotrophic factors and receptors in the immature and adult spinal cord after mechanical injury or kainic acid. J Neurosci 21:3457-3475.

Wietek C, O'Neill LA (2007) Diversity and regulation in the NF-kappaB system. Trends Biochem Sci 32:311-319.

Wigley R, Hamilton N, Nishiyama A, Kirchhoff F, Butt AM (2007) Morphological and physiological interactions of NG2-glia with astrocytes and neurons. J Anat 210:661-670.

Wilhelmsson U, Bushongt EA, Price DL, Smarr BL, Phung V, Terada M, Ellisman MH, Pekny M (2006) Redefining the concept of reactive astrocytes as cells that remain within their unique domains upon reaction to injury. Proc Nat Acad Sci USA 103:17513-17518.

Wilhelmsson U, Li L, Pekna M, Berthold CH, Blom S, Eliasson C, Renner O, Bushong E, Ellisman M, Morgan TE, Pekny M (2004) Absence of glial fibrillary acidic protein and vimentin prevents hypertrophy of astrocytic processes and improves post-traumatic regeneration. J Neurosci 24:5016-5021.

Williams SK, Franklin RJ, Barnett SC (2004) Response of olfactory ensheathing cells to the degeneration and regeneration of the peripheral olfactory system and the involvement of the neuregulins. J.Comp. Neurol. 470:50-62.

Wilms H, Hartmann D, Sievers J (1997) Ramification of microglia, monocytes and macrophages in vitro: influences of various epithelial and mesenchymal cells and their conditioned media. Cell Tissue Res 287:447-458.
Winslow MM, Crabtree GR (2005) Immunology. Decoding calcium signaling. Science 307:56-57.
Wofchuk ST, Rodnight R (1994) Glutamate stimulates the phosphorylation of glial fibrillary acidic protein in slices of immature rat hippocampus via a metabotropic receptor. Neurochem Int 24:517-523.
Wolff NA, Abouhamed M, Verroust PJ, Thevenod F (2006) Megalin-dependent internalization of cadmium-metallothionein and cytotoxicity in cultured renal proximal tubule cells. J Pharmacol Exp Ther 318:782-791.
Wolter S, Doerrie A, Weber A, Schneider H, Hoffmann E, von der Ohe J, Bakiri L, Wagner EF, Resch K, Kracht M (2008) c-Jun controls histone modifications, NF-kappaB recruitment, and RNA polymerase II function to activate the ccl2 gene. Mol Cell Biol 28:4407-4423.
Woo MS, Park JS, Choi IY, Kim WK, Kim HS (2008) Inhibition of MMP-3 or -9 suppresses lipopolysaccharide-induced expression of proinflammatory cytokines and iNOS in microglia. J Neurochem 106:770-780.
Woodhall E, West AK, Chuah MI (2001) Cultured olfactory ensheathing cells express nerve growth factor, brain- derived neurotrophic factor, glia cell line-derived neurotrophic factor and their receptors. Brain Res Mol Brain Res 88:203-213.
Woods A, Couchman JR (1992) Protein kinase C involvement in focal adhesion formation. J Cell Sci 101 (Pt 2):277-290.
Wroblewski R, Roomans GM, Kozlova EN (2000) Effects of dorsal root transection on morphology and chemical composition of degenerating nerve fibers and reactive astrocytes in the dorsal funiculus. Exp Neurol 164:236-245.
Wu CX, Zou Q, Zhu ZY, Gao YT, Wang YJ (2009) Intrahepatic transplantation of hepatic oval cells for fulminant hepatic failure in rats. World J Gastroenterol 15:1506-1511.
Wu J, Yang H, Qiu Z, Zhang Q, Ding T, Geng D (2010) Effect of combined treatment with methylprednisolone and Nogo-A monoclonal antibody after rat spinal cord injury. J Int Med Res 38:570-582.
Xiao BG, Xu LY, Yang JS (2002) TGF-beta 1 synergizes with GM-CSF to promote the generation of glial cell-derived dendriform cells in vitro. Brain Behav Immun 16:685-697.
Xu L, Sapolsky RM, Giffard RG (2001) Differential sensitivity of murine astrocytes and neurons from different brain regions to injury. Exp Neurol 169:416-424.
Xu L, Chock VY, Yang EY, Giffard RG (2004) Susceptibility to apoptosis varies with time in culture for murine neurons and astrocytes: changes in gene expression and activity. Neurol Res 26:632-643.
Xu XM, Chen A, Guenard V, Kleitman N, Bunge MB (1997) Bridging Schwann cell transplants promote axonal regeneration from both the rostral and caudal stumps of transected adult rat spinal cord. J Neurocytol 26:1-16.
Yagita Y, Sakoda S, Kitagawa K (2008) [Gene expression in brain ischemia]. Brain Nerve 60:1347-1355.
Yagita Y, Kitagawa K, Ohtsuki T, Takasawa K, Miyata T, Okano H, Hori M, Matsumoto M (2001) Neurogenesis by progenitor cells in the ischemic adult rat hippocampus. Stroke 32:1890-1896.
Yamamoto Y, Gaynor RB (2001) Therapeutic potential of inhibition of the NF-kappaB pathway in the treatment of inflammation and cancer. J Clin Invest 107:135-142.
Yamashima T, Tonchev AB, Borlongan CV (2007) Differential response to ischemia in adjacent hippocampalsectors: neuronal death in CA1 versus neurogenesis in dentate gyrus. Biotechnol J 2:596-607.
Yan H, Bunge MB, Wood PM, Plant GW (2001) Mitogenic response of adult rat olfactory ensheathing glia to four growth factors. Glia 33:334-342.
Yang H, Yang X, Lang JC, Chaum E (2006) Tissue culture methods can strongly induce immediate early gene expression in retinal pigment epithelial cells. J Cell Biochem 98:1560-1569.

Yang HY, Lieska N, Kriho V, Wu CM, Pappas GD (1997) A subpopulation of reactive astrocytes at the immediate site of cerebral cortical injury. Exp Neurol 146:199-205.
Yang L, Tao LY, Chen XP (2007) Roles of NF-kappaB in central nervous system damage and repair. Neurosci Bull 23:307-313.
Yang P, Hernandez MR (2003) Purification of astrocytes from adult human optic nerve heads by immunopanning. Brain Res Brain Res Protoc 12:67-76.
Yang P, Agapova O, Parker A, Shannon W, Pecen P, Duncan J, Salvador-Silva M, Hernandez MR (2004) DNA microarray analysis of gene expression in human optic nerve head astrocytes in response to hydrostatic pressure. Physiol Genomics 17:157-169.
Ye P, Popken GJ, Kemper A, McCarthy K, Popko B, D'Ercole AJ (2004) Astrocyte-specific overexpression of insulin-like growth factor-I promotes brain overgrowth and glial fibrillary acidic protein expression. J Neurosci Res 78:472-484.
Ye ZC, Sontheimer H (1999) Metabotropic glutamate receptor agonists reduce glutamate release from cultured astrocytes. Glia 25:270-281.
Yenari MA, Han HS (2006) Influence of hypothermia on post-ischemic inflammation: role of nuclear factor kappa B (NFkappaB). Neurochem Int 49:164-169.
Yi JH, Hazell AS (2006) Excitotoxic mechanisms and the role of astrocytic glutamate transporters in traumatic brain injury. Neurochem Int 48:394-403.
Yokota S, Imagawa T, Miyamae T, Ito S, Nakajima S, Nezu A, Mori M (2000) Hypothetical pathophysiology of acute encephalopathy and encephalitis related to influenza virus infection and hypothermia therapy. Pediatr Int 42:197-203.
Yu AC, Lee YL, Eng LF (1993) Astrogliosis in culture: I. The model and the effect of antisense oligonucleotides on glial fibrillary acidic protein synthesis. J Neurosci Res 34:295-303.
Yu AC, Wong HK, Yung HW, Lau LT (2001) Ischemia-induced apoptosis in primary cultures of astrocytes. Glia 35:121-130.
Zabel U, Henkel T, Silva MS, Baeuerle PA (1993) Nuclear uptake control of NF-kappa B by MAD-3, an I kappa B protein present in the nucleus. Embo J 12:201-211.
Zador Z, Stiver S, Wang V, Manley GT (2009) Role of aquaporin-4 in cerebral edema and stroke. Handb Exp Pharmacol:159-170.
Zafra F, Lindholm D, Castren E, Hartikka J, Thoenen H (1992) Regulation of brain-derived neurotrophic factor and nerve growth factor mRNA in primary cultures of hippocampal neurons and astrocytes. J Neurosci 12:4793-4799.
Zaheer A, Mathur SN, Lim R (2002) Overexpression of glia maturation factor in astrocytes leads to immune activation of microglia through secretion of granulocyte-macrophage-colony stimulating factor. Biochem Biophys Res Commun 294:238-244.
Zaheer A, Zaheer S, Sahu SK, Knight S, Khosravi H, Mathur SN, Lim R (2007) A novel role of glia maturation factor: induction of granulocyte-macrophage colony-stimulating factor and pro-inflammatory cytokines. J Neurochem 101:364-376.
Zalewski PD, Forbes IJ, Giannakis C, Cowled PA, Betts WH (1990) Synergy between zinc and phorbol ester in translocation of protein kinase C to cytoskeleton. FEBS Lett 273:131-134.
Zeng JW, Liu XH, Zhang JH, Wu XG, Ruan HZ (2008a) P2Y1 receptor-mediated glutamate release from cultured dorsal spinal cord astrocytes. J Neurochem 106:2106-2118.
Zeng JW, Liu XH, He WJ, Du L, Zhang JH, Wu XG, Ruan HZ (2008b) Inhibition of ATP-induced glutamate release by MRS2179 in cultured dorsal spinal cord astrocytes. Pharmacology 82:257-263.
Zhang H, Uchimura K, Kadomatsu K (2006) Brain keratan sulfate and glial scar formation. Ann N Y Acad Sci 1086:81-90.
Zhang HL, Gu ZL, Savitz SI, Han F, Fukunaga K, Qin ZH (2008) Neuroprotective effects of prostaglandin A(1) in rat models of permanent focal cerebral ischemia are associated with nuclear Factor-kappa B inhibition and peroxisome proliferator-activated receptor-gamma up-regulation. J Neurosci Res 86:1132-1141.

Zhang X, Polavarapu R, She H, Mao Z, Yepes M (2007) Tissue-type plasminogen activator and the low-density lipoprotein receptor-related protein mediate cerebral ischemia-induced nuclear factor-kappaB pathway activation. Am J Pathol 171:1281-1290.

Zhao H (2007) The protective effect of ischemic postconditioning against ischemic injury: from the heart to the brain. J Neuroimmune Pharmacol 2:313-318.

Zhou J, Sutherland ML (2004) Glutamate transporter cluster formation in astrocytic processes regulates glutamate uptake activity. J Neurosci 24:6301-6306.

Zhu C, Wang X, Huang Z, Qiu L, Xu F, Vahsen N, Nilsson M, Eriksson PS, Hagberg H, Culmsee C, Plesnila N, Kroemer G, Blomgren K (2007) Apoptosis-inducing factor is a major contributor to neuronal loss induced by neonatal cerebral hypoxia-ischemia. Cell Death Differ 14:775-784.

Zhu SM, Xiong XX, Zheng YY, Pan CF (2009) Propofol inhibits aquaporin 4 expression through a protein kinase C-dependent pathway in an astrocyte model of cerebral ischemia/reoxygenation. Anesth Analg 109:1493-1499.

Zlokovic BV (2008) The blood-brain barrier in health and chronic neurodegenerative disorders. Neuron 57:178-201.